ISAC-II OPERATION AND FUTURE PLANS

M. Marchetto, TRIUMF, Vancouver, BC V6T 2A3, Canada

Abstract

The ISAC-II superconducting heavy ion linac now accelerates radioactive ion beams with the highest gradient of any operating SC ion facility in the world and provides a 20 MV boost to the ISAC accelerated beams. The addition of a further 20 MV of SC linac, with cavities made in Canada, will be installed by the end of 2009. The ISAC-III project scheduled to begin in 2010 will see the installation of an additional driver beam of 50 MeV electrons to produce RIBs by photofission, an expanded target area, and new front-end ion accelerators to expand the capability to three simultaneous radioactive beams for experiments.

INTRODUCTION

ISAC at TRIUMF is one of the major existing facilities for the production of radioactive ion beams (RIB). There are two commonly used methods for RIB production [1].

The first one is the in flight or fragmentation method. The facility using this method has a main accelerator that accelerates heavy ions toward a thin target. The heavy ion breaks apart going through the target producing a variety of radioactive ions. The ions, already at the final velocity, are selected through a fairly complex mass separator system and sent to the experiment.

The second method is the isotope separation on line or ISOL method. In this case an accelerator, called a driver, accelerates light projectiles, the primary beam, toward a thick target. The light projectiles, protons or light ions, break the target nuclei producing neutral radioactive isotopes. These neutral atoms are then transported into a source where they are ionized and extracted at source potential. The radioactive ions are magnetically separated and post accelerated to reach the final energy requested.

The two methods are complementary. The in flight is a fast production method that allows to deliver isotopes of very short half-lives (ms or less) but with a beam of relatively large emittance . The ISOL method on the contrary produces high quality emittances but the complicated and relatively slow process reduces the possibility of extracting isotopes with few ms half-lives. The in flight methods RIB has energy of several tens of MeV/u while the ISOL method can deliver beam of few keV/u.

ISAC OVERVIEW

The ISAC facility at TRIUMF is an ISOL facility. It has the highest power (50 kW) primary proton beam. The overview of the facility is represented in Fig. 1. The ISAC facility produces the most intense beam for certain species, an example being the exotic ^{11}Li.

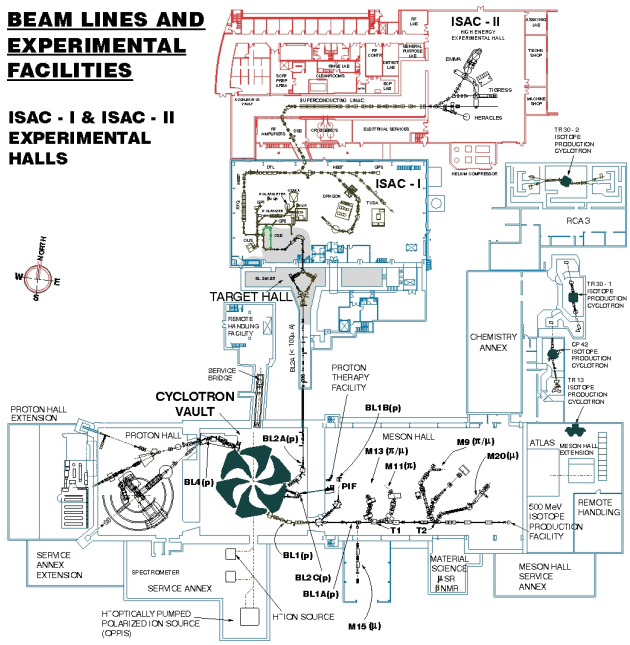

Figure 1: Overview of the TRIUMF site. The main machine is the H$^-$ 500 MeV cyclotron used also as driver of the ISAC facility.

The facility uses silicon carbide or tantalum targets for ion production. Two target configurations are available: low and high power respectively for proton beam powers up to 20 kW and 50 kW. Most recently beam production with a UOx target was successfully completed.

Driver

The TRIUMF H$^-$ cyclotron is the largest cyclotron in the world and has operated for almost 35 years. It accelerates H$^-$ ions up to an intensity of 250 μA to a maximum energy of 500 MeV. The H$^-$ are then stripped and protons are extracted in three different beam lines at different energies the maximum being 500 MeV. One of these beam line is dedicated for the ISAC radioactive beam production. In this case the beam is extracted at 500 MeV and up to 100 μA.

The simultaneous extraction of multiple beams with stable delivery is challenging. Nevertheless a 90% availability of the proton beam for the ISAC facility is regularly achieved.

The capability of multiple extractions can be expanded by refurbishing a fourth existing extraction beam line giving two simultaneous proton beams for RIB production [2] as represented in Fig. 2. This possibility together with an upgrade of the cyclotron [3] is one of the goals for the next

THE EUROPEAN XFEL SC LINAC PROJECT

R. Brinkmann, Deutsches Elektronen-Synchrotron (DESY), D-22607 Hamburg, Germany for the XFEL Team

Abstract

The European XFEL project is entering the construction phase, based on the very successful experience of the TESLA linac technology and the SASE FEL concept, now serving the FLASH user facility at DESY.

The EU-XFEL will be realized by a widespread international collaboration and it is also relevant for the ILC planning. A description of the overall layout of the facility, of the tchnical developments and industrialization efforts for the accelerator components, and of the international collaboration will be given.

INTRODUCTION

The XFEL was originally proposed as part of the TESLA facility, first in a version integrated with the linear collider using the same linac [1,2], in a later version with its own separate linac [3]. In February 2003 the German Government announced the decision that the XFEL should be realized as a European project, with at least 40% funding contributions requested from partner countries. After this decision an intense preparation phase followed in which DESY, together with partner institutes, pushed forward the work necessary to achieve the status of readiness for start of construction. Besides the optimization of the overall design, main objectives in this phase where preparations for the site and civil construction, industrialization of major technical components and detailed studies of beam physics and the FEL process. The XFEL has a strong link to the FLASH (VUV-FEL) facility at DESY [4 – 6], which is in nearly all respects (accelerator technology, FEL operation, photon beam lines and user experiments) truly a pilot facility for the future project.

The project organization at the international level is supervised by a steering committee (ISC) with members from all countries interested in participating in the project. In 2005 ISC nominated a European Project Team (EPT), with the main charge to deliver the technical and administrative documents required for the process of negotiations and decisions at the political level towards achieving the final go-ahead for the project. In July 2006, an updated Technical Design Report (TDR) was completed [7] and delivered to ISC. The progress in the negotiations with the partner countries on contributions to the project then led to the official go-ahead for project construction on June 5, 2007, on the basis of an initially de-scoped startversion of the facility (see below). The nominal construction cost (in year 2005 prices) of the start version amounts to 850 M€, to which approximately 90 M€ have to be added for project preparation and commissioning.

Up to date, 14 countries have made commitments to contribute to the project (Figure 1), summing up to a total of 1,060 M€ (on year 2005 basis). In addition to covering the cost for the startversion including preparation and commissiong, there remains an overhead which will with first priority be used to cover cost risks, but which may to a limited extent also permit to remove part of the initial de-scoping of the facility.

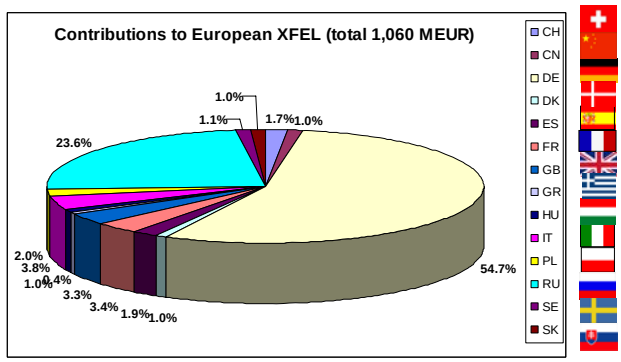

Figure 1: Distribution of funding contributions to the European XFEL project. Contributions are in cash as well as in-kind.

The administrative documents, in particular the Intergovernmental Convention, are essentially ready for signature by the partner countries. After that event, foundation of the XFEL company, of which all partners are shareholders, will take place. The company has the overall supervision and responsibility for the European XFEL and will also manage the civil construction and photon beam systems parts of the project. For the accelerator complex, an international consortium is being set up, which will contribute the entire accelerator and the related technical infrastructure essentially as an in-kind contribution to the project. At present 17 institutes from 10 of the XFEL member states have joined the consortium. DESY will provide approximately 60% of the in-kind contributions to the accelerator complex and act as the consortium coordinator.

LAYOUT AND PARAMETERS

The main components of the XFEL Facility are the injector, the linear accelerator, the beam distribution system, the undulators, the photon beam lines, and the instruments in the Experiments Hall (see Figure 2).

These components are distributed along an essentially linear geometry, 3.4 km long, starting on the DESY campus in the northwest part of the city of Hamburg, and ending in the neighbouring Federal State of Schleswig-

SNS SUPERCONDUCTING LINAC OPERATIONAL EXPERIENCE AND UPGRADE PATH*

Sang-ho Kim, ORNL, Oak Ridge, TN 37831, U.S.A.

Abstract

The Spallation Neutron Source (SNS) Superconducting Linac (SCL) has been providing a main acceleration in two different accelerating sections with 33 medium beta and 48 high beta superconducting radio-frequency (SRF) 6-cell cavities. The use of superconducting elliptical cavities for particles whose velocity are less than speed of light (beta<1), make this accelerator a very important milestone for learning operating conditions of this type of cavities. Since the SNS SCL is the first large-scale high energy pulsed-superconducting proton linac that provides high beam power utilizing H- beams, many aspects of its performance were unknown and unpredictable. A large amount of data has been collected on the pulsed behavior of cavities and cryomodules at various repetition rates and at various temperatures. This experience will be of great value in determining future optimizations of SNS as well in guiding in the design and operation of future pulsed superconducting linacs. This paper describes the details of the RF properties, performances, path-forward for the SNS power ramp-up goal, and upgrade path of the SNS superconducting linac.

INTRODUCTION

The SNS accelerator complex consists of a negative hydrogen (H-) RF volume source, a low-energy beam transport (LEBT) line with a first-stage beam chopper, a 4-vane radio-frequency quadrupole (RFQ) up to 2.5 MeV, a medium-energy beam transport (MEBT) line with a second-stage chopper, six drift-tube linac (DTL) tanks up to 87 MeV, four coupled-cavity linac (CCL) modules up to 186 MeV, a superconducting linac (SCL) with 11medium-beta cryomodules (up to 379 MeV) and 12 high-beta cryomodules (up to 1000 MeV), a high energy beam transport (HEBT) line, an accumulator ring with associated beam transport line, a ring-to-target beam transport (RTBT) line, and a mercury target. At a full duty, the linac will produce 38-mA peak, chopped H^- beam for 1-ms long at 60 Hz. In the ring, 700-ns long midi-pulse beam is accumulated over 1060 turns reaching an intensity of 1.5×10^{14} protons per pulse. After beam accumulation in the ring, the beam is extracted using the extraction kickers during 300-ns long midi-pulse gap in a single turn is transported to the mercury target through the RTBR line. Figure 1 shows the layout of the SNS.

A series of the beam commissioning, initiated in 2002 and completed in May 2006, was performed in seven commissioning runs for Front-End, DTL Tank 1, DTL Tanks 1-3, CCL, SCL, Accumulator Ring, and beam on target.

* SNS is managed by UT-Battelle, LLC, under contract DE-AC05-00OR22725 for the U.S. Department of Energy

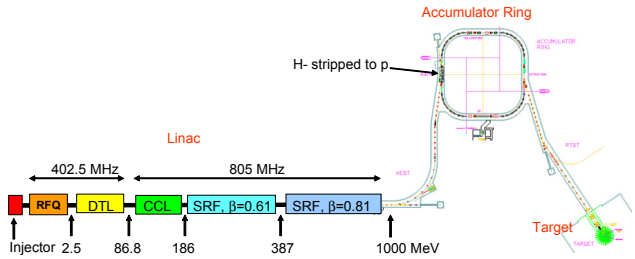

Figure 1: Layout of the SNS accelerator system.

Official SNS operations for scheduled neutron scattering experiments has been started since October 2006. The SNS is now nearly two years into the initial operations phase [1, 2].

The SRF cavities and the cryomodules were designed and developed at Jefferson Lab and installed at the SNS site in 2005. Major parameters are summarized in Table 1. As the first operational pulsed superconducting linac, many of the aspects of its performance were unknown and unpredictable. A lot of experiences and data have been gathered on the pulsed behavior of cavities and cryomodules at various repetition rates and at various temperatures during the commissioning of its components and beam operations. Careful balance between safe operational limits and the study of conditions, parameters and components that create physical limits has been achieved [3, 4]. The SCL is running at about 0.9-GeV output energy and is presently one of the most reliable systems in SNS. Figure 2 shows the accelerating gradients of SCL cavities at 60Hz in 2008 for the neutron production, which is set based on the 60 Hz collective limits achieved. Power ramp up plan to reach the design goal is set and various efforts are in progress.

Table 1: Major Design Parameters of the SNS SCL

Cryomodule Parameter	β=0.61 Section	β=0.81 Section
Output Energy (MeV)	379	1000
No. of Cryomodules	11	12
No. of cavities per cryomodule	3	4
Cavity Parameter	**β=0.61 Cavity**	**β=0.81 Cavity**
Geometric beta	0.61	0.81
EoT (MV/m)	10.1 at β=0.61	15.8 at β=0.81
Epeak (MV/m)	27.5	35.0
Hpeak (kA/m)	46.2 (580 Oe)	59.7 (750 Oe)
Q*Rs (Ω)	176	228
r/Q at design beta	279	483
Equivalent Cavity Length (cm)	68.2	90.6

PROGRESS IN THE BEAM COMMISSIONING OF J-PARC LINAC AND ITS UPGRADE PATH

M. Ikegami, KEK, Tsukuba, Ibaraki 305-0801, Japan

Abstract

The beam commissioning of J-PARC linac was started in November 2006, and its initial stage was completed in October 2007. Since then, we start to provide the linac beam for the beam commissioning of downstream facilities. During this period, we have performed occasional high-power demonstrations, where we have recently achieved the linac beam power of 12.7 kW (210 kW from RCS) for a limited period of time. We have also confirmed that the short-term beam stability and beam availability of the linac have already reached a sufficient level. The final goal of 1 MW from RCS is to be pursued though a staged upgrades.

INTRODUCTION

J-PARC (Japan Proton Accelerator Research Complex) is a multi-purpose high-intensity proton accelerator facility jointly constructed by KEK (High Energy Accelerator Research Organization) and JAEA (Japan Atomic Energy Agency). J-PARC accelerator consists of a 400-MeV linac, 3-GeV RCS (Rapid Cycling Synchrotron), and 50-GeV MR (Main Ring). Figure 1 shows the schematic layout of J-PARC facilities.

J-PARC linac serves as an injector for the entire J-PARC facility. The output beam from linac is injected into RCS, and that from RCS is delivered to both MR and a neutron production target. We also have a muon production target through which a proton beam penetrates before reaching the neutron target. Meanwhile, MR is accommodated with two beam extraction systems. One is a slow extraction system, and the other is a fast extraction system. The beam extracted with the slow extraction system is utilized for studies on hadron physics, and the fast-extracted beam is delivered to a neutrino production target for a long-baseline neutrino oscillation experiment. The final goal of the project is to deliver a 1-MW beam from RCS and 0.75-MW beam from MR.

To achieve the final goal, a phased approach is taken in the J-PARC project as discussed in a later section. We are currently in the first phase of the project, where the output energy from linac and MR are 181 MeV and 30 GeV, respectively. In this phase, the linac consists of a 50-keV negative hydrogen ion source, 3-MeV RFQ (Radio Frequency Quadrupole linac), 50-MeV DTL (Drift Tube Linac), and 181-MeV SDTL (Separate-type DTL). The schematic layout of the linac is shown in Fig. 2. The operation frequency of these accelerating cavities is 324 MHz, and the RF power is fed by 3-MW klystrons. Aside from these accelerating cavities, we also have two buncher cavities and two chopper cavities in MEBT (Medium Energy Beam Transport) between RFQ and DTL. In addition, two debuncher cavities are installed in the beam transport line between the SDTL exit to RCS, to which we refer as L3BT (Linac-to-3-GeV RCS Beam Transport). In 181-MeV operation, two SDTL tanks are temporarily utilized as debunchers.

At this point, the initial commissioning of RCS is approaching its completion [2]. The first neutron and muon beams were respectively produced in May and September 2008. Then, neutron production runs are to be started in December 2008. The initial commissioning of MR has recently been started with a beam storage mode, and the acceleration up to 30 GeV will be tried in December 2008 [3]. We plan to deliver the beam to the hadron experimental facility by February 2009, and to the neutrino production target by June 2009.

In this paper, we summarize the achieved performance in J-PARC linac after briefly reviewing its commissioning history. We also show the recent situations with emphasis on the stability of the beam operation and the machine activation experienced to date. Finally, we will present an upgrade path planned for J-PARC linac.

COMMISSIONING HISTORY AND PRESENT SITUATION

The beam commissioning of J-PARC linac was started in November 2006, and its initial stage was completed in October 2007 [4, 5, 6]. During the beam commissioning, the design beam energy of 181 MeV was achieved in January 2007. Then, the output beam power of 1.2 kW (3.3 % of the design value) was demonstrated in June 2007. From February to May 2007, fundamental tunings have been conducted including the phase scan tuning for the RF set-points [7, 8, 9], orbit correction, and transverse match-

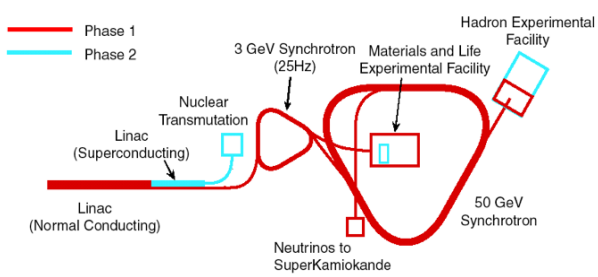

Figure 1: Schematic layout of J-PARC facility.

STATUS OF A HIGH CURRENT LINEAR ACCELERATOR AT CSNS

S.N. Fu, H.F. Ouyang, X.J. Yin, J. Li, J. Peng, Z.R. Sun, Y. Cheng
IHEP, Institute of High Energy Physics, Beijing 100049, China

Abstract

China Spallation Neutron Source (CSNS) consists of an H^- linac as an injector of a rapid cycling synchrotron of 1.6 GeV. The 324 MHz rf linac is designed with beam energy of 81 MeV and a peak current of 30 mA. The linac design and R&D are in progress. A test stand of a Penning ion source is under construction. RFQ technology has been developed in ADS study, with beam energy of 3.5 MeV, a peak current of 46 mA at 7% duty factor and a beam transmission rate more than 93%. The first segment of the DTL tank is under fabrication. A full-scale prototype of resonant high-voltage pulse power supply for klystron has been successfully demonstrated. This paper will introduce the design and R&D status of the linac.

INTRODUCTION

The CSNS accelerator is the first large-scale, high-power accelerator project to be constructed in China[1]. CSNS accelerator mainly consists of an H- linac and a proton rapid cycling synchrotron. It is designed to accelerate proton beam pulses to 1.6 GeV kinetic energy at 25 Hz repetition rate, striking a solid metal target to produce spallation neutrons, as schematically shown in Figure 1. The accelerator is designed to deliver a beam power of 120 kW with the upgrade capability up to 500 kW by raising the linac output energy and increasing the beam intensity, as listed in Table 1[2].

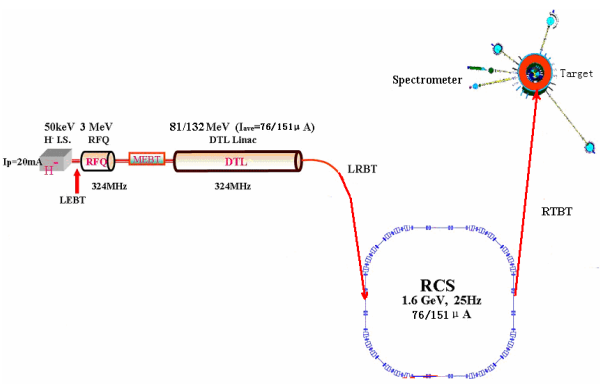

Figure 1: CSNS schematics.

This paper will introduce the design and R&D status of the linac. In the next section, physics design of the linac will be described. Then some R&D activities in the key technology, including ion source, RFQ, DTL and a new type of RF source power supply, will be briefly introduced.

Table 1: CSNS Primary Parameters in Baseline and Upgrade Phases

Project phase	I	II	II'
Beam ave. power, kW	120	240	500
Proton energy, GeV	1.6		
Ave. current, *I*, μA	76	151	315
Repetition rate, Hz	25		
Proton per pulse, 10^{13}	1.88	3.76	7.83
Pulse length, ns	<500		
Linac energy, MeV	81	132	230
Linac length, m	50	76	86
Linac rf freq. , MHz	324		
Macro ave. *I*, mA	15	30	40
Macro duty factor, %	1.1	1.1	1.7
Ring circumference, m	247	247	247
Ring filling time, ms	0.5	0.5	0.8
Uncontroled loss, W/m	< 1		

CSNS LINAC PHYSICS DESIGN[3]

CSNS linac consists of an H- ion source, an LEBT, a 3MeV RFQ linac at 324MHz RF frequency, an MEBT and a 324MHz DTL linac. The output beam of the DTL linac is 81MeV with peak current of 15mA in the first phase. CSNS upgrade plan has been taken into the physics design. Beam pulse current will be increase to 30mA or even 40mA, while the beam energy will be increased to 132MeV or even 230MeV respectively so as to keep an acceptable space charge tune spread during the injection into the RCS. Some space in the linac-RCS beam line is now reserved for the additional accelerating structure for the upgraded CSNS linac.

For a low beam loss during the injection to the RCS, injected beam needs to be chopped for pre-bunching in the ring RF bucket. The chopped beam pulse structure is illustrated in Figure 2. To realize such a macro-pulse of 468ns, a pre-chopper is designed in the LEBT. In the case that the chopping is not clear, another fast chopper may be added in the MEBT.

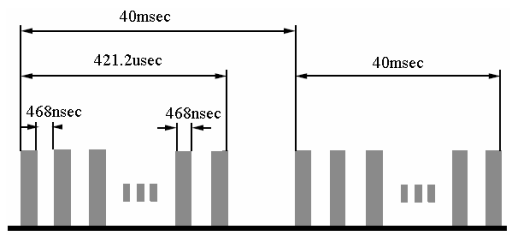

Figure 2: The linac beam pulse structure after chopping.

THE SARAF CW 40 MEV PROTON/DEUTERON ACCELERATOR

A. Nagler, D. Berkovits, I. Gertz, I. Mardor#, J. Rodnizki, L. Weissman,
Soreq NRC, Yavne 81800, Israel
K. Dunkel, F. Kremer, M. Pekeler, C. Piel, P. vom Stein,
Accel Instruments GmbH, Bergisch Gladbach 51429, Germany

Abstract

The Soreq Applied Research Accelerator Facility, (SARAF) is currently under construction at Soreq NRC. SARAF will be a multi-user facility for basic research, medical and biological research, neutron based non-destructive testing and radio-pharmaceuticals research, development and production. SARAF is based on a continuous wave (CW), proton/deuteron RF superconducting linear accelerator with variable energy (5–40 MeV) and current (0.04-2 mA). The accelerator is designed to enable hands-on maintenance, which implies beam loss below 10^{-5} for the entire accelerator. Phase I of SARAF consists of a 20 keV/u ECR ion source, a low energy beam transport section, a 4-rod RFQ, a medium energy (1.5 MeV/u) beam transport section, a superconducting module housing 6 half-wave resonators and 3 superconducting solenoids, a diagnostic plate and a beam dump. Phase II will include 5 additional superconducting modules. The ECR source is in routine operation since 2006 and the RFQ has been operated with ions and is currently under characterization. The superconducting module is installed in the beam line and its RF performance is being characterized. Phase I commissioning results, their comparison to beam dynamics simulations and beam dynamics simulations of Phase II are presented.

SARAF OVERVIEW

SARAF is currently under construction at Soreq NRC [1]. It will consist of a medium energy (up to 40 MeV) high current (up to 2 mA) RF superconducting linac of protons and deuterons, beam lines and a target hall with several irradiation stations for the abovementioned applications.

The facility schematic layout, its required parameters and a technical description of its components are given in Ref. 2. For a review of its operation concept and control system see Ref. 3.

Due to the technical novelty in the accelerator, the project has been divided to two phases. Phase I includes the ECR ion source, the RFQ, a prototype superconducting module (PSM), the design of the full accelerator (based on beam dynamics simulations [4]) and the design and risk reduction of the foreseen applications. Phase II includes construction of rest of the accelerator and its applications.

This paper presents recent commissioning results of phase I, including comparison to beam dynamics simulations [5], selected results of simulations for Phase II and a calculation of the expected residual activation due to beam loss in Phase II.

#mardor@soreq.gov.il

PHASE I COMMISSIONING

The SARAF accelerator is designed, manufactured, installed and commissioned by Accel Instruments GmbH [6], in close collaboration with Soreq NRC personnel.

Phase I is fully installed on site, as is shown from 2 views in Figs. 1 and 2.

Figure 1: Upstream view of Phase I as installed on site at Soreq NRC. From right to left: ECR ion source (EIS), Low energy beam transport (LEBT), RFQ and Prototype Superconducting Module (PSM).

Figure 2: Downstream view of Phase I of SARAF. From right to left: PSM, Diagnostic plate (D-Plate), low power (Beam dump 1, copper, 6 kW) and high power (Beam dump 2, tungsten, 20 kW) beam dumps.

THE INJECTOR SYSTEMS OF THE FAIR PROJECT

W. Barth
Gesellschaft für Schwerionenforschung, D-64291 Darmstadt, Germany

Abstract

The present GSI accelerator chain will serve as an injector for FAIR (**F**acility for **A**ntiproton and **I**on **R**esearch). The linear accelerator UNILAC and the heavy ion synchrotron SIS18 should deliver up to $1\cdot10^{12}$ U^{28+}-particles/sec. In the past two years different hardware measures and a careful fine tuning of the UNILAC resulted in an 35% increase of the beam intensity to a new record of $1.25\cdot10^{11}$ U^{27+}-ions per 100 µs or 2.3 10^{10} U^{73+}-ions per 100 µs. The increased stripper gas density, the optimization of the Alvarez-matching, the use of various newly developed beam diagnostics devices, and a new charge state separator system in the foil stripper section comprised the successful development program. The contribution reports results of beam measurements during the high current operation with uranium beams (beam pulse power up to 0.65 MW). The UNILAC-upgrade for FAIR will be continued by assembling a new front-end for U^{4+}, stronger power supplies for the Alvarez quadrupoles, and versatile high current beam diagnostics devices. Additionally, the offered primary proton beam intensities will be increased by a new proton linac, which should be commissioned in 2013. We acknowledge the support of the European Community – Research Infrastructure Activity under the FP6 "Structuring the European Research Area" program (CARE, contract number RII3-CT-2003-506395). Work supported by the European Community INTAS Project Ref. no. 06-1000012-8782.

INTRODUCTION

Meeting the FAIR science requirements higher intensities have to be achieved in the present GSI-accelerator complex, through faster cycling and, for heavy ions, lower charge state which enters quadratically into the space charge limit (SCL). The desired energy of up to 1.5 GeV/u for radioactive beam production is delivered by the synchrotron SIS 100, which also generates intense beams of energetic protons up to 30 GeV for pbar-production. Highly charged heavy ion beams with a maximum energy of 30 GeV/u have to be accelerated in the slower cycling synchrotron SIS 300. SIS 300 can also be used as a stretcher for radioactive beams, which can be injected, cooled, and stored in a system of rings with internal targets and in-ring experimentation.

Figure 1: The future accelerator facility FAIR at GSI in Darmstadt [1].

Table 1: FAIR-design Uranium Beam Parameters at UNILAC and SIS 18 Injection [2]

	HSI entrance	HSI exit	Alvarez entrance	SIS 18 injection	
Ion species	$^{238}U^{4+}$	$^{238}U^{4+}$	$^{238}U^{28+}$	$^{238}U^{28+}$	$^{238}U^{73+}$
El. Current [mA]	25	18	15	15.0	5.5
Part. per 100µs pulse	$3.9\cdot10^{12}$	$2.8\cdot10^{12}$	$3.3\cdot10^{11}$	$3.3\cdot10^{11}$	$5.0\cdot10^{10}$
Energy [MeV/u]	0.0022	1.4	1.4	11.4	
ΔW/W	-	$4\cdot10^{-3}$	$\pm1\cdot10^{-2}$	$\pm2\cdot10^{-3}$	
$\varepsilon_{n,x}$ [mm mrad]	0.3	0.5	0.75	0.8	
$\varepsilon_{n,y}$ [mm mrad]	0.3	0.5	0.75	2.5	

In the last years GSI put effort in increasing the uranium intensities delivered to the SIS 18. An advanced upgrade program for the UNILAC is still in progress to meet the FAIR requirements. For uranium (FAIR reference ion) the UNILAC has to deliver $3.3\cdot10^{11}$ U^{28+}-particles per 100 µs (see Table 1). Besides for a 15 emA $^{238}U^{4+}$ beam from the High Current Injector HSI [2] up to $5.5\cdot10^{10}$ U^{73+} particles should be delivered to the GSI heavy ion synchrotron SIS 18 (during 100 µs), while the SIS 18 SCL is reached by a 15 turn injection into the horizontal phase space.

In the 36 MHz-HSI [3] comprising ion sources of MEVVA-, MUCIS- or Penning-type, the IH-RFQ, a short 11 cell adapter RFQ (Super Lens), and two IH-tanks, the beam is accelerated up to 1.4 MeV/u. In the gas stripper section the charge state is increased and after charge separation the high intensity U^{28+}-beam is matched to the Alvarez DTL. After acceleration up to the final UNILAC-beam energy the transfer line (TK) to the synchrotron provides for a foil stripper and a new compact charge state separator system.

The UNILAC brilliance for proton beams is at least two orders of magnitude below the FAIR-requirements. For the proposed time sharing scenario proton beam intensities of 35 mA and an energy of 70 MeV are required. Accordingly, a dedicated proton injector linac [4] being designed within FAIR will be operated independently from the existing UNILAC.

The UNILAC serving as a high duty factor heavy ion linac for physics experiments is in operation since more than 30 years. After completion of the FAIR complex in 2015 the running time for the accelerator facility will be 20 years at least, while the UNILAC will then be in operation for more than 60 years. Different proposals for a new advanced short pulse, heavy ion, high intensity,

OVERVIEW OF THE HIGH INTENSITY NEUTRINO SOURCE LINAC R&D PROGRAM AT FERMILAB *

R. C. Webber#, G. Apollinari, J. P. Carneiro, I. Gonin, B. Hanna, S. Hays, T. Khabiboulline, G. Lanfranco, R. L. Madrak, A. Moretti, T. Nicol, T. Page, E. Peoples, H. Piekarz, L. Ristori, G. Romanov, C. W. Schmidt, J. Steimel, W. Tam, I. Terechkine, R. Wagner, D. Wildman
Fermilab, Batavia, IL 60510, U.S.A.
P. N. Ostroumov, ANL, Argonne, IL 60439, U.S.A.

Abstract

The Fermilab High Intensity Neutrino Source (HINS) Linac R&D program is building a first-of-a-kind 60 MeV superconducting H- linac. The HINS Linac incorporates superconducting solenoids for transverse focusing, high power RF vector modulators for independent control of multiple cavities powered from a single klystron, and superconducting spoke-type accelerating cavities starting at 10 MeV. This will be the first application and demonstration of any of these technologies in a low-energy, high-intensity proton/H- linear accelerator. The HINS effort is relevant to a high intensity, superconducting H- linac that might serve the next generation of neutrino physics and muon storage ring/collider experiments. An overview of the HINS program, machine design, status, and outlook is presented.

INTRODUCTION

Fermilab has long considered options to replace its aging 8 GeV injector complex to support future accelerator-based physics programs that will demand high intensity proton beams, including neutrino physics and muon storage ring/collider experiments. A technologically advanced, enhanced performance version of the classical Fermilab Linac/Booster system is a natural concept to pursue and a great deal of effort has been invested to develop the physics and engineering details of this option [1][2]. With recent advances in superconducting (SC) RF cavity science and technology, the possibility of a full 8 GeV linac became realistic. Plans for such a machine that would leverage the best aspects of RIA, SNS, and TESLA/ILC developments were born [3] and matured [4].

By late 2005, strong interest in pursuit of the International Linear Collider (ILC) and the U. S. high energy physics community's commitment to PEP-II B-Factory and Tevatron Collider operations left little room to support construction of an 8 GeV linac. Nevertheless, it was recognized that a machine of this caliber might be a key to maintaining a strong U.S. presence in accelerator-based physics before ILC construction. This provided the basis, in the name of neutrino physics, for R&D funding to pursue the novel technical aspects of the linac and thus the Fermilab High Intensity Neutrino Source (HINS) R&D linac.

HINS R&D SCOPE

The full scope of the HINS R&D program has included studies of various accelerator physics issues of importance to a facility expected to deliver high intensity, high energy beams for exploration of neutrino physics. With Fermilab steering the overall efforts, collaborating laboratories have also made important contributions. Argonne National Laboratory provides the major resources for the accelerator physics design and particle tracking simulations for both the HINS and the 8 GeV linacs. Argonne's experience in the design and development of SC spoke-type RF cavities [5] [6] serves as the foundation for Fermilab's entry into this technology and Argonne continues to provide resources for cavity processing in the construction phase. Lawrence Berkeley National Laboratory's participation in the HINS program has included studies of electron cloud issues, especially as related to the Fermilab Main Injector and Recycler Rings, development of linac Low Level RF system hardware and firmware, and design and fabrication of two buncher cavities for the HINS 2.5 MeV transport section. Brookhaven National Laboratory has reviewed an 8 GeV H- beam transport line design, provided consultation on H- injection and stripping, and built a prototype H- beam profile monitor based on laser neutralization to be used in the HINS Linac. The Oak Ridge Spallation Neutron Source has provided a copy of their Low Level RF system hardware modified for the HINS frequency.

This paper concentrates on the design, status and outlook for the HINS Linac.

HINS R&D LINAC OBJECTIVES

The HINS Linac R&D program will address accelerator physics and technology questions for a new concept, low-energy, high intensity, long-pulse H- SC linac. In particular, the specific goals of the program are to demonstrate:

- acceleration of beam using SC spoke-type cavity structures starting at a beam energy of 10 MeV
- use of high power RF vector modulators to control multiple RF cavities driven by a single high power klystron for acceleration of a non-relativistic beam
- control of beam halo and emittance growth with an axially symmetric optics design using solenoid focusing
- performance of a fast, 325 MHz bunch-by-bunch, beam chopper at 2.5 MeV

*Operated by Fermi Research Alliance, LLC under Contract No. DE-AC02-07CH11359 with the United States Department of Energy.
webber@fnal.gov

OVERVIEW OF RECENT RFQ PROJECTS *

A. Schempp
Institut für Angewandte Physik, J. W. Goethe-Universität, D-60486 Frankfurt am Main, Germany

Abstract

RFQs are the new standard injector for a number of projects. The development of the 4-Rod RFQ structure has led to interesting developments, which will be discussed with actual projects as examples. Recent work on the FAIR - p linac, the GSI - high charge state injector upgrade, the GSI - HITRAP, the new BNL - EBIS-RFQ, and the RFQ of the MSU-CW Reaccelerator will be presented and the status of these projects will be discussed.

INTRODUCTION

Accelerators have been developed as tools for atomic, nuclear and particle physics. From these technologies numerous applied research did develop. The "production" of secondary particles as purpose of a facility was another big step in accelerator technology, because the production rates can be increased by optimizing the beam energy and target arrangement and of course by increasing the beam current to the target.

In case of heavy ion beams the duty factor of the machines had to be large because of the limits of sources for (multiple charged) heavy ions. For protons and deuterons the beam currents from ion sources could be pushed up to the 100 mA region, so the duty factors of the accelerators could be modes tlike for spallation sources with beam powers of up to 1MW and the synchrotron injectors, drivers for neutron production or for sources of radioactive beams with beams of some kW.

Accelerators for radioactive beams have low power beams but require high duty factors for compensation of the low production rates.

The Frankfurt IAP was involved in the planning phase for GSI and the cooperation with GSI in the 70s by post accelerator structure applications (helix, spiral) could be kept up until today with respect to the FAIR project.

A big step were the new ideas about RFQs in the late 70s for low energy acceleration [1,2].

Application for heavy ions and lower frequency and the need for practical solutions led to the development of the 4-rod RFQ structure. First prototyps and beam tests were rather simple, but the big point was the chance to develop and built structures for other labs, at first GSI, DESY and MSI, which pushed the development and besides beam dynamics, the importance of issues like rf- and mechanical technologies and reliability.

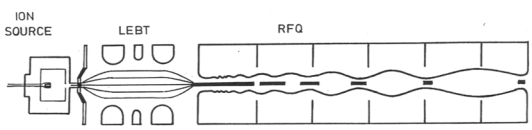

Figure 1: Scheme of a RFQ injector.

RFQ DESIGN

The design of RFQs is at first the choice of basic parameters like frequency, input output energy, which are mostly determined by the application or the ion source or the following bigger accelerator system.

Next steps in the beam dynamics design is the choice of electrode voltage U, beam current, input and output energy and emittances ε and the cell parameters along the RFQ: cell length L_i, aperture a_i, modulation m_i. The result is an RFQ with certain total length L and power consumption N which adiabatically bunches and focuses the dc beam from the ion source with small Δε and high transmission [3].

RFQ design is sometimes treated as being completed, when the beam dynamics design is finished. Especially for high power beams it is crucial to have a balanced design which takes into account the special rf-problems as well as the engineering to ensure tolerances, to handle the rf-losses, the beam with losses, the diagnostics and also maintenance possibilities and control.

While for smaller neutron generators RFQ aspects can dominate the choice e.g. of the frequency and length and rf-power consumption to simplify alignment and tuning, for bigger projects the optimization of the total accelerator, the availability of power sources and naturally costs will set some design input parameters and e.g. will increase the frequency to lower the charge per bunch, to avoid funneling and ease emittance growth and matching problems or reduce crucial beam losses.

Reducing losses and emittance growth and high duty factors or beam powers require even new solutions and prototype developments not showing up in beam dynamics simulation which sometimes are described as “physics design”.

To generate the quadrupole fields we use the 4 rod RFQ structure, which we have developed in Frankfurt It can be described as a chain of interlaced λ/2-resonators in π–0-mode. The electrodes can be typical rods, or small vane shaped electrodes. with unchanged rf-properties. The radial dimensions of the 4-rod RFQ are appr. half as for a 4-Vane TE_{210}-structure at the same frequency. Beam dynamics and experimental results for emittances and transmission are the same as for 4-Vane RFQs.

While the power consumption is also roughly the same, there are some advantages because the 4-rod structure cannot show dipoles and longitudinal coupling is stronger

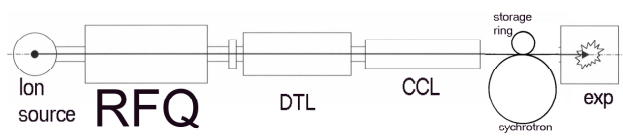

Figure 2: Accelerator system.

*supported by the BMBF

A COUPLED RFQ-DRIFT TUBE COMBINATION FOR FRANZ

A. Bechtold, U. Bartz, M. Heilmann, P. Kolb, H. Liebermann, D. Mäder, O. Meusel, H. Podlech, U. Ratzinger, A. Schempp, C. Zhang, IAP, J. W. Goethe-Universität, Frankfurt, Germany,
G. Clemente, GSI, Darmstadt, Germany.

Abstract

The Frankfurt Neutron Source at the Stern-Gerlach-Zentrum (FRANZ) [1] will comprise a short 175 MHz linac sequence consisting of a 1.75 m long 700 keV 4-rod type RFQ [2] followed by a 60 cm IH-DTL [3] for proton acceleration up to 2 MeV. The beam current is 200 mA at pulsed and up to 30 mA at c.w. operation. The aim is to have a very compact device driven by only one rf-amplifier to reduce costs and required installation space. A strong coupling between the RFQ and the IH resonators will be realized by a direct connection between the last stems of each resonator through the common end wall. The accelerators could also be driven separately by just removing the coupling. The distance between the end of the RFQ electrodes and the midplane of the first DTL gap is only 5 cm leaving some place for a x-y-steerer. Preliminary rf-simulations have been carried out together with accompanying measurements on rf-models.

INTRODUCTION

The coupling of different rf-components is very attractive for most recent accelerator development. It leads to more compact devices using a common rf-amplifier and control system. Thus the overall size and the costs of the set up can be reduced drastically.

Many examples are planned or already in existence. For instance a coupled RFQ-drifttube combination that has been developed for medical application at the HICAT (Heavy Ion Cancer Therapy) center in Heidelberg by the IAP, where a 4-rod-RFQ and a 2 gap rebuncher sequence are merged [4]. This concept has been applied recently to other treatment facilities by industry several times [5]. Coupled CH-DTL cavities are a major achievement in the development of the FAIR Proton Injector at GSI [6, 7].

Two coupled rf-systems with same resonance frequency can be driven in 0 or in π-mode, which can lead to very interesting applications. When they are excited both at the same time, the resulting beat resonance can be used to reduce thermal load where pulsed operation is not feasible like in the case of the former LEP normal conducting accelerator at CERN, where the accelerator cavity was coupled to a low loss spherical resonator [8].

Presently investigations on a resonant coupling between RFQ an IH-DTL for FRANZ are performed. Unlike the aforementioned medicine RFQ, both parts are tuned to the same resonance frequency and are clearly separated by means of a metallic wall.

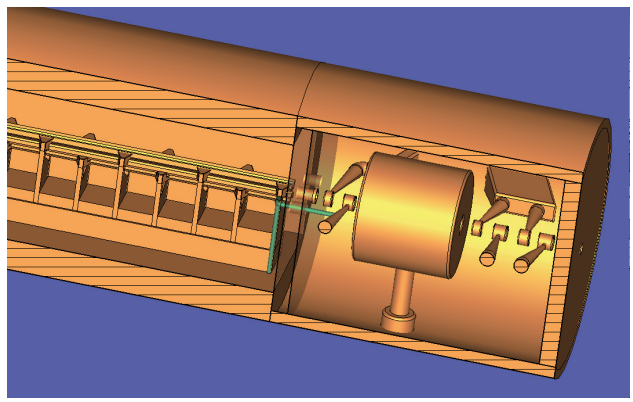

Figure 1: The coupled 4-rod-RFQ-IH-DTL structure. The coupling bridges are colored in green.

Table 1: Main Parameters

Operating frequency	175 MHz
Ion species	protons
Length of RFQ	1.75 m
Length of IH-DTL	0.6 m
Tank diameter IH	510 mm
Height of RFQ-Stems	145 mm
# of RFQ cells	97
# of matching in cells	4
# of IH-gaps	8
Input energy	120 keV
Input emittance (absolute) $\varepsilon_{x,y}$	150 π mm mrad
Electrode voltage (RFQ)	75 kV
Max. gap voltage of IH-DTL	300 kV
Exp. Power consumption RFQ	150 kW
Exp. Power consumption IH	45 kW
Current	max. 200 mA
Output energy RFQ	700 keV/u
Output energy IH-DTL	2 MeV
Coupling factor k	≈0.03

COUPLING

The distance between 0 and π-mode is given by $\Delta\omega = \omega_0 \cdot k$, where ω_0 is the uncoupled resonance frequency and k is the coupling strength. The coupling should be sufficiently strong ($k > 0.01$), to guarantee a good separation between the modes.

INJECTOR DEVELOPMENT FOR HIGH INTENSITY PROTON BEAMS AT STERN-GERLACH-ZENTRUM

O. Meusel, A. Bechtold, L.P. Chau, M. Heilmann, H. Podlech, U. Ratzinger, K. Volk, C. Wiesner
IAP, University Frankfurt/Main, Germany

Abstract

The Frankfurter neutron source at the Stern-Gerlach-Zentrum (FRANZ) uses a 2 MeV proton LINAC as a driver for the ^{7}Li(p,n) neutron production. A volume type ion source will deliver a 120keV, 200mA proton beam continuously. A LEBT section consisting of four solenoids is under construction to transport the beam and to match it into the acceptance of the RFQ. A chopper system between solenoid 2 and 3 will provide beam pulses with a length of about 50 to 100 ns with a repetition rate of up to 250 kHz. The RFQ and the following IH drift tube LINAC will be coupled together to achieve an efficient beam acceleration. Furthermore only one power amplifier will be needed to provide the RF power for both accelerator stages. The Mobley type bunch compressor will merge 8 micro bunches formed in the accelerator module to one single 1ns bunch with an estimated peak current of up to 9.6 A. A rebuncher will provide the post acceleration to final beam energy adjustable between 1.8 and 2.2 MeV. The whole system is optimized for high beam intensity causing high space charge forces. As a consequence new accelerator concepts and beam diagnostic concepts have to be developed.

INTRODUCTION

FRANZ comprises two experimental areas allow different types of neutron capture measurements. The compressor mode offer time of flight measurements in combination with a 4π BaF_2 detector array. The proton beam will be compressed to a 1ns pulse with a peak current of about 9.6 A and a repetition rate of 250 kHz. On the other hand activation mode uses a continuous neutron flux. Primary cw proton beams with a current up to 8 mA on solid targets and up to 30 mA on liquid metal targets as a later option are feasible.

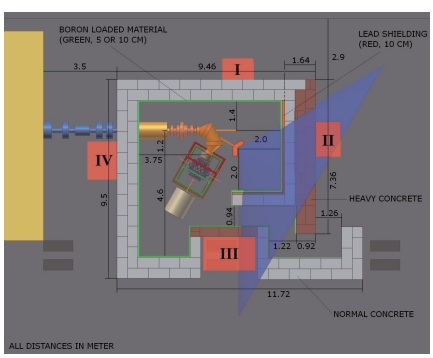

Figure 1: Scheme of the FRANZ facility with targets and detector and iradiation and neutron shielding.

FRANZ is not only a neutron generator but also a test bench for new accelerator and diagnostic concepts for intense ion beams. The envisaged proton beam properties on the target lead into a challenging accelerator design to overcome the space charge forces.

ION SOURCE

A volume type ion source was chosen for FRANZ to extract the proton beam from a hot filament driven gas discharge plasma [1]. Figure 2 shows this source type. The life time of the filament is limited about one month of operation. On the other hand the plasma temperature of a gas discharge at moderate arc power is as well as the confining magnetic field very low compared with other source types e.g. ECR sources. Therefore the beam emittance is small and gives the possibility to investigate causes of emittance growth during beam transport and acceleration along the whole LINAC.

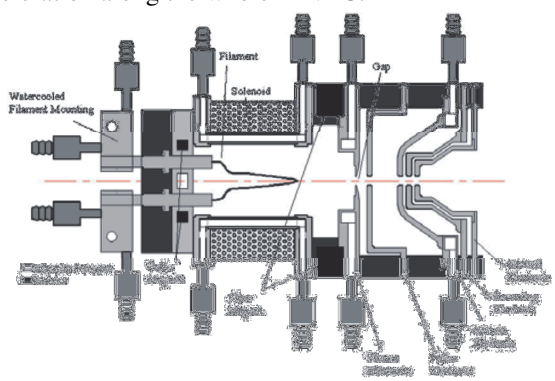

Figure 2: crossectional view of the volume type ion source under construction.

For the planned beam intensities a pentode extraction system keeps quite well the beam emittance during the extraction and pre acceleration phase when compared with other extraction schemes [2]. Figure 3 shows a preliminary numerical simulation of the beam extraction by the use of the IGUN code [3] and under respect of a multi species beam with approximately H^+ = 80%, H_2^+ = H_3^+ 10%.

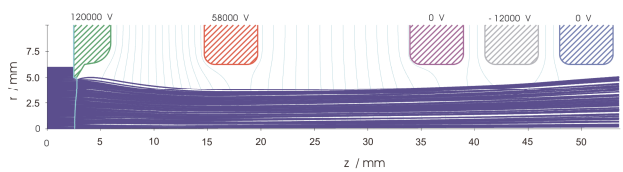

Figure 3: Illustration of a preliminary IGUN calculated beam profile along a pentode extraction system.

PERFORMANCE OF THE CONTROL SYSTEM FOR THE J-PARC LINAC

H.Yoshikawa, T.Suzuki, H.Sakaki, Y.Itoh, Y.Kato, M.Kawase, H.Sako, G.Shen, H.Takahashi, JAEA, Tokai-mura, JAPAN
S.Fukuta, MELCO SC, Tsukuba, JAPAN
S.Sawa, TOSS, Tokai-mura, JAPAN
H.Ikeda, VIC, Tokai-mura, JAPAN.

Abstract

LINAC of J-PARC began to operate in November, 2006, and a achieved an initial performance in January, 2007. Afterwards, the beam supply to RCS begins, and it is operating extremely with stability up to now[1]. The fundamental condition of the control system design is to defend the beam loss detecting it as early as possible because it controls the radiation by the large strength beam to the minimum. This requirement influences from the level of the basic function of high-speed interlock to the level of an advanced application that needs the predictive control. It describes what work distribution, how much man power were necessary for the control system construction.

CONCEPT OF DESIGN

The requirement to minimize the beam loss and to reduce the residual radiation makes large difference from the control system of a past experimental accelerator in the point that operating the trial and error is not permitted. This control system protects LINAC from miss-operation, but flexibility of operation absolutely must be kept for the development of 1MW operation[2]. We set the robustness of protection in the middle-ware, and set the free-stage enclosed that middle-ware for the application.

Basic policies of the strategy are :

- Middle-ware (process communication tools, device drivers, database libraries) gives the perfection as much as possible.
- Least making and maximum recycling by OOP is used.
- End user presents a necessary function of th program, and doesn't make the program itself.

At the debugging, it is severe to find bugs of middle-ware. It takes most of the debugging time that finding the reason of unexpected behaviour of poor libraries or cheep drivers. There is an idea with driver's structure simply to avoid this, too. However, it gives origin to an excessive complexity of a high-level application. We were initially given using EPICS. To make the best use of the advantage of the flat scope of EPICS records, we limited the use of record-link. The use of the record-link is a rapier, and it is necessary to use it under the total management. Even the record file should not be individually described. (Sometimes, the file written at the device test survives still.) The database application that confirmed parsing, matching and grammar was developed. End user, who are the expert of device or equipment, are not always good programmer, and don't know the detail of our function hierarchy. If sharing an individual application by the common device model is attempted, the quiet sleep at the term of all-day operation can be secured. We concentrated on the competent understanding of the function of the application that the user requested.

LINAC components are categorized into :

- Vacuum system (several kind of pumps, vacuum gauge, rough pumping system, gate valve, fast closing valve)
- RF cavity system (cavity, tuner, cooling water, temp meas.,)
- High-power RF source (klystron, HV-PS, LLRF, wave-guide, tuner)
- Magnet system (bend, q-singlet, doublet, steer)
- Monitor system (position, profile, current)

And, each device communicates with :

- Timing System (TS)
- Machine Protection System (MPS)
- Personnel Protection System (PPS)
- Parameter Data Base (DB1)
- Measurement Data Base (DB2)

We described all function of each cell in the matrix that is made of device column and sub-system line. On the result of this detailed examination, we aimed at sharing software by adapting low-level application of each device to common skeleton based on the machine model.

MPS and PPS was required very complicated function because J-PARC is a multi-purpose facility. Though it is preferable to achieve it by hardware logic, it is impossible to achieve it only by the relay logic. We decided using PLC for PPS, and FPGA is used for MPS to realize the required response time.

MAN POWER AND STRATEGY

The control system design started in 2002. It had 4 years to beam operation, but we aimed to use the actual application for factory test of individual equipment after three years. Requested man power was ;

- Five experts those who can develop device driver, process communication.
- Five programmers those who have a experience of medium scale application.

At the beginning, we started 8 members. Fortunately, 4 of us are ex-colleague of SPring-8 LINAC. Machine model, OOP driver and special needs of J-PARC LINAC became our common recognition at once. To cancel the lack of man power, the detailed design of network system was done in outsourcing. And the coverage of the

OPERATING EXPERIENCE OF THE J-PARC LINAC

Kazuo Hasegawa#, H. Asano, E. Chishiro, T. Hori, T. Ito, T. Kobayashi, Y. Kondo,
Y. Namekawa, H. Oguri, K. Ohkoshi, H. Suzuki, A. Ueno, M. Yamazaki,
J-PARC (KEK&JAEA), JAEA, Tokai, Ibaraki, Japan
S. Anami, Z. Fang, Y. Fukui, K. Ikegami, M. Kawamura, F. Naito, K. Nanmo,
H. Tanaka, S. Yamaguchi, J-PARC (KEK&JAEA), KEK, Tokai, Ibaraki, Japan

Abstract

The beam commissioning of the J-PARC linac started in November 2006 and 181 MeV acceleration was successfully achieved in January 2007. The linac has delivered beams to the 3 GeV Rapid Cycling Synchrotron for its commissioning, and then, the subsequent Main Ring Synchrotron and the neutron target commissioning. The linac uses a Cs-free LaB_6-driven ion source and 20 units of 324 MHz klystrons. As of June 2008, the operation times are about 3,000 and 6,000 hours for the ion source and the RF source, respectively. The operating experience of the linac is described.

INTRODUCTION

The J-PARC (Japan Proton Accelerator Research Complex) is a multipurpose facility with 1 MW class proton beam[1]. The facility is under construction at the JAEA/Tokai site as a joint project between the Japan Atomic Energy Agency (JAEA) and the High Energy Accelerator Research Organization (KEK). The J-PARC accelerator consists of a linac, a 3 GeV rapid cycling synchrotron (RCS), and a 50 GeV main ring synchrotron (MR). At the initial stage of the project, the linac accelerates a negative hydrogen beam up to 181 MeV with a current of 30 mA, a pulse width of 0.5 msec and repletion of 25 Hz.

The linac consists of an RFQ, a Drift Tube Linac (DTL) and a Separated-type Drift Tube Linac (SDTL). The features of the linac are described in [2]. High power conditioning of the cavities and beam test started in October and November 2006, respectively, then 181 MeV energy acceleration was achieved in January 2007. Since then, the linac beams have been used for the linac commissioning for its own, for the RCS commissioning, for neutron production, and for RF capture experiment at the MR.

We have adopted a three to four weeks commissioning cycle, which consists of a two or three week beam commissioning run and a one or two week interval. Adjusting the terms of intervals to accommodate appropriate maintenance periods, 17 beam commissioning cycles have been experienced from November 2006 to June 2008. Detailed beam commissioning results are described in [3].

FRONT END

The J-PARC linac uses a Cs-free, LaB_6-driven, multicusp H^- ion source[4]. The diameter and the length of the plasma chamber are 100 and 120 mm, respectively. The source plasma is confined by the multicusp magnetic field by 18 rows at the sidewall and four rows at the upper flange. The filament is a cylindrical spiral structure LaB_6 and the size is 29.5 mm and 49 mm in diameter and height, respectively.

Figure 1 shows the history of the ion source operation. During intervals between commissioning cycles, we have performed maintenance or ion source study. The pink and green bars denote the typical H^- beam current in the commissioning days and the ion source study days, respectively. The maximum beam current from the ion source is 38 mA at the arc duty factor of 0.8 % (0.32 msec in pulse width and 25 Hz). Since the commissioning tasks doesn't always require a high peak H^- beam current, the ion source has been operated either at the low current mode of 5 mA or at the high current mode of 30 mA. To keep the condition of the plasma chamber surface good, the ion source keeps running of the filament or beam extraction during the nighttime in the commissioning days. Operation time of the source has been reached to 3,360 hours as of June 2008.

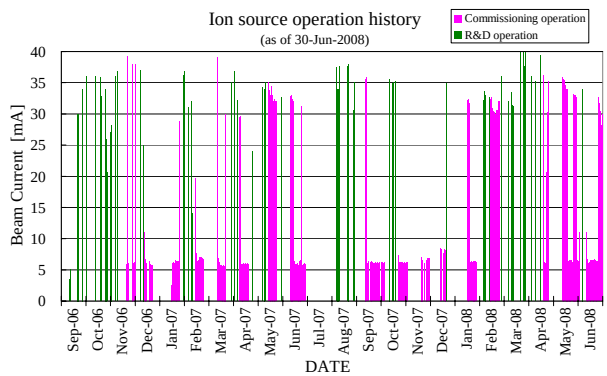

Figure 1: Operation history of the ion source.

On October 6 and December 18, 2006, filament had troubles of short-circuit to the neighboring spirals. The troubles were caused by filament deformation due to the arc power heating. Then the filament shape was modified to have a wider gap between spirals from 0.3 to 0.6 mm. We have not had similar troubles since then.

On August 21, 2007, we had a cutting off of the filament. We consider that the filament was broken by some strong mechanical stress because the filament showed no signs of remarkable consumption. The filament was replaced with a studious care. That filament lasted by June 28, 2008. The beam time was 2,030 hours,

#hasegawa.kazuo@jaea.go.jp

BEAM TEST RESULTS OF THE PEFP 20 MEV PROTON ACCELERATOR AT KAERI*

Yong-Sub Cho#, Han-Sung Kim, In-Seok Hong, Ji-Ho Jang, Dae-Il Kim, , Hyeok-Jung Kwon, Bum-Sik Park, Kyung-Tae Seol, Young-Gi Song, Sang-Pil Yun, KAERI, Daejon 305-353, Korea

Abstract

A 20 MeV proton accelerator, which consists of a 50 keV injector, a 3 MeV RFQ and a 20 MeV DTL, has been tested by Proton Engineering Frontier Project (PEFP) at Korea Atomic Energy Research Institute (KAERI). The operation conditions are 20 MeV, 20 mA peak current, 50 μs pulse length with a 1 Hz repetition rate due to the limited radiation shielding. The accelerator was tuned to reach to the above operating conditions. Moreover, an irradiation facility with external beam has been installed to supply the proton beam for the user and irradiation test. In this paper, we present results from tuning operation and the irradiation tests.

INTRODUCTION

The Korean Government launched the Proton Engineering Frontier Project (PEFP) in 2002 to help realize potential applications of high-power proton beams. The primary goal of the project is to develop a high-power proton linear accelerator to supply 100-MeV proton beams and to construct user beam line facilities, whose users can utilize proton beams with a wide range of energies and currents for their research and development programs [1]. In addition, the 100-MeV accelerator can be used as a proton injector for the next-stage high-power accelerators, such as a high-energy linac or rapid cycling synchrotron [2].

A 20-MeV proton linear accelerator has been developed as the front end of the 100-MeV accelerator, which consists of a 50-keV proton injector, a 3-MeV RFQ, a 20-MeV DTL, and RF systems, as shown in Fig. 1.

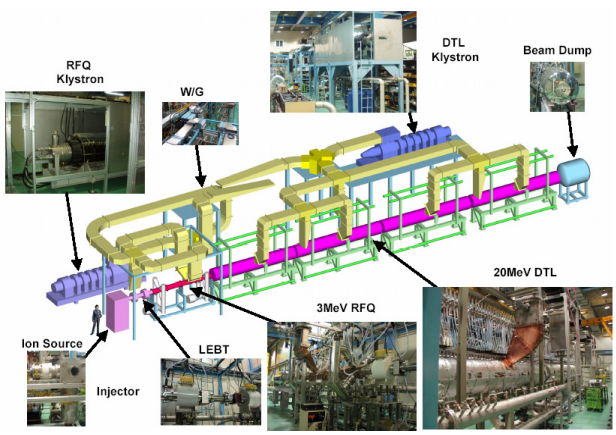

Figure 1: 20MeV proton linac at KAERI.

*Work supported by the Korea Ministry of Education, Science and Technology.
#choys@kaeri.re.kr

THE 20-MEV PROTON LINEAR ACCELERATOR

The Proton Injector [3]

The injector includes a duoplasmatron proton source and a low-energy beam transport (LEBT). The beam current extracted from the source reached a current of 50 mA. The extracted beam has a normalized emittance of 0.2 πmm-mrad from a 90% beam current, where the proton fraction is > 80%. To achieve pulsed operation, a high-voltage switch has been installed in the high-voltage power supply, whose rise and fall times are < 50 ns. The pulse length and the repetition rate can be easily changed using this semiconductor switch. The LEBT consists of two solenoid magnets that can filter the H^{2+} ions and two steering magnets that can control the beam's position and angle at the entrance of the RFQ.

The 3 MeV RFQ [4,5]

The PEFP RFQ is designed to accelerate a 20-mA proton beam using a voltage from 50 keV to 3 MeV and has the usual four-vane-type design. The entire structure is separated into two segments that are resonantly coupled for field stabilization. The RF power is fed into the cavity through two iris couplers in the third section.

A 3-MeV, 350-MHz PEFP RFQ has been fabricated, tuned, installed, and tested. The low-power field tuning satisfied the design requirements. High-power RF conditioning experiments for the RFQ were carried out up to a peak power of 450 kW, a pulse length of 80 μs, and a repetition rate of 1 Hz. The time required for this conditioning was about 8 h. The RF signals shown in Fig. 6 are the signals detected after the conditioning, which were very stable. Beam tests were carried out by adjusting the LEBT and the RF parameters.

The 20-MeV DTL

The PEFP 20-MeV DTL consists of four tanks that accelerate the 20 mA proton beam from 3 MeV to 20 MeV. The total length of the DTL is about 20 m. The PEFP DTL structures were designed for a beam duty of 24%, and the FFDD lattice configuration has a magnetic field gradient of 5 kG/cm and an effective field length of 3.5 cm.

The DTL was fabricated using electroplating technology for the tanks and e-beam welding technology for the drift tube. A laser tracker was used to align the drift tubes in the tanks. Figure 8 shows the inside of a tank. The tuning goals for the PEFP DTL were such that the deviation in frequency was less than ±5 kHz from the design value, and the field distribution was less than ±2 %

STABILITY OF NORMAL CONDUCTING STRUCTURES OPERATION WITH HIGH AVERAGE HEAT LOADING

V. V. Paramonov *, INR RAS, 117312 Moscow, Russia

Abstract

Instead of proved application of superconducting structures for high energy part of intense linear proton accelerators, Normal Conducting (NC) structures are still considered for medium and low energy parts below $200MeV$. Operation with accelerating rate of $\sim 4\frac{MeV}{m}$ and duty factor $\sim 5\%$ results for standing wave NC structure in an average heat loading of $\sim 30\frac{kW}{m}$. Due to the high heat loading an operating mode frequency shift is significant during operation. In this paper conditions for field distribution stability against small deviations in time of individual cell frequencies are considered. For $\frac{\pi}{2}$ structures these conditions were formulated by L. Young and Y. Yamazaki. General case of 0, $\frac{\pi}{2}$ and π operating modes is considered with common approach.

INTRODUCTION

In projects of modern particle accelerators NC structures are consideration for application with the strong heat loading due to high average RF power dissipation. It can be the sequence of a high accelerating gradient E_0T, or long RF pulse, or high RF pulse repetition rate or combinations of these factors. Together with bi-periodical (or compensated) structures, simple periodical structures with 0 or π operating modes are under consideration too due to a simpler design and construction. As it is known well, simple 0 or π mode structures are sensitive in electric field distribution to small deviations of cells frequencies. To ensure required accelerating field homogeneity, not so large number of simple structure periods $N_p \sim 5 \div 10$ should be in the cavity and coupling coefficient should be so high, as reasonable.

Nevertheless, let us suppose the cavity with the simple periodic or bi-periodic structure is tuned for required field distribution and another parameters. But during a high RF power operation a question of thermal stability arises.

THERMAL STABILITY

During a high RF power operation the temperature of the cavity increases and own cavity frequency f_0 decreases due to cavity expansion. For the fixed cooling conditions the cavity frequency shift is linearly proportional to the average dissipated RF power. For a heat loading of $\geq 20\frac{kW}{m}$ the cavity frequency shift df can be of $df \geq 2.0 \cdot 10^{-4} f_0$. The cavity frequency for high RF power operation should be adjusted by the change of cooling water temperature.

* paramono@inr.ru

Suppose we have a steady-state high RF power operation with a reference field distribution in the cavity. Let us suppose, that in one moment the cell with the number j got a small frequency deviation Δf_j due to some random reasons. Mostly possible reason is a fluctuation of a turbulent flow in cooling channels, because the turbulent flow is stable in average. For distinctness we will suppose $\Delta f_j < 0$, assuming cooling ability reduction. The small frequency change of the $j-th$ cell immediately will results in the change of the field distribution along the cavity and the change of relative field balance between cells. Depending on the structure dispersion properties, two options are possible.

In the first case the field in the $j-th$ cell relatively decreases. RF power dissipation in this cell decreases, the cell temperature decreases, the cell frequency increases, canceling initial cell frequency deviation. After some time the structure returns to operation with the reference field distribution. Such structures are thermally stable.

In the second case the field in the $j-th$ cell relatively increases. RF power dissipation in this cell also increases, the cell temperature increases, the cell frequency decreases, amplifying initial cell frequency deviation. Self-amplifying process starts. At least, such process can lead to the change in the filed distribution, because the cooling and control systems operate for the cavity as a whole. Such structures are thermally unstable.

Field distribution description

Suppose we know the total set of modes in the reference unperturbed cavity - frequencies f_ν and field distributions E_ν, H_ν, normalized as:

$$\int_V Z_0^2 H_n H_\nu^* dV = \int_V E_n E_\nu^* dV = \delta_{n\nu} W_0, \qquad (1)$$

where $Z_0 = \sqrt{\frac{\mu_0}{\epsilon_0}}$ and V is the cavity volume. The field distribution in the cavity with a small dimension deviation ΔV can be describe as [1]:

$$E = E_n + \sum_{\nu \neq n} E_\nu \frac{f_\nu^2}{f_n^2 - f_\nu^2} \frac{1}{W_0} \int_{\Delta V} (Z_0^2 H_n H_\nu^* - E_n E_\nu^*) dV. \qquad (2)$$

In all periodical accelerating structures the field distribution along the axis can be described as:

$$E_{m\nu} = E_{\nu 0} cos(m\nu\pi), \qquad (3)$$

where $E_{m\nu}$ is the field amplitude in the m-th cell, $\nu\pi$ is the phase shift per structure period. Here we assume the phase

STATUS OF THE LINAC4 PROJECT AT CERN

M. Vretenar, C. Carli, R. Garoby, F. Gerigk, K. Hanke, A.M. Lombardi, S. Maury, C. Rossi,
CERN, Geneva, Switzerland

Abstract

Linac4 is a new 160 MeV, 40 mA H^- accelerator which will be the source of particles for all proton accelerators at CERN from 2013. Its construction has started in 2008, as part of a programme for the progressive replacement or upgrade of the LHC injectors during the next decade. Linac4 will initially inject into the PS Booster and at a later stage into a 4 GeV Superconducting Proton Linac (SPL), which could ultimately be upgraded to high duty cycle operation. For this reason accelerating structures, RF infrastructure and shielding of Linac4 are dimensioned for higher duty cycle from the initial phase.

Linac4 is normal-conducting, 80 m long and consists of an RF volume ion source, an RFQ, a beam chopping section and a cascade of three different types of 352 MHz accelerating structures. Its main design requirements are high reliability, high beam brightness and low beam loss. The accelerator will be housed in an underground tunnel on the CERN Meyrin site, which can eventually be extended to the SPL, with equipment installed in a surface building above.

The main parameters, the status of the main components, the planning, the project organisation and the civil engineering infrastructure are presented.

THE CERN INJECTOR UPGRADE

A programme for the progressive replacement or upgrade of the LHC injectors has been recently defined at CERN [1]. The first goal of this programme is to increase the LHC luminosity beyond nominal by improving beam brightness from the injector complex, which is now the main limiting factor towards higher luminosity. A second motivation is the replacement of the present cascade of injectors, which has been built between 1959 and 1978 and in the past few years has been giving rising concerns for its long-term reliability, with a more modern, reliable and easier to maintain system, where transfer energies and beam parameters are optimised for the LHC needs. Moreover, new low energy accelerators can be made compatible with operation at higher beam power that could be required by future physics needs.

The present sequence of accelerators used as LHC injectors is based on a proton linac of a relatively low energy (Linac2, 50 MeV) followed by the 1.4 GeV PS Booster (PSB), by the 26 GeV Proton Synchrotron (PS) and finally by the 450 GeV Super Proton Synchrotron (SPS). The new injector sequence would use an H^- high-energy linear accelerator, the 4 GeV Low-Power Superconducting Proton Linac (LP-SPL), whose normal-conducting section of 160 MeV, to be built in a preliminary stage, is called Linac4 [2]. The LP-SPL can be eventually upgraded to a High-Power SPL operating at multi-MW beam power [3]. The SPL will be followed by a new 50 GeV Proton Synchrotron (PS2). Present and future injection lines are schematically presented in Fig. 1.

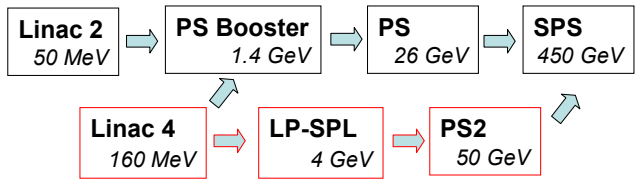

Figure 1: Scheme of the old and new LHC injectors.

A staged construction is possible because Linac4 can inject in a preliminary phase H^- ions into the existing PSB. The higher injection energy coupled with the benefits of H^- charge exchange injection are expected to increase brightness out of the PSB by a factor of 2, making possible a first increase in the LHC luminosity around 2013, when the nominal luminosity should have been attained in the LHC and a programme of upgrades to the ring and to the experiments aiming at higher luminosity could be implemented.

In June 2007, the CERN Council has approved the construction of Linac4 as a high-priority project for the period 2008-2013. At the same time, it has approved the detailed design of SPL and PS2, whose construction could start in 2012 and be terminated between 2015 and 2017

Linac4 will be housed in a 12 m deep underground tunnel, connected to the Linac2-PSB line. A surface equipment building will house klystrons and linac equipment. The Linac4 tunnel can be later on extended to the SPL. Figure 2 shows a view of the CERN Linac-PSB-PS complex, indicating the position of Linac4 and of the future extension to the SPL. Figure 3 presents the layout of the foreseen Linac4 infrastructure.

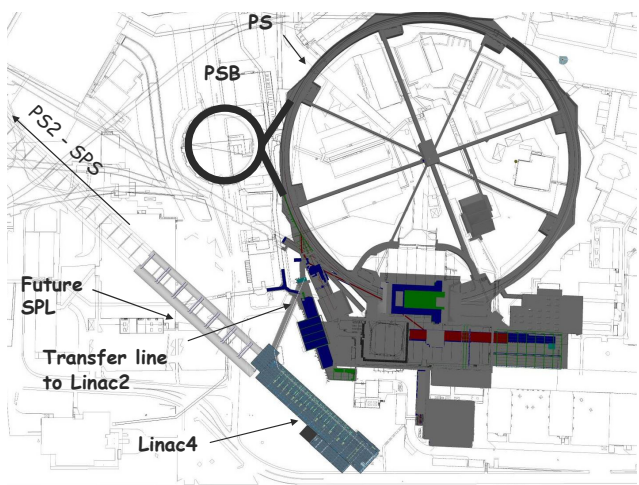

Figure 2: View of the PS Complex at CERN, showing the position of the new Linac4.

DEVELOPMENT OF A CELL-COUPLED DRIFT TUBE LINAC (CCDTL) FOR LINAC4

Y. Cuvet, F. Gerigk, G. De Michele, M. Pasini, S. Ramberger, M. Vretenar, R. Wegner, CERN, Geneva, Switzerland
E. Kenzhebulatov, S. Kryuchkov, E. Rotov, A. Tribendis, BINP, Novossibirsk, Russia
M. Naumenko, VNIITF, Snezhinsk, Russia

Abstract

The 352 MHz CCDTL will accelerate the Linac4 beam from 50 to 102 MeV. It is the first structure of this kind that will be used in a proton linac. Three short DTL-type tanks, each having two drift tubes, are connected by coupling cavities and form a chain of resonators operating in the stable π/2 mode. The CCDTL section is made of 7 such 5-resonator chains, each fed by a 1.3 MW klystron. Focusing quadrupoles are placed between tanks, easing their alignment with respect to a conventional DTL thus making the structure less sensitive to manufacturing errors. In order to validate the design and to develop the production technology, two prototypes have been constructed and successfully tested. The first prototype, built at CERN, consists of two half-cavities and one coupling cell, whereas the second, larger one, having two full cavities and one coupling cell, was built at VNIITF and BINP in Russia within the frame of an R&D contract funded by the ISTC Organisation. Both prototypes have been tested at CERN slightly beyond their nominal power level, at the design duty cycle of 10%. In this paper we present the results of high-power tests, the results of the technological developments prior to production, and the final design of the CCDTL.

INTRODUCTION AND BASIC DESIGN

The Cell-Coupled Drift Tube Linac (CCDTL) was originally developed at LANL as a structure providing higher shunt impedance than conventional Drift Tube Linacs (DTL) for intermediate-velocity particles [1]. In the original design the CCDTL was used at twice the basic linac frequency (800 MHz) and when the principle was tested on a CW prototype it appeared that surface power density was too large for stable operation. To avoid these problems, CERN started to develop a CCDTL at the basic linac frequency of 352 MHz and for applications as the Superconducting Proton Linac (SPL), limited at a duty cycle of less than 10% [2]. Different combinations were analysed and tested, to finally adopt for the Linac4 project [3] the CCDTL configuration shown in Fig. 1. This CCDTL is made of 3-gap DTL-like accelerating tanks, connected by off-axis coupling cells bridging the focusing quadrupoles. Whereas the shunt impedance of this CCDTL configuration remains similar to that of a DTL with permanent quadrupoles, its main advantages are the easy access, alignment and cooling of the quadrupoles and the simpler construction and alignment of the tanks, the drift tube alignment tolerances being no longer dominated by the tight requirements of the quadrupoles.

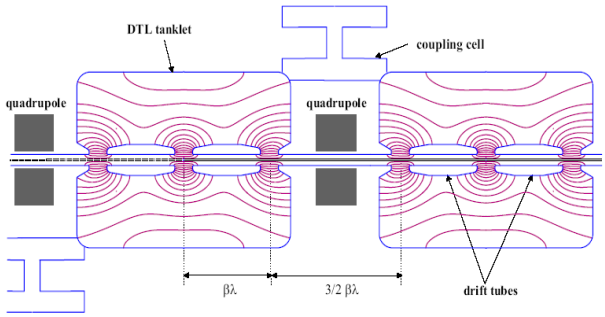

Figure 1: Linac4 CCDTL structure with indication of the electric field lines.

The RF configuration of Linac4 limits the peak power per resonator to about 1 MW. For this reason, the CCDTL tanks are grouped in modules of 3 tanks connected by two coupling cells (Fig. 2). The basic Linac4 CCDTL resonator is therefore made of 5 coupled cells operating in the π/2 mode. The CCDTL starts at 50 MeV, an energy that allows placing quadrupoles within the 3/2 βλ distance between neighbouring gaps. The geometry of the coupling cell and coupling slot is kept constant for all modules to simplify construction. This is achieved by shifting the end-walls of the tanks.

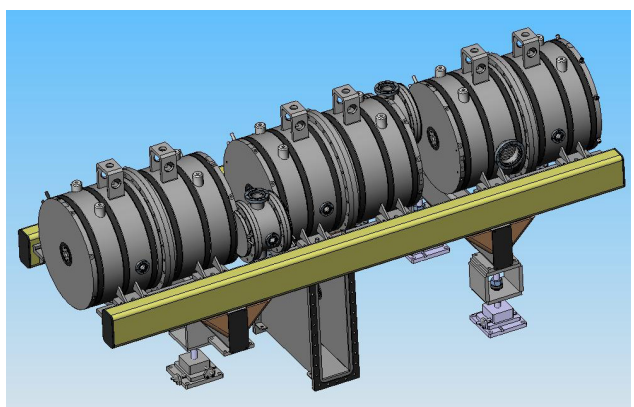

Figure 2: 3D view of a Linac4 CCDTL module with support structure and rectangular RF port.

At higher energies the shunt impedance of the CCDTL falls considerably, together with the coupling factor between CCDTL cells, inversely proportional to the stored energy per tank. Both these factors impose an upper energy limit of about 100 MeV for this structure.

STATUS OF THE RAL FRONT END TEST STAND

A.P. Letchford, M.A. Clarke-Gayther, D.C. Faircloth, D.J.S. Findlay, S.R. Lawrie, P. Romano, P. Wise (STFC RAL, Didcot, UK), F.J. Bermejo (Bilbao, Spain), J. Lucas (Elytt Energy, Madrid, Spain), J. Alonso, R. Enparantza (Fundación Tekniker, Elbr, Spain), S.M.H. Al Sari, S. Jolly, A. Kurup, D.A. Lee, P. Savage (Imperial College of Science and Technology, London, UK), J. Pasternak, J.K. Pozimski (Imperial College of Science and Technology, London; STFC RAL, Didcot, UK), C. Gabor, C. Plostinar (STFC ASTeC, Didcot, UK), J.J Back (University of Warwick, Coventry, UK)

Abstract

High power proton accelerators (HPPAs) with beam powers in the several megawatt range have many applications including drivers for spallation neutron sources, neutrino factories, waste transmuters and tritium production facilities. The UK's commitment to the development of the next generation of HPPAs is demonstrated by a test stand being constructed in collaboration between RAL, Imperial College London, the University of Warwick and the Universidad del Pais Vasco, Bilbao. The aim of the RAL Front End Test Stand is to demonstrate that chopped low energy beams of high quality can be produced and is intended to allow generic experiments exploring a variety of operational conditions. This paper describes the current status of the RAL Front End Test Stand.

BACKGROUND

In order to minimise the need for remote or active handling of accelerator components, beam loss in future HPPAs must be kept to levels comparable to those of current facilities. With beam powers an order of magnitude or more greater than those currently achieved, fractional beam loss must necessarily be reduced by a similar factor. Beam chopping is one approach to reducing loss and will be an important feature of the next generation of HPPAs.

Beam Chopping

In circular machines a significant source of beam loss occurs when the continuous linac beam is trapped and bunched in the ring RF bucket. Trapping efficiency can be improved with higher harmonic RF systems but to achieve the improvements necessary for MW scale beams, the linac beam must be chopped at the ring revolution frequency. This chopped beam allows for the ring RF bucket to be precisely filled with little trapping loss. The low levels of beam between bunches also reduces loss at extraction.

Everywhere downstream of the RFQ the linac beam has RF structure, this structure typically being at some 100s of MHz. Partially chopped bunches can occur in the linac if the chopping is not precisely synchronised with the linac beam RF bunch structure. With less charge than normal and possibly off axis or off momentum, these partially chopped bunches may lead to beam loss in the linac. The ideal is perfect chopping where the chopper switches on and off in the time between two successive linac beam bunches which is typically a few ns. This very fast switching requirement coupled with the increasing stiffness and power of the beam at higher energies dictates that chopping is carried out at the front of the linac, downstream of the RFQ at around 2.5 – 3 MeV.

Front End Test Stand

The Front End Test Stand (FETS) project at RAL [1][2][3][4] has several goals. The primary goal is to demonstrate a high quality, high current, chopped H^- beam. This is a generic objective and does not have a single future application in mind. FETS is funded by the Science and Technology Facilities Council (STFC) as part of their HPPA and Megawatt Spallation Source programme [5] and as a generic work package of the UK Neutrino Factory (UKNF) project [6].

A secondary goal of FETS is to encourage the study of accelerator technology within UK universities and foster international collaborations on HPPA research. High energy and particle physics has been well served by UK universities who are enthusiastic users of accelerator facilities and contributors to detector and physics projects however accelerator theory and technology has traditionally been less well served.

TEST STAND COMPONENTS

The front end test stand consists of an H^- ion source, magnetic low energy beam transport (LEBT), 324 MHz RFQ, medium energy beam transport (MEBT) chopper line and comprehensive diagnostics.

Ion Source

FETS will use an ion source based on the well-proven and highly successful Penning type H^- surface plasma source (SPS) [7] which is in routine operation on ISIS producing currents in excess of 50 mA at a duty factor of ~1%. Its use with an RFQ pre-injector has been previously demonstrated [8].

Following previous work which concentrated on increasing the current and duty factor of the source [9][10][11], recent work has focussed on understanding the beam transport and optics with a view to decreasing the emittance to the FETS specification. Considerable experimental and computational effort, using CST EM & Particle Studies [12] plus General Particle Tracer (GPT) [13], is leading to a much better understanding of the

A FAST CHOPPER FOR THE FERMILAB HIGH INTENSITY NEUTRINO SOURCE (HINS)*

R. Madrak, D. Wildman, FNAL, Batavia, Illinois, 60510, U.S.A.
A. Dymokde-Bradshaw, J. Hares, P. Kellett, Kentech Instruments Ltd., Wallingford, U.K.

Abstract

A fast chopper capable of kicking single 2.5 MeV H^- bunches spaced at 325 MHz, at rates greater than 50 MHz is needed for the Fermilab High Intensity Neutrino Source (HINS) [1]. Four 1.2 kV fast pulsers, designed and manufactured by Kentech Instruments Ltd., will drive a 0.5 m long meander made from a copper plated ceramic composite. Test results showing pulses from the first 1.2 kV pulser and meander results will be presented.

INTRODUCTION

As a demonstration of the feasibility of a high intensity 8 GeV proton source, Fermilab is constructing a 60 MeV H^- linac (HINS). This would serve as the front end to a superconducting 8 GeV linac, which would deliver beam to the Main Injector. Since the operating frequency of this linac is 325 MHz, not a multiple of the Main Injector's 53 MHz, we are compelled to chop out approximately one out of every six beam bunches. This avoids beam losses due to bunches which would not be captured in a Main Injector RF bucket.

The chopping is to be done in the 2.5 MeV (MEBT) section of the linac. This requires extremely fast (width < 6 ns) high voltage (±2.4 kV) pulses which propagate at the same speed as the beam (β=0.073) along a two plate deflecting "meander" structure. The requirement on the width is such that only one bunch at a time may be removed.

The two meander structures are 50 cm long, each with an impedance of 100 ohms. To obtain the necessary deflection, the beam must be kicked by the electric field (due to the high voltage pulse) for the entire length of the meander.

FAST PULSER

Fermilab has procured from Kentech Instruments, Ltd. [2] a prototype 500V pulser, in June 2006, and a 1.2 kV pulser in November 2007. The average chopping rate imposed by the HINS pulse parameters is close to 1MHz however the switching losses in high voltage (kilovolt) semiconductor switching devices becomes excessive at these pulse rates. In order to obtain fast rise and fall, together with a high pulse repetition rate, the output is generated from an array of custom packaged low voltage (100 volt) semiconductor switches. These relatively low voltage parts have a bandwidth of ~500MHz allowing nanosecond rise and fall times.

The 1.2 kV pulser is based on an array of twenty four 50V pulse cards. The cards are floating, each with an output impedance of ~2 ohms. This output from each card is transported by 12 parallel 25 ohm semi-rigid coax cables and is taken to a summing point. When combined, this yields the 1.2 kV, 50 ohm output.

Figure 1: Kentech 1.2 kV pulser.

Each card has a floating power supply together with PECL trigger logic, burst width and duty cycle limit circuitry and power supply monitoring, all of which are remotely controlled. The TTL burst pattern input trigger signal is regenerated in PECL circuitry on each card before being amplified to a 50V pulse output. Individual cards can be enabled or disabled for testing purposes and the correct operation of the card can be confirmed via the link.

The pulser incorporates load fault detection (open or short circuit) and has an embedded controller for set up and control functions. It may be operated in either a 1 ms or 3 ms mode, triggered by an arbitrary TTL pattern with the option of a 325MHz clocked data input. The maximum total on-time during a 1 ms burst is 0.75 ms. A photograph of the 1.2 kV pulser is shown in Fig. 1. Figure 2 shows the pulser output (attenuated by 60dB). The top scope photo shows several 1.2 kV pulses spaced by ~20 ns. The bottom shows a full 3 ms burst of this pulse pattern.

*Operated by Fermi Research Alliance, LLC under Contract No. DE-AC02-07CH11359 with the United States Department of Energy.

AN 8 GeV CW LINAC WITH HIGH POTENTIAL BEAM POWER*

Charles Ankenbrandt[a,c], Richard Baartman[b], Ivan Enchevich[a], Rolland P. Johnson[a#], Alfred Moretti[c], Sergei Nagaitsev[c], Michael Neubauer[a], Thomas Peterson[c], Milorad Popovic[c], Robert Rimmer[d], Gennady Romanov[c], Nikolay Solyak[c], Vyacheslav Yakovlev[c], Katsuya Yonehara[c]

[a]*Muons, Inc., Batavia, IL, USA*
[b]*TRIUMF, Vancouver, BC, Canada*
[c]*Fermi National Accelerator Laboratory, Batavia, IL USA*
[d]*Thomas Jefferson National Accelerator Facility, Newport News, VA, USA*

Abstract

Modern technology allows us to consider operating an 8 GeV SC linac in a CW mode to accelerate a high-current H^- beam. By using appropriate accumulation rings, the linac could provide simultaneous beams for direct neutrino production, neutrino factories, fixed target experiments, and muon colliders. Several other unique accelerator applications could also be served and improved by the same continuous beam, including studies of energy production and nuclear waste reduction by transmutation, rare muon decay searches, and muon catalyzed fusion. A comparison of CW and pulsed operation is strongly dependent on the choice of accelerating gradient, and a first look at refrigeration requirements for a gradient of 20 MV/m is included in this study. Methods for accumulating the beam from a CW linac to serve the special needs of the potential future Fermilab programs mentioned above are considered. In this paper we also examine the use of a cyclotron as a source of high current beams to reduce the cost and complexity of the linac front end. Although the refrigeration system would be large for 20 MV/m gradient, a 3 mA CW H^- beam at 8 GeV looks feasible, with potential beam power up to 24 MW to access the intensity-frontier for muon and neutrino physics and also be an essential step to an energy-frontier muon collider.

INTRODUCTION

Modern proton accelerators or storage rings use multi-turn H^- charge exchange injection and strip at high energy, where the Laslett tune shift is smaller, to achieve high proton bunch intensities. This approach has been used in several new machines, and the next step that is being proposed is to provide a powerful 8 GeV H^- linac that could feed any number of accumulation rings or accelerators for planned and as yet undreamt-of purposes.

A plan for Project-X [1], to replace the aging Fermilab 8 GeV rapid cycling Booster proton synchrotron, has centered on a 1.3 GHz superconducting (SC) linac, which could also act as a string test for the ILC. The purpose of this paper is to consider a CW H^- linac as an option for Project-X, which would not be limited by any ILC constraints and, by virtue of high potential 8 GeV beam power, be best suited to the needs of any future Fermilab research program. Nevertheless, as a large-scale SRF system, it would act as a significant demonstration of many aspects of ILC technology.

Since its design in the late 1960's, the Fermilab Booster has at times been both the world's most intense proton source and almost always the bottleneck in the Fermilab research program, where proton economics have determined which experiments could be scheduled or even were possible. If the Booster is replaced as planned, it will have served in this way for about 45 years. It is quite likely that its replacement will have a similar function for a similar time.

Recent studies of proton driver requirements for muon colliders and neutrino factories [2] have indicated that the present parameters for Project-X may limit these machines because the proton beam power will be insufficient and the repetition rate too low. Even with optimistic muon collection and cooling efficiencies, at least 4 MW of 8 GeV proton power will be required for muon collider designs. The natural repetition rate for muon machines is suggested by the muon lifetime in its final storage ring. For a 5 TeV center of mass collider, for example, the muon lifetime is about 50 ms so that the natural repetition rate is about 20 Hz. For lower energy storage rings, the natural repetition rate is higher.

For the study reported here, the RF gradient G has been chosen to be low enough such that resistive losses, proportional to G^2, are not too large. In the next section we calculate the wall-plug power for the case of G=20 MV/m for ILC-like RF structures. This is to be compared to the 25 to 30 MV/m presently favored by Project-X. A gradient of 20 MV/m implies a linac that would be about 27/20 times longer than the baseline, but has the compensating virtue of easier technology for the RF cavities and klystrons.

CW CRYO POWER REQUIREMENTS

CW operation results in much higher dynamic heating in the RF cavities and input couplers and higher cryogenic cooling power requirements. Table 1 shows a comparison of the power requirements for the components of a TESLA linear accelerator operated as a pulsed machine compared to CW operation.

*Supported in part by the US DOE under contracts DE-AC02-07CH11359 and DE-AC05-84ER40150 and STTR grant DE-FG02-08ER86350.
#rol@muonsinc.com

HIGH POWER TEST OF ROOM TEMPERATURE SPOKE CAVITIES FOR HINS AT FERMILAB *

W-M. Tam #, G. Apollinari, T. Khabiboulline, R. Madrak, A. Moretti, L. Ristori, G. Romanov, J. Steimel, R. Webber, D. Wildman, Fermilab, Batavia, IL 60510

Abstract

The High Intensity Neutrino Source (HINS) R&D program at Fermilab will build a new 65 MeV test linac to demonstrate new technologies for application in a high intensity hadron linac front-end. The HINS warm section is composed of an ion source, a radio frequency quadrupole, a medium energy beam transport and 16 room temperature Crossbar H-type (RT-CH) cavities that accelerate the beam to 10 MeV (=0.1422). The RT-CH cavities are separated by superconducting solenoids enclosed in individual cryostats. Beyond 10 MeV, the design uses superconducting spoke resonators. In this paper, we illustrate the completion of four RT-CH cavities and explain latest modifications in the mechanical and radio frequency (RF) designs. Cavities RF measurements and tuning performed at Fermilab are also discussed. Descriptions of the HINS R&D Facility including high power RF, vacuum, cooling and low level RF systems will be given. Finally, the history of RF conditioning and the results of high power tests of RT-CH cavities will be discussed.

INTRODUCTION

Fermilab is considering an 8 GeV superconducting H- linac with the primary mission of enabling 2 MW beam power from the 120 GeV Fermilab Main Injector for a neutrino program [1]. The front end linac in the energy range from 10 MeV to 400 MeV is foreseen as based on 325 MHz superconducting spoke resonators. New paradigms introduced into the front end design include the adoption of short, high field SC solenoids as primary lattice focusing elements and a low energy transition at 10 MeV from RT to SC RF acceleration. The HINS R&D program is underway to demonstrate these concepts in a 65 MeV prototype linac [2].

Our studies show that the most appropriate RT accelerating structure in the energy range 2.5-15 MeV is a CH type cavity [3, 4] operating at 325 MHz. We have successfully fabricated, fully dressed and high power tested the first three RT-CH resonators. The next one is now ready for high power tests. We are currently fabricating the remaining twelve resonators.

CAVITY RF DESIGN

The RF design of the RT-CH cavities is reported in [2, 3]. In order to accelerate the manufacture of the remaining twelve cavities, five different designs are used instead of twelve. So there are 2-3 identical cavities in each of the five groups. Due to the reduction in the overall efficiency of acceleration, the power loss in the warm section is increased by 2%.

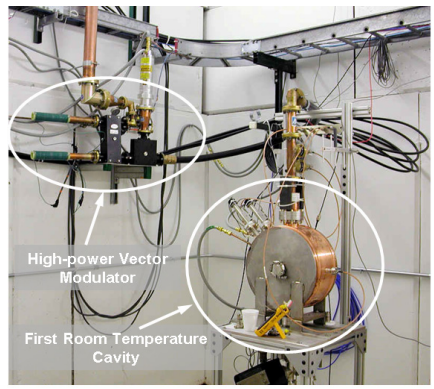

Figure 1: Cavity completed with coupler, tuners, cooling pipes, vacuum, and vector modulator.

RF POWER SYSTEM AND TEST STAND

The cavity under test is completed with a power coupler, a pair of motor-driven tuners (now reduced to one) and cooling pipes and is mounted on a test stand sitting inside a cavity test cave for radiation shielding purpose (See Fig.1). This cavity assembly is then leak-checked with helium and is connected to low conductivity water (LCW), vacuum pumps and gauges, high power RF directional coupler and cable, and low-level RF (LLRF) signal cables.

RF power is supplied by a 325 MHz 2.5 MW Toshiba E3740A klystron which is protected by a 2.5 MW circulator (See Fig.2). Two RF power lines, 25 kW and 250 kW, are available for the cavity test cave. The 25 kW line was used in the test.

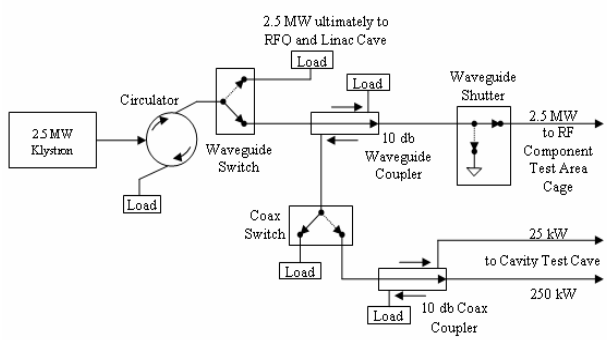

Figure 2: RF power and distribution system diagram.

*This work was supported by the U.S. Department of Energy under contract number DE-AC02-76CH03000.
#watam@fnal.gov.

FOCUSING SOLENOIDS FOR THE HINS LINAC FRONT END*

I. Terechkine#, G. Apollinari, J. DiMarco, Y. Huang, D. Orris, T. Page,
R. Rabehl, M. Tartaglia, J. Tompkins, FNAL, Batavia, IL 60510, U.S.A.

Abstract

The low energy part (front end) of a linac for the High Intensity Neutrino Source (HINS) project at Fermilab will use superconducting solenoids as beam focusing elements (lenses). The lenses for the conventional (room temperature) drift tube-type accelerating section of the front end require individual cryostats; in the superconducting accelerating sections, solenoids will be installed inside RF cryomodules. Some of the lenses in the conventional and superconducting section are equipped with horizontal and vertical steering dipoles. Lenses for the room temperature section are in the stage of production with certification activities ongoing at Fermilab, and a prototype lens for the superconducting section has been built and tested. Since each lens will be installed in the transport channel of the accelerator so that its magnetic axis is on the beamline, testing has also included alignment measurements.

This report summarizes design features, parameters, and test results of the focusing lenses.

INTRODUCTION

As part of the High Intensity Neutrino Source (HINS) program at Fermilab, building a high power H^- RF linac is under consideration [1]. At present, main R&D efforts are concentrated on development of accelerating and transport elements for the front end of the linac. To reduce beam losses through mitigation of halo formation in the front end (see [2]), superconducting solenoids will be used as focusing lenses [3]. There are three sections of the front end, which are identified by the type of 325 MHz RF structure used for acceleration. The first section uses low-beta, room temperature Crossbar H-type (CH) structures [4]; in this section, each focusing lens is in its own cryostat. For higher energies, superconducting spoke resonators are used with several of them in one cryostat [5]; focusing lenses in these sections are mounted in the same cryostats. There exist two types of superconducting sections in the linac: SS1 and SS2; focusing lenses for these sections differ in strength.

One of the major requirements for focusing lenses in the superconducting sections of the linac is low fringe field. To limit the power loss in walls of accelerating cavities, it is desirable to keep the magnetic field on the walls below 10 μT [6].

*Work supported by the U.S. Department of Energy under contract No. DE-AC02-07CH11359.
#terechki@fnal.gov

In each section of the linac, two styles of lenses are required: with and without embedded steering dipoles for horizontal and vertical correction of beam position.

A total of 53 focusing lenses will be built for the linac (including spares). Solenoids for the CH section are in the production stage, solenoids for the SS1 section are being prototyped, and design work is ongoing for the SS2 system.

CH SECTION FOCUSING SOLENOID

Focusing length of a solenoid-based focusing lens is given by the following expression:

$$F = \frac{8mU}{q \cdot \int_{-\infty}^{+\infty} B^2 dz}$$

where $\boldsymbol{m}$ is mass, $\boldsymbol{q}$ is charge, and $\boldsymbol{U}$ is the kinetic energy of the particles in the beam. For high intensity ion beams, it is essential to have the focusing period small; this requires high magnetic field, that only can be generated by superconducting systems. Basic requirements for the focusing lens include 20 mm warm bore diameter, the squared magnetic field integral $\int B^2 dz$ of ~1.8 T^2-m, with an effective length less than 0.1 m (normalized to the maximum magnetic field). Steering dipoles must have an integrated strength of ~0.25 T-cm to be able to compensate for uncertainties in the solenoid magnetic axis positioning of ~0.3 mm. Due to lack of space in the beamline, the dipoles must be placed inside of some of solenoids. To solve the fringe field problem, each solenoid is made of a main coil and two bucking coils with the direction of magnetic field opposite to that of the main coil. Design of the solenoid is described in [7] and [8]. Several prototypes of the focusing solenoid were tested before serial production started. Magnetic field distribution of a solenoid with embedded steering coils in the central and the fringe area is shown in Fig. 1. Here the measured field is compared to a model prediction; the data points from both sides of the magnet are overlaid. The squared field integral at 200A is 2.5 T^2-m, versus the predicted value of 2.4 T^2-m. The maximum current in the system (quench condition) is ~240 A; the required value of 1.8 T^2-m can be achieved at 170 A.

The measured magnetic field in the fringe field region (outside the solenoid) is also very close to the expected. At the nominal current of 170 A, for the solenoids with the embedded steering coils, the magnetic field in the area of the accelerating cavity (~150 mm from the solenoid center) is ~0.03 T; it is ~0.01 T for the solenoids without

STATUS OF THE LANSCE REFURBISHMENT PROJECT*

John L. Erickson, Kevin W. Jones and Michael W. Strevell
Los Alamos National Laboratory, Los Alamos, NM 87545, U.S.A.

Abstract

The Los Alamos Neutron Science Center (LANSCE) accelerator is an 800-MeV proton linac that drives user facilities for isotope production, proton radiography, ultra-cold neutrons, weapons neutron research and various sciences using neutron scattering. The LANSCE Refurbishment Project (LANSCE-R) is an ambitious project to refurbish key elements of the LANSCE accelerator that are becoming obsolete or nearing end-of-life. The conceptual design phase for the project is funded and underway. The 5 year, $170M (US) project will enable future decades of reliable, high-performance operation. It will replace a substantial fraction of the radio-frequency power systems (gridded tubes and klystrons) with modern systems, completely refurbish the original accelerator control and timing systems, replace obsolete diagnostic devices, and modernize other ancillary systems. An overview of the LANSCE-R project will be presented. The functional and operating requirements will be discussed, the proposed technical solutions presented, and the plan for successful project execution while meeting annual customer expectations for beam delivery will be reviewed.

INTRODUCTION

The LANSCE User Facility accelerator is capable of simultaneously accelerating protons or negative hydrogen ions to beam powers of up to 800 kW. A beam switchyard allows tailored time-structured beams to be delivered to the five distinct experimental areas.

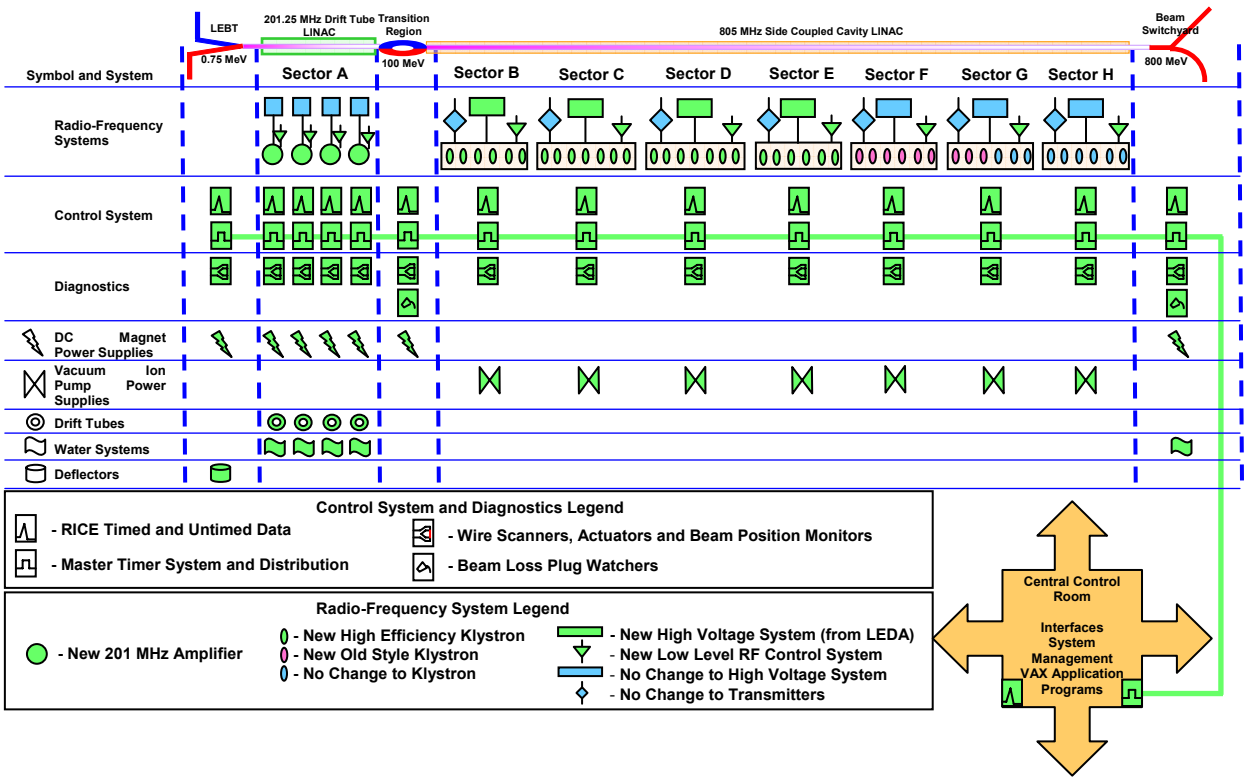

Figure 1: A summary diagram showing the scope of LANSCE-R.

Vision and Goals

LANSCE produces one of the highest beam currents in the world of medium energy protons to irradiate experimental targets directly or to produce intense pulses of spallation neutrons. LANSCE performs state-of-the-art experiments in proton radiography, nuclear science, and materials science.

Our goal is to provide safe, secure, environmentally-compliant, cost-effective performance in beam delivery that meets or exceeds metrics prescribed by our customers.

*Work supported by the U. S. Department of Energy, National Nuclear Security Administration, Contract No. DE-AC52-06NA25396 – Publication Release LA-UR-08-06209

OPERATIONAL STATUS AND FUTURE PLANS FOR THE LOS ALAMOS NEUTRON SCIENCE CENTER (LANSCE)*

Kevin W. Jones and Kurt F. Schoenberg, Los Alamos National Laboratory, Los Alamos, NM 87545, U.S.A.

Abstract

The Los Alamos Neutron Science Center (LANSCE) continues to be a signature experimental science facility at Los Alamos National Laboratory (LANL). The 800 MeV linear proton accelerator provides multiplexed beams to five unique target stations to produce medical radioisotopes, ultra-cold neutrons, thermal and high-energy neutrons for material and nuclear science, and to conduct proton radiography of dynamic events. Recent operating experience will be reviewed and the role of an enhanced LANSCE facility in LANL's new signature facility initiative, Matter and Radiation in Extremes (MaRIE) will be discussed.

INTRODUCTION

The Los Alamos Neutron Science Center (LANSCE) is a unique multidisciplinary facility for science and technology. The core of the facility is an 800-MeV linear accelerator system with demonstrated 1MW capability that presently accelerates up to 100kW of negative hydrogen ions with unique and highly variable timing patterns suitable for a wide variety of experimental programs. Five experimental areas form the core of the user facility. Four areas utilize the 800-MeV negative hydrogen ion beams directed by appropriate pulsed kicker systems: at the Manuel Lujan Jr. Neutron Scattering Center (Lujan Center) sixteen flight paths utilize pulsed thermal and epithermal neutrons produced at 20Hz by intense 0.29μs bursts of protons incident on a tungsten spallation target and moderated by water or liquid hydrogen; the Weapons Neutron Research Facility (WNR) provides the most intense source of high-energy neutrons in the world for neutron nuclear science and is an accepted world standard for irradiation of semiconductor electronics; the Proton Radiography Facility (pRAD) provides a unique facility for the study of shock-induced dynamic processes where shocks are driven by high explosives or projectiles; and the Ultra-Cold Neutron (UCN) facility uses a moderated solid deuterium target to generate intense pulses of ultra-cold neutrons for fundamental science research. The Isotope Production Facility (IPF) at 100 MeV utilizes a proton beam of up to 275 μA to produce proton-induced isotopes for medical imaging diagnostics and fundamental research. LANSCE continues a disciplined approach to both operations and maintenance that maintains operational performance and user satisfaction in a constrained funding environment.

*Work supported by the U. S. Department of Energy, National Nuclear Security Administration, Contract No. DE-AC52-06NA25396 – Publication Release LA-UR-08-06170

THE LANSCE USER FACILITY

The Lujan Center provides 11 neutron scattering instruments capable of studying materials structures of diverse items such as proteins, machinery components, powders, and single crystals using both elastic and inelastic techniques. Nuclear science is supported by three flight paths, one of which is equipped with a 4π detector used to measure thermal neutron capture cross sections on unstable nuclei. This suite of instruments applies and advances neutron scattering for both defense and academic research. Beam current to the Lujan target is nominally 100μA but can be as high as 125μA depending on ion source and accelerator optimization.

The WNR facility receives beam at 40-100Hz with a variable micro-pulse spacing (typically 1.8μs) to address the needs of LANSCE Users in the areas of basic and applied nuclear science. The pulse spacing permits resolution of frame overlap in the neutron spectra. This white neutron source (Target 4) is the most intense source of high-energy (<760 MeV) neutrons worldwide and is equipped with six flight paths that determine neutron energy using time-of-flight techniques. A key flight path used principally by industry users provides a neutron spectrum essentially identical to that of cosmic-ray neutrons to permit accelerated studies of single-event-upset sensitivity for the electronics and avionics industries. A related facility (Target 2) provides direct access to proton beams with energies up to 800 MeV for studies of proton-induced reactions and target irradiations for materials testing. This target station is also equipped with five neutron flight paths.

The pRAD facility provides a unique experimental technique for studies of dynamic processes. Up to 37 pulses of protons, each with approximately 10^9 particles per pulse, temporally spaced at appropriate intervals, are directed at a dynamic object. The scattering characteristics of each pulse are imaged by a collimator and magnetic lens system and recorded by a camera. This technique permits multi-frame radiographs of dynamic events driven by gas guns or high explosives. These radiographs permit the study of material dynamics and failure mechanisms under shock conditions.

The UCN facility accepts several full charge (~5μC) accelerator pulses separated by a period suitable for the moderation and bottling of the neutrons and compatible with average current limits, typically about 5-7 seconds. The ultra-cold neutrons are then directed through a guide to a decay volume where beta-decay parameters are measured.

OPERATIONAL EXPERIENCE OF THE SNS FRONT END AND WARM LINAC

A. Aleksandrov

Oak Ridge National Laboratory, Oak Ridge, TN 37830 USA

Abstract

The Spallation Neutron Source accelerator complex uses set of pulsed linear accelerators of different types to accelerate beam to 1GeV. The 2.5 MeV beam from the Front End is accelerated to 86 MeV in the Drift Tube Linac, then to 185 MeV in a Coupled-Cavity Linac and finally to 1 GeV in the Superconducting Linac. In the process of the commissioning and beam power ramp up many technical systems, as well as tuning algorithms, have deviated significantly from the original design. Our understanding of beam behavior has been evolving continuously and resulted in a steady reduction of fractional beam losses in the linac. In the same time new unexpected problems have been discovered, which are still in the process of investigation. In this paper we summarize our experience up to date and report on the current directions of experimental study, simulations, and development of tuning methods.

INTRODUCTION

The SNS Front End and warm linac consist of an H^- injector, capable of producing one-ms-long pulses with 38 mA peak current, chopped with a 68% beam-on duty factor and a repetition rate of 60 Hz to produce 1.6 mA average current, an 87 MeV Drift Tube Linac (DTL), a 186 MeV Coupled Cavity Linac (CCL), and associated transport lines. After completion of the initial beam commissioning at a power level lower than the nominal, the SNS accelerator complex is gradually increasing the operating power with the goal of achieving the design parameters in 2009 [1]. Results of the initial commissioning can be found in [2], and of the initial operation experience in [3]. At the time of this writing the Front End and warm linac routinely provides beam at 40% of the design average power.

FRONT-END PERFORMANCE

The front-end for the SNS accelerator systems is a 2.5 MeV injector consisting of the following major subsystems: an RF-driven H^- source, an electrostatic low energy beam transport line (LEBT), a 402.5 MHz RFQ, a medium energy beam transport line (MEBT), a beam chopper system, and a suite of diagnostic devices. The front-end is required to produce a 2.5 MeV beam of 38 mA peak current at 6% duty factor. The 1 ms long H^- macro-pulses are chopped at the revolution frequency of the accumulator ring (~1 MHz) into mini-pulses of 645 ns duration with 300 ns gaps.

Ion Source and LEBT

The ion source has been capable of satisfying peak and average beam current requirements for the power ramp up goals. At the time of this writing it produces 32mA 750us pulses at 60Hz. We do not expect significant difficulties in expanding the pulse width to the design value of 1200us. Increasing peak current to the nominal 38mA is more challenging but peak current higher than 40mA in 800us pulses has been demonstrated recently in dedicated tests [4].

The RF antenna life time and the possibility of catastrophic antenna failures still remains a concern. We implemented several interlock mechanisms to prevent a possible water leak into the LEBT chamber in case of antenna failure and have not had such events for the two last run periods. An external antenna source is being developed as a long term solution and the first experimental tests have shown promising results [4].

The long standing problem of electrical breakdowns in the electrostatic LEBT has not been fully resolved yet. An improved LEBT design, which does not have glue joints and has a better isolation between the chopper electrodes and the rest of the LEBT, was installed before the last run and demonstrated significant reduction of arc related chopper failures. As a long term solution we plan to use a magnetic LEBT which is in the early stages of development.

Chopper Systems

Beam chopping is performed by two separate chopper systems located in the LEBT and MEBT. The last lens in the LEBT is split into four quadrants to allow electrostatic chopping using the RFQ entrance flange as a chopper target. The LEBT chopper removes most of the beam charge during the mini-pulse gaps, and the traveling-wave MEBT chopper further cleans the gap to a level of 10^{-4} and reduces the rise and fall time of the mini-pulse to 10 ns. A chopper controller provides different patterns of chopped beam: “regular chopping”, “single mini-pulse”, “every n-th mini-pulse”, “blanking-off”, and “ramp up”. The chopper systems demonstrated design parameters during commissioning for the nominal chopping pattern at low average beam power. We encountered serious problems with both the LEBT and the MEBT choppers at higher beam power.

The main problem of the LEBT chopper is frequent damage to the high voltage switches by arcs in the electrostatic LEBT. Serial resistors were installed in the chopper circuitry for protection, resulting in significant

THE PROPOSED ISAC-III (ARIEL) LOW-ENERGY AREA AND ACCELERATOR UPGRADES

R.E. Laxdal, F. Ames, R. Baartman, M. Marchetto, M. Trinzcek, Fang Yan,
V. Zvyagintsev, TRIUMF*, Vancouver, BC, V6T2A3, Canada

Abstract

The ISAC-III proposal (now called ARIEL) is a ten year plan to triple the amount of radioactive ion beam (RIB) time at the facility. The plan includes the addition of two new independent target stations, a second 500 MeV proton beam line from the TRIUMF cyclotron and a new 50 MeV electron linac as a complementary driver to provide RIBs through photo-fission. A new mass-separator and low-energy beam-transport complex is foreseen to deliver the additional beams to the ISAC experimental facilities. A new linear accelerator section would provide the capability for two simultaneous accelerated RIBs to experimenters. This paper will describe the proposed installations in the low-energy transport and accelerator sections of the ISAC complex.

INTRODUCTION

In the ISAC-I facility[1] 500 MeV protons from the cyclotron at up to 100μA impinge on one of two production targets to produce radioactive isotopes. The isotopes are ionized and the resulting beam is mass-separated and transported in the low energy beam transport (LEBT) electrostatic beamline to either the low energy experimental area or through a series of room temperature accelerating structures (RFQ, DTL) to the ISAC-I medium energy experimental area. The RFQ accelerates ions with A/q$\leq$30 to 150 keV/u and the post-stripper variable energy DTL accelerates ions with A/q$\leq$6 up to 1.8 MeV/u. The accelerated beam can also be transported to the ISAC-II Superconducting Linear Accelerator (SC-linac)[3] for further acceleration above the Coulomb barrier. An ECR charge breeder (CSB) is presently being added to extend the mass range beyond A=30.

The cyclotron provides the highest power driver beam (50 kW) of any operating ISOL based facility. Two 50 kW target stations are available to reduce the switchover time between targets. But the present scientific output is oversubscribed with more experiments requested than available beam time would allow. The aim of the ISAC-III (ARIEL) proposal is to get more RIBs on target to produce more physics. Fundamental to the plan is the eventual delivery of three simultaneous RIBs to three experimental areas. The expansion requires the addition of two new driver beams - one from a second cyclotron proton beamline and one from a new high power electron linac[2]. Two new target areas with independent separators and a flexible beam delivery system would allow simultaneous operation of three production sources. A new accelerator front end including a second charge breeder provides a second simultaneous accelerated beam capability. The TRIUMF site with the prosposed addition is shown in Fig. 1.

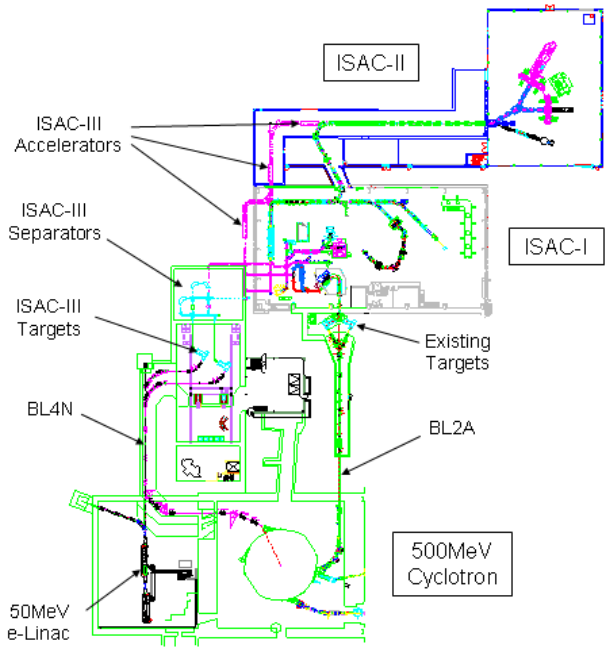

Figure 1: The TRIUMF site including the cyclotron, ISAC-I and ISAC-II and the proposed ISAC-III (ARIEL) facility. BL2A is the present proton line and the BL4N tunnel is proposed for the new ISAC-III driver beams.

MASS-SEPARATOR SWITCHYARD

It is useful to consider a switchyard that is capable of either low resolution, medium resolution or high resolution separation schemes depending on the experiment. In general reduced resolution schemes are desired since they reduce the tuning time required. The proposed configuration is shown in Fig. 2. Here each of the two target/source units has a pre-separator and individual transport lines directing the beams to a mass-separator switchyard. The beams after separation are directed to either one of two new vertical sections VS-2 or VS-3 for delivery to the upstairs experimental area. Standard ISAC LEBT electrostatic components are used to deliver the beam to either a Medium Resolution Spectrometer (MRS) or a High Resolution Spectrometer (HRS). The medium resolution leg has a resolution of ~2500 while the high resolution leg has a resolution

* TRIUMF receives funding via a contribution agreement through the National Research Council of Canada

ISAC-II SUPERCONDUCTING LINAC UPGRADE - DESIGN AND STATUS

R.E. Laxdal, R.J. Dawson, M. Marchetto, A.K. Mitra, W.R. Rawnsley,
T. Ries, I. Sekachev, V. Zvyagintsev, TRIUMF*, Vancouver, BC, Canada,

Abstract

The ISAC-II superconducting linac, operational since April 2006, adds 20 MV accelerating potential to the ISAC Radioactive Ion Beam (RIB) facility. An upgrade to the linac, in progress, calls for the addition of a further 20 MV of accelerating structure by the end of 2009. The new installation consists of twenty 141 MHz quarter wave cavities at β_0=11%. The cavities will be housed in three cryomodules with six cavities in the first two cryomodules and eight cavities in the last. A second Linde TC50 refrigerator has been installed and commissioned to provide cooling for the new installation. The design incorporates several new features as improvements to the existing cryomodules. A summary of the design and the current status of the cryomodule production and supporting infrastructure will be presented.

INTRODUCTION

The Radioactive Ion Beam (RIB) facility, ISAC, includes an ISOL production facility and a post-accelerator for delivery of beams from 150 keV/u to beyond the Coulomb barrier.[1] The post-accelerator consists of two room temperature devices, a 35 MHz RFQ for acceleration of ions with A$\leq$30 to 150 keV/u and a 106 MHz post-stripper DTL to energies fully variable from 0.15 to 1.8 MeV/u. A superconducting heavy ion linac[2] was added in 2006 to add a further 20 MV to the ISAC beam energy. The installation known as ISAC-II is the first phase in a planned three phase installation. The Phase I linac consists of 20 bulk niobium quarter wave cavities housed in five cryomodules. Each cryomodule consists of four cavities and one superconducting solenoid arranged symmetrically along the beamline with a diagnostic box and steering magnet located between the modules at the beam waist. Routine average operating gradients of 7 MV/m corresponding to peak surface fields of 35 MV/m are achieved. Eight of the cavities (the first two cryomodules) are β=0.057 and the other twelve are β=0.071.

A second phase now in progress will see the addition of another 20 MV of accelerating potential to extend the present energy range by the end of 2009. The new installation consists of twenty 141 MHz quarter wave cavities at β=0.11. The cavities will be housed in three cryomodules with six cavities in the first two cryomodules and eight cavities in the last. The cavities and cryomodules are now in fabrication. The plan is to install the completed and tested cryomodules during an extended shutdown of ISAC-II starting in Sept. 2009. The layout of ISAC-I and ISAC-II is shown in Fig. 1.

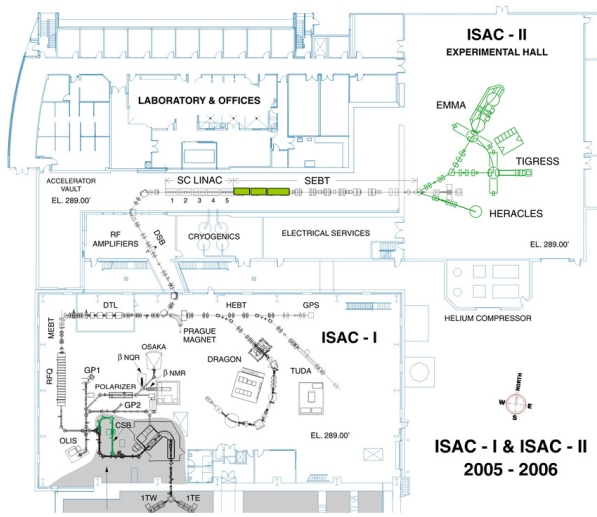

Figure 1: The layout of ISAC-I and ISAC-II. The Phase II SC-linac is highlighted.

CRYOMODULE DESIGN AND STATUS

The Phase II cryomodules are identical in many respects compared to the Phase I cryomodules. A key design choice was to maintain the philosophy of incorporating a single vacuum space for thermal isolation and beam/rf volumes. This has been the historic choice in the low-beta community (ATLAS, INFN-Legnaro, JAERI) but recent proposed facilities in development or assembly have chosen separated vacuum systems (SARAF, SPIRAL-II, FRIB). The decision to maintain a single vacuum comes from our experience with Phase I operation of the SC-linac. We have seen very little evidence of degradation in cavity performance over the first two years of operation even after repeated thermal and venting cycles. Procedures are followed to help mitigate cavity degradation: 1. Initial cavity treatment and overall assembly using HPWR and clean conditions 2. Vacuum materials and components to be free from particulate, grease, flux and other volatiles 3. Maintain a LN2 cooled cold trap upstream and downstream of the linac to prevent volatiles migrating from the beamline into the cryomodule 4. Cryomodule venting with filtered nitrogen 5. Pumping and venting of modules at slow rates to avoid turbulences.

All cryomodules are assembled in a 'dirty' assembly area to check the fitting of all components. Next the assembly is completely dismantled, all parts are cleaned in

* TRIUMF receives funding via a contribution agreement through the National Research Council of Canada

THE HITRAP DECELERATOR PROJECT AT GSI - STATUS AND COMMISSIONING REPORT

L. Dahl#, W. Barth, P. Gerhard, F. Herfurth, M. Kaiser, O. Kester, H.-J. Kluge, S. Koszudowski, C. Kozhuharov, G. Maero, W. Quint, A. Sokolov, T. Stöhlker, W. Vinzenz, G. Vorobjev, D. Winters
Gesellschaft für Schwerionenforschung, D-64291 Darmstadt, Germany

B. Hofmann, J. Pfister, U. Ratzinger, A. Sauer, A. Schempp
Goethe University, D-60438 Frankfurt, Germany

Abstract

For injection into the ion trap facility HITRAP, the GSI accelerator complex has the unique possibility to provide beams of highly stripped ions and even bare nuclei up to Uranium at an energy of 4 MeV/u. The HITRAP facility comprises linear 108 MHz-structures of IH- and RFQ-type to decelerate the beams further down to 6keV/u for capturing the ions in a large penning trap for cooling purpose. The installation is completed except the RFQ.

During commissioning periods in 2007 $^{64}Ni^{28+}$ and $^{20}Ne^{10+}$ beams were used to investigate the beam optics from the experimental storage ring extraction to the HITRAP double-drift-buncher system. In 2008 the IH-structure and the downstream matching section were examined with $^{197}Au^{79+}$ beam. Comprehensive beam diagnostics were installed: Faraday cups, tubular and short capacitive pick ups, SEM grids, YAG scintillation screens, a single shot pepper pot emittance meter, and a diamond detector for bunch shape measurements. Results of the extensive measurements are presented.

INTRODUCTION

Within the HITRAP project (Heavy Ion Trap) [1] trapped and cooled highly charged ions up to U^{92+} will become available for a variety of attractive experiments in atomic physics. As presented in Fig.1 heavy ions are produced, accelerated, and stripped in the GSI accelerator complex and are stored, decelerated, and cooled in the ESR (Experimental Storage Ring) down to 4 MeV/u. After extraction from the ESR, the ions have to be further decelerated down to 6 keV/u by 108.408 MHz structures [2,3]. An IH drift tube cavity operating in the H11(0) mode reduces the ion energy to 0.5 MeV/u and a 4-rod RFQ [4] degrades it finally to 6 keV/u. Phase matching into the IH structure is prepared by a DDB (Double-Drift-Buncher combination) of λ/4-resonators whereof the second one works at 216 MHz. A third rebuncher of spiral type is located between the decelerator tanks. Finally a low power spiral type debuncher integrated into the RFQ tank at the beam exit end reduces the beam energy spread for efficient beam capturing in the super conducting penning trap. The linear decelerator as sketched in Fig. 1 is installed in the re-injection channel between ESR and SIS (Heavy Ion Synchrotron).

STATUS OF INSTALLATIONS

Until September 2008 the HITRAP decelerator was being constructed except the RFQ tank. Magnet power

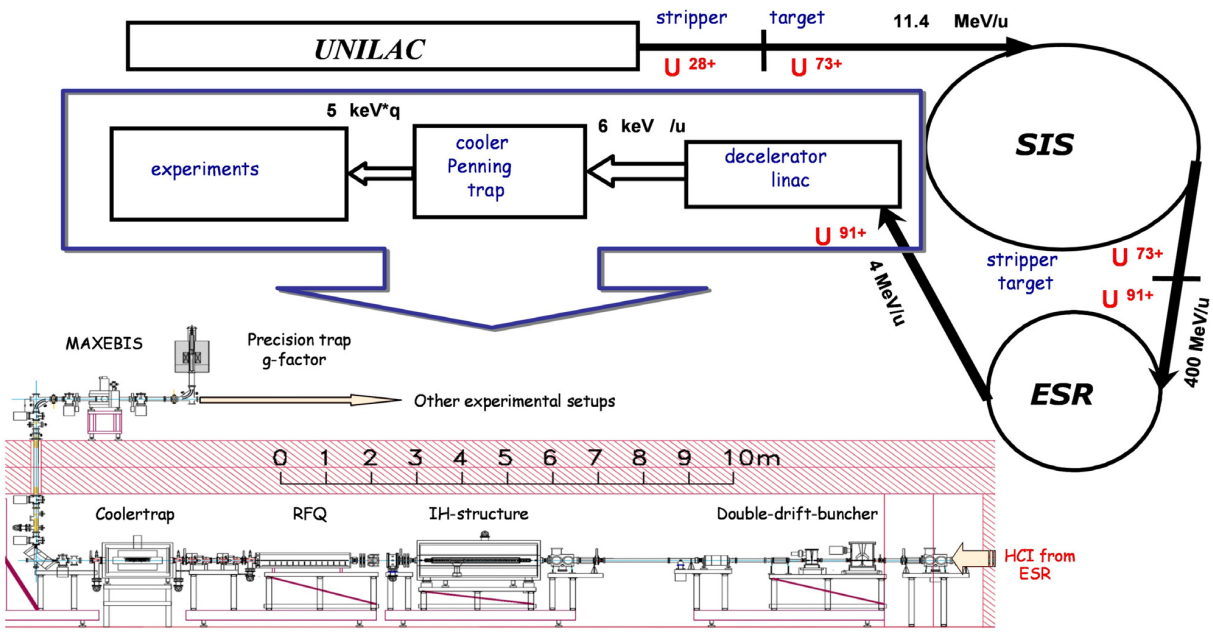

Figure 1: Production process of bare nuclei and HITRAP decelerator.

l.dahl@gsi.de

POST-ACCELERATOR LINAC DEVELOPMENT FOR THE RIB FACILITY PROJECT AT VECC, KOLKATA

Arup Bandyopadhyay, M. Mondal, H. K. Pandey, T. Mandi, A. Chakrabarti
Variable Energy Cyclotron Centre, 1/AF Bidhan Nagar, Kolkata 700064, India

Abstract

An ISOL (Isotope Separator On Line) type of RIB (Rare Ion Beam) facility is being developed at our centre. The post-acceleration scheme will consist of a Radio Frequency Quadrupole (RFQ) followed by a few IH LINAC cavities - further augumentation of energy using SC QWRs will be taken up at a later stage.

The first two IH cavities have been designed for 37.6 MHz frequency like the preceding RFQ to keep the RF defocusing smaller. Explosively bonded copper on steel has been used for the fabrication of the IH cavities and the inner components have been from of ETP grade (UNS C11000) copper. Also, we have adopted an octagonal cross-section for the cavity structure to avoid fabrication complicacies. The first and second cavity have inside lengths of 0.62 and 0.97 m respectively and the inside separation between two opposite sides of the octagon is 1.72 m.

Thermal analysis of the cavities has been carried out and cooling configurations have been optimized accordingly to control the temperature rise of the LINACs. Detailed mechanical analysis has been carried out to reduce the deflection of the LINAC components under various loads.

Design and fabrication aspects of these two cavities and results of the low power tests will be reported in this paper.

INTRODUCTION

Rare Ion Beams (ions of β-unstable nuclei) offer many new possibilities in different branches of accelerator based research. An ISOL type of RIB facility is being developed at our centre [1]. Light ion beams (p, α) from the K=130 cyclotron will be used as a primary beam for this facility. Also an electron LINAC is being developed at present which will open up the possibility of producing RIBs using photofission route. The primary reaction products will be ionised using an on line ion source and mass separated to choose the RIB of interest from the other reaction products. The RIBs will be accelerated from 1-97.5 keV/u using a heavy ion RFQ [2, 3, 4] operating at 37.6 MHz. Further acceleration up to 1.2 MeV/u will be done using IH LINAC cavities. The first two of these cavities have been designed and fabricated. Low power tests have also been performed. Design and fabrication aspects of these two cavities and results of the low power tests will be reported in this paper.

DESIGN REQUIREMENTS

The initial energy of the RIBs after the mass selection is 1.7 keV/u. The RIBs will be accelerated in stages - the first post-accelerator is a RFQ which accelerates up to about 98.7 keV/u at 37.6 MHz, followed by two IH cavities at the same frequency to reach 287 keV/u - all of them are designed for $q/A \geq 1/14$. This will be followed by one IH cavity designed for 75.2 MHz to reach 409.1 keV/u. There will be a charge stripper at this stage and this will be followed by three more IH cavities designed for $q/A \geq 1/7$ to reach around 1.2 MeV/u. Further acceleration using QWRs are being planned at present.

The intensity of RIBs is a prime concern as it is significantly lower than stable ion beams in most of the cases. So, the LINACs have been designed for high transmission efficiency of the ions. Many experiments require measurement of parameters at various energies and therefore the aim is to continuously vary the energy of the beam without significant loss of intensity or degradation of beam quality (spot size and energy width).

DESIGN PRINCIPLE

The acceleration method adopted in our design consists of classical negative synchronous phase small length LINACs with transverse focusing quadrupole triplets in between the cavities. Buncher cavities will also be accomodated where need arises. The cell parameters of the LINACs have been calculated by tracking trajectory of an ion having designed values of phase and velocity by integrating its equation of motion using static electric field obtained from *POISSON* code for a particular drift tube geometry – ignoring the details of the drift tube supports, ridges and cavity. With this drift tube (DT) and gap geometry, the cavity parameters have been optimised using *ANSYS*. The detailed beam dynamics have been studied using interpolated field from *ANSYS* using *VECLIN* code. Details of this design principle has been reported elsewhere [5].

The important parameters for the first two IH cavities are shown in Table 1. The frequency of first two LINACs has been kept same as that of RFQ to keep the RF defocusing smaller for low input energy. The shunt impedance and Q-values of the table are *ANSYS* results and the power has been calculated for a 60% shunt impedance value. The beam energy can be veried without any significant loss of intensity or degradation of beam quality. Fig. 1 shows two possible tunes for 286.8 keV/u energy - the case for good transmission (top) and good beam quality (bottom). This has of course still room for improvement by reducing the inter-tank separation.

TOWARDS THE DEVELOPMENT OF RARE ISOTOPE BEAM FACILITY AT VECC KOLKATA*

Vaishali Naik, Alok Chakrabarti, Arup Bandyopadhyay, Manas Mondal, Siddharta Dechoudhury, Hemendra Kumar Pandey, Debasis Bhowmick, Dirtha Sanyal, Tapatee Kundu Roy, J.S. Kainth, Tapan Kumar Mandi, Mahuya Chakrabarti, Prasanta Karmakar
Variable Energy Cyclotron Centre, 1/AF Bidhannagar, Kolkata, India

Abstract

An ISOL type Rare Isotope Beam (RIB) Facility is being developed at VECC, Kolkata around the existing K=130 room temperature cyclotron. In the first stage, the beam energy will be about 400 keV/u using an RFQ post-accelerator and three modules of IH-linacs. Subsequently the energy will be boosted to about 1.3 MeV/u. A separate LEBT line for material science experiments is planned. Some of the systems have already been installed and made operational. The LEBT line has been tested and stable ion beams accelerated to 29 keV/u with high efficiency in a 1.7 m RFQ. A 3.4 m RFQ and the first IH Linac tank are under installation in the post-acceleration beam line. In this contribution an overview of the present status of the facility will be presented.

INTRODUCTION

An ISOL type RIB facility is presently under construction at VECC Kolkata [1]. The K=130 cyclotron at VECC will act as mother accelerator for this facility. A schematic layout of the facility is shown in figure 1. The 1+ radioactive ions will be produced inside a thick target integrated ion-source, injected into an on-line Electron Cyclotron Resonance Ion source (ECRIS) for high charge state ionization, mass separated and then post accelerated in a Radio Frequency Quadrupole (RFQ) Linac and IH-Linacs. The production target and ECR based charge-breeder system lead to two beam lines. The first one, a low energy beam transport (LEBT) line is already installed and presently delivers stable ion beams of 29 keV/u energy at the end of a 1.7m RFQ linac. The second, post-acceleration beam line will accelerate the beams to 1.3 MeV/u using a longer, 3.4 m RFQ and a series of IH linear accelerators. In the first stage, the beam energy will be about 400 keV/u using three modules of linacs.

DESCRIPTION OF RIB FACILITY

Target Ion-Source

The first component is the Integrated Ion source. Radioactive nuclei will be produced inside thick targets using proton and α-particle beams from the K=130 cyclotron at VECC and ionized to 1+ charge state in the integrated surface ionization source. A possibility of using a multiple target Electron Beam Plasma ion-source is also being worked out. The low energy 1+ ion beam from the first ion-source will be injected into the ECR ion source for higher charge state (n+) production in the *charge breeder*.

We have undertaken a target R&D programme as we need to develop many kinds of thick targets for our facility. Since diffusion of radioactive species out of the target increases with temperature one usually selects refractory target compounds such as oxides and carbides for the target. Target materials can be deposited on Graphite matrices (RVCF fibres) that can withstand high temperature and have sufficient porosity to allow radioactive atoms to diffuse out [2].

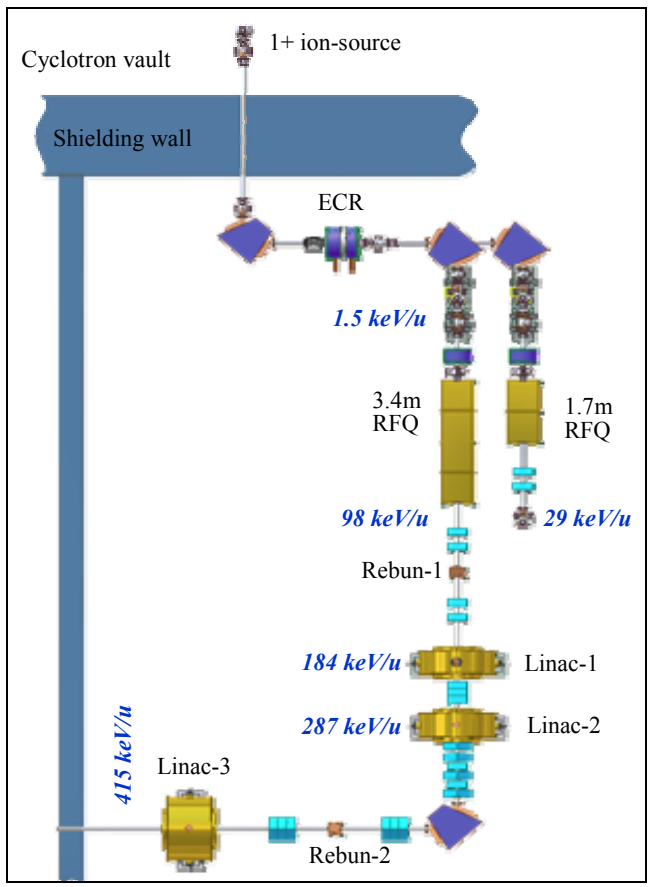

Figure 1: Layout of RIB facility.

Sintering & grain growth due to beam heating hinders the release of radioactive ions. Studies have shown that grain growth stays within limiting range if one starts with grain size of nano-metre range. Recent studies in case of ZnO have revealed that formation of a composite phase (Zinc silicate) resist the grain growth within the permissible limits even for 6 hrs heating at 1300 C[3].

*This is a VECC-DAE project

THE ALPI SUPER-CONDUCTING ACCELERATOR UPGRADE FOR THE SPES PROJECT*

P. A. Posocco†, Consorzio RFX, Padova and INFN/LNL, Legnaro, ITALY
G. Bisoffi, A. Pisent, INFN/LNL, Legnaro, ITALY

Abstract

The SPES project at Laboratori Nazionali di Legnaro foresees the construction of a RIB facility based on a fission target driven by a 40 MeV proton beam. After the ^{238}U carbide target the 1+ charged ions will be selected by a high resolution mass spectrometer, charge enhanced by a charge breeder and accelerated up to 10 MeV/A for ^{132}Sn. The present configuration of the Legnaro super-conducting accelerator complex (PIAVE injector and ALPI main accelerator) fits the requirements for SPES post acceleration too. Nevertheless an upgrade of its performances both in overall transmission and final energy is needed and a solution which minimizes the impact on the present structures will be presented.

INTRODUCTION

The super-conducting linac ALPI [1] is injected either by a XTU tandem or by the s-c PIAVE injector [2][3]. The linac (at the present 64 cavities and a total voltage of 48 MV) is build up in two branches connected by an achromatic and isochronous U-bend (Fig. 1). ALPI period consists in one triplet and 2 cryostats (4 cavities in each cryostat), and a diagnostic box (profile monitor and Faraday cup) in between.

The PIAVE-ALPI complex is able to accelerate beams up to A/q = 7. Higher A/q ions suffer from a too low injection energy to the medium-β cryostats, where the RF defocusing is too strong and the beam gets easily lost onto the cavity beam ports. In the last few years the average cavity accelerating field (E_{acc}) has been enhanced by more than a factor of two with respect to the original design value [4]. The strength of the focusing lenses on the other hand, has remained the same (20 T/m). Therefore, even for 6 < A/q < 7 it is hard to design a proper longitudinal beam dynamics such that it will not cause problems on the transverse plane. To fully exploit the available acceleration gradient, some improvements are required in the layout of both PIAVE and ALPI.

Referring to the cavity performances of Tab. 1 (expected in the next years), three subsequent upgrade scenarios may be envisaged, each one representing a step forward in the final energy (Fig. 2) and beam quality: 2009 for stable beams (funded), an intermediate and a final upgrade within the SPES project (not yet officially funded). For SPES, the Radioactive Ion Beam at 37.1 keV/A will be injected into PIAVE line upstream the SRFQs.

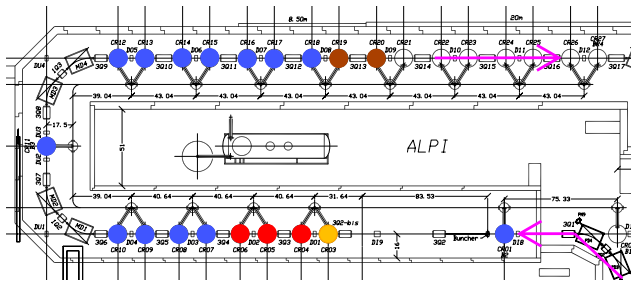

Figure 1: ALPI plan for 2009. The beam coming from PIAVE injector passes through the low-β (in orange and red), medium-β (blu) and high-β (brown) cryostats.

The beam dynamics of each scenario has been optimized for 4 < A/q < 7 thanks to several runs of PARMELA [5]: the beam behavior in the low-energy branch is highly non-linear due to the high gradients and strong Bessel components of the fields inside the cavities, therefore, in such conditions, simulation programs like Trace3D are simply ineffective.

Table 1: ALPI cavity performances for the upgrade scenarios. E_{acc} in MV/m.

cryostat	#	2009	inter	SPES I	SPES II
low-beta (β_o = 0.047 *and* β_o = 0.056), 80 MHz					
CR01-02	8	n/a	n/a	6	n/a
CR03	4	5	6	6	6
CR04-06	12	3.5	6	6	6
medium-beta (β_o = 0.11), 160 MHz					
CR07-18	44	4.2	4.5	4.5	4.5
high-beta (β_o = 0.13), 160 MHz					
CR19-20	8	5.5	5.5	5.5	5.5
CR21	4	n/a	5.5	5.5	5.5
CR22-23	8	n/a	n/a	n/a	5.5
total number		68	72	80	80

THE 2009 STATUS

The first ALPI cryostat (CR03) gently focuses the beam coming from PIAVE to the following cryostat. Hence, only a small acceleration is given to the beam by CRO3. The E_{acc} values of the following low-energy branch cavities are

* http://www.lnl.infn.it/ spes/
† piero.antonio.posocco@lnl.infn.it

PRESENT STATUS OF RIKEN HEAVY-ION LINAC

O. Kamigaito*, E. Ikezawa, M. Kase, M. Fujimaki, T. Fujinawa, N. Fukunishi,
A. Goto, H. Haba, Y. Higurashi, M. Kidera, M. Komiyama, R. Koyama†,
H. Kuboki, K. Kumagai, T. Maie, M. Nagase, T. Nakagawa, J. Ohnishi, H. Okuno,
N. Sakamoto, Y. Sato, K. Suda, T. Watanabe, K. Yamada, S. Yokouchi, Y. Yano,
RIKEN Nishina Center for Accelerator-Based Science, Wako-shi, Saitama 351-0198 Japan

Abstract

The RIKEN heavy-ion linac (RILAC) has been used as an injector for the RIKEN RI-Beam Factory (RIBF) since 2006. Results of the acceleration tests of ^{48}Ca and ^{238}U performed recently in the RIBF are reported; we got 270 pnA of ^{48}Ca at an energy of 114 MeV/u after the Intermediate-stage Ring Cyclotron (IRC). On the other hand, the intensity of the uranium beam is still far below the design goal. Therefore, we are planning to install a superconducting ECR ion source, which is under construction, on the high-voltage platform of the Cockcroft-Walton pre-injector. It will be possible to test this new pre-injector in April 2009. A plan to construct an alternative injector for the RIBF, consisting of an ECR ion source, an RFQ, and three DTLs, is also illustrated, which aims at independent operation of the RIBF experiments and super-heavy element synthesis.

INTRODUCTION

The RIKEN heavy-ion linac (RILAC), which has been operated since 1981, accelerates various kinds of ions by changing the rf frequency from 18 to 38 MHz in the continuous-wave (cw) mode. The voltage gain is 16 MV in the whole frequency range, and the acceptable mass-to-charge ratio (m/q) of the ions ranges from 5.5 at 38 MHz to 25 at 18 MHz. The original Cockcroft-Walton pre-injector to the RILAC was replaced by an RFQ pre-injector equipped with an 18-GHz ECR ion source in 1996.

In 2001, a booster linac for the RILAC was constructed, which consists of two variable-frequency resonators and four fixed-frequency resonators; the maximum energy of the RILAC facility has been increased to 5.8 MeV/u [1]. By using the high-intensity beams from the booster, experimental study has been started for searching super-heavy elements (SHE) since 2002. The beam time provided for the SHE experiments so far has exceeded 10,000 hours. The present layout of the RILAC facility is illustrated in Fig. 1.

On the other hand, commissioning of the RI-Beam Factory (RIBF) [2] started in 2006 [3], where the RILAC is used as an injector. Results of the acceleration tests performed recently in the RIBF are given in the next section, as well as a brief introduction of the RIBF accelerators.

RILAC AS RIBF INJECTOR

Figure 2 shows a conceptual layout of the accelerator chain of the RIBF, which consists of the RILAC injector and four booster cyclotrons (RRC, fRC, IRC and SRC) in a cascade. The fRC is exclusively used for very heavy ions such as uranium and xenon, where the rf frequency of the RILAC is fixed to 18.25 MHz and the beam energy at the exit of the SRC is 345 MeV/u. For medium-mass ions such as calcium and krypton, the fRC is skipped; it is possible to operate the accelerator chain in the variable-energy mode. There is another acceleration mode in the RIBF, where the AVF cyclotron (K70 MeV) is used as an injector for the acceleration of light ions such as deuteron and carbon.

In this year, acceleration tests were performed up to the exit of the IRC using ^{48}Ca and ^{238}U beams.

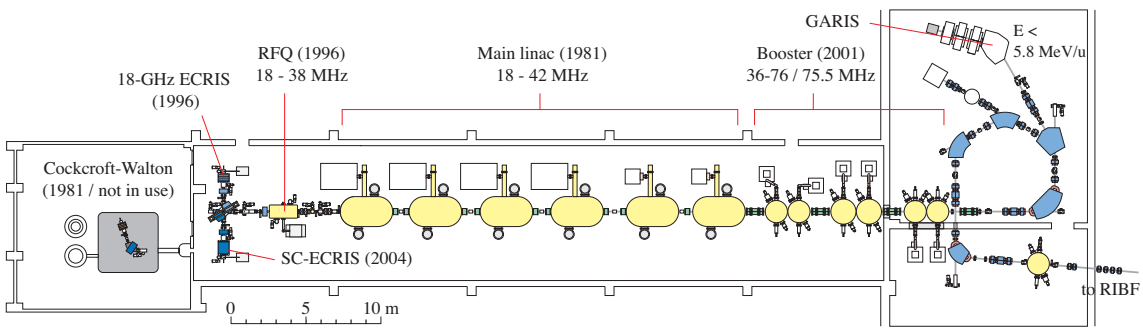

Figure 1: Plan view of the RIKEN Heavy-Ion Linac (RILAC).

* kamigait@riken.jp
† SHI Accelerator Service, Ltd.

LOW ENERGY SPREAD BEAM DYNAMICS AND RF DESIGN OF A TRAPEZOIDAL IH-RFQ *

Y.R. Lu†, Y.C. Nie‡ ,C.E. Chen, Z.Y.Guo, X.Q.Yan, K.Zhu, S.L.Gao, J.X.Fang
State Key Lab of Nuclear Physics and Technology, Peking University, 100871

Abstract

The methodology for a low energy spread RFQ beam dynamics design has been studied for C^{14+} AMS application This paper will present a low energy spread beam dynamics and RF design for a trapezoidal IH-RFQ (abbreviated T-IH-RFQ) operating at 104MHz at Peking University. $^{14}C^{+}$ will be accelerated from 40keV to 500keV with the length of about 1.1m. The designed transmission efficiency is better than 95% and the energy spread is as low as 0.6%. Combining the beam dynamics design, a T-IH-RFQ structure was proposed, which can be cooled more easily and has better mechanical performance than traditional RFQ. The electromagnetic field distribution was simulated by CST Microwave Studio (MWS). The simulation results show such T-IH-RFQ has higher operating frequency than normal four rods RFQ and/or IH-RFQs. The specific shunt impedance and the quality factor were also compared to these RFQ structures.

INTRODUCTION

RFQ, proposed by I.M.Kapchinsky and V.A.Teplyakov in 1970[1], has been used widely for many applications. It can focus, bunch and accelerate low energy beam, extracted from ion sources directly, over a mass range from proton to heavy ions such as uranium based on the RF electrical field of a modulated quadruple transport channel [2]. RFQ was used to ^{3}H Accelerator Mass Spectroscopy (AMS) firstly by LLNL in USA because of its inherent compact size [3]. RFQ based ^{14}C AMS application has been studying in recent years at the Institute of Heavy Ion Physics (IHIP), Peking University [4, 5]. The most critical problem is that the energy spread of full width at half magnitude (FWHM) for traditional RFQ is usually larger than 2% because of the process of adiabatic bunching and phase oscillation, which is too high for the particle identification in an AMS detector. So, ways must be found to reduce the energy spread of the output ^{14}C beam. The highest beam current of RFQ used for AMS ^{14}C facility is lower than 200μA, which is such low that the space charge effects can be ignored. Non-adiabatic bunching method should be used to make output beam energy spread low. A physical design of RFQ with 0.6% energy spread has been obtained through external bunching method by previous work at IHIP. A pre-buncher will be necessary in the injection system before RFQ to bunch beam length in the range of [-20°, 20°]. However, the bunching efficiency of a pre-buncher can only be 70~80%. As a result, the total transmission will be lower than most tandems based AMS facility even though no particle is lost in RFQ. An internal discrete bunching proposed by J.W.Staples at LBNL [6] is used to save additional RF power supply and buncher cavity. The low energy spread beam dynamics design for $^{14}C^{+}$ RFQ will be presented in this paper.

On the other hand, an IH-RFQ acceleration structure was proposed and studied. The four electrodes are supported by erect boards connected to the external cavity up and down. This new structure was named trapezoidal IH-RFQ according to its appearance. The trapezoidal IH-RFQ is easily cooled and will have good mechanical performance. Moreover, it will have higher resonant frequency than traditional IH-RFQ [7]. Simulations of the electromagnetic fields have been completed by CST Microwave Studio (MWS). RF characteristics is investigated, and geometrical parameters are optimised initially to make the shunt impedance and the quality factor as large as possible.

BEAM DYNAMICS DESIGN

According to Staples' method, the whole RFQ beam dynamics design is divided into five sections, radial matcher, buncher section, drift section, transition section and accelerator section. The radial matcher is similar to that of four-step method developed at LANL [8], which matches DC input beam to the time-varying transverse envelope at the entrance of RFQ. The buncher section is distributed over several cells while the modulation parameter m ramps from zero to a maximum and then back down to zero, which performs the function of bunching as a non-adiabatic buncher. The following several unmodulated cells make up of the drift section which allows the ideal beam bunch to form. In the transition section, the beam is accelerated slowly as the synchronous phase varies from -90º to its final value -30º. Finally, the designed energy is reached in the acceleration section. Significantly lowered longitudinal output emittance and slightly lowered transverse emittance can be obtained by this new design technique compared to previous methods, which has been proved by PARMTEQM.

* Supported by NSFC(19775009)
† Corresponding author yrlu@pku.edu.cn
‡ Current institute: Institute of Applied Physics, Frankfurt University, Frankfurt, Germany

AN INTERMEDIATE STRUCTURE SFRFQ BETWEEN RFQ AND DTL*

Y. R. Lu, J. E. Chen†, K. Zhu，X. Q. Yan, Z. Wang, Z. Y. Guo,
M. L. Kang, M. Zhang，J. Zhao, S. L. Gao, S. X. Peng, J. X. Fang
State Key Lab of Nuclear Physics and Technology, Peking University, 100871

Abstract

SFRFQ is an intermediate accelerating structure, which combines RFQ and DTL together, it can increase the accelerating efficiency at RFQ exit part by inserting gap acceleration between RFQ electrodes while providing strong focusing by RFQ focusing field. One prototype cavity has been manufactured and been used as a post accelerator of ISR RFQ to accelerate O+ from 1MeV to 1.6MeV in 1meter. A code SFRFQCODEV1.0 was developed for the beam dynamics design. The RF conditioning and full RF power test has been carried out. The intervane or gap voltage have reached 86kV at 29 kW with 1/6 duty cycle and repetition frequency 166Hz. The initial beam test results will also be presented in this paper.
PACS numbers: 29.20.Ej

INTRODUCTION

RFQ accelerators have been widely used in many applications. Because of increasing of the beam energy, beam accelerating efficiency goes down rapidly. Actually, Longer the RFQ length is, lower kinetic energy gain per unit length is; lower the injection energy of DTL is, much higher accelerating efficiency is; more accelerating gaps at DTL entrance means stronger transverse focusing is needed for the beam. Therefore several different accelerating structures, such as SP RFQ [1] in Russia and RFD [2] in U.S.A., have been studied in last decade to improve accelerating efficiency. The novel idea of Separated Function RFQ (SFRFQ) was first proposed by the RFQ group of IHIP (Institute of Heavy Ion Physics) at Peking university[3], based on the experience of ISR-RFQ 1000 (Integral Split Ring RFQ) [4][5][6]. Initial results of electro-magnetic calculation and dynamics proved the possibility and higher RF accelerating efficiency of SFRFQ structure[7].

To verify accelerating feasibilities of the SFRFQ structure, a simulation code SFRFQCODEV1.0[8] was developed for beam dynamics design. The prototype SFRFQ cavity will be used as a post-accelerator for ISR RFQ-1000 and accelerate O+ beam with ~mA peak current from 1MeV to 1.6MeV. This paper will present the beam line setup and related experimental results.

SFRFQ BEAMLINE SETUP

SFRFQ accelerating system consists of a 2.45GHz ECR ion source and LEBT, 1MeV ISR RFQ-1000, Magnetic Triplet, SFRFQ cavity, Analyzing Magnet and three beam Faraday cups. It is shown in Fig.1. Figure 2 shows the 2.45GHz ECR ion source and LEBT. 2.45GHz ECR ion source was made by permanent magnet. It can generate the axial magnetic field of 90~100mT in microwave discharging chamber, which is about 50mm in diameter and 50mm in length. LEBT consists of two electrostatic lenses with diameter of 80mm and 120mm respectively. The total extracted beam current can reach 5mA with extraction voltage 22kV, extraction aperture diameter of 5mm, O_2 gas inlet of 0.15sccm, electrostatic focusing voltage 19.6kV and 16.7kV respectively. The extracted O^+ ratio is about 0.6 and LEBT transmission is about 80%[9]. The beam emittance is about 0.12~0.16mm·mrad measured by Allison emmitance equipment.

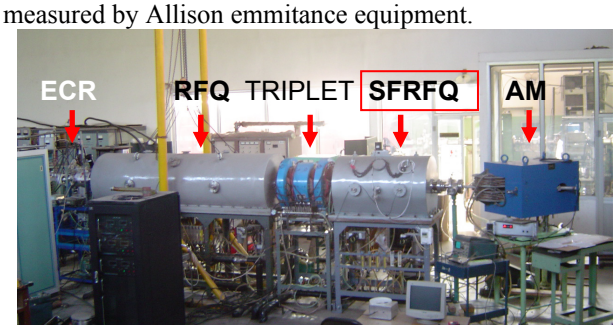

Figure 1: SFRFQ beam line setup.

The triplet has been designed to realize the beam matching in transverse. The figure 2 shows the magnetic gradient distribution along the triplet axis. It is only regret that longitudinal bunched beam length was expanded to nearly 150degree because of beam energy spread and longitudinal drifting. It asks an additional buncher to bunch the beam.

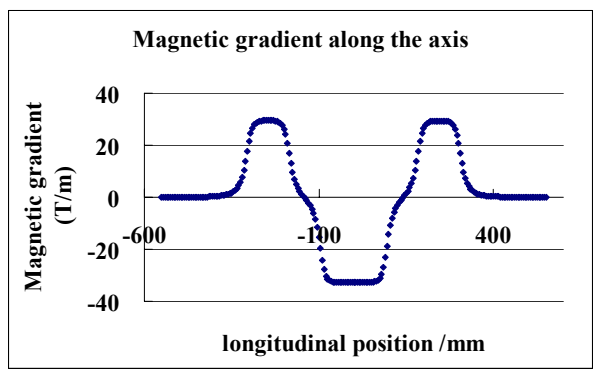

Figure 2: Magnetic gradient along the triplet axis.

The upgrade of beam test for 1MeV ISR-RFQ has been performed. The maximum output peak beam current at RFQ exit i.e. at the entrance of triplet is 2mA with sample

* Supported by NSFC 10455001
† Corresponding author: Chenje@pku.edu.cn

HEAVY ION INJECTOR FOR NICA/MPD PROJECT

V.V.Kobets, A.I.Govorov, G.V.Trubnikov, E.E.Donets, E.D.Donets, A.O.Sidorin, V.A.Monchinsky, I.N.Meshkov, JINR, Dubna, Russia

O.K.Belyaev, A.P.Maltsev, Yu.A.Budanov, I.A.Zvonarev, IHEP, Protvino, Russia

Abstract

General goal of the NICA/MPD project under realization at JINR is to start in the coming 5÷7 years an experimental study of hot and dense strongly interacting QCD matter and search for possible manifestation of signs of the mixed phase and critical endpoint in heavy ion collisions. The Nuclotron-based Ion Collider fAcility (NICA) and the Multi Purpose Detector (MPD) are proposed for these purposes. The NICA collider is aimed to provide experiment with heavy ions like Au, Pb or U at energy up to 3.5 x 3.5 GeV/u with average luminosity of 10^{27} $cm^{-2}\cdot s^{-1}$ and to provide collisions of light ions in the total energy range available with the Nuclotron. New injector designed for efficient operation of the NICA facility is based on Electron String Ion Source providing short (< 10 μs) and intensive (up to 10 mA) pulses of U^{32+} ions, one section of RFQ and four sections of RFQ Drift Tube Linac accelerating the ions at Z/A ≥ 0.12 up to 6.2 MeV/u of the kinetic energy. General parameters of the injector are discussed.

INTRODUCTION

General challenge of the NICA facility is to achieve a high luminosity level of heavy ion collisions in a wide energy range starting with about 1 GeV/u. To reach this goal the NICA injection chain has to deliver a single bunch of fully stripped heavy ions (U^{92+}, Pb^{82+} or Au^{79+}) at intensity of about $1\div1.5\cdot10^9$ ions [1]. The existing Nuclotron injection complex consists of HV fore-injector and Alvarez-type linac LU-20. The LU-20 accelerates the protons up to the energy of 20 MeV and ions at Z/A ≥ 0.33 up to the energy of 5 MeV/u [2]. Because of the limitation in charge to mass ration the LU-20 can not be used effectively for operation as a part of the NICA facility. Additionally, an effective stripping of the ions before injection into the Nuclotron requires their preliminary acceleration to an energy of a few hundreds of MeV/u. Therefore, realization of the NICA project presumes design and construction a heavy ion injector and intermediate booster synchrotron as new elements of the NICA collider injection chain. The injection chain optimization was started from the choice of an ion source and formulation of requirements to the linear accelerator.

ION SOURCE AND REQUIREMENTS FOR LINAC

We have considered a few types of the heavy ion sources – namely the Laser Ion Source (LIS), the Electron Beam Ion Source (EBIS), the Electron String Ion Source (ESIS) and the Electron Cyclotron Resonance (ECR) ion source.

The LIS has limitations in the kind of ions that can be produced. Additional obstacles, such as large beam emittance due to a large energy spread, target erosion and coating of mirrors, state of the art laser requirements, and very large pulse-to-pulse fluctuations of the beam current, set one thinking seriously about development of this type of the ion source presently.

The EBIS ion source chosen as the base of the new RHIC injector [3] has parameters close to the required ones and expected for the ESIS. General disadvantage of the EBIS is very high DC power of the electron beam. So, the EBIS proposed for the new RHIC injector requires of about 300 kW DC power for the operation and maximum charge state is limited because of the electron energy limitations. At the same time, the maximum DC power of the electron beam in the ESIS is about 200 W. By contrast to the EBIS, the ESIS source can provide heavy ions in very high charge states, like Au^{51+} or U^{64+} at practically same intensity as Au^{30+} or U^{32+}. The repetition frequency of ESIS operation in this mode is at the level of 1 Hz.

In view of the facts described above the decision to use the development of the ESIS as the baseline for the NICA project has been taken.

The possibility to work with ECR ion source as reserve option for the NICA facility operation is considered as well. To realize it the linac has to accelerate long heavy ions pulse generated in an ECR source for multiturn injection into the booster.

To provide optimization of the heavy ion injection chain and cover the polarized program of the NICA facility the injector-linac has to provide the following options of the operation:

- acceleration of the heavy ions at the charge state of 30+ ÷ 32+ at the intensity of $(2\div4)\cdot10^9$ ions and the pulse duration of 7 μs (the ion revolution period in the booster);
- acceleration of the heavy ions like Au^{51+} and U^{64+} at the intensity of $(2\div4)\cdot10^9$ and the pulse duration of 7 μs;
- acceleration of the heavy ions at the charge state of about 30+ ÷ 32+ at the current of 0.1 ÷ 0.2 mA and pulse duration up to 100 μs (operation with ECR source);
- acceleration of the polarized D^- ions at the current up to 1 mA and the pulse duration of about 1 ms.

The first option is chosen as the baseline for realization of U-U collision experiment. The pulse of $4\cdot10^9$ U^{32+} ions at 7 μs duration corresponds to the peak current of about

A SC UPGRADE FOR THE REX-ISOLDE ACCELERATOR AT CERN

M. Pasini*, S. Calatroni, N. Delruelle, M. Lindroos, V. Parma, P. Trilhe,
D. Voulot, F. Wenander, CERN, Geneva, Switzerland
R. M. Jones, Cockcroft Institute, Daresbury, UK and University of Manchester, Manchester, UK.
P. McIntosh STFC/DL/ASTeC, Daresbury, Warrington, Cheshire, UK

Abstract

The High Intensity and Energy ISOLDE (HIE-ISOLDE) proposal is a major upgrade of the existing ISOLDE and REX-ISOLDE facilities with the objective of increasing the energy and the intensity of the delivered radioactive ion beam. For the energy increase a staged construction of a superconducting linac based on sputtered quarter wave cavities is foreseen downstream of the present normal conducting linac. A funded R&D program has been launched at the end of 2007 in order to prepare a full Technical Design Report covering all the issues of such linac, including cavity prototyping and testing, cryomodule design, beam dynamics and beam diagnostics. We report here on the status and planning of the R&D activities for the SCREX-ISOLDE linac.

INTRODUCTION

Radioactive ion beam production at the ISOLDE facility at CERN is based on the ISOL (Isotope Separation On-Line) method where a max 2.8 kW proton beam, extracted at 1.4 GeV from the Proton-Syncrotron Booster (PSB), impinges upon a thick, high temperature target. The radioactive nuclei can be produced in two different target stations (GPS and HRS) via spallation, fission or fragmentation reactions. ISOLDE has been continuously developing targets and ion sources for four decades, introducing several new technologies (e.g. the resonance ionization laser ion source) so that there are now available more then 700 radioisotopes from 65 elements. These beams are accelerated to 60kV and steered to different experimental stations. In the present REX-ISOLDE facility [1] the RIBs are accelerated to higher energies with a compact Normal Conducting (NC) linac, making use of a special low energy preparatory scheme where the ion charge state is boosted so that the maximum mass to charge ratio is always $3 < A/q < 4.5$. This scheme consists of a Penning trap (REXTRAP), a charge breeder (REXEBIS) and an achromatic A/q separator of the Nier spectrometer type. The NC accelerator is designed with an accelerating voltage for a corresponding maximum A/q of 4.5 and it delivers a final energy of 3 MeV/u for $A/q < 3.5$ and 2.8 for $A/q < 4.5$. After charge breeding, the first acceleration stage is provided by a 101.28 MHz 4-rod Radio Frequency Quadrupole (RFQ) which takes the beam from an energy of 5 keV/u up to 300 keV/u. The beam is then re-bunched into the first 101.28MHz interdigital drift tube (IH) structure which increases the energy to 1.2 MeV/u. Three split ring cavities are used to give further acceleration to 2.2 MeV/u and finally a 202.56 MHz 9-gap IH cavity is used to boost and to vary the energy between $2.2 < E < 3$ MeV/u. Fig. 1 illustrate the scheme of the present linac.

The HIE-ISOLDE project contains three major parts: higher energies, improvements in beam quality and flexibility, and higher beam intensities. This requires developments in radioisotope selection, improvement in charge breeding and target-ion source development, as well as construction of the new injector for the PSB, LINAC4 [2]. The most significant improvement in the physics program [3] will come from the energy upgrade which aims at reaching a minimum energy of 10 MeV/u.

The present NC machine was developed in order to deliver beams at specific energies whilst taking advantage of the high accelerating gradient that pulsed NC IH structure could achieve. This concept is nevertheless not without some limitations: 1) limited energy variability; 2) operation restricted to pulsed mode; 3) inefficient use of the installed power when running light ions; 4) non variable longitudinal beam parameters, such as energy spread and bunch length.

To overcome the above limitations and to open the possibility of different longitudinal beam parameters, a superconducting linac based on Nb-sputtered SC Quarter Wave Resonators (QWRs) has been proposed [4]. The fact of having 2-gaps cavity independently phased assures both a very high flexibility in term of velocity acceptance and at the same time a small number of cavity types to cover the whole energy range.

THE SUPERCONDUCTING LINAC

The superconducting linac is designed to deliver an effective accelerating voltage of at least 39.6 MV with an average synchronous phase ϕ_s of -20 deg. This is the minimum voltage required in order to achieve a final energy of at least 10 MeV/u with $A/q = 4.5$. Because of the steep variation of the ions velocity, at least two cavity geometries are required in order to have an efficient acceleration throughout the whole energy range. A total number of 32 cavities are needed to provide the full acceleration voltage. The geometries chosen corresponding to *low* ($\beta_0 = 6.3\%$) and *high* ($\beta_0 = 10.3\%$) "β" cavities maintain the fundamental beam frequency of 101.28 MHz and their design parameters are given in Table 1. The design accelerating gradient aims at reaching 6 MV/m with a power consumption of 7 W per low β cavity and 10 W per high β cavity. These values have been already achieved by the two avail-

* matteo.pasini@cern.ch

BEAM DYNAMICS STUDIES FOR THE SCREX-ISOLDE LINAC AT CERN

M. Pasini*, D. Voulot, CERN, Geneva, Switzerland
M. A. Fraser, R. M. Jones, Cockcroft Institute, UK and University of Manchester, Manchester, UK

Abstract

For the REX-ISOLDE upgrade a superconducting linac based on 101.28 MHz Quarter Wave Resonators (QWRs) is foreseen downstream of the normal conducting (NC) linac. Currently the REX-ISOLDE linac can accelerate ions with a mass to charge ratio in the range of $3 < A/q < 4.5$ up to an energy of 2.8 MeV/u. The upgrade aims to reach a minimum final beam energy of 10 MeV/u for A/q=4.5 in two main stages. The first stage consists of installing two cryomodules loaded with 10 cavities able to reach 5.5 MeV/u at the end of the present linac and the second consists of replacing part of the existing NC linac and adding further cryomodules. We report here on a beam dynamics study of the accelerator for the two installation stages.

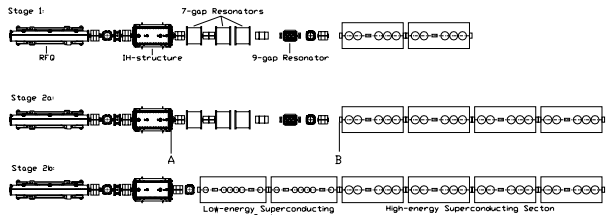

Figure 1: A Schematic of the HIE-ISOLDE linac stages. Stage 1 is shown at the top, while stage 2 can be split into two sub-stages depending on the physics priorities: the low energy cryomodules will allow the delivery of a beam with better emittance; the high energy cryomodule will enable the maximum energy to be reached.

INTRODUCTION

The REX-ISOLDE linac for the ISOLDE Radioactive Ion Beam facility at CERN [1] consists of a normal conducting linac where the RIB gets accelerated in different stages: a 101.28 MHz 4-rod Radio Frequency Quadrupole (RFQ) takes the beam from 5 to 300 keV/u, a 101.28 MHz interdigital drift tube (IH) structure boosts the beam energy up to 1.2 MeV/u, three 101.28 MHz split ring cavities accelerate to reach 2.2 MeV/u and a final 202.56 MHz IH structure is used to vary the energy between 2.2 and 3 MeV/u. The HIE-ISOLDE project [2] looks at the overall upgrade of the facility, i.e. an increase of the final energy of the radioactive ion beam, an improvement of the beam quality and flexibility and an increase of the beam intensity. The linac upgrade will consist of a superconducting machine [3] providing 39.6 MV of effective accelerating voltage with an average synchronous phase ϕ_s of -20 deg. utilising 32 101.28 MHz QWRs split into two families: *low* and *high* β cavities. The first stage of the upgrade plan consists of installing 10 high β cavities grouped in two cryomodules downstream of the present NC linac (stage 1). The second stage will be installed in two parts. Firstly, two more high β cryomodules will be added (stage 2a) downstream from those in stage 1 and secondly the split ring cavities and the 202.56 MHz IH cavity will be replaced with 12 low β cavities grouped in 2 cryomodules (stage 2b). Figure 1 shows a schematic of the different installation stages. The final energy for stage 1 and stage 2 is respectively 5.5 MeV/u and 10 MeV/u for A/q=4.5.

The focusing scheme foresees the employment of 200 mm long SC solenoids, which allow a high mismatch factor tolerance with respect to a standard triplet or doublet focusing scheme [4]. This brings a significant advantage for the tuning and operation of the machine. In fact, RIBs accelerators in general make use of a *high* intensity stable beam as a pilot beam with an A/q ratio that is as close as possible to the A/q of the wanted RIB. This is in fact necessary, since the very low RIB's intensity is practically invisible to conventional beam instrumentation. Once the pilot beam is established, a scaling action is performed and a focusing lattice with high mismatch tolerance guarantees better beam transport in the machine after scaling, where possible beam mismatch can occur. In addition, because SC solenoids allow the intermodule distance to be minimized, the longitudinal acceptance of the linac is not reduced and multi-charge state acceleration can be performed [5]. A schematic of the two cryomodules is shown in Figure 2. With this configuration the beam diagnostics instruments are ideally positioned at the beam waist location in the inter-cryomodule region where a pair of steering magnets will also be installed.

BEAM DYNAMICS SIMULATIONS

For the simulations of the complete HIE-LINAC (stage 2b) a 1 m long matching section with 4 quadrupoles between the first IH-structure and the first cryomodule is taken into account. It is important to keep this section as short as possible in order to minimize the longitudinal beam debunching. The input beam parameters for the simulations are constrained by the IH-cavity output beam and were calculated using `TRACE3D` [6]. The resonators were set to operate at a synchronous phase of -20 deg., and to increase the longitudinal phase spread capture at injection, the first resonator was phased at -40 deg. The last resonator in the first cryomodule was also re-phased, at -30 deg., in

* matteo.pasini@cern.ch

MULTIPLE USER BEAM DISTRIBUTION SYSTEM FOR FRIB DRIVER LINAC*

D. Gorelov# , V. Andreev, S. Chouhan, X. Wu, R. C. York,
NSCL/MSU, East Lansing, MI 48824, U.S.A.

Abstract

The proposed Facility for Radioactive Ion Beams (FRIB) [1] will deliver up to 400 kW of any stable isotope to Rare Isotop Beam (RIB) production target. Operational efficiency could, under certain conditions, be improved by a system that can distribute the beam current, variable in a large dynamic range, to several independent targets simultaneously. A possible FRIB Beam Switchyard (BSY) utilizes an RF kicker with subsequent magnetostatic septum system to split the beam on micro-bunch to micro-bunch basis. The micro-bunches can be differentially loaded at the front-end of the Driver Linac [2]. The detailed analysis of the beam dynamics performance in the proposed BSY system is presented.

INTRODUCTION

The effective use of the proposed FRIB facility [1] can under certain conditions be benefited by the ability to support simultaneous experiments. The stable isotope beams from the Driver Linac can be used for production of Radioactive Ion Beams (RIBs) using either Isotope Sepatation On Line (ISOL) or In-flight Particle Fragmentation methods to maximize yield of the corresponding species.

The discussed Beam Switchyard (BSY) will allow separation of the continuous stable ion beam from the Driver Linac into two independent channels on a micro-bunch by micro-bunch basis using an RF kicker followed by magnetic septum system.

The performance of this system was explored in details using three-dimensional electromagnetic fields for the RF kicker and a magnetostatic field distribution in septum magnet. As an alternative to the RF kicker, a DC septum magnet consisting of an array of thin wires and two electrodes can be used for lighter ions.

BEAM SWITCHYARD (BSY) SYSTEM

A proposed FRIB BSY design uses an RF kicker, an alternative DC bending dipole, and a septum magnet along the beam transport channel to either split the incoming stable beam into two beam lines with 50% intensity in each branch or to supply a single target with the full beam intensity (100 %) any of two production targets. The intensity of the two branches can be varied from 0% to 50% total beam intensity independently using the additional system of differential beam loading [2]. Figure 1 shows the layout of the proposed BSY system.

To minimize beam loss, quadrupole magnets in front of the RF kicker are provided to achieve reduced horizontal beam size at the entrance of the septum magnet. Both the RF kicker and the DC dipole have the same design deflection angle of ±1.5 mrad and will be used interchangeably for either splitting the incoming beam into two segments or direct all beam into one of the following beam lines. Given the beam micro-bunch frequency of 80.5 MHz, an RF kicker frequency of 120.75 MHz is appropriate to split the beam into two segments by kicking every other bunch in opposite transverse directions. A 10 m long drift space after the initial splitting point in RF kicker is required to generate enough spatial separation to accommodate a 10 mm thick septum in the septum magnet.

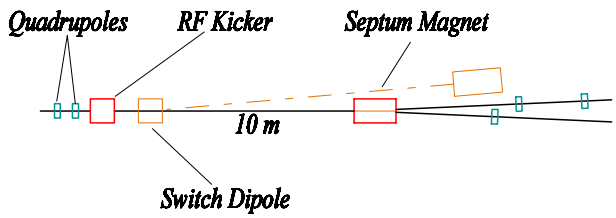

Figure 1: Layout of a proposed FRIB BSY system.

The performance of the proposed BSY system was evaluated by detailed beam dynamics simulations using the realistic three-dimensional (3D) distributions of the electromagnetic RF and magnetostatic fields in the system elements.

RF Kicker

The electromagnetic (EM) field calculations for the RF kicker were done using the computer code MAFIA. The resonant structure of the RF kicker is shown in Figure 2 and represents a “lumped circuit” consisting of two parallel plates (capacitance) and four stems (inductors).

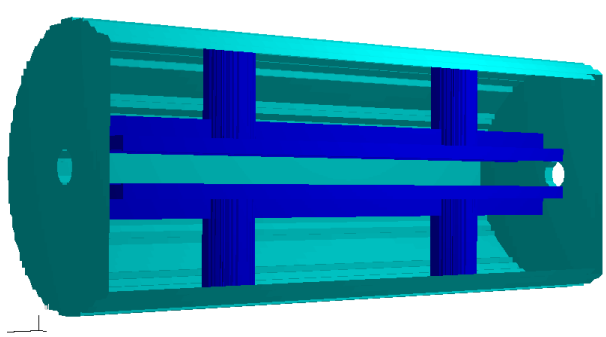

Figure 2: Three-dimensional view of the RF kicker.

The transverse electric field created between the plates deflects the beam in the direction perpendicular to the planes and parallel to the stems. Using two stems improves stiffness of the structure, simplifies cooling, and helps to equalize the longitudinal electric field

*Work was supported by the US DOE grant DE-FG02-04ER41324.
#gorelov@msu.edu

ESTIMATES OF ENERGY FLUENCE AT THE FOCAL PLANE IN BEAMS UNDERGOING NEUTRALIZED DRIFT COMPRESSION*

J. J. Barnard, LLNL, Livermore, CA 94550, USA, P. A. Seidl, J. E. Coleman, D. Ogata, LBNL, Berkeley, CA 94720, USA, D. R. Welch, Voss Scientific Corp., Albuquerque, NM, 87108, USA

Abstract

We estimate the energy fluence (energy per unit area) at the focal plane of a beam undergoing neutralized drift compression and neutralized solenoidal final focus, as is being carried out in the Neutralized Drift Compression Experiment (NDCX) at LBNL. In these experiments, in order to reach high beam intensity, the beam is compressed longitudinally by ramping the beam velocity (i.e. introducing a velocity tilt) over the course of the pulse, and the beam is transversely focused in a high field solenoid just before the target. To remove the effects of space charge, the beam drifts in a plasma. The tilt introduces chromatic aberrations, with different slices of the original beam having different radii at the focal plane. The fluence can be calculated by summing the contribution from the various slices. We develop analytic formulae for the energy fluence for beams that have current profiles that are initially constant in time. We compare with envelope and particle-in-cell calculations. The expressions derived are useful for predicting how the fluence scales with accelerator and beam parameters..

INTRODUCTION

Recently, experiments have been carried out on the Neutralized Drift Compression Experiment (NDCX) at Lawrence Berkeley National Laboratory to investigate the use of injected plasma into a final drift compression line, final focus magnet, and target chamber to eliminate the effects of space charge [1], which, in turn, allows for maximum longitudinal compression and transverse final focusing. These beams have short final pulse duration Δt_f and small focal spot radius r_{spot} (defined at $2^{1/2}$ times the rms radius, when averaged over all beam particles). Because of the possibility of creating high beam intensities in a short pulse, the beams are being used to generate so called warm dense matter (WDM) conditions [2,3]. The main figures of merit for experiments are the beam fluence (beam energy per unit area integrated over the pulse) E and Δt_f, since the attainable temperature is determined by E as long as Δt_f is much shorter than the hydrodynamic timescale for expansion. In this paper, we provide an analytic estimation of E which can be useful for designing experiments that maximize E.

In the following sections, we first describe a simplified model for a final drift and focus section. We then outline the derivation of the estimate and.compare with more detailed numerical calculations (envelope and particle in cell), and finally we describe how we have used these three approaches to help design experiments for NDCX at LBNL.

MODEL FOR ANALYTIC ESTIMATE

We assume that after the beam is accelerated to final velocity v_0, and energy qV_0 with charge state q, the beam exits the accelerator with 4 rms unnormalized transverse emittance ε. The beam passes through an induction bunching module gap that increases the velocity of the tail to v_t and decreases the velocity of the head to v_h. The "tilt" is defined as $\Delta \equiv (v_t - v_h)/v_0$. The beam drifts a distance L to the target, longitudinally compressing as it propagates, due to the tilt. A distance f from the target, when the beam has radius r_0 the beam enters a solenoid of strength B_{sol} and length l_{mag}, and exits the solenoid with the envelope converging angle r_1' and radius r_1, setting the beam onto a final trajectory that focuses onto the target with radius r_{spot}. . (Throughout this paper, envelope radii r, with or without subscripts, are defined as $2^{1/2}$ times the rms radius). A plasma is assumed to fill the drift section, the final solenoid and the target chamber (that includes the distance between the target and the solenoid). We further assume that the plasma density sufficiently exceeds the beam density so that the space charge forces within the beam are negligible. This implies that each slice of the beam retains the velocity $v \equiv v_0(1+\delta)$ it obtained in the bunching gap, and so each slice will have a slightly different focal length, and hence slightly larger focal spot at the target than the focal spot of the longitudinal center of the beam (δ=0). Although formal analytic solutions to the kinetic equations describing drift compression have been obtained [4], exact closed form-scaling relations for the fluence have not, as of yet, been derived.

ANALYTIC ESTIMATE OF FLUENCE *E*

The envelope equation for the beam radius r for a beam without space charge may be written: $r'' = -\frac{k_c^2}{4} r + \frac{\varepsilon^2}{r^3}$. Here $k_c = qB_{sol}/(mv)$, and prime is derivative with respect to longitudinal position z. Within the solenoid, the emitttance term is small relarive to the focusing term, so we may solve the envelope equation: $r_1 = r_0 \cos\frac{k_c z}{2} + \frac{2r_0'}{k_c}\sin\frac{k_c z}{2}$. We assume that $r_0'=0$, as the change in r' going through the solenoid is expected to be large. The condition that the beam comes to a focus at a distance after the magnet f-l_{mag} is: $r_1' = \left(r_0/\left(f - l_{mag}\right)\right)\cos k_c l_{mag}/2 = (k_c r_0/2)\sin k_c l_{mag}/2$. This may be expressed as: $\eta_{mag} = \theta\tan\theta/(1+\theta\tan\theta)$. Here $\eta_{mag} = l_{mag}/f$, and $\theta = k_c l_{mag}/2$. The contribution to the spot

UPGRADE OF THE UNILAC HIGH CURRENT INJECTOR RFQ

A. Kolomiets, S. Minaev, ITEP, Moscow, Russia
W. Barth #, L. Dahl, H. Vormann, S. Yaramyshev, GSI, Darmstadt, Germany

Abstract

For the operation of the GSI-accelerator chain as an injector for the future FAIR facility a considerable increase of the heavy ion beam intensity of up to a factor of 5 at the end of the UNILAC is required. The bottleneck of the whole UNILAC is the front-end system of the High Current Injector. It is shown that the transverse RFQ-acceptance can be significantly increased while the emittance growth can be reduced. Both goals are achieved with only a moderate change of the RFQ electrode geometry; the intervane voltage raised from 125 kV to 155 kV, but keeping the design limit of the maximum field at the electrode surface. The changed resonant frequency can be compensated with a relatively small correction of the carrying rings. The beam parameters in the final focusing elements of the LEBT were optimized together with the improved design of the input radial matcher; the length of the gentle buncher section was considerably increased to provide slow and smooth bunching resulting in a reduced influence of space charge forces. DYNAMION simulation with the modified electrode design resulted in an increase of the U^{4+}-beam current of up to 20 emA. It is planned to start the upgrade measure in spring 2009.

INTRODUCTION

In 1999 UNILAC passed a substantial upgrade - the Wideroe structure was replaced by the High Current Injector (HSI) [1]. The HSI consists of IH-type RFQ and two IH-DTL structures. The main goal of the upgrade project was to increase the U^{4+} beam current up to 15 emA. However the measured U^{4+} beam current behind the HSI never exceeded 6.5 mA. Detailed computer simulations using the DYNAMION code were performed to determine the source of beam intensity limitations [2]. The simulations were verified by beam parameters, measured during the whole period of HSI operation. The most important limitations were the following:

– lower brilliance of the injected beam in comparison with the design value;
– considerably mismatched beam at the RFQ-entrance due to the too high beam convergence required by original design;
– fast beam bunching in the RFQ gentle buncher section, leading to transverse emittance growth;
– strongly limited rf-voltage during the U^{4+} operation.

As a result, a partial RFQ upgrade program took place in 2004. It was mainly directed to the improvement of the rf-performance, but also included the new design of the input radial matcher (IRM), dedicated to optimize the beam dynamics in the focusing elements in front of the RFQ and to improve the matching itself [3].

The rf-performance of the HSI-RFQ was significantly improved after replacement of the electrodes. Minor changes in the IRM lead to 15% increase of the maximum beam intensity at the RFQ output (with the same beam, coming from the ion source). More than this, the results of the numerically calculated optimization of the RFQ electrode profile was confirmed and the beam dynamics codes were approved.

The FAIR program [4] requires increased beam intensities for the UNILAC as an injector. The HSI U^{4+} beam current has to be increased up to 18 mA. All previously obtained beam dynamics results confirmed that an essential RFQ electrode profile upgrade could provide for such requirements.

DESIGN OF THE HSI RFQ PROFILE

The main conditions for the new design are:

– maximum field at electrode surface should not exceed 320 kV/cm (existing design, U^{4+} -operation);
– total length of the electrodes must be exactly the same as in the existing design;
– operation frequency and other essential rf-parameters of the cavity must be kept, only minor adjustments of the resonant structure are acceptable.

It is clear, that an increase of the RFQ output beam current, keeping parameters of an injected beam, can be provided only by a corresponding increase of its transverse acceptance. The normalized transverse acceptance of the RFQ V_k can be expressed as:

$$V_k = \frac{1}{\lambda}\left(\frac{2}{m+1}\,\frac{R_0}{\rho_{\max}}\right)^2 \qquad (1)$$

with λ - wave length, m - modulation, R_0 - average distance from axis to electrode, ρ_{max} - maximum value of the normalized matched envelope. The value of ρ_{max} is defined mainly by the focusing parameter B, expressed through the maximum field at the electrode surface $E_{\max}$:

$$B = \frac{Ze}{A}\,\frac{1}{E_0}\,\frac{E_{\max}}{\chi R_0}\,\lambda^2 \qquad (2)$$

with χ - field enhancement factor, A,Z - mass and charge numbers, E_0 - rest energy. For flat electrodes with semicircular tips R_e it can be calculated by the formula

$$\chi = \sqrt{\frac{1}{2}\left(1+\frac{R_e}{R_0}\right)^2 + \frac{2T}{\pi}\,k\,R_0\,I_0\left(k\,\frac{R_0+R_e}{\sqrt{2}}\right)^2} \qquad (3)$$

with T - transit-time factor, $k = 2\pi/\beta\lambda$ - wave number, β - relative velocity of the particle, I_0 - modified Bessel function [5]. It follows from the expressions above, that the only way to keep the focusing parameter B constant,

Presenting author
W.Barth@gsi.de

THE NEW EBIS RFQ FOR BNL

M. Vossberg, J. Schmidt, B. Hofmann, A. Schempp, C. Zhang, IAP, Univ. Frankfurt, Germany
J. Alessi, D. Raparia, L. Snydstrup, BNL, Upton NY, U.S.A.

Abstract

A new RFQ is being built as a part of the new EBIS-Linac at BNL. The RFQ accepts highly charged ions from the EBIS ion source with energy of 17 keV/u and ion currents of up to 10 mA. The operation frequency will be 100.625 MHz. The design had been optimized to get a rather short structure with L_{RFQ} = 3.1 m with moderate electrode voltages of U_Q = 70 kV. The resonant insert has a cooled base plate and solid stems and vane-electrodes. The mechanical design is very stiff, with a precise base-structure. The top lid along the RFQ allows installation, alignment, inspection and maintenance.
After the mechanical alignment of the electrodes the longitudinal electrode voltage distribution will be adjusted with tuning plates between the stems. The properties of the RFQ, the results of the tuning and the status of the project will be discussed.

INTRODUCTION

Availability for beams for high energy heavy ion physics is limited by the properties and performance of the accelerator chain especially the low energy part, where beam intensities and emittances are set.

At RHIC the injector consists of a Tandem whose beam is transported to the AGS. The limitations of that injector, a combination of a dc, low beam current heavy ion machine, a long transport line with a typical pulsed proton high energy machine are obvious. Starting with negative ions, the mass range is also limited.

Plans for a new injector making use of the new developments of ion sources as well as rf-linacs have been discussed for a number of years. Now that modern injector scheme is being set up at BNL, which will lead to more reliable operation and improved capability especially for the RHIC and NSRL programs [1].

The EBIS ion source is perfectly matched to the operation pattern with its pulsed beam of highly charged ions. The RFQ accepts a low energy heavy ion beam, and bunches and accelerates it with high efficiency and low emittance growth [2]. The IH structure has been applied for heavy ion machines e.g. at GSI and CERN which have demonstrated operation with very high gradients resulting in a very efficient compact ion injector for a Synchrotron [3,4].

Figure 1 shows a layout of the new heavy ion injector linac with total length of appr. 12 m, which will provide ions with 2 MeV/u for a mass to charge ratio of up to A/q = 6.25.

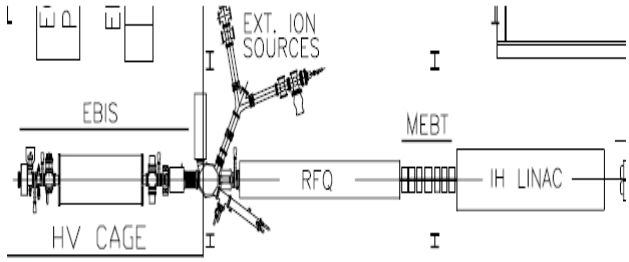

Figure 1: Layout of the EBIS Linac at BNL.

RFQ

The RFQ for the new EBIS-linac at BNL accepts highly charged ions from the EBIS ion source with energy of 17 keV/u and ion currents of up tp 10 mA. The operation frequency will be 100.625 MHz.

Beam Dynamics

The beam dynamics design does an adiabatic variation of the RFQ parameters to shape, bunch and accelerate the beam [5]. We optimized the design to get a rather short structure with L_{RFQ} = 3.1 m with moderate electrode voltage of U_Q = 70 kV.

Table 1: RFQ Beam Dynamics Design Parameters

Frequency	100.625 MHz
Input energy	17 keV/u
Output energy	0.3 MeV/u
Mass to charge ratio	6.25
Beam current	10 mA
Outp trans. emitt rms norm. 90%	< 0.38 π mm mrad
Output long. emittance 90%	< 220 deg keV/u
Transmission	98%
Electrode voltage	70 kV
RFQ length	3.1 m
Cell number	189
Aperture min - max	2.96-5.25 mm

Results of particle dynamics simulations show the RFQ output transmission and emittances for different beam input emittances and currents show low emittance growth and very high transmission also for I = 10 mA

*Work supported by the US Department of Energy and the National Aeronautic and Space Administration.

HEAVY ION RADIO-FREQUENCY QUADRUPOLE LINAC FOR VEC-RIB FACILITY

Siddhartha Dechoudhury, Vaishali Naik, Arup Bandyopadhyay, Manas Mondal, Hemendra Kumar Pandey, Tapatee Kundu Roy,Dirtha Sanyal, Debasis Bhowmick, Alok Chakrabarti

Variable Energy Cyclotron Centre,1/AF Bidhan Nagar, Kolkata 700 064, India

Abstract

Post acceleration of ion beams would be done in Radio Frequency Quadrupole (RFQ) LINAC for the upcoming Radioactive Ion Beam (RIB) facility at Variable Energy Cyclotron Centre (VECC), India. A 33.7 Mhz RFQ capable of accelerating stable as well as RI beams of q/A≥1/16 to about 30 keV/u has already been constructed and operational since September 2005. This has been installed in a dedicated beam line for doing material science experiments. Another 3.4 m long RFQ resonating at 37.8 Mhz and capable of accelerating heavy ion beams upto 98 keV/u have been fabricated which is to be installed in the beam-line for the VEC-RIB facility. The physical parameters, rf test along with the measurements of accelerated beams from RFQ would be presented.

DESIGN OF RFQ

We plan to accelerate beams with mass ranging up to A=150 in the VEC-RIB facility[1]. The radioactive atoms would be ionized in Electron Cyclotron resonance ion source(ECRIS) operating in "High B-mode". The ions would be then subsequently mass separated and accelerated in RFQ and Linac tanks[2]. ECRIS in principle would be able to deliver beams of around 15^{+} for uranium even in the on-line mode .Thus q/A≥ 1/14 seems to be a judicious choice for our RFQ. Normalized emmittance of ion beam has been taken to be 0.05 π cm mrad. Characteristic radius of 0.71 mm for the RFQ ensured a good transmission of the RI beams through the RFQ. The four-rod type structure have extended vanes supported on posts similar to the structure developed by Fujisawa[3]. The rods are placed at an angle of 45° with respect to conventional horizontal and vertical axes.

The beam dynamics simulation has been done using GENRFQ and PARMTEQ code. Optimization of different physical parameters was done keeping in mind the goal to achieve the desired acceleration with minimum vane length and maximum transmission efficiency. Initially the RFQ was decided to design for input beam of energy of 1keV/u and input bunch width of ±42° and final energy of 86 keV/u[4]. The RFQ was designed to resonate at frequency of 35 MHz. A half scale cold model was fabricated for RF measurements. The results show good agreement with the simulation using MAFIA. In the next stage we have designed and fabricated 33.7 MHz RFQ delivering beam of 29 keV/u to be installed in the dedicated beam line for material science experiments . As the first post accelerator, using the experience and expertise gathered with 33.7 MHz RFQ final 3.4 m RFQ accelerating RIB's to 98 keV/u have been fabricated.

33.7 MHz RFQ

Design Parameters

The RFQ is designed for an input dc beam of 1.38 keV/u, *q*/*A*=1/ 16, and resonant frequency of 33.7 MHz. The intervane voltage has been chosen to be 45.9 kV, which is about 1.12 times the Kilpatric limit for cw operation. With the interelectrode potential of 45.9 kV the calculated output energy comes out to be 29.06 keV/u for a vane length of 1.552 m. The radial matching section consists of 6 rf cells, and a total of 119 cells are needed to reach the energy. The synchronous phase in the acceleration section is chosen to be −30°. The calculated transmission efficiency is 95.8% for a beam current of 1 mA. The optimized physical parameters are shown in Fig.1. Energy width of the beam at the exit of RFQ is ± 0.67 keV/u.

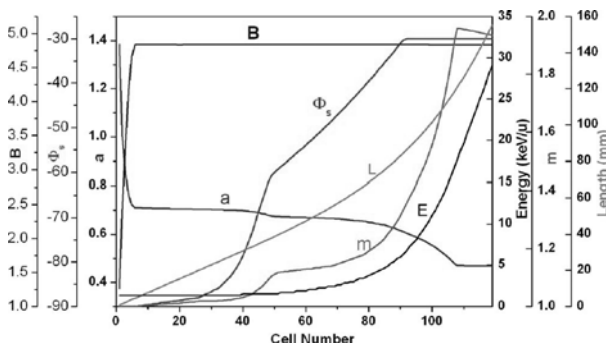

Figure 1: Optimised physical parameters variation along length of 33.7 MHz RFQ.

RF Analysis

MAFIA estimates resonant frequency, *Q*, and *Rp* values for the structure with unmodulated electrodes of the same characteristic radius to be 35 MHz, 9830, and 174 kΩ respectively. The measured resonating frequency is 33.7 MHz. The Q value measured using pick ups under 99% power reflection method is 5200.The tuning range of the tuner has been measured to be 100 KHz.

Beam Energy Measurement

Low energy beam transport line from ECRIS to RFQ consists of einzel lens,90°dipole for q/A selection and solenoid as matching element. The separation stage is designed for a dispersion of 1.84 cm. The ions are extracted from ECRIS at 1.38 keV/u. In the downstream

THE IFMIF-EVEDA RFQ: BEAM DYNAMICS DESIGN

M. Comunian, A. Pisent INFN/LNL, Legnaro (PD) Italy, E. Fagotti (Consorzio RFX, Padova)

Abstract

The IFMIF-EVEDA (Engineering Validation and Engineering Design Activities) project foresees the construction of a high intensity deuteron accelerator up to 9 MeV, with the characteristics required for the actual IFMIF facility. The linac will be installed in Rokkasho, and INFN is in charge of the construction of a 5 MeV, 125 mA, deuteron RFQ operating at 175 MHz. In this article the beam dynamics design of this challenging RFQ is described, namely the design, the main outcomes in terms of beam particles physics, and finally the study of mechanical and rf field error tolerances. The RFQ design method has been aimed to the optimization of the voltage and R0 law along the RFQ, the accurate tuning of the maximum surface field and the enlargement of the acceptance in the final part of the structure. As a result this RFQ is characterized by a length shorter than in all previous design, very low losses (especially at higher energy) and small RF power dissipation[1][2][3].

RFQ PARAMETERS AND DESIGN

The IFMIF EVEDA RFQ specification and the main design parameters are listed in Table 1.

Table 1: IFMIF RFQ Parameters

Particles	D+	
Frequency	175	MHz
Input Current	130	mA
RMS Input tr. emittance	0.25	N.mmmrad
Input/Output Energy	0.1/5	MeV
Max Surface Field (1.82 Kp)	25.6	MV/m
Length L	9.78	m (5.7 λ)
Voltage Min/Max	79/132	kV
Total Power with margins	1.6	MW
Mean aperture R_0(min/max)	4.1 / 7.1	mm
Trans. (WaterBag÷Gauss)*	99.1÷95.7	%
Power Loss(WaterBag÷Gauss)*	253÷1007	Watts
RMS Output Long. Emittance*	0.197	MeVdeg
RMS Output Tr. Emittance*	0.26	N.mmmrad

*Average of 10 Toutatis runs with 10^6 particles.

The design of such high current RFQ is very challenging due to the necessity to limit deuteron losses, keeping in particular extremely low the losses in the high energy part. The aim is to minimize the neutron production and the consequent activation of the RFQ structure.

Due to the high space charge effect at low energy. The value of input energy has been chosen of 0.1 MeV to maintain the value of maximum transverse current up to 200 mA until the end of Gentle Buncher;, this large margin guarantees small losses along the buncher formation process.

All the RFQ simulations here reported has been made by using the CEA code "Toutatis" [4].

Transverse Parameters Characterization

The IFMIF EVEDA RFQ beam dynamics study was aimed at minimizing beam losses at high energy, reducing the RFQ length and power consumption. The main parameters are plotted in fig. 1, the focusing force "B" at the beginning of RFQ is about 7, i.e. a very high value to compensate the high space charge force and keep the beam in a linear force fields. It is not possible to ramp the value of "B" in the shaper because we get a larger beam size and due to that same losses in the gentle buncher process. The normalized transverse acceptance of the RFQ in smooth approximation is defined by:

$$Acc = \frac{a^2\sigma_{T0}}{2\lambda}\sqrt{\left(1-\frac{B}{4\pi^2}\right)^3 \Big/ \left(1+\frac{B}{4\pi^2}\right)}$$

with λ the wavelength *a* small aperture,σ_{T0} phase advance at zero current and "B" the focusing factor expressed by:

$$B = \frac{qV}{mc^2}\frac{\lambda^2}{R_0^{\,2}} \quad and \quad \sigma^2_{T0} = \Delta_{RF} + \frac{B^2}{8\pi^2}$$

The variation of acceptance and "B" is therefore strictly connect to voltage and average aperture R_0 along the RFQ. For that reason a closed-form and continuous up to the 2nd derivative voltage law V(z) and R_0(z) was used.

$$V(z) = V_1 + (V_2 - V_1)\left(\frac{1}{2} + \frac{15}{8}\left(-\sin(\Delta z_{12}) - \frac{1}{3}\sin(3\Delta z_{12}) + \frac{1}{5}\sin(5\Delta z_{12})\right)\right)$$

$$R_0(z) = R_{01} + (R_{02} - R_{01})\left(\frac{1}{2} + \frac{15}{8}\left(-\sin(\Delta z_{34}) - \frac{1}{3}\sin(3\Delta z_{34}) + \frac{1}{5}\sin(5\Delta z_{34})\right)\right)$$

$$with \quad \Delta z_{12} = \frac{\pi}{6} - \frac{\pi(z-z_1)}{3(z_2-z_1)} \quad and \quad \Delta z_{34} = \frac{\pi}{6} - \frac{\pi(z-z_3)}{3(z_4-z_3)}$$

In this way it is possible to increase the voltage in a smooth way in the accelerator part and to have continuous variation of the phase advance per meter along the RFQ. The R0 and the voltage V are ramped after the Gentle Buncher, the V is increased for 4.4 meters instead the R0 are changed for 4.5 meters to reduce the surface fields and smoothing the phase advance change rate. The final value of the voltage V_2 is limited by the total available RF power, the final value of R0 allows to avoid the resonance $\sigma_T = \sigma_L$.

RF DESIGN OF THE IFMIF-EVEDA RFQ

F. Grespan, A. Palmieri, A. Pisent INFN/LNL, Legnaro (PD) Italy

Abstract

The RFQ of IFMIF-EVEDA project is characterized by very challenging specifications, with 125 mA of deuteron current accelerated up to 5 MeV. Upon beam dynamics studies, it has been chosen a law for the variation of R_0 and voltage along the structure; this law provides a significant reduction in terms of structure length, beam losses and rf power consumption. Starting from these outcomes, the rf study of the RFQ, aimed at determining the optimum design of the cavity shape, was performed. The stabilization issues were also addressed, through the analysis of the RFQ sensitivity to geometrical errors, by means of perturbative theory-based algorithms developed for this purpose . Moreover the determination of the main 3D details of the structure was also carried out. In this article the results of the rf studies concerning the above-mentioned topics are outlined.

RFQ PARAMETERS AND CAVITY DESIGN

The main RFQ parameters are listed in Table 1, and the 3D layout in Figure 1.

Table 1: IFMIF RFQ Input Design Parameters

Particles	D+	
Frequency	175	MHz
Input Current	130	mA
Energy (in-out)	0.1-5	MeV
Max Surface Field	25.2	MV/m (1.8 Kp)
Length L	9.78	m
Voltage min/max	79/132	kV
Mean aperture R_0	4.1 / 7.1	mm
Pole tip radius ρ	3.08/5.33	mm

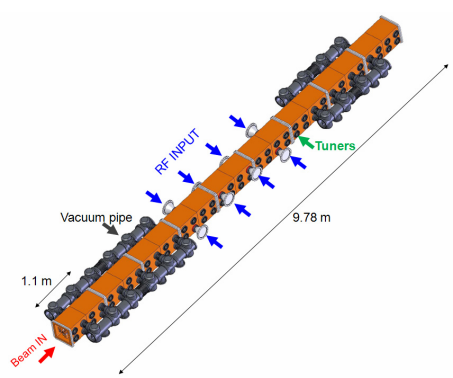

Figure 1: IFMIF RFQ schematic layout.

The IFMIF EVEDA RFQ beam dynamics study[1] was aimed at minimizing beam losses at high energy, reducing the RFQ length and power consumption. A closed-form and continuous up to the 2nd derivative voltage law V(z) was used. In this way it is possible to increase the voltage smoothly along the accelerator part and to have continuous cut-off frequency variations.

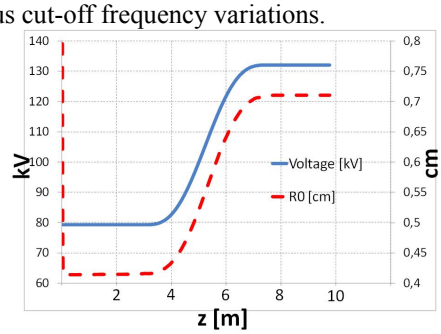

Figure 2: Mean aperture and voltage profile along the RFQ.

The goal of the cavity design was the optimization of the transverse section in order to match the local cut-off frequency with respect to local TE_{21} cut-off frequency f(z) variation due both to voltage and aperture variation, by varying the Vane Base Width 2·W1 along the RFQ with the usage of the RFQFISH routine. The minimum W value (1 cm) was chosen in order to allow cooling channel positioning and the maximum W1 value (1.5 cm) to avoid mechanical oscillations during machining. The upper flat surfaces H1 and H2 (9 cm) allow the positioning of tuners and RF couplers (Fig.3). Moreover the choice of the section was also dictated by the fact that a "square" shape of the RFQ cross-section allows, for a given frequency and R_0, a better volume/surface ratio and a subsequent Q improvement (about 10%) with respect to a "triangular" shape.

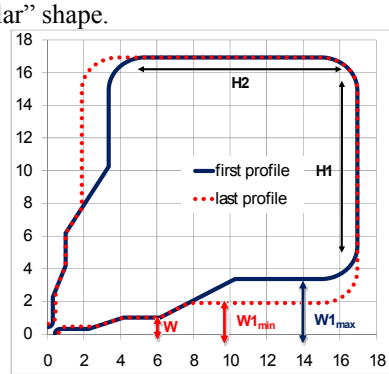

Figure 3: The variable shape of the RFQ section.

The main parameters obtained from the SUPERFISH optimization are summarized in Table 2.

FABRICATION AND TESTING OF TRASCO RFQ

E. Fagotti, Consorzio RFX, Padova, Italy and INFN/LNL, Legnaro, Padova, Italy
M. Comunian, A. Palmieri, A. Pisent, C. Roncolato, INFN/LNL, Legnaro, Padova, Italy
F. Grespan, Università degli studi di Milano, Milano, Italy and INFN/LNL, Legnaro, Padova, Italy
S. J. Mathot, CERN, Geneva, Switzerland.

Abstract

The Legnaro National Laboratory (LNL) is building the 30 mA, 5 MeV front end injector for the production of intense neutron fluxes for interdisciplinary application. This injector comprises a proton source, a low energy beam transport line (LEBT), a radio frequency quadrupole (RFQ) and a beam transport line designed to provide a 150 kW beam to the beryllium target used as neutron converter. The RFQ, developed within TRASCO project for ADS application, is designed to operate cw at 352.2 MHz. The structure is made of OFE copper and is fully brazed. The RFQ is built in 6 modules, each approximately 1.2 meter long. This paper covers the mechanical fabrication, the brazing results and acceptance tests for the various modules.

INTRODUCTION

The high intensity RFQ under construction at LNL, developed within TRASCO project[1] for ADS study, will be devoted to the application of Boron Neutron Capture Therapy (BNCT) for the treatment of skin melanoma[2]. The main RFQ nominal parameters are listed in Table 1.

Table 1: Main RFQ parameters

Parameter	Value	Unit
Energy In/Out	0.08/5	MeV
Frequency	352.2	MHz
Proton Current (CW)	30	mA
Emit. t. rms.n. in/out	0.20/0.21	mm-mrad
Emit. l. rms.	0.19	MeV-deg
RFQ length	7.13	m (8.4 λ)
Intervane Voltage	68	KV (1.8 Kilp.)
Transmission (Waterbag)	98.5	%
Q (70% of SF result)	7000	
Beam Loading	0.148	MW
RF Power dissipation	0.847	MW

The RFQ consists of three electromagnetic segments 2.4 meters long resonantly coupled via two coupling cells in order to reduce sensitivity to machining errors. Each module consists of two 1.2 meters long modules, which are the basic construction units.

In order to accelerate the 30 mA CW proton beam up to 5 MeV, the maximum amount of power expected to be delivered to the RFQ is about 995 kW (148 kW beam power + 847 kW dissipated power). The possibility of a ten percent voltage increase respect to the nominal is considered in the dissipated power value. The power is generated by one klystron and supplied to the RFQ by a WR2300 waveguide system. Due to the fact that each RF coupler is rated for a maximum of 140 kW[3], the RF power is split in eight ways via magic-Tee dividers. An artistic view of the integration of the RF distribution, vacuum system and support is presented in Fig.1.

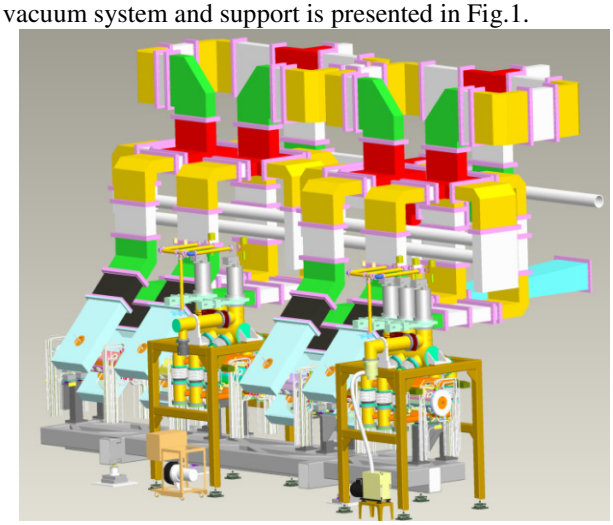

Figure 1: Integration of RFQ with ancillaries.

MECHANICAL FABRICATION AND BRAZING

Each module, built in OFE copper, is made of four main parts. The head flanges between modules and the rectangular vacuum flanges are made of SS (LN316). To reduce the number of brazing joints, the longitudinal cooling passages are deep-hole drilled from one side and closed with brazed plugs on the flat surfaces of the RFQ module (opposite to the coupling or end cells). Moreover, the vacuum grids with their cooling channels are directly machined on the copper bulk.

Two brazing steps occur. In the first the four main parts are brazed in horizontal position in a horizontal vacuum furnace, as well as the OFE plugs for the cooling channels. The brazing alloy is Ag68CuPd-807/810 (57.3% at., 38,4% at., 4.3% at.) and the brazing temperature is 815ºC. After first brazing, housings for the head flanges and the flat end surfaces (where the cooling channel plugs are located) are machined. In the second brazing cycle the head SS flanges, the inlet and outlet cooling water SS tubes, the SS supports for vacuum ports flanges and the SS flanges for couplers are brazed in vertical position in a vertical vacuum furnace. The

DESIGN OF A 2-BEAM TYPE IH-RFQ LINAC FOR HIGH INTENSE HEAVY ION BEAM ACCELERATIONS IN LOW ENERGY REGION

Takuya Ishibashi#, Noriyosu Hayashizaki, Toshiyuki Hattori,
Research Laboratory for Nuclear Research, Tokyo Institute of Technology, Tokyo, Japan

Abstract

For generating high intense ion beams from a linear accelerator (linac) stably, it is necessary to suppress the defocusing force between the charged particles. The defocusing force is extremely strong in low energy and high intense beams. Therefore, high intense ion beam acceleration in the low energy region is one of the most difficult conditions to achieve. One of the solutions is to suppress the defocusing force by dividing the high intense beam into several beams. Thus, a multibeam IH type Radio Frequency Quadrupole (IH-RFQ) linac has been proposed for the low energy and high intense beam acceleration. In particular, we have been developing a 2-beam type IH-RFQ cavity as a prototype of the multibeam type IH-RFQ.

INTRODUCTION

High intense ion beam acceleration in the low energy region is one of the most difficult conditions to achieve due to the space charge effect. As a solution for this problem, an idea has been proposed to divide a single, high intense beam into several beams, and merge these beams into a single high intense beam with higher energy. Toward this end, an accelerator technology for a heavy ion inertial confinement fusion driver has been studied [1-3].

There is a HIBLIC in Japan that serves as a conceptual design of the inertial confinement fusion reactor [1]. The design requires 16 RFQ linacs for the first acceleration stage because the maximum output current limit is estimated to be 35 mA in the conventional RFQ linac. In this case, a beam is accelerated in a cavity conventionally. Thus, if several beams can be accelerated in a cavity towards a cascade acceleration, this method would be better than the existing systems in terms of space and cost economy.

Therefore, multibeam type linacs, which consist of several beam channels in one cavity, have been studied. For instance, a multibeam type RFQ linac with an IH structure was proposed at GSI in Germany [4]. However, there have been no previous cases in which the actual machine was manufactured. Consequently, we have developed an IH-RFQ linac with two beam channels in one cavity as a prototype for the multibeam type linac.

DESIGN AND PARAMETERS

The external appearance of the 2-beam type IH-RFQ cavity is shown in Fig. 1, which consists of two sets of quadrupole electrodes. The RF electromagnetic field is stimulated by the TE_{111} mode as well as the IH cavity. The RFQ electric field is generated by four rods installed in each of the stems taking the polarity into consideration. We adopted a structure separated into three parts, a main frame and two semi cylinders, for ease in fabrication and modification of the electrodes.

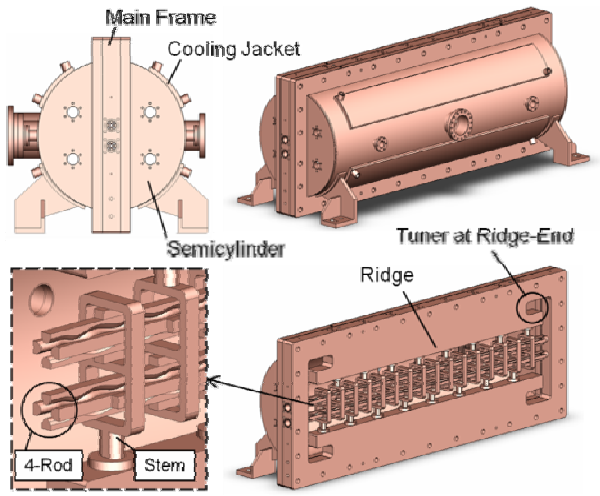

Figure 1: External appearance of the 2-beam type IH-RFQ.

The RFQ cavity can replace a resonance circuit equivalently, and the four gaps between the quadrupole electrodes in the RFQ are represented as the electrical capacitance in the resonance circuit. The resonance frequency is proportional to $(LC)^{-0.5}$. L and C are inductance and electrical capacitance in the cavity respectively. The electrical capacitance of the 2-beam type IH-RFQ cavity increases compared to the single beam type because the 2-beam type structure has two sets of quadrupole electrodes. This allows a comparatively low frequency to be achieved within a small cavity diameter. The cuts at the end of the ridge adjust the resonance frequency by changing the area of the magnetic flux surface and the inductance in the cavity.

Acceleration properties of the 2-beam type and the single beam type IH-RFQ linac were simulated [5]. The results demonstrated that the cavity diameter and length of the 2-beam type cavity are more compact than those of the single beam type cavity. The transmission of the 2-beam type cavity is 34% larger than that of the single beam type cavity, which has double the cross section of the beam channel in the 2-beam type. However, the beams from the multibeam type cavity need to be merged because the total emittance of the several output beams is too large for most applications to handle. There is a

ishibashi.t.aa@m.titech.ac.jp

THE RADIOFREQUENCY QUADRUPOLE ACCELERATOR FOR THE LINAC4

C. Rossi, P. Bourquin, J.-B. Lallement, A. M. Lombardi, S. Mathot, M. Timmins, G. Vandoni, M. Vretenar ,CERN, Geneva, Switzerland.
S. Cazaux, O. Delferriere, M. Desmons, R. Duperrier, A. France, D. Leboeuf, O. Piquet, CEA, Saclay, France.

Abstract

The first stage of acceleration in Linac4, the new 160 MeV CERN H^- injector, is a 352 MHz, 3-m long Radiofrequency Quadrupole (RFQ) Accelerator. The RFQ will capture a 70 mA, 45 keV beam from the RF source and accelerate it to 3 MeV, an energy suitable for chopping and injecting the beam in a conventional Drift Tube Linac. Although the RFQ will be initially operated at low duty cycle (0.1%), its design is compatible with higher duty cycle (10%) as the front-end for a possible high-intensity upgrade of the CERN linac facility.

The RFQ will be of brazed-copper construction and will be built and assembled at CERN. Beam dynamics design allows for a compact structure made of a single resonant unit. Field symmetry is ensured by fixed tuners placed along the structure. In this paper we present the RF and mechanical design, the beam dynamics and the sensitivity to fabrication and to RF errors.

INTRODUCTION

In Linac4 an RFQ is required to capture the beam extracted from the H^- ion source and accelerate it to an energy suitable for injection in the following DTL [1]. This energy must also be compatible with the operation of a chopper line, used to create a microstructure in the beam pulse. The initial Linac4 plans considered using the RFQ developed and built by CEA and IN2P3, for their IPHI project [2].

The possibility to adopt a lighter design, by reducing the injection energy and adopting a different acceleration profile, made CERN decide in 2007 to build a dedicated RFQ, which could profit from the tools and experience developed at CEA within the IPHI and SPIRAL2 projects, thus reducing the R&D cost and time. Besides, CERN has recently brazed the RFQ for the TRASCO project and therefore has contributed to the related mechanical design and gained access to this manufacturing experience [3].

BEAM DYNAMICS CONSIDERATIONS

The RFQ must initially be able to operate in Linac4 to fill the PS Booster, delivering beam pulses of 400 µs at 1.1 Hz, and, at a later stage, to fill a Superconducting Proton Linac (SPL) operated as LHC injector (1.2 ms, 2 Hz). In case a high intensity beam programme would be approved, the option is left open to operate with 400 µs, 50 Hz pulses. These different requirements represent an additional complication to the design. The specification parameters are listed in Table 1.

Table 1: Main Design Specification for the Linac4 RFQ, with rms Values of Emittance in the Two Planes

Linac4 RFQ Parameter	Min	Max	Units
Beam energy	3.0	3.0	MeV
Operating frequency	352.2		MHz
Peak beam current (pulse)	10	80	mA
RF duty cycle	0.08	7.5	%
Transverse emittance (in)	0.20	0.35	π mm mrad
Longitudinal emittance (out)	0.11	0.20	π deg MeV

The decision to designing a dedicated RFQ came after the chopper line elements had already been procured and assembly plans made. The output beam parameters of the new RFQ have to be similar to the IPHI ones or at least compatible with the existing chopper line. Other constraints on the design are the requirement to limit the RF power to 0.8 MW peak, corresponding to a single LEP klystron with a sufficient safety margin, and to keep the RFQ length around 3 m. This allows dividing the RFQ into 3 segments of 1 meter while keeping the overall length at 3.5 λ, thus allowing the direct coupling of the three RFQ sections without using coupling cells between sections.

The results of the redesign is a compact RFQ (3 m vs 6 m of IPHI) with an intra-vane voltage of 78 kV and a peak surface field of 34 MV/m (1.84 times the Kilpatrick limit). The main design parameters are shown in Figure 1.

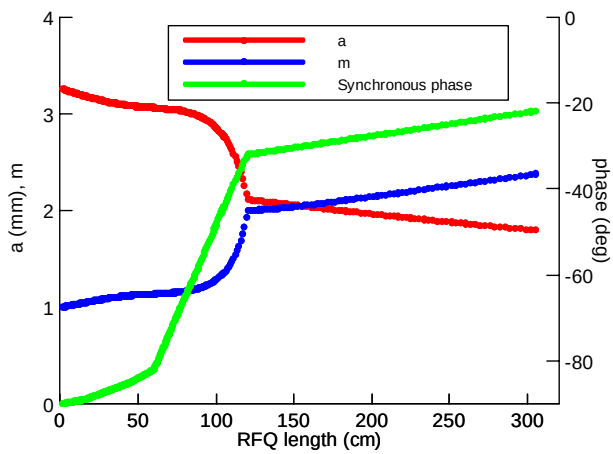

Figure 1: Graph of the synchronous phase, with the RFQ aperture a and modulation parameter m.

The considerable reduction in length was made possible by the lower injection energy, a higher focusing factor and a compromise on the current limit (80 mA vs. 100 mA). The beam quality for the nominal current is equivalent to that of the 6 m long IPHI RFQ. The value for the peak

THE FABRICATION AND INITIAL TESTING OF THE HINS RFQ*

G.Romanov#, G.Apollinari, B.Hanna, T.Khabiboulline, A.Lunin, A.Moretti T.Page, J.Steimel, R.Webber, D.Wildman, Fermilab, Batavia, IL 60510, USA
P.Ostroumov, ANL, Argonne, IL 60439, USA

Abstract

Fermilab is designing and building the HINS front-end test facility. The HINS proton linear accelerator consists of a normal-conducting and a superconducting section. The normal-conducting (warm) section is composed of an ion source, a 2.5 MeV radio frequency quadrupole (RFQ), a medium energy beam transport, and 16 normal-conducting crossbar H-type cavities that accelerate the beam to 10 MeV. Production of 325MHz 4-vane RFQ is recently completed. This paper presents the design concepts for this RFQ, the mechanical design and tuning results. Issues that arose during manufacturing of the RFQ will be discussed and specific corrective modifications will be explained. The preliminary results of initial testing of RFQ at the test facility will be presented and comparisons with the former simulations will also be discussed.

INTRODUCTION

Within the framework of the High Intensity Neutrino Source (HINS) program at FNAL, we plan to build and operate a portion of the Front End (up to energies of 90 MeV) as a technical feasibility proof of the proposal. A detailed description of the project and the current status is given in [1]. In the Front End test stand a four vane 325 MHz Radio Frequency Quadrupole (RFQ) will be used for bunching the beam and accelerating it from 50 keV to 2.5 MeV.

The technical specifications for the RFQ were developed by ANL/FNAL collaboration and are presented in Table 1.

Table 1. Initial Specifications for the RFQ Design

Input energy	50 keV
Output energy	2.5 MeV
Frequency, MHz	325
Accelerating beam current, mA	40
Peak surface field, kV/cm	<330
Acceleration efficiency,%	>95
Pulsed power losses in copper, kW	<450
Duty factor, %	1
Total length of vanes	302.428 cm
Average bore radius	3.4 mm
Input rms transverse emittance, normalized π mm mrad	0.25
Transverse emittance growth factor	<1.1
Longitudinal rms emittance, π keV deg	<150
Separation between operating and nearest dipole modes	>4 MHz

*This work was supported by the U.S. Department of Energy under contract number DE-AC02-76CH03000.
#gromanov@fnal.gov.

In this collaborative effort ANL was responsible for complete beam dynamic design resulting in a vane tip modulation table for machining. RF design with computational support from FNAL, mechanical design and manufacturing, preliminary tuning were delivered by AccSys Technology, Inc. Serious issues arose during manufacturing of the RFQ that prevented proper preliminary tuning. Intensive study has been undertaken to address the problem and specific corrective modifications have been done. Final RF measurements and testing of recently arrived RFQ have been performed by FNAL. The preliminary results of initial testing of RFQ at the test facility are presented.

DESIGN FEATURES

Similar to many other linear accelerators, the HINS proton accelerator requires an RFQ for initial acceleration and formation of the bunched beam structure. The HINS RFQ will operate at 325 MHz. The initially projected acceleration of ~40 mA pulsed current is considered a relatively moderate problem in the physics design of the RFQ. The design of the RFQ, MEBT and whole proton accelerator lattice has been iterated several times to satisfy more advanced RFQ beam specifications. Particularly, the longitudinal phase space beam emittance must be halo free to avoid excessive beam loss in the high energy section of the accelerator. As a part of this approach, axial-symmetric beam was requested at the RFQ output.

For RFQs longer than ~3l rf wavelengths, it is difficult to stabilize the operating field and damp field errors. To address this problem, modern RFQ designs include p-mode stabilizing loops (PISLs) [2]. PISLs complicate the resonator design and increase its cost; therefore we proposed to minimize the length of the RFQ resonator to allow using the end-wall dipole mode tuners for field

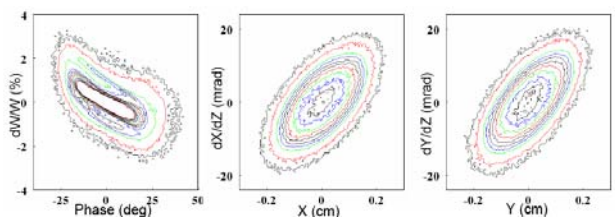

Figure 1: Phase space plots of accelerated beam. The outmost isoline contains 100%, the next one contains 99%.

stabilization that were successfully applied to several RFQs.

For the beam dynamics design, the RFQ is divided into three main sections: an input radial matcher, a main modulated vane section where bunching and acceleration

COMPLETE RF DESIGN OF THE HINS RFQ WITH CST MWS AND HFSS*

G. Romanov #, A.Lunin, Fermilab, Batavia, IL 60510, USA.

Abstract

Similar to many other linear accelerators, the High Intensity Neutron Source requires an RFQ for initial acceleration and formation of the bunched beam structure. The RFQ design includes two main tasks: a) the beam dynamics design resulting in a vane tip modulation table for machining and b) the resonator electromagnetic design resulting in the final dimensions of the resonator. The focus of this paper is on the second task. We report complete and detailed RF modeling on the HINS RFQ resonator using simulating codes CST Microwave Studio (MWS) and Ansoft High Frequency Structure Simulator (HFSS). All details of the resonator such as input and output radial matchers, the end cut-backs etc have been precisely determined. Finally in the first time a full size RFQ model with modulated vane tips and all tuners installed has been built, and a complete simulation of RFQ tuning has been performed. Comparison of the simulation results with experimental measurements demonstrated excellent agreement.

INTRODUCTION

Within the framework of the High Intensity Neutrino Source (HINS) program at FNAL, we plan to build and operate a portion of the Front End (up to energy of 62 MeV) as a technical feasibility proof of the proposal. A detailed description of the project and the current status is given in [1]. In the Front End test stand a four vane 325 MHz Radio Frequency Quadrupole (RFQ) will be used for bunching the beam and accelerating it from 50 keV to 2.5 MeV.

The complete beam dynamics design, resulted in a vane tip modulation table for machining, is described in [2]. The mechanical design concepts for this RFQ, tuning results, manufacturing of the RFQ in industry and the preliminary results of initial testing of RFQ at the Front End test stand are discussed in [3].

The electromagnetic design of RFQ resonators is rather complicated and requires essentially three-dimensional modeling. That, and also an additional complication with RF tuning because of some blunder made in the mechanical design of RFQ, urged us to develop a full length 3D RFQ model for simulation. Modern three-dimensional electromagnetic codes are now available and successfully used for RFQ design [4, 5, and 6]. This paper focuses exclusively on the computational technique of electromagnetic design. We report complete and detailed RF modeling on the HINS RFQ resonator using simulating codes CST Microwave Studio (MWS) and Ansoft High Frequency Structure Simulator (HFSS).

*This work was supported by the U.S. Department of Energy under contract number DE-AC02-76CH03000.

#gromanov@fnal.gov.

RFQ MODEL FOR ELECTROMAGNETIC SIMULATION

The basic parameters of the RFQ are given in table 1.

Table 1

Input energy	50 keV
Output energy	2.5 MeV
Frequency	325 MHz
Total length of vanes	302.428 cm
Average bore radius	3.4 mm

The RFQ design has several features that have been taken into account during electromagnetic simulations.

Instead of π-mode stabilizing loops (PISLs) usual for RFQs longer than ~3λ, where λ is the rf wavelength [7], FNAL's RFQ design uses the end-wall tuners - field stabilizers simpler than PISLs [8]. This method requires a precise knowledge of dipole mode spectrum, so simulating full length RFQ with end-wall tuners installed was needed.

Modulation of the vanes in the regular accelerating section of the RFQ is shown in Fig. 1. A variable modulation changes capacitive loading and therefore local frequency along RFQ as also reported elsewhere [4, 9, and 10]. In our RFQ the local frequency variation due to the modulation is significant, so the vane tip modulation has been included in the model.

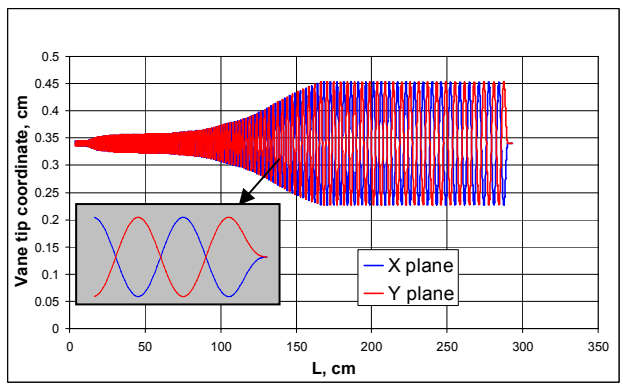

Figure 1: Vane tip modulation along RFQ. Radial matchers are excluded.

The output radial matcher is designed to form axially symmetric beam exiting the RFQ, and because of this special function it is different than the input radial matcher. Fig. 2 shows profile of the output radial matcher and imposed profile of the input matcher to compare with. The RFQ ends (cutbacks) can be tuned in simulations individually, but their combined effect on field flatness must be evaluated. Besides the end-wall tuners have

SIMULATION OF MULTIPACTING IN HINS ACCELERATING STRUCTURES WITH CST PARTICLE STUDIO*

G. Romanov #, Fermilab, Batavia, IL 60510

Abstract

Recently high power tests of the room temperature cross-bar H-type resonators (CH resonators) and high gradient tests of a superconducting single spoke resonator (SSR) have been performed under the High Intensity Neutrino Source (HINS) project at Fermilab. The resonators have shown a tendency of having multipacting at various levels of input power and therefore longer processing time. To provide insights for the problem, detailed numerical simulations of multipacting for these resonators have become necessary. New generation of accelerating structures like superconducting spoke resonators and room temperature CH resonators need a full 3D treatment. Simulations and study of multipacting in the resonators have been carried out using CST Particle Studio. The problematic regions and power levels have been identified for both types of resonators. This presentation will give the result of simulations and comparison with experimental data.

INTRODUCTION

Within the framework of the High Intensity Neutrino Source (HINS) program, we plan to build and operate a portion of the Front End (up to energy of 62 MeV) as a technical feasibility proof of the proposal. A detailed description of the project and the current status is given in [1]. The Front End of HINS, operating at 325 MHz, uses a mixture of warm copper structures and superconducting spoke resonators. After a standard RFQ [2], room-temperature crossbar H-type resonators are used to accelerate the beam from 2.5 to 10 MeV [3]. The use of short normal conducting resonators up to ~10 MeV reduces the number of different types of SC cavities and provides adiabatic beam matching. Three types of superconducting spoke resonators are used to accelerate protons from 10 MeV to 400 MeV [4].

Recently high power tests of the room temperature cross-bar H-type resonators (CH resonators) and high gradient tests of a superconducting single spoke resonator (SSR) have been performed [5,6]. The resonators have shown a tendency of having multipacting at various levels of input power and therefore longer processing time. To provide insights for the problem, detailed numerical simulations of multipacting for these resonators have become necessary. Simulations and study of multipacting in the resonators have been carried out using CST Particle Studio. Since CST PS is probably the first commercial code that can simulate realistic electron multiplication, the result of study is useful also as the code benchmarking.

*This work was supported by the U.S. Department of Energy under contract number DE-AC02-76CH03000.

#gromanov@fnal.gov.

MODEL PREPARATION

A general approach for mulipacting simulation was developed a while ago and it can be mapped to the three steps. These steps are performed in every case, with variations in execution, strategies for detailed implementation and numerical methods. The first step is the definition of the geometry and the calculation of the RF and static fields in this geometry. In a second step, a motion of large number of particles is tracked in the structure. And in a third and final step a multipacting behavior in the collection of particle tracking data is identified [7]. In CST PS, all three steps are smoothly integrated in one code.

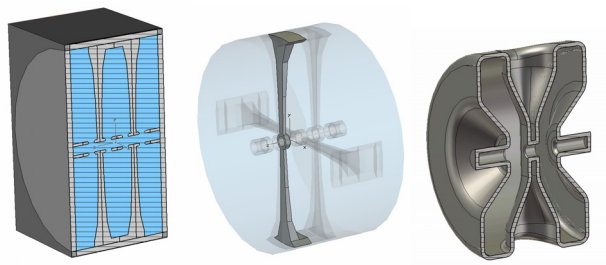

Figure 1: RT CH model consisting of background PEC, cavity components and vacuum filling is on the left. In the center a separate half of spoke is shown. Model of single spoke superconducting cavity SSR is on the right.

RF design for all HINS cavities was done with CST MicroWave Studio. The standard “vacuum” solid models from MWS can not be used “as is” in PS and additional manipulations are needed. First of all, the models before importing into PS from MWS had to be converted to more realistic models with metal walls (or developed from scratch). This is because the secondary emission properties in PS can be assigned to metal surface only, and PS does not recognize Perfect Electric Conductor background as a metal surface. Besides creating a model with metallic walls it is recommended to fill it with vacuum and make background of PEC as shown in Fig.1. This eliminates parasitic mode simulation outside a cavity. Usually several locations are suspicious as MP ones, so it is useful to build a cavity model consisting of separate parts and provide them with independent initial particle sources. It helps to evaluate MP on different surfaces independently.

The prepared models were imported first into MWS for field calculations (it is preferable because MWS has more

STATUS OF DPIS DEVELOPMENT IN BNL*

M. Okamura**, BNL, Upton, NY 11973, U.S.A.
J. Tamura**, Tokyo Inst. Tech, Meguro, Tokyo, 152-8550, Japan
T. Kanesue**, Kyushu University, Ito, Fukuoka, Ito, 819-0395, Japan
**RIKEN, Saitama, 351-0198, Japan

Abstract

Direct injection scheme was proposed in 2000 at RIKEN in Japan. The first beam test was done at Tokyo Institute of Technology using a CO_2 laser and an 80 MHz 4 vane RFQ in 2001, and further development continued in RIKEN. In 2006, all the experimental equipments were moved to BNL and a new development program was started. We report on our recent activities at BNL including the use of a frozen gas target for the laser source, low charge state ion beam production and a newly developed laser irradiation system.

INTRODUCTION

A laser ion source (LIS) is a leading candidate of heavy ion sources for providing intense highly charged beams for high-energy accelerators. The laser power can be deposited within a tiny area of the target material's surface and the evaporation process starts. Successively the evaporated gas absorbs the laser power and becomes plasma. Since the large laser power goes into a very limited volume, huge amount of the highly charged ions are produced. An emission from a table top small laser easily produce more than10^{12} W/cm^2 on a target surface and the total induced current reaches more than a few hundred A.

We have studied LIS since 2000. We proposed direct plasma injection scheme which enables high current heavy ion beam acceleration. More than 60 mA of carbon [1] and aluminum beam accelerations by an RFQ were demonstrated. We have also examined several laser systems and many targets species [2]. Using the measured plasma data, almost any desired species can be used for the LIS except helium gas.

In 2006, our group moved from RIKEN, Japan to BNL, USA with all the experimental equipments and we started a new development program in BNL. In this report, we briefly introduce our current activities related LIS and DPIS.

LASER EMISSION CONTROL

The laser emission control is important to gain good ion beam stability. We are currently using a tabletop Nd-YAG laser system, Thales-SAGA 230/10. When we started to use this laser, we were suffered by laser leakages. The laser consists of two laser cavities, a master oscillator and a power amplifier, and a Q-switch is installed at the oscillator to make a short pulse. The Q-switch controls a polarization and adjusts laser-firing timing. The laser media is pumped by flash lamps. A typical emission of the flash lamps is indicated as red curve in Fig. 1. The flash lamp emission lasts more than 200 μs and the Q-switch selects certain timing for releasing the pumped energy to maximize laser emission power.

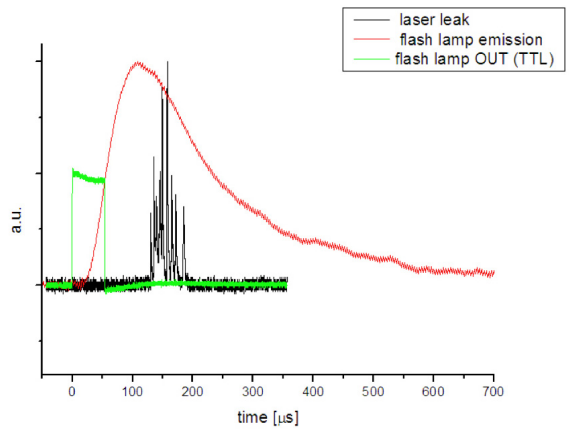

Figure 1: Flash lamp timing and laser leakage.

The laser emission pulse width is typically 6 ~ 9 ns. The flash lamps are always operated at 10 Hz for good stability and the laser emission is only controlled by the Q-switch. While the Q-switch is off position, the laser should not be emitted. However even Q-switch is turned off, very week laser emission exists. This leakage could not be sensed by a power meter. We observed the leakage by directly seeing the light from the plasma using an IR viewer. The leaking laser energy is very small but is enough to make plasmas and can damage the surface of the target since the leaked energy is concentrated onto a pinpoint by a focusing mirror. To avoid the pre-damage of the target due to the laser leakage, we installed a fast mechanical shutter in the laser path to the ion source. The shutter closes or opens within several ms and this speed is adequate to choose any desired laser pulses because the flash lamps are blinking at 10 Hz. So that the laser shots caused only by the Q-switch are transported to the ion source. Un-desired laser leakages from the un-fired blinking of the flash lamps are blocked. The ion beam stability was dramatically improved. However the laser shutter is not enough to eliminate the negative effects completely. Again in Fig. 1, you see the black plot which shows the time structure of the laser leakage when the Q-switch closed. The leakage still exists even in the same fired laser pulse. The Q-witch timing is usually selected to maximize the laser emitting power and typically around 180 μs behind the flash lamp control signal triggered.

*Work supported by U.S. DOE and RIKEN

DESIGN STUDY OF A DPIS INJECTOR FOR A HEAVY ION FFAG *

M. Okamura#, D. Raparia, BNL, Upton, NY 11973, U.S.A.
K. Ishibashi, Y. Yonemura, T. Kanesue, Kyushu University, Ito, Fukuoka 819-0395, Japan

Abstract

A new heavy ion injector linac is proposed for providing heavy ion beams to a fixed field alternating gradient (FFAG) accelerator in Kyushu University. A combination of the new intense laser source based injector and the FFAG will be able to accelerate high current ion beams with 100 Hz of a repetition rate. The planned average current reaches 7 μA with carbon 6+ beam.

A NEW INTENSE PULSED ACCELERATOR

To obtain large beam power within a limited space, cyclotrons have been chosen since they provide CW beams even with relatively small peak beam current. In this report, we propose a new approach to utilize comparatively large beam power using a laser ion source and a FFAG synchrotron accelerator.

Generally a synchrotron can have larger peak current than cyclotron has, however most of the time is occupied for ramping up and down the bending magnets in the operation and the beam pulse width is very limited. To increase the total beam power, it is effective to have high repetition rate. The maximum repetition rate is about 1 to 25 Hz for normal conducting synchrotrons [1]. Recently FFAG accelerators are being focused as high repetition synchrotrons and some FFAGs have already been built by KEK and Kyoto University groups both lead by Y. Mori [2]. It has been proved to operate it at 100 Hz in KEK and possibly it will run at 1 KHz. Also FFAG has large transverse acceptance and is expected to deliver large current.

A laser ion source (LIS) has an advantage to induce a powerful pulsed beam and can operate at high repetition rate which is restricted by a driver laser system. A typical flash lamp pumped solid laser can reach 100 Hz and a LED pumped laser easily achieves above 1 kHz operation with good stability. Hence both a laser source and a FFAG are operational at same high frequency range. Since a LIS can provide large current, beam losses in a transport line which connects from the ion source to a first stage accelerator, typically RFQ, was always tough issue. To overcome this difficulty caused by space charge effect, direct plasma injection scheme (DPIS) has been studied. Using the DPIS, several tens of mA heavy ion beams have been accelerated effortlessly in an RFQ [3]. A rapid cycle LIS with DPIS and a high current heavy ion RFQ suit a FFAG well to boost the beam power.

In Kyushu University, a new facility called “Center for accelerator and beam applied science” is established [4]. A new building was already constructed to accommodate a FFAG accelerator which was originally designed and constructed in KEK as a prototype 150 MeV FFAG. The installation of the FFAG to the new building is in progress. A small proton cyclotron will be used as an injector in the first stage and in the next stage we plan to install a new injector system to provide heavy ions for various application including medical, engineering studies and educational activities. A photo of the FFAG and its design parameters are shown in Fig. 1 and Table 1.

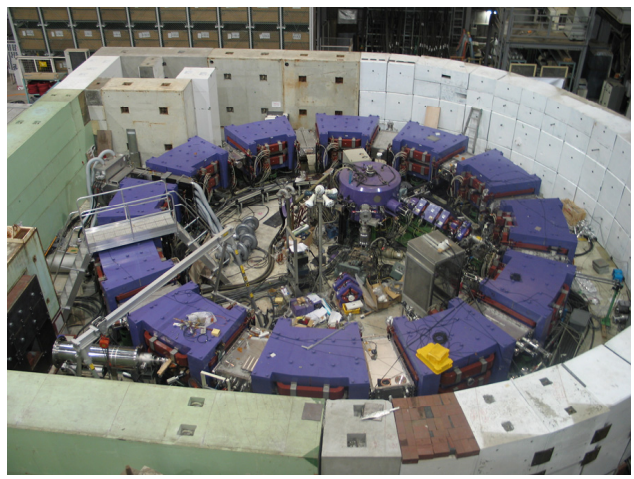

Figure 1: 150 MeV FFAG in KEK.

Table 1: Design Parameters of 150 MeV FFAG

Energy	10 – 125 MeV (proton) 2.5 – 31 MeV/u (C^{6+})
Type of magnet	Triplet radial (DFD)
Number of cell	12
Average radius	4.47 – 5.20 m
Magnetic field	Focus: 1.63 T Defocus: 0.78 T
Revolution Frequency	1.5 – 4.2 MHz (proton) 0.78 – 2.3 MHz (C^{6+})
Repetition rate	100 Hz (2 RF cavities)

The proposed heavy ion injector will accelerate fully stripped ion beams up to 2.5 MeV/u with the highest available current which will be induced by a conventional table top laser system with the DPIS.

LASER ION SOURCE

Beam Pulse Width

The harmonic number of the FFAG ring is one and revolution period at the injection energy is 1.28 μs. With single turn injection scenario, the required beam pulse

*Work supported by U. S. DOE
#okamura@bnl.gov

COMMISSIONING OF THE NEW GSI-CHARGE STATE SEPARATOR SYSTEM FOR HIGH CURRENT HEAVY ION BEAMS

W. Barth, L. Dahl, L. Groening, P. Gerhard, S. Mickat, M. Kaiser
Gesellschaft für Schwerionenforschung, D-64291 Darmstadt, Germany

Abstract

A dedicated charge separator system has been installed in the transfer line to the GSI synchrotron SIS18, replacing charge separation with a single 11 degree dipole magnet after a 25 m beam transport section. This was not adequate to meet the requirements during high current operation for FAIR: it only allows for charge state separation of low intensity and low emittance beams. With the new compact charge separator system emittance blow up and undesired beam losses for high intensity beam operation will be avoided. Additionally, a new beam diagnostics test bench is integrated to measure beam parameters (ion current, beam profile, beam position, transversal emittance, bunch structure and beam energy) for the injection into the SIS 18 in parallel to the routine operation in the transfer line. Results of commissioning with high intensity argon beams as well as with an uranium beam will be reported. We acknowledge the support of the EU-Research Infrastructure Activity under the FP6 "Construction of infrastructure for the FAIR-project" (co.-number 515876).

INTRODUCTION

In the transfer line (TK) to the GSI synchrotron SIS 18 the beam is stripped to higher charge states in a carbon foil, if high final energies from the SIS 18 are required. The TK is operated at 3 Hz pulse to pulse mode at maximum, with beams of different ion species and intensities, with or without stripping. A high current U^{28+}-beam of 15 emA (FAIR requirement) has a power of 1.5 MW (≤300µs pulse length). After stripping, undesired charge states with 85 % of the beam power must be separated and dumped. A newly developed stripper foil (with enlarged width) is loaded with 3 % of the beam power. To avoid evaporation in a single beam pulse, the beam is rapidly swept over its width of 55 mm. The UNILAC delivers beam emittances in the range of 5 to 20 µm, depending on the beam current. Emittance growth in the TK is caused by small angle scattering in the stripper foil, and by space charge forces, mainly in the section between the stripper and the charge separator (see Fig. 1). To minimize emittance growth, a narrow, vertically elongated beam spot (4 mm · 20 mm) is prepared, and the distance to the separator is kept as short as possible. [1]

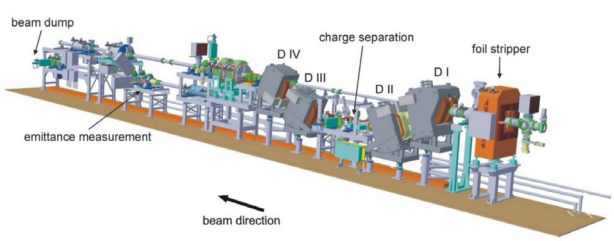

Figure 1: New charge state separator system integrated in the TK comprising the foil stripper, the four 35°-Dipole magnets (DI - DIV), and a beam diagnostics bench.

THE NEW CHARGE STATE SEPARATOR SETUP

The vertical magnetic bending system of the new charge state separator system consists of four 1.6 T-dipole magnets providing high resolution and a field homogeneity ≥ 99.97 %. Each of the four 35° H-type dipole magnets (D I - D IV) has a bending radius of 1.1 m. The first two dipoles have the same vertical and horizontal aperture, as well as D III and D IV. Rogowski profiles at the beam entrance and the beam exit assure independence of the magnetic flux density (up to 1.6 T) from the effective magnetic length. The gyration number of each coil is chosen to make use of three equal power supplies (650 A/380 V); the last two dipole magnets (with reduced gap height) are operated in a serial mode. All coils are equipped with correction coils to compensate remaining fields. [2] With a beam diagnostic bench behind D III high current beam measurements are accomplished to prepare for the injection of high intensity heavy ion beams into the synchrotron. Besides ion current the beam profile and position, the emittance, the beam energy and the bunch structure can be measured. Additionally, beam focusing using a quadrupole duplet and the correction of beam positions is provided in the 12 m diagnostic line. [3]

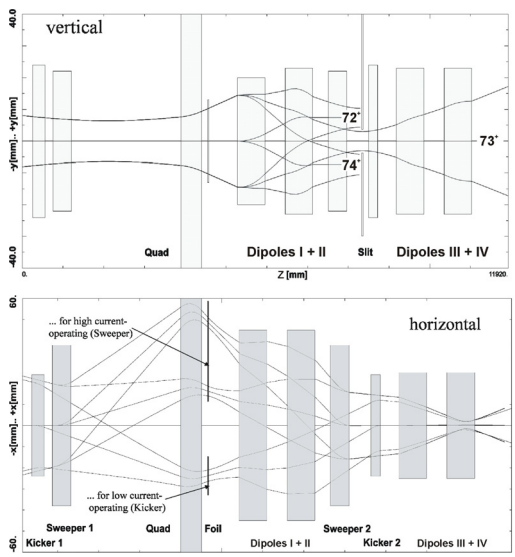

Figure 2: Beam dynamics layout of the new charge state separator system.

QUADRUPOLE MAGNET DEVELOPMENT FOR 132 MEV DTL OF CSNS

Yi Cheng, Xuejun Yin, Zhirui Sun, Keyun Gong, Shinian Fu
[1]IHEP, Institute of High Energy Physics, Chinese Academy of Sciences, Beijing 100049, China

Abstract

In the China Spallation Neutron Source (CSNS) linac, a conventional 324 MHz drift-tube linac (DTL) accelerating an H- ion beam from 3 MeV to 132 MeV has been designed with 1.05% duty, consisting of 7 tanks with a total length of approximately 59.6 m. Currently, R&D work has focused on the first module of Tank 1, which will have 29 drift-tubes (DT) each housing an electro-magnet quadrupole (EMQ). Some EMQs with SAKAE coil have been fabricated and are under rigorous magnetic measurements by means of Hall probe (HP), single stretched wire (SSW), rotating coil (RC) in order to verify the design specifications and fabrication technology. Magnetic measurements on the EMQs with iron cores made from the electrical-discharge machining (EDM) and the stacking method will be compared and discussed. Work has been implemented to reduce the alignment discrepancies between the geometric center of the DT and magnetic center of EMQ to within +/- 50 μm.

INTRODUCTION

Currently, a prototype cavity of the 1st module of Tank 1, of the 132MeV drift tube linac (DTL) for the proton linear accelerator for the CSNS has been constructed. A frequency of 324 MHz and a duty factor of 1.05% have been chosen for the RF structures. The design of the DTL was presented in reference [1]. Alongside with the construction of the DTL RF cavity, R&D work has also focused on the drift-tubes (DT) and the electro-magnet quadrupoles (EMQ). Presently, six EMQs with J-PARC type SAKAE coils [2] have been fabricated and are under rigorous magnetic measurements that includes the Hall probe (HP), single stretched wire (SSW) and rotating coil (RC) measurements, to verify the EMQ design specifications and fabrication technology and capabilities in the Institute of High Energy Physics (IHEP), Beijing. The design parameters for the EMQs and DTL Tank-1 are listed in Table 1.

Table 1: Design Parameters for EMQ and DTL Tank-1

EMQ		Tank 1 of DTL	
Parameter name	Parameter values	Parameter name	Parameter values
Beam aperture[mm]	15	Output energy [MeV]	21.76
Core outer diameter[mm]	59	Length [m]	7.99
Core length[mm]	35	Number of DTs	61
Magnetic field gradient[T/m]	75	RF power for each cell[MW]	1.41
Magnetic field effective length[mm]	40.96	Total RF power[MW]	1.97
Maximum excitation current[A]	530	Accelerating field strength[MV/m]	2.2-3.1
Field integral, *GL*[T]	3.07		
Coil resistance [mΩ]	9.08		

THE ELECTRO-MAGNET QUADRUPOLES (EMQ)

The six EMQ-magnets constructed consists of 3 EMQs with their iron cores made using the Stamped-Stacking Method (SSM), and 3 EMQs with their iron cores made using the Electrical Discharge Machining (EDM). DQ1#DW is the only EMQ that has its water gasket installed as shown in Figure 1.The results of the magnetic measurements for both EDM-made and SSM-made iron core EMQs will be presented, in order to illustrate their magnetic parameters' similarities and differences.

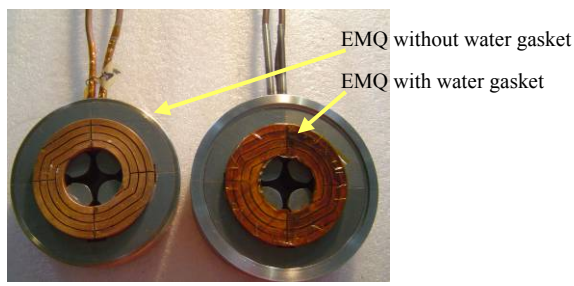

Figure 1: Photos of EMQ.

MAGNET MEASUREMENTS

Hall Measurements

From the HP measurement, the magnetic field profile along the beam-axis of the EMQ can be obtained at different x and y transverse positions. A typical result from the HP measurement is shown Figure 2.

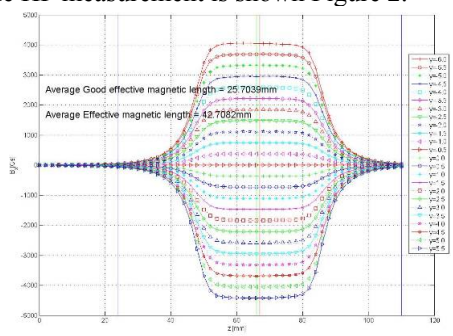

Figure 2: Typical HP measurement result on an EMQ.

The average effective magnetic length, $\overline{L_{eff}}$, is computed by taking the average of all the effective magnetic length obtained from each profile along the

DTL TANK DEVELOPMENT OF 132 MeV LINAC FOR CSNS

Zhirui Sun, Xuejun Yin, Keyun Gong, Jun Peng, Shinian Fu
IHEP, Institute of High Energy Physics, Beijing 100049, China

Abstract

A conventional 324 MHz DTL has been designed for China Spallation Neutron Source (CSNS) to accelerate H^- ion beam from 3MeV to 81MeV and up to 132MeV in its second phase. There are 7 tanks in the 132MeV DTL and currently the R&D of the first tank is under progress. In the design, tank-1 has a tilt field distribution partial for obtaining the most effective energy gain and keeping the low Kilpatrick parameter. This tank is under fabrication and the manufacture technique was verified by the measurement results. Concerning of the difficulty of tuning a partial tilt field distribution, the complex RF measuring and tuning procedure is introduced.

INTRODUCTION

China Spallation Neutron Source (CSNS) mainly consists of an H^- linac and a rapid cycling synchrotron of 1.6GeV[1]. The DTL linac are designed in two phases, with energy of 81MeV for phase I and 132MeV for phase II. R&D program for some key technologies involves a prototype of the first unit of the DTL tank, which is the most difficult section in the whole DTL linac. A 3-meter module covers an energy range from 3MeV to 8.9MeV. The tilt field is designed in this module with an electrical field from 2.2MV/m to 3.1MV/m. The electrical field will keep 3.1MV/m after tilt part through whole DTL tank. Concerning the difficulty in tuning this kind of RF field, a procedure for measuring and tuning the tank is designed. In this paper, we will introduce the progress of module tank fabrication and RF tuning procedure.

DTL CAVITY DESIGN

The main parameters of the CSNS DTL are listed in Table 1. There are four tanks for phase I and additional three tanks for phase II. The first tank is composed of three short module tanks, and the first module tank is under manufacturing.

Table 1: DTL main parameters

	CSNS-I	CSNS-II
Input Energy (MeV)	3	3
Output Energy (MeV)	81	132
Chopping rate (%)	50	50
Average I (μA)	75	150
Pulse Current (mA)	15	30
RF frequency (MHz)	324	324
Repetition frequency(Hz)	25	25
Duty factor (%)	1.05	1.05

Mechanical parameters for this unit are listed in Table 2. In the drift tube, the electromagnetic quadrupole (EMQ) is used to supply a gradient 75T/m focusing strength in maximum. The focusing periods are designed as the FD lattice and each drift tube contains one quadrupole.

Table 2: The parameters of first module tank

Tank length (m)	2.85
Energy range (MeV)	3-8.88
Average E_0 (MV/m)	2.2 ~ 3.1
Synchronous phase (deg)	-30 ~ -25
Tube face angle (deg)	0 ~ 9 ~ 14
Tank inner diameter(mm)	566.27
Cells number	29
No. of Slug tuners	4
Bore radius (mm)	6
DT diameter (mm)	148

TANK MANUFACTURE

The tank body was made of carbon steel with a copper inner surface. To develop the technology, we tried various approaches with some short test tanks. At the beginning, an explosive bonding technology was tested. A thin copper plate was tightly bonded with a steel tank in the inner surface. Since the tank had many ports and holes for vacuum and for holding drift tubes, here the bonding condition was not as good as the inner surface, resulting in vacuum leakage at some ports. Then we turned to adopt the technology of the Periodic Reverse (PR) copper electroforming method. It has been successful for both inner surface and all ports/holes. Figure1 shows the 2.8m tank module after electroforming. The inner copper surface was polished and the ports are now under fine machining for high accuracy and high flatness. There are twelve straight water cooling channel embedded into tank out-wall. Size of the channel is 26mm×13mm. The tank end plate is separated into two parts for water cooling with opposite water flow direction. Water channels on the end plate are shown in Figure 2.

Figure 1: The first module tank is under fine machining after copper electroform.

DRIFT TUBE LINAC DESIGN AND PROTOTYPING FOR THE CERN LINAC4

S. Ramberger, N. Alharbi, P. Bourquin, Y. Cuvet, F. Gerigk, A.M. Lombardi, E. Sargsyan, M. Vretenar, CERN, Geneva, Switzerland, A. Pisent, INFN/LNL, Legnaro, Italy

Abstract

The Drift Tube Linac (DTL) for the new linear accelerator Linac4 at CERN will accelerate H^--ion beams of up to 40 mA average pulse current from 3 to 50 MeV. It is designed to operate at 352.2 MHz and at duty cycles of up to 10 %, if required by future physics programmes. The accelerating field is 3.2 MV/m over the entire length. Permanent magnet quadrupoles (PMQs) are used as focusing elements. The 3 DTL cavities consist of 2, 4 and 4 section of about 1.8 m each, are equipped with 35, 41 and 29 drift tubes respectively, and are stabilized with post-couplers. Several new features have been incorporated in the basic design. The electro-magnetic design has been refined in order to reduce peak field levels in critical areas. The mechanical design aims at reducing the complexity of the mechanical structure and of the adjustment procedure. Drift tubes and holders on the tanks that are machined to tight tolerances do not require adjustment mechanisms like screws or bellows for drift tube positioning. A scaled cold model, an assembly model and a full-scale prototype of the first half section have been constructed to validate the design principles. The results of metrological and RF tests are presented.

INTRODUCTION

The Linac4 DTL will accelerate H^--ion beams of up to 40 mA average pulse current from 3 MeV to 50 MeV in 3 accelerating cavities over a length of 18.7 m. The RF cavities operating at 352.2 MHz and at duty cycles of up to 10% are 520 mm in diameter with drift tubes of 90 mm diameter and 20 mm beam aperture.

The drift tubes are equipped with permanent magnet quadrupoles (PMQ) with an FFDD lattice in cavity 1 and an FD lattice in cavity 2 and 3. PMQs have the advantage of small size at medium magnetic gradients without the need for current supply wires or power converters. To ease matching for beam currents below nominal, electromagnetic quadrupoles are placed in each of the intertank sections. Latest design parameters are shown in Table 1.

ELECTRO-MAGNETIC DESIGN

The electro-magnetic design aims at an acceleration with high constant average field E_0 of 3.2 MV/m over all gaps with a high effective shunt impedance per unit length ZT^2. While it is a typical DTL concept to ramp E_0 in the first cavity in order to adiabatically capture the beam longitudinally [1], the choice of high constant E_0 aims at maximizing the energy acceptance to the incoming beam and leads to a more compact design [2].

Table 1: DTL Cavity Parameters

Parameter	Cavity 1 / 2 / 3
Cells per cavity	36 / 42 / 30
Maximum surface field	1.6 / 1.4 / 1.3 Kilp
Synchronous phase	-30 to -20 / -20 / -20 deg
RF peak power per cavity	0.95 / 1.92 / 1.85 MW
RF beam / peak power	1.88 MW / 4.7 MW
Focusing scheme	FFDD / FD / FD
Quadrupole length	45 / 80 / 80 mm
Number of sections	2 / 4 / 4
Length per cavity	3.63 / 7.38 / 7.25 m

A particular advantage of ramping E_0 are lower peak fields at lower beam energies where earlier designs showed increased breakdowns [3]. Several parameters might be of influence: comparably large surfaces of flat opposing faces on consecutive drift tubes, more outgassing due to larger overall surfaces including the cavity end-wall, an incoming beam with a higher number of stray particles, magnetic fields close to surfaces of shorter drift tubes.

Recent studies for muon cooling where strong accelerating and magnetic fields have to be combined, emphasize the importance of the latter [4]. The PMQs that will be used for the DTL design have a peak magnetic surface field of 0.5 T which in the shortest drift tubes falls close to the area of peak electric fields.

In order to reduce breakdown probability in the first cells, the peak electric field therefore has been reduced by 30% by increasing the gap length. The cells are tuned by the face angle. At longer drift tubes the peak electric field can be ramped to values that allow for optimum effective shunt impedance (Fig. 1). In this way, the same advantage of lower peak fields in the first cells is achieved as when ramping E_0.

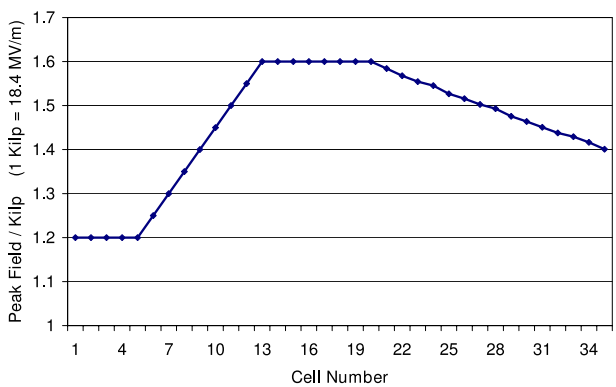

Figure 1: The peak field is reduced in the first cells.

DEVELOPMENT OF INVESTIGATIONS ON THE MILAC HEAVY ION LINEAR ACCELERATOR

V.O.Bomko, O.F.Dyachenko, O.M.Yegorov, A.P.Kobets#, M.S.Lesnykh, K.V.Pavlii, Z.Ye.Ptukhina, V.M.Reshetnikov, S.S.Tishkin, O.V.Zabotin, B.V.Zajtsev, B.M.Zinchenko, V.G.Zhuravlev, National Science Center "Kharkov Institute of Physics and Technology", Kharkov, Ukraine

Abstract

On the Kharkov heavy ion linear accelerator MILAC works are carried out with heavy ion beams accelerated to 8.5 MeV/u, and development of new methods for acceleration and investigations on modernization of accelerating structures [1].

MILAC LINEAR ACCELERATOR

The Kharkov ***multicharge ion linear accelerator*** (MILAC) is a unique physical and technology complex that consists the first prestripping section PSS-15 (Fig. 1, p. 2), second prestripping section PSS-4 (Fig. 1, p. 5), main section MS-5 (Fig. 1, p. 3) and the system of the ion irradiation (Fig. 1, p. 8). The structural scheme of the accelerator is given in the Fig.1.

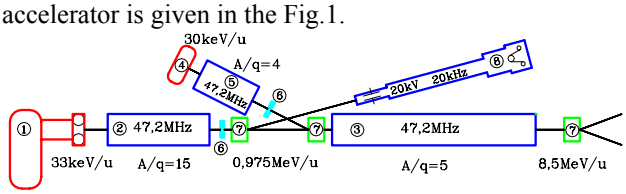

Figure 1: The structural scheme of the MILAC.

At the main and two pre-stripping sections of the MILAC linear accelerator the accelerating DTL structure on the H-wave of interdigital type (IH-structure). was applied [2].

The characteristic feature of the main section MS-5 (Fig. 1, p. 3) is its electrodynamic characteristics. An effective method was developed for adjusting the cells of the accelerating structure using additional current-carrying rods located at an angle to the supporting rod (Fig.2).

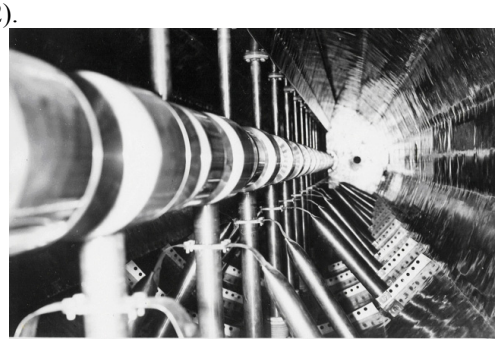

Figure 2: Accelerating structure MS-5.

This method of adjusting the inductive accelerating cell parameters allowed formation of a uniform accelerating field distribution along the structure. From one hand, this allowed to increase significantly the acceleration rate, and from the other, to form the paths of the uniform filed distribution of the controllable extension which gives a possibility to obtain the beams of intermediate energies [3]. Additionally, a method was developed for adjusting the field distribution using the ending resonance adjusting device, which represent quarter wave oscillators; on the side of the oscillator facing the side wall of the cavity a control piston is placed which can move in longitudinal direction. Such systems are installed on the input and output ends of the cavity.

The main section MS-5 11 m in length with 42 drift tubes, of which 21 contain magnetic quadrupoles gives a possibility to accelerate ions with A/q≤5 from 0.975 to 8.5 MeV/u. Total acceleration rate in the prestripping section is 3.2 MeV/m.

Second pre-stripping section PSS-4 (Fig. 1, p. 5) for accelerating only light ions with A/q≤4 from 30 keV/u to 1 MeV/u is developed. In this new section irregular interdigital (IH) accelerating structure with beam focusing by radiofrequency field (alternating phase focusing with stepped changing the synchronous phase along the focusing period) are used. After stripping this beam will be output on the acceleration line of the main MILAC section (Fig. 1, p. 3) and accelerated up to 8.5 MeV/u.

The problem of adjustment accelerating structure PSS-4 was especially difficult in connection with the non-uniform of lengths of cells mention above in structure of the focusing periods and increasing character of distribution of an accelerating field along the accelerator. Therefore it was required to apply a combination of various tuning methods The new effective inductance-capacitor tuning devices (contrivance) as rods located on the drift tube side, opposite to their holders are developed [4]. At the certain design the exact local tuning of cells is possible for carrying out not only selection of contrivance length, but also by change of a corner of their disposition concerning an axis of drift tube holders (Fig.3.).

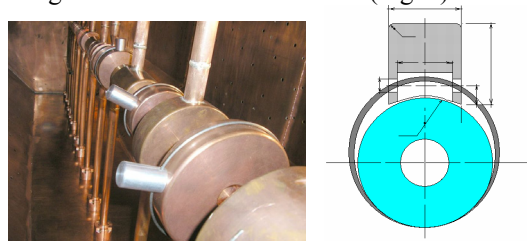

Figure 3: Accelerating structure PSS-4 with contrivance.

The high efficiency such inductance-capacitor tuning system allows to receive required electro-dynamic characteristics of accelerating structure at an identical small diameter of drift tubes, that considerably simplifies

#kobets@kipt.kharkov.ua

LINAC OPERATIONS AT FERMILAB

L. Allen, FNAL, Box 500, Batavia, IL 60510 USA

Abstract

The Fermilab Linac has been delivering unprecedented amounts of beam for HEP. The addition of Main Injector, three high intensity high repetition rate experiments and the 120 GeV Fixed Target Programs have increased the repetition rates from 0.33Hz. to a maximum of 7.5 Hz. and it is expected to increase further. The intensity accelerated by the Booster is 5 E12 protons per pulse. The effects on radiation levels and operational reliability and developments helping both to cope with the higher rates and make the beam more useful to Booster will be discussed.

THE PROBLEM

As the demand for higher booster intensity and repetition rate began to ramp up, the Booster was operating at about 65% efficiency. Because the Linac discards the first ten μsec of beam it needed to accelerate almost 1 E13 H- ions per pulse. Today after many improvements to the Linac and Booster, booster efficiency is 90% and only 7.7 E12 per pulse are required from Linac.

IMPROVEMENTS

In the late 1990's Milorad Popovic [1] accurately modeled the high energy linac quadruples. Using this data he was able to make significant reductions in losses. The match to the Booster was also improved.

In 2001 an experiment [2] was performed measuring the effect of linac beam current on booster efficiency. At that time the Linac normally accelerated 50ma. and injected 11 turns into the Booster. During the experiment, linac beam current was reduced to 30ma. and The Booster was tuned with up to 20 turns injected. The Booster operated at the same or better efficiency at the lower current. As a result, linac beam current was reduced to 40 ma. and as a result of further booster improvements to 36 ma.

As a result of these improvements, linac beam losses have decreased dramatically. The parameter D7LMSM is the sum of all the loss monitors in the RF area. In 2000 D7LMSM was >20. The improvements noted plus constant tuning has reduced the total losses to the 10 to 12 region for the H- ion source and less than ten for the I- ion source.

To get a better measurement of the linac energy on a day to day basis a device called the Velocity Meter [3] has been installed in the 400 MeV Line. By measuring the beam phase between two Griffin [4] detectors it measures flight. While it is not calibrated in energy, it does alert one to energy changes. Before this monitor was installed it was impossible to determine if an energy drift was causing booster efficiency to decline.

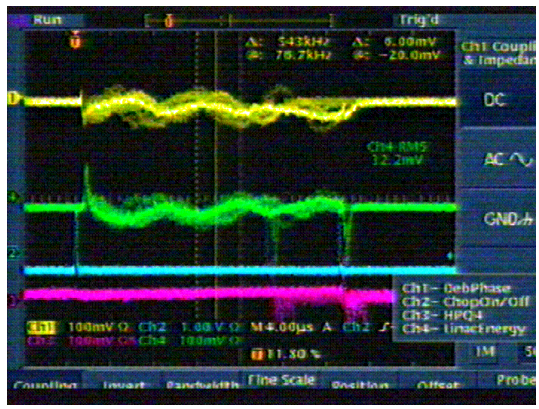

Figure 1: Velocity meter scope traces.

The output signal (in green) viewed on an oscilloscope can detect an energy swing during the pulse or an overall energy shift. The computer reads this parameter and automatically changes the RF phase in the final RF module to correct the energy. Using this method has stabilized the linac energy and made booster tuning more repeatable.

A Bunch Length Monitor [5] was also installed in the 400 MeV Line. It has been empirically determined that booster needs this device to read less than .85 nsec. for good operation. Linac has been tuned so that it averages approximately .83 nsec. The low energy buncher. medium energy buncher and the phase difference between the Low Energy Linac(LE Linac) and High Energy Linac(HE Linac) are the most common adjustments to control this.

CONTINUING PROBLEMS

Looking at the trace in Fig. 1 one notices an oscillation. The oscillation is at approximately 130 kHz and is a real energy effect. We can see this in the HE Linac RF phase and at times in the gradient. There is a program underway, lead by Ken Quinn, to locate and repair the source of this oscillation.

There is a slow drift of some parameter in the LE Linac. The signature of this drift indicates that it is RF related. The gradients have independent readings but intertank phase does not. The drift does not appear to be the gradient because the independent readings do not change at the same time. The lack of independent readings has made looking at phase difficult. The fix is to vary the phase of LE Tank 5. This both changes the output energy of the LE Linac and the phase difference between the LE Linac and the HE Linac.

As mentioned earlier the Linac discards the first 10μsec. of beam each pulse. This is the time it takes for the feedback systems in the LE Linac to settle in. During this time the beam is unreliable and dumped. This beam usually has slightly higher losses than the later beam sent

RE-PHASING OF THE ISAC SUPERCONDUCTING LINAC WITH COMPUTED VALUES

M. Marchetto, R.E. Laxdal, Fang Yan TRIUMF, Vancouver, BC V6T2A3, Canada

Abstract

The ISAC superconducting linac is a fully operational machine that routinely provides beam to experiments. The linac consists of twenty superconducting independently phased cavities housed in five cryomodules. The initial tune is done manually aided by MATLAB routines to phase the linac and set the correct optics. From the initial tune we calculate the gradient at which each cavity operates based on the energy gain, the transit time factor and the geometry of the cavity itself. Then in the event of a gradient change of one or more cavities we can calculate the RF phase shift of each downstream cavity using the initial gradients, the known geometry of the entire linac and assuming linearity of the RF controls. This possibility has been investigated and we have demonstrated that the calculated phase shift can be implemented automatically thus avoiding a complete retune of the machine. In this paper we will present the calculations and the results of the online tests.

INTRODUCTION

The ISAC facility at TRIUMF (Fig. 1) has at present the most intense driver available for ISOL based radioactive ion beams (RIB) production. The RIBs can be delivered to three experimental areas; one using the beam at source potential (60 kV), the other two using post accelerated beam.

In the ISAC I facility the beam is accelerated through a chain composed of an RFQ injector followed by an IH drift tube linac (DTL). The DTL is design as an energy variable machine [1] being able to deliver all the energies ranging between 150 keV/u and 1.8 MeV/u. The DTL injects also the beam in the ISAC II linac at 1.5 MeV/u.

In the ISAC II facility the beam is accelerated by means of a superconducting (SC) linac operating at 106.08 MHz [3]. The present installation of the SC linac is composed of five cryomodules each housing four superconducting cavities and one superconducting solenoid. The cavity voltages are set to operate each at a fixed power of 7W, for a total of ∼20MV of acceleration. The twenty cavities are independently phased at -25° synchronous phase in sequence starting from the first one. The number of cavities turned on determines the final energy. The tuning time for the SC linac can be as long as four hours although tuning algorithms are being developed to reduce this time. The ISAC II linac is going to be upgraded by the end of 2009 adding twenty more cavities housed in three cryomodules [2]. In this case there is an increased motivation to look for more tuning aids.

In order to maximize the integrated beam at the experiment it is essential to reduce the downtime as much as possible. One possible source of downtime is the retuning of

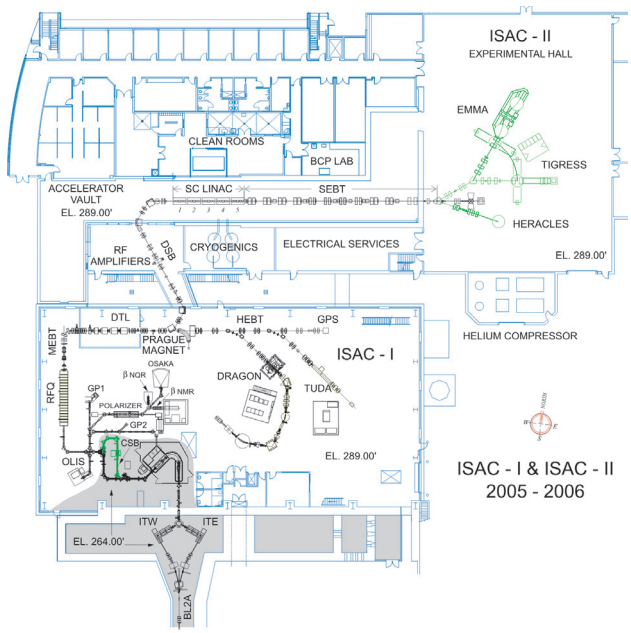

Figure 1: Overview of the ISAC facility at TRIUMF. The ISAC II linac is superconducting while in ISAC I they (RFQ and DTL) are normal conducting.

the superconducting linac in case one cavity (or more) experiences a drop of the accelerating gradient. In this paper we call this generic event a cavity failure without specifying the cause. In this case it is possible to recalculate the difference in time of flight and hence the shift of the RF phase for each cavity downstream of the faulty one. In order to calculate the phase shifts we need to know the geometry of the linac, the transit time factor of the cavities and the accelerating gradients. The transit time factor is known from radio frequency simulations of the cavity geometry. The geometry of the linac is also known by design. The operating gradients of each cavity are calculated based on the energy gain measured from the initial tuning of the linac.

ONLINE MEASUREMENT

In order to validate the calculated values of the rephasing routine the first cavity is turned off and online RF phases are manually reset for the nineteen cavities downstream. Four separate runs are completed using different ion beams, meaning also that the energy gain after each cavity is different from one run to another due to different A/Q. These four series together with their original phase setting give the online phase shift for cavity one off. Fig. 2 represents the calculated time of flights (TOF) before and after cav-

THE SPIRAL 2 SUPERCONDUCTING LINAC

R. Ferdinand, T. Junquera, SPIRAL2/GANIL Caen
P. Bosland, PE Bernaudin CEA Saclay
H. Saugnac, G. Olry IPN Orsay
Y. Gómez-Martínez LPSC Grenoble

Abstract

The SPIRAL 2 superconducting linac is composed of 2 cryomodule families, basically one of low beta, called Cryomodule A, and one of high beta, called Cryomodule B. The low beta family is composed of 12 single cavity cryomodules. The high energy section is composed of 7 cryomodules hosting 2 cavities each. According to beam dynamics calculations all the cavities will operate at 88 MHz: one family at β=0.07, and one at β=0.12. The design goal for the accelerating field Eacc of the SPIRAL 2 QWRs is 6.5 MV/m. The configuration, cavities and cryomodule tests and status are described.

INTRODUCTION

The GANIL's SPIRAL 2 Project [1] aims at delivering high intensities of rare isotope beams by adopting the best production method for each respective radioactive beam. The unstable beams will be produced by the ISOL "Isotope Separation On-Line" method via a converter, or by direct irradiation of fissile material.

The driver will accelerate protons (0.15 to 5 mA – 33 MeV), deuterons (0.15 to 5 mA – 40 MeV) and heavy ions (up to 1 mA, Q/A=1/3 14.5 MeV/u to 1/6 8.5 MeV/A). It consists of high performance ECR sources, a RFQ, and the superconducting light/heavy ion linac. The driver is also asked to provide all the energies from 2 MeV/u to the maximum designed value.

Figure 1 : SPIRAL2 superconducting linac – 2 QuaterWave Resonator (QWR) families.

The superconducting linac is composed of cryomodules type A developed by CEA-Saclay, and cryomodules type B developed by IPN-Orsay. Both types of cavities will be equipped with the same power coupler specified for a maximum power into the cavity of 12.8 kW@6.5MV/m, which is developed in a third laboratory, LPSC-Grenoble. The coupler must handle 100% reflected power at maximum incident power.

All the components of the series (cavities and cryomodules) will be fabricated in the industries. Couplers conditioning, cavities chemical treatments, HPR rinsing in clean room, assembly, and RF tests of the cavities in vertical cryostat and RF power tests of the cryomodules will be made in the respective 3 labs.

CRYOMODULES A - β=0.07

Details of the cavity and cryomodule design were described in [2,3].

The cavity tuner works by cavity deformation perpendicularly to the beam axis. This design saves room in the beam axis direction. The cavity mechanical design was optimized in order to reach a full tuning range of ±25 kHz at 4 K, without plastic deformation of the niobium cavity.

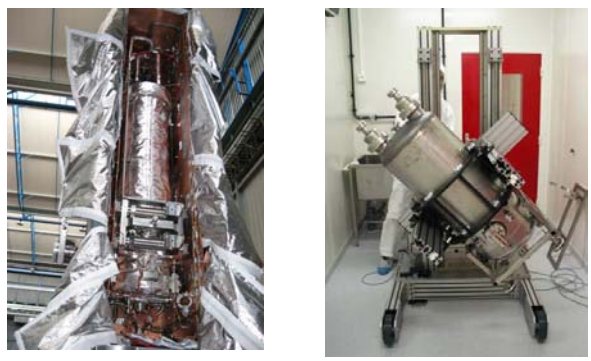

Figure 2 : Cavity A with MLI and B in clean room.

Each cavity A will be feed by 5 to 10 kW solid state RF amplifier [4]. The first cavities of this low beta section working at low accelerating field (≈ 0.49 MV/m, 0.5 kW) will require less power than the last cavities of the section.

At present, one cavity prototype and a qualifying cavity have been tested in vertical cryostat. Whereas the prototype reached the specifications, the qualifying cavity performances were not as good as expected. The maximum accelerating field, 11 MV/m, was much higher that needed, but the Q_0 value was a factor 10 below the acceptable value, about 2 10^8 (see Figure 3).

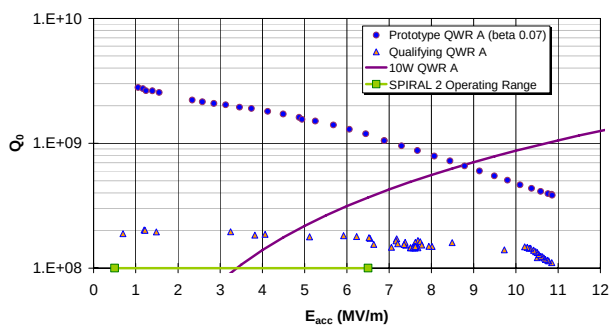

Figure 3: prototype and qualifying QWR A cavity in vertical cryostat.

Several tests were performed to localise the dissipating defects without success. We could determine that this defect is not located at the cavity extremities, at the

EXPERIENCE WITH STRIPPING CARBON FOILS IN ALPI SUPER-CONDUCTING ACCELERATOR

P. A. Posocco*, Consorzio RFX, Padova, and INFN/LNL, Legnaro, ITALY
D. Carlucci, A. Pisent, M. Poggi, INFN/LNL, Legnaro, ITALY

Abstract

The super-conducting linac ALPI, injected either by a XTU tandem or by the s-c RFQ of PIAVE, is composed by 3 cryostats of bulk-Nb cavities (β_o = 0.056) and 13 cryostats of Nb-sputtered-on-Cu cavities (β_o = 0.11 and β_o = 0.13), for a total of 64 cavities and an equivalent voltage of 35 MV. The linac is build up in two branches connected by an achromatic and isochronous U-bend. In January 2007 a stripping station equipped with carbon foils of different thickness was placed after 6 cryostats, before the U-bend, to test the feasibility of acceleration and transport of a charge enhanced beam. The study was performed with 4 different beams (Ca, Ar, Zr and Xe) and a complete data analysis has been carried out.

INTRODUCTION

ALPI (Acceleratore Lineare Per Ioni) [1] is a super-conducting linac running since 1995 at LNL, Legnaro. The structure of this booster (see Fig. 1) is comprised of two branches (low and high-energy branch) connected by an achromatic and isochronous U-bend. There are three families of cavities, 12 β_o = 0.056 of bulk Nb, 44 β_o = 0.11 and 8 β_o = 0.13 of Nb-sputtered-on-Cu, 4 cavities in each cryostat. At present the low-β cryostats reach an average accelerating field of 3.5 MV/m, the medium-β 4.2 MV/m and the high-β 5.5 MV/m, resulting in a total available voltage of 48 MV [2]. The effective voltage reaches ~ 35 MV due to a careful beam dynamics optimization.

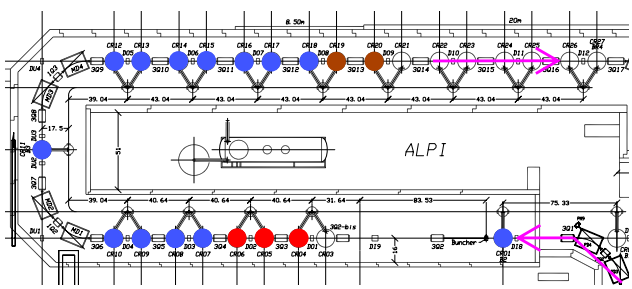

Figure 1: ALPI plan. The beam coming from PIAVE injector passes through the low-β (in red), medium-β (blu) and high-β (brown) cryostats.

The linac period is made by one triplet and 2 cryostats with a diagnostics box (profile monitor and Faraday cup) in between. In January 2007 it was decided to place a stripper station in the center of the low-energy branch period, at the both transverse and longitudinal focal point in order to reduce undesired emittance growths. Hence, the diagnostics box DO4 was modified to held the device.

The position along the accelerator was chosen to optimize the overall energy gain: the energy before the stripping is about 3 MeV/A, enough to enhance the charge state by 50% for the medium/high mass ions (see Fig. 2), and the remaining accelerating voltage is 2/3 of the total voltage. This means that the final energy of the stripped beam is 20 ~ 30% higher than the unstripped one.

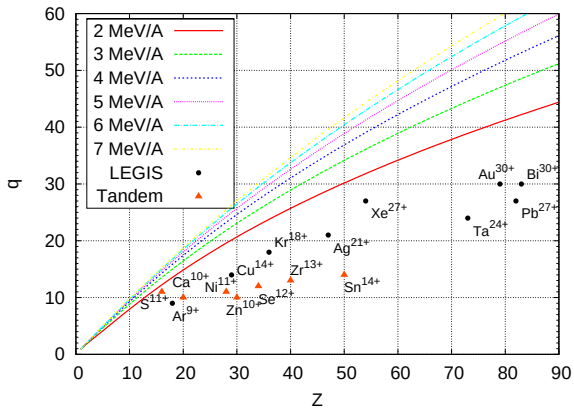

Figure 2: Most probable charge state from stripper as function of Z and energy compared to some examples of available ions out of LNL Tandem injector or foreseen for the new LEGnaro ecrIS (LEGIS).

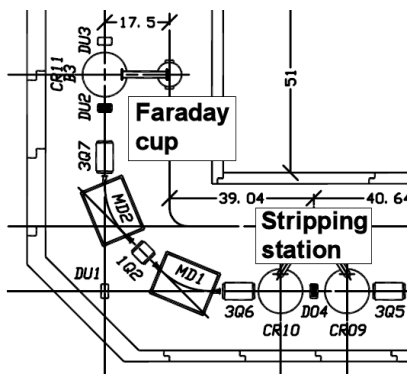

Figure 3: ALPI layout around the stripper station. The beam focalized in the diagnostic box D04 is stripped and then selected by the two dipoles MD1 and MD2.

* piero.antonio.posocco@lnl.infn.it

PLANS FOR A SUPERCONDUCTING H- LINAC (SPL) AT CERN

O. Brunner, S. Calatroni, E. Ciapala, R. Garoby, F. Gerigk , A.M. Lombardi, R. Losito, V. Parma, C. Rossi, J. Tuckmantel, M. Vretenar, W. Weingarten, CERN, Geneva, Switzerland

Abstract

As part of the upgrade of the LHC injector complex at CERN, the construction of a 4 GeV Superconducting Proton Linac (the SPL, in fact an H- accelerator) is planned to begin in 2012. Depending upon physics requests, it should be upgradeable to 5 GeV and multi-MW beam power at a later stage. The construction of Linac4, its low energy front end, has started at the beginning of 2008. A full project proposal with a cost estimate for the low power version of the SPL aimed at improving LHC performance has to be ready for mid-2011. As a first step towards that goal, essential machine parameters like RF frequency, cooling temperature and accelerating gradient have recently been revisited and plans have been drawn for designing and testing critical components.

INTRODUCTION

The foreseen upgrade of the LHC injector complex [1] will entail the construction of PS2, a new 50 GeV synchrotron and of the SPL as its injector. The SPS will not be replaced, but it will be significantly upgraded. The layout of these new accelerators on the CERN site has been decided [2] and Linac4 [3], the SPL front-end, is being built at its final location (Fig. 1).

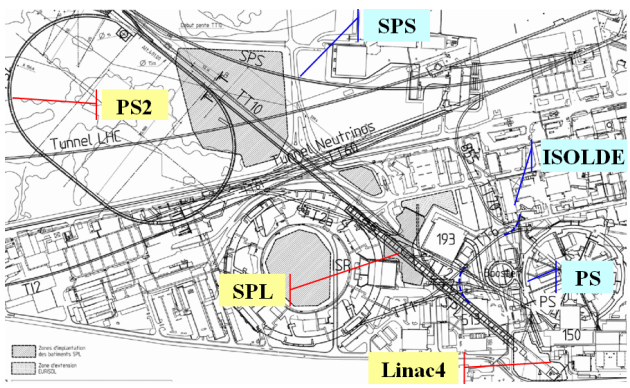

Figure 1: Layout of the new injector complex.

The flexibility and the potential of evolution of the SPL will make it an important asset for physics in the future [4]. As injector of PS2, only a 4 GeV low power version of the SPL is needed ("the "LP-SPL"). For a neutrino facility, the LP-SPL would have to be upgraded to 5 GeV and 4 MW of beam power, and accompanied with an accumulator and a compression ring to meet the required time structure of the beam [5]. For a Radioactive Ion Beam Facility of the next generation [6], a similar beam power would also be required at 2.5 GeV. A summary of the specifications of the accelerator in its different possible phases of implementation is given in Table 1.

As a first step in the preparation for the project proposal to be submitted to the CERN Council by mid-2011, the choice of the basic parameters of the SPL [7] has been revisited during the past months in view of optimizing synergy with the worldwide development effort on superconducting accelerating structures cavities. The RF frequency was therefore reconsidered, as well as the cooling temperature of the superconducting cavities and the foreseeable accelerating gradients [8, 9, 10].

Table 1: Main Characteristics of the Successive Phases of Realization of the SPL

	LP-SPL	**SPL (5 GeV)**	**SPL (2.5 GeV)**
Users	PS2 ISOLDE	+ ν facility	+ RIB facility
T [GeV]	4	5	2.5
P_{beam} [MW]	0.2	4	4
F_{rep} [Hz]	2	50	50
I_{source} [mA]	40	80	80
Chopping	yes	yes	no
I_{av} [mA]	20	40	40
T_{pulse} [ms]	1.2	0.4	0.8

DESIGN OPTIONS

The RF frequency of 352 MHz has been selected for Linac4, because it is very well matched for use in the low energy front end of a proton linac and because of the large inventory of RF hardware available at that frequency since the decommissioning of LEP. Hence only harmonics of 352 MHz can be considered for acceleration after Linac4 (160 MeV). The three design options which have been compared [9] (Table 2) were especially aimed at analysing the interest of 1408 MHz which is close to the frequency used in the ILC and X-FEL projects.

An updated survey of recent experimental results, confirmed the 2006 conclusion [7, 10] that the maximum accelerating gradient of bulk Niobium cavities only depends on geometry ($\beta_{geometrical}$) and on the quality of the surface treatment techniques, and not on the RF frequency. It is therefore assumed when comparing the length of the different options that the superconducting elliptical cavities operate at an accelerating gradient corresponding to the same peak surface field of 50 MV/m, as in a β=1 cavity with an accelerating gradient of 25 MV/m. Their characteristics are given in Table 3.

The "Nominal" option in Table 2 is a slightly improved version of the SPL design published in 2006 [7]. It uses only 2 types of 5 cell elliptical cavities and has a length of 439 m.

THE STATUS OF THE MSU RE-ACCELERATOR (ReA3)*

X. Wu†, C. Compton, S. Chouhan, M. Doleans, W. Hartung, D. Lawton,
G. Machicoane, F. Marti, P. Miller, J. Ottarson, M. Portillo, R. C. York, A. Zeller and Q. Zhao
National Superconducting Cyclotron Laboratory, Michigan State University, E. Lansing, MI 48824, U.S.A.

Abstract

The Re-accelerator ReA3 [1] being developed at the Michigan State University is a major component of a novel system proposed to first stop the high energy Rare Isotope Beams (RIBs) created using Coupled Cyclotron Facility (CCF) by the in-flight particle fragmentation method in a helium filled gas system, then increase their charge state with an Electron Beam Ion Trap (EBIT) charge breeder, and finally re-accelerate them to 3 MeV/u to provide opportunities for an experimental program ranging from low-energy Coulomb excitation to transfer reaction studies of astrophysical reactions. The accelerator system consists of a Low Energy Beam Transport (LEBT) with an external multi-harmonic buncher, a radio frequency quadrupole (RFQ), a superconducting linac, and a High Energy Beam Transport (HEBT). The superconducting linac will use quarter-wave resonators with β_{opt} of 0.041 and 0.085 for acceleration and superconducting solenoid magnets for transverse focusing. The paper will discuss the recent progress of R&D and beam dynamics studies for ReA3.

INTRODUCTION

Isotope Separation On-line (ISOL) and Projectile Fragmentation (PF) are the two methods used to produce high quality RIBs for the nuclear science. Since 1989, the NSCL has been using the PF method with great success to produce fast RIBs for nuclear structure and nuclear reaction experiments, especially after the completion of the CCF and the A1900 Fragment Separator in 2001. For ReA3, RIBs from the EBIT will have an initial energy of 12 keV/u and an initial emittance of 0.6 π mm-mrad. The ReA3 is required to accelerate RIBs with charge-to-mass ratios (Q/A) ranging from 0.2 to 0.4 and to achieve a final energy ranging from 0.3 to 3 MeV/u. The nuclear astrophysics experimental program requires the beam bunch width and the energy spread for the RIBs on the experiment target within 1 ns and 1 keV/u, respectively, which corresponding to a small longitudinal emittance of ~0.25 π keV/u-ns. The ReA3 accelerator system consists of four segments: a Low Energy Beam Transport (LEBT) system to transport, bunch and match the RIBs from the EBIT to the RFQ, an RFQ for initial beam acceleration and focusing, a superconducting linac system for RIBs acceleration to the desired energy, and a High Energy Beam Transport (HEBT) system to deliver the RIBs to an experimental area with the required beam parameters. The entire ReA3 accelerator system will be located on a balcony in the NSCL high bay area.

*Work supported by Michigan State University and NSF
#xwu@nscl.msu.edu

LEBT

The ReA3 LEBT will transport, bunch and match RIBs from the EBIT into RFQ. An electrostatic triple Bender is implemented in the LEBT in order to allow a stable ion source (SIS) on a high voltage platform to deliver $^4He^{1+}$ beam into the RFQ for SC linac tuning and diagnostics calibrations. It is also capable to deliver RIBs from the EBIT directly to a low energy experiment area as well as accept RIBs from a possible 2nd EBIT in the future upgrade. Figure 1 shows the layout of the ReA3 LEBT. Electrostatic quadrupoles and a solenoid magnet are used to provide transverse focusing for both RIBs and stable beam. In addition, there are four beam diagnostics stations in the LEBT for proper beam transverse and longitudinal matching into the RFQ. To achieve a small longitudinal emittance, an external Multi-Harmonic Buncher (MHB) is used in the LEBT, which has been constructed and tested at MSU recently [2].

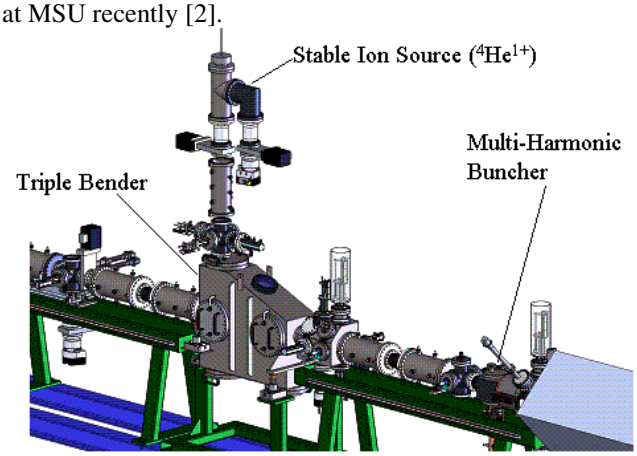

Figure 1: The layout of the ReA3 LEBT.

Figure 2 shows the structure of the triple bender. It consists of three 75° spherical benders and two 15° parallel plate kickers. The spherical bender has a bend radius of 250 mm and a gap of 80 mm. For a maximum initial accelerating voltage of 60 kV, potentials of ±19.2 kV are required to bend beam by 75°. The parallel plate kicker has a gap of 120 mm, and requires potentials of ±9.3 kV to deflect beam by ±15°. Herzog shunt plates grounded to the vacuum chamber are used for limiting the fringe electric fields at the entrance and exit of the electrodes. A gap of 12 mm separates the shunt plates and the electrodes. COSY INFINITY [3] and SIMION [4] were used for beam simulations and optimizations of the shape of the electrodes and the shunt plates.

LINAC FRONT-END UPGRADE AT THE CANCER THERAPY FACILITY HIT

M. Maier#, W. Barth, B. Schlitt, A. Orzychevkaya, H. Vormann, S. Yaramyshev

GSI, Darmstadt, Germany

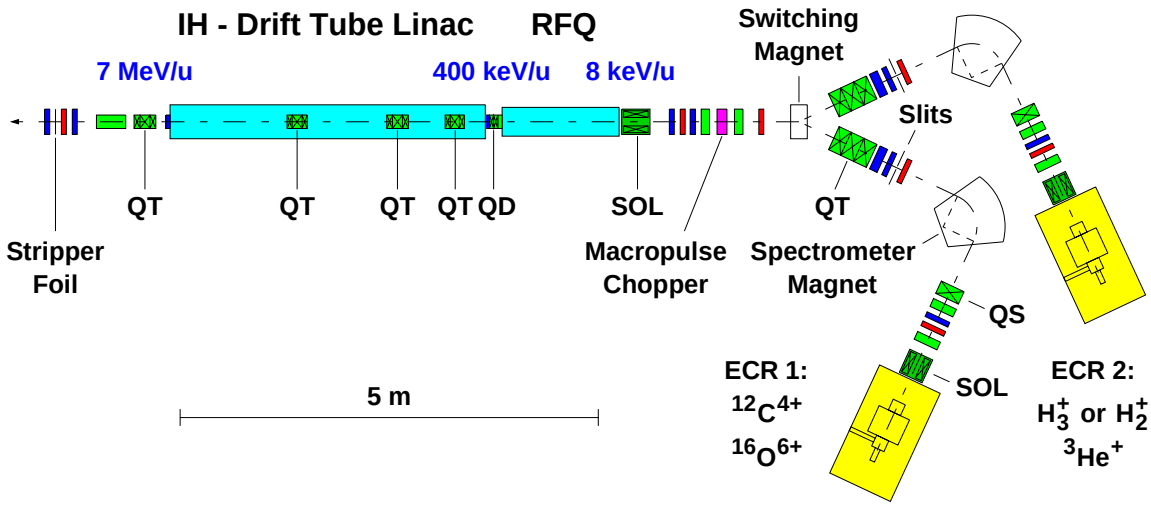

Figure 1: Layout of the Injector Linac [1]. QS = Quadrupole singulet, QT = Quadrupole triplet, SOL = solenoid, magnetic focusing and steering magnets (green), profile grids and the tantalum screen (red), and the beam current monitors (blue).

Abstract

A clinical facility for cancer therapy using energetic proton and ion beams (C, He and O) has been installed at the Radiologische Universitätsklinik in Heidelberg, Germany [1]. It consists of two ECR ion sources, a 7 MeV/u linac injector, and a 6.5 Tm synchrotron to accelerate the ions up to 430 MeV/u. The linac [2] comprises a 400 keV/u RFQ [3] and a 7 MeV/u IH-DTL [4] operating at 216.8 MHz and has been commissioned successfully in 2006 [5]. Yet the overall achieved transmission through the injector linac did not ecxeed 30 % due to a mismatch of the beam at the RFQ entrance. Thus a detailed upgrade programm has been started to exchange the RFQ with a new radial matcher design, to correct the missalignment and to optimize beam transport to the IH-DTL. The aim is to achive a sufficient overall linac transmission above 60%. Since August 2008 the new RFQ is at a test setup in Risø, Danmark. There a test bench comprising a full ion source and LEBT setup to commission the RFQ has been installed by Danfysik.

INTRODUCTION

The commissioning of the injector Linac [5] shown in Figure 1 was performed in three consecutive steps for the LEBT, the RFQ, and the IH-DTL.

Because of the low transmission (~30 %) achieved for the injector Linac an upgrade program was initiated in 2007. The timeline of the commissioning and the upgrade program is given in Table 1.

Table 1: Timeline of the HIT Linac Commissioning and the Linac Front-end Upgrade Program

2006 Apr.-Dec.	HIT Linac commissioning
2007 Aug.	RFQ design study measurements and solenoid exchange
2007 Nov.	New stiffened tank copper plated
2007 Dec.	RFQ input radial matcher design ready and approved
2008 May	Machining of the electrodes at NTG workshop
2008 Jun.	Assembly and RF tuning at the Univ. of Frankfurt
2008 Sep.–Oct.	Rebuncher adjustment and commissioning in Risø, Danfysik
Outlook	
2009	Integration of the new RFQ at HIT

LINAC FRONT-END UPGRADE

As a result of the Linac commissioning and excessive beam dynamics simulations the reasons for the low RFQ transmission were found to be:

- The poor performance of the ion sources,
- field errors of the Solenoid matching the beam to the RFQ,
- RFQ input radial matcher section and
- the deformed electrodes due to mechanical stress on the tank.

As first the Solenoid matching the beam to the RFQ has been exchanged and the result is shown in Figure 3.

C^{6+} ION HYBRID SINGLE CAVITY LINAC WITH DIRECT PLASMA INJECTION SCHEME FOR CANCER THERAPY

Toshiyuki Hattori, Taku Ito, Noriyosu Hayashizaki, Takuya Ishibashi, Liang Lu, Jun Tamura, Rui Kobori, Masahiro Okamura[1)], E.Osvath[2)], D.Biro[2)], D.Hollanda[2)], L. Kenez[2)]
Research Laboratory for Nuclear Reactors, Tokyo Institute of Technology,Tokyo, Japan
1) Collider-Accelerator Department, Brookhaven National Laboratory, New York, USA
2) Sapientia –Hungarian University of Transylvania, Tirgu-Mures, Romania

Abstract

We succeeded to accelerate more than 18mA of C^{6+} ions with Direct Plasma Injection Scheme (DPIS) of YAG laser in 2004. We believe that these techniques are quite effective for pulse accelerator complexes (linac and synchrotron) such as heavy ion cancer therapy. We study a new hybrid single cavity C^{6+} linac for heavy ion cancer therapy. This hybrid linac, combined with radio frequency quadrupole (4rod-RFQ) electrodes and drift tube electrodes into a single cavity, is able to downsize the linac system and reduce the peripheral device. High intensity beam of C^{6+} by DPIS have many advantage for the synchrotron of heavy ion cancer therapy. We will present the design procedures of this hybrid linac, which is base on a three-dimensional electromagnetic field simulation.

INTRODUCTION

In order to verify DPIS, accelerator test was carried out using Tokyo Institute of Technology (Titech) RFQ heavy ion linear accelerator and CO_2 laser heavy-ion source in 2001. The accelerated carbon beam obtained 9.2mA of C^{4+} was much higher than designed currents. [1-4] To confirm the capability of the DPIS, we designed and fabricated a new RFQ linac to accommodate 100mA of carbon beam collaboration The Institute of Physical and Chemical Research and Frankfurt University. We succeeded to accelerate very intense carbon ions with the DPIS in 2004. The peak current reached more than 60mA of C^{4+} and 18mA of C^{6+} by CO2 and YAG laser, respectively [5-9]. Fig. 1 shows photographs of Titech RFQ linac and 100 mA Test RFQ linac. We believe that these techniques are quite effective for pulse accelerator complexes such as linear accelerator and synchrotron. The accelerator complexes are heavy ion cancer therapy and heavy ion inertial fusion.

We are studying a new hybrid single cavity linac [10] for Boron Neutron Capture Therapy. This hybrid linac, combined with radio frequency quadrupole electrodes and drift tube electrodes into an interdigital-H (IH) type single cavity, is able to downsize the linac system and reduce the peripheral device. From these matters, we propose a small Hybrid Single Cavity (HSC) linac for injector of heavy ion cancer therapy.

Titech RFQ linac 100 mA Test RFQ linac

Figure 1: Titech RFQ linac in 2001 and 100 mA Test RFQ linac in 2004 succeeded to accelerate high intensity beam by DPIS.

ND-YAG LASE ION SOURCE

A Nd-YAG laser with a wavelength of 1060nm is used for this ion source. The pulse duration is 15ns(FWHM) and its energy is 400mJ. Fig.2 shows charge state distribution of Carbon ion with about 400mJ. Fig.3 shows laser power dependence of charge state distribution of Carbon ion. From these data, C^{6+} ions were produced 40%. C^{6+} ion beam have pulse width of about 2 μ s and about 200mA at injection point of 4 rod of RFQ.

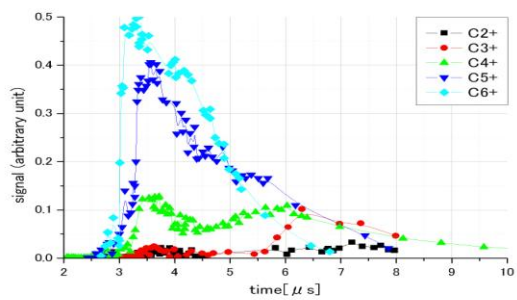

Figure 2: Charge state distribution of the Carbon ion with about 400mJ of YAG laser.

thattori@nr.titech.ac.jp

QUALITY IMPROVEMENT OF LASER-PRODUCED PROTONS BY PHASE ROTATION AND ITS POSSIBLE EXTENSION TO HIGH ENERGIES*

Akira Noda, Yoshihisa Iwashita, Hikaru Souda, Hiromu Tongu, Akihisa Wakita
ICR, Kyoto University, Gokano-sho, Uji-city, Kyoto, 611-0011, Japan
Hiroyuki Daido, Masahiro Ikegami, Hiromitsu Kiriyama, Michiaki Mori, Mamiko Nishiuchi, Koichi Ogura, Satoshi Orimo, Alexander Pirozhkov, Akito Sagisaka, Akifumi Yogo
JAEA/Kansai, 8-1, Umemidai, Kizugawa-city, Kyoto, 619-0215, Japan
Toshiyuki Shirai, NIRS, 4-9-1, Inage-ku, Chiba-city, Chiba, 263-8555, Japan

Abstract

Energy spread compression scheme for laser-produced ions by phase rotation with the use of an RF electric field synchronized to the pulse laser has been proved in principle for rather lower energies up to ~2 MeV. Its extension to higher energy around 200 MeV has been investigated with multi-gap structure assuming higher frequency of L-Band (~1.3 GHz). RF defocusing effect worried about at lower energy was found to be manageable at such a higher energy if the laser-produced-protons are well treated just after production at the target

INTRODUCTION

Based on recent rapid development of high-power short-pulse laser with the use of Chirped Pulse Amplification, laser-produced ion beam has been proposed to be utilized as an injection beam of a medical synchrotron for cancer therapy replacing the RF linac as shown in Fig.1 [1]. For that purpose, however, the characteristics of laser-produced ion beam are not well suited. The energy spread of the laser-produced ion beam has been almost 100 % without a rather sophisticated treatment of the production target [2] or additional radial focusing scheme [3], which seems not to be suitable for operation by a tolerable repetition (~1 Hz) with good reproducibility as is required from medical use.

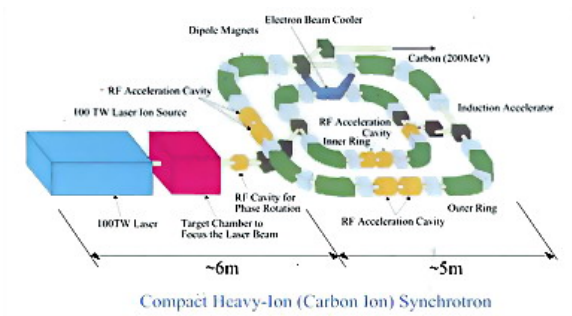

Figure 1: Layout of a medical synchrotron for cancer therapy replacing an injector linac by laser-produced ion beam.

*This work has been supported by Advanced Compact Accelerator Development from MEXT of Japanese Government and the 21st COE of Kyoto University, Center for Diversity and Universality in Physics.
#noda@kyticr.kuicr.kyoto-u.ac.jp

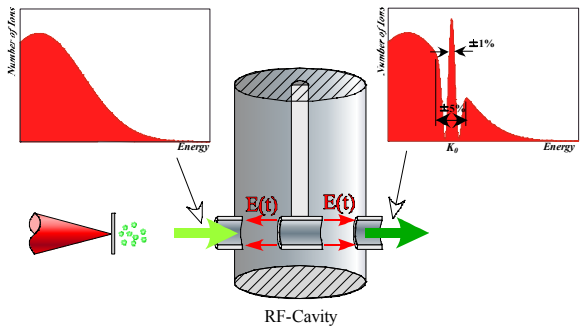

Figure 2: Illustration of the phase rotation principle.

In order to manage such a situation, a phase rotation scheme of the laser-produced ion beam with the use of an RF electric field synchronized to the pulse laser has been proposed [1]. In Fig.2, a basic concept of the phase rotation of phase rotation is illustrated. Utilizing the phase difference caused by the speed difference among ions with different energies, faster and slower ions are decelerated and accelerated, respectively in order to be put together into a central peak. Such an idea of energy spread compression of laser-produced ions by phase rotation has already been experimentally demonstrated with use of a rather smaller peak power (~10 TW) pulse laser, J-LITEX [4, 5]. Recent experiments with use of higher peak power (~100TW) laser, J-KAREN, has extended the energy of laser-produced proton up to ~4 MeV and also given us the information on the radial focusing/defocusing of such protons by the RF electric field created with the phase rotation cavity [6]. In the present paper, capability of multi-gap structure cavity for phase rotation has been considered for the case of

Table 1: Main Parameters of the Two Gap Resonator

Structure		λ/4 with 2 gaps
RF Frequency		80.6MHz (83.7MHz)
Applied Power		<30kW
Dimension	Outer Conductor	ID200mm×~1100mm
	Inner Conductor	ϕ40 mm×~700 mm
	Drift Tube	ID50×100mm
	Gap	20mm
RF Tuner		Cover ~250 kHz
Water Cooling		Keep Temperature with in 0.5°

THE FEASIBILITY OF LOW-ENERGY ELECTRONUCLEAR POWER PLANT

Yu.A. Svistunov, M.F. Vorogushin (D.V. Efremov Institune, 196641, St.Petersburg, Russia),
I.V. Kudinovich (A.N. Krylov Shipbuilding Research Institute, 196158, Moskovskoye Shosse, 44, St.Petersburg, Russia)

Abstract

There are examined prospects and challengers associated with the development of low-energy electronuclear power plant eliminating any possibility of uncontrolled chain fission reaction through fission in subcritical reactor with an additional neutron source. The neutron source is anticipated to be a heavy-element target irradiated with a beam of protons accelerated to several hundreds of mega-electron-volts. The intensity of external neutron source for an electronuclear reactor rated under 200-400 MW may be much less than for greater ones, and that allows reducing accelerator performances to limits that are already run in the world industry. Potential applications of such electronuclear plants include municipal, industrial and other electricity, and heat supply utilities in remote areas. The same engineering philosophy may be used on solving of the nuclear waste transmutation problem.

INTRODUCTION

Thermal power N_T which is picked out in active zone of a subcritical reactor with an outer neutron source and effective multiplying factor K_{ef} is determined by formula

$$N_t = \frac{I_p n_0}{e} \cdot \frac{K_\infty}{1 - K_{ef}} \cdot \frac{E_f}{\nu} \quad (1)$$

where E_f - energy which is picked out under fussion of one fuel nucleus; υ - average number of neutrons from one act of fission; K_∞ - multiplying factor of infinite reactor; I_p - average current of accelerator; n_0 - number of neutrons which are produced by one particle after interaction with target. It is supposed now that for save of nuclear safety K_{ef} must be not more than 0.98. During the active zone campaign K_{ef} can decrease due to change of the fuel isotope composition (fuel burning out, toxic effect etc.) One expect K_{ef} will decrease to 0.95 for fast neutron reactor. Results of modeling of active zones of gas-cooled reactor with multiplying target and K_{ef} =0.96 give release of thermal power 200 MW for intensity of outer source $4.2 \cdot 10^{17}$ n/s. This intensity may be achieved for I_p =5mA and yield of neutron n_0 =13. Such yield neutrons can obtain from (UN+W) target under proton energy E_p =200-400 MeV. 200 MeV spread depend on incompleteness of experimental data, possibilities to use K_{ef} >0.96, cascade zone etc. There is consider proton linac as outer source of neutrons. Alternative variant is to use cyclotron as energy amplifier. Among contemporary cyclotrons PSI (or such type cyclotron) may provide 1 MW beam and required conversion "proton-neutron". But cost of such machine and weight will be well higher than 200-400 MeV, 5 mA proton linac. On the other hand cyclotron with energy 400 MeV and 5 mA current could consider as alternative of rf linac for stationary nuclear power station. Conclusions of workshop [1] show that at present creation of 5 mA cyclotron has more problems than creation of rf linac with the same current.

LINEAR ACCELERATOR

A probable scheme of such proton linac is given on fig.1 It includes: RF volume source, LEBT, 4-vane spatially-homogeneous strong focusing structure (RFQ), alternating phase focusing structure (APF DTL), coupled cavity linac structure (CCL). APF DTL structure is IH-cavity with thick holders turned on right angle in each following sell and magnetic lenses in drift tubes [2].

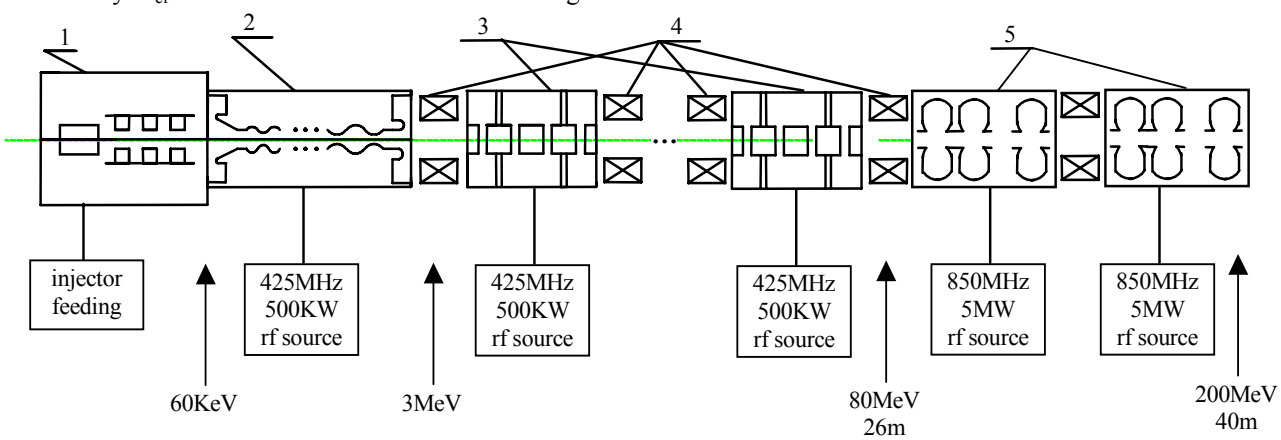

Figure 1: Layout of linac. 1 - ion source and LEBT 2 - spatially-homogeneous strong focusing structure (RFQ) 3 - alternating phase focusing structure (APF DTL) 4 - coupled cavity linac structure (CCL) 5 - focus lenses

CW PROTON LINAC FOR THE BNCT APPLICATION

Donald A. Swenson, Linac Systems, LLC, Albuquerque, NM

Abstract

A 2.5-MeV, 20-mA, cw, proton linac for the Boron Neutron Capture Therapy medical application is under construction at Linac Systems. The system consists of a 25-keV microwave ion source, a solenoid lens based low energy beam transport system, a 0.75-MeV RFQ linac, a 2.5-MeV RFI linac, and the necessary service systems. Because of the superb low energy capabilities of the RFI structure, the RFQ linac need only go to 0.75 MeV, resulting in a cavity dissipation of 74 kW for the RFQ section. Because of the high rf efficiency of the RFI structure, the cavity dissipation is only 35 kW for the RFI section. Extensive thermal studies have been made to accommodate these cw heat load. The beam power is 50 kW. The rf power system is designed for an average power output of 200 kW. The RFQ and RFI sections are coupled into a single resonant unit by a quarter-wave-stub resonant coupler. The combination is driven at a single point in the RFQ structure. The total length of the linac is 2.84 meters.

INTRODUCTION

There are very few cw linacs in the world. Our proprietary linac structures offer the best chance to realize a commercially viable cw linac product. Features of our patented Rf Focused Interdigital (RFI) linac structure make it practical to consider cw linac systems for applications requiring very high average beam intensities. BNCT and Isotope Production are two such medical application. Solid state materials modification is another such application.

A 2.5-MeV, 20-mA, cw, proton linac for the Boron Neutron Capture Therapy (BNCT) medical application is under construction at Linac Systems. The system consists of a 25-keV microwave ion source, a solenoid lens based low energy beam transport (LEBT) system, a 0.75-MeV RFQ linac, a 2.5-MeV RFI linac, and the necessary service systems. This 2.84-m linac system is shown in Fig. 1.

The largest engineering challenge for cw operation is the removal of the heat generated by the cw operation. To mitigate this problem, we have performed extensive thermal management studies on the critical parts of the system. The highest power density in the RFQ linac structure is the RFQ bar supporting strut. The highest power density in the RFI structure is the main drift tube support stem.

Because of the superb low energy capabilities of the RFI structure, the RFQ linac need only go to 0.75 MeV, resulting in a cavity dissipation of only 65 kW (30% beyond theoretical) for the RFQ section. Because of the high rf efficiency of the RFI structure, the cavity dissipation for the RFI section is only 35 kW (30% beyond theoretical). The beam power is 50 kW. The total rf power required is 150 kW. The two linac structures are resonantly coupled, providing a single drive point for the combination. The details of this coupler are presented in another paper at this conference[1].

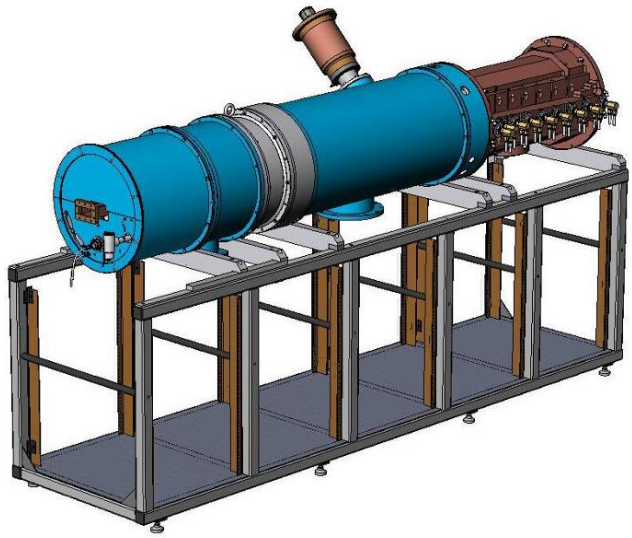

Figure 1: Cw proton linac.

Abundant quantities of epithermal neutrons are produced when the 50 kW, 2.5-MeV proton beam falls on a solid lithium target, which is under design and fabrication at Linac Systems. The details of this target are presented in another paper at this conference[2].

THE INJECTION SYSTEM

The first section of this accelerator is an ion source and low-energy beam transport (LEBT) system. The ion source is a microwave ion source which produces a 25-keV, 30-mA, dc, proton beam with low emittance and high proton fraction. A drawing of the injection system is shown in Fig. 2. The total distance from the ion source to the RFQ is 540 mm.

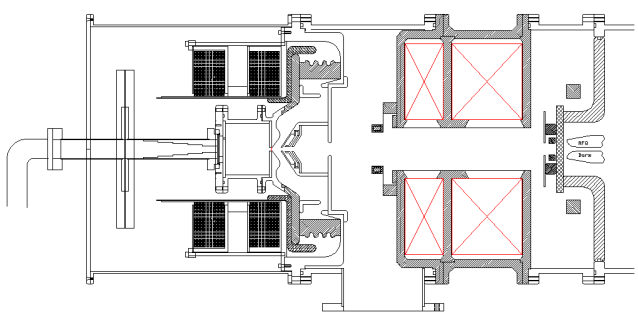

Figure 2: Injection system.

HIGH-POWER LITHIUM TARGET FOR ACCELERATOR-BASED BNCT

Carl Willis*, John Lenz, Donald Swenson, Linac Systems LLC, Albuquerque, NM 87109, USA

Abstract

A water-cooled conical target for producing neutrons via the ^{7}Li(p,n)^{7}Be reaction at 2.5 MeV is under development at Linac Systems. The target is intended to accept an expanded 50-kW beam from an rf linac, and is predicted to meet the intensity requirements for practical accelerator-based boron neutron capture therapy (BNCT) in concert with Linac Systems' CW RFI linac[1]. Lithium metal targets present well-known physical and mechanical challenges at high beam power density that are addressed in our design. CFD modelling indicates that the peak lithium temperature can be held below 150°C with a water flow rate near 80 kg min^{-1} and corresponding pressure drop of 170 kPa. The target prototype has been fabricated and is undergoing thermal-hydraulic testing using an electron beam at the Plasma Materials Test Facility, Sandia National Laboratories.

INTRODUCTION

The ^{7}Li(p,n)^{7}Be reaction on lithium metal, at energies in the range of 1.9-3.0 MeV, has desirable properties as a potential source of neutrons for BNCT. Yield is high, typically reported in the range of 8-9 $\times$ 10^{14} n A^{-1} s^{-1} at 2.5 MeV. Neutron energy is low; at 2.5 MeV, the flux-weighted mean neutron energy is only 330 keV.

Despite nuclear advantages, lithium presents thermal challenges in a high-power-density target. The solid is preferable on account of the corrosive and mobile nature of the liquid, but its 180°C melting point necessitates careful cooling. Recent experimental attempts at using solid lithium in targets have elucidated other difficulties. Taskaev[2] operated a 10-cm-diameter planar copper-backed lithium target with a 25-kW beam, finding that blistering of the copper substrate by beam-implanted hydrogen limited target lifetime to under a day.

Linac Systems is developing a unique solid lithium target for a 2.5-MeV, 20-mA beam. In this paper we focus on the target prototype mechanical design and some results of experiment and modelling pertaining to the thermal hydraulics of the heat removal system.

TARGET DESIGN AND FABRICATION

Design Criteria and CFD Modelling

Several basic functional requirements for our target were stipulated to guide the design:

- The proton beam is an 8-cm-diameter stationary (i.e. not rastered or rotated), magnetically-expanded, "waterbag" distribution produced by an rf linac.
- Peak surface temperature must not exceed 150°C to keep lithium layer solid (including safety margin).
- Liquid water coolant will be used with inlet temperature of 20-30°C, outlet pressure of 101 kPa.
- Symmetry of target system about the beam axis is desirable to simplify neutron dosimetry and treatment planning calculations.

The concept born from these requirements consists of a 10-cm diameter conical heat exchanger with water channels on the exterior that mates with a coolant manifold. This concept is illustrated in Figure 1.

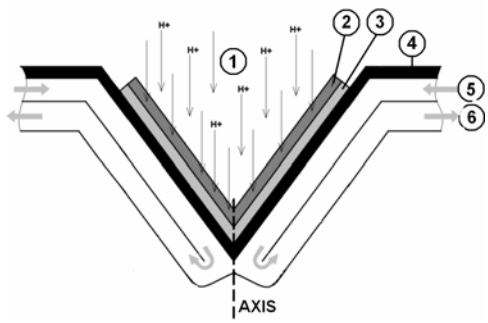

Figure 1: Protons (1) strike a 50-µm lithium metal layer (2) that is deposited on a Pd anti-blistering substrate (3), supported by a channelized conical heat exchanger (4). Coolant (5) flows through a conical-annular duct that encompasses the channels of the heat exchanger; reverses at the apex; returns via an outer conical-annular duct, and exits (6).

Design of the channelized heat exchanger was carried out with the aid of the CFD packages FLUENT, CFDesign, and COSMOS FloWorks. Simulations examined the effects of channel dimensions, number of channels, heat exchanger material, and apex-region geometry upon the coolant flow, pressure drop, and pumping power needed to meet the target surface temperature requirement. Initial studies focused on designs with straight tangential channels, but we determined that helical channels would offer superior performance (Figure 2). Copper was selected as the only viable heat exchanger material. In simulations comparing identical aluminium and copper heat exchangers, copper conferred a ~40°C target temperature improvement over aluminium for given coolant flow rates.

Modelling concluded with the acceptance of a copper heat exchanger design with 20 2-mm helical channels. According to the FloWorks models, this design will hold the target surface temperature below 150 °C by means of 80 kg min^{-1} of water flow with 170 kPa pressure drop. Such a requirement is easily met with a small centrifugal pump.

*Willis.219@osu.edu

BENT SOLENOID TUNING SIMULATIONS FOR THE COMET BEAMLINE.*

A. Kurup, Imperial College London, UK / FNAL, Batavia, USA

Abstract

The COMET experiment beamline uses bent superconducting solenoids for the muon transport and the spectrometer used to analyse the decay electrons from stopped muons. The bent solenoid includes not just a solenoid field but also a vertical dipole field. It is therefore important to have the ability to tune the field distribution. However, since the field distribution is mainly determined by the geometry it is difficult to adjust once the solenoids have been constructed. A cost effective method to provide tuning capability of the field distribution of the bent solenoids is proposed and the results of simulations presented.

INTRODUCTION

The COMET [1] experiment aims to investigate COherent Muon to Electron Transitions by nuclear capture. This requires having a very precisely controlled muon momentum spectrum on a target that will stop the muons and the electron momentum spectrum produced by coherent $\mu \rightarrow e$ transitions needs to be accurately measured. The COMET experiment utilises bent solenoids for the muon transport and the electron spectrometer. However, helical trajectories in a curved solenoid drift in the vertical direction. In order to compensate for this vertical drift an additional dipole field in the vertical direction is applied. In the COMET design this is done in a cost effective way by tilting the solenoids. The downside to using this method is that the relative magnitude of the vertical dipole field component is given by the geometry, which is fixed after the solenoid has been manufactured. It may be necessary to tune the magnitude of the vertical dipole component after manufacture to correct for manufacturing tolerances and thermal contraction due to cooling the magnets to superconducting operating temperatures.

This paper investigates the possibility of having some control over the vertical dipole component by powering alternate solenoids with a different current. The simulations presented aim to demonstrate whether this method could provide the ability to control the momentum distribution, vertical dispersion and composition of the beam at the stopping target. For these simulations, only the muon transport has been considered and only the simple scenario where all solenoids in the bent transport channel have identical geometries and only two different power supplies are used.

* This work has been supported by The Royal Society as a joint project between Imperial College London and Osaka University. The author would also like to thank the members of the COMET collaboration for all their help.

G4BEAMLINE FIELD DISTRIBUTION

Initial simulations were done using G4Beamline [2] by taking the existing baseline design of the COMET beamline. The geometry was altered to include the tilt of the solenoids but all other parameters were kept the same. Figure 1 shows the model that was simulated and Fig. 2 shows the tilt of the solenoids, which is $1.43°$. All the solenoids

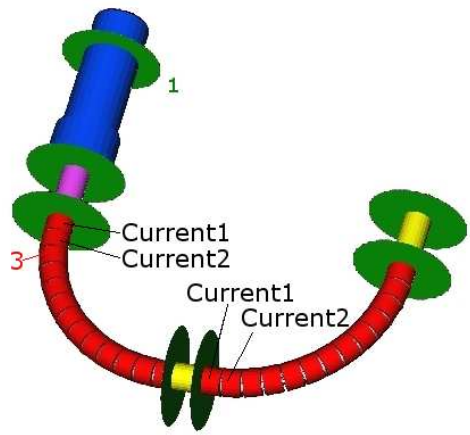

Figure 1: G4Beamline model of the muon transport channel. The blue solenoids are the pion capture channel, the red solenoids are the bent, tilted solenoids for pion decay and muon transport and the final yellow solenoids end just before the stopping target. The virtual detector (green circle) labelled 1 shows the position of the pion production target. Alternate solenoids in the transport channel (in red) were powered with a different current. Field measurements were made at the centre of the solenoid labelled 3.

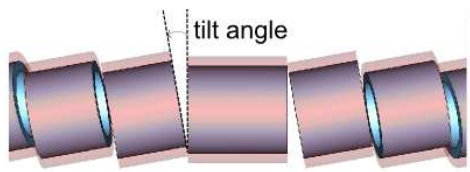

Figure 2: Drawing of the bent, tilted muon transport channel of the COMET beamline showing the tilt used to produced the vertical dipole field. The tilt angle shown here is exaggerated as the angle used in the simulations is $1.43°$.

in the G4Beamline simulations are ideal solenoids composed of infinitely-thin current sheets. Four different scenarios for powering the bent, tilted solenoids were investigated, see Table 1.

STATUS OF MICE: THE INTERNATIONAL MUON IONIZATION COOLING EXPERIMENT

Dazhang Huang#, Daniel M. Kaplan, IIT, Chicago, IL 60616 USA
Michael S. Zisman, LBNL, Berkeley, CA 94720 USA

Abstract

A key unanswered question in particle physics is why the universe consists only of matter. It is believed that CP violation in the lepton sector is the answer. The best tool to find this is a muon-based neutrino factory. Muons can also be used for an energy-frontier collider that would fit on an existing laboratory site. Since muons are produced as a tertiary beam, their phase space and energy spread are large and must be reduced (cooled) to create a usable beam. Ionization cooling, comprising momentum loss in material followed by RF reacceleration, is the only suitable technique. A transverse cooling channel is merely a linac with absorbing material in the beam path. To demonstrate an understanding of the physics and technology issues, MICE will test a section of cooling channel exposed to a muon beam derived from the ISIS synchrotron at RAL. The muon beam line is now installed and commissioning is under way. Fabrication of cooling-channel components and the required detector systems has begun. A successful demonstration will go a long way toward proving the value of muon beams for future accelerator-based particle physics experiments.

INTRODUCTION

Muon ionization cooling is the only practical method for preparing high-brilliance beams needed for a neutrino factory or muon collider. It reduces the transverse phase space of muons sufficiently to permit subsequent acceleration and storage in a practical acceleration system. This key enabling technology will be demonstrated experimentally for the first time in the Muon Ionization Cooling Experiment (MICE).

MICE is an experimental program to establish the feasibility and performance of ionization cooling. The approach is to measure precisely the emittance of 140–240 MeV/c muon beams both before and after an ionization-cooling cell. Implementing such a system will tell us about the subtleties of fabrication of the required components and, after comparing our results with detailed simulation predictions, will provide a validated tool for designing and optimizing the performance of a future neutrino factory and/or muon collider cooling channel.

The experiment is currently under construction at the Rutherford Appleton Laboratory (RAL) in the UK.

MICE BEAM LINE AND SCHEDULE

The secondary muon beam line at RAL's ISIS synchrotron is being built to meet the needs of MICE. The line will provide muon beams in the range of 140–240 MeV/c momentum, with normalized transverse emittance values in the range of 1–10 π mm-rad. The muon beam will be momentum-selected and transported to the MICE apparatus (see Fig. 1). Particle identification ensures better than 99.9% muon purity. Via magnet settings and a Pb diffuser of adjustable thickness, the transverse emittance of the input muon beam can be tuned. The input 6D emittance is measured [1] in a magnetic spectrometer comprising a five-station scintillating-fiber tracker mounted within a 4 T superconducting (SC) solenoid. The tracker determines x, x', y, y', and particle energy. The time-of-flight (TOF) counters measure the sixth phase space coordinate, t. The cooling cell consists of low-Z absorbers and normal conducting (NC) RF cavities, along with SC coils to provide strong focusing for the beam. The final emittance is measured in a second spectrometer system identical to the first one. Electrons from muon decay are eliminated from the data by calorimetry.

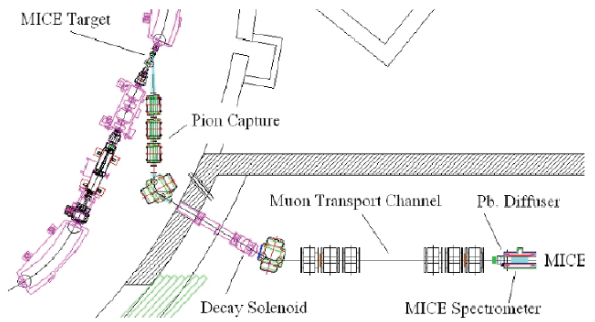

Figure 1: MICE beam line at ISIS, with two bending magnets and three quadrupole triplets.

The most important part of MICE is the cooling cell (see Fig. 2). It comprises three absorber–focus-coil (AFC) modules [2,3] and two RF–coupling-coil (RFCC) modules [4] (Fig. 3). Each hydrogen absorber contains about 20 L of liquid and is enclosed within a pair of room-temperature safety windows (Fig. 4) [5].

A pair of focus coils is employed to focus the muon beam, which results in a low equilibrium emittance for the channel. While hydrogen is best, for emittance far from equilibrium, a more practical absorption medium may be LiH, or Be. MICE is therefore designed to test both liquid and solid absorbers over a range of beta-function values. Critical hydrogen system issues are:

1. safety
2. use of the thinnest possible metal containment windows
3. hydrogen storage

A commercial metal-hydride storage system will be tested at RAL.

huangd@iit.edu

HIGH GRADIENT EXCITATION AND RF POWER GENERATION USING DIELECTRIC LOADED WAKEFIELD STRUCTURES*

M.E. Conde#, S. Antipov, F. Franchini, W. Gai, R. Konecny, W. Liu, J.G. Power, Z. Yusof,
ANL, Argonne, IL 60439, U.S.A.
F. Gao, IIT, Chicago, IL 60616, U.S.A.
C. Jing, Euclid Techlabs LLC, Solon, OH 44139, U.S.A.

Abstract

Dielectric loaded wakefield structures are being developed to be used as high gradient accelerator components. The high current electron beam at the Argonne Wakefield Accelerator Facility (AWA) was used to excite wakefields in cylindrical dielectric loaded wakefield structures in the frequency range of 8 to 14 GHz, with pulse duration of a few nanoseconds. Short electron bunches (13 ps FWHM) of up to 86 nC drove these wakefields, and accelerating fields as high as 100 MV/m were reached. Similar structures were used to extract RF power from the electron beam; however, in this case they were traveling-wave structures, driven by electron bunch trains of up to 16 bunches. RF pulses of up to 40 MW were measured at the output coupler of these structures. The AWA electron beam was also used to drive the cavity modes in a metallic standing-wave structure designed and built by SLAC / KEK (originally meant to be powered by a klystron).

INTRODUCTION

The Argonne Wakefield Accelerator Facility (AWA) is dedicated to the study of electron beam physics and the development of accelerating structures based on electron beam driven wakefields [1]. In order to carry out these studies, the facility employs a photocathode RF gun capable of generating electron beams with high bunch charges and short bunch lengths (up to 100 nC with a bunch length of 13 ps FWHM). This high intensity beam is used to excite wakefields in the structures under investigation. The wakefield structures presently under development are dielectric loaded cylindrical waveguides with operating frequencies between 8 and 14 GHz.

The facility is also used to investigate the generation and propagation of high brightness electron beams, and to develop novel electron beam diagnostics.

The AWA electron beam is also used in laboratory-based astrophysics experiments; namely, measurements of microwave Cherenkov radiation and beam induced fluorescence of air [2].

AWA FACILITY

The AWA high intensity electron beam is generated by a photocathode RF gun, operating at 1.3 GHz. This one-and-a-half cell gun typically runs with 12 MW of input power, which generates an 80 MV/m electric field on its Magnesium cathode surface. A 1.3 GHz linac structure increases the electron beam energy, from the 8 MeV produced by the RF gun, to 15 MeV. The charge of the electron bunches can be easily varied from 1 to 100 nC, with bunch lengths of 2 mm rms, and normalized emittances of 30 to 200 π mm mrad.

The AWA laser system consists of a Spectra Physics Tsunami oscillator followed by a Spitfire regenerative amplifier and two Ti:Sapphire amplifiers (TSA 50). It produces 1.5 mJ pulses at 248 nm, with a pulse length of 2 to 8 ps FWHM and a repetition rate of up to 10 pps. A final KrF Excimer amplifier is optionally used to increase the energy per pulse to 15 mJ. The generation of electron bunch trains (presently up to 16 bunches) requires each laser pulse to be divided by means of beam splitters into a laser pulse train.

HIGH GRADIENT WAKEFIELD GENERATION

We have recently built and tested four dielectric loaded wakefield structures. Each one consists of a cylindrical dielectric tube inserted into a cylindrical copper waveguide. The dielectric material is either a ceramic known as cordierite, or quartz. The insertion of metallic end-pieces with a cut-off frequency above the operating frequency, makes these devices operate as standing-wave structures. A weakly coupled field probe (-60 dB) near the outer diameter of the dielectric cylinders serves to monitor the wakefields generated by the driving electron bunches, and to verify the absence of electric breakdown. Table 1 shows some parameters of four wakefield structures tested.

Table 1: Parameters of Standing-Wave Structures

SW Structure	# 1	# 2	# 3	# 4
Material	Cordierite	Cordierite	Cordierite	Quartz
Dielectric constant	4.76	4.76	4.76	3.75
Freq. of TM01n	14.1 GHz	14.1 GHz	9.4 GHz	8.6 GHz
Inner radius	5 mm	5 mm	2.75 mm	1.9 mm
Outer radius	7.49 mm	7.49 mm	7.49 mm	7.49 mm
Length	102 mm	23 mm	28 mm	25.4 mm
Maximum charge	46 nC	86 nC	86 nC	75 nC
Maximum gradient	21 MV/m	43 MV/m	78 MV/m	100 MV/m

*Work supported by the U.S. Department of Energy under contract No. DE-AC02-06CH11357.
#conde@anl.gov

TRAINS OF SUB-PICOSECOND ELECTRON BUNCHES FOR HIGH-GRADIENT PLASMA WAKEFIELD ACCELERATION

P. Muggli, UCLA, Los Angeles, California;
M. Babzien, BNL, Upton, Long Island, New York;
M.J. Hogan, SLAC, Menlo Park, California;
E. Kallos, USC, Los Angeles, California;
K. Kusche, J.H. Park, V. Yakimenko, BNL, Upton, Long Island, New York

Abstract

In the plasma wakefield accelerator (PWFA), high quality accelerated electron bunches can be produced by injecting a witness bunch behind a single drive bunch or a train of N bunches. To operate at large gradient the plasma density must be in the 10^{17}/cc range, corresponding to a typical bunch separation of the order of the plasma wavelength or $\sim 100\mu$m. We have demonstrated that such a sub-picosecond temporal bunch structure can be produced using a mask to selectively spoil the emittance of temporal slices of the bunch*. The bunches spacing, as well as their length can be tailored by designing the mask and choosing the beam parameters at the mask location. The number of bunches is varied by using an adjustable width energy limiting slit. The bunches spacing is measured with coherent transition radiation interferometry. Experimental results will be presented and compared to simulations of the bunch train formation process with the particle tracking code ELEGANT.

* P. Muggli *et al.*, to appear in Phys. Rev. Lett. (2008).

CONTRIBUTION NOT RECEIVED

BEAM DYNAMICS SIMULATIONS FOR A 15 MEV SUPERCONDUCTING ELECTRON LINAC COUPLED TO A DC PHOTO-INJECTOR

D. Guilhem, J-L. Lemaire, S. Pichon
CEA, Département de Physique théorique et Appliquée
Bruyères Le Châtel, 91297 Arpajon, Cedex, France

Abstract

A 15 MeV accelerator scheme based on a DC photo-injector and a RF superconducting linac has been proposed as a new facility for radiography applications.
The beam operating condition is a limited number of bunches up to twenty electron micro-pulses of 100 ps time duration and 200 nC bunch charge at 352 MHz repetition rate.

The overall beam dynamics simulation process based on LANL POISSON-SUPERFISH and PARMELA codes, is presented and the results will be reviewed.

INTRODUCTION

A new versatile scheme based on well-tested technologies has been studied in the purpose to produce flash X-ray pulses from very intense electron beams impinging a high Z material target [1].
This machine consists to a DC photo-injector coupled to a RF superconducting accelerator. A final beam transport allows tight beam focusing on the target. Electrons bunches are emitted from a photocathode driven by a 266 nm wavelength laser and extracted up to the energy of 2.5 MeV in a DC gun. The beam is accelerated in a 352 MHz RF-cavity to a final energy of 15MeV (Fig. 1). Among several applications, one requires a total accelerated charge of 1µC. In this scope, we studied two beam distributions in time: either ten electron bunches carrying 100 nC each (pulse time duration of 28 ns) or five electron bunches carrying 200 nC each (pulse time duration 13 ns).

Beam dynamics have been computed using a simulation chain based on LANL codes POISSON-SUPERFISH [2] and PARMELA [2]. The optimizations of the photo-injector beam transport and the final focusing on the target are presented. The results for the whole machine simulation are reviewed for the two different configurations.

BEAM DYNAMICS CHART

Our beam dynamics study is based on the LANL POISSON-SUPERFISH and PARMELA codes. We have linked them together through a graphical interactive interface which was developed specifically for this use (Fig. 2). POISSON-SUPERFISH first computes electromagnetic field maps of the photo-injector, the RF cavity and final focusing. These results are used as input data in PARMELA to calculate the beam dynamics along the machine. We have developed coupling and post processing tools compatible with CEA-PLOTWIN software (*.plt) [3] which allows powerful, interactive and friendly viewing of the beam behaviour.

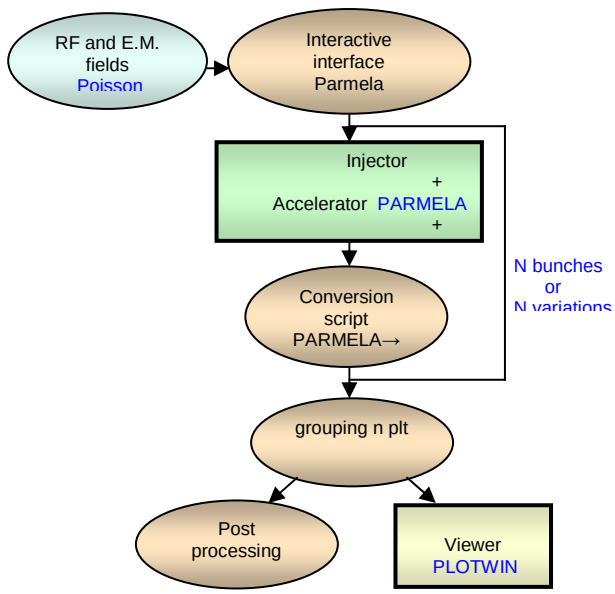

Figure 2: Beam dynamics simulation chart.

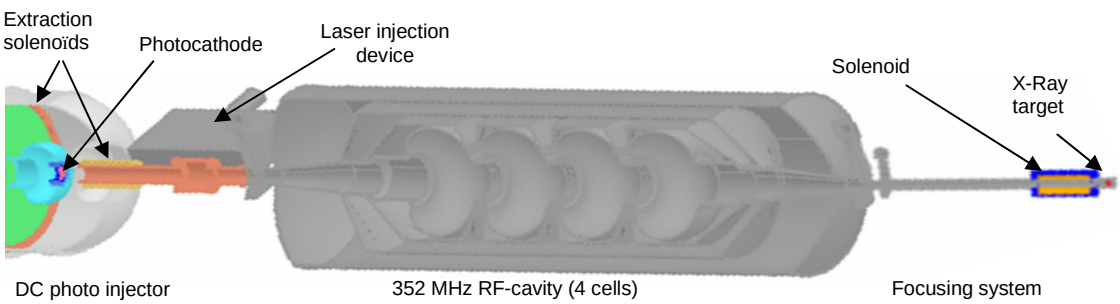

Figure 1: Scheme for the 15MeV RF proposed machine.

BEAM DYNAMICS AND ERROR STUDIES OF THE SPIRAL2 DRIVER ACCELERATOR

P. Bertrand, GANIL, Caen, France
J-L. Biarrotte, L. Perrot, CNRS / IPN Orsay, France
D. Uriot, CEA Saclay, France.

Abstract

After a detailed design study phase (2003-2004), the SPIRAL2 project at GANIL (Caen, France) was officially approved in May 2005, and is now in its phase of construction, with a project group including the participation of many French laboratories (CEA,CNRS) and international partners. The SPIRAL2 facility is composed of a multi-beam driver accelerator (5mA 40MeV deuterons, 5mA 33Mev protons, 1mA 14.5MeV/u heavy ions), a dedicated building for the production of Radioactive Ion Beams, the existing cyclotron CIME for the post acceleration of the RIBs, and new experimental areas. In this paper we focus on the beam dynamics and error studies dedicated to the SPIRAL2 accelerator part of the project, from the ECR sources to the High Energy Beam Lines which have been recently updated.

INTRODUCTION

The SPIRAL2 facility is now in its construction phase with huge progress for many parts of the machine as explained in [1]. In parallel, many beam dynamics calculations have been performed in order to extend the possibilities of the accelerator, and to take into account new demands of experimental physics.

As indicated table 1, the Spiral2 accelerator will deliver a huge variety of beams, at various intensities and energies, which constitutes a great challenge.

Table 1: Beam Specifications

beam	P+	D+	ions	ions
Q/A	1	1/2	1/3	1/6
Max. I (mA)	5	5	1	1
Min. output W (Mev/A)	2	2	2	2
Max output W (Mev/A)	33	20	14.5	8
CW Max. beam power (kW)	165	200	44	48

Our beam dynamics reference program is the well known TRACEWIN code [2]. It allows us to simulate the machine from the source to the final target, with a huge number of pseudo-particles. All the simulations can use 3D electromagnetic maps of magnets and cavities which are presently under construction, and the beam optimization uses the set of diagnostics which will be effectively used in the real machine. Moreover we project to incorporate (part of) TRACEWIN into the control system as an essential component of the tuning process.

SPIRAL2 INJECTOR

LEBT Lines and RFQ

The beam dynamics of the LEBT has been explained in detail in [3] and there is no recent modification. However we have investigated in detail the behaviour of the beam for various estimated values of the space charge compensation: this aspect is crucial when we manage the duty cycle and keep perfect bunches with a combination of ECR source, slow chopper and RFQ pulsations.

The 88 MHz 4-vane RFQ accepts charge/mass ratio between 1 and 1/3, and is designed for a very high transmission, in particular in the case of Deuterons at full intensity. We have checked that the 99% transmission was kept with or without space charge.

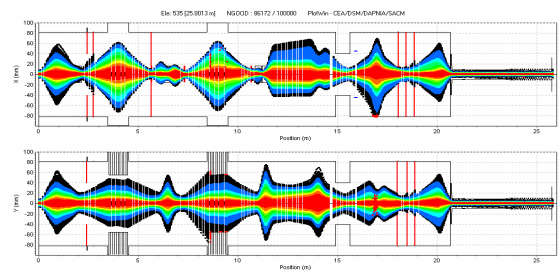

Figure 1: LEBT transport and RFQ acceleration for 1mA 1/3 heavy ions.

MEBT Line

The SPIRAL2 MEBT (Fig. 2) is a complex 8 meters transfer line with the following fundamental functions:

- Transverse/longitudinal matching into the linac
- Fast chopping system and associated beam stop
- Drift for a future connexion of a q/A=1/6 injector
- Movable slits for halo elimination.

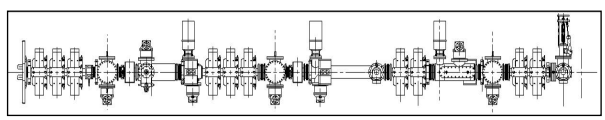

Figure 2: SPIRAL2 MEBT design.

The MEBT beam energy is fixed to 0.75 Mev/u, which corresponds to 7.5 kW for 5mA D+. Beam dynamics have been performed for all types of ions, using particle distributions from LEBTs and the RFQ, using quadrupole and rebuncher 3D maps and with linac matching (fig.3).

Calculations with use of the fast chopper have been performed in parallel with the development of the device.

BEAM DYNAMICS SIMULATION OF THE LOW ENERGY BEAM TRANSPORT LINE FOR IFMIF/EVEDA

N. Chauvin*, O. Delferrière, R. Duperrier, R. Gobin, P.A.P. Nghiem, D. Uriot,
CEA, IRFU, F-91191 Gif-sur-Yvette, France.

Abstract

The purpose of the IFMIF-EVEDA (International Fusion Materials Irradiation Facility-Engineering Validation and Engineering Design Activities) demonstrator is to accelerate a 125 mA cw deuteron beam up to 9 MeV. Therefore, the project requires that the ion source and the low energy beam transport (LEBT) line deliver a 140 mA cw deuteron beam with an energy of 100 keV and an emittance of 0.25 π.mm.mrad (rms normalized) at the entrance of the RFQ. The deuteron beam is extracted from a 2.45 GHz ECR source based on the SILHI design. A LEBT with a two solenoids focusing system is foreseen to transport and adapt the beam for the RFQ injection. In order to validate the LEBT design, intensive beam dynamics simulations have been carried out using a parallel implementation of a particle-in-cell 3D code which takes into account the space charge compensation of the beam induced by the ionization of the residual gas. The simulations results (in particular from the emittance growth point of view) performed under several conditions of gas species or gas pressure in the beam line are presented.

INTRODUCTION

The International Fusion Materials Irradiation Facility (IFMIF) will produce a high flux (10^{18}n.m^{-2}.s^{-1}) of 14 MeV neutron dedicated to characterization and study of candidate materials for future fusion reactors. A solution based on two high power cw accelerator drivers, each delivering a 125 mA deuteron beam at 40 MeV to a liquid lithium target, is foreseen [1].

In the first phase of IFMIF, called EVEDA (Engineering Validation and Engineering Design Activities), a 125 mA cw/9 MeV deuteron demonstrator accelerator will be constructed, tested and operated at Rokkasho-mura, in Japan [2]. This accelerator is composed by an ECR (Electron Cyclotron Resonance) ion source, a low energy beam transport (LEBT) line, a RFQ (100 keV to 5 MeV) [3], a matching section, a superconducting Half Wave Resonator cavities section (5 MeV to 9 MeV), and a high energy beam line equiped with diagnostic plate and a beam dump. This paper will focused on the LEBT section of the EVEDA project.

The purpose of the LEBT is to transport the 140 mA/100 keV deuteron beam extracted from the ECR source to the RFQ. In order to design the LEBT parameters and to optimize the beam injection in the RFQ, beam dynamics simulations have been performed.

* Nicolas.Chauvin@cea.fr

LOW ENERGY BEAM LINE LAYOUT

ECR Ion Source and Extraction System

The beam intensity and reliability required for the IFMIF project have lead to the choice of an ECR ion source to produce the deuteron beam. The IFMIF source, based on the SILHI design, will operate at 2.45 GHz [4]. The extraction system has been optimized to increase the total beam intensity from 150 mA to 175 mA in order to meet the 140 mA D^+ requirements, as D_2^+ and D_3^+ are also produced in the ECR source. The extraction energy has also been increased from 95 keV to 100 keV, and a four electrode system has been calculated to minimize the D^+ divergence. In order to decrease the risk of high voltage breakdown, the maximum of the extraction electric field has been kept around 100 kV/cm.

Table 1: Beams Parameters after the Extraction System

Extracted Species	Intensity (mA)	Emittance (π mm.mrad)
D^+	141	0.064
D_2^+	26.5	0.043
D_3^+	8.8	0.042

The particle distributions after the source are derived from their tracking through the extraction system. Those beam distributions, of which main parameters are summarized in table 1, have been taken as inputs for the LEBT simulations. More precisely, the simulations start with a part of source extraction system, computed with AXCEL-INP [5], in order to get relevant boundary condition.

Low Energy Beam Transport Line

The optics for the LEBT is based on a dual solenoids system. The 3D magnetic field maps of the solenoids (pole length: 300 mm), computed by finite elements method, have been included in the simulations.

The total length of the beam line, from the plasma electrode to the RFQ entrance is 2.05 m (see Fig.1). A pumping system and beam diagnostics as movable Faraday cup and emittance measurement could be inserted between the two solenoids. A regulating valve is also foreseen in order to inject a controlled flux of a specific gas in the beam line.

PARAMETER DESIGN AND BEAM DYNAMICS SIMULATIONS FOR THE IFMIF-EVEDA ACCELERATORS

P. A. P. Nghiem*, N. Chauvin, O. Delferrière, R. Duperrier, A. Mosnier, D. Uriot,
CEA/DSM/IRFU, 91191 Gif-sur-Yvette Cedex, France
M.Comunian, INFN/LNL, Legnaro, Italy. C. Oliver, CIEMAT, Madrid, Spain.

Abstract

One major system of IFMIF (International Fusion Materials Irradiation Facility) is its accelerator facility, consisting of two 175 MHz CW accelerators, each accelerating a deuteron beam of 125 mA to the energy of 40 MeV. This high power beam, 10 MW, induces challenging issues that lead to plan a first phase called EVEDA (Engineering Validation and Engineering Design Activity), where only the portion up to 9 MeV of one accelerator will be constructed and tested. For these accelerators, the Parameter Design phase is about to be completed. Particular efforts have been dedicated to minimise the space charge effect that can strongly increase the beam size via the halo, and the losses that can prohibit the requested hand-on maintenance. This paper presents the status of these studies.

INTRODUCTION

In the future Fusion Demonstration Reactor (DEMO), the materials surrounding the plasma will be submitted to a very intense neutron flux, so that their atoms can be displaced up to hundreds of times more than with those of present fusion materials. In order to test and qualify the material behaviour under such severe irradiations, the International Fusion Materials Irradiation Facility (IFMIF) is planned, with the purpose of delivering an intense neutron flux, generated by the impact of an accelerated deuteron beam on a liquid lithium target. One major system of IFMIF is its accelerator facility, consisting of two 175 MHz CW accelerators, each accelerating a deuteron beam of 125 mA to the energy of 40 MeV. The total power delivered at the target is 10 MW. One important challenging specification of these accelerators is therefore their very high intensity, which must nevertheless be reconciled with the requested hands-on maintenance imperative. That is why a first phase called Engineering Validation and Engineering Design Activity (EVEDA) is now starting, where a prototype accelerator will be constructed and tested, consisting of only the portion up to 9 MeV of one IFMIF accelerator. For these accelerators, the parameter design and beam dynamics simulations are now well engaged. Two topics have been particularly scrutinised: characterisation and minimisation of the space-charge effect, very critical in the low energy part, and of the losses, very critical in the high energy part. Different solutions have been studied, and the choices between them are either done or underway. In this paper, after having given the general layout, the status of those studies is presented for each accelerator section.

LAYOUT & CHALLENGING ISSUES

The layout and general parameters of IFMIF and EVEDA accelerators are given in Fig.1. D+ particles are extracted from the ion source at 100 keV, then properly focused by the LEBT in order to be injected into the RFQ where they are bunched and accelerated to 5 MeV. The MEBT matches the RFQ output beam in transverse and longitudinal to that required by the superconducting HWR-Linac. Composed of 4 cryomodules housing solenoids and accelerating cavities, the Linac accelerates particles to the final energy of 40 MeV, where the HEBT transports the beam to the lithium target while giving it the required dimensions and homogeneity. For the prototype accelerator, only the first cryomodule will be constructed, and a special HEBT sends the resulting 9 MeV beam with the right dimensions to a beam dump, while allowing to measure its characteristics.

For Beam dynamics studies, the TraceWin package code(including PARTRAN and TOUTATIS) [1] is used as the common code between the different sections, where multiparticle trackings are performed under a strong space charge regime. Given the very high

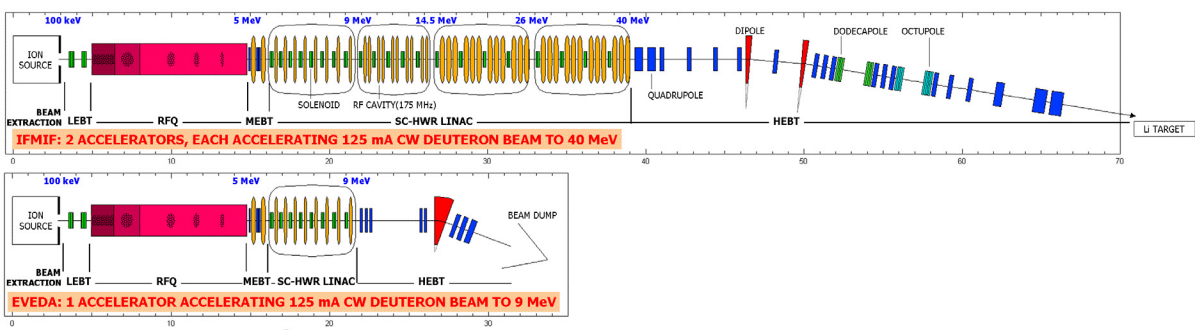

Figure1: General layout of the IFMIF-EVEDA accelerators.

BEAM DYNAMICS SIMULATIONS OF SUB-PS ELECTRON BUNCH PRODUCED IN A PHOTO-INJECTOR

R. Roux
LAL, bâtiment 200, Université Paris-Sud, 91898 Orsay, France.

Abstract

A growing number of experiments require low emittance ultra-short electron bunches in the 100 fs range (rms value) for the production of coherent light or the injection into a plasma for laser-plasma acceleration. Especially in the last case it is highly desirable to have a compact accelerator; hence a strong experimental activity is carried out to get such a beam directly from a photo-injector. We have performed beam dynamic simulations using the PARMELA code to study the performances of the alphaX photo-injector installed in the University of Strathclyde in UK*. This RF gun is aimed to produce electron bunches which have 100 pC of bunch charge, 100 fs bunch length and 1 π mmmrad transverse emittance. We will show the results of systematic parametric studies as a function of charge and laser pulse duration as well as the natural evolution of the beam phase space as a function of the distance from the photo-cathode.

INTRODUCTION

Up to now the preferred way to get very short bunch is to use a magnetic chicane but this could lead to a degradation of the emittance due to the emission of coherent synchrotron radiation. Moreover it is difficult to make a compact beamline in such a scheme. Some experiments as alphaX [1] in the University of Strathclyde strive to produce X ray in the SASE [2] regime with a very short accelerator which the length is roughly 7 meters. The idea is to inject a very short electron bunch coming from a photo-injector into a laser-plasma [3] accelerating cell to bring it at 1 GeV over few millimeters instead of ≈ 30 m in classical linear accelerators. In order to get an efficient acceleration in the plasma, the specification on the bunch length must be absolutely fulfilled. So the purpose of this study is to investigate the behaviour of sub-ps electron bunches directly issued from the photo-injector using numerical simulations.

PARMELA SIMULATIONS

PARMELA is a well-known code used for beam dynamics in linacs which takes into account the space charge force effect. It was created by Los Alamos National Laboratory and modified at LAL by B. Mouton to include, for instance, the photo-injectors.

*We acknowledge the support of the European Community-New and Emerging Science and Technology Activity under the FP6 "Structuring the European Research Area" programme (project EuroLEAP, contract number 028514).

AlphaX Photo-injector

The alphaX photo-injector is made of 2.5 cells at 3 GHz resonant frequency. This gun designed at the Eindhoven University of Technology [4] exhibits two noticeable features. First, the shape of irises is elliptical because, according to the RF simulations, the surface electrical field is reduced by a factor 2 with respect to the more usual cylindrical shape. So one hopes to operate the gun at gradient higher than 100 MV/m without electrical breakdowns. Secondly the RF power is sent to the gun via a coaxial "doorknob" antenna in a coupler at the output of the gun. In this way the gun keeps a perfect cylindrical symmetry in order to avoid possible degradation of the emittance rising in non-symmetric coupling.

Simulations in PARMELA are performed with the electrical field of alphaX calculated with the 2D RF code SUPERFISH. Results are shown in table 1 for 6000 macro-particles used in the simulation.

Table 1: Results of PARMELA simulations at the output of the gun, input parameters are (rms value): Q = 100 pC, laser has a Gaussian profile, radius = 1.4 mm cut at 10 mm and pulse duration = 100 fs cut at 500 fs. The peak electrical field is 92 MV/m and the phase is chosen to optimise the energy gain, rms value.

Beam radius (mm)	3.1
Bunch length (fs)	206
Energy (MeV)	6.2
Normalized Emittance (πmmmrad)	4.2
Energy spread (%)	0.172

In this case the specifications are not fulfilled, the emittance being 4 times higher and the bunch length 2 times bigger. About the emittance there is a way to significantly reduce the effect of the space charge forces thanks to a uniform transverse profile instead of a Gaussian shape for the laser. The same technique can be applied along the longitudinal axis. But before to show the results of the improvements with a square distribution, one may wonder about the validity of these calculations. Indeed most of simulations are usually performed with electron bunches which the length is in the picosecond range.

Test of PARMELA

Up to now there are no measurements of sub-ps bunches produced directly from the gun to compare with PARMELA simulations. But it is possible to check if the results of PARMELA are at least in agreement with the

BENCHMARKING OF MEASUREMENT AND SIMULATION OF TRANSVERSE RMS-EMITTANCE GROWTH ALONG AN ALVAREZ DTL

L. Groening, W. Barth, W. Bayer, G. Clemente, L. Dahl, P. Forck, P. Gerhard,
I. Hofmann, G. Riehl, S. Yaramyshev, GSI, D-64291 Darmstadt, Germany
D. Jeon, SNS, ORNL, Oak Ridge, TN 37831, USA
D. Uriot, CEA IRFU, F-91191 Gif-sur-Yvette, France

Abstract

Transverse emittance growth along the Alvarez DTL section is a major concern with respect to the preservation of beam quality of high current beams at the GSI UNILAC. In order to define measures to reduce this growth appropriate tools to simulate the beam dynamics are indispensable. This paper is on benchmarking of three beam dynamics simulation codes, i.e. DYNAMION, PARMILA and PARTRAN against systematic measurements of beam emittance growth for different machine settings. Experimental set-ups, data reduction, the preparation of the simulations, and the evaluation of the simulations will be described. It was found that the mean value of final horizontal and vertical rms-emittance can be reproduced well by the codes.

INTRODUCTION

In the last decades many beam dynamics computer codes were developed [1] in order to simulate emittance growth along a linac. Several benchmarking studies among codes have been performed [2, 3, 4] generally assuming idealized conditions as initial Gaussian distributions, equal transverse emittances, matched injection into a periodic lattice, and small longitudinal emittance with respect to the rf-bucket size. In case of an operating linac most likely non of these conditions is met. To apply simulation codes to a realistic environment a benchmark activity was started aiming at the simulations of beam emittance measurements performed at a DTL entrance and exit, respectively. The studies were performed at the GSI UNILAC [5]. For the simulations three different codes were used: DYNAMION [6], PARMILA (V 2.32) [7], and PARTRAN [8]. A more detailed description of the campaign is given in [9].

EXPERIMENT SET-UP AND PROCEDURE

Intense beams are provided by MEVVA, MUCIS, or CHORDIS sources at low charge states with the energy of 2.2 keV/u. An RFQ followed by two IH-cavities (HSI section) accelerates the ions to 1.4 MeV/u using an rf-frequency of 36 MHz. A subsequent gas-stripper increases the average charge state of the ion beam. Final acceleration to 11.4 MeV/u is done in the Alvarez DTL section operated at 108 MHz. The increase of rf-frequency by a factor of three requires a dedicated matching section preceding the DTL. It comprises a 36 MHz buncher for longitudinal bunch compression, a 108 MHz buncher for final bunch rotation, a quadrupole doublet for transverse compression, and a quadrupole triplet for final transverse beam matching.

The Alvarez DTL comprises five independent rf-tanks. Transverse beam focusing is performed by quadrupoles in the F-D-D-F mode. Each drift tube houses one quadrupole. The periodicity of the lattice is interrupted by four inter-tank sections, where D-F-D focusing is applied. Acceleration is done -30° from crest in the first three tanks and -25° from crest in the last two tanks.

Figure 1 presents the schematic set-up of the experiments. Beam current transformers are placed in front of

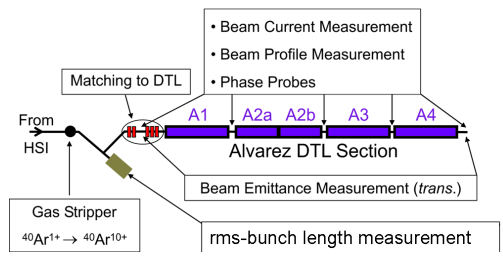

Figure 1: Schematic set-up of the experiments.

and behind the DTL as well as horizontal and vertical slit/grid emittance measurement devices. The total accuracy of each rms-emittance measurement including its evaluation is estimated to be 10%. A set-up to measure the longitudinal rms-bunch length is available in front of the DTL [10]. It measures the time of impact of a single ion on a foil. This time is related to a 36 MHz master oscillator. The resolution is 0.3° (36 MHz).

The HSI was set to obtain 7.1 mA of $^{40}Ar^{10+}$ in front of the DTL being space charge equivalent to the UNILAC design beam of 15 mA of $^{238}U^{28+}$. Horizontal and vertical phase space distributions were measured in front of the DTL. The longitudinal rms-bunch length was measured at the entrance to the DTL. The DTL quadrupoles were set to zero current transverse phase advances σ_o ranging from 35° to 90° in steps of 5°. Due to space charge the phase advances in all three dimensions were depressed. The transverse depression reached from 21% (90°) to 43% (35°). Afterwards the quadrupoles and bunchers preceding the DTL were set to obtain full transmission and to minimize low energy tails of the beam. For each value of σ_o hori-

INTEGRATION OF FRINGE FIELD ALPHA MAGNETS INTO THE V-CODE BEAM DYNAMICS SIMULATION TOOL*

Sylvain Franke**, Wolfgang Ackermann, Bastian Steiner, Thomas Weiland,
Technische Universität Darmstadt, Institut für Theorie Elektromagnetischer Felder,
Schlossgartenstraße 8, 64289 Darmstadt, Germany,

Joachim Enders, Christoph Heßler, Yuliya Poltoratska,
Technische Universität Darmstadt, Institut für Kernphysik,
Schlossgartenstraße 9, 64289 Darmstadt, Germany

Abstract

The design process and the operation of particle accelerator machines can advantageously be assisted by fast online beam dynamics simulations because of its flexible parameter variation combined with nearly simultaneous solution responses providing a detailed insight into the actual machine status. Based on the moment approach a fast tracking code named V-Code has been implemented at TEMF. At the Superconducting DArmstädter LINear ACcelerator S-DALINAC the V-Code is used during the design process of the injector for the new 100 keV polarized electron source but is also supposed to be employed at the control system. For these purposes an implementation of fringe field alpha magnets is mandatory. In this paper a summary of issues regarding the implementation complemented with simulation results will be provided.

INTRODUCTION

At the Superconducting DArmstädter LINear ACcelerator (S-DALINAC) a new 100 keV polarized electron source is currently being installed. Therefore, a new low energy injection concept has to be designed. The most important components of the injector are a polarized electron source, an alpha magnet and a Wien filter used for spin rotation together with various beam forming elements. The polarized electrons extracted vertically from a photo cathode are bent into the horizontal injector beam line with the help of an alpha magnet. Unlike a classical alpha magnet designed as a half quadrupole given for example in [1], the hyperbolic poles of the installed alpha magnet are supplemented by a dipole like extension in order to achieve a 90° bending angle. In Fig. 1 a schematic computational model of the realized alpha magnet is visualized. Within the V-Code simulation tool the beam line is represented as a consecutive alignment of separate independent beam line elements. This procedure allows to simulate even a very long beam line with minimum requirements to the computer memory. In order to be able to simulate the hole injector an implementation of alpha magnets was missing so far.

* Work supported by DFG through SFB 634.
** franke@temf.tu-darmstadt.de

NUMERICAL MODEL

The V-Code simulation tool is based on the moment approach to beam dynamics. Instead of using the particle distribution itself this method applies a discrete set of moments of the particle distribution. The time evolution of each moment can be deduced from the VLASOV equation when suitable initial conditions are given and all essential external forces are known. These forces are given by the LORENTZ equation in combination with the distribution of electric and magnetic fields obtained during a preprocessing step.
The required three-dimensional field distribution in the immediate vicinity of the particle trajectory can be reconstructed from extracted one-dimensional field components by means of a TAYLOR series expansion. This allows to considerably reduce the size of the required field data inside a specific beam line element.
A precise description of the numerical model is given in [2]. Details about its implementation in V-Code are published for example in [3] and [4].

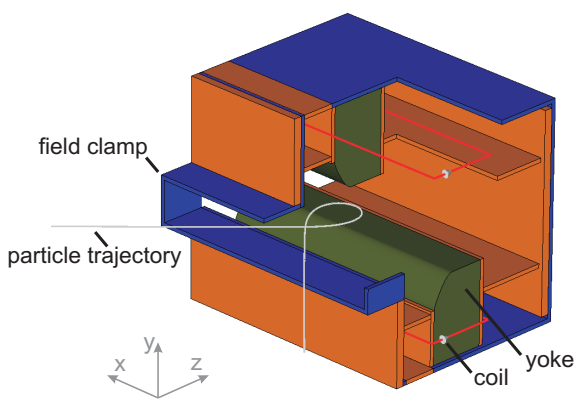

Figure 1: Schematic computational model of an α-magnet including the excitation coils and the high permeable yoke. For visualization reasons the upper corner of the housing and the yoke have been cut away. Additionally, a typical particle trajectory is specified as a reference path.

BEAM DYNAMICS STUDIES ON THE EURISOL DRIVER ACCELERATOR

A. Facco, A. Balabin, R. Paparella, D. Zenere, INFN-Laboratori Nazionali di Legnaro, Padova, Italy; D. Berkovits, J. Rodnizki, SOREQ, Yavne, Israel; J. L. Biarrotte, S. Bousson, A. Ponton, IPN Orsay, France; R. Duperrier, D. Uriot, CEA/Saclay, France; V. Zvyagintsev, TRIUMF, Vancouver, Canada

Abstract

A 1 GeV, 5 mA cw superconducting proton/H^- linac, with the capability of supplying cw primary beam to up to four targets simultaneously by means of a new beam splitting scheme, is under study in the framework of the EURISOL DS project which aims to produce an engineering-oriented design of a next generation European Radioactive beam facility. The EURISOL driver accelerator would be able to accelerate also a 100 μA, ^{3}He beam up to 2.2 GeV, and a 5 mA deuteron beam up to 264 MeV. The linac characteristics and the status of the beam dynamics studies will be presented.

INTRODUCTION

The EURISOL-DS project [1] aims at the design of a last generation Radioactive Ion Beam (RIB) facility for nuclear physics experiments, based on the ISOL method, to be constructed in Europe [2]. This facility is based on a 1 GeV, 5 mA primary proton beam feeding 4 RIB production targets. One of them (the high power target) will include a 4 MW neutron converter, able to receive most of the beam power and to create an intense neutron flux to the RIB target. The three remaining ones will accept a proton beam up to 100 kW for RIB production through direct reactions. The radioactive ions will be then extracted from the sources, selected and post-accelerated to the required energy (up to 150 MeV/A) by means of a superconducting linac.

One of the main requirements for the driver accelerator is the possibility of feeding more than one target in parallel, possibly in cw mode with finely tunable intensity to avoid destructive thermal shocks. No apparatus was available for this operation when the EURISOL-DS study started.

New requirements for the Driver, proposed after the first year of studies by the Beam Intensity Calculations Task group with the aim of opening new lines of experiments, are the possibility of delivering to the direct targets a 2 GeV, 100 μA ^{3}He beam, and to a new target station a 250 MeV, 5 mA deuteron beam. This could be accomplished with a rather limited effort taking advantage of the structure of the EURISOL Driver, based on short, independently phased cavities, which allows a rather wide beam velocity acceptance.

EURISOL DRIVER LAYOUT

The EURISOL Driver is a superconducting (SC) linac that includes 5 different sections: Injector, Low-β section, medium-β section, high-β section and CW Beam Splitter (Fig. 2). The lengths of the injector and of the SC part are 12 m and 247 m, respectively, while the 4-way beam splitting section is 55 m long. An additional extraction sector is located at the beginning of the high-β section, giving a beam line for 264 MeV deuterons. All cryostats are planned to work at 4.5K.

Injector

The injector design is rather similar to the SARAF one [3], with modifications required by the different beam types (Fig. 1). Two ion sources are used. The first one is a TRIUMF-type multicusp H^- source [4], located in the straight LEBT line. The second one is an ECR source for production of Deuterons (5 mA) and doubly charged ^{3}He (0.1 mA) beams, located in the 90° LEBT branch to allow A/q selection. The minimum beam parameters at the sources output are listed in Table 1.

Table 1: LEBT Input Beams Specifications

beam	H^-	$^3He^{++}$	D^+
E (keV/A)	20	20	20
I (mA)	6	0.2	6
ε_x, ε_y (π mm mrad rms norm.)	0.125	0.125	0.1

The LEBT includes 6 solenoids and one dipole. An electron trap is foreseen at the RFQ injection.

The 176 MHz RFQ, resembling the SARAF one, is 3.8 m long and must be able to operate in cw mode. It allows acceleration up to 1.5 MeV/A, requiring a maximum power of 300 kW for acceleration of the Deuteron beam.

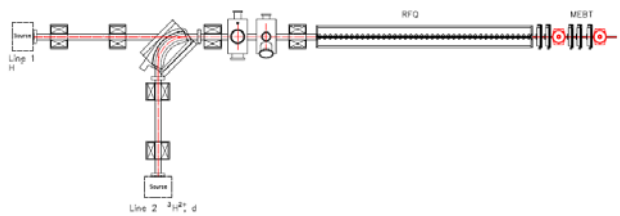

Figure 1: Injector RFQ and MEBT schematic layout.

Little emittance growth and relatively small size and cost are its main characteristics, at the price of a not spectacular transmission (92% accelerated beam for H^- and 95 % for D and ^{3}He). However, this appears to be fully acceptable for our application. The transmitted, but not accelerated RFQ particles (about 3%) are lost in the MEBT which is used to match the RFQ beam to the superconducting linac in order to prevent halo formation. The MEBT includes 5 quadrupole magnets and 2 normal conducting HWR bunchers.

TRANSVERSE BEAM MATCHING AND ORBIT CORRECTIONS AT J-PARC LINAC

H. Sako#, A. Ueno, T. Ohkawa, Y. Kondo, T. Morishita, JAEA, Tokai, Japan
M. Ikegami, H. Akikawa, KEK, Tsukuba, Japan

Abstract

In high intensity H^- beam of J-PARC LINAC, precise control of transverse beam dynamics is extremely important to suppress beam loss. Transverse matching has been performed at several matching sections in LINAC, which consist of knob quadruple magnets (QM's) and wire scanners (WS's) for profile measurements. Mismatch factors of less than 5% have been achieved. Matching of Twiss parameters and dispersion at the RCS injection point has been also done with quadruple magnets at L3BT injection region with beam profiles measured with WS's and also multi-wire profile monitors (MWPM's) at RCS. Orbit corrections along the whole LINAC have been done with steering dipole magnets in the upstream of beam position monitors (BPM's). Orbit deviations were suppressed within 1mm in the whole LINAC.

TRANSVERSE MATCHING

The strategy of the LINAC transverse matching is as follows;

1. At MEBT1, we fit transverse and longitudinal Twiss parameters and emittance at the MEBT1 entrance.
2. Then, using the beam parameters, an initial QM field pattern at matching sections through LINAC and electric field and phase settings of Buncher 1 and 2 at MEBT1 is calculated requiring matching conditions with a model (TRACE3D).
3. Applying the calculated settings to QM's and Bunchers, we measure beam profiles from most upstream (MEBT1) to most downstream (L3BT injection section) in turn at each matching section. At sections after MEBT1 QM field is corrected to fulfil matching conditions.

The LINAC has 7 matching sections, each of which consists of 4 or more upstream QM's and 4 or more downstream WS's. At MEBT1, only fitting of initial beam parameters is done. At RCS injection section, special matching procedure is performed which is described later. At the rest of matching sections; SDTL entrance, MEBT2, L3BT straight, L3BT arc, L3BT collimator sections, lattices are periodic at each WS position; where the following common procedure has been applied.

1. Fit the XAL online model [2, 3] to measured horizontal and vertical beam widths at 4 WS's by varying (α_x, α_y, β_x, β_y, ε_x, ε_y) at an upstream position from the QM's. The fit is done with a response matrix calculated with the model.
2. Corrections of 4 QM field are calculated to require that α_x, α_y, β_x, β_y agree at each WS. The calculation is done by applying the response matrix calculated with XAL [2].
3. The above procedures 1 and 2 are iteratively applied until convergence.

In MEBT1, Procedure 1 is replaced by 1';

1'. In addition to transverse parameter (α_x, α_y, β_x, β_y, ε_x, ε_y), longitudinal parameters (α_z, β_z, ε_z) are varied to fit simultaneously beam widths at 4 WS's at MEBT1 and transverse emittance and Twiss parameters measured at a double-slit emittance monitor at MEBT1 bend line [4].

In L3BT injection section, Procedure 2 is replaced by;

2'. QM's after the collimator section (L3BT QM62-79) are used to tune transverse Twiss parameters and dispersion at the RCS injection point of the charge exchange foil.

These procedures are done with a newly developed application called "matcher" [2].

SDTL to L3BT Collimator Sections

Measured emittance is shown in Fig. 1 at 5 mA and 30 mA at all sections. At 5 mA, measured 1 σ emittance at 5 mA is 0.17 πmm-mrad and 0.25 πmm-mrad at 30 mA.

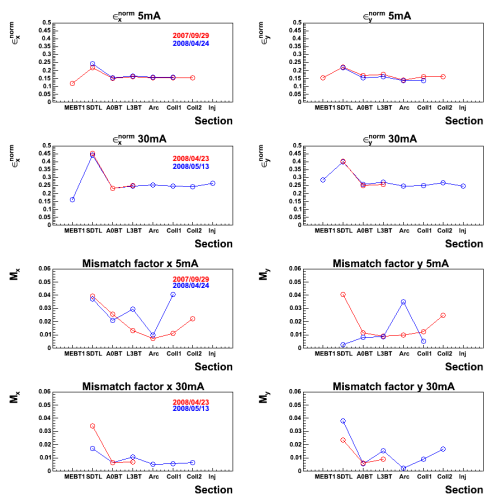

Figure 1: Normalized 1 σ emittance at 5mA (first row) and 30 mA (second row) in horizontal (left) and vertical (right) directions. Mismatch factors at 5 mA (third row) and 30 mA (forth row) in horizontal (left) and vertical directions (right).

Red and blue lines show matching results at two different periods, which proves good reproducibility of the matching procedure. Emittance growth at the SDTL entrance has been observed 5 mA and more enhanced at 30 mA. Mismatch factors of less than 5% have been achieved at 5 mA and 30 mA.

DEVELOPMENT OF MODULATING PERMANENT MAGNET SEXTUPOLE LENS FOR FOCUSING OF PULSED COLD NEUTRONS*

Masako Yamada, Yoshihisa Iwashita, Masahiro Ichikawa, Hiromu Tongu, Hiroshi Fujisawa (ICR, Kyoto University, Uji Kyoto Japan), Hirohiko M. Shimizu, Takashi Ino, Kenji Mishima, Kaoru Taketani, Takahiro Morishima, Suguru Mutou, Tamaki Yoshioka (KEK, Ibaraki Japan), Takayuki Oku, Kenji Sakai, Takenao Shinohara, Jun-ichi Suzuki (JAEA, Ibaraki, Japan), Katsuya Hirota, Yoshie Otake, Hiromi Sato (RIKEN, Wako, Saitama), Yoshichika Seki (Kyoto University, Kyoto), Sinsuke Kawasaki, Hidetoshi Otono, Sachio Komamiya (The University of Tokyo), Satoru Yamashita, Yoshio Kamiya (ICEPP, Tokyo), Peter Geltenbort (ILL, Grenoble, France)

Abstract

Cold neutron beams can be focused by a strong sextupole magnetic field. A permanent magnet sextupole lens whose focusing strength can be synchronously modulated at the rate of pulsed cold neutron beams is under development. This device should keep the focal point for pulsed neutron beams whose wavelength spreads as a function of time of flight. This kind of device improves the utilization of valuable neutrons and saves experiment time and costs. It will raise linac based small neutron sources as a good counter part to large powerful neutron facilities. Experimental results that were obtained at Institute Laue-Langevin (ILL) are also described.

INTRODUCTION

Neutron beams are well known as powerful probes for both material science and fundamental physics. The applicable research field, however, is limited by the low intensity of the neutron beams. Meanwhile, the efficiency of a neutron beam has recently been much improved by techniques such as neutron optics [1-6], time of flight (TOF) method, and so on.

Among such neutron optics devices, a magnetic lens can focus neutron beams on such targets as samples and/or detectors by using interaction between the neutron's magnetic dipole moment and the sextupole field. When we apply the TOF method to pulsed neutrons for increasing the efficiency of each experiment, the wavelength range to be covered is in the order of a few times. The time dependence of the wavelength λ is proportional to t (time of flight of a neutron). Then we should modulate the field gradient proportional to t^{-2} in order to keep the focal length Z_f fixed independent of λ. With these aspects, we are developing a modulating permanent magnet sextupole lens (PMSx) for focusing of pulsed neutron beams with chromatic aberration suppressed. The sextupole lens is composed of permanent magnets (NdBFe) because they can generate a strong magnetic field within limited space.

This lens increases the intensity of neutron beams on a target to reduce an experiment time with sufficient count rate and to increase the spatial resolution. Then neutron probe applications can be widely extended, for example, even the linac-based small neutron source now under development becomes practical.

FOCUSING OF PULSED NEUTRONS BY SEXTUPOLE MAGNET

The origin of the focusing force is the interaction between neutron's magnetic dipole moment and the external magnetic field [7-9]. A sextupole component of magnetic field B can be written as:

$$|B| = G'/2\left(x^2 + y^2\right) \qquad (1)$$

where G' is a positive value indicating the strength of the gradient of magnetic field. In the sextupole field, neutrons feel the thrusting force proportional to the distance from the magnetic centre and their equation of motion is a simple harmonic oscillator described as

$$\frac{d^2x}{dt^2} = -\omega^2 x, \quad \frac{d^2y}{dt^2} = -\omega^2 y, \quad \frac{d^2z}{dt^2} = 0 \qquad (2)$$

where $\omega^2 = G'\alpha$, $\alpha = |\mu_n/m_n| = 5.77$ m^2 s^{-2} T^{-1}, μ_n is magnetic dipole moment and m_n is the mass of neutron, in case the neutron spin is parallel to the local magnetic field [7-8]. When the ambient magnetic field is strong and changes slow enough (adiabatic condition), the spin direction follows the magnetic field direction. Because the magnetic dipole moment of the neutron is connected to the spin, the polarity of the force changes in accordance

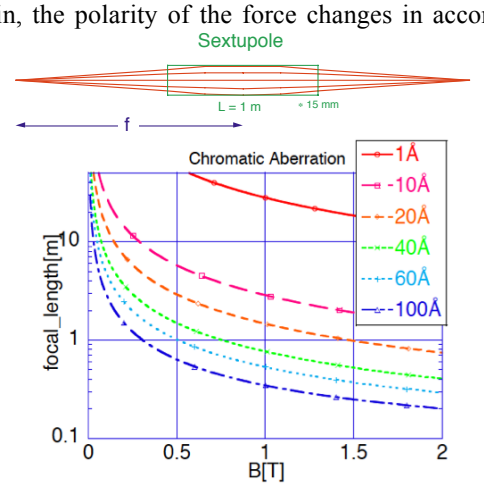

Figure 1: Focusing of neutrons by sextupole magnet and chromatic aberration.

*Work partially supported by the Ministry of Education, Science, Sports and Culture, Grant-in-Aid for Scientific Research (A), 18204023(2006) and 19GS0210.

MULTIPACTING SIMULATION IN RF STRUCTURES

M.A.Gusarova, V.I.Kaminsky, S.V.Kutsaev, M.V.Lalayan, N.P.Sobenin, MEPhI, Moscow, Russia
L.V.Kravchuk, S.G.Tarasov, INR, Moscow, Russia

Abstract

A new computer code for 3D simulation of multipacting phenomenon in radio frequency (RF) structures is developed. Simulation results in various RF devices are compared with theoretical calculations and experimental measurements.

INTRODUCTION

Design of accelerating cavities, input power couplers and other RF devices for the charged particle accelerators should provide the conditions of multipactor discharge elimination or suppression. The multipactor effect is a phenomenon in radio frequency (RF) devices (cavities, waveguides and others), where, under certain conditions, secondary electron emission in resonance with an alternating electric field leads to exponential electron multiplication, possibly damaging and even destroying the RF device.

Currently, there are three general approaches for suppressing multipactor discharge: conditioning of the components by the discharge, coatings and other surface treatments, and geometrical modifications. Proper design and geometry choice are the most powerful methods for multipactor suppression. Geometry modification results in electromagnetic field pattern changes. Latter leads to electrons trajectories distortion that breaks resonant conditions for multipactor discharge.

The code MultP–M is a tool that allows the analysis of multipacting in fully 3 dimensional RF structures and the modification for multipactor suppression

MULTP-M

The main window MultP-M is presented on Fig. 1. The code was programmed using Object Pascal in Delphi environment.

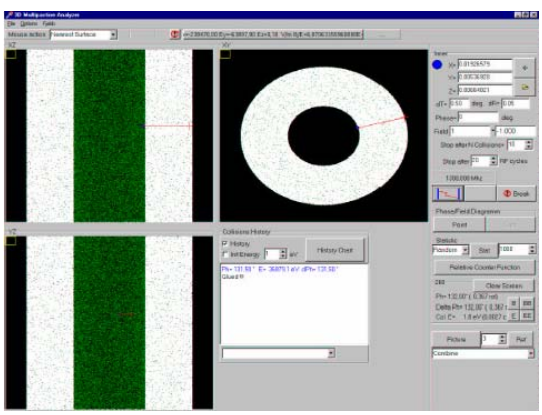

Figure 1: The main window. Example: single trajectory in a coax cavity.

MultP–M is the succeeding code for MultP [1, 2]. The latter was upgraded to get more functionality.

The code MultP–M is a tool that allows the analysis of multipacting in fully 3-dimensional RF structures. It solves the non-relativistic equation of motion of electrons in time harmonic rf fields. MultP–M does not contain a field solver, but it provides an interface to import the field-map from a text-file. The external field solver must be able to export field-maps to text-files, and it is strongly recommended that it uses a conformal mesh (mesh-points coincide with the boundary). MultP-M takes into account the RF device operation mode and allows simulation both for standing and traveling waves.

The resulting trajectories can be analyses by means of electron counter function and various statistics (statistics - particle counter, statistics - impact energy distribution, statistics - distribution of impact phases, statistics - the collision counter, statistics - finding trajectories with more than n impacts). All parameters used in the calculation (field level ranges, SEY, initial energy of electron, electron emission phases, initial number of particles, minimal collision, frequency, and limitation of number of field periods for calculation) are assigned by user.

The final decision whether multipacting is possible or not is up to the user.

Testing of MultP-M

As the test several narrow rectangular waveguides were simulated. For the narrow rectangular waveguides it is possible to do the theoretical estimation of the electric field strength threshold providing the conditions to multipactor discharge (equation 1). Resonance sizes of discharge gaps h(k) can be calculated using expression (2).

$$E_0 = \frac{\omega}{e}\sqrt{\frac{W_1 m}{2}} \quad (1) \qquad h(k) = \frac{eE_0 k\pi}{m\omega^2} \quad (2)$$

Here h - distance between the wide walls of waveguide, k - multipactor order, W_1 - energy of primary electron providing SEY > 1. These equations are rather simple and leave out the electron's initial phase and velocity spread.

Two rectangular waveguides were studied namely copper waveguides of 70x3.5 mm and 70x2.1 mm operated on 1.3 GHz.

Fig. 2 illustrates direct modeling results for 70x3.5 mm waveguide presented in two cross sections in xy and yz planes. The region subject to multipactor electrons burst is marked with dark blue.

ANALYSIS OF INPUT COUPLER ASYMMETRY INFLUENCE ON BEAM DYNAMICS IN ACCELERATORS WITH SUPERCONDUCTING CAVITIES

S.V.Kutsaev, M.V.Lalayan, V.A.Makarov, N.P.Sobenin, MEPhI, Moscow, Russia
V.I. Shvedunov, SINP MSU, Moscow, Russia
A.A.Krasnov, A.A.Zavadtsev, ScanTech Sciences, LLC, Affiliate in Russia, Moscow

Abstract

An investigation of input coupler asymmetry influence on electron beam dynamics in energy recovery linacs (ERL) with superconducting cavities was carried out. There were several types of input power couplers – coaxial and waveguide, asymmetric and symmetric considered. Using numerical simulation the electromagnetic fields distribution in accelerating cavity with input coupler was found and transverse deflecting impulse was calculated. RTMTRACE code was adapted for beam dynamics modeling.

INTRODUCTION

Choice of asymmetric geometry for RF-power input coupler for accelerator leads to transverse components of EM-field on the beam axis, which are responsible for a transverse impulse deflecting particles from the axis and making the beam emittance grow. To estimate the influence of the current effect on beam dynamics a notion of the beam kick is introduced. Numerically it is characterized by a ratio of Lorenz force integral normalized by charge and integral of longitudinal accelerating component of EM-field. Integration is made along the trajectory of the beam center. One must also take into account transit-time factor.

$$kick = \frac{V_t}{V_{acc}} = \frac{\int \left(E_y + eH_x\right)dx}{\int E_z dz} \qquad (1)$$

Calculation of beam emittance change due to field asymmetry in the beam region can be performed by analytical formula, which is given in [1]. More precise results can be obtained by modeling of beam dynamics, i.e. by solving motion equations for all beam particles in the field distribution obtained. RTMTRACE software was used for that task. It was originally designed for electron beam dynamics simulation in microtron [2]. Further developments made it possible to use RTMTRACE for calculation of other accelerating structures. One has to provide EM-field calculated using external software and exported to file in a special format for dynamics modeling. Also, to calculate structures considered below initial program was modified and compiled to produce an executable file.

COAXIAL INPUT COUPLER

Calculations were made for structures with coaxial and waveguide input couplers presented in Fig. 1.

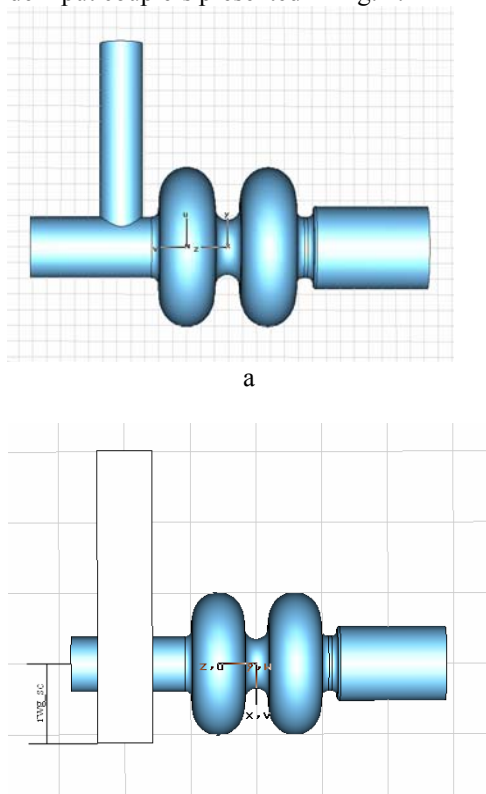

a

b

Figure 1: Coaxial and waveguide input couplers.

Calculation for a structure with a single coaxial input coupler (Fig.1, a) was performed to compare results with those given in [1]. During field calculation manual mesh optimization was performed in order to increase the number of mesh nodes in the beam region. Finally mesh with 160000 elements was used for field calculation, 10000 nodes corresponded to the beam region. Fig.2 presents the components of EM-fields in asymmetric coaxial input coupler calculated for perfect electric wall set as boundary condition. Similar calculations were made for a perfect magnetic wall.

CALCULATIONS OF TARGETS FOR ADS USING GEANT-4

R.S. Kolevatov, I.V. Kudinovich, A.N. Krylov Shipbuilding Research Institute,
Moskovskoe Shosse 44, 196158, St. Petersburg Russia
Yu.A. Svistunov, D.V. Efremov Research Institute of Electrophysical Apparatus,
Metallostroy Road 3, 196641 Metallostroy, St. Petersburg, Russia

Abstract

Calculations of neutron production in metallic targets bombarded by protons with energies up to 1 GeV in framework of GEANT-4 are presented. Calculations of neutron production in targets of large size, dependencies of neutron yields on target dimensions and spatial distribution of energy deposited in the target, intended for working out ADS targets with multiplying blankets are also presented.

INTRODUCTION

Accelerator driven systems (ADS) as powerful spallation sources of neutrons can find their application in nuclear power engineering for transmutation of long-living radioactive waste, production of new elements and substances with fission capability and for power generation. In hybrid reactor also called energy amplifier (EA) - fission reaction takes place in sub-critical reactor while the necessary density of neutron flux is provided by the spallation neutron source.

Costs, dimensions and weights as well as power consumption of accelerators required in a large extend depend on the output power of EA. Installations with high (about 1GW) power output for their operation require beams of protons accelerated up to the energies of 1GeV and higher with intensities of hundreds of mA. Beams of charged particles with mentioned characteristics one can get only using unique expensive accelerator machines. However EA of 200-400MW output require substantially lower intensities of neutron sources. This fact allows one to make use of accelerators producing beams of several hundred MeV and few mA current which can be copiously produced by industrial means.

In our work on the basis of calculations performed within GEANT-4 framework (v.9.1) we present neutron yield for different metal targets (Cu,Fe,Ta,W, Pb) bombarded by proton beam with energies from 300 MeV up to 1 GeV and spatial distribution of heat deposited in target.

GEANT-4 (v.9.1) developed by CERN is a program package (a set of C++ libraries) designed for modelling particle interactions with matter on the Monte-Carlo basis [1]. GEANT-4 can be used with different types of projectiles, materials and geometry of targets (detectors) and user is free to choose models for physical processes involved according to the task, which he is working at.

In our calculations we take into account electromagnetic processes, i.e. multiple scatterings off nuclei and ionization losses of charged particles, together with nuclear processes. For modelling of high-energy hadron—nucleus interactions we choose Bertini intranuclear cascade model for the very first cascade stage of interaction (approx. 10^{-23} s). Excited nucleus formed after this first stage rather emits hadrons (cascade-exciton and evaporation models are used respectively for pre-equilibrium and equilibrium states of excited nucleus) or breaks up instantly (multifragmentation or Fermi break-up for light nuclei). Interaction of neutrons having energies lower than 20 MeV with matter is described by parameterization-driven models based on ENDF/B-IV neutron cross section libraries.

Interaction of particles with matter within GEANT-4 is modelled on step-by step basis, at each step characteristics of generated track can be extracted and processed. To obtain our results we process up to 10000 of primary proton tracks.

Computation error was determined according to root mean square deviation (RMS) of the quantity of interest, determined using same set of values for the quantity obtained by Monte-Carlo. That is, for N events and RMS value of D computation error on 3σ level for quantity X can be determined according to central limit theorem as

$$\Delta X = 3D/\sqrt{N} \qquad (1)$$

Table 1 represents comparison of experimental data on neutron yields from target bombarded by protons with GEANT-4 computations.

Table 1: Average Neutron Yield m from Cylindrical Lead Targets per 1 Proton

Target dimensions D×L cm	E_p, MeV	*m*, n/p GEANT-4	*m*, n/p experimental data	Reference (experimental data)
10.0×60	17	3.65±0.52	3.13±0.06	[2]
10.2×61	70	7.53±0.80	8.0±0.4	[3]
			6.4±0.3	[2]
	40	9.47 ±0.87	9.0	[4]
	20	14.99±1.02	11.8±0.6	[3]
			11.7±0.4	[2]
			13.3	[4]
	60	21.28±1.19	16.6±0.8	[3]
			16,8±0,5	[2]
			17.7	[4]
0.4×61	70	8.46±0.88	8.7±0.4	[5]
	20	16.24±1.14	13.9±0.7	[5]
	60	24.63±1.38	20.3±1.1	[5]

Comparison of GEANT-4 evolved quantities confirms a possibility to apply the toolkit for practical calculations of targets for ADS.

END TO END BEAM DYNAMICS AND RF ERROR STUDIES FOR LINAC4

G. Bellodi, M. Eshraqi, J-B. Lallement, S. Lanzone, A.M. Lombardi, E. Sargsyan, CERN, Geneva, Switzerland
R. Duperrier, D.Uriot, CEA, Gif-sur-Yvette, France

Abstract

Linac4 is a normal conducting H^- linac to be built at CERN as a new injector to the PS Booster and later on as a front end of a possible MultiMegaWatt Linac Facility. The layout consists of a H^- RF source, a magnetic LEBT, a RFQ (accelerating the beam from 45 keV to 3 MeV), a chopper line, a conventional Drift Tube Linac (from 3 MeV to 50 MeV), a Coupled Cavity Drift Tube Linac (from 50 MeV to 102 MeV) and a π-mode structure (PIMS, from 102 to 160 MeV), all operating at a frequency of 352 MHz. End-to-end beam dynamics simulations have been carried out in parallel with the codes PATH and TRACEWIN to optimise the design and performance of the accelerator and at the same time to guarantee a cross-check of the results found. An extensive statistical campaign of longitudinal error studies (static and dynamic) was then launched for validation of the proposed design and to assess the maximum level of RF jitter/inaccuracies (in both phase and amplitude) the system can tolerate before beam quality at injection in the PS Booster - and later in the Superconducting Proton Linac (SPL)- is compromised.

LINAC4 LAYOUT

A 2 MHz RF volume source and 1.9m long 2-solenoid LEBT supply the initial H^- beam at 45 keV (a 400 μs long pulse at 2 Hz repetition rate for 80 mA current). This is first accelerated to 3 MeV by a 352 MHz RFQ, before entering a 3.6 m long chopper line consisting of 11 EM quadrupoles, 3 bunchers and 2 deflecting plates. Here micro-bunches are removed from the pulse to achieve a cleaner injection of the Linac4 beam in the PS Booster ring downstream. The beam is then accelerated to 50 MeV by a 352 MHz conventional Drift Tube Linac (DTL), composed of 3 separate tanks each fed by one klystron. There are 111 drift tubes, each equipped with a Permanent Magnet Quadrupole. The DTL is followed by a Cell-Coupled Drift Tube Linac, which takes the beam to 102 MeV through a series of 7 modules (21 tanks coupled by 3's) operating at 352 MHz and powered by individual klystrons. Transverse focusing is provided by 21 electromagnetic quadrupoles placed between tanks. Acceleration to the final energy of 160 MeV is then carried out by 12 Pi-Mode Structure (PIMS) tanks at 352 MHz, each composed of 7 cells, and 12 EM quadrupoles. The first 4 tanks are powered individually, while the last 8 are coupled in pairs onto a same klystron. The last 2 tanks have a lower nominal accelerating field, to allow for the possibility of energy painting at injection in the PSB [1]. The layout here described is the result of several revisions of previous designs [2], the main changes being in the values of the transition energies and in the final choice for one single frequency (352 MHz), to make for a simpler design.

END-TO-END BEAM DYNAMICS

Each section of Linac4 has been studied and optimized independently before a campaign of end-to-end simulations was launched to identify overall bottlenecks and limitations. The codes PATH[3], TRACEWIN[4], TOUTATIS[5], and PARMTEQ[6] have been used for these studies, providing mutual crosscheck of the results.

The H^- beam pulse current from the source is 80 mA, and the duty cycle is 0.1% in an initial phase when Linac4 is used as injector of the PS Booster ring, and a duty factor of 6% for a later use as front end for the SPL (value used for the safety and loss studies).

Space charge effects dominate at low energy, causing some beam degradation and losses in the RFQ and chopper line. The RFQ can accelerate with <5% losses beams in the 20-100 mA range, with 8% transverse emittance growth for 70 mA current. The chopper line consists of two deflecting plates housed inside quadrupoles and driven at an effective voltage of 500V to remove 133/352 micro-bunches in the pulse, which are kicked onto a conical shaped dump. About 5% of the unchopped beam is lost here, whereas the fraction of chopped beam that is transmitted past the dump into the Linac, and might need to be eliminated at the lowest possible energy is ~0.05%. The beam current available at the end of the chopper line would thus be 65 mA per pulse without chopping, and 40mA with chopping on.

After the dump the beam is matched into the first tank of the DTL, with a FFDD focusing scheme. Most of the transverse emittance growth (almost 20%) occurs at this transition, when after a relatively slow phase advance

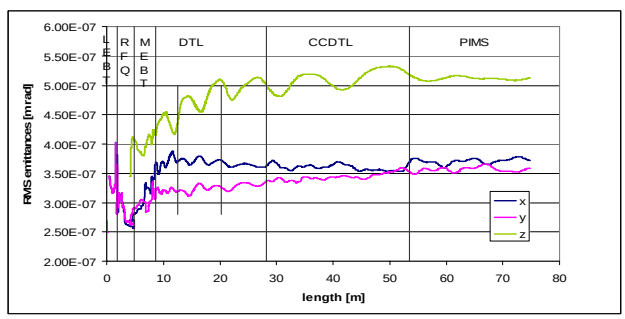

Figure 1: Transverse and longitudinal RMS emittance growth along the chopper line and Linac.

STATUS OF LONGITUDINAL BEAM DYNAMICS STUDIES IN CTF3

H. Shaker, Institute for research in fundamental science, Iran; CERN, Switzerland
E. Adli, University of Oslo, Norway; CERN, Switzerland
R. Corsini, A. Dabrowski, A. Latina*, T. Lefevre, P. K. Skowronski, F. Tecker, P. Urschutz#, CERN, Switzerland

Abstract

The aim of the CLIC Test Facility CTF3, built at CERN by an international collaboration, is to address the main feasibility issues of the CLIC electron-positron linear collider technology by 2010. One key-issue studied in CTF3 is the generation of the very high current drive beam, used in CLIC as the RF power source. It is particularly important to simulate and control the drive beam longitudinal dynamics in the drive beam generation complex, since it directly affects the efficiency and stability of the RF power production process. In this paper we describe the ongoing effort in modelling the longitudinal evolution of the CTF3 drive beam and compare the simulations with experimental results. Our study is based on single bunch simulation.

INTRODUCTION

The result of PARMELA [1] for the injector (see Fig. 1) was used as the input for PLACET [2] simulation code and for a 1-D analytical model using MathCAD. By these simulation codes, the CL (CTF3 Linac) from girder 3 in the injector (see Fig. 1), CT and CTS lines (See Fig. 1) were simulated. Measurements of the bunch length in CT and CTS lines by using RF deflector of delay loop in the CT line and OTR screen in the CTS line were done and were compared to the result of the simulation.

Table 1: Simulation Codes Comparison

PARMELA	MathCAD	PLACET
Injector, Chicane	Girder 3, Chicane, DBA†, CT & CTS lines	DBA, INFN-Frascati chicane
Space charge	No space charge	No space charge
No wake field	Wake field	Wake field
Longitudinal & Transverse	Longitudinal	Longitudinal & Transverse
No CSR‡	No CSR	CSR

SIMULATION

Injector

In the Injector, the electron beam is produced by a DC electron gun, is bunched at 1.5 or 3 GHz by the bunching system and is accelerated to about 18 MeV.

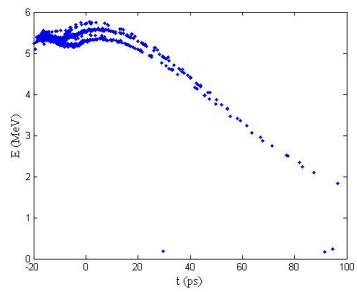

Figure 2: The result from PARMELA after girder 2 and the input for MathCAD.

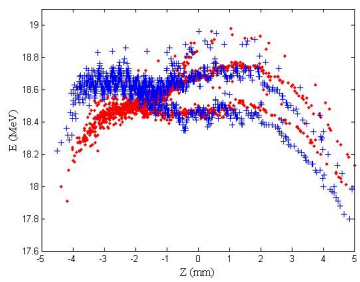

Figure 3: The result from MathCAD (no wake field) and PARMELA (+) after the injector, between z=-5 and z=5 mm. The rest will be cut in the chicane of girder 4.

Fig. 3 shows a good agreement between MathCAD and PARMELA result. In Fig. 13 you will see a little difference in the final bunch length, after the INFN-Frascati chicane.

The main reason for this difference is the space charge effect that is included in PARMELA and it is not included in MathCAD. The space charge effect is even less and hence insignificant in other parts of the machine where the energy is higher.

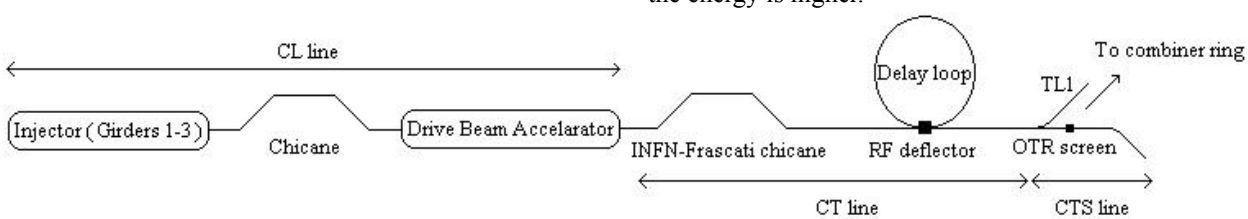

Figure 1: Layout of CTF3 from the injector to the combiner ring.

*Presently at Fermilab, #Presently at Siemens, †Drive Beam Accelerator, ‡Coherent Synchrotron Radiation.

PARTICLE DYNAMICS CALCULATIONS AND EMITTANCE MEASUREMENTS AT THE FETS *

J. Pozimski[1+2 #],A. Letchford[2] , J. Back[3], Dan Faircloth[2], S. Jolly[1] C. Gabor[4], C. Plostinar[4]
[1]Imperial College London, United Kingdom, [2]Rutherford Appleton Laboratory, Oxford, United Kingdom, [3]Warwick University, Coventry, [4]ASTeC United Kingdom

Abstract

In order to contribute to the development of high power proton accelerators in the MW range, to prepare the way for an ISIS upgrade and to contribute to the UK design effort on neutrino factories [1,2], a front end test stand (FETS) is being constructed at the Rutherford Appleton Laboratory (RAL) in the UK [3]. The aim of the FETS is to demonstrate the production of a 60 mA, 2 ms, 50 pps chopped beam at 3 MeV with sufficient beam quality. The results of numerical simulations of the particle dynamics from the charge separation dipole behind the ion source to the end of the MEBT will be presented. Previous measurements showed that the emittance of the beam delivered by the ion source exceeded our expectations by more than a factor of three [4]. Since then various changes in the beam extraction/post accelerator region reduced the beam emittance by nearly a factor of two. Simulations of the particle dynamics in the FETS based on distributions gained from recent measurements of the transversal beam emittance behind the ion source will be presented and the results for different input distributions discussed.

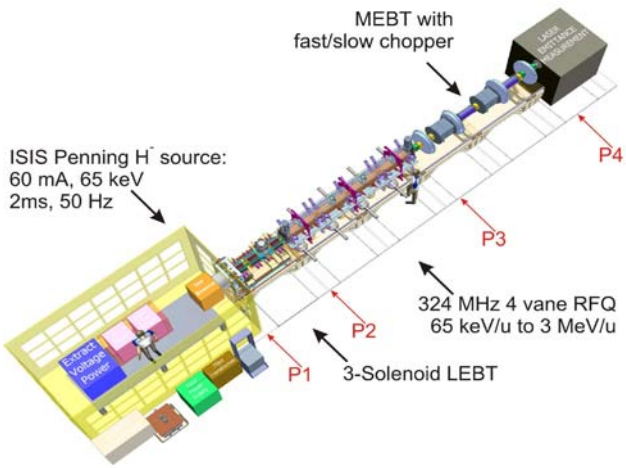

Figure 1: Schematic layout of the FETS set up. For the positions indicated (P1 behind post acceleration at the entrance of the LEBT [z=0mm], P2 at the entrance of the RFQ [z=1770mm], P3 at the RFQ exit [z=5770mm] and P4 at the end of the MEBT [z=10580mm]) the phase space distribution of the beam has been determined with GPT and TRACEWIN.

INITIAL PARTICLE DISTRIBUTION

The ion source development program, based on the highly successful ISIS H⁻ ion source at RAL, has already shown encouraging results. The aim is to increase the ion current from 35mA to 70mA, to increase the pulse length from 250µs to 2ms and to improve the beam quality [5]. In order to compare the recent status of the improvement of the ion source emittance and the consequences for the beam transport through the FETS end-to-end simulations have been performed for an idealized (shown in figure 2) and a real measured space phase distribution (shown in figure 3) based on pepper-pot emittance data.

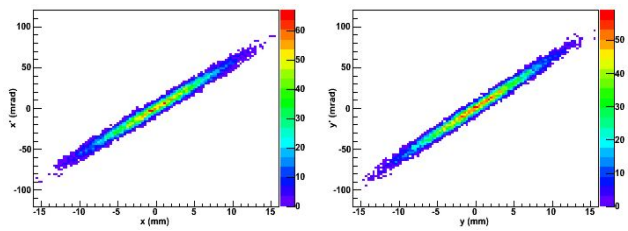

Figure 2: Input particle distribution into the LEBT (P1) for an ideal waterbag beam (input 1) ($\varepsilon_{x,rms}$=0.25 πmmmrad; $\varepsilon_{y,rms}$=0.25 πmmmrad).

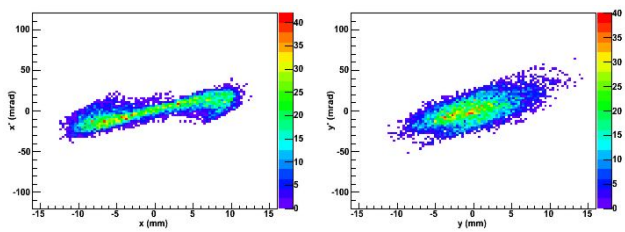

Figure 3: Input particle distribution into the LEBT (P1) for a measured beam distribution (input 2) ($\varepsilon_{x,rms}$=0.58 πmmmrad; $\varepsilon_{y,rms}$=0.52 πmmmrad).

LEBT SIMULATION AND RESULTS

A 3 solenoid LEBT system similar to the one used at the ISIS injector is under construction and the calculated 3D field distribution of the solenoids (figure 4) is used for particle transport simulation of the LEBT using the GPT code [6, 7].

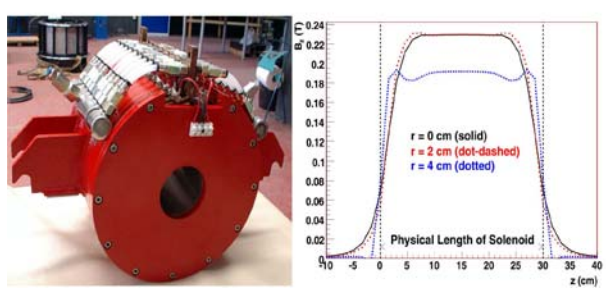

Figure 4: Left: one of three LEBT solenoids for FETS. Right: Magnetic field distribution in the z direction for different radii.

BEAM DYNAMICS AND WAKE-FIELD SIMULATIONS FOR HIGH GRADIENT ILC LINACS

C.J. Glasman & R.M. Jones; Cockcroft Institute, Daresbury, WA4 4AD, UK; University of Manchester, Manchester M13 9PL, UK

Abstract

Higher order modes (HOMs) are simulated with finite element and finite difference computer codes for the ILC superconducting cavities. In particular, HOMs in KEK's Ichiro type of cavity and Cornell University's Reentrant design are focused on in this work. The aim, at these universities and laboratories, is to achieve an accelerating gradient in excess of 50 MV/m in 9-cell superconducting cavities whilst maintaining a high quality and stable electron beam. At these gradients, electrical breakdown is an important cause for concern and the wakefields excited by the energetic electron beams are also potentially damaging to the beam's emittance. Here we restrict the analysis to performing detailed simulations, on emittance dilution due to beams initially injected with realistic offsets from the electrical centre of the cavities. We take advantage of the latest beam dynamics codes in order to perform these simulations.

INTRODUCTION

The main superconducting (SC) linacs of the ILC will accelerate electron (positron) beams from energies of 5 (15) GeV to a center of mass energy of 500 GeV at collision. Efficient operation of the machine demands high luminosity collisions which are achieved by accelerating a train of 2625 low emittance bunches particles. This low emittance must of course be preserved in transport through the main linacs and beam delivery system to the interaction point.

Here we consider the main positron linac where the beam quality can be degraded and the emittance can be diluted due to a number of factors including energy spread, phase jitter in cavities, beam position feedback errors, quadrupole magnet misalignments and wakefield effects. We focus on the dilution in the transverse emittance due to long range transverse wakefields. In this case the wakefields are excited by the relativistic particle beam and consist of a series of higher order modes [1]. These wakefields have the potential to not only dilute the emittance, but can also cause a beam beak up instability (BBU) [2].

The ILC will employ superconducting cavities operating at gradients at 31.5 MV/m. It is envisaged that the cavity design will be the TESLA type which has been developed at DESY over a long period [3]. TESLA is a relatively mature design, however there are still significant concerns regarding the limited yield and reproducibility of high gradient cavities.

There is also a concerted international effort focused on increasing the gradient of the SC cavities. Reshaping the cavity has allowed the accelerating gradient to be increased without pushing the magnetic field past the quenching limit (~180 mT) on the walls of the cavity [4]. This has allowed cavity designs which in theory will sustain accelerating gradients in excess of 50 MV/m. There is also a recent design which minimizes both the electric field as well as the magnetic field on the walls of the cavity [5].

In practice only single-cell cavities have reached these gradients, at Cornell University [6] with the Reentrant design and at KEK with the Ichiro design [7]. Complete 9-cell cavities are in the process of being fabricated and tested for both designs with a view to achieving similar gradients. The new high gradient designs operate at the same accelerating frequency as the baseline TESLA design. Furthermore the cavity shapes are similar to that of the TESLA design.

However, the perturbations of the cavity geometry are expected to give rise to a modification of the mode distribution. With this in mind, we carefully investigated the kick factors and mode frequencies in the alternative designs. The transverse long range wakefield experienced by the bunch train is given by:

$$W_T(t) = 2\sum_p K_p \sin(\omega_p t) e^{\frac{-\omega_p t}{2Q_p}}$$

where $\omega_p/2\pi$, K_p and Q_p are the modal frequencies, kick factors [1] and damping Qs respectively for the dipole mode p.

These modes have been simulated in detail [8, 9] using parallel finite difference and finite element codes GdfidL [10] and Analyst [11] and this data has been used as input for beam dynamics simulations presented herein, using the codes Lucretia [12] and Placet [13]. The codes track particle bunches through the lattice of the linac in which the energy is increased from 15 GeV to 250 GeV.

The envelope of the transverse long range wakefield is displayed in Fig. 1 with a damping Q imposed on all modes of 10^5 for the Ichiro cavity. Here it is evident that after 500 bunches (~50 km) the wake has decayed by 6 orders of magnitude. Thus, in all beam dynamics simulations 500 bunches is sufficient to account for the interaction between the wakefield and the multi-bunch train. We report on the results of these simulations in the next section.

BEAM DYNAMICS SIMULATIONS

In constructing the main linacs of ILC approximately 16,000 cavities will be required. Fabrication of these cavities is expected to introduce random errors in the geometry and thereby alter the modal frequencies and kick factors for each cavity. These errors are in fact

SCATTERING MATRIX SIMULATIONS OF FIELDS AND DISPERSION RELATIONS IN SUPERCONDUCTING CAVITIES FOR XFEL AND ILC

I. Shinton and R.M. Jones; Cockcroft Institute, Daresbury, WA4 4AD, UK;
University of Manchester, Manchester, M13 9PL, UK

Abstract

The globalised cascaded scattering matrix technique is a well proven, practical method that can be used to simulate large accelerating RF structures in which realistic fabrication errors to be incorporated in an efficient manner without the necessity to re-mesh the entire geometry. The globalised scattering matrix (GMS) technique allows one to obtain the scattering matrix for a structure. The method allows rapid e.m. field calculations to be obtained. Results are presented on monopole mode fields and dispersion relations calculated from direct and analytical methods. Analytical approximate results are also presented for the equivalent shunt susceptance of an iris loaded structure.

INTRODUCTION

In large accelerating structures such as the ILC beam break up and emittance dilution are major design concerns; hence the need to be able to accurately model large fractions of these structures in which effects such as wakefields, trapped modes, coupler kicks have been taken into consideration. GSM has been shown in previous works [1-3] to be capable of being employed to accurately model such large scale structures.

MODE MATCHING USING GSM

Mode matching is an established technique [4-5] which has been applied to various accelerator problems for sharp transitions consisting of adjoining wide narrow (WN) sections [6-10]. The mode matching technique relies upon splitting the structure into a series of sub-regions (WN or NW regions) in which an analytical solution of Maxwell's equations is given in terms of a series expansion over a set of orthogonal modes. The field solutions are then obtained by matching the field at the interfaces. In principle there are an infinite number of modes excited at a junction. In a practical application of the technique we truncate the series with an appropriate ratio of the modes in the narrow to wide section. Indeed, numerous studies have been preformed on the relative convergence phenomena to determine the optimal ratio of modes [11].

A MODE MATCHING GSM TECHNIQUE FOR FIELD DETERMINATION

The mode matching procedure presented here differs from previous studies. We will consider the case for a propagating monopole mode launched form one port. We derive an analytical relation for the S matrix for a WN or a NW junction. Let us consider the circular WN junction with n modes in region I (wide) and m modes in region II (narrow) where m<=n. We shall denote "b" as the radius of the wide region and "a" as the radius of the narrow region. Analytical electromagnetic fields $\vec{e}$ in a circular beam waveguide are provided in [12]. The characteristic scalar product is given by $\bar{a}_{nm} = \int_S e_n \cdot \hat{e}_m \partial\Gamma$ (over the aperture S) and this evaluates to:

$$\bar{a}_{nm} = \frac{2a^2\chi_n J_0(\chi_{0n}a/b)}{b^2 J_1(\chi_{0n})\left((\chi_{0n}a/b)^2 - \chi_m{}^2\right)} \quad (1)$$

where χ_{0n} is the nth root of $J_0(\chi_{0n})$. For a = b the normalisation in [12] corresponds to $\bar{a}_{nm} = \delta_{nm}$ (where δ is the Kronecker delta function). The S matrix at the transition is obtained by mode-matching the fields in terms of the modal amplitudes at each transition:

$$S_{21} = 2\left(U + \hat{Z}\bar{a}^t Y \bar{a}\right)^{-1} \hat{Z}\bar{a}^t Y \quad (2)$$

$$S_{11} = \bar{a}S_{21} - U \quad (3)$$

$$S_{22} = 2\left(U + \hat{Z}\bar{a}^t Y \bar{a}\right)^{-1} - U \quad (4)$$

$$S_{12} = \bar{a}\left(U + S_{22}\right) \quad (5)$$

In the above equations U, $Z = Y^{-1}$ is the identity and impedance matrix, respectively. Using Eqs. 1-5 the S matrix of a structure decomposed into WN and NW transitions can be obtained. The e.m field in any structure can be subdivided into one of three different regions, as depicted in Fig. 1. Region 1 lies between z=0 and z=1, here the S matrix consists of the GSM formed z=z1 and z=z3.

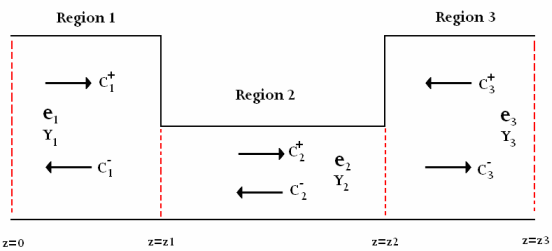

Figure 1: Sketch of WNW transition illustrating incident and reflected modes.

Any subsection of a structure will be classified as a region 2 section, only the first and last sections are classified as region 1 and 3 respectively. The S matrix of any region 2 subsection consists of a propagating matrix representing the infinite propagating wave series S_{21}^0 and a reflected matrix S_{11}^0 representing the infinite reflected wave series both which are decaying within the subsection [3]. Here the superscripts I and II represent the GSM's left and

END-TO-END SIMULATION OF THE SNS LINAC USING TRACK*

B. Mustapha#, P.N. Ostroumov
Argonne National Laboratory, 9700 S. Cass Ave, IL 60439, U.S.A.

D. Jeon
Oak Ridge National Laboratory, 1 Bethel Valley Rd, Oak Ridge, TN 37831, U.S.A.

Abstract

To simulate the SNS linac using the beam dynamics code TRACK and to benchmark the results against the recent commissioning data, we have updated TRACK to support SNS-type elements such as DTL's and CCL's. After successfully implementing and simulating the DTL section of the SNS linac, we have implemented the CCL section and the high energy superconducting (SCL) section up to 1 GeV. Results from end-to-end TRACK simulations of the SNS linac including the RFQ will be presented and discussed.

INTRODUCTION

In an effort to benchmark the beam dynamics code TRACK [1] againt experimental data from existing linacs, such as the SNS linac, we have updated the code to support new elements such as DTLs and CCLs. We previously reported the results of TRACK simulations for the SNS MEBT and DTL [2]. Recently, we implemented a new subroutine for the simulation of CCL tanks. After building the CCL, SCL and HEBT lattices, we were able to perform end-to-end simulations from the RFQ to the HEBT right before the stripping foil.

After briefly describing the SNS linac lattice, results of the RFQ simulations using TRACK are presented and compared to simulations using the RFQ design code Parmteq [3]. The method of implementing CCL tanks is then presented followed by results of end-to-end simulations of the linac from the MEBT to the HEBT. Possible future developments are discussed at the end.

THE SNS LINAC

The SNS accelerator facility [4] is designed to provide a 1 GeV, 1.4 MW proton beam to a liquid mercury target for neutron production. The accelerator complex consists of a H− injector capable of producing 38 mA peak current, a 1 GeV linac, an accumulator ring and associated beam transport lines to experimental areas. The linac consists of a 2.5 MeV, 38mA H− front-end injector, a six-tank 402.5 MHz DTL to accelerate the beam to 87 MeV, a four-module 805 MHz Coupled Cavity Linac (CCL) to accelerate the beam to 187 MeV, and a superconducting linac (SCL) to accelerate the beam to 1 GeV. Figure 1 shows a schematic layout of the SNS linac.

* This work was supported by the U.S. Department of Energy, Office of Nuclear Physics, under Contract No. DE-AC02-06CH11357.
# mustapha@phy.anl.gov

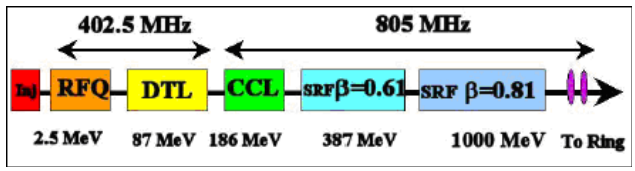

Figure 1: Schematic layout of the SNS linac.

SIMULATIONS OF THE RFQ

The design parameters of the SNS RFQ [5] are summarized in Table 1. According to these parameters the RFQ lattice was generated using Parmteq from which the TRACK lattice was derived. The simulations were performed using both Parmteq and TRACK. Table 2 compares the calculated transmissions for a 0 mA beam and the actual operating current of 32 mA [6]. We notice differences between TRACK and Parmteq that should be further investigated. However, the two codes agree reasonably well on the output beam parameters. Figure 2 compares the phase space plots at the end of the RFQ and Table 3 compares the values of the normalized rms emittances.

Table 1: Design parameters of the SNS RFQ.

Type	4 vane
RF Frequency	402.5 MHz
Voltage	83 kV
N. Of Cells	448
Length	3.723 m
Beam	H-
Input Energy	65 keV
Output Energy	2.5 MeV
Peak Output Current	52 mA
Long. Emittance	103 deg-keV
Trans. Emittance: N-RMS	0.21 mm-mrad
Design Transmission	> 90 %

Table 2: RFQ transmission for different beam currents calculated using both Parmteq and TRACK.

Current	Parmteq	TRACK
0 mA	99.4 %	98.5 %
32 mA	97.3 %	91.4 %

MONTE CARLO SIMULATION OF TOUSCHEK EFFECTS IN A LINAC BEAM *

A. Xiao†, M. Borland, ANL, Argonne, IL 60439, USA

Abstract

We present a Monte Carlo method implemented in the code `elegant` [1] for simulating Touschek scattering effects in a linac beam. The local scattering rate and the distribution of scattered electrons can be obtained from the code. In addition, scattered electrons can be tracked to the end of the beamline and the local beam loss rate and beam halo information recorded. This information can be used for beam collimation system design.

INTRODUCTION

The Touschek effect is a single Coulomb scattering effect between charged particles in a beam. For a relativistic beam, a small change of transverse momentum results in a much larger change of longitudinal momentum, as the momentum change is increased by the Lorentz factor γ. When the change exceeds the machine's momentum acceptance, the scattered particle is lost.

The Touschek effect is well understood in storage rings and has been largely ignored for linac beams in the past due to the negligible loss rate. However, this is not the case for an intense electron bunch with ultra-low emittance and very short bunch length that passes through a linac with a very high repetition rate, as occurs in proposed Energy Recovery Linacs (ERLs) [2]. This is a concern for a possible ERL upgrade of the APS, since the radiation shielding of the ring is not designed for high continuous loss rates [3].

Previously, a preliminary theoretical analysis [4] was performed using Piwinski's formula [5]. To better determine the scattered electron distribution and determine precisely the electron loss rate and loss position, we have included a Monte Carlo simulation method in `elegant` for studying the Touschek scattering effect.

In this paper, we review the theory of Touschek scattering, then describe the method used for the Monte Carlo simulation. The scattering rates calculated from the Monte Carlo simulation and Piwinski's formula are compared. The strategy used for calculating beam loss rate and location in `elegant` is then explained. Finally, we give an application example to a proposed APS ERL lattice design.

THEORY DESCRIPTION

In the center-of-mass (CM) system [1], the probability of one of the two encountered electrons being scattered into a solid angle $d\Omega^*$ is given by the differential Møller cross section [6]

$$\frac{d\sigma^*}{d\Omega^*} = \frac{r_e^2}{4\gamma^{*2}}\left[\left(1+\frac{1}{\beta^{*2}}\right)^2 \frac{4-3\sin^2\Theta^*}{\sin^4\Theta^*} + \frac{4}{\sin^2\Theta^*} + 1\right], \tag{1}$$

where r_e is the classical electron radius; γ^* and β^* are the relative energy and velocity of scattered electrons in the CM system, respectively; Θ^* is the angle between the momenta before and after scattering; and $d\Omega^* = \sin\Theta^* d\Theta^* d\Psi^*$.

The total scattering rate R is given by the integration over all possible scattering angles and over all electrons in the bunch. In the CM system,

$$R^* = 2\int |v^*|\sigma^*\rho(\vec{x}_1^*)^*\rho(\vec{x}_2^*)^* dV^*, \tag{2}$$

where v^* is the scattered electrons' velocity, σ^* is the total Møller cross section, $\vec{x}^* = (x^*, y^*, z^*, p_x^*, p_y^*, p_z^*)$, $\rho(x_i^*)^*$ is the electron phase-space density, and $dV = dx^*dy^*dz^*dp_{x1}^*dp_{y1}^*dp_{z1}^*dp_{x2}^*dp_{y2}^*dp_{z2}^*$. σ^* is integrated over the solid angle $d\Omega^*$ with $\Theta^* \in (0, \frac{\pi}{2}]$, $\Psi^* \in [0, 2\pi]$:

$$\sigma^* = \int_0^{2\pi}\int_0^{\pi/2} \frac{d\sigma^*}{d\Omega^*}\sin\Theta^* d\Theta^* d\Psi^*. \tag{3}$$

The reason for $\Theta^* \in (0, \frac{\pi}{2}]$ is that, if one electron is scattered into the region $0 < \Theta^* \le \frac{\pi}{2}$, then the other is scattered into the region $\frac{\pi}{2} \le \Theta^* < \pi$. The factor "2" in Equation (2) includes both regions.

For the problem we are interested in, we assume that $p_x \ll p_z$ and $p_y \ll p_z$, which means that the Lorentz transformation is mainly taking place along the z direction, and σ^* is parallel to the z^*-axis. Transforming to the laboratory coordinate system gives

$$|v|\sigma = \frac{|v^*|}{\gamma}\frac{\sigma^*}{\gamma} \tag{4}$$

and

$$R = 2\int |v|\sigma\rho(\vec{x_1})\rho(\vec{x_2})dV, \tag{5}$$

with

$$dV = dx_\beta dy_\beta d\Delta z dx'_{\beta 1}dx'_{\beta 2}dy'_{\beta 1}dy'_{\beta 2}d\Delta p_1 d\Delta p_2. \tag{6}$$

Ignoring coupling, for an electron bunch with Gaussian distribution, the electron's density in phase space $(x_\beta, x'_\beta, y_\beta, y'_\beta, \Delta z, \Delta p/p_0)$ is given by

$$\rho = \frac{N\beta_\beta}{8\pi^3\sigma_\sigma\sigma^2{}_\beta\sigma^2{}_\beta}\exp\left\{-\frac{\Delta z^2}{2\sigma^2} - \frac{1}{2\sigma^2}\frac{\Delta p^2}{p_0^2}\right\} \times \exp\left\{-\frac{x_\beta^2+(\alpha_x x_\beta+\beta_x x'_\beta)^2}{2\sigma^2{}_\beta} - \frac{y_\beta^2+(\alpha_y y_\beta+\beta_y y'_\beta)^2}{2\sigma^2{}_\beta}\right\}, \tag{7}$$

* Work supported by the U.S. Department of Energy, Office of Science, Office of Basic Energy Sciences, under Contract No. DE-AC02-06CH11357.

† xiaoam@aps.anl.gov

[1] For clarity, we use (*) to denote all quantities in the CM system, as opposed to quantities in the laboratory coordinate system.

STUDY OF IBS EFFECTS FOR HIGH-BRIGHTNESS LINAC BEAMS *

A. Xiao†, ANL, Argonne, IL 60439, USA

Abstract

Intrabeam scattering (IBS) may become an issue for linac-based fourth-generation light sources such as X-ray free-electron lasers and energy recovery linacs (ERLs), both of which use high-brightness electron beams with extremely small emittance and energy spread. Any degradation of this extremely high beam quality could significantly reduce the machine's performance. We present here a strategy first used in the code `elegant` [1] for simulating IBS effects for high-brightness linac beams. We also present an application to a possible ERL upgrade of the Advanced Photon Source.

INTRODUCTION

Particles in a beam exchange energy between transverse and longitudinal oscillations due to Coulomb scattering. Depending on the scattering angles, the process leads to a diffusion in beam size (intrabeam scattering or IBS) or beam loss (Touschek effect).

The theory of IBS is discussed in several publications [2, 3]. A number of codes (e.g., ZAP [4], MAD-X [5]) have been developed for calculating the beam size growth rates. In the past, particle densities were not very high, so the growth times were much longer than the time spent traversing a typical linac. Thus, codes were designed for the stored beam case only with a constant beam energy. Linac-based fourth-generation light sources, such as X-ray free-electron lasers and Energy Recovery Linacs (ERLs [6]), require a high-brightness electron beam with extremely small emittance and energy spread. Any degradation of the beam quality could significantly reduce the machine's performance. Since the IBS growth time becomes much shorter for a high-brightness beam, IBS effects may become an issue even for a linac beam.

To investigate this issue, we modified the IBS calculation in `elegant` to include vertical dispersion effects and added the ability to handle acceleration. We applied our code to a proposed APS-ERL [7, 8] upgrade lattice also. Our results show that the IBS effects is moderate with the designed beam parameters.

CALCULATION OF IBS GROWTH RATES

A detailed formalism for intrabeam scattering, taking into account the variation of lattice functions with azimuth, has been developed by Bjorken and Mtingwa [3]. The expression of emittance growth rate τ_d in the direction d (x, y, or z) is given by (3.4) in [3] as:

$$\frac{1}{\tau} = \frac{\pi^2 c r_0^2 m^3 N ln\Lambda}{\gamma\Gamma} f,$$

$$f = \left\langle \int_0^\infty \frac{\lambda^{1/2} d\lambda}{\sqrt{|A|}} \left\{ TrL^d Tr[A^{-1}] - 3Tr[L^d (A)^{-1}] \right\} \right\rangle, \quad (1)$$

where c is the speed of light, r_0 is the classical particle radius, m is the particle mass, N is the number of particles per bunch (or in the beam for unbunched case), $ln\Lambda$ is a Coulomb logarithm, γ is the Lorentz factor, Γ is the 6-dimensional invariant phase-space volume of the beam,

$$\Gamma_B = (2\pi)^3 (\beta\gamma)^3 m^3 \varepsilon_x \varepsilon_y \sigma_p \sigma_z \qquad (bunched)$$

$$\Gamma_U = 4\pi^{5/2} (\beta\gamma)^3 m^3 \varepsilon_x \varepsilon_y \sigma_p (2\pi R) \quad (unbunched), \quad (2)$$

and $A = (L + \lambda I)$, with

$$\begin{aligned} L &= L^x + L^y + L^z, \\ L^x &= \frac{\beta}{\varepsilon} \begin{pmatrix} 1 & -\gamma\phi_x & 0 \\ -\gamma\phi_x & \gamma^2(\frac{D^2}{\beta^2} + \phi_x^2) & 0 \\ 0 & 0 & 0 \end{pmatrix}, \\ L^y &= \frac{\beta}{\varepsilon} \begin{pmatrix} 0 & 0 & 0 \\ 0 & \gamma^2(\frac{D^2}{\beta^2} + \phi_y^2) & -\gamma\phi_y \\ 0 & -\gamma\phi_y & 1 \end{pmatrix}, \\ L^z &= \frac{\gamma^2}{\sigma^2} \begin{pmatrix} 0 & 0 & 0 \\ 0 & 1 & 0 \\ 0 & 0 & 0 \end{pmatrix}. \end{aligned} \quad (3)$$

Here, $\phi_{x,y} = D'_{x,y} + \frac{\alpha_{,} D_{,}}{\beta_{,}}$; $\varepsilon_{x,y}$ and $\sigma_{p,z}$ are beam distribution related quantities; and $\beta_{x,y}, \alpha_{x,y}, D_{x,y}, D'_{x,y}$ are local optical functions.

Equation (3), which includes vertical dispersion effects, is used in `elegant` for calculating the beam size growth rate. We found there are missing terms in MAD-X in the expressions for $a_{x,y}$ and $b_{x,y}$ used in formula (8) in [9], as confirmed by the developer [10]. The following equations show the differences between a_x in `elegant`,

$$\begin{aligned} a_x &= 2\gamma^2 \left(\frac{H}{\varepsilon} + \frac{H}{\varepsilon} + \frac{1}{\sigma^2} \right) - \frac{2\beta}{\varepsilon} - \frac{\beta}{\varepsilon} \\ &\quad - \frac{\beta_{,} H}{H_{,} \varepsilon} + \frac{\beta}{H_{,} \gamma^2} \left(\frac{2\beta}{\varepsilon} - \frac{\beta}{\varepsilon} - \frac{\gamma^2}{\sigma^2} + \frac{6\beta}{\varepsilon} \gamma^2 \phi_x^2 \right) \end{aligned} \quad (4)$$

* Work supported by the U.S. Department of Energy, Office of Science, Office of Basic Energy Sciences, under Contract No. DE-AC02-06CH11357.

† xiaoam@aps.anl.gov

ORTHOGONAL BASIS FUNCTION APPROXIMATION OF PARTICLE DISTRIBUTION IN NUMERICAL SIMULATIONS OF BEAMS *

Balša Terzić†, NICADD, Northern Illinois University, DeKalb, IL 60115, USA

Abstract

Numerical simulations of charged particle beams require an approximation to the particle distribution being simulated. We present a mathematical formalism for approximating two-dimensional (2D) particle distribution using a basis composed of scaled and translated Gauss-Hermite (STGH) functions. It is computationally efficient, because it only requires the values of the particle distribution at $(N+1)\times(M+1)$ nodes, where N and M are the highest basis function retained in the expansion in each coordinate. After outlining the mathematical formalism for the expansion, we compare it to the cosine expansion which is currently used in a code simulating coherent synchrotron radiation. The advantages of the STGH approximation over the cosine expansion are demonstrated by comparing the computational costs and execution times, as well as manifesting that unphysical fluctuations in the tail of the approximation which plague cosine expansion are not a factor in the new method. All these features make the STGH approximation valuable for N-body codes simulating the dynamics of multiparticle systems.

INTRODUCTION

The normalized Gauss-Hermite functions are given by

$$\psi_n(v) = \frac{1}{\sqrt{2^n n!\sqrt{\pi}}} H_n(v) e^{-v^2}, \qquad (1)$$

where the $H_n(v)$ are the Hermite polynomials. They are orthonormal on $(-\infty,\infty)$ with the weight $w(v)=e^{v^2}$:

$$\int_{-\infty}^{\infty} \psi_n(v)\psi_m(v)e^{v^2}dv = \delta_{nm}, \qquad (2)$$

where δ_{nm} is a Kronecker delta. The basis composed of Gauss-Hermite functions $\{\psi_n\}_{n=0}^N$ are often used in various areas of physics, because of their relationship to normal distribution. The Gauss-Hermite spectral methods, while possessing some useful properties, only yield good approximation when scaled. Scaled Gauss-Hermite functions have been used earlier in the context of beam simulations [1, 2, 3]. While most of our motivation and justification for using scaled Gauss-Hermite function coincides with theirs, the mathematical formalism and computational implementation we present here are different. In the new method: (i) no underlying ellipsoidal distributions are assumed; (ii) the computation of the scaled Gauss-Hermite expansion here is done in a more direct and efficient way; (iii) the Poisson equation and the self-fields are directly obtained, without an expensive multidimensional integration. The results reported in the earlier work – most notably appreciable increase in accuracy and computational efficiency over the existing particle-in-cell (PIC) codes – gives us a reasonable expectation that the approach we present here is indeed superior to the existing gridless approaches. The efforts to integrate this 2D formalism into an existing 2D beam simulation code, as well as extending it to 3D and implementing a full 3D gridless N-body code as an alternative to PIC codes, are currently underway [4].

* Work supported by the Department of Defense under contract N00014-06-1-0587 with Northern Illinois University.

† bterzic@nicadd.niu.edu

SCALED AND TRANSLATED GAUSS-HERMITE BASIS

The 2D gaussian-type functions (i.e., functions which decay at infinity at least like $\exp\left(-px^2-qy^2\right)$, with p,q some positive constants) can be well-approximated by a finite Gauss-Hermite expansion

$$f(x,y) = \sum_{n=0}^{N}\sum_{m=0}^{M} a_{nm}\psi_n(\alpha_1(x-\bar{x}))\psi_m(\alpha_2(y-\bar{y})), \qquad (3)$$

where $\alpha_1,\alpha_2>0$ and $\bar{x}$, $\bar{y}$ are constants. In solving differential equations, it is important to be able to express derivatives of the function in the same basis. This is achieved via recurrence relations of Gauss-Hermite polynomials [6]:

$$\begin{aligned} H_{k+1}(z) &= 2zH_k(z) - 2kH_{k-1}(z), \qquad (4)\\ H_k'(z) &= 2zH_{k-1}(z). \end{aligned}$$

This ability to express coefficients of the derivatives of the function in terms of coefficients of the function itself renders solving the Poisson equation in this basis trivial.

In pseudo-spectral methods, such as the collocation method used in [5], the optimal pseudo-spectral points are the roots of the $H_{N+1}(x)$ and $H_{M+1}(y)$, denoted by $\{\gamma_j\}_{j=0}^N$ and $\{\beta_k\}_{k=0}^M$, respectively. The collocation points are arranged in descending order, i.e., $\gamma_0>\gamma_1>\ldots>\gamma_N$ and $\beta_0>\beta_1>\ldots>\beta_M$. If the eq. (3) is satisfied at the collocation points, then it can be written as

$$f(\tilde{\gamma}_j,\tilde{\beta}_k) = \sum_{n=0}^{N}\sum_{m=0}^{M} a_{nm}\psi_n(\gamma_j)\psi_m(\beta_k), \qquad (5)$$

where $0\le j\le N$, $0\le j\le M$, and

$$\tilde{\gamma}_j = \frac{\gamma_j}{\alpha_1}+\bar{x}, \qquad \tilde{\beta}_k = \frac{\beta_k}{\alpha_2}+\bar{y}. \qquad (6)$$

THE OPEN ARCHITECTURE SOFTWARE INTEGRATION SYSTEM (OASIS) FOR CREATING PBO LAB MODULES

G. H. Gillespie and B. W. Hill
G. H. Gillespie Associates, Inc., P. O. Box 2961, Del Mar, CA 92014, USA

Abstract

A specialized software package has been developed that enables the rapid implementation of custom beam optics modules that run in the Particle Beam Optics Laboratory (PBO Lab™). PBO Lab is a commercially available software application that supports a suite of accelerator codes for design, operations, and personnel education. The intuitive and easy-to-use graphic user interface (GUI) is largely responsible for the popularity of PBO Lab. The Open Architecture Software Integration System, or OASIS, builds upon the capability of PBO Lab to host a suite of different codes. OASIS provides an innovative framework that allows users to readily create new PBO Lab modules without writing or compiling any source code. OASIS has been used to develop several new modules for PBO Lab. This paper presents a summary of the OASIS framework and describes some of the features used in creating a new PBO Lab module for one example optics code.

INTRODUCTION

PBO Lab has been used to support beamline design, personnel training, and accelerator operations for over a decade and delivers a suite of Application Modules that implement a variety of trusted optics codes [1]. The PBO Lab GUI provides a common graphic user interface for creating and editing iconic object-based computer models of accelerators and beamlines.

OASIS leverages the mature software framework utilized by PBO Lab [2], and extends its capabilities to provide users with a familiar environment from which to create their own PBO Lab Application Modules [3]. The PBO Lab Beamline Object Model [4] is the underlying persistent representation that allows multiple optics codes with varying input/output requirements to utilize a single beamline model description. Multiple optics codes run side by side in PBO Lab's sophisticated drag-and-drop graphic user interface. PBO Lab generates the native input and processes the native output, for the different optics codes, from a single beamline model.

THE OASIS FRAMEWORK

The OASIS framework is a collection of abstract and concrete classes, and their interfaces which comprise a generic subsystem used to implement Application Modules in PBO Lab. It provides a reusable, generic OASIS Module, or "OModule," that encapsulates the user interface and data interface functionality required for running in the multi-module PBO Lab environment. Figure 1 illustrates the abstract layer diagram for the PBO Lab/OASIS application framework. User developed Application Modules are implemented dynamically in PBO Lab with this generic reusable Application Module (OModule) design pattern.

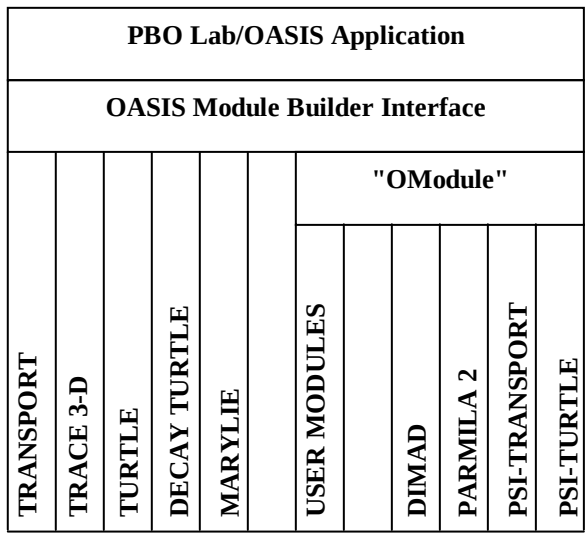

Figure 1: Layer diagram for PBO Lab Framework and Open Architecture Software Integration System.

An OModule has both a user interface component and a computational component. The user interface component is created in the OASIS Module Builder Interface which is an extension to the drag-and-drop PBO Lab GUI. The computational component may be a library (.dll) or executable (.exe) application. No source code needs to be compiled or linked to use the Application Module in PBO Lab.

OASIS MODULE BUILDER

The OASIS Module Builder Interface, used to create PBO Lab Application Modules, is an intuitive extension of the standard PBO Lab interface, providing users with a familiar environment to create custom Application Modules that run seamlessly in the PBO Lab GUI without writing or compiling any source code. The OASIS Module Builder is itself a very specialized PBO Lab Module: it is a Module for the specification of other Application Modules. The OASIS Module Builder provides an interactive environment to incrementally create and test Application Modules in the PBO Lab GUI. Detailed specifications to fully define the requirements for the generation of a native input file for

AN INNOVATIVE GRAPHIC USER INTERFACE FOR PARMILA 2

G. H. Gillespie and B. W. Hill
G. H. Gillespie Associates, Inc., P. O. Box 2961, Del Mar, CA 92014, USA

Abstract

A new graphic user interface (GUI) has been created for the PARMILA 2 program. PARMILA 2 is an advanced version of the historical PARMILA program originally developed to design and model drift tube linear (DTL) accelerators. PARMILA 2 expands upon that capability to support the design and simulation of coupled cavity linear (CCL) accelerator structures, coupled-cavity drift tube linac (CC-DTL) structures, superconducting accelerator structures, as well as DTL structures and transport lines that can include magnetic, radiofrequency and electrostatic beam optics elements. A new software package called the Open Architecture Software Integration System, or OASIS™, has been used to develop an innovative graphic interface for the PARMILA 2 program. OASIS provides a framework for developing custom modules for the Particle Beam Optics Laboratory (PBO Lab™) software. The framework can be used to create new PBO Lab modules *without the need for writing or compiling any source code*. Tools in the OASIS software were utilized to define the GUI features of the new PARMILA 2 module. Existing PARMILA 2 executables, including Parmila.exe, Lingraf.exe and readdst.exe, have been linked to GUI commands utilizing other tools within the OASIS framework. This paper presents an overview of the new PARMILA 2 module and illustrates some of the GUI features.

INTRODUCTION

PARMILA (Phase and Radial Motion in Ion Linear Accelerators) is a well established computer code [1] used for the design and simulation of proton (and heavier particle) linear accelerators. The program has a long history and the version 2 developed at the Los Alamos National Laboratory includes design capabilities for drift tube linacs (DTLs), coupled cavity linacs (CCLs), coupled cavity drift tube linacs (CCDTLs) and several types of superconducting linac structures [2, 3]. One challenge to users of PARMILA has been acquiring a good knowledge of the detailed input file format required by the program. The development of an intuitive, easy-to-use graphic interface for PARMILA 2, as an Application Module of the Particle Beam Optics Laboratory (PBO Lab), directly addresses that challenge.

PBO Lab is a modular suite of commercial software applications which has Application Modules that support a variety of particle beam optics programs and other accelerator-related codes [4]. Each optics program Application Module incorporates a specific particle beam optics modeling or simulation program. Available modules include TRANSPORT [5], TURTLE [6], MARYLIE [7], TRACE 3-D [8] and DECAY-TURTLE [6]. Other modules are also available, including an Optimization Module utilizing the NPSOL [9] and MINOS [10] nonlinear constrained optimization programs, and specialized modules for modeling electrostatic elements [11] and traveling wave accelerator components [12]. PBO Lab provides a common graphic user interface (GUI) for constructing and editing iconic object-based computer models of accelerators and beamlines. The common GUI for optics programs in PBO Lab simplifies the task of carrying out calculations for a given beamline. PBO Lab assures that the input files for every optics program represent the same beamline, and PBO Lab will automatically display graphical results that may otherwise require post-processors. Users do not need to construct input files in the format required by a specific program -- PBO Lab takes care of all the needed bookkeeping, and the object model automatically creates the necessary input files following simple menu commands issued by a user.

PBO LAB PARMILA-2 MODULE

The requirements to develop a workable GUI for PARMILA were outlined some years ago [13] and a prototype concept was described at the 1994 Linac Conference [14]. For a variety of reasons, further progress was limited until a new approach for creating optics code GUIs for PBO Lab became available. The new approach was provided by the Open Architecture Software Integration System, or OASIS. Developed under the auspices of the U. S. DOE Small Business Innovation Research (SBIR) program, OASIS [15] provides the type of reusable framework required for rapidly creating PBO Lab Application Modules without the need to write any new source code, for either the GUI (PBO Lab) or the associated physics code (e.g. PARMILA). In brief, OASIS is a new PBO Lab Module that is used to create additional PBO Lab Modules, where the GUI and related object model themselves provide the creative framework.

The document (or start up) window for the PARMILA-2 Module is basically the same as that for any other PBO Lab Module. Figure 1 illustrates an example document window which has an iconic description of a drift tube linac (DTL) model displayed. The DTL model was created by using the "drag and drop" construction kit of the PBO Lab software. Several custom features of the PARMILA-2 Module are pointed out in Figure 1.

SIMULATION OF EMITTANCE GROWTH USING THE UAL STRING SPACE CHARGE MODEL

Richard Talman, Cornell University, Ithaca, NY, USA, Nikolay Malitsky, Brookhaven National Laboratory, Upton, NY,USA, and Frank Stulle, CERN, Geneva, Switzerland

Abstract

Evolution of short intense electron bunches passing through bunch-compressing beamlines is simulated using the UAL (Unified Accelerator Libraries) string space charge formulation.[1] Excellent agreement is obtained with results obtained experimentally at CTF-II, the CERN ``Compact Linear Collider" test facility[2]. The 40 MeV energy of these data is low enough for Coulomb and Biot-Savart forces to be important and high enough for coherent synchrotron radiation and centrifugal space charge forces to be important. UAL results are also compared with CSRtrack [3] results for emittance growth in a 50 MeV "standard" chicane. Vertical space charge forces are found to be important in this (low energy) case.

CALCULATIONAL MODEL

Particles are treated as strings as regards their fields but as points as regards their dynamics. Bunch evolution is treated as standard tracking but with intrabeam scattering. The force on particle A due to the (properly-retarded) field of the string associated with particle B is expressed in terms of (closed-form) elliptic integral functions. In the (rare) case when the bunch straddles a magnet edge all particles are assumed to be on the same side of the edge as A. All results have become essentially independent of the number N of macroparticles for N>400, but N-values as great as 3200 have been used in some cases. Summed over all B, for every particle A there are N impulses, making N-squared calculations per evolution step. Even so, all calculations have been done on a laptop.

CSR (coherent synchrotron radiation) results from self-work of the bunch acting on itself---validity of Newton's third law requires the inclusion of field momentum. All static (electric and magnetic) forces plus all coherent longitudinal (CSR) and transverse CSCF (centrifugal space charge force), as well as radiative effects, are included. Since there is no need for "regularization" to suppress singularity, bends and drifts are treated homogeneously. Extreme relativistic approximations (such as neglect of vertical forces) are avoided.

SIMULATION OF CTF-II MEASUREMENTS

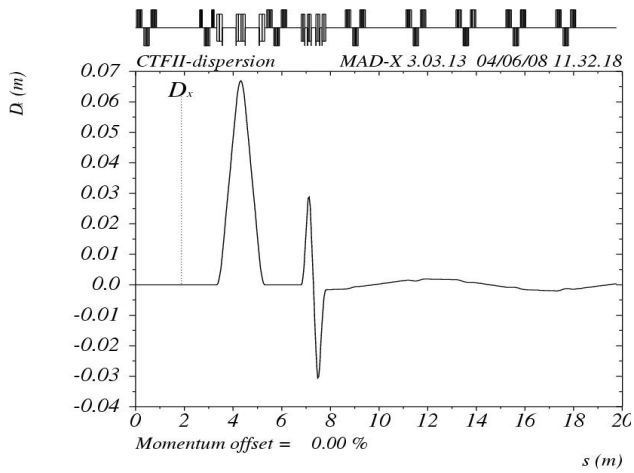

Figure 1: Beamline dispersion, showing "compressor" chicane (C shape) and "shielded" chicane (S shape).

Emittance growth in a bunch compressor has been studied experimentally[2] at the CTF-II (CERN Compact Test Facility), shown in Fig. 1, using electrons of energy 40 MeV. No shielding of CSR by vacuum chamber walls was detected, and the present simulation assumes this to be true. Input and output momentum spectra are shown in Fig. 2. Substantial momentum spreading is visible.

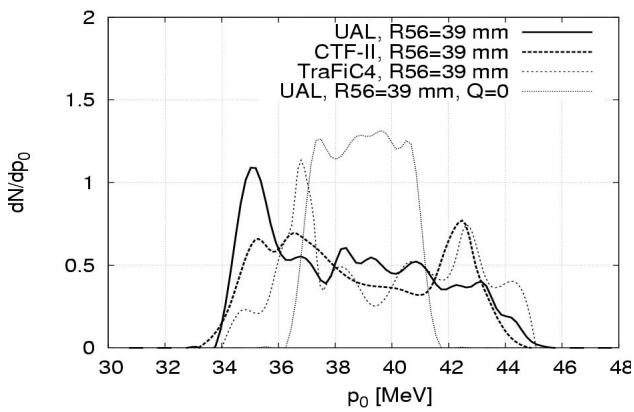

Figure 2: Bunch momentum spread at beamline output with no space charge (narrow square pulse) and with Q=10nC, as measured (label CTF-II) and as simulated by UAL and by (an early version of) TraFiC4.

ELECTRON BEAM DYNAMICS IN THE DARHT-II LINEAR INDUCTION ACCELERATOR*

Carl Ekdahl, E. O. Abeyta, P. Aragon, R. Archuleta, G. Cook, D. Dalmas, K. Esquibel, R. Gallegos, R. Garnett, J. Harrison, J. Johnson, E. Jacquez, B. Trent McCuistian, N. Montoya, S. Nath, K.Nielsen, D. Oro, L. Rowton, M. Sanchez, R. Scarpetti, M. Schauer, G. Seitz, V. Smith, and R. Temple, LANL, Los Alamos, NM 87545, USA

H. Bender, W. Broste, C. Carlson, D. Frayer, D. Johnson, C. Y. Tom, C. Trainham, and J. Williams, NSTec, Los Alamos, NM 87544, USA

B. Prichard and M. Schulze, SAIC, San Diego, CA 92121, USA

T. Genoni, T. Hughes, and C. Thoma, Voss Scientific, Albuquerque, NM 87108, USA

Abstract

The DARHT-II linear induction accelerator (LIA) accelerates a 2-kA electron beam to more than 17 MeV. The beam pulse has a greater than 1.5-microsecond flattop region over which the electron kinetic energy is constant to within 1%. The beam dynamics are diagnosed with 21 beam-position monitors located throughout the injector, accelerator, and after the accelerator exit, where we also have beam imaging diagnostics. We discuss the tuning of the injector and accelerator, and present data for the resulting beam dynamics. We discuss the tuning procedures and other methods used to minimize beam motion, which is undesirable for its application as a bremsstrahlung source for multi-pulse radiography of explosively driven hydrodynamic experiments. We also present beam stability measurements, which we relate to previous stability experiments at lower current and energy.

INTRODUCTION

The 2-kA, 17-MeV DARHT-II linear induction accelerator (LIA) is unique in that its beam pulse has a long, 1.6-μs flattop during which the kinetic energy varies by less than ±1%. A kicker cleaves four short pulses out of this long pulse, and these are converted to bremsstrahlung for multi-pulse flash radiography of high explosive driven hydrodynamic experiments.

The long-pulse 2-kA beam is produced in a 2.5-MV diode. A diverter switch (crowbar) is incorporated to shorten the 2-μs flat-top pulse to as little as 200 ns flat-top (Fig. 1). After leaving the diode, the beam is accelerated by six induction cells to ~3.5 MeV, and then enters a transport zone designed to scrape off the long rise time, off-energy beam head. As in previous experiments [1,2,3], this beam-head clean-up zone (BCUZ) was configured to pass almost the entire beam head. The main LIA has 68 induction cells that have been upgraded to provide enough potential to accelerate the beam to more than 17 MeV. Each accelerating cell incorporates a solenoid to provide the focusing field for beam transport, as well as dipoles for beam steering.

The solenoids in the injector cells are tuned so that none of the off-energy electrons in the ~500-ns beam head are lost, even in the absence of accelerating fields. The solenoids through the main accelerator were tuned to transport a matched beam through a field increasing to more than 1 kG on axis to suppress beam breakup (BBU).

The tunes for the DARHT-II magnetic transport were designed with two envelope codes, XTR [4] and LAMDA [5]. These solve the beam-envelope differential equations keeping terms that are dropped from the usual paraxial approximation [6]. Initial conditions for XTR and LAMDA were provided by simulations of the space-charge limited diode using the TRAK gun-design code [7] and the LSP particle-in-cell code [8].

Non-invasive DARHT-II beam diagnostics, such as beam position monitors (BPM), are used on every shot [2,3]. Invasive diagnostics, such as a magnetic spectrometer and beam current profile imaging, are only occasionally used [1,2,9].

RESULTS

There was no loss of beam current through the LIA during the time that the accelerating cells were energized, as shown in Fig. 1, which is an overlay of beam current measurements though the injector and accelerator for a single shot. The ~7-MHz oscillation on the beam head is the result of large capacitances and inductances on the diode structure. The loss of some current in the beam head as it transited the BCUZ is evident. For these data, the current was terminated by the crowbar, which was timed to coincide with the end of the accelerating cell pulse. The red cursors in Fig. 1 delineate the 1.6-μs flattop used for the four radiography pulses. Slight beam loss in the BCUZ during the risetime is evident. Figure 2 shows the electron kinetic energy measured with our magnetic spectrometer. The kinetic energy of the accelerated beam exceeds 17.0 MeV for more than 1.6 μs. For this measurement five of the LIA cells were turned off, which reduced the energy by ~1.3 MeV from that expected with all 74 cells.

ARTIFICIAL INTELLIGENCE RESEARCH IN PARTICLE ACCELERATOR CONTROL SYSTEMS FOR BEAM LINE TUNING*

Martin Pieck†, Los Alamos National Laboratory, NM 87544, USA

Abstract

Tuning particle accelerators is time consuming and expensive, with a number of inherently non-linear interactions between system components. Conventional control methods have not been successful in this domain, and the result is constant and expensive monitoring of the systems by human operators. This is particularly true for the start-up and conditioning phase after a maintenance period or an unexpected fault. In turn, this often requires a step by step restart of the accelerator. Surprisingly few attempts have been made to apply intelligent accelerator control techniques to help with beam tuning, fault detection, and fault recovery problems. The reason for that might be that accelerator facilities are rare and difficult to understand systems that require detailed expert knowledge about the underlying physics as well as months if not years of experience to understand the relationship between individual components, particularly if they are geographically disjoint. This paper will give an overview about the research effort in the accelerator community that has been dedicated to the use of artificial intelligence methods for accelerator beam line tuning.

BEAM LINE TUNING

A typical accelerator beam line includes trim magnets for steering, quadrupole magnets for focusing, Faraday cups and stripline detectors for measuring current, and profile monitors for measuring beam size and position. Beam loss monitors give information about loss of beam through miss-steering. Unfortunately, real systems rarely work as they are designed. Problems arise from imperfect beam production, residual magnetic fields, poorly modeled beam behavior, misplaced or flawed control elements, and changes to the design or use of the facility after it has been built. Beam line designers consider these problems and build diagnostic components into the beam lines. Profile monitors and current detectors are used to measure beam parameters throughout the line to provide information for verifying or correcting beam characteristics. Even so, imperfect detectors, system errors, and noise due to various effect cause beam line control to be difficult at best. Surprisingly, few attempts have been made to apply intelligent accelerator control techniques to help with beam tuning, fault detection, and fault recovery problems.

PREVIOUS AI ATTEPMPTS TO ACCELERATOR CONTROL

An early example of AI technology applied to accelerator control can be found in Higo et al. [1]. In this work a rather simple objective of maintaining a given system or operation condition has been discussed. AI is relevant here for dealing with the complex problems of generalized hysteretic and stochastic effects.

Weygand [2] reports on a development for a knowledge-based, domain specific expert system at Brookhaven National Laboratory. The purpose of the expert system is to aid in the control of the Heavy Ion Transfer line (HITL) and in turn to minimize down time after a change in running conditions or the start of a new run. Due to the complexity of the expert system it was divided up into three domains (control, device beam influence, and device cause and effect segment). Separate from that is the goal-solving mechanism of the program. This goal-solving function takes a specified high level goal, and then, by developing a tree of sub-goals, attempts to solve the given goal via a hill-climbing technique. However, the system doesn't take into account that conditions may change during the execution of the solution.

Other attempts at intelligent control for accelerators include the ISIS tune advisor (Schultz et al. 1990), the LAMPF Beam Loss Expert (Clearwater et al. 1986), and a learning system based on RL4 (Clearwater et al. 1990). The ISIS tune advisor and LAMPF Beam Loss Expert were both expert systems for indirect control which were never implemented as general or real-time control solutions. The learning system used knowledge-based induction for off-line learning of beam position monitor placement, but was not implemented as a general learning algorithm.

Neural networks have been applied to accelerator control for actual manipulation of control parameters as well as for simulation. Howell et al. [3] used neural networks for modeling and control of a negative-ion accelerator source at Los Alamos National Laboratory to predict the beam characteristics of the source for given changes in control settings. However, the success was rather limited.

Brown [4] developed an automated controller based on an artificial neural network and evaluated its applicability in a real-time environment. This capability was developed within the context of a small angle negative ion source on the Discharge Test Stand at Los Alamos National Laboratory. Using no knowledge of operating conditions, the controller begins acquiring rough snapshot of the

*This work has benefited from the use of the LANSCE at LANL. This facility is funded by the US DOE and operated by LANS for NSSA under Contract DE-AC52-06NA25396.

† pieck@lanl.gov

PARALLEL 3D FINITE ELEMENT PARTICLE-IN-CELL CODE FOR HIGH-FIDELITY RF GUN SIMULATIONS*

A. Candel†, A. Kabel, L. Lee, Z. Li, C. Limborg, C. Ng,
G. Schussman, R. Uplenchwar and K. Ko
SLAC, Menlo Park, CA 94025, USA

Abstract

SLAC's Advanced Computations Department (ACD) has developed the first high-performance parallel Finite Element 3D Particle-In-Cell code, Pic3P, for simulations of RF guns and other space-charge dominated beam-cavity interactions. As opposed to standard beam transport codes, which are based on the electrostatic approximation, Pic3P solves the complete set of Maxwell-Lorentz equations and thus includes space charge, retardation and wakefield effects from first principles. Pic3P uses advanced Finite Element methods with unstructured meshes, higher-order basis functions and quadratic surface approximation. A novel scheme for causal adaptive refinement reduces computational resource requirements by orders of magnitude. Pic3P is optimized for large-scale parallel processing and allows simulations of realistic 3D particle distributions with unprecedented accuracy, aiding the design and operation of the next generation of accelerator facilities. Applications to the Linac Coherent Light Source (LCLS) RF gun are presented.

INTRODUCTION

The Office of Science in the U. S. DOE is promoting the use of High Performance Computing (HPC) in projects relevant to its mission via the 'Scientific Discovery through Advanced Computing' (SciDAC) program which began in 2001 [1]. Since 1996, SLAC has been developing a parallel accelerator modeling capability, first under the DOE Grand Challenge and now under SciDAC, for use on HPC platforms to enable the large-scale electromagnetic and beam dynamics simulations needed for improving existing facilities and optimizing the design of future machines.

METHODS

In the following, a brief introduction to the employed methods for solving the full set of Maxwell's equations in time domain in the presence of charged particles is given.

Maxwell Finite Element Time-Domain

In our approach, Ampère's and Faraday's laws are combined and integrated over time to yield the inhomogeneous vector wave equation for the time integral of the electric field:

$$\varepsilon\frac{\partial^2}{\partial t^2}\int_{-\infty}^{\mathbf{t}}\mathbf{E}\,\mathrm{d}\tau+\nabla\times\mu^{-1}\nabla\times\int_{-\infty}^{\mathbf{t}}\mathbf{E}\,\mathrm{d}\tau=-\mathbf{J},\quad(1)$$

where $\mathbf{E}$ is the electric field intensity, $\mathbf{J}$ is the electric current source density, and ε and μ are the electric permittivity and magnetic permeability.

The computational domain is discretized into curved tetrahedral elements and $\int_{-\infty}^{t}\mathbf{E}\,\mathrm{d}\tau$ in Eq. (1) is expanded into a set of hierarchical Whitney vector basis functions $\mathbf{N_i}(\mathbf{x})$ up to order p within each element:

$$\int_{-\infty}^{t}\mathbf{E}(\mathbf{x},\tau)\,\mathrm{d}\tau=\sum_{i=1}^{N}e_i(t)\cdot\mathbf{N_i}(\mathbf{x}).\quad(2)$$

For illustration, $N_2=20$ and $N_6=216$. After accounting for boundary conditions at domain boundaries and between neighboring elements, a global number of expansion coefficients is obtained, representing the field degrees of freedom (DOFs) of the system.

Substituting Eq. (2) into Eq. (1), multiplying by a test function and integrating over the computational domain Ω results in a matrix equation, second-order in time. The unconditionally stable implicit Newmark-Beta scheme [2] is employed for numerical time integration. The resulting sparse positive definite system matrix is distributed over the compute nodes and is either factorized with a direct solver for smaller problems, or the linear system is solved iteratively at each time step with a conjugate gradient method with suitable preconditioners.

At a given moment in time, the electric field $\mathbf{E}$ and the magnetic flux density $\mathbf{B}$ are then easily obtained from the solution vector $\mathbf{e}$:

$$\mathbf{E}(\mathbf{x})=\sum_{\mathbf{i}}(\partial_{\mathbf{t}}\mathbf{e})_{\mathbf{i}}\cdot\mathbf{N_i}(\mathbf{x})\quad(3)$$

and

$$\mathbf{B}(\mathbf{x})=-\sum_{\mathbf{i}}(\mathbf{e})_{\mathbf{i}}\cdot\nabla\times\mathbf{N_i}(\mathbf{x}).\quad(4)$$

* Work supported by the U.S. DOE ASCR, BES, and HEP Divisions under contract No. DE-AC002-76SF00515.
† candel@slac.stanford.edu

BEAM DYNAMICS AND WAKE-FIELD SIMULATIONS FOR THE CLIC MAIN LINACS

V. F. Khan, R.M. Jones, Cockcroft Institute, Daresbury, WA4 4AD, UK
and University of Manchester, Manchester, M13 9PL, UK

Abstract

The CLIC linear collider aims at accelerating multiple bunches of electrons and positrons and colliding them at a centre of mass energy of 3 TeV. These bunches will be accelerated through X-band linacs, operating at an accelerating frequency of 12 GHz. Each beam readily excites wake-fields within the accelerating cavities of each linac. The transverse components of the wake-fields, if left unchecked, can dilute the beam emittance. The present CLIC design relies on heavy damping of these wake-fields in order to ameliorate the effects of the wake-fields on the beam emittance. Here we present initial results on simulations of the long-range wake-fields in these structures and on beam dynamics simulations. In particular, detailed simulations are performed, on emittance dilution due to beams initially injected with realistic offsets from the electrical centre of the cavities.

INTRODUCTION

The CLIC scheme aims at colliding electrons and positrons at a centre of mass energy of 3 TeV. The main accelerating cavities of CLIC are normal conducting copper structures, designed to operate at 12 GHz. As the beam transits these accelerating cavities it receives a tranverse momentum kick which has the potential to result in serious beam disruption. This kick is proportional to the a^3, where "a" is the iris dimension. It is interesting to note that for the CLIC scenario the average iris is ~3.0 mm compared to 35 mm for the ILC superconducting cavities (which operate at an L-band frequency of 1.3 GHz). Thus, the kick imparted to the beam in the CLIC design is a factor of 1600 greater than that of the ILC cavities. Clearly, the wake-field will require careful suppression and the impact on emittance dilution will necessitate a beam dynamics study including realistic fabrication tolerances.

The present baseline design for CLIC relies on heavy damping (with Qs as low as 10) in order to suppress these wake-fields. The wake-field suppression in this case entails locating the damping materials in relatively close proximity to the location of the accelerated beam. Here a strategy originally employed for the NLC [1] in which moderate damping is imposed (Q~500) together with detuning of the characteristic modes of the structure is used. The potential advantage of this alternative method lies in the ability to locate the damping materials outside the immediate vicinity of the beam and to provide a means of diagnosing the location of the beam and cell misalignments from the radiation at the damping ports [2].

We have already considered a design in which we prescribed a Gaussian dipole mode distribution with an optimised bandwidth of 3.3 GHz for the first band together with interleaving of successive structures [3]. The detuning resulted in a wake-field which was suppressed by almost two order of magnitude at the first trailing bunch in the CLIC train of 312 bunches. In this work we focus on the parameters of the present baseline design known as CLIC_G which consists of 24 cells. We retain the dimensions of the end cells and the intermediate cells are modified with a view to enforcing a Gaussian distribution in the kick factor weighted distribution [1]. Enforcing a fixed geometry to the end cells results in a reduced dipole mode bandwidth. As a consequence of this fixed dipole bandwidth the wake-field at the first few trailing bunches is insufficiently damped. Interleaving successive structures results in an improved overall suppression in the wake-field. Nonetheless, even with 8-fold interleaving of structures the envelope of the wake-field is still unsatisfactory. To ameliorate the effect of this wake-field on emittance dilution we have modified the structure geometry with a view to locating the first few trailing bunches at the zero crossing point in the wake-field. To assess the practicality of this method we have undertaken a series of beam dynamics simulations entailing tracking the beam through the complete CLIC main linac. We present initial results on this study herein. The RMS of the sum wake-field also provides evidence as to whether beam break up (BBU) is occurring and we study this parameter also.

BASELINE CLIC STRUCTURE

The fundamental parameters of the present baseline structure known as CLIC_G are delineated in Table 1. From an analysis of electrical breakdown the group velocity of the fundamental mode should be kept as small as is commensurate with a practical filling time. With this in mind, the geometry of the end cells is invariant to within a factor of ~10%. Intermediate cells are varied in

Table 1: Parameters of updated CLIC baseline structure CLIC_G [4].

Structure	CLIC_G
Frequency (GHz)	12
Average iris radius/wavelength <a>/λ	0.11
Input /Output iris radii (mm)	3.15, 2.35
Input /Output iris thickness (mm)	1.67, 1.0
Group velocity (% c)	1.66, 0.83
Number of cells per cavity	24
Bunch separation (rf cycles)	6
Number of bunches in a train	312

PREDICTION OF 4ν=1 RESONANCE OF A HIGH INTENSITY LINAC*

D. Jeon#, SNS, ORNL, Oak Ridge, TN 37831, U.S.A.
I. Hofmann, L. Groening, G. Franchetti, GSI, Darmstadt, Germany

Abstract

The 4ν=1 resonance of a linac is demonstrated when the depressed tune is around 90°. It is observed that this fourth order resonance is dominating over the better known envelope instability and practically replacing it. Simulation study shows a clear emittance growth by this resonance and its stopband. Experimental measurement of the stopband of this resonance is proposed and conducted in 2008 using the UNILAC at GSI. This study will serve as a benchmarking and guidance for the experiment.

INTRODUCTION

Recently many high intensity linacs have been designed or constructed like the SNS (USA) [1], J-PARC (Japan) [2], or people are trying to increase the intensity of existing linacs such as the UNILAC of GSI (Germany) [3]. For the high intensity linacs, it is the utmost goal to minimize the beam loss of halo particles by avoiding or minimizing contributions of various halo formation mechanisms. One such mechanism is the envelope instability [4]. So far the high intensity linac design such as the SNS linac has avoided the $\sigma_{ot} = 90°$ phase advance because of the envelope instability [1].

Until 1998, mismatch was the primarily studied mechanism of halo formation. Late 1998, Jeon found a case of halo formation induced by the $2\nu_x$-$2\nu_y$=0 resonance from the space charge potential in the ring [5]. Further studies of halo formation and/or emittance growth by space charge and resonances are reported in [6] and by space charge coupling resonance studies of linac such as [7]. Besides these, halo formation by non-round beam was reported [8] and halo formation by rf cavity [9].

In this paper, we will report about a collaborative effort between FAIR-GSI and SNS concerning the 4ν=1 resonance of a high intensity linac. We are preparing for an experiment to measure the stop-band of this resonance using the UNILAC at GSI. Numerical simulation is performed with 50 000 to 100 000 macroparticles with the PARMILA code [10]. Space charge tune shift is about -20°.

THE LINAC FOURTH ORDER RESONANCE

The study shows that the 4ν=1 resonance occurs when the phase advance with space charge σ is slightly lower than 90° for a linac just like a ring through the space charge octupole potential for a variety of beams including Gaussian, waterbag, etc.. For the phase advance with space charge σ > 90°, no resonance effect is observed, as shown in Fig. 6.

Crossing the Resonance from Below 90 °

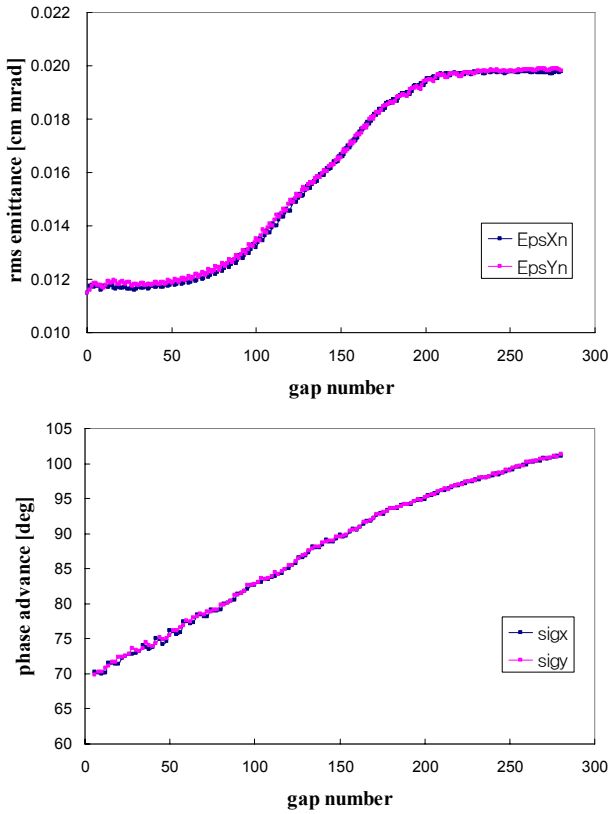

Figure 1: Top plots display rms emittance vs gap number and bottom plots the phase advance with space charge when the beam crosses the resonance from below.

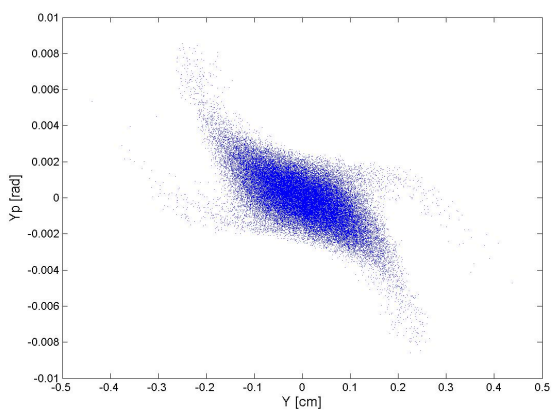

Figure 2: Plot of the beam distribution in Y phase space at the 96th gap. Transport of beam particles along the separatrices is observed.

* See acknowledgement
#jeond@ornl.gov

TRANSVERSE MATCHING OF THE SNS LINAC BASED ON PROFILE MEASUREMENTS *

Dong-o Jeon#, Oak Ridge National Laboratory, Oak Ridge, TN37831, U.S.A.

Abstract

For a high intensity linac such as the SNS linac, it matters to match transversely adequately to minimize the beam mismatch and potential beam loss. The technique of doing the matching using the wire-scanners in series was employed [1]. It was verified that matching was improved through the matching technique based on the beam profile measurements from wire-scanners in series.

INTRODUCTION

The Spallation Neutron Source (SNS) linac accelerates intense H^- beams to energy of 1-GeV, delivering more than 1.4 MW of beam power to the neutron production target [2]. Being a high intensity linac, a primary concern is the uncontrolled beam loss and radio activation of accelerator components. Mismatch generating beam halo, it is important to accomplish adequate level of transverse matching between sections of linac.

When emittance measurement device is available, minimization of rms emittance proves to be effective in doing the matching as for the SNS DTL (Drift Tube Linac) tank 1 commissioning [3].

Alternatively wire-scanners installed in series can be used to transversely matching between two different structures of the SNS linac [4,1]. During the beam operation runs, the matching technique based on beam profile measurements was tested and the results are presented here. The previous work [5] was for a relatively low beam current around 15 mA. This study is focused on the performance for high current (~ 32 mA) and for an incoming beam with a large envelope oscillation.

MATCHING DTL TO CCL

We applied the technique based on profile measurements to matching the Drift Tube Linac (DTL) to the Coupled Cavity Linac (CCL). The beam energy is 86.6 MeV coming out of DTL. The peak beam current used for the measurement was 34 mA. We performed a Gaussian fit to the measured beam profile and obtained its beam size σ. By fitting the beam envelope from the Trace3D code to the wire-scanner profile data, we obtained the input beam Courant-Snyder parameters β and α, and the beam emittance ε, as shown in Fig. 1. With the beam parameters of the incoming beam determined, the matching quadrupoles are optimized using the Trace3D code to do the matching.

The first four wire-scanners were used by the matching program to predict a better matching. This matching technique is robust for quite high peak current beam.

* SNS is managed by UT-Battelle, LLC, under contract DE-AC05-00OR22725 for the U.S. Department of Energy.

#jeond@ornl.gov

Figure 1 shows the data before the matching exercise and Fig. 2 the data after the matching. The solid circles in Figs. 1 and 2 represent profile measurements from wire-scanners in CCL module 1 and 2. The blue color represents the x beam size and the red the y beam size. It is clear that the matching in x plane is improved significantly and that a slight improvement is observed in y plane (y plane was already close to well matched condition). We observe an overall improvement in matching. The measured normalized rms emittances are ε_x=0.283 and ε_y=0.320 [mm mrad] of the equivalent uniform beam distribution having the same rms beam size as the beam profile.

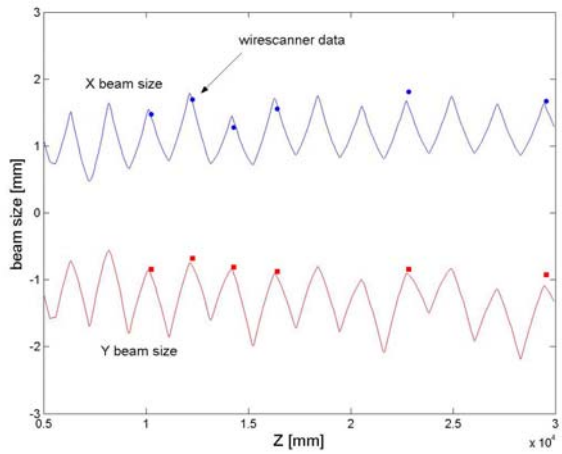

Figure 1: Plots of beam profiles before matching DTL to CCL. Solid lines are plots of beam size σ [mm] from the Trace3D program and solid circles are wire-scanner profile data. The peak beam current is 40 mA.

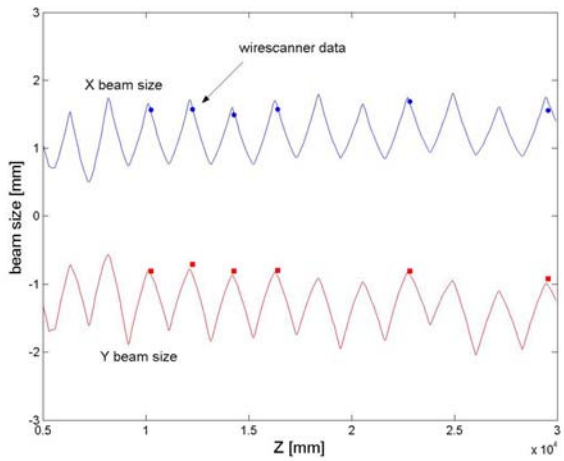

Figure 2: Plots of beam profiles after matching DTL to CCL. Solid lines are plots of beam size σ [mm] from the Trace3D program and solid circles are wire-scanner profile data.

PHASE LAW OF A HIGH INTENSITY SUPERCONDUCTING LINAC*

D. Jeon# and J. Galambos, SNS, ORNL, Oak Ridge, TN 37831, U.S.A.

Abstract

The importance of a proper phase law is recognized to tune the synchronous phase of each superconducting cavities of a high intensity proton superconducting linac such as the SNS linac. The factors to be optimized are 1) maximizing the longitudinal acceptance 2) better matching throughout the linac and 3) achieving maximum beam energy. The driving force behind this study is how to effectively control the large voltage fluctuation from cavity to cavity, achieving low beam loss and high beam quality.

INTRODUCTION

Recently many high intensity linacs have been designed or constructed like the SNS (Spallation Neutron Source) [1], and J-PARC (Japan) [2]. Part of the SNS linac is a pulsed superconducting linac (SCL) accelerating from 186 MeV to 1 GeV. There is a significant spread of the cavity field from cavity to cavity as shown in Fig. 1. Besides, there are cavities turned off for various reasons. If the synchronous phase is set to design values which assumes uniform cavity voltage, cavity field variation and off cavities lead to significant perturbation to the beam, potentially leading to beam loss. So the goal is how to 1) preserve beam quality, 2) minimize beam loss and 3) get as high beam energy as possible. In this paper, we report the important factors to be considered in achieving the three goals.

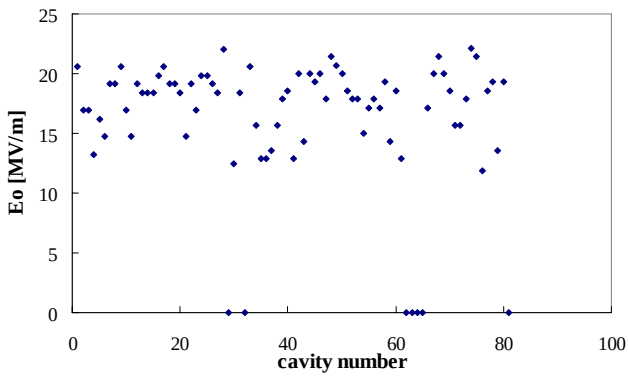

Figure 1: Plot of cavity field Eo vs. cavity number. Quite significant variation is observed besides that six cavities are off.

IT MATTERS HOW TO SET THE PHASE

Each superconducting cavity of the SNS linac is fed by individual klystron, leaving us a lot of freedom how to set the phase of each cavity. One approach is to vary the synchronous phase ϕ_s of each cavity to compensate the variation of Eo from cavity to cavity, hoping to provide smooth focusing across the superconducting linac. We call this method "Smooth Focusing Optics (SFO)" for the sake of convenience. The other approach is to fix the synchronous phase of most of the cavities to design values and vary the phase of a handful of carefully chosen cavities only. We call this method "Constant Phase Optics (CPO)". Figure 2 shows how the synchronous phase of each cavity is set for the two optics.

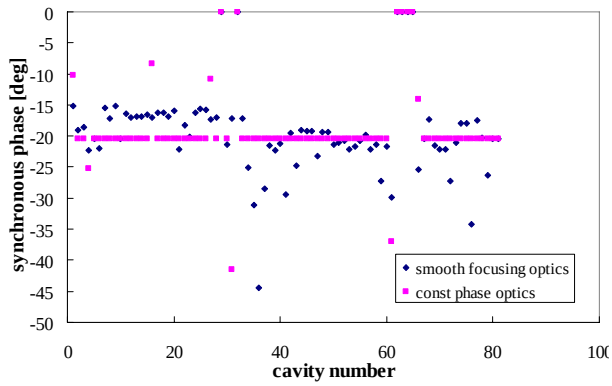

Figure 2: Plot of synchronous phase of the smooth focusing optics in blue and that of the constant phase optics in magenta. Phase of cavities that are off is set to zero in the plot.

Longitudinal Acceptance Matters

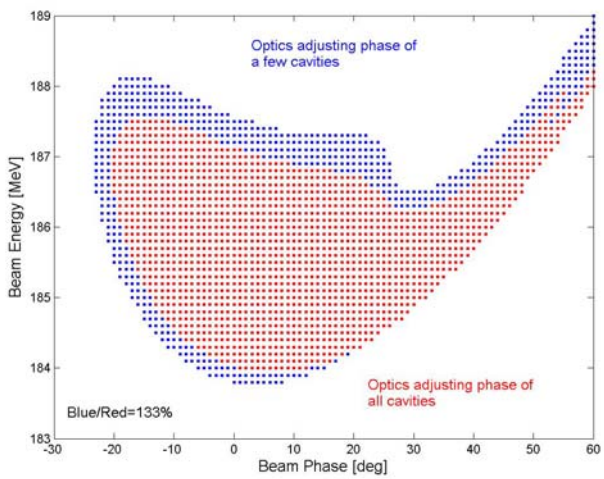

Figure 3: Longitudinal acceptance of the two optics. The constant phase optics in blue produces 33 % bigger acceptance than the smooth focusing optics in red.

* SNS is managed by UT-Battelle, LLC, under contract DE-AC05-00OR22725 for the U.S. Department of Energy.
#jeond@ornl.gov

PRECISE CONTROL OF COOLING WATER SYSTEM FOR STABILIZATION OF 125 MEV LINAC AT LEBRA*

T.Sakai#, T.Kuwada, M.Inagaki, I.Sato, ARISH, Nihon University, Tokyo, 102-8251, Japan
T.Tanaka, K.Hayakawa, Y.Hayakawa, Y.Takahashi, K.Nakao, K.Nogami, LEBRA, Nihon University, Funabashi, 274-8501, Japan

Abstract

The 125-MeV linac at the Laboratory for Electron Beam Research and Application (LEBRA) in Nihon University has been used for the generation of the near-infrared FEL and the Parametric X-ray Radiation (PXR). Currently the FELs from 0.855 to 6μm and the PXR X-rays from 5 to 20keV are available at LEBRA.

Precise experiments using the light sources require a high stability in both the wavelength and the intensity of the lights. Though the linac was operated with the cooling water stabilized at 30±0.2°C, periodical fluctuation of the electron beam energy and the beam orbit suggested that the stability of the cooling water temperature was not sufficient. With this condition a large fluctuation (±15%) was observed for the PXR intensity.

After the improvement of the fine cooling water system and the water flow path, fluctuation of the cooling water temperature at the supply head of the accelerating tubes and the electromagnets was suppressed to within ±0.01°C. As a result of the improvement the PXR intensity fluctuation at the X-ray output port has been suppressed to within ±2% for the operation over several hours.

INTRODUCTION

Research of a high performance electron linac for the generation of Free Electron Laser (FEL) and Parametric X-ray Radiation (PXR) has been continued at the Laboratory for Electron Beam Research and Application (LEBRA) of Nihon University as a joint research with the High Energy Accelerator Research Organization (KEK) [1],[2]. The experiments using coherent X-rays or FELs generally require a high stability electron beam in order to keep high spatial definition and stability of wavelength and intensity.

The electron beam from the linac at LEBRA was stabilized with the klystron RF phase feedback and the beam energy feedback systems [3]. Then the work on the beam stabilization has been devoted to the improvement of the linac cooling water system, because it was found that the effect of the temperature change in the linac cooling water was not sufficiently suppressed by the feedback systems. This paper reports on the achievement of the precise stabilization for the accelerator cooling water temperature and the resultant effect on the stability of the light sources.

*Work supported by Nihon University Research Grant for Assistants and Young Researchers (2007), and "Academic Frontier" Project for Private Universities: matching fund subsidy from MEXT, Japan, 2000-2004 and 2005-2007.
#sakai@lebra.nihon-u.ac.jp

LEBRA 125MEV ELECTRON LINAC

The linac consists mainly of the 100kV DC electron gun, the pre-buncher, the buncher and the three 4m long regular accelerating structures. The accelerating RF has been powered by two S-band klystrons (the peak output power of 20MW has been achieved at the repetition rate of 12.5Hz and the pulse duration of 20μs) [4]. After the improvement of the linac cooling system the accelerating structures, the bending magnet coils and the PXR Si target crystal have been cooled with the water precisely controlled by a single fine cooling unit. On the other hand, the klystrons, the klystron focus coils and the RF dummy loads have been cooled with the coarse cooling water. The layout of the LEBRA electron linac is shown in figure 1, and the specifications of the linac are listed in table 1.

The saturated FEL lasing has been obtained in the wavelength region of 0.855-6μm, with the maximum macropulse output energy of approximately 60mJ/pulse at a wavelength of 1725nm [1]. The PXR generator covers the X-ray energies from 5 to 20 keV by using Si(111) planes as the target and the second crystals[2]. These light sources have been used for the variety of user's experiments [2],[5].

Table 1: Specifications of the LEBRA Electron Linac

Maximum Energy	125	MeV
DC gun voltage	-100	kV
Accelerating RF frequency	2856	MHz
Klystron peak RF power	30	MW
Number of klystrons	2	
Macropulse duration	5~20	μs
Repetition rate	2~12.5	Hz
Macropulse beam current	200	mA
Energy spread(FWHM)	0.5~1	%

PROBLEMS IN THE COOLING WATER SYSTEM

The diagram of the original water flow path in the cooling system for the LEBRA linac is shown in figure 2. The water temperature in the fine cooling system was 30 ±0.2°C at the normal operation. The fluctuation of the PXR intensity measured using an ion chamber was approximately ±15% of the average value, strongly depending on the change in the cooling water temperature. By adjusting the control parameters of the fine cooling

CONTROL SYSTEMS FOR LINAC TEST FACILITIES AT FERMILAB*

J. Patrick and S. Lackey, Fermilab, Batavia, IL, U.S.A.

Abstract

Fermilab is constructing superconducting RF test facilities for development of technologies to be used in future linear accelerator projects. Two of these facilities, the High Intensity Neutrino Source, (HINS) and the New Muon Laboratory, (NML) are proto-type linacs which will run with beam. Originally the NML facility was primarily an R&D facility for the proposed International Linear Collider. Now both HINS and NML are focused on R&D for the Project X [2] high intensity proton linac proposed for Fermilab. The requirements for these facilities vary but all involve collaboration and flexibility for integrating various new instruments. Tight timing requirements and automation are also required. Some facilities require integration into the existing Fermilab controls system. The controls also must be robust so as not to interfere with the main purpose of the facilities. We will outline the plan for accomplishing this task as well as the current status.

STATUS AND REQUIREMENTS

HINS

HINS (High Intensity Neutrino Facility) [2] is a 60 MeV proton or H- accelerator being built in the Meson Detector Building at Fermilab. It consists of an ion source, RFQ, room temperature and superconducting RF cavities, focusing solenoids, and diagnostic instrumentation. It is initially using an instance of the SNS low level RF system [3] to control the klystron. This =and a desire to create graphical user interfaces easily without programming resulted in the decision to use EPICS for the HINS control system. The SNS LLRF system will be replaced with a new design within a year to accommodate longer pulse lengths and control multiple cavities per klystron using vector modulators.

As in any pulsed machine, it is important to be able to correlate data from the various front ends and instruments. Special time stamping which includes either pulse identification and/or synchronization across computers will be required.

NML

The NML facility is intended to test cryomodules developed for the ILC or the proposed Project X linac. Initially RF testing on a single cryomodule will be performed with no beam. Eventually the facility will support electron beam operation through 3 cryomodules at energies up to 750 MeV. The NML facility is a stand alone system which will not have to interoperate with the rest of the Fermilab complex. The low level RF system presently in use is from DESY and was developed in the DOOCs control system. There may be equipment which other laboratories may bring for testing purposes but the main objective of this facility will be the testing of the cryomodules themselves. The correlation of data by RF pulse is a requirement for NML as well.

The aggressive schedule demands that especially the cryogenic system and RF system be controllable this fall. Depending on the funding profile, beam will come somewhat later. For this reason, the Fermilab Control System will be used at NML.

There is an NML control room with operator consoles but it will most likely not be manned 24 hours per day so some oversight at least during off hours will be required.

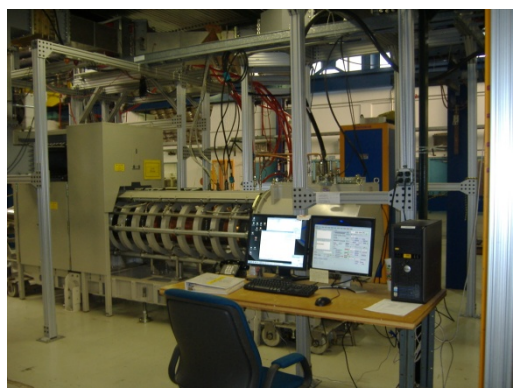

Figure 1: HINS Console and Klystron.

HTS

The Horizontal Test Stand is also in the Meson Detector Building and has been operating for the past year. The purpose of this facility is to test dressed cavities at full RF power before they are installed in cryomodules. It makes use of the DOOCs based low level RF system as well as EPICs input/output controllers for processing loops and interfacing to systems such as vacuum and high level RF interlocks and control.

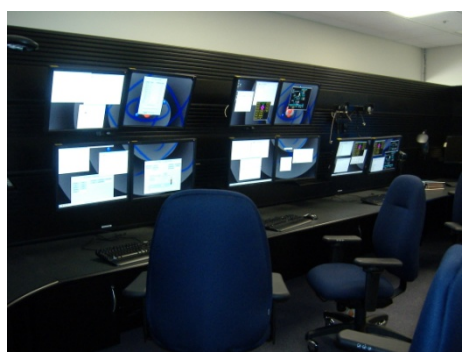

Figure 2: NML Control Room.

* Operated by Fermi Research Alliance, LLC under Contract No. DE-AC02-07CH11359 with the United States Department of Energy

THE DARHT DATA ACQUISITION, ARCHIVAL, ANALYSIS, AND INSTRUMENT CONTROL SYSTEM (DAAAC), AND NETWORK INFRASTRUCTURE.*

R. Archuleta, L. Sanchez, LANL, Los Alamos, NM 87545, USA

Abstract

The Dual Axis Radiographic Hydrodynamic Test Facility (DARHT) at Los Alamos National Laboratory is the world's most advanced weapons test facility. DARHT contains two linear accelerators for producing flash radiographs of hydrodynamic experiments. High-speed electronics and optical instrumentation are used for triggering the accelerators and collecting accelerator data. Efficient and effective diagnostics provide basic information needed to routinely tune the accelerators for peak radiographic performance, and to successfully monitor the accelerators performance. DARHT's server and network infrastructure is a key element in providing shot related data storage and retrieval for successfully executing radiographic experiments. This paper will outline the elaborate Data Acquisition, Archival, Analysis, and Instrument Control System (DAAAC), as well as the server and network infrastructure for both accelerators.

INTRODUCTION

The DARHT facility consists of two accelerators, DARHT-I and DARHT-II. The data acquisition systems are elaborate and heavily instrumented with beam and pulse power diagnostics. Since accelerator data storage and retrieval is crucial in monitoring and executing radiographic experiments, the server and network infrastructure must be isolated and reliable.

DATA ACQUISITION SOFTWARE

DARHT-I and DARHT-II use the Data Acquisition, Archival, Analysis, and Instrument Control System (DAAAC, V4.0) software package from Voss Scientific [1]. This software is used for automating remote instrumentation setup and control, documentation, data archival, and data analysis. The DAAAC software runs on computers running the Windows XP operating system.

The user interface consists of five modules; Archive, Acquire, Analyze, CalMan, and NetCom which operate as one system (see Figure 1).

* This work supported by the US National Nuclear Security Agency and the US Department of Energy under contract DE-AC52-06NA25396
LA-UR-08-06026

The Archive module is the database management tool which allows users to select databases, import or export data, and organize and transfer data. This module manages the various databases that have been created under DAAAC. It provides access to waveforms, images, single point data, informational notes, and accelerator diagnostic data logs that have been stored into a particular database. The Analyze module is the data analysis display tool which is used for examining and processing waveforms, single point data, images, informational notes, and accelerator diagnostic data logs.

Raw and processed data is shown by this module after the data is captured by the Acquire module and processed by the CalMan module. Once the data is displayed by this module it can be examined using tools that apply directly to the data presentation. These tools include such mechanisms as cursors, combining data into single plots, sub-sampling data or computing Figures of Merit (FOMs). In addition to FOMs, there are other tools for performing various mathematical functions. The Acquire module manages instrumentation communication, and controls acquisition sequence and automatic data processing. The CalMan module is used for documenting every channel's signal path, providing a graphical display of the test setup, and organizing the signal line components. The NetCom module is the mechanism that coordinates actions between the other DAAAC modules and the Microsoft Structured Query Language (SQL) Database. The DAAAC architecture uses inter-process communication (IPC) to exchange information between the five modules to operate as a single integrated system [1].

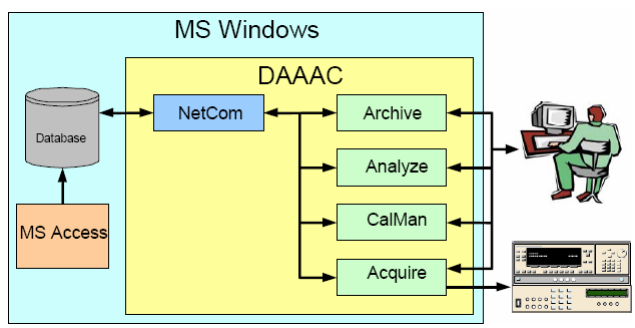

Figure 1: The DAAAC modules.

An additional DAAAC embedded piece of software is the Data Migration tool which migrates data from each accelerator SQL database into Microsoft Access database files. This migration allows for remote users to access the data without having SQL software to poll data from the SQL database elevating the risk of data loss and

THE DUAL AXIS RADIOGRAPHIC HYDRODYNAMIC TEST (DARHT) FACILITY PERSONNEL SAFETY SYSTEM (PSS) CONTROL SYSTEM*

E. Jacquez, LANL, Los Alamos, NM 87545, U.S.A.

Abstract

The mission of the Dual Axis Radiograph Hydrodynamic Test (DARHT) Facility is to conduct experiments on dynamic events of extremely dense materials.

The PSS control system is designed specifically to prevent personnel from becoming exposed to radiation and explosive hazards during machine operations and/or the firing site operation. This paper will outline the Radiation Safety System (RSS) and the High Explosive Safety System (HESS) which are computer-controlled sets of positive interlocks, warning devices, and other exclusion mechanisms that together form the PSS.

BASIC OPERATIONAL OVERVIEW

Physical barriers and alarms are interlocked to the PSS. Door interlocks are located throughout the building. Other physical barriers include the Firing Point boundary fence, interlocked firing point gates, and perimeter warning lights and sirens.

The PSS logic is shown in Figure 1. The PSS is passive in that no external arming, conditioning, or operator intervention is required other than selecting the operational mode and executing the sweep.

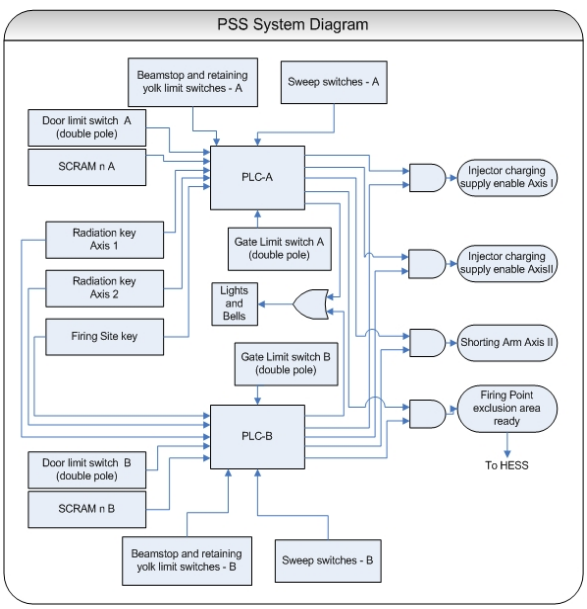

Figure 1: System diagram of PSS.

*This work supported by the US National Nuclear Security Agency and the US Department of Energy under contract DE-AC52-06NA25396
LA-UR-08-06022

A physical inspection, or sweep, of all exclusion areas ensures that affected hazardous areas are clear of personnel before any hazardous operation begins.

SCRAM actuators that inhibit radiation production are located throughout all potential radiation areas.

Located before the beam exit of each accelerator hall, the beamstop is designed to block the beam from reaching beyond the thick-walled accelerator halls. The beamstops allow beam production internal to the accelerator halls and inhibit radiation from reaching the firing point.

The PSS inhibits radiation production and explosive permissions depending on the modes of operation selected. The modes of operation for each axis are described below in Table 1.

Table 1: Operations Modes

Mode	Activities
0	beam off
1	beam in the accelerator hall
2	beam in the hall and on the firing point
3	beam in the hall on the firing point in combination with explosives operations on the firing point

The entire facility operation must be defined by the mode for each axis i.e., Mode 1, 1 (Axis I Mode 1, Axis II Mode 1; Mode 1, 3 (Axis I Mode 1, Axis II Mode 3); etc). The mode of operation defines the requirements for personnel exclusion in an area and therefore procedural sweep patterns. The PSS software controls are programmed to allow certain modes for each axis depending on the mode of the other axis. The modes of operation are shown below in Figure 2.. Up to two modes may be selected simultaneously, depending on the modes selected in Table 1 of this document.

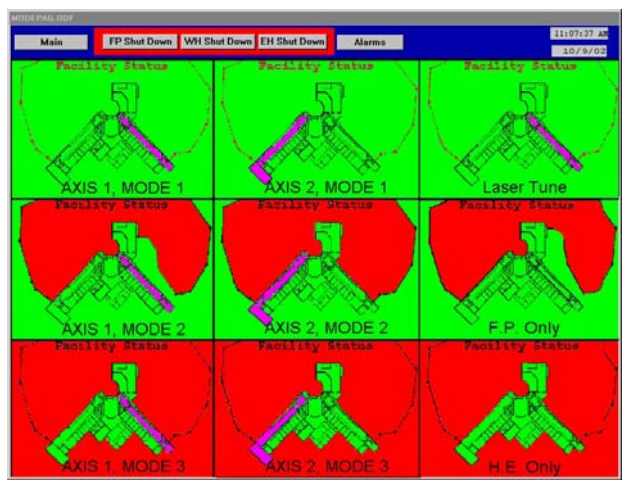

Figure 2: Mode select page.

UNIQUE FEATURES OF THE J-PARC LINAC AND ITS PERFORMANCE - LESSONS LEARNT

A. Ueno#, J-PARC, JAEA, Tokai, Naka, Ibaraki, 319-1195, Japan

Abstract

The J-PARC (Japan Proton Accelerator Research Complex) linac has been successfully commissioned up to its design energy of 181MeV and almost the first stage design peak intensity of 30mA. The following unique methods and hardware features adopted in the J-PARC linac are explained and those results are presented in this paper. The surface production dominating Cs-free H^- IS (Ion Source) with magnetic focus LEBT (low energy beam transport), macro-beam-pulse shaping method related with the J-PARC 30mA-RFQ (Radio Frequency Quadrupole linac) design, a stable one-shot operation method, beam suspending method for machine protection, RF-chopper system related with the operation parameter of the RFQ, one-turn injection into the following J-PARC RCS (Rapid Cycling Synchrotron), transverse matching using TRACE3D PMQ (Permanent Magnet Quadrupole) elements approximating the fringe field effects of the electro-quadrupole magnets, PR (Periodic Reverse) electroforming for high-duty compact DTQ (Drift Tube Quadrupole) coil and thick pure plating of DTL (Drift Tube Linac) and SDTL (Separated-type DTL) and 2 cavity behaviour of SDTL fed with one Klystron.

OVERVIEW OF J-PARC LINAC

As shown in Fig. 1, the J-PARC linac consists of 34 accelerating cavities (RFQ, DTL1~3, SDTL1A~15B), IS, LEBT, MEBT1 (Medium Energy Beam Transport 1) and beam transport to RCS [1]. Since the uncoupled SDTLnA and B (n=1~15) are fed RF-power by one klystron, 19 klystrons are used for acceleration. At the J-PARC first stage, the J-PARC linac accelerates an H^- beam with a peak intensity of 30mA up to the energy of 181MeV with a pulse width of 500μs and a repetition rate of 25Hz.

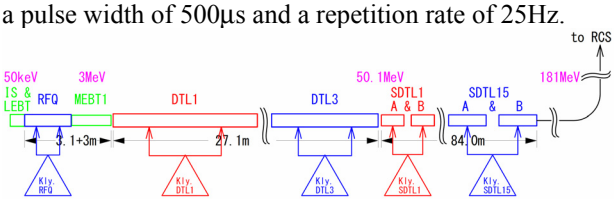

Figure 1: Scheme of J-PARC linac.

SURFACE PRODUCTION DOMINATING CS-FREE IS & MAGNETIC FOCUS LEBT

In almost all of IS's for high intensity H^- accelerators, Cs is seeded on PE (Plasma Electrode) in order to increase H^- production efficiency. Since the thickness of the Cs layer affects to the efficiency greatly, it is not so easy to keep H^- intensity constant with the Cs seeded H^- IS. Also the frequency of sparking in high-voltage gaps of IS or RFQ is increased by the Cs. For stable operation, Cs-free IS is adopted for J-PARC. In order to minimize emittance growth by using SCN (Space-Charge Neutralization) measured as more than 90% [2], the magnetic focus LEBT composed of two solenoid and one ejection angle correction magnets is adopted. A schematic drawing of the IS and LEBT is shown in Fig. 2.

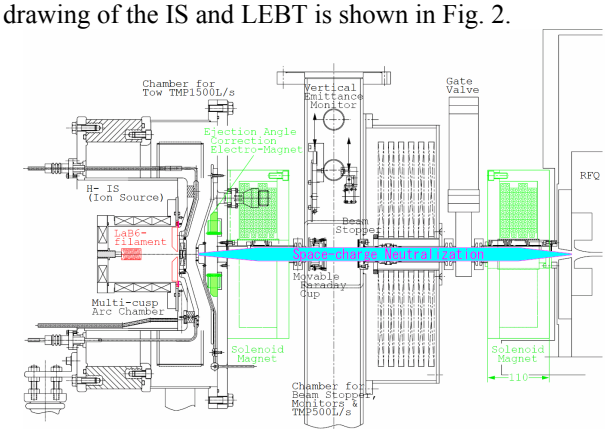

Figure 2: Schematic drawing of IS and LEBT.

On 1995, in a Cs-free IS, a 16mA H^- beam was produced by using a cylindrical arc-chomber (D150mm, L150mm), a LaB_6-filament, a PE shown as Fig.3(a) and an arc-current of 220A [3]. Although the plasma density was increased by using a smaller arc-chamber (D100mm, L125mm) and a higher arc-current of 290A, the intensity had been limited to 16mA by using the PE shown as Fig. 3(b), for two years. After the success of 4mA intensity increase by only increasing the temperature of PE with a thermal insulator ceramics flange shown as Fig. 3(c), various shapes of PE's shown in Fig. 3 were examined by the assumption of that surface H^- production was dominating. Finally, a 38mA H^- beam was produced by using PE shown as Fig.3(h) [4]. The H^- production efficiency seems to be increased mainly by the deoxidization of PE surface made of Mo with the high temperature measured as about 500°C in H_2 gas.

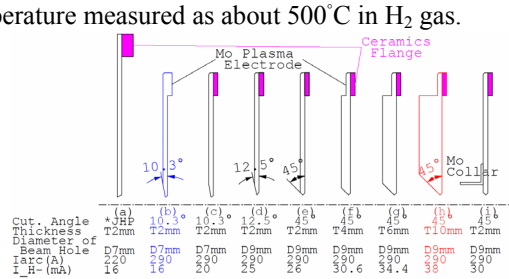

Figure 3: Various shapes of PE's examined.

MACRO-BEAM-PULSE SHAPING & BEAM SUSPENDING METHODS

In order to avoid emittance rotation problem during the rise-time of SCN, macro-beam-pulse shaping by kicking the beam transversely is not available in magnetic focus

#akira.ueno@j-parc.jp

STATUS OF THE CONSTRUCTION OF THE SPIRAL2 ACCELERATOR AT GANIL

Tomas Junquera # on behalf of the Spiral 2 project team, IPN (CNRS/IN2P3, Univ. Paris Sud)
91400 Orsay, France

Abstract

The Driver Accelerator for the SPIRAL2 Radioactive Ion Beam facility at GANIL (Caen, France) is in the construction phase. Following the initial phase of prototyping development, the series production of major components was recently launched. Important decisions have also been recently taken concerning buildings, RIB operational aspects and related safety requirements.

INTRODUCTION

The GANIL laboratory (CNRS-CEA) in Caen (France) is one of the major radioactive and stable-ion facilities for nuclear physics, astrophysics and interdisciplinary research in the world. Since the first beams delivered in 1983 the performances of the GANIL accelerator complex, was constantly improved with respect to the beam intensity, energy and available detection systems. A major improvement was the construction of a new Cyclotron dedicated to the production and acceleration of Radioactive Ion Beams (RIB), the Spiral 1 project, which entered into operation in 2002.

Following the recommendations of international committees, the French Minister of Research took the decision in May 2005 to construct a new facility (Spiral 2) in order to enlarge the range of accelerated ions by production of high intensity RIB. On the 1st of July 2005, the construction phase of SPIRAL2 was launched within a consortium formed by CNRS, CEA and the region of Basse-Normandie in collaboration with French, European and international institutions.

The importance of the availability of Radioactive Ion Beams (RIB) has been often underlined in the last years. NuPECC (Nuclear Physics European Collaboration Committee) and ESFRI (European Strategy Forum on Research Infrastructures) established roadmaps and recommendations for the next generation of facilities in Europe. FAIR in GSI laboratory in Darmstadt (Germany) and Spiral 2 in GANIL laboratory are among the selected projects. Both projects are complementary and are based on two different RIB production methods: FAIR is based on In-Flight Fragmentation techniques, while Spiral 2 uses the Isotope Separation on Line (ISOL) techniques.

THE SPIRAL 2 PROJECT

The radioactive neutron rich beams will be mainly produced via the fission process induced by fast neutrons in a depleted Uranium Carbide (UCx) target (11g/cm3 density), with the aim of 5.10^{13}-10^{14} fissions/s [1]. For this purpose a high intensity CW driver accelerator will deliver 40 MeV (5 mA) to a thick Carbon target (Converter), and produce a very high neutron flux on the UCx target. The fission process will release radioactive atoms which are ionized and extracted from a target/ion-source system. The produced RIB are finally sent to either a low energy experimental hall, or driven towards a charge breeder and post-accelerated by the existing CIME cyclotron (Spiral 1).

The possibilities offered by the driver accelerator, with its capability to accelerate a large range of high intensity CW ion beams (Table 1 and 2), have opened new complementary opportunities to the Spiral 2 project:

- High intensity stable beams, i.e. Ar, Kr, etc
- Neutron experiments, i.e. time of flight
- Interdisciplinary researchs, i.e. solid state, biology, etc

Table 1: Driver Accelerator Beams

beam	p+	D+	ions	ions
Q/A	1	1/2	1/3	1/6
I (mA) max.	5	5	1	1
Womin(Mev/A)	2	2	2	2
Womax(Mev/A)	33	20	14.5	8.5
CW max beam power (KW)	165	200	44	48

Table 2: Driver Accelerator Characteristics

Total length: 65 m (without HE lines)
D+ : ECR ion source
Heavy Ions: ECR Ion Source
Slow and Fast Chopper
RFQ (1/1, 1/2, 1/3) & 3 re-bunchers
12 QWR beta 0.07 (12 cryomodules)
14 QWR beta 0.12 (7 cryomodules)
1 KW Helium Liquifier (4.2 K)
Room Temperature Q-poles
30 Solid State RF amplifiers (10 & 20 KW)

PROGRESS IN THE CONSTRUCTION OF THE SPIRAL 2 FACILITY

During the last two years (oct. 2006-sept 2008) the activities have evolved in two main directions:

1. Preparation and adoption of decisions around the project phases, considering the different beam users and the main project goals, the consequences on buildings and the safety aspects.

2. Construction and tests of main components of the driver accelerator, essentially the Injector and the SC Linac

junquera@ipno.in2p3.fr

CERN LINAC UPGRADE ACTIVITIES

A. M. Lombardi, CERN, Geneva, Switzerland.

Abstract

In its June 2007 session the CERN Council has approved the White Paper, which includes construction of a 160 MeV H^- linear accelerator called Linac4, and the study of a 4 GeV Superconducting Proton Linac (SPL). Linac4 will initially replace Linac2 as the injector to the PS Booster, improving its performance up to the levels required for producing the ultimate LHC luminosity. In a later stage, Linac4 is intended to become the front-end of SPL in a renewed injection chain for the LHC, which could be progressively constructed over the next decade. After briefly introducing the motivations and layout of the new injector chain, the talk will present the characteristics of the new linacs and give an overview of their main technical features and the R&D activities pursued within the HIPPI Joint Research Activity.

INTRODUCTION

In its June 2007 session the CERN Council has approved the White Paper "Scientific Activities and Budget Estimates for 2007 and Provisional Projections for the Years 2008-2010 and Perspectives for Long-Term", which includes construction of a 160 MeV H^- linear accelerator called Linac4, and the study of a 5GeV, high beam power, superconducting proton Linac (SPL).

Both those activities aim at rejuvenating the present proton injectors which –although well-performing for the time being - date from the 60-70s and are working, since some years, well beyond their design intensity and very close to their technical limits.

PRESENT LHC INJECTORS

All the protons at CERN are produced by a duoplasmatron ion source giving in excess of 300 mA of beam current, composed by about 2/3 of protons [1]. The source provides a 100-150 μs beam with a repetition rate of 1.1 Hz. The beam, extracted at 90 keV, is further accelerated by a Linac (Linac2) up to 50 MeV and then injected in the 4 rings of a 25 m radius synchrotron, called the CERN PS Booster (PSB). The PSB, commissioned in 1972, brings the beam energy to 1.4 GeV and injects in another synchrotron, 100 m in radius, called the Proton Synchrotron (PS). CERN PS was commissioned in 1959 and accelerates the beam up to 26 GeV. All the above accelerators are located on the original CERN Meyrin site and serve several experimental facilities like ISOLDE, the antiprotons facility (AD), nTOF and the experiments in the East Area [2].

A fraction of the proton pulses from the PS is sent to the Super Proton Synchrotron (SPS), 1000 m in radius, to be accelerated to 450 GeV and then, amongst other, be injected in the Large Hadron Collider (LHC). The SPS was commissioned in 1976. A sketch of the present CERN accelerator is shown in Fig 1.

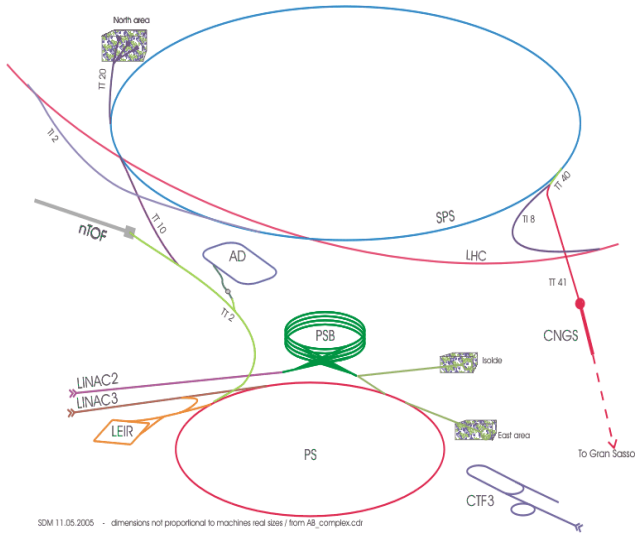

Figure 1: Layout of the present LHC proton injectors.

Linac2 and the Reasons for Its Upgrade

Linac2 [3] was commissioned in 1978 and it consists of a three Alvarez-type Drift Tube Linac (DTL) tanks, operating at the frequency of 202.56 MHz. Electromagnetic quadrupoles are housed inside the 128 drift tubes necessary to bring the beam energy from 0.75 to 50 MeV. Until 1993 the pre-injector was a 750 kV Cockcroft-Walton, which was then replaced by a 4-vane Radio Frequency Quadrupole (RFQ2) [4], capable of delivering almost 200 mA of protons to the DTL. Linac2 is working at a current well beyond its design limit (150 mA) and the RF hardware is working at its technical limit. Besides, the output energy of 50 MeV is too low for any further current increase in the PSB, limited by space charge detuning at injection.

All the above reasons motivate the construction of Linac4 [5], accelerating H^- to an energy of 160 MeV, which halves the space charge detuning at PSB injection and allows charge exchange injection.

Upgrade of the Injectors

Linac4, which is approved to provide H^- for the PSB operation in 2013, can be the first stage of a more global injector upgrade, which includes a Superconducting Proton Linac (SPL) [6] delivering a 4 GeV beam to a new synchrotron (PS2). PS2 could inject in the SPS at 50 GeV opening the potential for a higher proton beam flux from the SPS [7]. A technical design study on SPL and PS2 are due to be completed by 2011 when a decision on further upgrades could be taken. The layout on the Meyrin site [8] is shown on Fig.3. In the next two sections the ongoing activities for Linac upgrades will be described.

LASER ACCELERATION OF QUASI-MONOENERGETIC MeV-GeV ION BEAMS

J.C. Fernandez, LANL, Los Alamos, New Mexico

Abstract

Laser interactions with thin solid targets can produce sheath fields of tens of TV/m, which have been used to accelerate ions to several MeV with ps pulse lengths, high currents, and low transverse emittance. While previous results have had 100% energy spread, recent experiments using foils coated with a few monolayers have produced quasi-monoenergetic beams with 17% energy spread near 3 MeV. Such beams may be of interest as injectors or sources. Simulations show the potential for acceleration to hundreds of MeV or GeV energies using very thin foils.

CONTRIBUTION NOT RECEIVED

LINAC R&D FOR THE ILC TECHNICAL DESIGN REPORT

M. C. Ross, Fermilab, Batavia

Abstract

The International Linear Collider (ILC) Technical Design Report (TDR) is scheduled for publication in 2012. The TDR will include an updated ILC baseline technical design description, results from critical R&D programs in support of key parameter choices, and one or more models for a Project Implementation Plan with an associated value estimate. The focus of linac R&D is to: 1) achieve the specified superconducting rf cavity accelerating gradient of 35 MV/m with a corresponding production yield, 2) design and test cryomodule assemblies that include "plug-compatible" sub-components with specified interfaces, and 3) demonstrate system performance with nominal ILC high intensity beams. In keeping with the international nature of the project, R&D is underway at ILC partner institutions with results and infrastructure that are shared throughout the project effort. This paper describes the technical challenges to be addressed and summarizes ongoing activities and plans.

CONTRIBUTION NOT RECEIVED

ILC SITING IN MOSCOW REGION NEAR DUBNA AND ILC RELATED ACTIVITY AT JINR

Yu. Budagov, Yu. Denisov, I. Meshkov, G. Shirkov, A. Sissakian, G. Trubnikov, JINR, Dubna, 141980, Russia

Abstract

The investigations on ILC siting in the Dubna region and ILC technical activity at JINR are presented. International intergovernmental status of JINR, stable geological and plain relief conditions, comfortable location and well developed infrastructure create a set of advantages of the JINR site in the neighborhood of Dubna. The shallow layout of accelerator tunnel makes it possible to use a communication gallery at the surface instead of second one. This is an effective way of significant cost reduction of all conventional facilities and explicit labor of the project.

Besides JINR physicists take part in several fields of activity in ILC: works on photo injector prototype, participation in design and construction of cryomodules, laser metrology, etc. [1].

INTRODUCTION

The last Global Design Effort (GDE) and ILC Steering Committee (SC) meetings took place at JINR, in Dubna on June 3-7, 2008. These meetings were dedicated to ILC convention facilities and siting and were focused at proposals of JINR [2]. The meetings finished with helicopter flight for leaders of ILC SC and GDE along the ILC possible layout (Fig. 1).

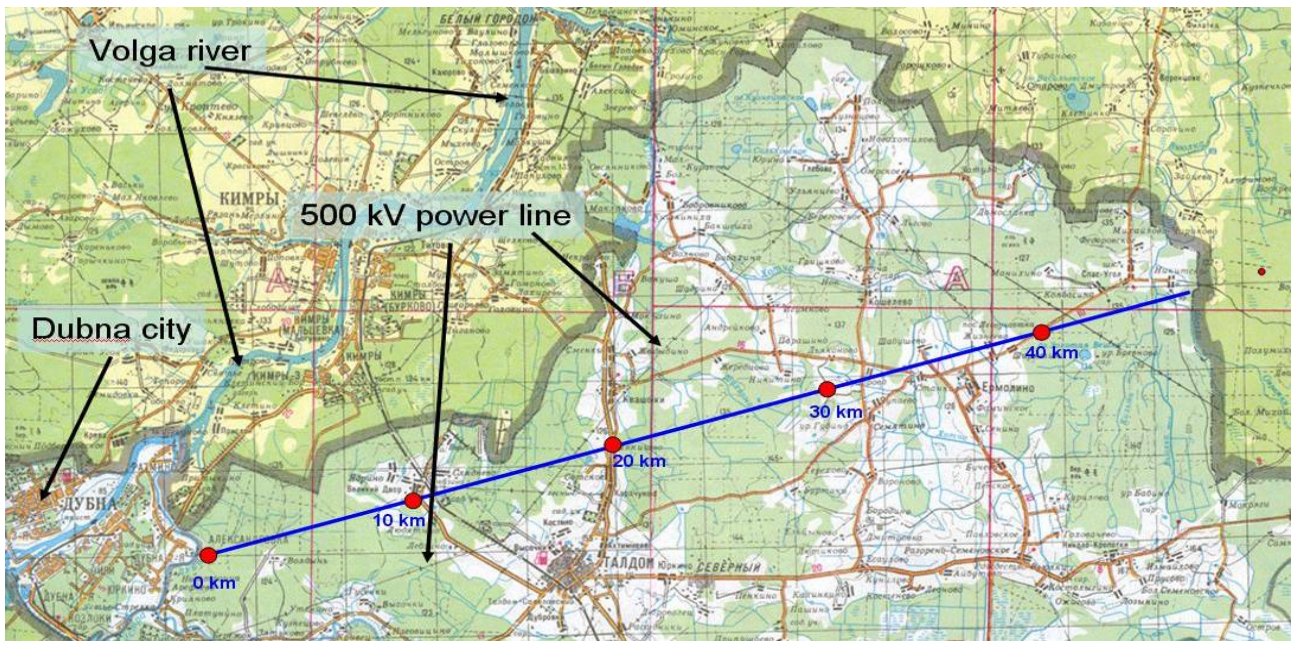

Figure 1: Planned location for ILC near Dubna, Moscow region.

The international scientific community has demonstrated a considerable interest to the proposal of ILC construction in Russia, in Dubna region, where JINR has essential benefits and privileges as an International Intergovernmental Organization and has a unique experience of organization and successful realization of large-scale research projects based on wide cooperation of scientific centers and industrial enterprises of many countries.

Taking into account that the ILC project is considered by the international scientific community as a strategic priority in the field of high energy physics after the LHC era, the International Scientific Council of the JINR has supported the idea of ILC siting in the Dubna region and has recommended to take part in preparation of the collider project. These recommendations had been approved by the Committee of Plenipotentiaries of the JINR Member States. The ILC project and it's siting in the Dubna region have been discussed and supported at different meetings of the Russian Academy of Sciences (RAS).

The initiative to host the ILC in the Dubna site has been strongly supported by the Moscow region governor B. Gromov.

DUBNA SITE DESCRIPTION

The ILC linear accelerator is proposed to be placed in the northern part of Moscow region to the north-east from the existing scientific center JINR in the town Dubna (Fig. 1). This area is thinly populated, the path of the accelerator traverses only two small settlements and a railway with light traffic between the towns Taldom and

STATUS AND FUTURE PROSPECTS OF CLIC

S. Döbert, for the CLIC/CTF3 collaboration, CERN, Geneva, Switzerland

Abstract

The Compact Linear Collider (CLIC) is studied by a growing international collaboration. Main feasibility issues should be demonstrated by 2010 with the CLIC Test Facility (CTF3) constructed at CERN. The CLIC design parameters have recently been changed significantly. The rf frequency has been reduced from 30 GHz to 12 GHz and the loaded accelerating gradient from 150 MV/m to 100 MV/m. A new coherent parameter set for a 3 TeV machine will be presented.

The status and perspectives of the CLIC feasibility study will be presented with a special emphasis on experimental results obtained with CTF3 towards drive beam generation as well as progress on the high gradient accelerating structure development.

The frequency change allows using high power x-band test facilities at SLAC and KEK for accelerating structure testing at 11.4 GHz. The design gradient of 100 MV/m has been achieved in a recent test at SLAC with a very low breakdown-rate.

INTRODUCTION

There is a consensus in the community of high energy particle physicists that LHC physics results need to be complemented in the future by experiments done with a high-energy lepton collider in the TeV centre-of-mass energy range [1]. A promising candidate for such a facility is CLIC, a linear collider aiming at a centre-of-mass energy of 3 TeV and a luminosity in the range of 10^{34} cm^{-2} s^{-1} presently studied by a large international collaboration [2, 3].

In a linear collider the particles have to be accelerated in a single pass to the final energy, 80% of the facility length is used for acceleration. Naturally the emphasis for the R&D on CLIC is on the rf system which has to reach a maximum accelerating gradient and efficiency to keep the length and cost limited. The CLIC scheme uses high-frequency normal conducting accelerating structures and a two beam scheme to cope with these challenges. In 2007 the rf frequency has been reduced from 30 GHz to 12 GHz and the accelerating gradient from 150 MV/m to 100 MV/m for CLIC. This change was motivated by high gradient constraints found experimentally which made the ambitious goal of 150 MV/m unrealistic. A general optimization study taking into account these rf constraints showed that the new parameters represent an optimum with respect to luminosity and cost [3].

The CLIC Test Facility CTF3 [4] is being built at CERN by the CTF3 collaboration to investigate and demonstrate the key technical issues of the CLIC scheme. This feasibility study should conclude in 2010 with a Conceptual Design Report for CLIC.

COMPACT LINAER COLLIDER CLIC

The compact linear collider CLIC uses high-frequency high-gradient normal conducting rf accelerating structures to accelerate the electrons. An accelerating gradient of 100 MV/m at 12 GHz allows to keep such a facility bellow a length of 50 km. The 12 GHz rf power needed to energize the accelerating structures is extracted from a drive beam running parallel to the main beam. This two beam scheme is an efficient and less costly way to provide the rf power needed for acceleration as compared to the use of 12 GHz klystrons. In order to achieve the luminosity needed for the experiments the electrons and positron beams need to be produced with extremely small emittances, accelerated and transported without significant degradation and finally focused to spot sizes in the nm range. The main parameters of CLIC can be found in table 1.

Table 1: CLIC Main Parameters

Centre of mass energy	3	TeV
Luminosity (in 1% energy)	$2*10^{34}$	cm^{-2} s^{-1}
Number of particles per bunch	$3.72*10^{9}$	
Bunch separation	0.5	ns
Number of bunches per train	312	
Proposed site length	48.4	km
AC to beam power efficiency	7.2	%

The Facility Layout

A schematic layout of CLIC is shown in figure 1. A central injector complex prepares the ultra low emittance beams needed for high luminosity collisions. The complex contains the positron and polarized electron sources, pre-damping and damping rings, bunch

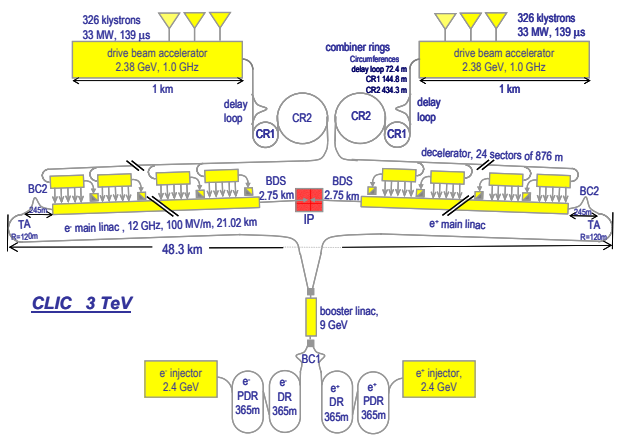

Figure 1: Schematic CLLC layout (not to scale).

DESIGN AND PERFORMANCE OF L-BAND AND S-BAND MULTI BEAM KLYSTRONS

Y. H. Chin, KEK, Tsukuba, Japan.

Abstract

Recently, there has been a rising international interest in multi-beam klystrons (MBK) in the L-band and S-band, with active development taking place. These MBKs are developed by industries such as Toshiba, Thales and CPI for the European X-FEL project or at the Naval Research Laboratory for high-power, low-voltage, broadband radar/radio communication systems. Some of them are already in operation at full specification and are commercially available. MBKs have distinctive advantages to conventional single-beam klystrons in their ability to produce high power with high efficiency and large bandwidth at lower voltage in compact body. This paper reviews the design and performance of these multi-beam klystrons, and describes future development plans.

INTRODUCTION

Klystrons have been always the major sources of high power RF in particle accelerators. The development of new types of klystrons has made large and important contributions in achieving significant advances in energy outreach of linear accelerators. The historical growth in klystron power in the past 60 years since WWII shows that the output power increases 10-fold every 14 years. Recent projects and proposals of high-energy super-conducting linacs demand high power klystrons with high efficiency (60-70%) and long pulse duration (an order of 1ms). The peak power delivered by a long pulse Single-Beam Klystron (SBK) is limited by the high voltage that its gun can withstand. A lower cathode voltage (more exactly speaking, the maximum surface electric field in the gun region) is desirable to ensure reliable operation without gun arching or voltage breakdown. However, in a single-beam klystron, the simultaneous optimization of output power, voltage and efficiency is nearly impossible, since the pervenace determines the relationship of all other operating parameters and even an achievable maximum efficiency of the tube.

When one designs a single-beam klystron for a given output power P_{out}, he first has to choose the pervenace, p, given by $p=I/V^{3/2}$, where I is the beam current from a cathode and V is the cathode voltage. The pervance indicates how much beam current comes out of the cathode when the voltage V is applied between the cathode and the anode. There is the empirical relation between the perveance and the achievable highest efficiency, η_{max}, given by [1]

$$\eta_{\max}\,(\%) = 78 - 16 \times p\,(\mu\text{-perveance}). \qquad (1)$$

Figure 1 illustrates this relationship. This figure indicates that a lower perveance beam with weaker space-charge forces enables stronger bunching and thus consequently higher efficiency.

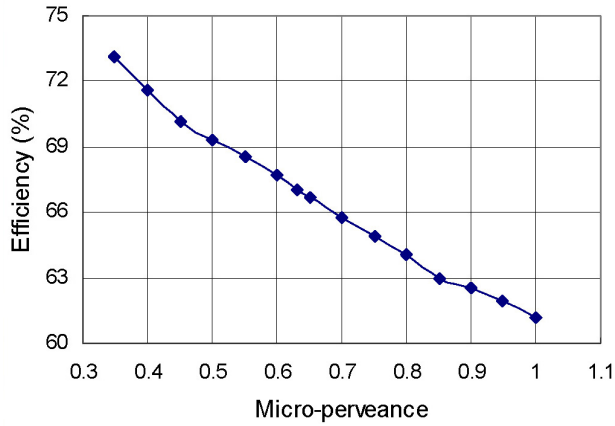

Figure 1: The empirical relation between the perveance and the achievable highest efficiency, η_{max}.

Once the efficiency ($\eta \le \eta_{\max}$) of the tube is assumed, the cathode voltage is determined from the relation

$$P_{out} = \eta IV = \eta p V^{5/2}. \qquad (2)$$

In this circumstance, only way to increase the output power without increasing the voltage, or reduce the voltage without reducing the output power, is to increase the perveance, i.e., the beam current. However, a high perveance is strongly undesirable since (1) it provides a lower efficiency (2) it requires a larger cathode current loading resulting in a shorter cathode lifetime (see Fig.2) (3) it requires stronger magnetic fields for beam focusing which can lead higher system volume and weight (4) it has a higher risk of gun oscillation and gun arching. In conclusion, the choice of perveance in a single-beam klystron is always a compromise between high power and efficiency and tube reliability.

A breakthrough solution to this gridlock is to use multiple low perveance beamlets in parallel in the same vacuum envelop. The number of beamlets introduces a new degree of freedom in parameter space. In a Multi-Beam Klystron (MBK), a high current electron beam is separated into multiple parallel beamlets,

- each with a sufficiently low current density (perveance) to ensure efficient electron bunching and a high efficiency,
- while the high total perveance of beam current provides the required high output power.

POSITRON BEAMS PROPAGATION IN PLASMA WAKEFIELD ACCELERATORS

Patric Muggli
University of Southern California, Los Angeles, CA 90089, USA

Abstract

Preservation of beam emittance is a concern in all accelerators. The formation of a beam charge halo in a plasma wakefield accelerator (PWFA) driven by a single positron bunch is observed. This phenomenon is also observed in numerical simulations. These simulations indicate that it results in significant emittance growth of the positron bunch. We discuss theses results as well as possible means to preserve the positron emittance.

INTRODUCTION

In conventional accelerators using magnetic optics and rf waves in resonant cavities to focus and accelerate particles, positive and negative charge particles can be accommodated by merely a change of current sign in the magnets and phase in the rf.

In plasma-based accelerators (PBAs) the plasma itself sustains the focusing and the accelerating fields. Plasmas are composed of particles of opposite charge, electrons and protons or ions, but of very different mass. Therefore, the light electrons are the mobile species, while the heavier ions are usually considered as immobile on the time scale of an electron plasma period. In the linear theory of PBAs where the relative plasma density perturbations $\delta n/n_e$ (n_e the background plasma density) and wakefield amplitudes are small, the plasma wave is also symmetric for opposite sign charges, providing a simple 90° phase shift of the wave or wake.

However, the nonlinear or blowout regime of PBAs [1] offers some striking advantages over the linear regime for accelerating electrons. In this regime all the plasma electrons are blown out of a volume encompassing the drive and the witness beam. This regime is reached when the drive particle bunch density n_b is much larger than the plasma density: $n_b >> n_e$, or when the drive laser intensity exceeds a threshold value. In this regime the accelerated beam propagates in a pure ion column that acts as a long focusing element free of geometric aberrations. Also, the accelerating field ($\approx \delta n/n_e$) is larger than in the linear regime. In fact, all current PBA experiments operate in this regime. These experiments have shown emittance preservation of the incoming beam [2,3], matching of the beam to the plasma focusing [3], and energy doubling of 42 GeV incoming electrons in only 85 cm of plasma [4], all the above in beam driven PBAs or plasma wakefield accelerators (PWFAs). Acceleration of electron bunches to hundreds of MeVs with narrow energy spread was also demonstrated in this regime in PBAs driven by intense laser pulses or laser wakefield accelerators (LWFAs) [5,6,7]. In this case, access to the nonlinear regime is necessary since the source for the accelerated beam is the trapping of the plasma electron triggered by the breaking of the plasma wave. In recent all these experiments the accelerating gradient exceeded 50 GV/m.

POSITRON BEAMS IN PLASMAS

The situation is very different for the acceleration of positron beams in plasmas. No blowout regime exists because the mobile plasma species is still the electrons, and to focus the positron beam by partial charge neutralization the plasma electrons have to flow through the positron bunch. As a result, in uniform plasmas the electrons do not form a large region (of the order of the plasma wavelength cubed as in the case of an electron bunch) where the wakefield can be uniform enough to accelerate the positron bunch with low energy spread and to focus it while preserving its low incoming emittance. This is true whether the drive beam is a laser pulse or a particle bunch. For instance, simulations indicate that the accelerating field driven by single bunch positron beams is smaller [8] than that driven by an electron bunch with similar parameters. Also, emittance growth of the incoming bunch along the plasma is expected as a consequence of the non-linear focusing force exerted by the plasma onto the bunch. Acceleration and propagation of positron beams in plasmas have not been studied as extensively as they have been with electrons. This is of course due primarily to the fact that short, high current positron bunches are not readily available, except at the Stanford Linear Accelerator Center (SLAC).

The acceleration of positrons in the wakefield driven by a single positron bunch has been demonstrated [9]. The focusing of a positron beam by a short, high-density gas jet plasma was also demonstrated [10]. The effect of the propagation of the same positron beam along a L_p=1.4 m, low density ($<10^{12}$ cm^{-3}) plasma column was studied in detail with picosecond time resolution along the ≈10 ps long bunch [11]. However, in these experiments the product of plasma density and plasma length ($n_e L_p < 3\text{x}10^{12}$ m^{-2}) was too small for the beam to significantly evolve in its transverse dimensions along the plasma.

In order to gain large amounts of energy (>10 GeV) the positron beam will have to propagate through a long (L_p>2 m), dense ($n_e > 10^{16}$ cm^{-3}) plasma, since accelerating gradients of 5 to 10 GV/m are desirable. The effect of the non-ideal wakefield will therefore accumulate and emittance preservation is an open question.

We present here some experimental and simulation results demonstrating the formation of a beam halo around a single positron bunch propagating through a 1.4-

CONTROL, STABILITY AND STAGING IN LASER WAKEFIELD ACCELERATORS

D. Panasenko, LBNL, Berkeley, California

Abstract

Laser driven plasma wakefields have recently accelerated electron beams with quasi-monoenergetic energy distributions and with gradients of ~100 GV/m. Stabilization and optimization of beam quality are now essential. Recent LBNL experiments have demonstrated control of self trapping, resulting in reproducible bunches at 0.5 GeV. Further optimization has been demonstrated using plasma density gradients to control trapping, producing beams with very low absolute momentum spread at low energies. Simulations indicate that use of these beams as an injector greatly improves accelerator performance and experiments are now underway to demonstrate such staging, which will be a crucial technology for laser driven linacs. This talk will cover recent progress in LWFAs to obtain more reproducible, higher quality beams and also cover staging prospects for high energy laser linacs.

CONTRIBUTION NOT RECEIVED

STATUS AND UPGRADE PLAN OF 250 MeV LINAC AT CLS

X.F. Shen, M.S. de Jong, L.O. Dallin, R.M. Silzer and T. Summers

CLS Inc., University of Saskatchewan, Saskatoon, SK S7N 0X4, Canada

Abstract

The Canadian Light Source (CLS) 250 MeV linac, originally constructed in the 1960's, serves as the injector for the 2.9 GeV synchrotron radiation facility [1] located on the University of Saskatchewan campus. The linac has operated reasonably well for routine operation of the light source. However, the long-term goal of operating the CLS storage ring in top-up mode will place increased demands on the linac for stability and availability that cannot be met with the existing system.

Consequently, an upgrade is planned over the next two years to get higher beam stability, reliability and reproducibility. In this paper, the existing linac system will be described and the planned upgrade will be reported.

INTRODUCTION

The 150 MeV linac, with three Varian accelerating sections, was originally constructed in the mid-1960's for nuclear physics research in the Saskatchewan Accelerator Laboratory. In the 1980's, the linac was upgraded to 300 MeV with the addition of three SLAC-type accelerating sections.

In 1999, the nuclear physics research program was shut down, and the linac was incorporated into the injection chain for the 2.9 GeV synchrotron storage ring of Canadian Light Source. In this upgrade the control system was partially modified to use the EPICS system with the exception of the electron gun and modulator high voltage control. The timing, trigger system and instrumentation were also upgraded. Linac operation for the injector only requires short bunch trains (less than 200 ns) with repetitions rates less than 2 Hz. Extensive changes to the modulators were made including the pulse-forming-networks (PFNs) the high voltage power supplies and thyratrons. Some ion pumps and CCGs were upgraded in the vacuum system. About 15% of the magnet power supplies were changed to fit new requirements. The video deflector was modified to produce bunch train lengths of up to 136 ns, corresponding to 68 bunches at 500 MHz. Figure 1 shows the 250 MeV linac tunnel with the 220 kV electron gun.

LINAC STATUS

Linac Structures and Parameters

The linac consists of a high-current gun with a buncher section (manufactured by Haimson) and six 2856 MHz rf sections, and is operated at 250 MeV. After the linac, there is an Energy Compression System (ECS), which reduces the 1% energy spread from the linac by a factor of 10, followed by a transport line to the 2.9 GeV booster synchrotron for the main storage ring.

The electron gun can provide up to 1A beam current at 220 keV. In normal operation, the gun emits 125 mA peak beam current. The buncher section compresses the bunch phase to about 12º and increases beam energy to 13 MeV [2]. Beam current at this point is about 70 mA. There are three Varian style acceleration sections that can provide approximately 50 MeV and three SLAC style sections which provide 40 MeV per section. Each section is supplied RF power by an ITT 8568 klystron.

The linac main parameters are listed in Table 1. The linac is shown in Fig. 1. The linac control schematic is shown in Fig. 4.

Table 1: General parameters of the CLS injector linac.

Type of structure	TW disc-load WG
Frequency	2856 MHz
Length of section	3 m and 5 m
Total number of section	3(3m) & 3 (5m)
RF source	
Peak power of klystron	20 MW
Number of klystrons	6
RF pulse length	2.5 μs
Main Linac Beam	
Energy	250 MeV
Beam Current	60 mA
Beam Pulse Length	2 ns ~136 ns
Repetition Rate	1 Hz
Energy spread (without ECS)	<1.0%
Energy spread (with ECS)	0.1%

ARIEL AND THE TRIUMF E-LINAC INITIATIVE, A ½-MW ELECTRON LINAC FOR RARE ISOTOPE BEAM PRODUCTION

S. Koscielniak, F. Ames, R. Baartman, R. Dawson, J. Drozdoff, Y. Bylinsky, K. Fong, A. Hurst, D. Karlen, R. Keitel, R. Laxdal, F. Mammarella, M. Marchetto, L. Merminga, A.K. Mitra, K. Reiniger, T. Ries, R. Ruegg, I. Sekachev, G. Stinson, V. Verzilov
TRIUMF*, 4004 Wesbrook Mall, Vancouver, BC V6T 2A3, Canada

Abstract

TRIUMF, in collaboration with university partners, proposes to construct a megawatt-class electron linear accelerator (e-linac) as a driver for U(γ,f) of actinide targets for nuclear astrophysics studies, and ^{9}Be(γ,p)^{8}Li for beta-NMR materials science. The e-linac is part of a broader proposal for an expansion of the TRIUMF rare isotope beams capability through a new facility to be named ARIEL. The e-linac design and prospects for funding are elaborated.

INTRODUCTION

TRIUMF, in its Five Year Plan 2010-2015 proposes to build the Advanced Rare IsotopE Laboratory (ARIEL) to augment the Rare Isotope Beam (RIB) science program at the ISAC facility. ARIEL, Figure 1, will have four major components: (i) an electron linac photo-fission driver, (ii) a new target hall to be located in a western extension of the existing ISAC building, (iii) a new proton beam line from the H- cyclotron, and (iv) a new RIB "front end". The accelerators and target station(s) will be connected by new 60 metre long beam lines in a common tunnel. The project will be staged. In the first stage, a 100 kW capable linac, a single target station, the e and p beam lines, ion sources and mass analyzers and RIB transport lines to the existing ISAC RFQ and linacs will be constructed. The second stage occurs in the 2015-2020 Plan: the electron linac and target station are upgraded to the full 1/2 –MW capability, an additional target station is added, and the "front end" is completed by the addition of new RIB accelerators, thus facilitating up to three simultaneous RIB, two of which may be accelerated beams. The science program is sketched in Ref.[1] and concepts for the e-linac design and RIB front end are presented in Refs.[2,3].

Ariel is a fictional sprite who appears in Shakespeare's play *The Tempest*. The counterpart of Ariel's master *Prospero* is the ISAC science program with its suite of world-class experimental apparatus eager to command the production of more beams and new beams. Adding the electron linac will double the RIBs, and adding the new proton beam line and second target station will triple the RIB production and science output. The '-el' ending of Ariel translates in Hebrew as 'God,' placing Ariel inline with benevolent spirits; and indeed the new accelerator will bring many benefits to TRIUMF.

*TRIUMF receives federal funding via a contribution agreement through the National Research Council of Canada.

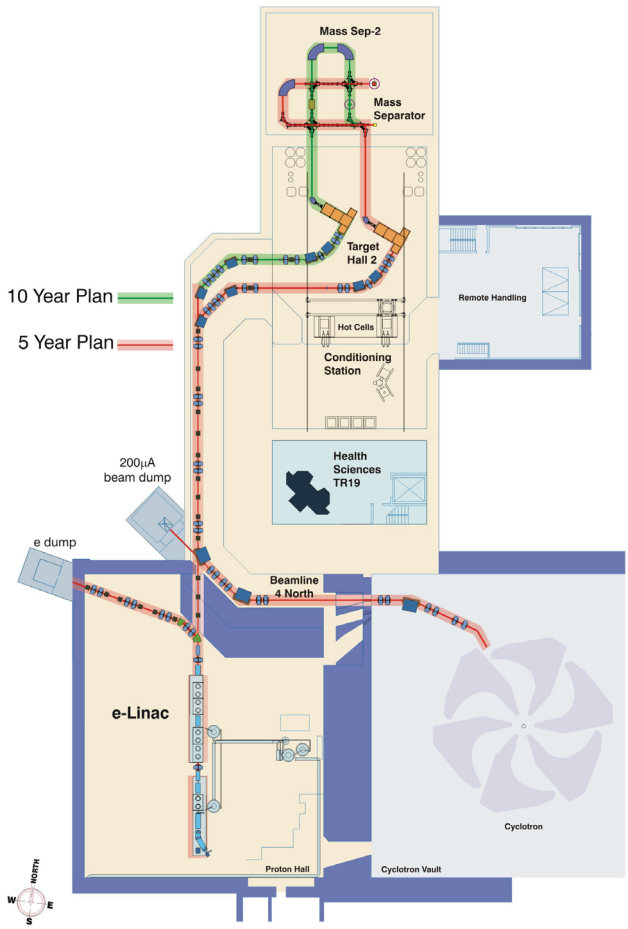

Figure 1: ARIEL infrastructure and layout.

- New Science: nuclear physics with neutron-rich RIBs, and ^{9}Be(γ,p)^{8}Li production for β-NMR studies in Materials and Molecular Sciences.
- An independent driver for RIB production that complements the cyclotron proton driver.
  - Implements strategy of multiple beams (e, p) to multiple users to accelerate science output.
  - E-linac will operate through annual cyclotron shutdowns providing a strong year-round RIB experimental program.
- Leverages valuable existing infrastructure:
  - Proton Hall, shielded vault with services
  - World-class experimental apparatus (detectors)
  - Builds further SCRF expertise base from β«1, 100 MHz, 4K quarter-wave structures to β=1, 1 GHz, 2K elliptical structures.

PROPOSAL FOR A 15 MeV SUPERCONDUCTING ELECTRON LINAC FOR THE DEINOS PROJECT

J-L. Lemaire, P. Balleyguier, D. Guilhem, J-L Flament, V. Le Flanchec, M.Millerioux, S. Pichon
CEA, DAM, DIF, Bruyères le Châtel, 91297 Arpajon, Cedex, France

Abstract

The design of a 15 MeV, 2 kA peak current, electron accelerator for the DEINOS project is presented. It is dedicated to a new radiographic facility. The accelerator is based on a DC photo-injector and a RF superconducting linac. Up to twenty electron micro-pulses, 100 ps time duration and 200 nC bunch charge are emitted at 352 MHz repetition rate from a Cs_2Te photocathode and accelerated to 2.5 MeV in the DC diode before injection into a superconducting linac.

A general description of the main accelerator components and the beam dynamics simulations are presented.

INTRODUCTION

The former DEINOS project which name stands for "**DE**monstrateur d'**IN**jecteur **O**ptimisé pour un accélérateur **S**upraconducteur**"** was consisting of a DC photo-injector coupled to a RF superconducting accelerator (Fig. 1). It is a new versatile scheme based on rather well tested technologies. It has been proposed to produce flash X-ray pulses from very intense electron beams impinging on a high Z material target. A final beam transport allows tight beam focusing on the conversion target [1].

In order to meet the specifications of the radiographic need, 2 µC- 51 MeV- 60 ns, compactness and low cost, the machine could be made of the assembly of a 352 MHz RF linear accelerator and a photo-injector, provided the photo-injector delivers the proper bunches.

Electrons bunches are emitted from a Cs_2Te photocathode driven by a 266 nm wavelength laser and extracted in a DC gun. A pulsed power supply made of a prime power, a Blumlein and coaxial transmission lines drives the diode accelerating voltage.

The voltage applied to the accelerating gap of the diode can reach a value up to 2.5 MV. Time duration of the voltage plateau is set by the Blumlein to be 60 ns.

A short drift section between the photo-injector and the linac allows room for the injection of the photocathode laser beam, a vacuum valve and beam diagnostics.

Optimizations of the photo-injector, the RF accelerator and radiographic parameters led to a design for which the accelerator machine could deliver 20 bunches at 352 MHz. Each bunch of 100 ps time duration would carry 100 nC. This can be done with a UV laser illuminating the photocathode in synchronism with the linac RF in order to recapture the bunches in the RF cavities without any losses.

All the main technical issues that were identified to building the photo-injector (large size diameter and high quantum efficiency Cs_2Te photocathodes, UH Vacuum level - 10^{-10} mbar, high voltage insulator barrier, electron gun and diode geometry, stability of the high voltage driver and stability of the laser) could be worked out with this new demonstrator, at lower budgetary cost. A new orientation has been decided for the project in order to build a reduced scale model.

Then a 15 MeV accelerator scheme based on the early architecture consisting of a DC photo-injector and a superconducting RF linac made of only one cavity, has been proposed as a new facility for radiography applications.

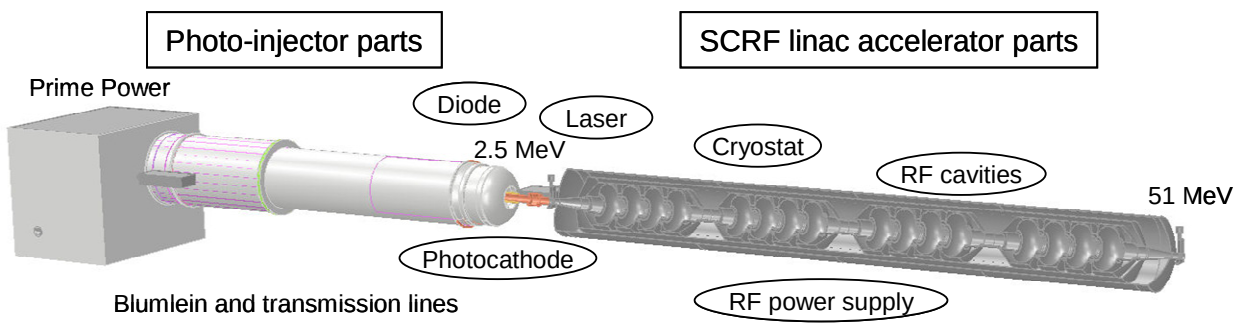

Figure 1: Artist's view of the DEINOS project.

STATUS OF THE CTF3 PROBE BEAM LINAC CALIFES

F. Peauger, D. Bogard, G. Cheymol, P. Contrepois, A. Curtoni, G. Dispau, M. Dorlot, W. Farabolini, M. Fontaine, P. Girardot, R. Granelli, F. Harrault, JL. Jannin, C. Lahonde-Hamdoun, T. Lerch, PA. Leroy, M. Luong, A. Mosnier, F. Orsini, C. Simon, DSM/Irfu, CEA Saclay, France, S. Curt, K. Elsener, V. Fedosseev, G. Mcmonagle, J. Mourier, M. Petrarca, L. Rinolfi, G. Rossat, E. Rugo, L. Timeo, CERN, Geneva, Switzerland, R. Roux, LAL, Orsay, France

Abstract

The CLIC project based on the innovative Two Beams Acceleration concept is currently under study at CTF3 where the acceleration of a probe beam will be demonstrated. This paper will describe in details the status of the probe beam linac called CALIFES. This linac (170 MeV, 0.9 A) is developed by CEA Saclay, LAL Orsay and CERN. It has been installed in the new experimental area of CTF3 to deliver short bunches (1.8 ps) with a charge of 0.6 nC to the CLIC 12 GHz accelerating structures. We report new results of beam dynamic and RF simulations considering the new CLIC parameters. The construction of CALIFES in the CLEX building is presented. Recent measurements from the laser system are discussed. Details about the HV modulator tests and the power phase shifter fabrication will be described and the start of commissioning will be also reported.

INTRODUCTION

The electron linac CALIFES [1] (Figure 1) will produce both single bunch and bunch train spaced by 0.66 ns to X-band structures in order to perform various tests such as beam kick due to RF breakdown or dipole mode excitation, in addition with the Two Beam Acceleration demonstration. The main linac parameters have been updated and are shown in Table 1.

Table 1: CALIFES main parameters.

Parameters	Value
Final linac e⁻ energy	170 MeV
Emittance rms	< 20 π mm.mrad
Energy spread (single bunch)	< ± 2%
Energy / Phase deviation (multi-bunch)	< ± 1% / < 10 ° at 12 GHz
Number of bunches Nb	1 – 32 - 226
Bunch charge (single/ multi bunch)	0.6 nC / 6 nC/Nb
Initial/final bunch length	5.3 / 1.8 ps, 1.6 / 0.5 mm
Transverse beam size	0.6 mm x 0.6 mm
Bunch spacing	0.66 ns / 1.5 GHz
Train length	21 – 150 ns
Train spacing (rep. rate)	5 Hz

BEAM DYNAMIC AND TRANSIENT RF SIMULATIONS

Due to fact that the flat top duration of the compressed RF pulse (1.3 µs) is close to the structure filling time (1.23 µs), the accelerating field profile must be precisely

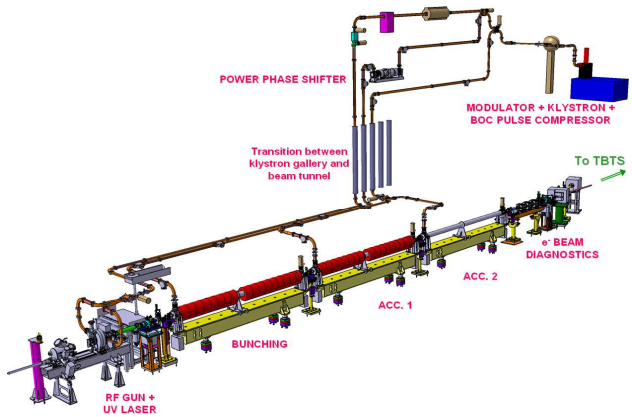

Figure 1: 3D layout of CALIFES.

computed (Figure 2). With a drive frequency slightly above the centre frequency (+ 150 MHz), the filling of the structure is nearly complete after a pulse propagation of 5.5 µs. A quasi steady state is reached and no major changes of the beam quality are expected.

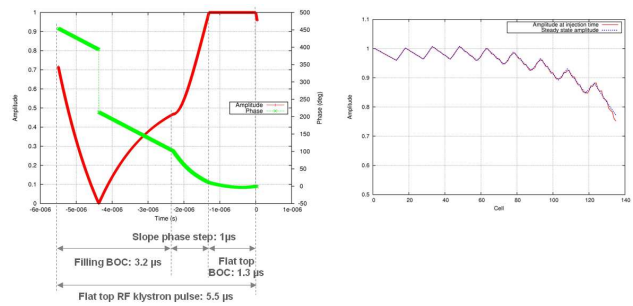

Figure 2: RF pulse shape after compression (left) and amplitude field profile after 5.5 µs (right).

In single bunch operation, simulations showed that the transverse profile at the end of the linac are $x_{rms} \sim y_{rms} \sim$ 0.6 mm. The bunch length at the end of the linac is z_{rms} = 0.176 mm and the emittance is 13.04 mm.mrad. The final linac energy is 169.6 MeV/c with an energy spread of $\Delta P/P$ = 1.006 %.

In multi bunch operation, we calculated a total energy deviation between the first and last bunch of 5.4 % at 170 MeV and a phase deviation of 15.5° at 12 GHz. The bunch charge will be reduced with the number Nb of bunches, Qb < 6 nC / Nb, such a way that both energy and phase deviations are smaller than respectively 1% and 10° at 12 GHz.

THE NEW SINGLE BUNCH INJECTOR FOR ELSA

F. Klarner, S. Aderhold, O. Boldt, W. Hillert,
Electron Stretcher Accelerator, Physikal. Institut, Nussallee 12, 53115 Bonn

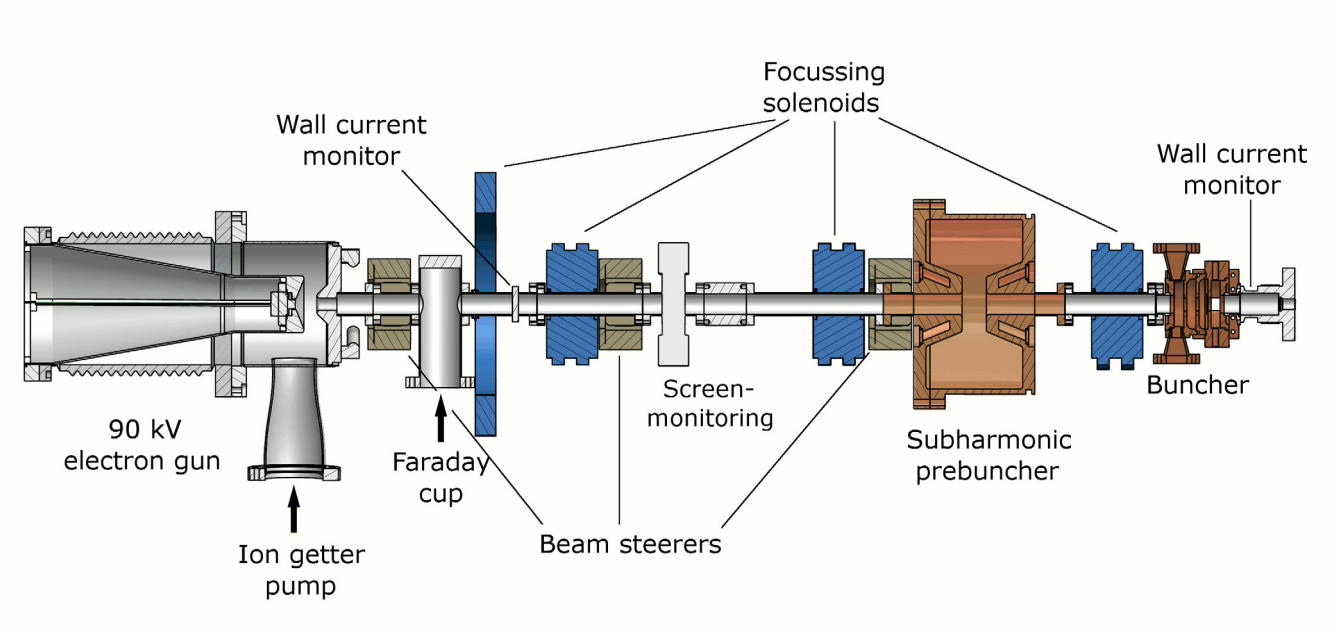

Figure 1: Overview of the new injection system which will be installed at the linear accelerator LINAC I at ELSA.

Abstract

Since 1966 a Varian manufactured injector is in use at the ELSA accelerator facility of the University of Bonn for several experiments investigating the subnuclear structure of matter.

The new injector for Linac 1 currently under construction at ELSA is expected to operate in a single bunch mode of 2 A beam current. This mode gives the possibility of deeper background studies in the experimental setup of the CB experiment sponsored by the "Deutsche Forschungsgesellschaft" and to investigate single bunch instabilities within the Helmholtz alliance "Physics at the Terascale". Also, a 2 µs long pulse mode of 500 mA beam current will be available for normal thermionic electron service. The injector delivering a single bunch was designed and optimised with EGUN and numerical simulations based on the paraxial equations. The compression of the pulses created by a pulsed thermionic 90 kV gun is achieved by a 500 MHz prebuncher as well as a β-matching travelling wave buncher running at the linac frequency.

90 KV ELECTRON GUN

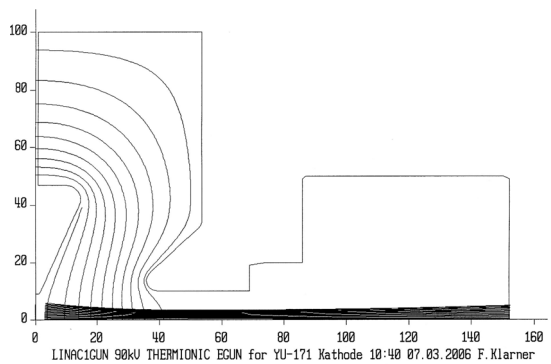

Figure 2: Gun geometry r vs. z in mm with equipotential lines and space charge limited electron rays calculated with EGUN for an anode voltage of 90 kV.

The 90 kV gun is based on a design used in the SBTF test facility at DESY. The design of the cathode conus was adjusted with the computer code EGUN to fulfill the requirements of 2 A single pulse and 500 mA long pulse operation. With a 34 mm wide anode cathode gap this gun has a perveance of 0.16 $\mu A/V^{3/2}$ and delivers a 4.3 A space charge limited current at 90 kV. The EGUN

IMPROVING THE SUPERCONDUCTING CAVITIES AND OPERATIONAL FINDINGS AT THE S-DALINAC*

R. Eichhorn#, A. Araz, M. Brunken, J. Conrad, H.D. Graef, M. Hertling, F. Hug, C. Klose, C. Liebig, M. Konrad, T. Kuerzeder, M. Platz, A. Richter, S. Sievers and T. Weilbach
S-DALINAC, Institut fuer Kernphysik, TU-Darmstadt, D-64293 Darmstadt, Germany

Abstract

After 15 years operating the S-DALINAC the design quality factor for the superconducting cavities has still not been reached. Currently, the cavities are heat treated at 850 C in an UHV furnace installed in Darmstadt three years ago. We will report about the furnace, the heat treatment procedure and the results of subsequent surface resistance measurements.

Prior to the heat treatment the field flatness of some of the 20 cell elliptical cavities has been measured, leading to unexpected operational findings to be reported: operating and frequency-tuning the cavity for several years led to heavy distortions of the field flatness. This might be an indication that the frequency tuning of the cavity done by compressing the cavity longitudinally, does not act uniformly on each cell even though the cavity is only supported at the end cells. The paper will close with a status report on machine operation and modifications undertaken during the last two years.

INTRODUCTION

The superconducting Darmstadt electron linear accelerator S–DALINAC was put into operation in 1987. It consists of ten superconducting 20 cell niobium cavities, operated at 2 K at a frequency of 2.9975 GHz. With a design accelerating gradient of 5 MV/m and a design quality factor of $3{\cdot}10^9$ in cw operation, the final energy of the machine is 130 MeV which is reached when the beam is recirculated twice [1]. The layout of the S–DALINAC is shown in Fig. 1.

The first set of cavities was built in the 80's at Interatom using low RRR material, so the observed performance regarding the gradient and the quality factor was rather poor [2]. Accordingly, a second set of cavities was ordered in the 90's made from RRR 300 material.

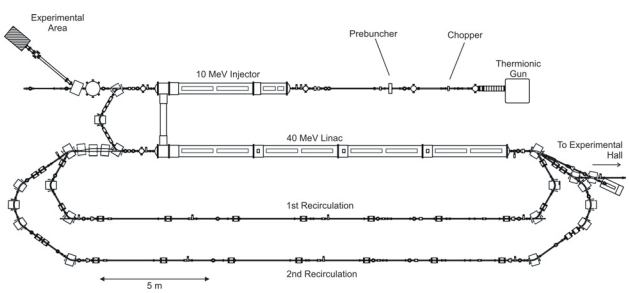

Figure 1: Floor plan of the S-DALINAC.

These cavities, welded at Dornier, are used since then. All of them reach the design gradient, some exceeding it by more than 50% [3]. The accelerator performance however did not benefit from this improvement: Due to the limited refrigerator power of some 100 Watt and the rather low Q of the cavities (typically below $1{\cdot}10^9$) the cavities have to be operated below their maximum gradients. Many measures have been taken in the past [4], all of them helped improving the Q but none was able to solve the problem completely.

CAVITY FIRING

The high temperature vacuum firing has proven to be an inherent part of the surface preparation of superconducting cavities. This procedure is applied to stress anneal the niobium and to remove hydrogen from the material inoculating cavities against the "Q disease" during their operation. The S-DALINAC niobium cavities were heat treated at 750 C after their commissioning as well. However recent studies have shown that the niobium is still contaminated by hydrogen which can be explained by doubting the temperature measurement during the first firing.

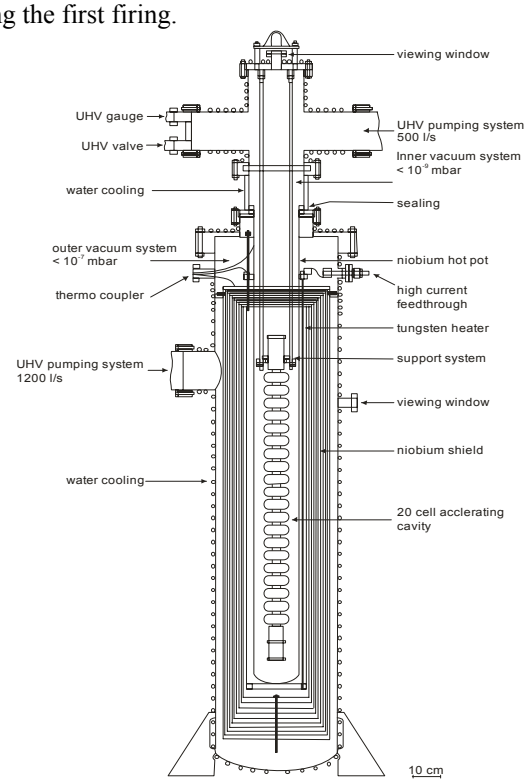

Figure 2: Side view of the UHV furnace in Darmstadt.

*Work supported by the DFG through SFB 634
#eichhorn@ikp.tu-darmstadt.de

THE POWER AND POLARISATION UPGRADE PROJECT AT THE S-DALINAC INJECTOR*

R. Eichhorn#, R. Barday, U. Bonnes, M. Brunken, C. Eckardt, J. Conrad, J. Enders, H.D. Graef , C. Heßler, T. Kuerzeder, C. Liebig, M. Platz, Y. Poltoratska, M. Roth, S. Sievers, T. Weilbach, S-DALINAC, IKP, TU Darmstadt, Germany
W. Ackermann, W. F. O. Mueller, B. Steiner, T. Weiland, TEMF, TU Darmstadt, Germany
K. Aulenbacher, IKP. University of Mainz, Germany
J. Fuerst, ANL, Argonne, IL 60439, U.S.A.

Abstract

The current upgrade for the injector mainly involves the superconducting rf part. In order to increase the maximum current from 60 µA to 150 or 250 µA the power coupler design had to be modified, resulting in major changes in the whole cryo-module.

Second, an additional polarized electron source (SPIN) has been set-up at an offline test area. There, the polarized electrons are produced by photoemission at a strained GaAs cathode on a 100 kV platform. The test beamline includes a Wien filter for spin manipulation, a Mott polarimeter for polarization measurement and additional diagnostic elements. We will give an overview to the project, report on the status and present first measurement results including the proof of polarisation.

INTRODUCTION

The superconducting Darmstadt electron linear accelerator S-DALINAC [1] is a recirculating linac, using ten superconducting niobium cavities at a frequency of 2.9975 GHz. It was first put into operation in 1987. Running at a temperature of 2 K the main acceleration is done by ten 20 cell elliptical cavities with a design accelerating gradient of 5 MV/m. The first pair of those cavities is used in the injector section of the machine. Behind this section it is possible to use the beam for nuclear physics experiments with a maximum energy of 10 MeV or the beam can be bent into the main linac. With its two recirculations and an energy gain of 40 MeV per pass the maximum design energy of the S-DALINAC is 130 MeV which can be used for several experiments in the adjacent experimental hall. The layout of the machine is shown in Fig. 1.

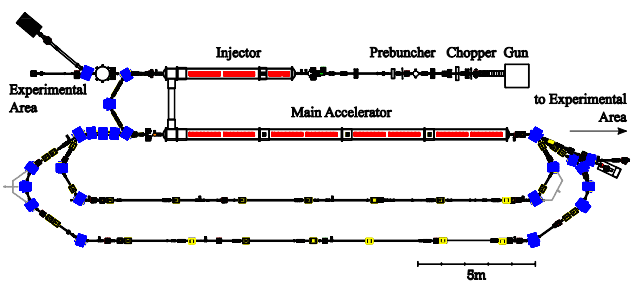

Figure 1: Floor plan of the S-DALINAC.

*Work supported by the DFG through SFB 634
#eichhorn@ikp.tu-darmstadt.de

POWER UPGRADE

The S-DALINAC uses cryostat-modules with two cavities per module. Each cavity has an rf input coupler, which is capable of a maximum power of 500 W. Assuming a 5 MV/m gradient the beam current is limited to 60 µA for the injector and 20 µA for the main linac, which might be higher for lower beam energies.

For future astrophysical experiments behind the injector, beam currents of 150 µA and above as well as energies of up to 14 MeV are demanded. Therefore, modifications in the injector linac had to be made.

New Power Couplers

The first step was to design and build new power couplers providing the necessary rf power of up to 2 kW to the cavities. While the existing couplers are coax-to-coax couplers [2] and limited to 500 W, the newly designed couplers are of waveguide-to-coax type [3]. One essential design feature of the old coupler was kept, namely the minimized transversal fields being a major concern in the low energy part of the accelerator. This was accomplished by using two diaphragms, reducing the excitations of the transverse electromagnetic fields in the beam pipe below -40 dB.

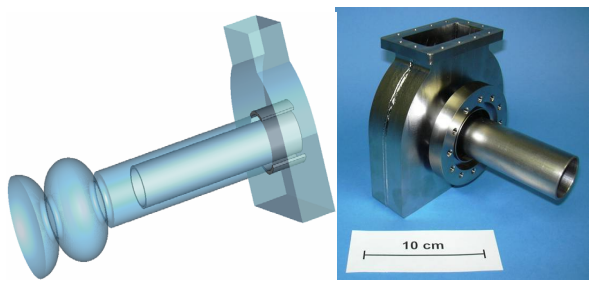

Figure 2: The design and the finally fabricated waveguide-to-coax coupler for the injector upgrade.

Figure 2 gives on the left side an impression, how the coupling from waveguide to coax and to the cavity along its cut-off tube is realized. The external quality factor of $5 \cdot 10^6$ ensures acceleration of beam currents ranging from 150 to 250 µA.

The coupler was made out of bulk niobium. The fabrication including the EB-welding was done by the FZ Juelich. Currently, the chemical cleaning of the couplers is underway.

RECENT CHANGES TO THE e^+/e^- INJECTOR (LINAC II) AT DESY

M. Hüning#, M. Schmitz, DESY, Hamburg, Germany

Abstract

The Linac II at DESY consists of a 6A/150kV DC electron gun, a 400 MeV primary electron linac, an 800 MW positron converter, and a 450 MeV secondary electron/positron linac.

The Positron Intensity Accumulator (PIA) is also considered part of the injector complex accumulating and damping the 50 Hz beam pulses from the linac and transferring them with a rate of 6.25 Hz or 3.125 Hz into the Synchrotron DESY II. The typical positrons rates are $6 \cdot 10^{10}$/s.

DESY II and Linac II will serve as injectors for the two synchrotron light facilities PETRA III and DORIS. Since PETRA III will operate in top-up mode, Linac availability of 98-99% is required. DORIS requires positrons for operation. Therefore during top-up mode positrons are required for both rings. In order to maintain its reliability over the operation time of the new facility PETRA III, the major components of the linac were renovated. Some components were redesigned taking into account experience from 30 years of operation.

INTRODUCTION

The Linac II was built in the late 1960s to provide electrons and positrons for the Deutsches Elektronen Synchrotron (DESY) at higher energies (200 MeV) than the at that time existing linac (50 MeV) [1]. It consisted of 14 S-band travelling wave structures operating at 2.998 GHz and 20 MW input power and 4 µs pulse duration. The setup was modified since by introducing SLED (SLAC energy doubler) cavities for pulse compression and injecting into the Particle Intensity Accumulator (PIA). PIA was built to achieve short damping times for the positrons to be injected into the electron/positron storage ring collider PETRA. The pulse compression scheme enabled an energy increase to 450 MeV and allowed reduction of RF stations to 12, but required together with the high revolution frequency of PIA a reduction of beam pulse duration.

Today DESY II with its injector Linac II provides electrons and positrons for the synchrotron radiation facility DORIS, the synchrotron radiation facility under construction PETRA III, and for test beam targets inside DESY II. The injection into HERA via PETRA II is shut off, but there is an option to inject directly into HERA if there is the requirement by future projects.

LINAC OVERVIEW

Injection System

The primary electron beam is produced by a 120 kV pulsed DC diode gun. Beam pulses of up to 6 A and 4 µs duration are produced. The cathode is made by a thoriated tungsten plug, heated by a 3 kV, 1.2 kW bombarder. For best performance the cathode plug has to be carborized.

An electrostatic chopper forms beam pulses of 2 ns to 30 ns duration, depending on the operation conditions. In electron mode the primary beam is used directly, which reduces the required average beam current. A 2.998 GHz prebuncher cavity is fed by a portion of the first structure's forward RF power drawn from a directional coupler. The beam then enters the first accelerator section, which is not tapered.

Accelerator Sections

The linac sections are 5.2 m long travelling wave S-band structures, operating at 2.998 GHz. They are constant gradient structures with an on-axis load. Therefore the last six of their 154 cells are coated with an absorbing material and add little to the total accelerating voltage. The fill-time of the structures is 740 ns. The original structures were replaced by a design made for the S-Band Linear Collider Test Facility [2].

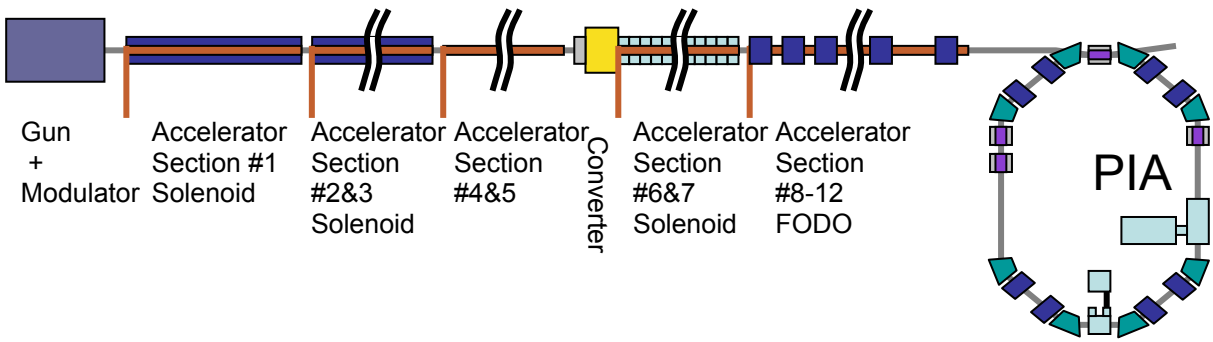

Figure 1: Schematic layout of the Linac II at DESY. The 6 A primary beam is produced in a 120 kV pulsed DC gun and directed onto a converter target at approximately 400 MeV. The secondary beam is accelerated to 450 MeV and injected into the Positron Intensity Accumulator (PIA).

corresponding author: markus.huening@desy.de

DEVELOPMENT OF TIMING AND CONTROL SYSTEMS FOR FAST BEAM SWITCH AT KEK 8 GeV LINAC

K. Furukawa*, M. Satoh, T. Suwada, KEK, Tsukuba, 305-0801, Japan
T. Kudou, S. Kusano, MELCO SC, Tsukuba, 305-0045, Japan
A. Kazakov, GUAS/SOKENDAI, Tsukuba, 305-0801, Japan
G. Lei, G. Xu, IHEP, Beijing, 100049, China

Abstract

The 8 GeV Linac at KEK provides electrons and positrons to Photon Factory (PF) and B-Factory (KEKB). Simultaneous top-up injections have been considered for both PF and KEKB rings in order to improve the injection efficiency and the experimental stability. Therefore, fast beam-switching mechanisms are being implemented, upgrading the timing and control systems. While the old timing system provides precise timing signals for 150 devices, many of the signals are now dynamically switched using an event system. A new scheme has been developed and tested to enable double-fold synchronization between rf signals. Fast controls of low-level rf, beam instrumentation, kickers, a gun, and beam operation parameters are also upgraded for fast and precise tuning of those parameters. The system has been developed since 2006, and is being deployed under the beam operation in 2008.

INTRODUCTION

The KEK Linac injects electron and positron beams with different characteristics into four storage rings, KEKB-HER, KEKB-LER, PF and PF-AR. It takes 30 seconds to 2 minutes in order to switch the beam modes, depending on the magnet standardization [1]. When the beam development study is performed at PF ring for example, the experiment at KEKB is disturbed. Especially with the crab cavities installed at KEKB, the luminosity tuning is sensitive to the constant beam conditions at the both HER and LER rings and simultaneous injection to those rings is preferable. At the same time, the top-up injection is increasingly demanded at the PF ring in order to achieve higher-quality experimental data.

Thus, the fast beam-mode switching system has been designed and implemented [2]. In the system many hardware pieces of equipment are installed including pulsed magnets, fast rf system, and so on. Beam optics development is also performed in parallel to support the wide dynamic range of beam energy and charge, namely 3-times different energy and 100-times different charge.

Control and timing systems is upgraded as well to meet the requirement of the beam-mode switch in 50Hz (20ms). In order to notify the switching event globally along the 600-m Linac, an event system has been introduced [3]. It has been tested since 2006 and installed for the operation in autumn 2008. The system enables fast switching of many parameters of timing-signals, magnets, microwave systems, and beam instrumentations.

FAST BEAM-MODE SWITCHING

There are a few beam modes defined at the Linac. It took more than 30 seconds for more than 20 items to switch. And it is considered important to switch at least following beam modes.

- KEKB HER : 8 GeV electron, 1.2-nC, 2 bunches.
- KEKB LER : 3.5 GeV positron, 1.2 nC, 2 bunches (10-nC primary electron).
- PF ring : 2.5 GeV electron, 0.1 nC, 1 bunch.

Here, 2 bunches in a pulse are separated by 96 ns. A fast switch of those beam modes is challenging because the dynamic range of the beam characteristics is very large. An adaptive beam optics scheme is being developed. In order to enable this scheme several hardware components had to be improved. And following parameters are changed within 20ms.

- Magnet: a pulsed bending magnet, several pulsed steering magnets, and a pulsed positron capture coil.
- Microwave: phase and timing of low-level rf, timing of high-power rf.
- Gun: grid-pulser selection, bias voltage, pico-second timing.
- Beam instrumentation: synchronized and fast beam-position-monitor read-out, pulse selection for wire-scanners and streak-cameras.
- Injection: selection of septa and kickers, interface to bucket selection systems.
- Operation: beam stabilization feedback, beam mode sequence pattern generation, mode-dependent parameter manipulation and archiving.

In order to achieve synchronized controls over Linac and beam transport lines for KEKB and PF, a global event notification system has been installed. Errors are not allowed because of safety reasons as the beam power varies 10 to 100 times [4]. The parameters for each mode have to be manipulated easily to optimize the beam tuning and the physics experiment conditions. It almost corresponds to building of three virtual accelerators.

* < kazuro.furukawa @ kek.jp >

PULSE-TO-PULSE MODE SWITCHING OF KEKB INJECTOR LINAC

T. Kamitani*, K. Yokoyama, T. Sugimura, K. Kakihara, M. Ikeda, A. Shirakawa, S. Ohsawa,
T. Suwada, K. Furukawa, M. Satoh, M. Kikuchi, T. Mimashi, N. Iida,
KEK, Tsukuba, Japan

Abstract

Electron and positron injections from the KEKB injector linac to storage rings have been switched in a typical cycle of five minutes. The switching involves a mechanical movement of a positron production target from and to a beam line. It prevents from faster switching, like pulse-to-pulse switching. A target assembly with a small hole beside a target material and four pulse steering magnets are installed. For positron injection pulses, the pulse steering magnets are off and electron beams irradiate the target to produce positrons. While, for electron injection pulses, the pulse steering magnets are excited to create a orbit bump in order for the electron beams to go through the hole and bypass the target. This paper describes details of a system for the pulse orbit bump and results from recent beam studies.

INTRODUCTION

The KEKB injector linac supplies electron and positron beams to the KEKB storage rings HER (8.0 GeV e-), LER (3.5 GeV e+) and to the two synchrotron radiation facility rings PF (2.5 GeV e-) and AR (3.1 GeV e-) as well. Each ring requires different beam properties; a time-structure, a particle charge, an energy and an intensity. Parameter setting of the linac, called as "injection mode", is switched for an appropriate beam to be generated, accelerated and sent into a selected ring. In this mode switching, parameters like a choice of the pre-injector, electron gun settings, magnet currents, acceleration phases, rf pulse timings and so forth are changed. Mode switching between the electron and the positron injection for HER and LER rings is frequent in typically 5 minutes cycle. Each switching takes 30 seconds in completing to change parameters. Most of the linac operation time is occupied for KEKB continuous injection. It is interrupted by injections to PF (once a day) and to AR (twice a day), each takes 15 minutes to fill up the storage ring. Switchings from KEKB to PF or AR and its reverse have taken a few minutes until recently, since it needed to change a current slowly for a large bending magnet to keep its hysteresis cycle. However, recently, a demand of continuous PF injection was brought up for keeping its storage current constant. It is beneficial for some synchrotron radiation users, but it was not compatible with the KEKB continuous injection. To solve this issue, much efforts have been made to realize quasi-simultaneous electron injection to KEKB HER and to PF [1]. It can be achieved by injecting both beams from the same pre-injector, installing a pulse bending magnet and a new beam transfer line for PF, pulse-to-pulse switching of acceleration rf phases for 8.0 GeV and 2.5 GeV beam energies, setting up focusing and steering magnets compatible for these different beam energies [2]. This unification of these two injection modes has almost been completed and it will be used for an autumn run this year (2008).

Next step of the unification is that of the KEKB electron and positron injections. Positrons are produced by irradiating a metal target with electron beams. A target is placed on a beam line halfway across the KEKB linac. The target is retracted from the beam line during an electron injection and inserted during a positron injection. Mechanical movement of the target takes a few seconds. It is desirable keep constant storage currents in both of electron ring and positron ring for a beam collision tuning to achieve superior luminosity. To realize pulse-to-pulse switching of the electron and positron injection modes, it was proposed to use a target assembly with a small hole beside a target material in order to fix it on a beam line and to let electron beams bypass through the hole with pulse steering magnets only for electron injection pulses.

In the following chapters, details of the target assembly, the pulse steering magnets and recent results of beam studies are given.

TARGET BYPASS ORBIT FOR PULSE-TO-PULSE MODE SWITCHING

Target Bypass Orbit

In designing a bypass orbit to avoid the target retraction, first considered has been a large orbit bump to bypass not only the target but positron focusing solenoids and a capture system. It needed an independent bypass beam line apart more than 300 mm from the original beam line and also huge pulse magnets to bend 4-GeV electron beams in large angle. Thus, it was too costly. More practical and economical solution was to make a small hole in a target assembly beside the target material and to make a bump orbit of only some millimeters height. This small orbit bump can be contained in a present beam ducts and in apertures of accelerating structures. Fig. 1 shows a bypass orbit bump and a beam line layout around the positron production target. A component denoted as PT21T in the figure is a positron production target and the thick green lines show an aperture of the target hole. Center of the hole is 5.2 mm aside horizontally from a beam line center. Focusing quadrupoles setting is based on a candidate beam optical calculation which is compatible for HER and PF injections. A purple line shows a bump orbit and red

* takuya.kamitani@kek.jp

OBSERVATIONS OF TWO MICROBUNCHES AFTER A 180-DEGREE ARC SECTION AT THE KEKB LINAC

Y. Ogawa#, M. Yoshida, KEK, Tsukuba, Japan

Abstract

The KEKB linac [1] continuously injects 8-GeV electron and 3.5-GeV positron beams into the KEKB rings: HER (high energy ring) and LER (low energy ring). The energy spread of the 8-GeV electron beam, which is accelerated to an energy of 1.7-GeV at a 180-degree arc section and reaccelerated after this arc to a final energy of 8 GeV, is optimized by adjusting rf acceleration phases so as to assure efficient injections. When rf phases after the arc are slightly changed or drifted for some reasons, the beam not only shows larger energy spreads but also indicates two clusters on a beam profile monitor located at large energy dispersions. In this connection, a longitudinal beam profile was measured before and after the arc section with streak-camera systems utilizing OTR (Optical Transition Radiation). The observed bunch shape clearly shows a two-microbunch structure, suggesting that it could be generated in the arc section. Various experimental data as well as some CSR-related speculations are presented.

INTRODUCTION

In high-luminosity machines like the KEKB factory, stable beam injections are absolutely essential to retaining the optimum luminosity. The injection efficiency is quite dependent upon the quality of injected beams, especially upon the energy spread. Thus the energy spread of the electron beam for the KEKB has been always kept at a minimum enough for stable injection by adjusting rf acceleration phases.

The KEKB electron beam is accelerated to an energy of 1.7-GeV at a 180-degree arc section and reaccelerated after the arc to a final energy of 8 GeV (Fig. 1). During tuning processes of the energy spread, we have found that the energy profile at the end of the linac shows peculiar behaviour, splitting into two clusters if the rf phases after the arc are not optimized, while we have not observed the same phenomenon before the arc section. Although the phenomenon itself is quite stable and reproducible, we examined as a first step the rf system looking for some unstable components, but did not find any causes attributed to the rf system. Meanwhile we have taken various observation data concerning this phenomenon, which are reported in this paper together with some CSR-related speculations.

EXPERIMENTAL CONFIGURATION

A schematic view of the experimental setup is shown in Fig. 2. The parameters relevant to the 8-GeV single-bunched electron beam are summarized in Table 1. The energy profile of the beam is observed by a screen monitor using an alumina fluorescent plate (AF995R, Desmarquest Co.) located at the 8-GeV energy-analyzer line; the energy separation of the two clusters is measured by changing rf phases of appropriate accelerator sections corresponding to an energy range of about 5 GeV. The time structure of the bunch is investigated with streak-camera systems (Hamamatsu Photonics K. K.) utilizing OTR located before and after the arc, which have a time resolution of two or three picoseconds.

Table 1: Beam Parameters

Energy	8 GeV
Acceleration Frequency	2856 MHz
Charge	1 nC (single bunch)
Bunch Length (σ)	4.7 ps (single bunch)
Energy Spread (σ)	0.05 %
Emittance $\gamma\beta\varepsilon$ (σ)	0.31 mm
Maximum Repetition	50 pps
Energy at the Arc Section	1.7 GeV

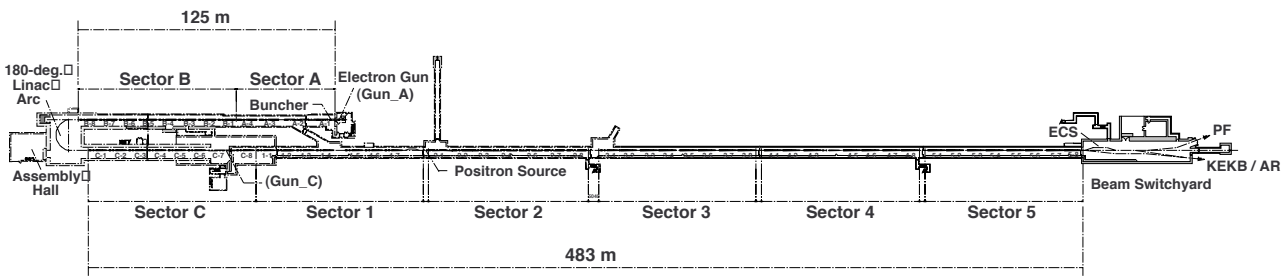

Figure 1: Layout of the KEKB linac. The KEKB electron beam is accelerated to an energy of 1.7-GeV at a 180-degree arc section and reaccelerated after the arc to a final energy of 8 GeV.

#yujiro.ogawa@kek.jp

DESIGN AND PERFORMANCE OF OPTICS FOR MULTI-ENERGY INJECTOR LINAC

Y. Ohnishi*,T. Kamitani, N. Iida, M. Kikuchi, K. Furukawa, M. Satoh, K. Yokoyama, and Y. Ogawa,
KEK, Tsukuba, Japan

Abstract

KEK injector linac provides an injection beam for four storage rings, KEKB high energy electron ring(HER), low energy positron ring(LER), PF-AR electron ring, and PF electron ring. The injection beams for these rings have different energies and intensities. Recently, a requirement of simultaneous injection among these rings arises to make a top-up injection possible. Magnetic field of the DC magnets to confine the beam to the accelerating structures can not be changed during a pulse-to-pulse, although the beam energy can be controlled by fast rf phase shifters of the klystrons. This implies that a common magnetic field of the bending magnets and the quadrupole magnets should be utilized to deliver beams having different characteristics. Therefore, we have designed a multi-energy optics for the KEKB-HER electron ring(8 GeV, 1 nC/pulse), the PF electron ring(2.5 GeV, 0.1 nC/pulse), and the KEKB-LER positron ring(3.5 GeV, 0.4 nC/pulse). We present a performance of the multi-energy injector linac for the PF ring and the KEKB-HER.

INTRODUCTION

A new injection scheme has been developed, which is so called a pulse-to-pulse injection with multi-energy linac for the KEKB-HER, the KEKB-LER, the PF ring. The pulse-to-pulse injection means that the beam can be switched and injected to the desired rings within 20 msec at a minimum duration. However, the beam energy is different among these rings. Difficulties arise from that most of magnets can not change the magnetic field by a pulse-to-pulse duration. Therefore, we have developed a new optics to use a common magnetic field for the different beam energies, such as 2.5 GeV for the PF and 8 GeV for the KEKB-HER. The KEKB-LER injection has been still tested and under development in this scheme, however, the strategy is a similar way of the PF and the KEKB-HER.

The injector linac has 7 sectors, A-sector and B-sector before 180° arc(J-arc) and 1-sector to 5-sector after the J-arc. The energy of the J-arc is 1.7 GeV and the multi-energy scheme focuses on the region from the C-sector to the 5-sector. A pulse bend is placed in the 5-sector and the 2.5 GeV beam is kicked out to the transport line of the PF ring, while the 8 GeV beam passes through the ECS(the energy compression system) to the KEKB-HER transport line.

* Email: yukiyoshi.onishi@kek.jp

OPTICS

A fundamental block of the linac is an acceleration unit that consists of an S-band klystron and four 2 m-long accelerating structures. The klystron drives these accelerating structures which have a common phase of the microwaves. The accelerating structures in the acceleration unit have the same field gradient in principle. Eight acceleration units make a sector, typically. A sub-booster supplies microwaves to each klystron in the sector and adjusts the phase for a beam passage.

A doublet or a triplet of quadrupole magnets is placed in every one or two acceleration unit and makes a cell of a periodic lattice. In the case of an electron injection, an electron beam is accelerated from 1.7 GeV up to 4.8 GeV between the C-sector and the 3-sector. A positron target to make a positron beam is placed in the 2-sector. In the case of a positron injection, a primary electron beam hits the positron target and positrons are generated by means of electro-magnetic showers. On the other hand, a small hall(ϕ=3 mm) is placed in the vicinity of the target so that an electron beam can pass through the positron target for the electron injection. In order to make this possible, it is necessary to squeeze the beta function at the hall as small as possible and to make a local bump orbit by using pulse steerings in the horizontal plane.

The electron beam injected to the PF ring is decelerated down from 4.8 GeV to 2.5 GeV between the 3-sector and the 5-sector, while the electron beam is accelerated up to 8 GeV for the KEKB-HER. In the multi-energy region, the phases of the sub-boosters are shifted by 180° approximately between the acceleration and the deceleration. In practice, an off-crest phase typically shifted by 6° from the crest phase is used to compensate the energy difference between the head and the tail of a bunch due to the wake field. The deceleration phase is

$$\phi_{dec} = \phi_{acc} + 180^\circ - 2\Delta\phi, \quad (1)$$

where $\Delta\phi$ is the phase shift from the crest phase. Further more, a few klystrons in the 3-sector would be a stand-by mode to adjust the beam energy so as to be 2.5 GeV. The stand-by mode implies an off-timing trigger for the beam passage. Both the 2.5 GeV and 8 GeV beam would be adjusted by the energy-feedback system[1] precisely. The energy feedback system consists of a set of two klystrons and adjust the phase. The off-crest phases are used in the opposite side of the crest for each klystron to compensate the energy spread. Those sub-boosters and the energy feedback system utilize a phase shifter with a solid-sate device and can change the phase by a pulse-to-pulse duration.

PRESENT STATUS OF THE KEK INJECTOR UPGRADE FOR THE FAST BEAM-MODE SWITCH

M. Satoh# for the IUC* Accelerator Laboratory, High Energy Accelerator Research Organization (KEK), 1-1 Oho, Tsukuba, Ibaraki, 305-0801

Abstract

The KEK Linac provides the four different quality beams for the four independent rings. The KEK Linac upgrade aiming a fast beam-mode switch operation is now in progress so that the KEKB continuous injection and PF top-up injection can be carried out at the same time. In this paper, we will report the present status of the KEK Linac upgrade in detail.

INTRODUCTION

The KEK Linac provides the beams of the different modes sequentially with four storage rings (KEKB 3.5 GeV positron/ 8 GeV electron, Photon Factory (PF) 2.5 GeV electron and Advanced Ring for pulse X-rays (PF-AR) 3 GeV electron).

For a typical operation, the PF and PF-AR need the beam injection twice a day on scheduled time. On the other hand, the KEKB rings are operated by the continuous injection mode (CIM) for keeping the stored current almost constant. In the CIM operation, the switch time between the electron and positron modes takes about a half minute so that all settings of magnet power supplies, RF phases and timings should be changed according to the electron and positron beam properties. In the near future, the PF top-up operation will be started to enhance the integrated photon flux. For these reasons, the linac upgrade is strongly required for a fast beam-mode switch [1, 2, 3 and 4].

Figure 1 shows the schematic drawing of ultimate fast beam-mode switch operation. In this operation scheme, we will change only the minimum parameters of the timing signals and Low-Level RF (LLRF) phases, and all the rest of parameters like DC magnet settings are never changed even for the different beam-mode. In the final stage of the linac upgrade, the beam mode can be changed in every 50 Hz of an arbitrary beam-mode pattern.

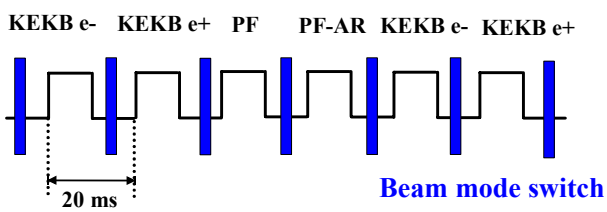

Figure 1: Schematic drawing of fast beam mode.

masanori.satoh@kek.jp
* Injector Upgrade Committee: Cross-functional team for the injector upgrade from PF/ KEKB and Linac members

UPGRADE PLAN

Outline

This project is a phased upgrade, and the phase-I has been already completed in the summer of FY2005. The detailed upgrade phases are shown in following sub-sections.

Phase-I

In the phase-I, the new PF-BT line has been constructed for shortening the beam-mode switch time between the KEKB and PF modes. Here, the initialization procedures of the energy compensation system (ECS) bends are required since the original DC switch bend was placed downstream of the ECS bends. In order to bypass the ECS, a new DC switch bend has been installed by removing four accelerating structures, and a new PF-BT line of 60-m-long has been constructed [5].

After the phase-I, the beam-mode switch between the KEKB and PF modes does not need to change the ECS parameters. The round trip mode switch time including PF injection was reduced by half from 5.5 min. to 2.5 min. In addition, the beam injection efficiency has been increased.

Phase-II

The phase-II aims to perform the fast beam-mode switch between the KEKB electron and PF modes up to 50 Hz. For the phase-II and later, we will use the new operation scheme called “Multi-Energy Linac” [6 and 7]. In this scheme, the common magnet settings are used for the different beam modes. The adjustment of the beam energy is performed by a fast control of LLRF phase. Though PF ring injection requires the 2.5 GeV electron, the beam is accelerated up to about 5 GeV in the multi-energy scheme. After then, the beam energy is adjusted to 2.5 GeV by using the deceleration RF phases. This method is effective for enlarging the common optics region. The result of a preliminary machine study shows that this scheme is feasible for a realistic beam operation. In this autumn, the more detailed machine study will be carried out to develop the daily operation parameters.

Phase-III

In the phase-III, the fast beam-mode switch will include the KEKB positron mode. In the current operation, the positron production target is controlled by a mechanical movement. For the fast beam-mode switch between the electron and positron modes, the positron target with a

PRESENT STATUS OF THE BEPCII LINAC

Pei Guoxi* for BEPCII-Linac Group
Institute of High Energy Physics, IHEP, Beijing, P. O. Box 918, 100049, China

Abstract

After the major upgrades in 2005, the BEPCII injector linac has been commissioning and working smoothly for more than two years. A 1.89GeV, 61.5mA positron beam at the linac end has been obtained, and the highest injection rate into the ring of 80mA/min. at 50pps is reached, much higher than the design goal of 50mA/min. The machine is working stably, and the mal function was only about 2% in the past two years, including the system test and the commissioning.

INTRODUCTION

The BEPCII [1] is a factory type e^-e^+ collider with a luminosity of $1\times10^{33}\,cm^{-2}s^{-1}$ in the Tau-Charm energy region (2-5 GeV). On-energy injection scheme with an injection rate of > 50mA/min (almost twenty times of BEPC number) for e^+ beam requires the existing BEPC injector linac be upgraded with higher performance [2]. The BEPCII linac major upgrades were completed in 2005, and we got the first positron beam of ~50mA on March 19th. On December 23rd, 2007, an acceptance test group organized by the Chinese Academy of Sciences has fully checked the linac beam performance. The measured beam energy, current, emittance, energy spread, orbit and energy stabilities were well reached their design goals, as shown in Table 1.

Table 1: The Design and Reached Beam Performance

		Design	Reached
Beam Energy (GeV)		1.89	1.89
Beam Current (mA)	e^+	37	66
	e^-	500	550
Emittance (1σ,μm)	e^+	0.40	0.35 (x) 0.27(y)
	e^-	0.10	0.097 (x) 0.079 (y)
Energy spread (1σ,%)	e^+	0.50	0.37
	e^-	0.50	0.30
Repetition rate (Hz)		50	50
Beam orbit stability(mm)		0.30	≤0.15
Beam energy stability (%)		0.15	≤0.05
e^+ injection rate(mA/min.)		50	61.5

OPERATIONAL STATUS

From October, 2006, up to now, the BEPCII only had two shut down time [3, 4, 5]. One was from early August to early October, 2007, which was for the BEPCII interaction region installation. We also took this chance to replace 5# RF unit's waveguide, which was badly damaged and confined the high power transmission. The other one was from March to May, 2008, for the BESIII installation. General speaking, in almost 20 months, the linac performance was excellent. The mal function including those happened at system test and commissioning time was only about 2%. The positron beam current at the linac end exceeded 60mA, which is good for a much higher injection rate. The injection rate of 61.5mA/min. listed in Table 1 was an average number. Actually, the peak value often reached 80mA/min. at 50pps as mentioned in the abstract, which indicates the injector linac's capability. The switch time for electron and positron modes change was less than 10 seconds. And the highest electron energy has reached 2.7GeV, so in the operation for the BERF early this year the top off injection at 2.5GeV with one RF unit stand-by has been adopted as shown in Fig. 1.

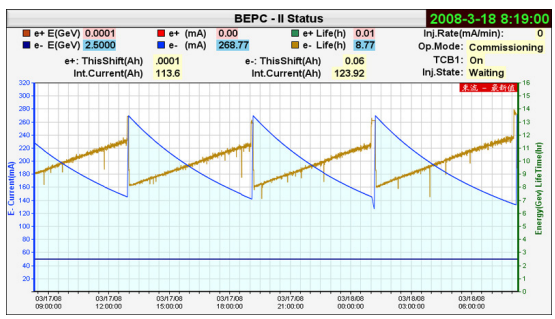

Figure1: The plot for top off injection.

In what follows we will present some details concerning the beam as well as machine stability issues.

Beam Orbit Stability

There are 19 BPMs along the linac. With these BPMs we can easily observe the beam position and the orbit stability. Figure 2 shows a good electron orbit at BPM5 and BPM14, the jitter is less than 0.1mm (1σ).

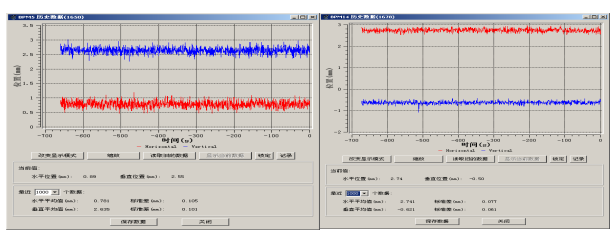
BPM5 BPM14
Figure 2: Beam position stability at BPMs 5 and 14.

Beam Energy Stability

The beam energy stability can be measured by the BPMs located at a large dispersion region in the beam

STATUS OF AN AUTOMATIC BEAM STEERING FOR THE CLIC TEST FACILITY 3*

E. Adli†, R. Corsini, A. Dabrowski, D. Schulte, S.H. Shaker,
P. Skowronski, F. Tecker, R. Tomas, CERN, Geneva, Switzerland

Abstract

An automatic beam steering application for CTF 3 is being designed in order to automatize operation of the machine, as well as providing a test-bed for advanced steering algorithms for CLIC. Beam-based correction including dispersion free steering have been investigated. An approach based on a PLACET on-line model has been tested. This paper gives an overview of the current status and the achieved results of the CTF3 automatic steering.

INTRODUCTION

The Compact LInear Collider (CLIC) study has shown that advanced beam-based correction will be needed to reach nominal performance of several parts of the collider [1], [2]. The CLIC Test Facility 3 (CTF3) has been constructed at CERN in order to demonstrate feasibility of several key concepts of CLIC [3]. New areas are added to CTF3 for each new phase, making operation more complicated, and it is therefore of significant interest to ease the operation of this machine. The purpose of the work described here is thus two-fold:

- test of correction algorithms devised for CLIC on a real machine
- aid operation of CTF3 by automating beam steering (currently performed by hand)

CORRECTION APPROACHES

The correction algorithms investigated here are "all-to-all" (A2A) and dispersion-free steering (DFS) [4]. In this paper we use "correction" and "steering" interchangeably. Both algorithms can be implemented using response matrices. Their effect when applied to a defined lattice segment is ideally:

- A2A: steers the beam to get BPM zero-readings, by simply inverting the response matrix of the nominal machine optics
- DFS: minimizes the difference of dispersive trajectories, using responses corresponding to optics with different $\Delta p/p$; weighted against A2A

Matrix inversion for both candidates is performed in the Least-Squares sense, using SVD. Smoothing can be introduced by taking out corrector modes corresponding to small singular values, effectively smoothing out noise effects. Furthermore, defect BPMs and/or correctors can be taken easily into account by zeroing rows and/or columns of the response matrix. A2A and DFS then find the global solution within the defined lattice segment (this is why we say "all-to-all" rather than "1-to-1").

For quick and effective correction computer model generated responses are needed. With model-based steering, one can perform all-to-all steering for a lattice segment in few tens of seconds. In comparison, to obtain machine responses in CTF3 takes from 1/4 h to 1/2 h per optics, per plane, totaling to hours if one wants to do dispersion-free steering. On the other hand, model-based steering require a good correspondence model/machine, and obtaining the needed model accuracy might be challenging.

TEST-CASE: THE CTF3 LINAC

The CTF3 linac, characterized by operation with full beam-loading [5], was chosen as "test-lattice", because of higher applicability wrt. [1], [2]. We apply correction on a straight part of the linac, with regular lattice structure consisting of 11 girders ("nr. 5" to "nr. 15"), where each girder supports a quadrupole triplet, one corrector coil, and one BPM, as shown in Figure 1. For girders 5,6,7,11,12,13 and 15 there are in addition two accelerating structures, fed by one klystron, located between the corrector and the BPM.

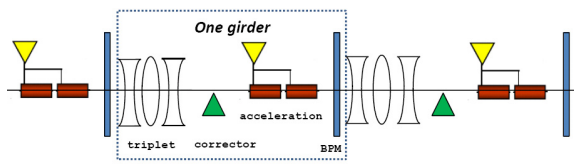

Figure 1: Structure of the CTF3 linac (not to scale).

Dispersion and Emittance Growth

Dispersion measurement and DFS were in this work performed by scaling magnet currents. We therefore consider only dispersion building up from the start of the test-lattice (we do not consider, and cannot mitigate, upstream dispersion). There are no powered dipoles in the test-lattice, so the dispersion comes mainly from parasitic dispersion due to quadrupole offsets (we also get a small contribution from the correctors, dispersion due to incoming beam offset/angle and due to transverse wakes). We note that our 11 cell lattice accomodates little more than a single betatron-oscillation, and we therefore expect dispersion to be small, even for the uncorrected case (no resonant build-up possible). The CTF3 component alignment tolerance is 100 μm

* Work supported by the Research Council of Norway and the Commission of the European Communities under the 6th Framework Programme 'Structuring the European Research Area', contract number RIDS-011899.
† Erik.Adli@cern.ch, University of Oslo and CERN

DESIGN OF THE TAIL CLIPPER COLLIMATOR FOR CTF3

R. Chamizo, H. H. Braun, N. Chritin, D. Grenier, J. Hansen, Y. Kadi, L. Massidda,
Th. Otto, R. Rocca, R. Zennaro, CERN, Geneva, Switzerland.

Abstract

The CERN CLIC Test Facility (CTF3) aims at assessing the feasibility of the future multi-TeV Compact Linear Collider (CLIC). The CTF3 Tail Clipper Collimator (TCC) will serve to adjust the bunch train length of the beam extracted from the combiner ring, in combination with a fast kicker magnet. In addition, the TCC will operate, when required, as an internal beam dump. The challenge of the TCC design is to meet the requirements of both collimation and dump operational modes for a low energy e^- beam (100-300MeV) of 35A peak intensity. The TCC collimator will be installed in January 2009 in the TL2 transfer line of CTF3. This paper describes the final design of the TCC and the main issues related to its integration in the line.

INTRODUCTION

The CTF3 facility [1] is a demonstrator of the technical feasibility of the key concepts of the novel CLIC RF power source, e.g., generation of high-charge, high-frequency electron bunch trains by beam combination and operation with a fully-loaded drive-beam accelerator. The CTF3 facility includes a 70 m long linac followed by a 42 m delay loop, an 84 m combiner ring (CR) and a CLic EXperimental area (CLEX). The TCC is a combined collimator/dump and will be installed in the transfer line from the CR to the CLEX. It will serve to shorten the pulse length of the accelerated beam for 12 GHz RF generation in the CLEX (collimation mode). A fast kicker magnet [2] will deflect vertically an adjustable fraction of the pulse length. The TCC will absorb the deflected pulse while the rest will be transferred to the CLEX. The TCC will also serve to intercept the full beam (dump mode) for safe installation work in the CLEX. The main beam parameters considered for the design of the TCC are summarized in Table 1.

Table 1: CTF3 Beam Parameters Relevant for the TCC Design

Particles	e^-	
Beam energy @ TCC	150	MeV
Repetition rate	0.8 – 5.0	Hz
Incoming pulse duration	140	ns
Peak beam pulse current	35	A
Beam size range (rms, 1σ)	σh=2-5; σv=1	mm
Beam deflection @ TCC	>6	mm
Average beam power	3.7	kW

THE TCC DESIGN

Thermo-Mechanical Considerations

The dump mode of the TCC represents the most demanding case of operation from the thermo mechanical point of view and it has been considered as the determining condition for the design. The TCC will intercept a 150MeV e^- beam of average power equal to 3.7kW. In the collimation mode, the absorbed power will be less than this.

In order to determine the most appropriate material for the TCC jaw, detailed studies with the Monte-Carlo code FLUKA were performed for assessing the amount of energy deposited on the TCC. Fig. 1 shows the temperature profile (instantaneous) in the jaw after one pulse impact (beam: 150MeV, 5 pulses/s, 3.7kW) for Aluminium, Graphite and Glidcop® jaws.

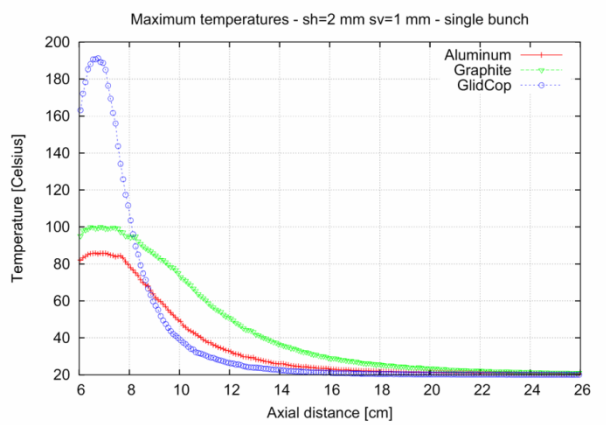

Figure 1: Temperature profile in the TCC jaw after one pulse impact for the studied materials.

Previous thermo-mechanical studies [3] have concluded that, structurally, the most critical case of impact occurs during an impact placed below 1.3mm from the jaw surface. The thermal loads calculated with FLUKA were given as input to an ANSYS® FE model of the TCC jaw, reproducing this particular case. The results obtained are summarized in Table 2.

Table 2: Temperature and Internal Stresses Obtained by ANSYS Simulation for the Studied Materials

e^- beam (σh=2 - σv=1, mm), 150Mev, 3.7kW, 5 pulses/s	Al	Glidcop	Graphite
Yield Strength (MPa)	55	255	30
ΔT (140ns) (ºC)	58	166	78
Maximum stress (140ns) (MPa)	79	265	2

THE 150 MeV PULSE ELECTRON LINAC WITH 1 mA AVERAGE CURRENT*

M.I. Ayzatsky, A.N. Dovbnya, V.N. Boriskin, I.V. Khodak, S.G. Kononenko, V.A. Kushnir, V.V. Mytrochenko, S.A. Perezhogin, Yu.D. Tur. Kharkov, NSC/KIPT, Kharkov, 61108, Ukraine

Abstract

The project of the accelerator driven subcritical assembly facility is under development in the National Science Center "Kharkov Institute of Physics and Technology". The important component of the facility is an electron linac with the particles energy of 100…200 MeV and average beam current of 1 mA. In this paper we focus on the S-band electron linac design. The accelerator scheme includes the injector based on evanescence waves, RF chopper, five accelerating structures and energy compression system. The calculation results of accelerating structure performances and linac systems are considered in the paper.

INTRODUCTION

The developing facility consists of the linac, the system of the beam transport to the target complex, the neutron-producing target and the subcritical assembly of the fuel elements.

Using of the linac as the subcritical assembly driver makes a number of demands. The electron energy at the linac exit must be 100-200 MeV. On the one hand, it provides rather high yield of the neutrons, and on the other hand - the volume of the neutron target will be large enough for the energy density decrease and the target cooling conditions improve. The existing high-frequency linac power supplies and the injector systems allow obtaining the average current at such linac exit in the necessary electron energy range near 1 mA. Considerable average beam power (about 100 kW) obviously demands minimizing the high-energy particles loss during their acceleration and transport.

THE FACILITY POSITION AND STRUCTURE

The linac will be placed in the building of the linac LU-2000 in NSC KIPT. Such placing of the complex doesn't need the new fundamental construction, allows using the existing engineer infrastructure after its major reconstruction. The existing power system allows power supplying of all systems of the linac. New equipment placing is possible after the demounting of the existing equipment. The accelerating sections of the developing linac will be placed after the 36th section of the linac LU-2000. The layout of the linac main parts is presented in Fig. 1.

The accelerator itself consists of the electron source, injector (I), five S-band accelerating sections (1s-5s) and the system of energy compression (SEC). The system of energy compression includes the debuncher (D) and the compensation accelerating section (CS). At the accelerator exit there are placed the magnetic electron energy analyzer (M1) and the dipole magnet (M2), providing the electron beam injection into the transport system to the target complex. The main elements for the beam focusing are the short solenoid on the first section (S) and the doublets of the quadruple lenses, placed on each section. The beam current transformers and the beam position monitors will be placed after the injector and each section exit.

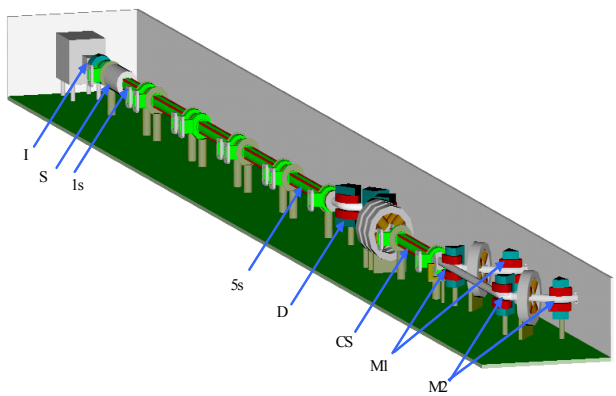

Figure 1: Placing of the accelerator main elements.

The accelerator RF power supply system is planned to be created at the base of six klystrons SLAC 5045 (produced by SLAC, USA). Proceeding from the average beam power 100 kW, the current pulse repetition rate and the pulse duration are chosen 300 pps and 3.0 μs respectively. In this context the standard mode of the klystron SLAC 5045 will have to be changed (see Table 1).

Table 1: Klystron parameters

Parameter	Standard mode	Required mode
RF frequency, MHz	2856	2856
Pulse repetition rate, pps	≤ 180	300
Max. pulse RF power, MW	67	29.9
RF pulse duration, μs	3.5	3.2
Average RF power, kW	37	31.2

* Work supported by STCU project P233

INJECTOR OF INTENSE ELECTRON BEAM

M. Ayzatskiy, V. Mytrochenko NSC/KIPT, Kharkov, 61108, Ukraine

Abstract

The results of beam dynamic simulation in a S-band injector that can be used for creation of the powerful electron linac are presented in the report. The injector consists of a diode electron gun with beam current of up to 2 A at energy of electrons of 25 keV, the klystron type prebuncher and the three cavity buncher. In the buncher, due to the special choice of eigen frequencies of resonators, maximal amplitude of the field on the axis of resonators exponentially increases from the first (downstream of the beam) resonator to the last resonator. It allows to realize an effective bunching the intensive electron beam and accelerating it to relativistic velocities. For achievement a low transversal beam emittance the injector is placed into the external magnetic field. The injector provides more than 1 A of beam current with particle energies of about 1 MeV. Attention is paid to research of transients and stability of injector work.

INTRODUCTION

Often it is necessary to provide ampere range beam at an exit of the pulsed electron S-band linacs with high beam power because a duty factor of pulsed klystron amplifiers is about 0.1%. Use of relatively low voltage electron guns (several tens of kilovolts) in a linac injector facilitates obtaining high reliability of the linac at compact linac dimensions. Bunching system based on evanescent waves (see for example [1]) is very suitable to generate electron bunches from continuous beam emitted from a cathode of such low voltage gun as well as to accelerate particles to relativistic velocities. The above mentioned bunching system comprised of five cells has exponential rise of on-axis field from the entrance of the electron beam into the buncher to the it exit. This rise is provided by correspondent choice of cell dimensions. To provide flexibility of the system at bunching and accelerating of the ampere range electron beam it was decided to change the first two cells of the buncher with a klystron type prebuncher and drift space. To prevent degradation of transversal beam emittance the prebuncher and buncher are placed into solenoidal magnetic field. This paper is devoted to brief description of simulation algorithms of beam dynamics in a system comprised of the prebuncher and the three cell buncher as well as to review of simulation results.

SIMULATION ALGORITHMS

The POISSON/SUPERFISH [2] group of codes was used to calculate characteristics of resonance and magnetic systems of the injector. Simulation of electron motion in the injector was performed using the PARMELA [3] code. Beam parameters of the ampere range diode gun [4] was calculated with EGUN [4] code. Study of unsteady self consistent beam dynamics in the injector were performed both with technique [6] and with developed by us program COUPLRES. Technique [6] solves self-consistent equations of field excitation in axially symmetrical cavities both by an electron beam and by an external RF generator. The PARMELA code is used in this technique to simulate particle motion in evaluated field to get needed data at each temporal step of the equation solution. This technique takes into account only one mode of a cavity field.

COUPLRES (COUPLing RESonators) allows to describe unsteady processes arising at interaction of electron beam with electromagnetic systems that can be represented as a chain of coupled cavities. This code is elaborated on a base of mathematical model that is development of the coupled cavity model by correct taking into account self-consistent beam dynamics in fields excited both by external sources and by particles itself. At the moment the model takes into account only fields that are symmetrical relatively the main direction of beam propagation. The base of the model is decomposition of a considered electromagnetic system into closed volumes and representation of fields inside of the volumes as an expansion into a series of eigen functions (solenoidal and potential) of closed cavities. Particles are injected into a simulated system at certain moments of time. A set of equations to be analyzed consists of particle motion equations and equations for expansion amplitudes (differential equations for basic oscillations and algebraic ones for non-resonant modes).

A developed variant of the code is applicable to describe systems that can be decomposed into cylindrical volumes. In this case there are analytical expressions for the eigen functions. The Runge-Kutta method is used to solve both equations of motion and equations for amplitudes of basic oscillations. At solution of the last equations values of current and charge integrals are kept constant over RF period of the fundamental frequency. Quasi-coulomb fields are represented as expansion into series of solenoidal and potential functions and are evaluated at frequencies $\omega \approx 0$ and $\omega \approx \omega_0$, where ω_0 is frequency of a RF source.

The merit of the code is a possibility to take into account influence of all eigen modes at simulation of time beam dynamics. This feature allows to make an analysis of injector operation stability at bunching and accelerating of intense electron beams.

SIMULATION RESULTS

Simulations were carried out to attain two aims. On the one hand in was necessary to find configurations both the resonance and magnetic system of the injector that provide effective bunching of the ampere range electron

COMMISSIONING THE DARHT-II ACCELERATOR DOWNSTREAM TRANSPORT AND TARGET*

Martin Schulze, SAIC, Los Alamos, NM 87544, USA
E. O. Abeyta,, R. Archuleta, J. Barazza, D. Dalmas, C. Ekdahl, W. Gregory, J. Harrison, J. Johnson, E. Jacquez, P. Marroquin, B. Trent McCuistian, R. Mitchell, N. Montoya, S. Nath, K. Nielson, R. Ortiz, L. Rowton, R. Scarpetti, G. Seitz, M. Schauer,
Los Alamos National Laboratory, Los Alamos, NM 87545, USA
R. Anaya, G Caporaso, F. Chambers, Y.J. Chen, S. Falabella, G. Guethlein, B. Raymond, R. Richardson, J. Watson, J. Weir
Lawrence Livermore National Laboratory, Livermore, CA 94550
H. Bender, W. Broste, C. Carlson, D. Frayer, D. Johnson, and C. Y. Tom,
N.S. Tech, Los Alamos, NM 87544, USA
T. P. Hughes, C. Thoma,
Voss Scientific, Albuquerque, NM 87108, USA

Abstract

The DARHT-II accelerator [1] produces a 2-kA, 17-MeV beam in a 1600-ns pulse. After exiting the accelerator, the pulse is sliced into four short pulses by a kicker and quadrupole septum and then transported for several meters to a tantalum target for conversion to x-rays for radiography. We describe the commissioning of the kicker, septum, transport, and multi-pulse converter target. The results of beam measurements made during the commissioning of the downstream transport are described.

INTRODUCTION

The DARHT–II accelerator beam parameters are 17-MeV and 2.0 kA with a flattop of 1.6 microseconds. The DARHT–II downstream transport was commissioned at reduced energy and current in early 2007 [2]. The beam parameters were 8-MeV and 1.1 kA with a flattop of 1.6 microseconds.

The downstream transport system for the DARHT-II accelerator is designed to extract four short pulses (20-100 nsec) from the 1.6 microsecond beam and deliver these pulses to an x-ray production target for radiography. Figure 1 provides a schematic illustration of the downstream transport beamline.

The high level requirements imposed on the downstream transport are outlined below:

- Deliver four pulses over 1.5-1.6 μsec
- Spot sizes less than 2.3 mm 50% MTF
- Dose format exceeding 100 R, 100 R 100 R and 300 R in each successive pulse

Each of these requirements were met and reproduced over multiple shots. These results will be described. High quality radiographic images with the DARHT-II accelerator impose additional requirements on the beam quality, in particular, the beam motion over flattop. This issue and the methods used to minimize the that have been used to address them are discussed.

*Work supported by USDOE under contract DE-AC52-06NA25396

LAYOUT AND OPTICS

The beam from the accelerator is focused using the first and third solenoids to produce a small waist at the entrance to the quad septum. This effectively decouples the accelerator from the remainder of the downstream transport. The beam enters the kicker and is either directed downward to the beam dump with a DC bias dipole magnet or the fast kicker is energized to direct the beam straight ahead. The bias dipole deflects the beam by 1-1.5 degrees. This deflection is magnified with a large aperture septum quadrupole tuned to defocus the beam in the vertical plane resulting in a net deflection of about 15 degrees. This also results in a large beam size on the dump which reduces the power density to acceptable levels. A dipole magnet further deflects the beam into the dump. The kicked beam enters the septum quadrupole on axis and the nominally round beam profile becomes elliptical. The function of the small Collins quadrupoles following the septum quadrupole is to transform this elliptical beam back to a round profile. The purpose of the remaining solenoid is to transport the beam to the final focus solenoid which delivers a tightly focused beam to the target.

There are four semi-independent regions in the downstream transport. The first region is from the accelerator to the septum quadrupole and the settings of the first and third solenoids. The second region is the transport to the septum dump. This defines the required settings of the bias dipole, septum quad and the septum dipole. The third region includes the four Collins quadrupoles that are used to return the beam back to round. The forth region consists of a transport solenoid and a final focus solenoid to produce a small beam size on target. The last transport solenoid was not used.

Beam position and current measuring diagnostics are located throughout the downstream transport. Beam profile imaging stations were located at the accelerator exit, between the 1st and 2nd Collins quadrupole magnets, and after the 4th solenoid.

DIGITALLY CONTROLLED HIGH AVAILABILITY POWER SUPPLY

David MacNair, Stanford Linear Accelerator Center, Menlo Park, CA

Abstract

This paper reports the design and test results on novel topology, high-efficiency, and low operating temperature, 1,320-watt power modules for high availability power supplies. The modules permit parallel operation for N+1 redundancy with hot swap capability. An embedded DSP provides intelligent start-up and shutdown, output regulation, general control and fault detection. PWM modules in the DSP drive the FET switches at 20 to 100 kHz. The DSP also ensures current sharing between modules, synchronized switching, and soft start up for hot swapping. The module voltage and current have dedicated ADCs (>200 kS/sec) to provide pulse-by-pulse output control. A Dual CAN bus interface provides for low cost redundant control paths. Over-rated module components provide high reliability and high efficiency at full load. Low on-resistance FETs replace conventional diodes in the buck regulator. Saturable inductors limit the FET reverse diode current during switching. The modules operate in a two-quadrant mode, allowing bipolar output from complimentary module groups. Controllable, low resistance FETs at the input and output provide fault isolation and allow module hot swapping.

OVERVIEW

The next linear collider will require several thousand magnet power supplies. This is a far greater number then any linear accelerator has used to date. To achieve equivalent or better availability of the beam will require improved availability of all systems. Significant increases in availability can come from improved reliability of modules, but an order of magnitude improvement can only come from redundant modules.

Power supplies will consist of parallel power modules in a N+1 redundant arrangement. Individual modules can fail without causing the power supply to lose regulation of the magnet current. Individual modules must provide for fault isolation to allow the power supply to operate with a failed module. The isolation will also allow for hot swapping of modules.

The individual modules will be autonomous so that there is no single point of failure. A digital controller will provide module control and fault detection. The controller provides a dual CAN bus interface for redundant power supply control.

POWER MODULE

The power supply architecture is based on shared central bulk AC-DC power supplies with redundant buck regulators for each load. The power supplies are assumed to be in the 5 to 50 kW range consisting of redundant 1 to 10 kW modules. The modules will provide a voltage regulated output set by CAN bus broadcast messages from redundant magnet current regulators. The modules will use buck regulators with FETs in place of free wheeling diodes. This provides lower conduction losses and eliminates the non-linear discontinuous conduction region at low current. The two quadrant operation allows two power supplies operating with complimentary outputs to drive bipolar loads.

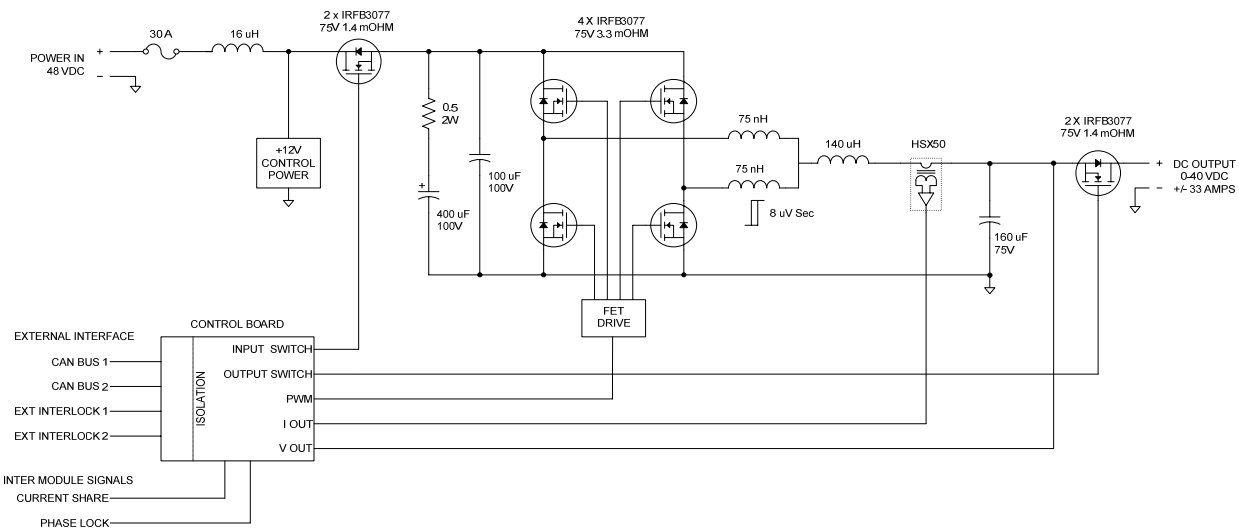

Figure 1: Two quadrant DC-DC converter with input and output FET switches.

*Work supported by the U.S. Department of Energy under contract number DE-AC02-76SF00515. SLAC-PUB-13415

RF CONTROL AND LONGITUDINAL BEAM STABILITY IN ENERGY RECOVERY LINACS

A. Neumann, M. Abo-Bakr, J. Knobloch, BESSY GmbH, Berlin

Abstract

Most concepts for next generation light sources base on linear accelerators (linac) due to their excellent beam properties. In case of high electron energies and extreme average currents Energy Recovery Linacs (ERL) are mandatory. In this paper we investigate the rf field stability in a generic superconducting, cw operated ERL. By using rf control cavity simulations and longitudinal beam dynamics the influence of rf field stability on the energy recovery process is analyzed. Since the ERL aims for a small net beam loading cavities are operated at a high loaded quality factor. Therefore they are operated at a low bandwidth and are very susceptible to microphonics detuning. We considered the field stability under the influence of limited rf power, mechanical cavity detuning, varying beamloading, synchronization deviations and varying bunch parameters at injection into the linac. The resulting temporal and energy jitter at the linac end will be transformed in the return arc and leads to rf phase deviations on the return path. Implications of varying beam loading on the ERL performance are examined.

CONTRIBUTION NOT RECEIVED

OPTIMIZATION OF LATTICE FOR AN ERL UPGRADE TO THE ADVANCED PHOTON SOURCE*

M. Borland†, V. Sajaev, ANL, Argonne, IL 60439, USA

Abstract

An Energy Recovery Linac (ERL) is one possibility for an upgrade to the Advanced Photon Source (APS). In addition to the linac itself, our concept involves a large turn-around arc (TAA) at 7 GeV that would eventually accommodate many new beamlines. Previously, we based the TAA design on isochronous triple-bend achromat (TBA) cells, since these are expected to provide some immunity to the effects of coherent synchrotron radiation. In the present work, we compare the previous TBA-based design to a new design based on double-bend achromat (DBA) cells, in terms of emittance growth, energy spread growth, and energy recovery. We also explore the trade-off between optimization of the beta functions in the straight sections and minimization of emittance growth.

INTRODUCTION

An ERL [1] upgrade to the APS promises a revolutionary improvement in x-ray properties. In previous work [2] we made use of a TBA-based cell design for the TAA for the ERL upgrade. This choice was inspired by the desire to make an isochronous system with cancellation of coherent synchrotron radiation (CSR) effects [3, 4]. However, we found that CSR effects were very small, even as we increased the charge in the beam. Hence, we hypothesized that perhaps a simpler cell design might be acceptable. In this paper, we show results for a DBA-based design and compare these to the previous TBA-based design. (The APS ring portion of the ERL is necessarily DBA, since we don't propose to replace the APS ring. However, for simplicity we'll refer to "TBA" or "DBA" designs based on the optics design used for the non-APS portions.)

We also noted previously that with smaller beta functions at the insertion devices, x-ray brightness might be increased beyond what was predicted in [2]. In the second part of this paper, we explore the potential benefit and issues related to smaller beta functions.

NEW ARC DESIGN

To develop the new arc design, we started with the APS cell including the Decker distortion[5], since this cell design is close to what we want. We then used `elegant` [6] to evolve this cell as follows: (1) Bending angle per cell of $\pi/24$ (48 cell turn around), just as for the TBA design. (2) $\eta_x = \eta'_x = 0$ in straights. (3) Increase space for insertion devices (IDs) from 4.8 m to 8 m. (4) $\beta_x \approx \beta_y \leq 5\mathrm{m}$ at center of ID straights. (5) Mean arc radius of 230 m, just as for the TBA design. (6) Minimize the I_2, I_3 and I_5 radiation integrals. (7) Similar maximum lattice beta functions as the TBA design, e.g., $\sim 25\mathrm{m}$. As Figure 1 shows, it was possible to make $\beta_x \approx \beta_y \approx 3\mathrm{m}$, which has advantages for brightness compared to the $\beta_x = 12\mathrm{m}$ and $\beta_y = 4.7\mathrm{m}$ values for the TBA. It is likely this could be achieved in the TBA only by moving away from the CSR canceling tunes and perhaps giving up isochronicity.

We attempted to simplify the DBA cell by having doublets on each side of the ID instead of triplets. We did not find a solution that had satisfactory emittance growth and beta functions. Hence, the promise of the DBA to simplify the cell structure didn't bear fruit. We eliminate one dipole magnet, but the dipoles are longer.

We also performed a DBA-based design of the arcs ("transport arcs") that bring the beam into and out of the APS ring. The constraints are very similar to those just listed, except there is no need for long straight sections. The mean radius was 75 m with a total bending angle of 72 degrees in 8 cells, as in the TBA design.

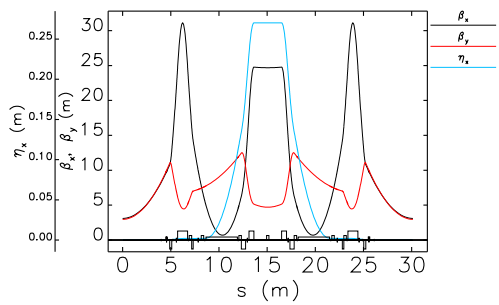

Figure 1: Optics for turn-around arc DBA cell.

TRACKING COMPARISON

The next step is to compare tracking results for the DBA and TBA designs. We are interested in absolute energy loss, energy droop (deviation from reference), energy spread increase, and emittance increase. Mechanisms involved are classical, incoherent, and coherent synchrotron radiation. All the tracking studies used `Pelegant` [7] and the high-coherence-mode beam parameters [8], i.e., 0.1 μm initial normalized emittance with a 2-ps rms bunch length. For consistency with previous work, we assumed an initial

* Work supported by the U.S. Department of Energy, Office of Science, Office of Basic Energy Sciences, under Contract No. DE-AC02-06CH11357.

† borland@aps.anl.gov

GROWTH OF DENSITY MODULATIONS IN AN ENERGY RECOVERY LINAC LIGHT SOURCE DUE TO COHERENT SYNCHROTRON RADIATION AND LONGITUDINAL SPACE CHARGE*

M. Borland †, ANL, Argonne, IL 60439, USA

Abstract

An Energy Recovery Linac (ERL) is one possibility for an upgrade to the Advanced Photon Source (APS). Such a system involves not only a long linac, but also long transport lines with many dipole magnets. Since the bunches are short, we may expect that coherent synchrotron radiation (CSR) and longitudial space charge (LSC) will have an effect on the beam dynamics. Although previous studies have shown minimal effects for an initially quiet beam distribution, the possibility of a microbunching instability seeded by initial density modulation must be evaluated. We present and discuss simulation results showing the growth of density modulations in two possible lattices for an ERL upgrade of the APS.

INTRODUCTION

The first hint that CSR could amplify initial density modulations in a beam in a single-pass system came from modeling [1] of the Linac Coherent Light Source (LCLS) with `elegant` [2]. Subsequently, theoretical analysis [3] for the TESLA Test Facility predicted an even more severe problem when LSC was included. This was subsequently confirmed by modeling with `elegant` for the LCLS [4]. What is critical in the LCLS and other similar systems is the alternation between long linear accelerators in which LSC effects accumulate and one or more bunch compression systems in which CSR effects act.

An ERL [5] upgrade to the APS promises a revolutionary improvement in x-ray properties. We have developed a concept for an "ultimate" ERL upgrade to the APS [6] that involves a long, single-pass 7-GeV linac and a large 7-GeV turn-around arc. The potential for build-up of CSR and LSC effects in such a system seems clear, due to the length of the linac and transport line, as well as the large number of dipole magnets. In addition, the bunch duration is relatively short ($\sim$2 ps rms) and the normalized emittance is very small ($\sim$ 0.1 μm), as is the rms fractional momentum spread ($\sim$ 0.02%). Like the LCLS and other high-performance injectors, the ERL injector is likely to be driven by a shaped laser pulse [7], which opens up the possibility that significant density ripples will be imparted to the beam at the cathode. Hence, in spite of the low charge (under 100 pC), there is reason to be concerned about potential microbunching growth.

We've investigated this for two possible optical configurations of the ERL: (1) The original "TBA" configuration [6, 8], with triple-bend-achromat (TBA) cells outside the APS and double-bend-achromat (DBA) cells inside the APS. (2) A new DBA configuration, with DBA cells throughout. A comparison of these configurations is offered elsewhere in these proceedings.

In the present work, we begin our simulations at the 10-MeV point. Full simulations starting at the cathode are obviously desirable, but beyond our scope at this time.

SIMULATION METHODS

The approach we have taken is very similar to what was done for LCLS and FERMI [9, 4, 10], where we obtained a growth curve for density modulations. We performed a series of simulations for various bunch charge, modulation wavelength, and modulation depth with CSR, LSC, and linac longitudinal wakefields. CSR was included using `elegant`'s line-charge model [11, 12], including CSR in drift spaces. This model includes the transient build-up of CSR in each dipole, but does not include shielding. Shielding will in fact have some effect on the "bulk CSR," i.e., CSR at the wavelengths related to the overall bunch length [13]. However, it will have a significantly diminished effect at the shorter wavelengths corresponding to density modulations.

LSC was included using an impedance-based method [4]. An LSC kick was added after each linac structure as well as at the center of each ID straight section. This made use of a newly-added feature in `elegant`, namely, the ability to insert an LSC kick that integrates the effect of an LSC applied over a user-specified length of the beamline. This approach is valid as long as the relative longitudinal motion of particles is not too great, which is the case when we place kicks at each ID straight section.

Control of noise is essential to getting reliable results. We followed the algorithm in [4, 10] fairly closely: 1. Choose a density modulation wavelength and depth. We used depth values between 0 and 10%, inclusive. The 0% runs are helpful in baselining the effects of noise. 2. Choose the bin size to be 1/24$^{\text{th}}$ of the wavelength. This means the Nyquist frequency is 12 times the wavelength. 3. Set the low-pass noise filter cutoff to 1.5 times the modulation frequency. Combined with item 2, we smooth and interpolate features at the modulation frequency on the

* Work supported by the U.S. Department of Energy, Office of Science, Office of Basic Energy Sciences, under Contract No. DE-AC02-06CH11357.

† borland@aps.anl.gov

EXPLORING BENEFITS OF USING RF DEFLECTION FOR SHORT X-RAY PULSE GENERATION FOR AN ENERGY-RECOVERY LINAC UPGRADE TO THE ADVANCED PHOTON SOURCE*

V. Sajaev#, M. Borland, ANL, Argonne, IL 60439, U.S.A.

Abstract

One option for the Advanced Photon Source (APS) upgrade is an energy-recovery linac (ERL). In its main operating mode, the ERL rms bunch length would be two picoseconds. Even though this bunch length is already a factor of 20 shorter than the present APS bunch length, some experiments might benefit from even shorter x-ray pulses. For the APS storage ring, we plan to use an rf deflection technique [1] to generate one-picosecond-long x-ray pulses. In this approach, an rf cavity is used to deliver a longitudinally dependent vertical kick to the electron beam and then a pair of slits is used to slice the vertically streaked x-ray beam (see Figure 1). Here, we investigate the possibility and benefits of utilizing this technique to generate shorter x-ray pulses in an ERL.

ANALYSIS

Let's consider the beam motion after the first cavity, which provides time dependent vertical kick:

$$y_0'(t) = \frac{V}{E}\sin(\omega t) \approx \frac{V}{E}\omega t\,,$$

where V is the deflecting cavity voltage, ω is the deflecting cavity frequency, E is the beam energy, and we have assumed that the beam is short enough to stay within the linear part of the rf waveform. At the location of the undulator, the beam will have the following coordinates [2]:

$$y_{ID}(t) = \frac{V\omega t}{E}\sqrt{\beta_{RF}\beta_{ID}}\sin(\psi)\,,$$

$$y_{ID}'(t) = \frac{V\omega t}{E}\sqrt{\frac{\beta_{RF}}{\beta_{ID}}}\left(\cos(\psi) - \alpha_{ID}\sin(\psi)\right),$$

where β and α are Twiss functions, and ψ is the betatron phase advance. These equations describe the vertical position and angle of the beam slice located at longitudinal position t. Each beam slice has beam size σ_y and divergence $\sigma_{y'}$. Considering the undulator radiation divergence σ_θ, the photon beam position and its vertical size a distance L down the beamline are

$$y_L(t) = y_{ID}(t) + y_{ID}'(t)\cdot L =$$

$$= \frac{V\omega t}{E}\left(\sqrt{\beta_{RF}\beta_{ID}}\sin(\psi) + L\cdot\sqrt{\frac{\beta_{RF}}{\beta_{ID}}}\left(\cos(\psi) - \alpha_{ID}\sin(\psi)\right)\right),$$

$$\sigma_L^{\,2} = \sigma_y^{\,2} + L^2\left(\sigma_{y'}^{\,2} + \sigma_\theta^{\,2}\right).$$

* Work supported by the U.S. Department of Energy, Office of Science, Office of Basic Energy Sciences, under Contract No. DE-AC02-06CH11357.

#sajaev@aps.anl.gov

At this point, an asymmetrically cut crystal can be used to compress the photon pulse as shown in Figure 2. Such a crystal performs horizontal sheering as shown by the red arrows, and the resulting minimum pulse length after the crystal is $\sigma_s = \sigma_y/\tan(\vartheta)$. The same length can be achieved by using slits instead of the crystal to slice the beam along the horizontal axis. The minimum achievable pulse length is

$$\sigma_t = \frac{\sigma_L}{dy_L(t)/dt} =$$

$$= \frac{\frac{E}{V\omega}\sqrt{\sigma_y^{\,2} + L^2\left(\sigma_{y'}^{\,2} + \sigma_\theta^{\,2}\right)}}{\left(\sqrt{\beta_{RF}\beta_{ID}}\sin(\psi) + L\cdot\sqrt{\frac{\beta_{RF}}{\beta_{ID}}}\left(\cos(\psi) - \alpha_{ID}\sin(\psi)\right)\right)}.$$

There are two phase-advance values between the cavity and the undulator that simplify the expression above by zeroing the sine or cosine term. One can see that having *sin(ψ)* equal zero rather than *cos(ψ)* allows for achieving shorter pulses assuming reasonable values for beta functions and distance to the beamline optics. The expression can be simplified for this case as follows:

$$\Delta t = \frac{E}{V\omega}\sqrt{\frac{\beta_{ID}}{\beta_{RF}}}\sqrt{\sigma_{y'}^{\,2} + \sigma_\theta^{\,2}}\,. \qquad (1)$$

This expression is the same as obtained in Ref. [3] with the addition of a beta function ratio. Looking at this equation, one can see what steps are necessary to achieve as short a pulse as possible: higher rf voltage and frequency, smaller ratio of beta functions, and smaller electron beam size divergence and undulator radiation divergence.

Figure 1: Schematic of the rf deflection approach to producing a short pulse.

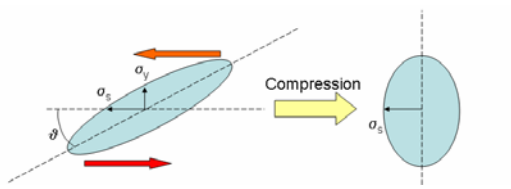

Figure 2: Illustration of pulse compression and minimum achievable pulse length.

SIMULATION OF LINEAR LATTICE CORRECTION OF AN ENERGY-RECOVERY LINAC DESIGNED FOR AN APS UPGRADE*

V. Sajaev#, ANL, Argonne, IL 60439, U.S.A.

Abstract

An energy recovery linac (ERL) is a possible candidate for an upgrade of the Advanced Photon Source (APS). Our ERL design includes full-energy linac, large turn-around arc that could accommodate new x-ray beamlines, and APS itself. In total, the beam trajectory length would be close to 3 km. The ERL lattice has a strong focusing to limit emittance growth, and it includes strong sextupoles to keep beam energy spread under control and minimize beam losses. As in storage rings, trajectory errors in sextupoles will result in lattice perturbations that would affect delivered x-ray beam properties. In storage rings, the response matrix fit method is widely used to measure and correct linear lattice errors. Here, we explore the application of the method to the linear lattice correction of ERL.

INTRODUCTION

Linear optics measurement and correction using response matrix fit is well known and widely used on modern circular machines. The purpose of this work is to simulate the application of the same method to a non-closed beamline.

Theoretically, there is no big difference between response matrix measurement for closed and non-closed beamlines. The orbit equations are well-known and look similar (top equation is for non-closed trajectory and bottom is for closed trajectory, θ – is the kick strength):

$$x(s) = \theta\sqrt{\beta_s\,\beta_\theta}\,\sin(\psi_s - \psi_\theta)\,,$$

$$x(s) = \frac{\theta}{2\sin(\pi\nu)}\sqrt{\beta_s\,\beta_\theta}\,\cos(\psi_s - \psi_\theta - \pi\nu)\,.$$

The measured trajectories in both cases depend on beta functions and phase advances and therefore could be used to derive linear optics. The main practical difference is that in the case of non-closed beamline, the response matrix is triangular with zeros in the top right triangle.

SIMULATION DETAILS

At APS, we have been using response matrix fit method for many years [1]. We added an option of working with non-closed trajectories to our existing program. From our experience, we know that at APS the main source of focusing errors are non-zero orbits in sextupoles and we also know that the focusing errors from sextupoles cannot be precisely represented by nearest quadrupoles [2]. Therefore we decided to include sextupole displacements in error simulation. The following set of errors was used for simulations:

* Work supported by the U.S. Department of Energy, Office of Science, office of Basic Energy Sciences, under Contract No. DE-AC02-06CH11357.

#sajaev@aps.anl.gov

Table 1: Errors used in Calculations

Quadrupole gradient error	0.1 %
Quadrupole tilt	0.001 rad
Sextupole X and Y displacement	1 mm
Corrector calibration error	5 %
Corrector tilt	0.001 rad
BPM calibration error	2 %
BPM tilt	0.001 rad
BPM measurement noise	1 μm

Sextupole displacements were chosen rather large because trajectory errors in sextupoles are defined not by the accuracy of sextupole alignment but by the accuracy of nearest BPM offset which could be large. The errors were generated using Gaussian distribution with 2 sigma limit.

For optics correction simulation we used only APS portion of the ERL because the Turn-Around Arc design has not been finalized to a level of BPM and corrector locations. The lattice of the APS portion is described in [3], the lattice functions of one APS sector are presented in Figure 1. The main difference from the present APS storage ring lattice is zero dispersion in ID straight sections to decrease electron beam size dependence on energy spread. The APS consists of 40 nearly identical sectors.

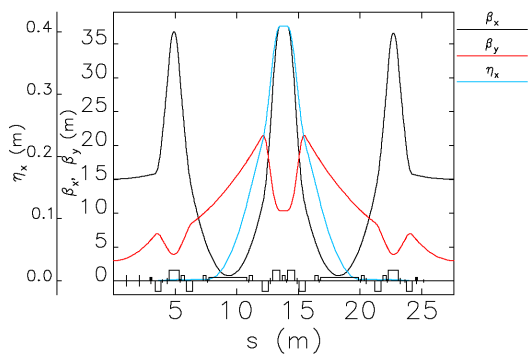

Figure 1: Lattice functions of one sector of the APS portion of the ERL.

Special attention was paid to the choice of correctors used for response matrix measurement in our simulations. APS storage ring has 8 correctors and 11 BPMs per sectors (in most sectors). Presently, for real measurements we use only 27 correctors in each plane (out of 320) evenly distributed along the ring and all BPMs. We limit the number of correctors in order to save measurement time and also to limit the size of the fitting problem. If all the correctors were used, the size of the response matrix derivative would be 15 Gb, which would be too big. Our experience shows that with 27 correctors we still have

STATUS OF HIGH CURRENT R&D ENERGY RECOVERY LINAC AT BROOKHAVEN NATIONAL LABORATORY *

D. Kayran#, D. Beavis, I. Ben-Zvi, M. Blaskiewicz, J.M. Brennan, A. Burrill, R. Calaga, P. Cameron, X. Chang, A. Drees, G. Ganetis, D.M. Gassner, J. Grimes, H. Hahn, L. Hammons, A. Hershcovitch, H.-C. Hseuh, A. Jain, R. Lambiase, D. Lederle, V.N. Litvinenko, G. Mahler, G. McIntyre, W. Meng, T.C. Nehring, B. Oerter, C.-I. Pai, D. Pate, D. Phillips, E. Pozdeyev, J. Reich, T. Roser, T. Russo, A. Sharma, Z. Segalov, J. Smedley, K.S. Smith, T. Srinivasan-Rao, Tuozzolo, G. Wang, D. Weiss, N.W. Williams, Q. Wu, K. Yip, A. Zaltsman, BNL, Upton, NY, USA,
H.P. Bluem, M. Cole, A. Favale, D. Holmes, J. Rathke, T. Schultheiss, AES, Medford, NY, USA,
A. Todd, AES, Princeton, NJ, USA,
J. Delayen, W. Funk, L. Phillips, J. Preble, JLab, Newport News, VA, USA

Abstract

An ampere class 20 MeV superconducting Energy Recovery Linac (ERL) is under construction at Brookhaven National Laboratory (BNL) [1] for testing concepts for high-energy electron cooling and electron-ion colliders. One of the goals is to demonstrate an electron beam with high charge per bunch (~ 5 nC) and extremely low normalized emittance (~ 5 mm-mrad) at an energy of 20 MeV. Flexible lattice of ERL loop provides a test-bed for testing issues of transverse and longitudinal instabilities and diagnostics of intense CW e-beam. The superconducting 703 MHz RF photoinjector is considered as an electron source for such a facility. At first we develop the straight pass (gun -- 5 cell cavity -- beam stop) test for the SRF Gun performance studies. Then the novel injection line concept of emittance preservation at the lower energy will be tested at this ERL. In this paper we present the status and our plans for construction and commissioning of this facility.

INTRODUCTION

The R&D ERL facility at BNL aims to demonstrate CW operation of ERL with average beam current in the range of 0.1-1 ampere, combined with very high efficiency of energy recovery. The ERL is being installed in one of the spacious bays in Bldg. 912 of the RHIC/AGS complex.

The ERL R&D program is started by the Collider Accelerator Department (C-AD) at BNL as an important stepping-stone for 10-fold increase of the luminosity of the Relativistic Heavy Ion Collider (RHIC). Furthermore, the ERL R&D program extends toward a possibility of using 10-20 GeV ERL for future electron-hadron/heavy ion collider, eRHIC [2].

Future RHIC upgrades define the goals for the R&D ERL development to test: 1) Test the key components of the High Current ERL based solely on SRF technology; 2) 703.75 MHz **SRF gun** test with 500 mA current; 3) 5-cell **SRF linac** test with HOM absorbers; 4) Single turn - 500 mA test the beam current stability criteria for CW operation; 5) Test the attainable ranges of electron beam parameters in SRF ERL; 6) Demonstrate beam quality close to that required for RHIC electron cooling and scalability to eRHIC.

GENERAL LAYOUT OF R&D ERL

The R&D ERL design (shown in Fig. 1) has one turn: electrons are generated in the superconducting half-cell gun and injected into the main superconductive linac. Linac accelerates electrons up to 15-20 MeV, when electron bunch pass through a one turn re-circulating loop with achromatic flexible optics [3].

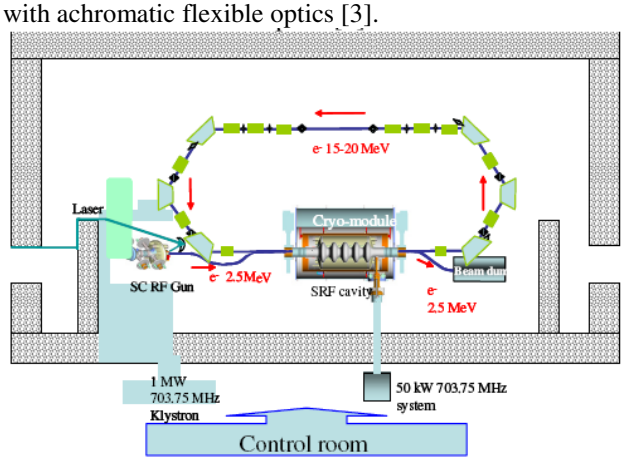

Figure1: Layout of the R&D energy recovery linac in the shielded vault.

The photocathode is located in a high electric field for immediate acceleration of the electrons to as high energy as possible, reducing emittance degradation due to strong space charge force. Furthermore, liner part of space charge effects is compensated by applying a suitable external solenoid magnetic field.

In nominal recovery operation regime the path-length of the loop provides for 180 degrees change of the RF phase, causing electron deceleration (hence energy recovery) down to injection energy. The decelerated beam separates from the higher energy beam and goes to the beam-dump.

ERL INJECTOR

The electron injector is a central part of any ERL that

* Work performed under the auspices of the US Department of Energy
# dkayran@bnl.gov

ELECTRON LINAC BASED COHERENT RADIATION LIGHT SOURCE PROJECT AT OPU*

S. Okuda#, Y. Sakamoto, R. Taniguchi, T. Kojima, Radiation Research Center, Osaka Prefecture Univ., Sakai, Osaka 599-8570, Japan

Abstract

The coherent radiation from an electron bunch of a linear accelerator (linac) has continuous spectrum in a submillimeter to millimeter wavelength range and has an intense pulsed electric field. The purpose of the present work is to establish a new light source of the coherent synchrotron and transition radiation from the electron beams of a 18 MeV S-band linac at Osaka Prefecture University (OPU). The pulse shape of the radiation has been evaluated from the electron bunch shape. The system of the light source has been optimized. The light source will be applied to the excitation of various kinds of matters and to the pump-probe experiments using the electron beam and the coherent radiation.

INTRODUCTION

The coherent radiation from a short electron bunch of a linac has continuous spectrum in a submillimeter to millimeter wavelength range at a relatively high peak-intensity. After the first observation of the coherence effect in synchrotron radiation the radiation processes have been investigated.

The peak intensity of the coherent radiation is extremely high compared with those of the other light sources. The coherent synchrotron and transition radiation light sources have been applied to absorption spectroscopy for various kinds of matters [1-4], especially for matters with relatively strong light absorbance. Recently, the absorption spectroscopy system using the coherent transition radiation from the electron beams of the L-band electron linac under relatively simple configurations has been established at Kyoto University Research Reactor Institute [5], and has been generally used for experiments.

As well as the applications as probes the high peak intensity and the short pulse shape of the radiation are expected to be used for excitation of matters and time-resolved experiments. Such applications are not performed so far.

The present work has been performed to establish the new coherent radiation light source applied to the excitation of matters and the pump-probe experiments.

COHERENT RADIATION LIGHT SOURCE

Synchrotron and transition radiation from short electron bunches of a linac becomes coherent and highly intense at wavelengths longer than the bunch length. It has a continuous spectrum in a submillimeter to millimeter wavelength range. The wavelength range of the radiation is determined by the length and the shape of the electron bunch. In general cases the wavelengths correspond to the terahertz and the lower frequencies of light. The peak intensity of the coherent radiation is extremely high compared with those of the other terahertz light sources.

The coherent synchrotron radiation is emitted as a linearly polarized, unipolar and pulsed electric field. The pulse shape of the electric filed is determined by the electron bunch shape. In our previous work investigating the electron bunch form factors from the coherent radiation spectra the bunch shape of an linac beam has been found to be approximated as triangular [6]. The light pulse has a short length corresponding to the bunch length, typically within a few picosecond in the case of the electron bunch of an S-band linac. It might be possible to use the coherent transition radiation for obtaining the similar pulsed light as well as the coherent synchrotron radiation.

The coherent radiation induces intense pulsed electric field in a matter and results in the excitation of it. In the case of the coherent radiation the electric field induced in a matter is expected to be more than 10 MV/cm.

LIGHT SOURCE SYSTEM

The new light source for the excitation of matters and the pump-probe experiments by using a 18 MeV S-band electron linac at OPU has been investigated.

OPU Electron Linac

The accelerator system of the OPU S-band linac is schematically shown in Fig. 1. Pulsed electron beams are injected from a thermionic triode gun with a cathode-grid assembly. The maximum energy, pulse lengths, the maximum pulse repetition rate of the beam are 18 MeV, 5 ns-5 μs and 500 pulses/s, respectively. The accelerated beam is bent to an underground irradiation room, where the energy spectrum of the beam is measured. In this

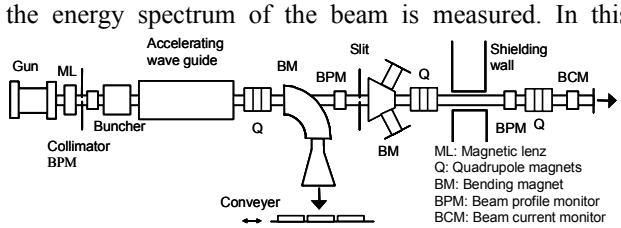

Figure 1: Schematic diagram of the OPU electron linac system.

*Work supported in part by the program of KEK for supporting accelerator research activities in universities, and KAKENHI (20360421).

#okuda@riast.osakafu-u.ac.jp

ENHANCEMENTS TO THE DIAMOND LIGHT SOURCE PRE-INJECTOR LINAC

C. Christou, S. J. Singleton and V. C. Kempson, Diamond Light Source, Oxfordshire, UK

Abstract

Modifications have been made to the Diamond pre-injector linac to improve beam stability and to increase the scope of operation of the system. New modes of operation are described and RF stability studies are presented. Operational experience is summarised, and options for future development are considered.

MODES OF OPERATION

The DLS pre-injector is a 3 GHz, 100 MeV linac delivering up to 3 nC in a bunch train of up to 1000 ns, or a single bunch of up to 1 nC. It has a bunching section and two identical accelerating structures driven by two Thales TH2100 klystrons, and a thermionic DC gun [1].

Beam from the linac is delivered through a full-energy booster to the 3 GeV storage ring. For user operation, beam is injected as required, usually topping up twice a day to the present operating level of 225 mA. During fills the linac and booster are cycled together at 5 Hz

Linac single-bunch operation has recently been incorporated into the Diamond top-up application [2] and into an automated single bunch filling routine for the storage ring, both implemented in Python. For both applications, the linac gun and booster extraction timing is set each shot so that the bunch is injected into the bucket with lowest charge relative to a programmed fill pattern. Linac bunch charge is kept constant for top-up, but is programmed during the single bunch fill to generate a smooth fill in the minimum time: high-charge bunches are first injected into empty buckets, and charge is reduced as the bucket approaches its target. Bunch charge is controlled by setting the bias on the triode gun, as illustrated in Figure 1. Top-up uses low bunch charge, whereas single bunch fill covers the entire range. Single bunch injection efficiency into the booster is 80% at low bunch charge falling to below 50% at high bunch charge. Injection efficiency studies are continuing, with attention being paid to booster chromaticity on injection [3].

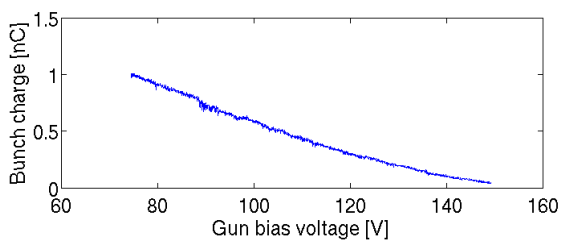

Figure 1: Single bunch charge as a function of gun bias.

Since the beginning of user operations in January 2007 most storage ring fills for user operation have used the multibunch mode of the linac, with trains of 144 buckets injected every 120 buckets over two-thirds of the ring. The 24 bucket overlap overcompensates for the 30 ns rise-time of the linac long-pulse envelope, and generates small peaks in the storage ring fill pattern [4]. The single bunch fill generates a very smooth fill, as shown in Figure 2. The smooth fill from buckets 100 to 600 is much better than that could be achieved by multibunch injection. This figure also illustrates the hybrid fill, which can be routinely generated for users on request. Hybrid fill may be generated by a multibunch two-thirds fill followed by single bunch injection, or by using the single bunch fill for the entire fill. Switching fill modes is quicker, because of the higher charge available in multibunch mode, but the automatic single bunch fill is simpler to carry out.

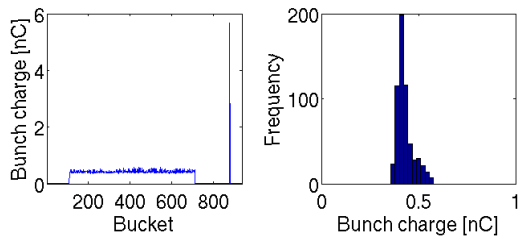

Figure 2: Hybrid fill generated using single bunch fill and histogram of bunch charge over two-thirds fill.

Long-duration tests of linac and booster reliability have been carried out in preparation for routinely offering top-up to users. Figure 3 summarises a continuous linac and booster run (with three short breaks for storage ring fills), showing a very reliable bunch charge delivered to the booster with a mean and standard deviation of 0.125 nC and 0.014 nC respectively over 24 hours.

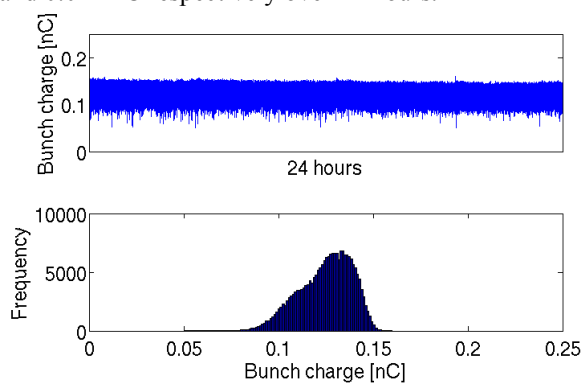

Figure 3: 24 hour run of linac and booster showing the beam delivered to the booster (top) and histogram of bunch charge (bottom).

A recent test of the complete top-up application is summarised in Table 1. At the start of top-up the gun bias was set so that the number of shots per top-up cycle was around 10 to reduce the variation in charge along the bunch train to 10% or less while minimising the

NORMAL CONDUCTING OPTIONS FOR THE UK'S NEW LIGHT SOURCE PROJECT

C. Christou, R. Bartolini, J.-H. Han, H. Huang and J. Kay
Diamond Light Source, Oxfordshire, UK

Abstract

This paper considers the design of a normal-conducting linac FEL in the context of the UK's New Light Source project. Capabilities and limitations of this approach are illustrated by reference to a 3 GeV S-band linac design. The effects of high repetition rate operation and RF jitter are considered.

THE NEW LIGHT SOURCE PROJECT

The UK's New Light Source (NLS) project [1] was launched in April 2008 to consider the scientific case and develop a conceptual design for a possible next generation light source. The outline facility design will be agreed by January 2009 following consultation with the user community throughout 2008 after which a design report and proposal for funding will be prepared for submission in October 2009.

A high (> 400 Hz) repetition rate of single pulses demands superconducting linac technology operating in continuous-wave. Normal conducting linac technology is however significantly cheaper, allowing a higher energy to be reached for a given cost. Design studies are ongoing for both normal conducting and superconducting linacs. This paper reviews the options for a normal conducting NLS design; a companion paper reviews the superconducting approach [2].

LINAC LIGHT SOURCE PROJECTS

There has been much recent interest in the use of normal conducting technology for linac FELs. Most projects in construction or development use the well-proven S-band technology used at SLAC for several decades whereas SCSS exploits C-band technology developed in the JLC(C) programme. LCLS and SCSS are scheduled for completion in 2009 [3] and 2011 [4] respectively. The study presented here considers an S-band linac for NLS, although X-band technology has not been ruled out, particularly considering possible technology developments following the decision to change the CLIC design frequency to 12 GHz [5].

NORMAL CONDUCTING TECHNOLOGY

Virtually all high-power klystrons operating today are driven by line-type modulators using a reactive pulse forming network (PFN) and a thyratron switch. The line-type modulator can be the dominant cost driver in a linac [6]. The self-terminating nature of the line-type discharge limits the modulator operation: the pulse length can only be changed by switching the connections to multiple PFNs, and the trailing edge of the pulse is usually not sharp since it depends on the discharge of multiple reactive elements. The modulator cannot drive loads of different impedances, and the thyratron has a limited operational lifetime. The overall efficiency of a line-type modulator is as low as 50% to 60% and the thyratron is a single-point of failure of the modulator.

An approach that would mitigate many of these problems in NLS is the use of an Insulated Gate Bipolar Transistor (IGBT) switch together with a solid state induction modulator: this is a stack of small pulse transformers in which the primaries of the cores are driven in parallel by separate sets of IGBT switches and capacitors operated at relatively low voltage (2-4kV). The high voltage is developed at the secondary in series [7].

Repetition rate of a line type modulator and klystron is limited by modulator charging rate or thyratron recovery time. Incorporation of an IGBT switch increases the available repetition rate from the modulator and power dissipation in the klystron is then the limiting factor.

Table 1: High Power Klystrons of Interest to NLS

Manufacturer	Thales	Toshiba	SLAC
Model	TH2155	E3730A	XL4
Waveband	S-band	S-band	X-band
Frequency	2998 MHz	2856 MHz	11.42 GHz
Peak power	45 MW	50 MW	50 MW
Efficiency	44%	45%	40%
Gain	54 dB	51 dB	50 dB
Pulse length	3.5 μs	4 μs	1.5 μs

Table 1 shows high power klystrons available in S-band and X-band. S-band klystrons already exist that separately satisfy high average and high peak power demands. The enhanced collector cooling that is provided in the former needs to be combined with a high peak power klystron, and manufacturers have indicated their readiness to supply this; repetition rates of up to 400 Hz are envisaged. A redesign of the klystron gun to reduce the arcing rate is also being discussed.

Table 2: Comparison of the DESY Type II Linac and SLAC 3 m Accelerating Structures available at 2998 MHz

Property	DESY structure	SLAC structure
Length	5.2 m	3.0 m
Shunt impedance	51.5 MΩ/m	52 MΩ/m
Attenuation	0.5 Neper	0.49 Neper
Mode	2π/3	2π/3
Q	14000	12500
Filling time	740 ns	690 ns
Number of cells	156	89

The two main types of S-band accelerating structure that are readily available are the DESY type II and SLAC 3 m ones; these structures are compared in Table 2.

SIMULATIONS ON IMPACT OF THE 3.9 GHZ RF SECTION ON THE MULTI BUNCH EMITTANCE AT FLASH

Y. Kot, DESY, Hamburg, Germany.

Abstract

In order to compensate nonlinear distortions of the longitudinal phase space a RF section operated at three times the 1.3 GHz frequency of the existing TTF cavities is foreseen in the next phase of FLASH. Four modules of a nine cell 3.9 GHz cavities will be installed right after the first accelerating module ACC1. These cavities could cause additional long-range wake fields which would affect the multi bunch (MB) beam dynamics leading to increase of the MB emittance. The MB emittance at the end of the linac is determined by the strength of the transverse wake fields in the RF system. These so called higher order modes appear after any off-axis moving bunch, which could happen either due to the cavities misalignment, or by transverse position fluctuations of the injected bunches. It is intended to damp them by means of the HOM couplers, which can reduce the damping time by factor of 10^5. The misalignment of the cavities offsets is expected to be limited by 0.5 mm rms. The paper describes the results of the simulations on the dependence of the MB emittance on cavities misalignment offsets and damping strength of the HOM couplers in the planned 3.9 GHz RF section.

INTRODUCTION

In the next phase of FLASH it is planned to install four modules of a nine cell 3,9GHz cavities right after the ACC1 at 14-19meter. These cavities would cause additional long-range wake fields which could affect the multi bunch beam dynamics leading to the increase of the multi bunch emittance.

It is transverse long-range wake fields which determine the multi bunch emittance at the end of the LINAC. They appear after any off-axis moving bunch which could happen either due to the cavities offset misalignment, or by transverse position fluctuations of the injected bunches. According to the design of the cavities setup the precision of 0.5mm rms could be achieved, whereas the fluctuations of the transverse positions of the injected bunches could be kept well below this value.

In order to damp the wake fields HOM couplers will be installed which will reduce the damping time by the factor of 10^{-5}. The MB emittance blow up is also mitigated due to the RF focussing since each cavity acts as a focussing quadrupole in both vertical and horizontal planes simultaneously. This effect could play an important role if the change of the energy per cavity is not negligible compared to the bunch energy.

Thus the resulting transverse multi bunch emittance is a subject to equilibrium between the strength of the transverse wake fields due to bunch positions offsets from the cavity axis on the one side and damping strength of the wake fields due to HOM couplers on the other side.

We have simulated the MB beam dynamics for the FLASH beam line with the new 3rd harmonic RF section. The meaning of the RF focussing for the MB dynamics at FLASH has been also investigated. The results will be shown in this paper.

THEORY AND MODEL

Formulas and Theory

The technical characteristics of both 1,3GHz and 3,9GHz cavities has been described in [3] and [1,2] respectively.

The calculations of the wake fields have been fulfilled according to the following formulas:

$$W_{\parallel}^{(m)}(s) = -\sum_n \omega_n \left(\frac{R^{(m)}}{Q}\right)_n \cos\left(\omega_n \cdot s/c\right)\exp\left(-1/\tau_n \cdot s/c\right)$$

$$W_{\perp}^{(m)}(s) = c\sum_n \left(\frac{R^{(m)}}{Q}\right)_n \sin\left(\omega_n \cdot s/c\right)\exp\left(-1/\tau_n \cdot s/c\right)$$

where $W_{\parallel}^{(m)}$ and $W_{\perp}^{(m)}$ are the longitudinal and transverse wake fields accordingly, $\omega_n = 2\pi f_n$ - the frequency of the mode, $R^{(m)}$ the impedance, Q the quality factor and τ_n the lifetime of the mode. In the simulations the lowest four passbands of the monopole (m=0), dipole (m=1) and quadrupole (m=2) modes for the longitudinal and dipole (m=1) and quadrupole (m=2) modes for the transverse wake fields has been considered.

The strength of the wake fields decays in time according to the natural mode lifetime τ_{n0}. If the external damping of the higher order modes provided, the lifetime reduces according to:

$$\tau_n \rightarrow dampingfactor \cdot \tau_{n0}$$

The energy deviation and the transverse kick of the bunch j due to the wake fields of the previous bunches can be then computed as:

$$\Delta E(s_j) = -eq\sum_{i<j} W_{\parallel}^{(0)}(s_j - s_i) - eq\sum_{i<j}\left(x_j x_i + y_j y_i\right)W_{\parallel}^{(1)} + \mathrm{K}$$

$$\vec{\theta}_j = \frac{eq}{E_j}\sum_{i<j}\left(x_i\vec{e}_x + y_i\vec{e}_y\right)W_{\perp}^{(1)}(s_j - s_i) + \ldots$$

LATTICE STUDIES FOR THE XFEL-INJECTOR

Y. Kot, V. Balandin, W. Decking, C. Gerth, N. Golubeva, and T. Limberg,
DESY, Hamburg, Germany

Abstract

The XFEL injector building has a length of 74.3 meters and is divided by 2.5m long concrete shielding wall. The section upstream the shielding wall will have a length of 42.3m and give place for the gun, accelerating module, a possible 3rd harmonic section, laser heater and the beam diagnostics section. At its end the possibility for the beam dump is foreseen so that the tuning of the beam in the injector becomes possible without any impact on the subsequent parts of the XFEL. Each of these components sets certain requirements on beam optics which may compete with each other.

Since there are two injectors foreseen for the XFEL the injector will be vertically displaced by 2.75 m from the linac. The displacement of the beam line takes place downstream the shielding over the distance of 20m by means of the so called dogleg – a combination of two four cells arcs (8 cell system). It is important there to optimize cells in such an order that the chromatic effects don't impact the beam quality noticeably. In this paper we describe the solution for the beam optics at the XFEL injector.

INTRODUCTION

The XFEL injector plays a crucial role for the beam quality along the subsequent transport of the beam through the XFEL. Therefore it is important to have the possibility for both the understanding of the beam parameters at the injector as well as for the flexible change of the beam parameters there. For the tuning and analysis of the beam parameters the section upstream the shielding wall is foreseen. At the end of this section a possibility for a separate beam dump will be given so that the tuning of the beam may proceed without any impact on the actions at the other sections of the XFEL. The section is about 42.3m long and has to give place for numerous components. They are the gun and gun diagnostics, accelerating module, 3rd harmonic RF section, laser heater, transverse deflecting structure (TDS) and the diagnostics section with four OTR monitors. Besides, a spare place of about 2.4m at the end of the section is needed in order to provide the change of the absorber body. Each of these components sets certain requirements on the beam optics, which may compete with each other. Since a very short length of the beam line of less than 40 meters for this purpose available the design of the beam optics at the injector becomes a challenging problem for the investigations.

Downstream the shielding wall the beam will be vertically displaced by 2.75m over the beam line length of 20m. Since the vertical displacement takes place one has to be cautious with the choice of the magnet arrangement there so that the optics doesn't affect the chromatic features of the beam noticeably.

We describe the possible optics solution for the XFEL injector in which these considerations and requirements of each component on the optics have been taken into account.

REQUIREMENTS ON OPTICS AT THE LASER HEATER

The purpose of the laser heater is to enhance the uncorrelated energy spread of the electron beam which would lead to the increase of the Landau damping and thus reduce the sensibility of the beam to the sources of the instabilities during the bunch acceleration and transport through the linac [1].

However not only the net value of the uncorrelated energy spread plays an important role for the effectiveness of the Landau damping but also the form of the energy distribution in the bunch. It has been found [1] that the laser beam size has to be equal or slightly larger than the transverse size of the electron beam to provide an effective Landau damping. This condition would require a reasonable matching of both laser and electron beams and thus sets constraints on the optics at the laser heater.

The possibility to suppress the microbunching instability by means of the laser heater has been discussed in [1]. The design of the laser heater for the XFEL injector has been described in [2]. It was found that the optics at the laser heater has to been chosen in such a way that the electron beam size doesn't change a lot during the transport through the undulator. Since the length of the undulator is L=0.5m the change of the beta-function along the undulator can be than roughly estimated according to the formula:

$$\Delta\beta[m] \approx -2\alpha L = -\alpha$$

The transverse beam size goes as $\sqrt{\beta}$ so that the reduction of the beta function by factor of 2 (i.e. α=0.5β) causes the change of the transverse beam size by approximately 30%. This boundary, though floating, has been proven to be a reasonable limitation on the α-function at the laser heater.

The smallest acceptable value for the beta function at the undulator is set by the condition of the stable laser beam spot size. The Rayleigh length shouldn't be shorter than the undulator length. Furthermore both beams should have the same transverse size. If one assumes the smallest possible transverse size of the laser and therefore also of the electron beam one gets for the design emittance of 1.0mm mrad that the beta function shouldn't be smaller than 7m along the undulator.

STATUS OF THE 3RD HARMONIC SYSTEMS FOR FLASH AND XFEL IN SUMMER 2008

E. Vogel[3], A. Bosotti[2], W. Decking[3], M. Dohlus[3], H. Edwards[1], E. Harms[1], M. Hoffmann[3], M. Huening[3], J. Iversen[3], K. Jensch[3], T. Khabiboulline[1], G. Kreps[3], T. Limberg[3], A. Matheisen[3], W.-D. Moeller[3], P. Pierini[2], K. Rehlich[3], A. Schmidt[3], J. Sekutowicz[3], D. Sertore[2] and W. Singer[3] for all third harmonic collaborators
[1]Fermi National Accelerator Laboratory (Fermilab), Batavia, Illinois, 60510 USA
[2]Istituto Nazionale di Fisica Nucleare (INFN), LASA, 20090 Segrate (Milano), Italy
[3]Deutsches Elektronen Synchrotron (DESY), Notkestraße 85, 22607 Hamburg, Germany

Abstract

Ultra short bunches with high peak current are required for the creation of high brilliance coherent light in the VUV and x-ray range in undulators. At the Free Electron Laser in Hamburg (FLASH) and the European x-ray free electron laser (XFEL) they are obtained by a two stage bunch compression scheme based on acceleration off the rf field crest and transverse magnetic chicanes. The deviation of the rf field's sine shape from a straight line leads to long bunch tails and reduces the peak current. This effect can be eliminated by adding a third harmonic rf system [1, 2, 3]. This paper gives an overview on the actual status of the beam dynamical examinations, as well as on the development of the third harmonic sub-systems like modules, cavities and radio frequency systems for FLASH and the XFEL. For an basic overview on the activities we refer to [3].

INTRODUCTION

At the linear accelerator based free electron lasers FLASH and XFEL bunches are generated by a normal conducting photocathode rf gun and then accelerated by a superconducting linear accelerator. While passing through undulators the bunches emit high brilliance coherent light. The emission process requires high electron peak currents and small transverse emittances. Collective effects restrict the minimum full width bunch length obtained from the photocathode rf gun. The high peak currents are obtained by compressing the bunch length in the first part of the superconducting accelerator (Fig. 1).

Accelerating the bunches off the rf field crest results in an energy chirp from the bunch head to the tail. In the bunch compressors the trajectory of the bunch head becomes longer than the trajectory of the bunch tail resulting in a compressed bunch due to the different transit time. Both the sinusoidal accelerating wave and non-linear collective effects lead to asymmetric bunches with reduced peak current and long tails. By adding a higher harmonic rf system, the voltage seen by the bunches and the collective effects may be linearised. The bunch compression becomes much more effective.

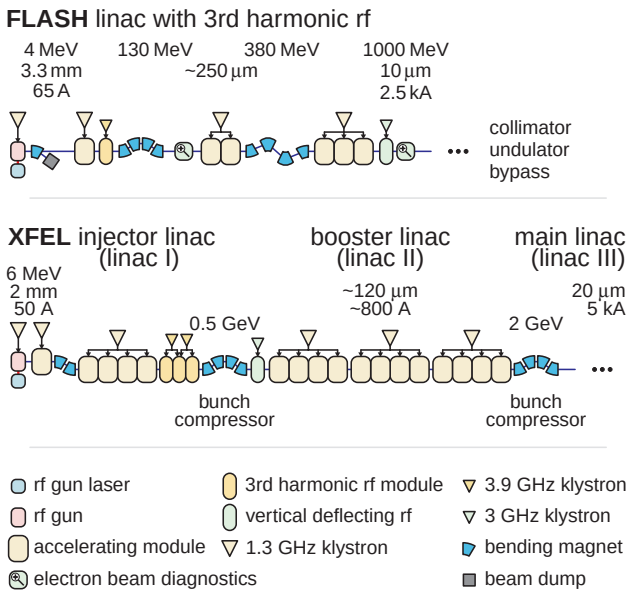

Figure 1: Sketch of the FLASH accelerator and the first part of the European XFEL accelerator.

BEAM DYNAMICS

Beam passing a third harmonic section suffers from coupler kicks, short range (intra bunch) and long range (bunch to bunch) effects. For the XFEL we decided to use a coupler arrangement where every second cavity is rotated around the cavity longitudinal axis [3, fig. 4] resulting in a transverse beam blow up in the order of 2%. The FLASH configuration or all couplers at the same side would result in a blow up by 40% and 100%, respectively. The r.m.s. of the difference between the cavity cell centre and the beam trajectory has to be below 0.3 mm for keeping the transverse blow up due to transverse wake fields below 5%. Long range effects caused by the lower frequency higher order modes (HOMs) are damped by the cavity HOM absorbers. Higher frequency HOMs can be trapped in a string of cavities with different spectra for the frequencies above 10 GHz. The effects on the beam are expected to be cured by an arrival time feedback system [4] and we can go without beam pipe HOM absorbers inside modules. Absorbers between modules should be sufficient.

NEW EXPERIMENTAL RESULTS FROM PITZ*

F. Stephan[#], G. Asova[§], J. Bähr, C. Boulware, H.J. Grabosch, M. Hänel, L. Hakobyan[$], Y. Ivanisenko, M. Khojoyan[$], M. Krasilnikov, B. Petrosyan, S. Riemann, S. Rimjaem, T. Scholz, A. Shapovalov[&], R. Spesyvtsev, L. Staykov[§], DESY, 15738 Zeuthen, Germany
K. Flöttmann, S. Lederer, DESY, 22607 Hamburg, Germany
D. Richter, BESSY, 12489 Berlin, Germany
J. Rönsch, Hamburg University, 22761 Hamburg, Germany
F. Jackson, STFC Daresbury Laboratory, United Kingdom
P. Michelato, L. Monaco, C. Pagani, D. Sertore, INFN Milano – LASA, 20090 Segrate, Italy

Abstract

The **P**hoto **I**njector **T**est facility at DESY, **Z**euthen site, (PITZ) was built to develop and optimize high brightness electron sources for Free Electron Lasers (FELs) like FLASH and the European XFEL. Last year, an electron beam with a very low transverse projected emittance of 1.26 mm mrad for 1 nC charge (100% RMS) was demonstrated [1, 2, 3]. In the shutdown last winter, a major upgrade of the facility took place where many new diagnostics elements were installed and almost all components in the beamline were repositioned. In addition, a new RF gun cavity with improved water cooling was installed and conditioned. It is the first RF gun where the surface cleaning was done with a dry-ice technique instead of high-pressure water rinsing. It showed a 10 times lower dark current emission than its precursor gun, even at cathode gradients as high as 60 MV/m. Also a new photo cathode laser system with higher bandwidth was installed, which so far has produced Gaussian laser pulses of 2.1 ps FWHM.
This contribution will summarize the transverse emittance measurements in 2007, the upgrade of the facility, dark current measurements from the new dry-ice cleaned RF gun cavity and quantum efficiency measurements of Cs_2Te photo cathodes.

INTRODUCTION

SASE-FELs for short photon wavelengths require electron sources providing particle beams with very good beam properties. Therefore, DESY is operating and continuously extending a photo injector test facility at its Zeuthen site (PITZ). It contains an 1½ cell L-band RF gun with cathode load-lock system and solenoids for space charge compensation, a laser system able to generate trains of electron pulses including temporal and transverse laser beam shaping, a booster cavity and many beam diagnostics systems for the characterization of the electron beam at different beam energies.

In the first section of this paper measurements of very low transverse emittance are summarized. These data have been taken in summer 2007 with a facility setup that was mainly unchanged since beginning of 2006. From autumn 2007 to spring 2008 a major upgrade of the facility took place and the current setup is shortly described in the second section. During the shutdown a new RF gun cavity treated with a dry-ice surface cleaning technique was commissioned at an accelerating gradient of 60 MV/m which is reported in the third section. In the fourth section recent quantum efficiency measurements of Cs_2Te photo cathodes are presented.

EMITTANCE MEASUREMENTS FROM SUMMER 2007

The transverse normalized projected emittance is of paramount importance for electron sources driving FELs. In summer 2007 it was measured at a bunch charge of 1 nC for gun cavity prototype 3.2, which was the first RF gun operated at PITZ with about 60 MV/m maximum accelerating gradient at the cathode. This cavity was cleaned with high-pressure water rinsing. Although the level of dark current at the maximum gradient was high (see details in commissioning section) this did not have a major influence on the emittance measurements when using the single slit measurement technique at a distance of 4.3 m from the photo cathode. Details of the measurement procedure and the data analysis are described in references [1, 2, 3]. An extensive experimental scan of different machine parameters resulted in an absolute minimum of the transverse normalized projected emittance for the following conditions: The gun was operated at a maximum accelerating gradient at the cathode of about 60 MV/m. The RF phases for gun and booster where set to maximum mean momentum gain. The beam momenta were 6.44 MeV/c downstream the gun and 14.5 MeV/c downstream the booster. The Cs_2Te cathode number 90.1 was used with a laser beam of about 0.36 mm rms spot size (approximate flat-top transverse shape) and an approximately flat-top temporal distribution of about 20 ps FWHM with 6-7 ps rise/fall time. The main scan parameter is the main solenoid current. A bucking magnet is always used to zero the magnetic field on the cathode. The measurement results of two different shift crews are shown in Figure 1. The repeatability is a few percent.

* This work has partly been supported by the European Community, contracts RII3-CT-2004-506008 and 011935, and by the 'Impuls- und Vernetzungsfonds' of the Helmholtz Association, contract number VH-FZ-005.
[#] Frank.Stephan@desy.de
§ on leave from INRNE, Sofia.
$ on leave from YERPHI, Yerevan.
& on leave from MEPHI, Moscow.

MIR-FEL WITH 4.5-CELL THERMIONIC RF-GUN

T. Kii#, H. Zen, K. Higasimura, R. Kinjo, K. Masuda, H. Ohgaki

Institute of Advanced Energy, Kyoto University, Gokasho, Uji, Kyoto 6110011, JAPAN

Abstract

We have constructed a compact Mid-Infrared Free Electron Laser (MIR-FEL) facility, Kyoto University FEL (KU-FEL) for advanced energy researches. The KU-FEL, consisting of an S-band thermionic RF gun, a 3 m accelerator tube and a planer undulator, aims to generate 4-13 μm tunable FEL. The most serious problem in using the thermionic RF gun for FEL facilities is unstable beam loading owing to back-streaming electrons in the RF gun. In order to overcome the problem, we have developed beamloading compensation methods realized by amplitude modulated RF and slight detuning of the resonant frequency of the RF gun. The first lasing was successfully achieved on March, 2008 at 12.4 μm and the FEL power saturation at 13.6 μm was observed on May. 2008.

INTRODUCTION

A tunable and coherent light source in the MIR (mid-infrared) range is useful tool for a research on molecular dynamics, designing a functional material, which are key techniques for "sustainable energy science". Thus in the Institute of Advanced Energy, Kyoto University, we have developed a compact MIR-FEL (Free Electron Laser) facility[1] with a thermionic RF gun. A use of the thermionic RF gun is aimed to realize a cost effective, compact, easily operable FEL facility.

Facility Design

The FEL system has been constructed in the Laboratory for Photon and Charged Particle Research, Institute of Advanced Energy, Kyoto University. Schematic drawing of the FEL facility is shown in Fig. 1. Total area of the facility is 350 m^2 including klystron gallery, control room and experimental hall. In order to reduce a construction cost, height of a radiation shielding wall made of concrete is reduced to 2.5 m and stairs are used to access to the accelerator room instead of a shielding door. Part of the shielding wall consists of cubic concrete blocks of 1 m^3 which can be moved to install large devices in the accelerator room. The KU-FEL was constructed in 2006[2] and commissioning was started in Dec. 2007.

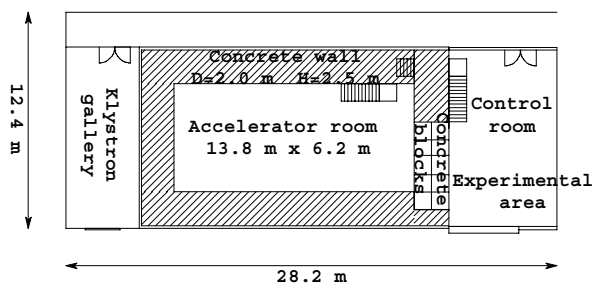

Figure 1: Schematic drawing of the KU-FEL facility.

#kii@iae.kyoto-u.ac.jp

KU-FEL System

The FEL system consists of an S-band 4.5 cell thermionic RF gun driven by a 10 MW klystron, a 3 m travelling wave accelerator structure driven by a 20 MW klystron, beam transport system, a Halbach type undulator of 1.6 m, and an optical resonator. Figure 2 shows a schematic drawing of the system. The FEL wavelength of from 4 to 13 μm is expected with electron-beam energy of from 20 to 40 MeV.

A thermionic RF gun is a key device for constructing economical and compact FEL facility, because it does not need any expensive multi-bunched stable short pulsed UV laser for a photocathode RF gun or additional beam bunching system for a DC RF gun. However, a serious problem of back-bombardment limits macro-pulse duration. The back-bombardment problem is described as follows. Some electrons which escape from acceleration phase change their direction in the RF gun. And the cathode surface temperature increases due to bombardment of the back-streaming electrons. As a result, the number of extracted electron increases, and the beam loading increases. Then the beam energy decreases. In case for our 4.5 cell thermionic RF gun, the maximum pulse duration which can pass the 'dog-leg' section shown in Fig. 2 was less than 1 μs, when the cathode temperature was set to extract the electron beam more than 100 mA at the exit of the 'dog-leg' section.

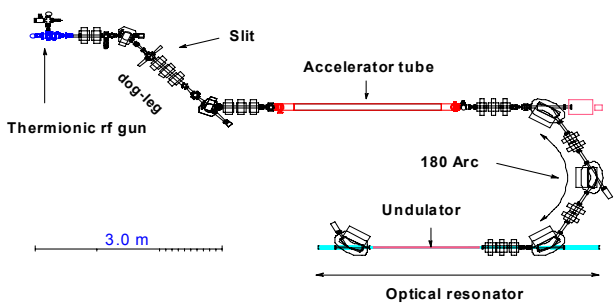

Figure 2: Layout of KU-FEL system.

BEAMLOADING COMPENSATION

In case of a low-gain resonator linac FEL, which consists of an undulator and a couple of mirrors, an

STATUS OF THE LINAC-800 CONSTRUCTION AT JINR

N.I. Balalykin, V.V. Kobets, A.G. Kobets, I.N. Meshkov, V.F. Minashkin, G.I. Sidorov,
V.G. Shabratov, G.D. Shirkov, G.V. Trubnikov
JINR, Moscow region, 141980, Dubna, Russia

Abstract

800 MeV electron linac (LINAC-800) is under construction at JINR. It will be used as a driver for Volume FEL and as a test bench for commissioning of elements of the ILC. Presently the electron injector is commissioned and the electron beam of 50 keV of the energy at current of about 15 mA was obtained. The results of the injector operation at nominal parameters (400 keV, 300 mA) and commissioning of the first accelerating section at 20 MeV are discussed.

THE LINAK-800 PROJEKT

The LINAC-800 project is being under development at the JINR, Dubna, Russia. It is based on an accelerator facility presented to JINR by the NIKHEF, Amsterdam.

Project will be accomplished with the construction of a complex of free electron lasers covering continuously the spectrum from far infrared down to ultraviolet (of about 150 nm) [1]. The far-infrared coherent source will cover continuously the submillimeter wavelength range.

Realization of this project will not require a significant modification of the JINR infrastructure. In Table 1 we present a summary of the radiation properties from coherent radiation sources being planned to build in project. Notations G1-G4 refer to the FEL oscillators, and FIR stands for the far-infrared coherent source.

ACCELERATOR LINAC-800

The electron beam with necessary parameters for the Free Electron Laser will be generated with the electron linac, which is a modified version of the Medium Energy Accelerator (MEA) transferred to JINR from NIKHEF[2]. The energy of electrons at the linac exit is 800 MeV and peak current of 30-60 A, with subharmonic buncher of the frequency of 476 MHz, a buncher at the frequency of 2856 MHz and 24 acceleration sections, which are combined in 14 acceleration stations (A00 – A13). To operate FEL, one needs an injector with a special subharmonic prebuncher. Such an injector has to be developed at JINR.

MEA Injector

To start the linac operation and test its condition, we plan to use the MEA injector consisting of an electron gun, chopper, prebuncher and buncher [2].

The electron gun (Table 2) has a dispenser thermocathode with the diameter of 8 mm. Its heater current is 15 A at the heater filament voltage of 12 V. The cathode lifetime is of the order of 20 thousand hours. The gun optics elements contain Pierce electrode at the cathode potential, control electrode and acceleration tube, which has 15 diaphragms forming homogeneous acceleration field. Linear potential distribution along the tube is provided with the divider, the voltage between two neighbour diaphragms is of the order of 30 kV. One can "close" the gun by applying the voltage of –150 V between the cathode and control electrode. The gun is operated in a pulsed mode by applying voltage pulses of +6 kV amplitude between the cathode and control electrode.

Table 1: Summary of Radiation Properties from Coherent Radiation Sources in Project

	FIR	G1	G2	G3	G4
Radiation wavelength [μm]	150-1000	20-150	50-30	1-6	0.15-1.2
Peak output power, [MW]	10-100	1-5	1-5	3-15	10-20
Micropulse energy, [μJ]	500	50-200	25-100	25-100	50-100
Micropulse duration (FWHM),[ps]	5-10	10-30	10	10	3-5
Spectrum bandwidth (FWHM),[%]		0.2-0.4	0.6	0.6	0.6
Micropulse repetition rate, [MHz]			19.8/ 39.7/ 59.5		
Macropulse duration, [μs]			5-10		
Repetition rate, [Hz]			1-100		
Average output power (max.), [W]	10-50		0.2-1		

Table 2: The Electron Gun Parameters

Scheme	Triode
Type of cathode: Diameter, [mm] Heater: voltage, [V] current, [A]	Dispenser 8 0-12 0-15
Electron energy, [keV]	400
Peak current, [A]	0.45
Cathode current stability	$1.5 \cdot 10^{-3}$
Beam diameter, [mm]	1.5
Normalized emittance (1σ), [π·mm·mrad]	8

LINEAR ACCELERATOR FOR THE PSI-XFEL FEL3 BEAMLINE

Y. Kim*, A. Adelmann, B. Beutner, M. Dehler, R. Ganter, R. Ischebeck, T. Garvey
M. Pedrozzi, J.-Y. Raguin, S. Reiche, L. Rivkin, V. Schlott, A. Streun, and A. F. Wrulich
Paul Scherrer Institute, CH-5232 Villigen PSI, Switzerland

Abstract

To supply coherent, ultra-bright, and ultra-short XFEL photon beams covering a wide wavelength range from 0.1 nm to 7 nm, three FEL beamlines will be constructed in the planned PSI-XFEL facility. The FEL1 beamline will use a 6 GeV normal conducting S-band linac to generate hard X-rays from 0.1 nm to 0.7 nm, while the FEL2 beamline will use a 3.4 GeV linac to supply X-rays from 0.7 nm to 2.8 nm. However, the FEL3 beamline is designed to supply spatially as well as temporally coherent soft X-rays from 1.8 nm to 7 nm with the High-order Harmonic Generation (HHG) based seeded High Gain Harmonic Generation (HGHG) scheme. In this paper, we describe an injector, bunch compressors, beam diagnostic sections, and linacs for the FEL3 beamline, which is based on a 2.5 cell S-band RF gun and a 2.1 GeV linac.

INTRODUCTION

Since 2003, the Paul Scherrer Institute (PSI) has been developing two key technologies to realize the advanced and compact PSI-XFEL facility within about 930 m long space [1]. One is the high voltage pulser based advanced Low Emittance Gun (LEG), and the other is the Cryogenic Permanent Magnet in-vacuum Undulator (CPMU) with a small gap of about 5 mm and a short period of about 15 mm [2]. A prototype CPMU will be installed at the Swiss Light Source in 2011. Since required slice beam parameters for FEL1 and FEL2 beamlines are challenging, we have been concentrating our efforts to develop the advanced LEG [1]. In 2007, a 500 kV pulser based LEG test facility was constructed at PSI, and recently, we have performed various machine studies there [1–3]. In parallel, a 250 MeV injector test facility will be constructed by the end of 2009 to develop advanced accelerator technologies for the future 6 GeV PSI-XFEL project [1, 4]. In the first phase of the 250 MeV injector test facility, a CTF3 RF gun based photoinjector will be tested, and in its second phase, a 1 MV pulser based advanced LEG will be tested. Additionally, an upgrade of the HHG based seeding with a CPMU in the 250 MeV injector test facility is under discussion. To saturate the FEL3 beamline effectively, a low slice energy spread is more important than a low slice beam emittance. Due to a much lower overall bunch length compression factor, the CTF3 RF gun is expected to supply a lower slice energy spread than the advanced LEG. Therefore the RF gun will be used as a dedicated gun to drive the FEL3 beamline. However, the advanced LEG will be used to drive the FEL1 and FEL2 beamlines, where a low slice emittance is the most critical beam parameter to get saturation with 60 m long undulators. In this paper, we describe the CTF3 RF gun based linac to drive the PSI-XFEL FEL3 beamline.

* Mail : Yujong.Kim@PSI.ch

OPTIMIZATION OF DRIVING LINAC

From our recent thermal emittance measurements at the LEG test facility, we find that the thermal emittance of a diamond turned copper cathode is about 0.2 μm for an rms laser spotsize on the cathode of about 330 μm at 40 MV/m [2, 3]. To optimize the CTF3 RF gun based injector, we used the measured value. Since the thermal emittance depends on the rms laser spotsize and the gradient on the cathode by the Schottky effect, the thermal emittance in the CTF3 RF gun was re-scaled to about 0.2 μm by choosing a smaller rms laser spotsize of about 270 μm at 100 MV/m [2, 4]. To compensate the projected emittance growth due to the linear space charge force in a drift space between the gun and the booster linac and to satisfy two special conditions for the invariant envelope matching in the booster, we have optimized the gradient of the RF gun, the magnetic field of the main gun solenoid, and gradients of the booster linac [4,5]. Details on the optimization of the CTF3 RF gun based injector are described in reference [4], and its optimized beam parameters are summarized in Table 1 where all emittances are normalized rms values, and all energy spreads are rms ones. According to ASTRA simulations, the optimized normalized projected and central slice emittance before the first bunch compressor (BC1) are about 0.35 μm and 0.32 μm, respectively.

Since the initial peak current from the RF gun is about 22 A, the peak current is increased to about 1.6 kA by two bunch compressors (BC1 and BC2) as shown in Figs. 1, 2, 3, and 4(middle left) and as summarized in Table 1. To minimize the projected and slice emittance growth due to the space charge forces, the bunch length is initially compressed from 840 μm to 55 μm by BC1 at 256 MeV. Then the beam is accelerated to a much higher beam energy of about 1469 MeV, where the bunch length is re-compressed down to 14 μm by BC2. To control the emittance growth at BC1 due to Coherent Synchrotron Radiation (CSR), we used special optimization methods which are described in references [4, 6]. Additionally, to control the horizontal emittance growth at BC2 due to CSR, we chose a higher horizontal beta-function of about 65 m in front of BC2 and a strong focusing horizontal beta-function in BC2 to make a beam waist at the end of the fourth dipole as shown in Fig. 2(bottom) [6]. Since the projected energy spread is

SUPERCONDUCTING OPTIONS FOR THE UK'S NEW LIGHT SOURCE PROJECT

P.A.McIntosh#, R.Bate, C.D.Beard, D.M.Dykes and S.Pattalwar, STFC Daresbury Laboratory, Warrington, WA4 4AD, UK

Abstract

The UK's New Light Source (NLS) project was officially launched on April 11th 2008 [1], which will be based on advanced conventional and free electron lasers, with unique and world leading capabilities. User consultation exercises have already been initiated to determine the fundamental photon output requirements for such a machine. In order to match possible requirements for high repetition rates (> 1 kHz), a series of Superconducting RF (SRF) linac options have been investigated, reflecting varied beam loading conditions and possible beam energy scenarios.

INTRODUCTION

Superconducting RF (SRF) is becoming the technology of choice for the next generation of particle accelerators, both for basic energy science programmes such as conventional synchrotron radiation sources (i.e. diamond, TLS, SSRF and SOLEIL), and also for high energy physics collider machines (i.e. LHC and ILC). This paper assesses possible existing SRF cryomodule design solutions for a number of SRF linac based accelerators that have been developed specifically for FEL applications around the world; which include single-pass (XFEL and BESSY-FEL), recirculating (CEBAF) and energy recovery (ALICE) configurations. A companion paper deals with alternative normal conducting linac solutions for NLS [2].

The design requirements for an SRF linac differ for every application, as typically for single pass configurations, beam-loading is relatively weak and RF infrastructure costs are not as significant compared to more heavily beam-loaded linacs. It then becomes more cost effective to recirculate and/or to remove the beam-loading component completely by operating in energy-recovery mode. Dynamic RF cryogenic loads will typically dominate for these types of linacs and so considerable cost savings can also be gained using multi-pass schemes to attain higher energies. A recirculating option is also being investigated for NLS in order to assess potential capital and operational cost savings.

CEBAF UPGRADE CRYOMODULE

A series of three cryomodules have been constructed as part of JLab's efforts to increase CEBAF's availability and reliability. These provide additional acceleration for the FEL and produce prototypical cryomodules for the 12 GeV Upgrade. The first two constructed were based on the initial "Upgrade Cryomodule" design [3,4]. Both containing 7-cell cavities based on the original CEBAF cavity cell shape operating at 1.5 GHz, with a design expectation of > 70 MeV of acceleration. The third cryomodule, dubbed "Renascence," incorporates several design changes in order to provide more than the 108 MeV capability required for the 12 GeV upgrade of CEBAF [5] (see Figure 1).

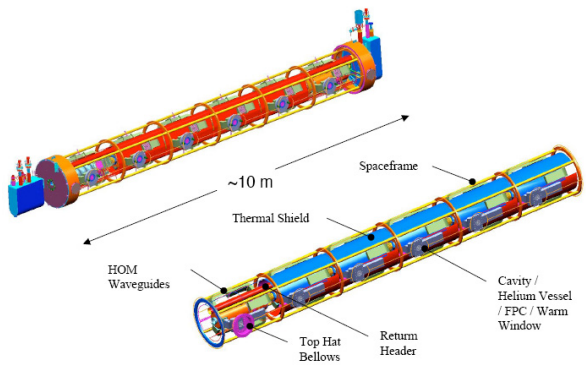

Figure 1: JLab Renascence Cryomodule.

XFEL CRYOMODULE

The XFEL Cryomodule consists of eight TESLA cavities in a string with a large helium gas return pipe as the backbone of the structure which the cavities are supported from (see Figure 2). Optimisation of the cryomodule design has been taken place to develop the module capable of reaching nearly 280 MV of acceleration, fed by a MW class multibeam klystron. In order to minimise the cryogenic load, XFEL is pulsed with a 1% duty factor to achieve a final operating energy of 20 GeV [6].

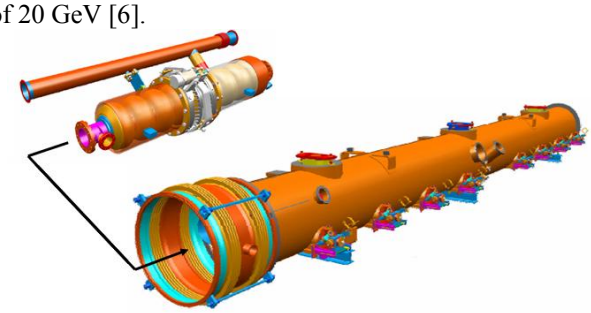

Figure 2: XFEL Cryomodule.

BESSY-FEL CRYOMODULE

The TESLA/XFEL cavity and cryomodule technology was developed for pulsed operation, although most of the system is equally suited for CW mode. There are a number of modifications that must be implemented to

#p.a.mcintosh@dl.ac.uk

HIGH REPETITION RATE ELECTRON INJECTORS FOR FEL-BASED NEXT GENERATION LIGHT SOURCES

B.L. Militsyn*, C.D. Beard, J.W. McKenzie, STFC Daresbury Laboratory, Warrington, UK.

Abstract

Several laboratories concentrate their efforts on the development of high repetition rate FEL-based next generation light sources. One particular concept under development at STFC Daresbury Laboratory specifies high brightness electron bunches with a charge of 0.2 nC which arrive with a repetition rate of up to 1 MHz. As emittance of the bunches should not exceed 1 mm·mrad, traditional grid modulated thermionic injectors, similar to the ones used at ELBE or FELIX, may not be used. We consider three options of high repetition rate injectors based on photocathode guns - a high voltage DC gun, a 3½-cell superconducting RF gun and a normal conducting VHF gun, recently proposed at LBNL. We analyse practical injector schemes for all three guns and provide the results of beam dynamic simulations. We also discuss the photocathodes which may be used in each gun, as this critical component defines achievable beam parameters and operational efficiency of the injectors.

INTRODUCTION

High brightness electron beams which are required for the operation of next generation light source may be delivered by three types of electron injectors – a high voltage DC photocathode gun, a very high frequency NCRF gun and a SRF gun. The first two options deliver relatively low energy (500-750 keV) beams and require additional velocity bunching and acceleration with a booster to an energy of 10 MeV in order to inject into the main linac. A SRF gun delivers beams with the required energy without additional acceleration. However, this leads to less flexibility in emittance compensation at different bunch charges. We consider the injectors for operation in CW mode with high beam repetition rate with a bunch charge of 200 pC as is the case for the UK's New Light Source (NLS) project [1].

Simulations

Beam dynamic simulations have been carried out for the three guns considered using ASTRA through the injector system to 10 MeV, then through the first module of the main linac to 120 MeV. Initial thermal emittance was included in all the simulations.

The main linac module consists of eight 9-cell TESLA-type 1.3 GHz superconducting cavities. All cavities except the first have been set to provide an average accelerating gradient of 17 MV/m and a phase of -20° to provide a beam with the necessary longitudinal phase space profile for the bunch compression system. There are two quadropoles to match the beam from the injector into the main linac. The injector parameters were optimised using a multi-objective genetic algorithm with a non-dominated sorting approach.

*b.l.militsyn@dl.ac.uk

HIGH VOLTAGE DC GUN

High voltage DC guns with GaAs photocathodes illuminated with laser light of wavelength 532 nm are used at a number of laboratories worldwide to feed energy recovery linac (ERL) based FELs. These include TJNAF [2] and Daresbury Laboratory [3]. An extra high voltage gun is under development at Cornell University [4]. Originally designed for operation at high (up to 100 mA) average currents, DC guns may be relatively easily adopted for operation at low (typically less than 1 mA) currents specific for NLS.

One disadvantage of DC guns is that the field strength on the cathode is restricted to 10-12 MV/m in order to minimise field emission. This rules out obtaining high emission current density and limits the minimum beam size at given bunch charges. However, the low energy spread of emitted electrons from GaAs photocathodes allows high brightness beams to be produced.

GaAs based photocathodes require XHV vacuum conditions to avoid surface contamination which restricts the cathode lifetime. Under ideal vacuum conditions the operational life time is defined by ion back-bombardment, which is proportional to the total extracted charge. Experiments have shown that the maximum charge extracted does not exceed a few hundred coulombs [5] which means that for an average current of 0.2 mA the operational life time will be at a level of 1–2 months. This is acceptable as modern guns are equipped with integrated load-lock photocathode preparation facilities [6] that allow replacement of the photocathode within half an hour and reduce the possibilities of vacuum contamination.

Alkali photocathodes operating in visible light are more stable to vacuum contaminations than GaAs [7]. For example, their lifetime in the presence of oxygen is two orders of magnitude higher than GaAs. However, their resistance to ion back-bombardment is not known, and investigation of their operation in DC photocathode guns is now in progress at Daresbury.

Simulations

A 500 keV DC electron gun with a focussing electrode was modelled in CST Studio/POISSON [8] and the on-axis field map was used as an input to ASTRA. The initial laser pulse used has a 4 mm diameter flat-top transverse profile and a 20 ps flat-top longitudinal profile.

DC guns provide electron bunches with a temporal profile similar to that of the initial laser pulse but quickly

DEVELOPMENT OF A BEAM LOSS MONITOR SYSTEM FOR THE LCLS UNDULATOR BEAMLINE*

W. Berg#, J. C. Dooling, A. Pietryla, and B.-X. Yang, Advanced Photon Source,
Argonne National Laboratory, Argonne, IL 60439 USA
H.-D. Nuhn, Linac Coherent Light Source, Stanford Linear Accelerator Center,
Menlo Park, CA 94025 USA

Abstract

A beam loss monitor (BLM) system based on the detection of Cerenkov radiation has been developed at the Advanced Photon Source (APS) for the Linear Coherent Light Source (LCLS) free-electron laser (FEL). The electron beam will vary in energy from 4.6 to 13.6 GeV with a bunch charge of 0.2 to 1.0 nC and a maximum repetition rate of 120 Hz. In order to limit radiation-induced demagnetization of the undulator permanent magnets, the BLM will provide beam-loss threshold detection as part of the Machine Protection System (MPS). The detector incorporates a large-volume (30 cm^3) fused-silica Cerenkov radiator coupled to a photo-multiplier tube (PMT). The output of the PMT is conditioned locally by a charge amplifier and then digitized at the front end of the MPS electronics. During commissioning, the device will be calibrated by inserting a 1-micron aluminum foil into the beam, upstream of the undulator magnets. Tests of a prototype BLM system showed that the detector and electronics are functional. Initial results from computer simulations support the proposed calibration scheme and indicate of the need for a dense population of BLM devices.

INTRODUCTION

APS is developing a beam loss monitor detector as a component of the LCLS Machine Protection System. The BLM is intended to protect the FEL undulator magnets from potential damage resulting from localized and distributed electron beam losses. Detection of a loss event above threshold will limit the beam pulse rate. A secondary usage of the BLM system is to track and archive the radiation dose. The data will be analyzed for correlation to any observed demagnetization or damage in the undulator magnets.

Initially, five detector modules will be distributed throughout the length of the 33 undulator magnets. Calibration of the system will be based on computer simulation using MARS [1, 2] and empirically verified during machine commissioning. Some of the relevant specifications of the electron beam are listed in Table 1.

SYSTEM OVERVIEW

Electron beam loss is measured by collecting Cerenkov radiation generated in a quartz radiator from a high-energy electron shower. The Cerenkov light propagates through the radiator to the UV glass entrance window (185-850 nm) of a single PMT for detection. The PMT output is conditioned locally by an interface module (IM) incorporating a charge amplifier. The amplifier integrates the PMT charge output pulse and converts the signal to a voltage pulse. The output of the amplifier is transmitted over a coaxial line to the MPS instrumentation racks, where signal filtering and a/d conversion is performed. Further signal processing, distribution, threshold detection, and system validation is handled by the MPS.

Table 1: Electron Beam Specifications

Beam Parameter	Value
Max. repetition rate	120 Hz
Beam charge	0.2 - 1.0 nC
Normalized emittance	2.0 - 3.0 μm rad
Beam energy	4.6 - 13.6 GeV
FWHM bunch duration	0.25 - 0.48 ps

BEAM LOSS DETECTOR

The detector design shown in Fig 1 is conceptually derived from a design for the PEP II B-Factory at SLAC [3]. A quartz Cerenkov radiator was chosen over conventional scintillation materials for better immunity to scintillation effects from the high-power x-ray beam emanating from the undulator. The radiator is cut from a single boule of synthetic crystalline quartz. Military-grade fused silica (MIL-G-174B) is used to limit impurities that may result in premature browning of the material from radiation exposure. The tuning fork geometry was chosen so the radiator would cover the surface area of the

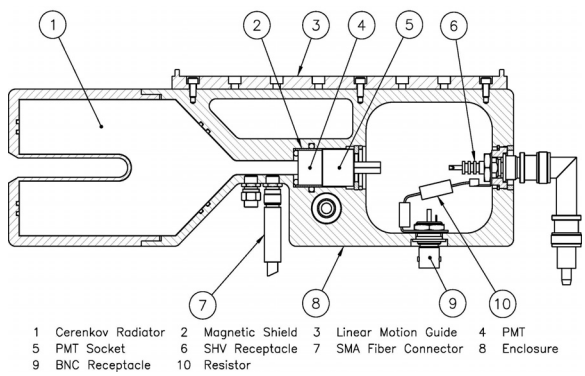

Figure 1: Cross section view of the BLM detector configuration with the component call outs.

*Work supported by U.S. DOE, Office of Science, Office of Basic Energy Sciences, under contract number DE-AC02-06CHI11357.
#berg@aps.anl.gov

THE NPS-FEL INJECTOR UPGRADE*

J.W. Lewellen#, W.B. Colson, S.P. Niles, Naval Postgraduate School, Monterey, CA
W.S. Graves, Massachusetts Institute of Technology, Cambridge, MA
T.L. Grimm, A.E. Bogle, Niowave, Inc., Lansing, MI
T.I. Smith, Stanford University, Stanford, CA

Abstract

The Naval Postgraduate School (NPS) has begun the design and assembly of the NPS Free-Electron Laser (NPS-FEL). As part of this effort, the original DC gun-based injector system from the Stanford Superconducting Accelerator has been moved to NPS and is being refurbished and upgraded to operate as a photoinjector. Design work has begun on a new, SRF, quarter-wave resonator based cavity that can serve as either an energy booster or photocathode gun.

The overall NPS-FEL design parameters are for 40-MeV beam energy, 1 nC bunch charge, and 1 mA average beam current, built as an energy-recovery linac in its final configuration [1]. As we move towards this goal, the injector system will be incrementally upgraded to add photocathode capability, have a higher final beam energy, and improve the beam brightness, to meet the needs of the overall experimental program.

OVERVIEW

The NPS-FEL is based around key components from the Stanford Superconducting Accelerator (SCA). These include:

- two, Stanford/Rossendorf cryomodules, each of which contains two, TESLA-type 9-cell 1.3-GHz cavities;
- four, 10-kW 1.3-GHz CW klystrons;
- a 240-kV gridded DC thermionic injector, with subharmonic buncher;
- the FIREFLY electromagnetic undulator; and
- assorted power supplies and magnets.

At present, the 240-kV SCA injector has been moved to NPS and is being prepared for beam in a temporary facility. This will serve as a platform for initial experiments while the main NPS-FEL vault is being constructed.

The nominal voltage gain in the TESLA structures is 10 MV per structure. The structures are matched for β~1, so injecting a 240-kV beam (β~0.73) results in significant phase slip and consequent reduction of maximum beam energy, as was observed at the SCA [2]. An injection voltage of 1.5 MV (β~0.97) will significantly reduce the phase slip during injection into the first linac structure, increasing final voltage and probably also helping to preserve beam quality. Higher injection beam energies are also desirable from the standpoint of constructing ERL return-loop beam merges.

* Funding for this work was provided by the Office of Naval Research, and the High-Energy Laser Joint Technology Office
# jwlewell@nps.edu

Also, while reliable and robust, the gridded DC injector places limits on both the charge per bunch that can be extracted, and on the quality of the beam produced.

For these reasons, we intend to gradually upgrade the NPS-FEL injector system, including diagnostics, from the original 240-kV DC gun to a superconducting RF photoinjector capable of generating nC bunches at 1.5 MeV (kinetic), with good transverse beam quality.

The incremental upgrade process will also allow us to continually perform experiments of interest in low-energy beam transport and cathode characterization.

DC GUN

The original SCA injector beam source is a 2-stage, 240-kV DC gun with a Pierce-type geometry and gridded cathode, shown schematically in Figure 1.

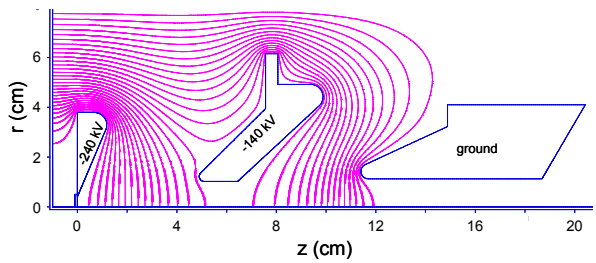

Figure 1: SCA DC-gun electrode geometry and equipotentials.

In the nominal configuration, with a potential difference of 100 kV between the cathode and first anode, the gradient at the cathode center is ~ 1.4 MV/m. The maximum radius of the cathode is 4mm, defined by the inner radius of the Pierce-type electrode ring.

Initial Configuration

As installed in the SCA, the gun was followed by a 260-MHz prebuncher and series of focusing solenoids, with approximately 3m from the cathode to the entrance of the first TESLA-type cavity. To configure the line as a photoinjector, the first solenoid lens and prebuncher will be moved downstream by approximately 13 cm (5") to install a laser injection port. For the initial series of experiments, the prebuncher will be removed and replaced with diagnostics, such as screens and slits for emittance measurement.

The first drive laser will be a Continuum Minilite-II Q-switched Nd:YAG laser [3]. This laser has a maximum repetition rate of 15 Hz, and a relatively long (relative to the RF period of the linac) pulse duration of ~ 5 ns (FWHM). The laser is appropriate for an initial series of

GENERATION OF FEMTOSECOND BUNCH TRAINS USING A LONGITUDINAL-TO-TRANSVERSE PHASE SPACE EXCHANGE TECHNIQUE*

Yin-e Sun[1], Philippe Piot[1,2]
[1]Accelerator Physics Center, Fermi National Accelerator Laboratory, Batavia IL 60510, USA
[2] Department of Physics, Northern Illinois University, DeKalb, IL 60115, USA

Abstract

We demonstrate analytically and via numerical simulations, how a longitudinal-to-transverse phase space manipulation can be used to produce a train of femtosecond electron bunches. The technique uses an incoming transversely-modulated electron beam obtained via destructive (e.g. using a multislits mask) methods. A transverse-to-longitudinal exchanger is used to map this transverse modulation into a temporal modulation. Limitation of the proposed method and scalability to the femtosecond regime are analyzed analytically and with the help of numerical simulation. Finally, a proof-of-principle experiment is discussed in the context of the Fermilab's A0 photoinjector.

INTRODUCTION

Modern applications of the accelerator often call for certain phase space distribution which sometimes can be achieved from the phase space manipulation within one or two degrees of freedom. For example, the production of comb bunches, i.e. a bunch consisting of a train of microbunches, could open the path toward compact light source operating in the super-radiant regime at a wavelength comparable or larger than the typical density modulation. The generation of such beams by shaping the photocathode drive laser of a photoemission electron source were explored via numerical simulations [1, 2]. An alternative method using an interceptive mask located in a dispersive section was experimentally demonstrated [3]. Each of these methods has its limitations: the method based on shaping the photocathode drive laser distribution is prone to space-charge effects which are prominent at low energy and wash out the impressed modulation; the other techniques have limited tunability. In this paper, we present a more general technique for tailoring the current profile to follow certain distribution: first the transverse beam profile is modulated using a mask in the beamline, then beam goes through a longitudinal-to-transverse phase space exchange [4, 5, 6], resulting in a longitudinally modulated beam.

* Work supported by by the Fermi Research Alliance, LLC under Contract No. DE-AC02-07CH11359 with the U.S. Department of Energy and by Northern Illinois University under Contract No. DE-AC02-76CH00300 with the U.S. Department of Energy.

THEORETICAL BACKGROUND

Our method is illustrated in Fig. 1: an incoming electron bunch is transversely intercepted by a mask with transmission function $T(x, y)$. The mask can have different patterns for various desired beam current profiles. In order to generate the comb bunches, we use a plate with multi vertical slits located upstream of an emittance exchanger beamline. The exchanger beamline consists of a dipole mode rf cavity flanked by two identical doglegs [5, 6]. The beam horizontal projection is mapped into the longitudinal (temporal) current density profile at the end of the emittance exchanger.

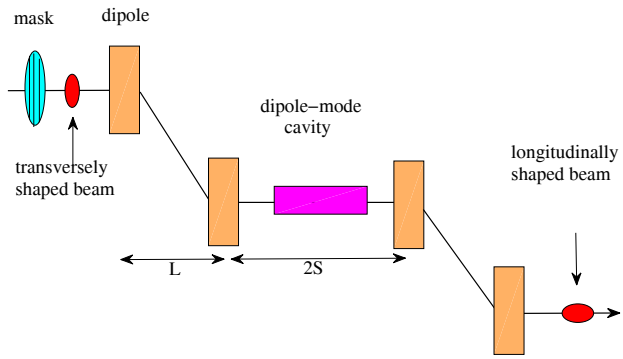

Figure 1: Overview of the proposed technique to produce relativistic electron bunch with arbitrary current profile.

A simple model based on the thin lens approximation for the transfer matrix associated to the dipole and cavity can be elaborated to give insights on the technique. In (x, x′, z, δ) phase space, the transfer matrix of a dogleg is

$$M_D = \begin{pmatrix} 1 & L & 0 & -L\alpha \\ 0 & 1 & 0 & 0 \\ 0 & -L\alpha & 1 & L\alpha^2 \\ 0 & 0 & 0 & 1 \end{pmatrix}, \quad (1)$$

where L is the drift distance between the two dipoles, and α is the bending angle. The matrix associated to a dipole-mode cavity with strength k is

$$M_C = \begin{pmatrix} 1 & 0 & 0 & 0 \\ 0 & 1 & k & 0 \\ 0 & 0 & 1 & 0 \\ k & 0 & 0 & 1 \end{pmatrix}. \quad (2)$$

LINAC DESIGN FOR AN ARRAY OF SOFT X-RAY FREE ELECTRON LASERS*

A.A. Zholents#, E. Kur, G. Penn, Ji Qiang, M. Venturini, R. P. Wells, LBNL, Berkeley, CA 94720, U.S.A.

Abstract

The design of the linac delivering electron bunches into ten independent soft x-ray free electron lasers (FELs) producing light at 1 nm and longer wavelengths is presented. The bunch repetition rate in the linac is 1 MHz and 100 kHz in each of ten FEL beam lines. Various issues regarding machine layout and lattice, bunch compression, collimation, and the beam switch yard are discussed. Particular attention is given to collective effects. A demanding goal is to preserve both a low beam slice emittance and low slice energy spread during acceleration, bunch compression and distribution of the electron bunches into the array of FEL beamlines. Detailed studies of the effect of the electron beam microbunching caused by longitudinal space-charge forces and coherent synchrotron radiation (CSR) have been carried out and their results are presented.

LATTICE AND DESIGN PARAMETRS

The accelerator is schematically shown in Figure 1. It consists of an injector, a laser heater, a bunch compressor, two main linacs, a harmonic linearizer linac, and a beam switch yard (spreader) into ten FELs (not shown).

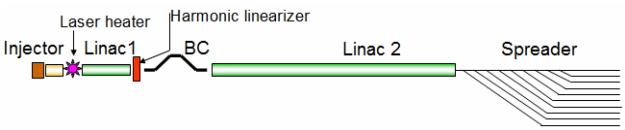

Figure 1: A schematic of the accelerator. Elements of the machine include the injector, laser heater, first linac, harmonic linearizer, bunch compressor, second linac, and spreader. The entire length of the machine is ~ 650 m.

The electron beam energy after injector at the entrance of the laser heater (LH) is ~ 40 MeV and the peak current is ~ 70A. The electron peak current after bunch compressor (BC), located behind the first linac (L1) and harmonic linearizer (HL) at a ~ 250 MeV beam energy point, is ~ 1 kA. The requirement for tunability of FELs outputs using APPLE-II undulator with adjustable helicity, in particular the FELs covering wavelengths from 1.5 nm to 1 nm, largely determines the lowest final beam energy ~ 2.4 GeV at the exit of the second linac (L2). However, surprisingly, this energy only weakly depends on a size of a minimal gap in APPLE-II undulator [1] (see Figure 2).

According to the user requirements the accelerator must accommodate with sufficient flexibility three operation modes depending on the x-ray pulse length, i.e the long pulse from 500 fs to 100 fs, the medium pulse from 100 fs to 10 fs and the short pulse of 10 fs and shorter. Because of a limited space, only the long pulse option requiring the long electron bunch is discussed here in detail. Other important electron beam parameters include the normalized slice electron beam emittance < 1 μm and the slice rms energy spread ~ 100 keV.

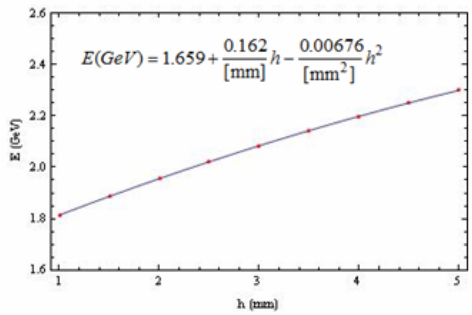

Figure 2: The electron beam energy that supports production of the x-rays within the range of wave lengths from 1 nm to 1.5 nm as a function of the size of the beam-stay-clear gap *h* in APPLE-II undulator.

Figure 3 shows one plausible alignment for a linac tunnel leading into the array of FELs located on the existing flat site in LBNL previously occupied by BEVATRON. It is also possible to begin the tunnel at a further point allowing more space for a linac.

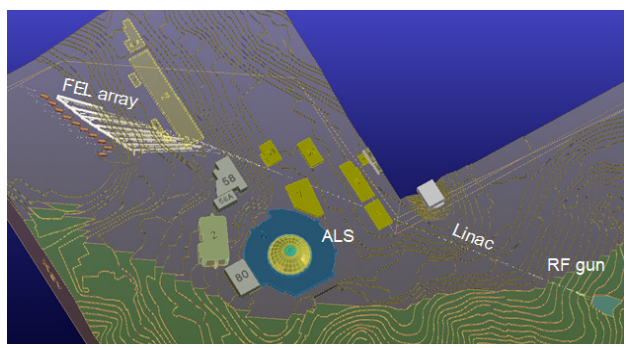

Figure 3: Bird view on East tunnel option for a linac, spreader and FEL array.

The linac lattice functions beginning from the end of the injector are shown in Figure 4. Large beta-functions are used in several locations along the L2 for convenience of the collimation of halo particles. This is important as we plan for up to 1 mA average electron current. A small horizontal beta-function <10 m is used at the forth bending magnet of the bunch compressor in order to minimize the impact of CSR on the beam emittance. It is considered that TESLA cryomodules with 1.3 GHz linac structures will be used in L1 and L2 with the energy gain

*Work supported by the U.S. Department of Energy under Contract No. DE-AC02-05CH11231.
#AAZholents@lbl.gov

MANIPULATING THE TWO-STREAM INSTABILITY FOR EFFICIENT TERAHERTZ GENERATION*

K. Bishofberger, B. Carlsten, R. Faehl; LANL, Los Alamos, NM 87544

Abstract

Particle beams have exhibited a two-stream instability for many decades; this undesirable trait has been well-understood for many years. We propose creating a scheme that uses a beam of electrons with two distinct energies that will develop the two-stream instability as a bunching mechanism. By controlling the beam parameters and seeding them with a low-level rf signal, a gain as high as 2.5 dB per centimeter is predicted. We show the theory behind this concept and recent progress in a developing experiment.

INTRODUCTION

Terahertz-frequency sources have been the holy grail of mm-wave research for many years now. In the recent past, a great deal of emphasis has been placed on developing these sources for a variety of applications [1].

Terahertz generally refers to a range of several hundred GHz through perhaps 10 THz, which lies in a band that has shorter wavelengths than electronics and conventional structures, yet longer than the atomic scale. Because of this, sources in this band have eluded conventional electronics and atomic techniques (e.g. lasers) and remain an unexplored region of the EM spectrum.

Yet the number of applications of terahertz manipulation is vast and growing. Typically, these include remote sensing, communications, three-dimensional imaging, and directed energy. Discussions of THz applications are published frequently; they will not be regurgitated here [1,2].

The most common approach to building a high-power source that reaches to 1 THz is typically a TWT-type device, where an electron beam is pushed through a comb-like structure, and the coupling of the beam with the vanes generates traveling waves of a wavelength nearly matching that of the structure. However, the structure and the efficiency of coupling scale very poorly to short wavelengths.

We propose a terahertz-generation scheme that eliminates the need for any problematic structure while providing high-average power output to satisfy the desires of the THz-based applications.

PHYSICAL DESCRIPTION

Figure 1 shows a three-dimensional model of the experiment currently being fabricated. The total beamline length, represented by the blue and red lines, is only a couple feet long. Two electron guns produce electron beams of slightly different energy. These beams are bent by a (green) dipole so that they merge and co-propagate. Then they get bent again and collected in a large-aperature collector.

The next section describes the theory of the interaction, and shows that Coulombic bunching should occur during the mixing process. These space-charge waves will radiate via coherent synchrotron radiation at the second bend. Instead of being dependent on shot noise to begin the process, we expect to steal a small percentage of the output radiation and reflect it back on the initial beam using one (yellow) mirror and a diffraction grating.

Seeding the beams at a specific frequency will allow that mode to self-select in the amplification process. Meanwhile, the majority of the radiative beam will be collected and analyzed. A number of variations are possible (frequency-modulated input, multi-mode mixing, etc), but in all cases, the setup is significantly less complex than conventional TWT-type techniques.

LINEAR THEORY

We start by separating out the dc and ac components of each beam's density and velocity:

$$\eta_j = \eta_{0j} + \tilde{\eta}_j \,, v_j = v_{0j} + \tilde{v}_j \,, \text{and } E = E_0 + \tilde{E} \,,$$

The continuity equation, Lorentz' law, and Poisson's equation can be written:

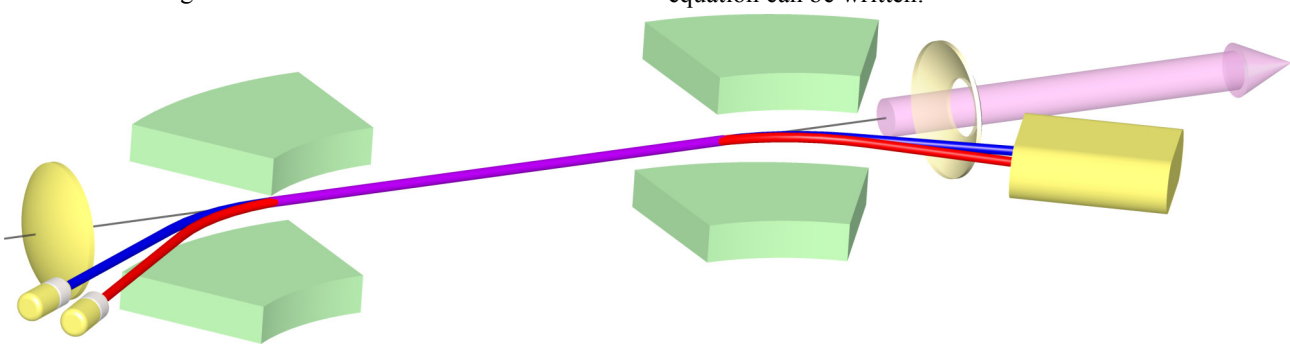

Figure 1: Model of the experimental beam layout. The two electron guns generate beams of slightly higher (blue) and lower (red) energies, which are then mixed (purple) through the interaction region. This middle portion is about 10-cm long, and the total apparatus is less than one meter in length.

IDENTIFYING JITTER SOURCES IN THE LCLS LINAC*

F.-J. Decker, R. Akre, A. Brachmann, W. Colocho, Y. Ding, D. Dowell, P. Emma, J. Frisch, S. Gilevich, G. Hays, P. Hering, Z. Huang, R. Iverson, K.D. Kotturi, A. Krasnykh, C. Limborg-Deprey, H. Loos, S.D. Molloy, H.-D. Nuhn, D. Ratner, J. Turner, J. Welch, W. White, J. Wu,
SLAC, Stanford, CA 94025, USA

Abstract

The beam stability for the Linac Coherent Light Source (LCLS) Free-Electron Laser (FEL) at Stanford Linear Accelerator Center (SLAC) is critical for good X-Ray operation. Although stability tolerances are met or very close to the specification [1,2], there is some transverse and longitudinal jitter in the beam [3]. Here we discuss identifying these jitter sources by different methods like correlations, frequency spectrum analysis or other methods for finally eliminating or reducing them.

MECHANICAL SOURCES

Understanding some of the jitter sources for the LCLS requires going back in history and looking at the sources and their solutions, which played out during running the SLC (SLAC Linac Collider) [4-7]. There was 10 Hz structural quadrupole vibration, which coupled from the longitudinal to the vertical 100 times stronger, since the quadrupole was mounted not below its center of gravity [4,5]. Additional clamps stiffened that motion and eliminated this frequency. Early frequency checks on the LCLS motion indicated some jitter power at 10 Hz, which could be traced to some clamps fallen in disrepair, like not be tightened down or even missing altogether, which was quickly fixed. The main sources, which drive this motion with mainly white noise jitter, are big accelerator structure water pumps. The asynchronous motors run at 3540 rpm 59 Hz [6,7], which when unbalanced, can be directly seen, or with 30 Hz beam rate aliased down at 1 Hz (see Fig. 1). 12% of the jitter power is at 1 Hz (8% at 4.4, 5% at 7 Hz).

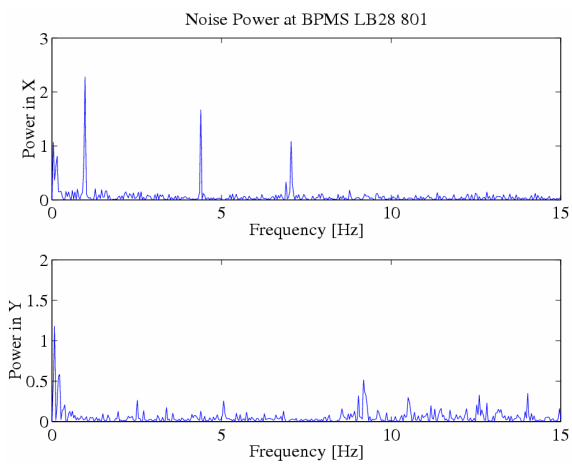

Figure 1: Power spectrum of a Beam Position Monitor (BPM) in the Linac indicates noise at 1.0, 4.4 and 7.0 Hz.

By plotting just the power at 1 Hz versus the length of the Linac z [6], we can pinpoint the location where a pump might be bad. Direct vibration data measured on top of the quadrupole can confirm this, and excessive variations of the pump water pressure can be even measured during running the beam.

Quantitative Analysis

A more quantitative approach is achieved in the following way. Only the 1-Hz-component of the FFT power spectrum (Fig. 1) is selected and the inverse FFT is taken. This gives a cleaned up 1-Hz sin curve (with some modulation, if more than one frequency bin was chosen). Now we take the peak-to-peak (p-p) difference (max – min) and plot this 1-Hz-difference orbit for all BPMs versus z or versus the BPM number (Fig. 2).

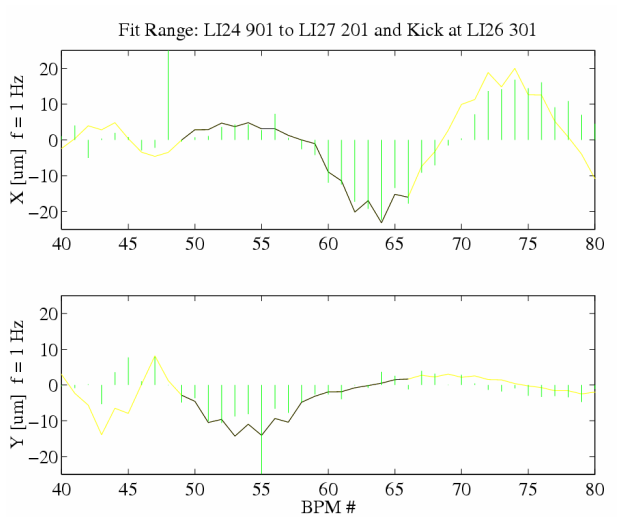

Figure 2: BPM orbit difference for only the 1 Hz component. A part (black curve) was fitted to the data allowing a kick at BPM # 59 (Li26 301).

The fitted kick angle was θ = -0.52 µrad in x and -0.18 µrad in y for a problem at Li26 301 BPM. The observed quadrupole vibration on top of the magnet was 2.3 µm RMS. These two numbers can be compared using the following equation

$$\theta = \frac{0.03}{E\,[\mathrm{GeV}]} * BL\,[\mathrm{kG\text{-}m}] \qquad (1)$$

where E (6.2 GeV) is the energy at that point and BL is the integrated field strength of an effective dipole kick. This kick is assumed to be produced by a nearby quadrupole B (-9.4 kG) and a vibration offset Δy. Using the above numbers Δy results to 11.4 µm (p-p).

* Work supported by US DOE contract DE-AC02-76SF00515.

THE ELECTRON BUNCH INITIAL ENERGY PROFILE ON A SEEDED FREE ELECTRON LASER PERFORMANCE*

Juhao Wu†, Alexander W. Chao, SLAC, Menlo Park, CA 94025, USA
Joseph J. Bisognano, Synchrotron Radiation Center, UW-Madison, Stoughton, WI 53589, USA

Abstract

A single-pass high-gain x-ray free electron laser (FEL) calls for a high quality electron bunch. In particular, for a seeded FEL, and for a cascaded harmonic generation (HG) FEL, the electron bunch initial energy profile is crucial for generating an FEL with a narrow bandwidth. After the acceleration, compression, and transportion, the electron bunch energy profile entering the undulator can acquire temporal non-uniformity. We study the effects of the electron bunch initial energy profile on the FEL performance.

VLASOV-MAXWELL ANALYSIS FOR AN INITIAL VALUE PROBLEM

The photoinjector generated electron bunch has a very small energy spread and small emittance. During the acceleration, bunch compression, and transportation, the electron bunch can acquire RF curvature, second order effect in the chicane, and collective effects, which will all lead to energy profile to be nonuniform. Further more, the electron bunch is subject to microbunching instability [1]. Thus, the electron bunch coming into the undulator can have an energy modulation. We study the energy profile nonuniformity on the free electron laser (FEL).

To analyze the start-up of a seeded FEL amplifier we use the coupled set of Vlasov and Maxwell equations which describe the evolution of the electrons and the radiation fields [2]. This approach is used as well for the Self-Amplified Spontaneous Emission (SASE) FEL [3]. We will work with a one-dimensional system analytically.

Vlasov-Maxwell Equations

We follow the analysis and notation of Refs. [3, 4, 2]. Dimensionless variables are introduced as $Z = k_w z$, $\theta = (k_0 + k_w)z - \omega_0 t$, where $k_0 = 2\pi/\lambda_0$, $\omega_0 = k_0 c$, and $k_w = 2\pi/\lambda_w$ with λ_0 being the radiation wavelength, λ_w being the undulator period, and c being the speed of light in vacuum. We also introduce $p = 2(\gamma - \gamma_0)/\gamma_0$ as the measure of energy deviation, with γ the Lorentz factor of an electron in the electron bunch, and γ_0 the resonant energy defined by $\lambda_0 = \lambda_w(1 + K^2/2)/(2\gamma_0^2)$, for a planar undulator, where the undulator parameter $K \approx 93.4 B_w \lambda_w$ with B_w the peak magnetic field in Tesla and λ the undulator period in meter. The electron distribution function is $\psi(\theta, p, Z)$ with $\psi_0(\theta, p, Z)$ describing the slow varying unperturbed component. The FEL electric field is written as $E(t, z) = A(\theta, Z)e^{i(\theta - Z)}$ with $A(\theta, Z)$ being the slow varying envelope function.

The one-dimensional linearized Vlasov-Maxwell equations are,

$$\frac{\partial \psi}{\partial Z} + p\frac{\partial \psi}{\partial \theta} - \frac{2D_2}{\gamma_0^2}\left(Ae^{i\theta} + A^* e^{-i\theta}\right)\frac{\partial \psi_0}{\partial p} = 0, \quad (1)$$

and,

$$\left(\frac{\partial}{\partial Z} + \frac{\partial}{\partial \theta}\right) A(\theta, Z) = \frac{D_1}{\gamma_0} e^{-i\theta} \int dp \psi(\theta, p, Z), \quad (2)$$

where in SI units, $D_1 = e a_w n_0 [JJ]/(2\sqrt{2} k_w \varepsilon_0)$, $D_2 = e a_w [JJ]/(\sqrt{2} k_w m c^2)$, with e and m being the charge and mass of the electron; $\varepsilon_0 \approx 8.85 \times 10^{-12}$ F/m being the vacuum permittivity; n_0 being the electron beam density; and $[JJ] = J_0[a_w^2/2(1 + a_w^2)] - J_1[a_w^2/2(1 + a_w^2)]$ where the dimensionless rms undulator parameter $a_w \equiv K/\sqrt{2}$. Equation (1) gives a general solution as

$$\begin{aligned} \psi(\theta, Z, \gamma) &\approx \psi_0(\theta - pZ, \gamma) \\ &+ \int_0^Z dZ' \frac{2D_2}{\gamma_0^2} A[\theta - p(Z - Z'), \gamma] e^{i[\theta - p(Z - Z')]} \\ &\times \frac{\partial \psi_0[\theta - p(Z - Z'), \gamma]}{\partial p}. \end{aligned} \quad (3)$$

Plugging Eq. (3) into Eq. (2), we have

$$\begin{aligned} \left(\frac{\partial}{\partial Z} + \frac{\partial}{\partial \theta}\right) A(\theta, Z) &= \frac{D_1}{\gamma_0} e^{-i\theta} \int dp \psi_0(\theta - pZ, \gamma) \\ &+ (2\rho)^3 e^{-i\theta} \int dp \int_0^Z dZ' A[\theta - p(Z - Z'), \gamma] \\ &\times e^{i[\theta - p(Z - Z')]} \frac{\partial \psi_0[\theta - p(Z - Z'), \gamma]}{\partial p}, \end{aligned} \quad (4)$$

with $(2\rho)^3 = (2D_1 D_2)/\gamma_0^3$, the Pierce parameter ρ [5, 6].

Initial Energy Imperfectness

To model an energy imperfectness in the electron bunch coming into the undulator, we assume that the initial distribution function is

$$\psi_0 = \delta[p + g(\theta_0)] = \delta[p + g(\theta - pZ)], \quad (5)$$

where $g(\theta_0)$ is a general function.

* Work supported by the US DOE contract DE-AC02-76SF00515.
† jhwu@SLAC.Stanford.EDU

DESIGN AND OPTIMIZATION OF ELECTRON BUNCH ACCELERATION AND COMPRESSION*

Juhao Wu†, Paul J. Emma, SLAC, Menlo Park, CA 94025, USA,
Robert A. Bosch, Kevin J. Kleman,
Synchrotron Radiation Center, University of Wisconsin – Madison, Stoughton, WI 53589, USA

Abstract

For electron bunches driving a hard x-ray free electron laser, the electron bunch high qualities should be preserved as well as possible in the acceleration and compression. For typical configuration, the electron bunch is accelerated in RF cavity and compressed in magnetic chicane. Besides the RF curvature and high-order optics terms in a chicane, the collective effects during the bunch acceleration, transportation, and compression can further distort the phase space. Among these collective effects, the coherent edge radiation dominates and governs the macroscopic bunch property. We study these effects and discuss their implication to general LINAC design and optimization.

TWO-STAGE LINAC BUNCH COMPRESSOR SYSTEM

After the electron bunch born from the cathode, it is accelerated and compressed by bunch compressors to achieve high peak current for x-ray free electron laser (FEL) [1]. Typically, there are two bunch compressor chicanes to achieve good stability. In the following, we will use BC1 to stand for the first chicane, and BC2 for the second. The accelerator RF waveform introduces RF curvature on a finite electron bunch, which needs a harmonic cavity to linearize the longitudinal phase space. The bunch compressor also introduces second order effect. Besides, the collective effects: geometric wakefield in LINAC, and coherent radiation wakefield in a bunch compressor will also affect the bunch compression. Recently, it was identified that the coherent edge radiation (CER) is the main source of impedance to govern the electron bunch macroscopic properties [2]. To illustrate the related concepts for RF acceleration and bunch compression, we first show some details of one stage of acceleration and bunch compression.

The electron beam is first accelerated, hence $E(z_0) = E_0(1+\delta_0) + eV\cos[\varphi + kz_0]$, where z_0 is the longitudinal coordinate of a certain electron with respect to the reference electron, $z_0 < 0$ is in the head, and $z_0 > 0$ is in the tail; $k = 2\pi/\lambda$ is the RF wavenumber for a wavelength of λ. We define the energy of the reference electron as $E_1 = E_0 + eV\cos[\varphi]$, so that the relative energy deviation of the electron with longitudinal coordinate z_0 is

$$\begin{aligned}\delta &\approx \frac{E_0}{E_1}\delta_0 - \frac{2\pi eV\sin\varphi}{\lambda E_1}z_0 - \frac{2\pi^2 eV\cos\varphi}{\lambda^2 E_1}z_0^2 \\ &\equiv \mathcal{A}\delta_0 - \mathcal{B}z_0 - \mathcal{C}z_0^2. \end{aligned} \quad (1)$$

Now, the beam is chirped and sent through the chicane. In the thin lens approximation, the path length difference after the chicane reads $\Delta s \sim [\theta_0/(1+\delta)]^2 L_2$, where L_2 is half of the drift distance for a symmetric chicane, and θ_0 is the bending angle. Hence, after the chicane, the particle internal coordinate reads

$$z = z_0 + \delta(R_{56} + T_{566}\delta), \quad (2)$$

where in the thin lens approximation, $T_{566} = -3R_{56}/2$. In a 4-dipole (or 3-dipole) magnetic chicane, the high energy particle travels a short path, hence for compression, the tail particles should have higher energy than that of the head particles. For convention of the tail with coordinate z larger than that of the head, this means that the chirp slope $-\mathcal{B} > 0$, so that $R_{56} < 0$.

To find the bunch length after the chicane, we plug Eq. (1) into Eq. (2) to get

$$z \approx \mathcal{A}R_{56}\delta_0 + (1 - \mathcal{B}R_{56})z_0 + (\mathcal{B}^2 T_{566} - \mathcal{C}R_{56})z_0^2. \quad (3)$$

Assuming a longitudinal uniform beam, we have

$$\begin{aligned}\sigma_z^2 \approx \left(\frac{E_0}{E_1}\right)^2 R_{56}^2\sigma_{\delta_0}^2 + \Bigg[\left(1 - \frac{2\pi R_{56}eV\sin\varphi}{\lambda E_1}\right)^2 \quad (4)\\ + \left(\frac{6\pi^2 R_{56}eV}{\sqrt{5}\lambda^2 E_1}\right)^2\left(\frac{2T_{566}eV\sin^2\varphi}{R_{56}E_1} - \cos\varphi\right)^2\sigma_{z_0}^2\Bigg]\sigma_{z_0}^2,\end{aligned}$$

where $\langle z_0^4\rangle = (9/5)\sigma_{z_0}^4$. Seen in Eq. (4), even if we choose a right R_{56} to minimize the bunch length according to the term quadratic in σ_{z_0}, the term quartic in σ_{z_0} will change the bunch length. This is brought up by the RF curvature. To remove the RF curvature effect, for LINAC Coherent Light Source (LCLS) setting, we install a X-band cavity, which is operated at the 4^{th} harmonic of the other S-band cavities. After L0- and L1- and the LX-linac, the energy of the electron reads

$$\begin{aligned}E &= E_0(1+\delta_0) + eV_0\cos[\varphi_0 + kz_0] \\ &+ eV_1\cos[\varphi_1 + kz_0] + eV_x\cos[\varphi_x + k_x z_0]. \end{aligned} \quad (5)$$

This leads to

$$\delta \equiv \frac{E - E_2}{E_2} \approx \mathcal{D}\delta_0 + \mathcal{E}z_0 + \mathcal{F}z_0^2 + \mathcal{G}z_0^3, \quad \text{where} \quad (6)$$

$$E_2 = E_0 + eV_0\cos(\varphi_0) + eV_1\cos(\varphi_1) + eV_x\cos(\varphi_x), \quad (7)$$

$$\mathcal{E} = -\frac{e}{E_2}[kV_0\sin(\varphi_0) + kV_1\sin(\varphi_1) + k_x V_x\sin(\varphi_x)], \quad (8)$$

$$\mathcal{F} = -\frac{e[k^2V_0\cos(\varphi_0) + k^2V_1\cos(\varphi_1) + k_x^2V_x\cos(\varphi_x)]}{2E_2}, \quad (9)$$

* Work supported by the US DOE contract DE-AC02-76SF00515.
† jhwu@SLAC.Stanford.EDU

DESIGN OF MICROWAVE UNDULATOR CAVITY*

Muralidhar Yeddulla, Sami Tantawi, SLAC, Menlo Park, CA 94061, USA

Abstract

Static magnetic field undulators are capable of producing quasi-monochromatic synchrotron radiation of very high brightness. However, it is not possible to quickly change the properties such as polarization of the radiation in a static undulator. It is possible to construct an undulator using microwaves instead of static magnets where the electron beam is undulated by both electric and magnetic fields of an rf wave. A major advantage with a microwave undulator is that the radiation properties can be changed very quickly. The biggest challenge in developing a microwave undulator is in keeping the rf losses low. We are designing a microwave undulator with the aim of achieving at least a tenth of the flux obtained by the BL13 static magnetic field Elliptical Polarized Undulator in the SPEAR ring. We have considered circular waveguide modes and hybrid HE_{11} mode in a corrugated waveguide as possible candidates for the microwave undulator. It is found that a corrugated waveguide has the lowest rf losses with a very desirable field profile. It is also possible to use this device for a linac driven FEL. Our analysis of the corrugated waveguide cavity for the rf undulator will be presented.

INTRODUCTION

In general, an undulator consists of a highly relativistic electron beam wiggled in the presence of a periodic undulating magnetic (or electromagnetic) fields producing synchrotron radiation. Highly successful modern undulator based synchrotron sources are based on periodic permanent magnetic fields. However, due to the intrinsic limitations of magneto static fields the polarization of the radiation fields and the undulator period cannot be controlled. These limitations can be overcome if high power rf waves are used instead of static magnetic fields in the undulator. However, the necessary rf power sources required to realize a microwave undulator capable of delivering synchrotron radiation comparable to a magneto static undulator was not available in the past. Recently a 500 MW X-band rf source was developed for the Next Linear Collider [2]. Combined with the advances in overmoded rf components and systems [3] led to the idea of the possibility of a practical rf undulator presented in this work. The same idea can be extended to LINAC driven rf FEL.

We are designing a microwave undulator for the SPEAR3 storage ring at SLAC. In a storage ring a static undulator would be *on* all the time giving rise to higher brightness. In order to be competitive, the microwave undulator we are designing should generate at least a tenth of circularly polarized radiation flux that can be generated by a static undulator. We have considered smooth wall circular waveguide structures operating in the TE_{11} and TE_{12} modes and a corrugated waveguide operating in the HE_{11} - mode as possible candidates for the design of the undulator [4]. Our study has shown that the HE_{11} - mode offers superior loss characteristics compared to other modes and can be operated at relatively lower power levels.

In order to generate the necessary field strength to undulate the 3 GeV electron beam in the storage ring, the rf power flow in the waveguide would be in the order of giga watts. To achieve such power levels rf energy can be stored inside a waveguide cavity to obtain the required levels of field strength by only compensating for the waveguide losses which can be within achievable power levels. It is a computationally intensive problem to design a corrugated waveguide cavity using numerical methods such as Finite Element Methods (FEM). As the corrugated waveguide can be regarded as a series of smooth cylindrical waveguides with discontinuities in radius, it can be analyzed using mode matching techniques that require moderate computational resources which is presented in this work.

RADIATION IN A MICROWAVE UNDULATOR

In a Circularly Polarized Standing Wave (CPSW) microwave undulator, due to the fact that the rf energy is confined in a cavity, the electron beam interacts with both the forward and backward wave with respect to the electron motion inside the cavity. The transverse electron velocity (normalized to speed of light in free space) is given by [1],

$$\beta_x(z) + i\beta_y(z) = -\frac{K}{\gamma} \sum_{n=-\infty}^{\infty} [J_n(\delta) + J_{n+1}(\delta)] \cdot \exp\left\{ i \left[k/\bar{\beta}_{||} + (2n+1)k_{||} \right] z \right\}, \quad (1)$$

where

$$\delta = \frac{K^2}{2\gamma^2} \frac{k}{k_{||}}, \quad (2)$$

$K = eE_w/m_0c^2k_{||}$ is the normalized amplitude of the rf wave, E_w is the amplitude of the rf wave, m_0 is the mass of an electron, c is the speed of light in free space,γ is the relativistic factor, k is free space wave number and $k_{||}$ is the axial wave number of the rf wave inside the waveguide.

From Eq. (1) we see that a CPSW microwave undulator, in general, is a combination of several harmonic motions and would radiate in several harmonics unlike a static

* Work supported by Department of Energy, USA

STATUS OF THE NPS FREE-ELECTRON LASER*

J.W. Lewellen#,1, W.B. Colson[1], S.P. Niles[1], T. Smith[1,2]
[1] Naval Postgraduate School, Monterey, CA 93943
[2] Stanford University, Stanford, CA 94305

Abstract

The Naval Postgraduate School (NPS) is in the process of designing and constructing a free-electron laser (FEL) laboratory to pursue FEL-related research and introduce students to modern accelerator and FEL technology. The laboratory will pursue research on high-brightness injectors, fundamental and applied beam dynamics, energy recovery linear accelerators, as well as FEL experiments.

The accelerator will be based around two, Stanford-Rossendorf type cryomodules, each of which houses two, 9-cell TESLA-type cavities. RF power will be provided by four, 10-kW CW L-band klystrons. With a nominal beam current of 1 mA, this provides an energy gain of 10 MV per structure. Intended operating modes include single-pass, energy recovery linac, and 2-pass microtron.

This paper provides an introduction to the NPS-FEL program goals, site and vault layout, and preliminary experimental plan.

PROGRAM GOALS

The Naval Postgraduate School has committed to the construction and operation of a free-electron laser and accelerator physics laboratory, NPS-FEL.

One of the primary missions of the NPS-FEL will be student education. NPS grants Master's and Ph.D. degrees in a variety of disciplines, including physics, mechanical and electrical engineering. Accelerators by their nature require multidisciplinary efforts to construct, operate and characterize; thus, the NPS-FEL represents an opportunity for cross-disciplinary study and research.

The NPS-FEL experimental program is intended to address technical challenges relevant to next-generation accelerator, light source and FEL design, and study topics of fundamental interest in accelerator physics. There is, naturally, substantial overlap, such as beam merger design, coherent synchrotron radiation effects, beam halo formation, etc.

FACILITY

Location

The NPS-FEL laboratory will be located at an existing building at the Monterey Pines golf course, a Navy-owned facility adjacent to the NPS main campus (see Figure 1). The NPS-FEL laboratory building is one of several research buildings at Monterey Pines, including a jet-engine test laboratory, several wind tunnels, oceanographic laboratories, machine shops, and a flash X-ray facility.

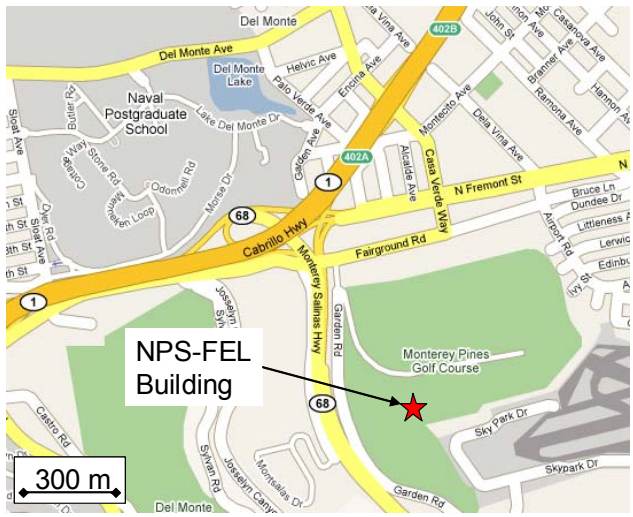

Figure 1: NPS-FEL facility location relative to the Naval Postgraduate School campus.

Site Preparation

The laboratory building is a metal-frame structure with steel side-panel walls and a concrete slab foundation, which until recently served as a laboratory and repair bay for an autonomous underwater vehicle (AUV) research program. The AUV laboratory move was completed in June 2008.

Site preparation began in early 2008 with the installation of a new electrical substation near the building, capable of supplying an additional MW for power supplies, cryogenic systems, and RF power sources.

Renovation for the NPS-FEL will include addition of an on-grade radiation shield vault, replacement and insulation of the building skin, and reconstruction of the interior laboratory and office space.

Interior Layout

The building is a rectangle approximately 40' (12.2 m) wide by 162' (49.4 m) long. There is a secondary pad to one side of the main foundation, approximately 22' (6.7 m) square, that will serve as a base for the eventual cryogenics plant.

The shield vault will take approximately half of the building, with the remaining half being dedicated to laboratory and office space. Figure 2 shows a conceptual sketch of the building layout; the vault design and interior space allocation have not been finalized as of this writing, however.

* Work supported by the Office of Naval Research and the Joint Technology Office for High-Energy Lasers
# jwlewell@nps.edu

EXPERIMENTAL CHARACTERIZATION AND OPTIMIZATION OF HIGH-BRIGHTNESS ELECTRON BEAM AT THE NSLS SDL

X. Yang, J. B. Murphy, H. Qian, S. Seletskiy, Y. Shen, and X. J. Wang,
National Synchrotron Light Source, BNL, Upton, NY 11973, U.S.A.

Abstract

The Source Development Laboratory (SDL) at the National Synchrotron Light Source (NSLS) is a laser linac facility dedicated for laser seeded FEL and beam physics R&D. The SDL consists of a RF synchronized Ti:sapphire laser, a BNL photocathode RF gun, a four-magnet chicane bunch compressor, and a 300 MeV linac. To further improve the performance of the laser seeded FEL at the NSLS SDL, we have carried out a systematic experimental characterization of the high-brightness electron beam generated by the photocathode RF gun. We will present the experimental studies of transverse emittance of electron beam as a function of RF gun phase and solenoid magnet for electron beam charge ranging from 350 pC to 1 nC.

INTRODUCTION

Small transverse emittance, high peak current, and small energy spread are keys for achieving high energy gains in the seeded FEL experiments. The electrons with a small energy spread and low space-charge-induced emittance are emitted from the photocathode surface with a strong RF field (~100MV/m). The quick acceleration of the electron beam in a photoinjector prevents thermalization of the beam's phase space. However, the emittance growth, due to the RF and the space-charge effects, occurs in the RF gun. In particular, the transverse emittance increases close to the cathode surface due to transverse defocusing space-charge force. We use a spatial laser shaping to produce a nearly flat-topped charge density electron beam, and a 9ps long Gaussian laser pulse to reduce the longitudinal space charge force. As an example, after a 1.6-cell RF gun with a space-charge emittance compensation solenoid magnet developed in the Brookhaven National Laboratory (BNL) [1,2], a transverse normalized rms emittance of 4 mm•mrad with 1nC of bunch charge was obtained.

Optimization of operating parameters of the RF gun, such as the laser injection phase and the space-charge compensation are required for the generation of a high-brightness electron beam. We have carried out a systematic experimental characterization of the transverse emittance of electron beam as a function of RF gun phase and solenoid magnet for electron beam charge ranging from 350 pC to 1 nC.

EXPERIMENTAL SETUP

The SDL accelerator features a 6MeV BNL gun, two SLAC-type traveling-wave accelerating structures providing 70MeV followed by a 4 dipole chicane and three more accelerating structures with a final energy of up to 250MeV [3]. A spectrometer dipole after the last structure enables energy spectra and time resolved measurements [4]. The RF gun consists of a half cell and a full cell. A magnesium cathode is located on the side of the half cell. A single solenoid magnet is mounted at the exit of the RF gun to compensate for the transverse emittance growth due to the space-charge effect.

The beam transverse emittance was measured downstream of the 4th accelerating structure with a standard quadrupole scan technique. The beam size was measured on a YAG crystal downstream of a quadrupole magnet which was varied so that the beam passed and a data translation 8-bit frame grabber both synchronized

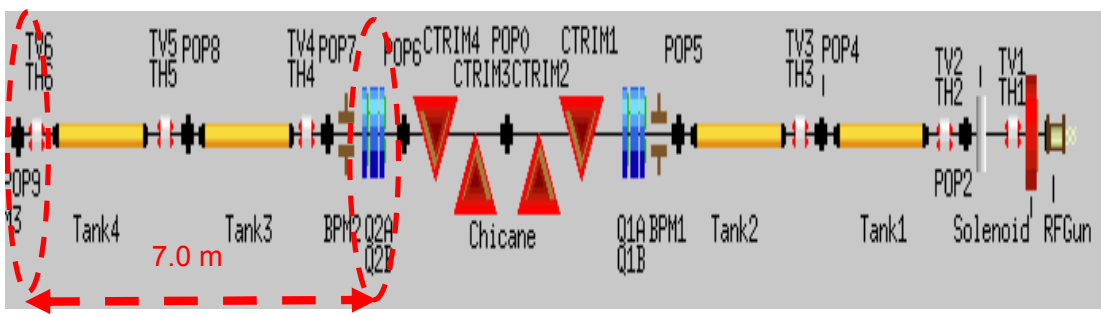

Figure 1: Schematic diagram of the experimental arrangement.

DEVELOPMENT OF THE CONTINUOUSLY ADJUSTABLE PERMANENT MAGNET QUADRUPOLE FOR ATF2

Takanori Sugimoto, Yoshihisa Iwashita, Masahiro Ichikawa, Masako Yamada, Ichiro Kazama
(ICR Kyoto Univ. Uji Kyoto) and Toshiaki Tauchi (KEK, Ibaraki)

Abstract

A quadrupole magnet for the final focus system of the International Linear Collider (ILC) is required specific properties, that is comparatively 'compact' (because the crossing angle of the Interaction Point (IP) of ILC is planned to be very small (~14mrad) and so out-going beam-line is installed passing close by the Final Focus Quadrupole (FFQ)), 'solid and stable' (so that beams with the very small beam-size at IP (~several nm in y-plane) needed can be realized and be handled stably) and so on. A super-conducting magnet scheduled now is not always suitable for that, for instance because of a huge cryostat needed outside of it (since it may have the mechanical vibrations due to liquid helium flow and also the magnet. This may prove not to be good). Since the continuously field-strength adjustable Permanent Magnet Quadrupole (PMQ) designed by Gluckstern [1][2] satisfies these properties, we are developing FFQ of this type for ILC, and for ATF2 (the Acceleration Test Facility 2) firstly.

However the magnet of this type has a risk of x-y coupling more greatly influenced than magnets of other types. For it is five discs singlet, which comprises five PMQ discs with appropriate skew each other. A nominal beam for ILC has different scales in x-plane and y-plane, so we need to avoid x-y coupling sufficiently.

We estimated the effect of field-error brought by skew of each PMQ disc. Then we used the way of calculation of transfer matrices neglecting fringe field and multipoles except for Q. In addition we produced this type of the magnet experimentally and measured field-strength and harmonics in the magnet. Then we fabricated an instrument measuring harmonics of fields in the magnets. The harmonic analysis is discussed compared with the estimation above.

We explain these schemes and show the conclusion. At the same time we are adjusting and aligning the magnets for reducing errors. We fabricated a jig then, so we explain it too.

INTRODUCTION

Since recent development for a PMQ enables high degree of field strength, a PMQ can be used as a focus magnet for a high-energy beam. However a focus magnet requires the tuning of field strength for the sake of practical beam energy and focal length. A five-discs-singlet configuration proposed by Gluckstern works as a PMQ, whose strength is continuously adjustable. Each disc of a Gluckstern's PMQ comprises a PMQ, and the field strength in it is altered by rotating the discs with respect to each other (Fig. 1). Though x-y coupling effect caused by a skew of each disc can be theoretically cancelled in this design, fabrication errors and rotation errors alter the situation. The effect of x-y coupling may prove fatal to a beam whose size in x-plane and y-plane are considerably different as in a case at IP of ILC.

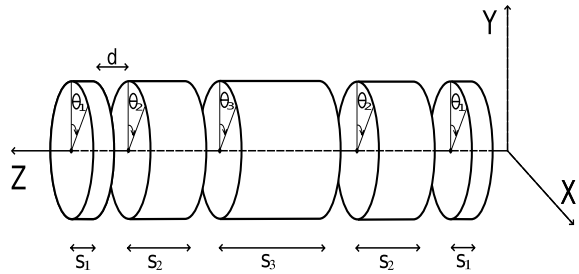

Figure 1: A Gluckstern's PMQ.

Though six parameters exist in the five-discs-singlet, five conditions constrain these parameters. So only one parameter is free. Using this parameter total field strength is continuously adjustable. The five constraint conditions are as follows.

- The absolute values of three rotation angles of five discs are the same. It should be noted that this statement represents two constraint conditions. The statement is namely
$$\theta \equiv \theta_1 = -\theta_2 = \theta_3 . \quad (1)$$
- The minimum of the total focusing force is decided. Here we chose the minimum zero, and strength of focusing is approximated in proportion to length of the magnetic filed. Then this constraint condition is
$$2s_1 - 2s_2 + s_3 \equiv S_0 . \quad (2)$$
We decided S_0 to be zero here.
- The maximum of the total focussing force is decided. We chose the maximum the value needed by ATF2. The total focussing force is represented as the total length when field gradients of discs are the same and decided. By the way, with the aim at ILC we are planning to choose the same total length and smaller bore of discs.
$$2s_1 + 2s_2 + s_3 \equiv S_t . \quad (3)$$
Here S_t is 220mm.
- In order to cancel the effect of x-y coupling at all angles of discs, the proportion of the lengths of discs should be optimized. In this optimization we used the proportion of the length of first and fifth discs to the total length.
$$\lambda \equiv s_1 / S_t . \quad (4)$$
Here λ is 0.07877.

ESTIMATION OF ERRORS

We estimated an x-y coupling effect caused by three types of errors associated with each disc, namely a rotation error, a length error and a shift. This estimation

OPTIMUM FREQUENCY AND GRADIENT FOR THE CLIC MAIN LINAC ACCELERATING STRUCTURE

A. Grudiev, H. H. Braun, D. Schulte, W. Wuensch, CERN, Geneva, Switzerland

Abstract

Recently the CLIC study has changed the operating frequency and accelerating gradient of the main linac from 30 GHz and 150 MV/m to 12 GHz and 100 MV/m, respectively. This major change of parameters has been driven by the results from a novel main linac optimization procedure. The procedure allows the simultaneous optimization of operating frequency, accelerating gradient, and many other parameters of CLIC main linac. It takes into account both beam dynamics (BD) and high power RF constraints. BD constraints are related to emittance growth due to short- and long-range transverse wakefields. RF constraints are related to RF breakdown and pulsed surface heating of the accelerating structure. The optimization figure of merit includes the power efficiency, measured as a ratio of luminosity to the input power, as well as a quantity proportional to total cost.

INTRODUCTION

From almost the very beginning of CLIC [1] the operating frequency of the main linac accelerating structure was 30 GHz which gave a compromise between the efficiency and peak power, and and machinability and wakefield considerations. The original gradient was 80 MV/m for a 2 TeV collision energy. Eventually it was increased to 150 MV/m [2] in order to reach the CLIC design luminosity and energy (~10^{35} cm^{-2}sec^{-1} and 3 TeV, respectively) in a power-efficient way and with an affordable site length. Since then several attempts have been made to find a better choice of the frequency and gradient for CLIC [3, 4].

In [4], a new optimization procedure has been used which is based on the interpolation of the accelerating structure parameters allowing millions of structures to be analyzed. The demanding beam dynamics requirements, a short-range transverse wakefield limit and long-range transverse wakefield suppression, are taken into account as well as high-power rf effects such as, rf breakdown and rf pulsed surface heating. The results indicated that 18 GHz and 100 MV/m are a better choice for CLIC if the ratio luminosity to the input power is considered to be paramount. Two things limited the validity of the results: first was the absence of a cost analysis and second was the lack of high gradient experimental data at 30 GHz. The latter difficiency called into question the frequency scaling of the rf breakdown constraints used in the optimization.

In this report, the extension of the optimization procedure described in [4] to include both a parameterized cost model and updated rf constrains is presented. Finally, the results of the CLIC main-linac accelerating structure using the new optimization are presented and discussed.

PARAMETERIZED COST MODEL

In the new parameterized cost model , the total cost is given by the sum of the investment cost and the exploitation cost for 10 years. It is calculated as a function of several parameters of the linac: the repetition frequency f_{rep}, the RF pulse energy for the whole linac W, the accelerating gradient E_{acc}, the structure length L, the operating frequency f and the rf phase advance per cell $\Delta\varphi$.

The model uses as a reference point a cost estimate which was done for a 30 GHz, 150 MV/m machine as described in [5]. Cost are scaled with the assumption that the cost per meter of accelerating structure varies according to the function

$$C_{\mathrm{acc}} = C_{mat} \cdot (f/30\mathrm{GHz})^{-3/2} + C_{mach} \cdot (f/30\mathrm{GHz})^{3/2} \cdot (\Delta\varphi/60^0)^{-2/3}$$

C_{acc} is the cost per meter of accelerating structure, C_{mat} *is* the material cost per meter of accelerating structure of the reference and C_{mach} is the cost of structure machining and assembly of the reference. This rule is based on scaling the required machining time and material mass and was benchmarked with the procurement costs of prototype structures at 30 GHz and 11.4 GHz. The effect of structure length L was modeled assuming that costs per meter of accelerator scale in proportion to $L^{-2/3}$. For other quantities like tunnel, magnet and instrumentation costs a simple linear scaling with cost ~E_{acc}^{-1} is assumed. The main cost of the drive beam the is determined by the total RF energy per machine pulse, which directly affects the number of required klystrons and modulators. The average RF power affects the total required charging power supply capacity. Electricity costs are based on the integrated consumption over 10 years of operation with 200 days per year and 95% up-time. The same unit costs were used as in estimates for the ILC [6].

UPDATED RF CONSTRAINTS

The following three rf constraints have been used in the optimization:

1. Surface electric field: $E_{surf}^{\max} < 380$ MV/m
2. Pulsed surface heating: $\Delta T^{\max} < 56$ K
3. Power: $P_{in}/C \cdot \tau_p^{1/3} \cdot f < 156$ MW/mm/ns$^{2/3}$

Here $E_{surf}^{\max}$ and $\Delta T^{\max}$ refer to maximum surface electric field and maximum pulsed surface heating temperature rise in the structure respectively. P_{in}, τ_p and f denote input power, pulse length and frequency respectively. C is the circumference of the first regular iris. The value used for the power constraint (3) is different from the one used in the previous optimization [4].

The original concept of power over circumference (P/C) as a limit for travelling wave rf breakdowns [7]

BEAM OPTICS STUDIES AND COMMISSIONING STATUS OF CTF3

P. K. Skowronski, R. Corsini, S. Bettoni, S. Doebert, F. Tecker, CERN, Geneva, Switzerland
D. Alesini, C. Biscari, INFN/LNF, Frascati, Italy
Yu-Chiu Chao, TRIUMF, Vancouver, Canada

Abstract

The objective of the CLIC Test Facility CTF3 is to demonstrate the feasibility issues of the CLIC two-beam technology. CTF3 consists of an electron linac followed by a delay loop, a combiner ring and a two-beam test area. One issue studied in CTF3 is the efficient generation of a very high current drive beam, used in CLIC as the power source to accelerate the main beam to multi-TeV energies. The beam current is first doubled in the delay loop and then multiplied by a factor four in the combiner ring by interleaving bunches using transverse deflecting rf cavities. The combiner ring and the connecting transfer line have been put into operation in 2007, and the remaining parts, namely decelerating section, probe beam linac and test beam line in 2008. In this paper we give the status of the commissioning, present the results of the combination tests and illustrate in some detail the beam optics measurements, including response matrix analysis, dispersion measurement and applied orbit correction algorithms. We discuss as well the observation of a vertical beam break-up instability which is due to the vertical transverse mode in the horizontal RF deflectors used for beam injection and combination. We outline the attempted methods to mitigate the instability and their effectiveness.

THE CTF3 COMPLEX

The CLIC technology [1] is believed to be the only practical path to multi-TeV colliders. The experimental program of the present CLIC Test Facility (CTF3) [2], aims to confirm its feasibility. In particular the generation and use of the high-current drive beam [3].

CTF3 is build at CERN by an international collaboration which at present includes 24 institutes from 14 countries [4]. Its construction is almost completed and a large part of the facility is already commissioned. It re-uses the infrastructure and most of the hardware of the former LEP Pre-Injector, LPI (see Fig. 1).

CTF3 consists of a 70 m long drive-beam linac followed by two rings, where the beam current is multiplied by a factor eight: a 42 m delay loop and an 84 m combiner ring. The drive beam is then delivered to the CLic EXperimental area (CLEX) to produce 12 GHz RF power for structure tests. In the same area, the CALIFES linac provides a probe beam for a Two-Beam Test Stand (TBTS) and a decelerator (Test Beam Line – TBL) will be used for drive beam stability studies. The detailed description of the facility can be found in [2,5].

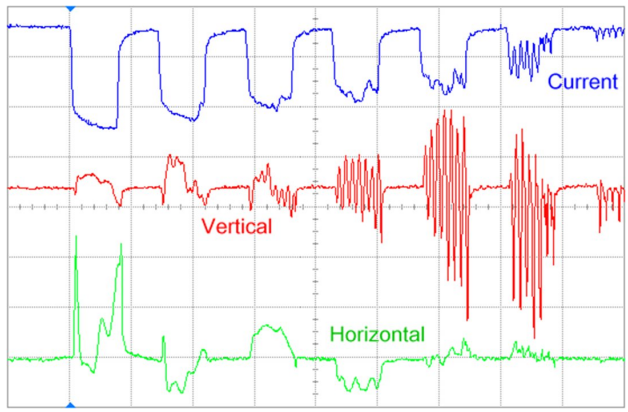

Figure 1: Traces of the beam current (upper line), vertical position (middle) and horizontal position (lower) in the ring, a clear indication of the vertical instability.

COMMISSIONING STATUS

In 2003-2004 the injector, the linac, the mid-linac power station and the end-of-linac magnetic chicane were installed and commissioned. Full beam-loading operation was established [6]. The resulting beam is remarkably stable, with no sign of beam break-up. An RF-to-beam efficiency of 94 % has been experimentally verified later on [7]. The first part of the linac is routinely used since 2005 as a source of 30 GHz RF power. Up to 100 MW can be produced in the PETS, and transported to the test stand with ~ 70 % efficiency. The delay loop was installed during 2005 and commissioned in 2006. Five 140 ns long bunch-trains were injected into the delay loop and combined with the following train, thus doubling the beam current [8]. In 2006 a short period was dedicated to the commissioning of the newly installed TL1. Short pulses of 200 ns were used. The beam was rapidly transported to the end of the line and a current of 3 A could be injected in the ring first straight section.

The combiner ring installation was completed at the beginning of 2007. Commissioning of the combiner ring began in 2007, with several interruptions for repairs and installation work [9], and still continues with the goal to reach nominal beam parameters. Several problems in the hardware and in the optics model were identified, mainly through beam measurements, and eventually fixed, including wrong BPM calibration and connections, quadrupole cabling errors, switched polarities and wrong current calibrations. The alignment of magnets and vacuum chamber elements was also re-checked and corrected when necessary. During 2007 we could finally obtain a beam circulating for several turns in the ring, albeit with non-negligible losses. A fast beam instability in the vertical plane (see Fig.1) was indeed discovered

DESIGN AND FABRICATION OF CLIC TEST STRUCTURES

R. Zennaro, A. Grudiev, G. Riddone, A. Samoshkin, W. Wuensch, CERN, Geneva, Switzerland
S. Tantawi, J. W. Wang SLAC, Menlo Park, USA
T. Higo KEK, Tsukuba, Japan

Abstract

Demonstration of an accelerating gradient of 100 MV/m at a breakdown rate of 10^{-7} is one of the key feasibility issues of the CLIC study. A high power RF test program both at X-band (SLAC and KEK) and 30 GHz (CERN) is under way to develop accelerating structures which reach this performance. The centrepiece of the testing program is the nominal CLIC accelerating structure [1], but also includes structures with different RF parameters, with and without wakefield damping waveguides and made with different fabrication technologies. The latter structures address as directly as possible the different aspects of the nominal CLIC structure. The design and objectives of the various X-band and 30 GHz test structures are presented and their fabrication methods and status are reviewed.

INTRODUCTION

The accelerating structure test program is one of the highest priority activities of the CLIC study [2]. The two main aims of the testing program are to validate the present CLIC structure design, CLIC_G [1], and to acquire data from different structures which can be used to both improve the understanding of and validate models of fundamental high power limits [3, 4, 5] and the effect on performance of different aspects of the design, such as the presence of HOM damping waveguides.

One of the main objectives for the structure is a loaded gradient of 100 MV/m with a 10^{-7} breakdown rate at the design pulse length. A second important objective is that the long range transverse wakefields be suppressed at the position of the second bunch to $W_{t,2} \leq 6.6$V/pC/mm/m for a bunch population $N=4*10^9$. In the CLIC structure this suppression is provided by combination of HOM damping waveguides located in each accelerating cell and detuning. Finally, the short range wakefield, which is determined by the aperture of the irises and is proportional to the bunch charge must remain below the threshold provided by the beam dynamics study.

The test structures can be organized into four groups: the VG1 family which is based on the design of the former nominal CLIC structure, CLIC_G family which is based on the present CLIC structure, the C10 family which is used to investigate specific issues in a simple constant impedance design with reusable couplers and 30 GHz structures which are now dedicated to the study of new ideas and to acquire more data for the understanding of the breakdown physics.

THE VG1 FAMILY

The design of vg1 is derived from the CLIC_C, a former CLIC nominal structure CLIC_C is strongly tapered with a group velocity which drops from 2.4%c to 0.65%c (values for the damped versions). The tapering results in a surface electric field of 300 MV/m in the last cell for the unloaded case as shown in Figure 1. Vg1 is a shortened version of CLIC_C, and is composed of the first 18 regular cells in order to limit the field on the surface to 265 MV/m for the unloaded case. The surface field for the loaded case is anyhow equivalent in the two cases as shown in Figure 1.

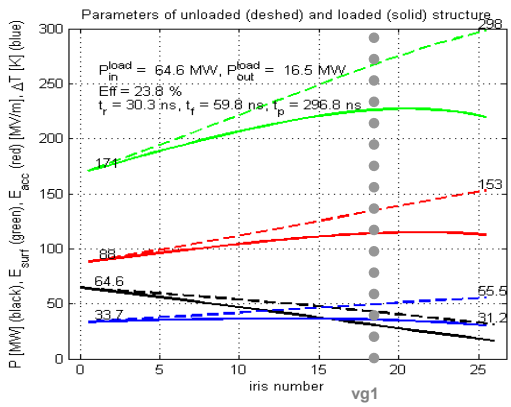

Figure 1: CLIC_C with accelerating gradient (MV/m, red), field on surface (MV/m, green), power (MW, black) and pulsed surface heating (K, blue) along the structure. vg1 extends to cell 18.

The reduction in the number of cells has as consequence not only in the reduction of peak surface electric field, but also a reduction in the efficiency of the structure which drops to only 18% from the original 24% of CLIC_C as shown in Table 1.

Table 1: Vg1 main parameters (undamped version).

Name	T18_vg2.6_disk
Frequency (GHz)	11.424
N cell	18+2
Phase advance/cell (deg)	120
Iris aperture ain,out (mm)	4.06/2.66
Iris thickness din,out (mm)	2.897/1.314
Vgin/out (%c)	2.61/1.02
Tfilling (ns) (full structure)	36
Pin unloaded (MW) (100 MV/m)	55.5
Pin loaded (MW) (100 MV/m)	63.7
Pulse length (ns)	267.4
P/c (Wu)	15.0
Efficiency (%)	17.7

A KICKER DRIVER EXPLOITING DRIFT STEP RECOVERY DIODES FOR THE INTERNATIONAL LINEAR COLLIDER

F. Arntz, M.P.J.Gaudreau, M. Kempkes, Diversified Technologies, Inc., Bedford, MA USA
A. Krasnykh, Stanford Linear Accelerator Center
A. Kardo-Sysoev, Ioffe Institute of Physics, Russia

Abstract

Diversified Technologies, Inc. (DTI), under a SBIR grant from the U.S. Department of Energy[1], is developing a driver for a kicker TEM strip-line deflector which inserts and extracts charge bunches to and from the electron and positron damping rings of the International Linear Collider. The ultimate ILC damping ring kicker driver must drive a 50 Ohm load (a 50 Ohm terminated TEM deflector blade) at 10 kV, with 2 ns flat-topped pulses at a 3 MHz rate, within one-millisecond bursts occurring at a 5 Hz rate. The driver must also effectively absorb high-order mode signals emerging from the deflector itself.

In this paper, DTI describes the design of the kicker driver involving high voltage DSRDs (Drift Step Recovery Diodes) and high voltage MOSFETs. The development system will produce 5 kV pulses, which otherwise will satisfy the ILC requirements, as a precursor to the full 10 kV system. Because of the high 3-MHz pulse rate required, this design employs an all-electronic, rather than magnetic, approach to pulse compression.

BACKGROUND

Every particle accelerator requires "kickers" – electromagnetic deflectors that pulse on to divert (kick) bunches of particles out of their trajectory onto new beam paths, targets, detectors, or other instrumentation. Kickers must reach the intended deflection field between particle bunches, control that field for a finite time, and return to zero field to avoid affecting the next bunch. The drivers for these kicker deflectors, therefore, must be capable of providing the required current pulses into the kicker impedance at demanding rates.

This effort is focused on the use of very fast Drift Step Recovery Diodes (DSRDs), driven by a MOSFET pulser, to obtain bursts of identical energetic pulses at a 3-MHz pulse rate - well beyond that attainable by magnetic pulse compression.

The pulse rate must be 3 MHz for a burst duration of one millisecond, with a bursts repetition rate of 5 Hertz (i.e. the average PRF is 15,000 Hertz). The essential objective of the project is to develop highly repetitive, high-voltage, 2 ns pulses for deflecting packets of electrons and positrons from their respective damping rings (6 km circumference rings) into the 40-km long ILC linear collider, and for nearly simultaneous replenishing of the packets of charge in the damping rings. An increment of deflection will be imparted by a symmetric pair of shaped parallel deflection blades of 30-cm length, pulsed in opposition at 10 kV each for two nanoseconds.

(Ten stages of such deflection will be necessary to produce the overall "kick" required.) Within each guide comprised of the two 30-cm deflector blades and their environment, each TEM wave produced by the two pulse generators traverses from the entrance to the terminus of the guide. Matching 50-Ohm resistors terminate the deflector blades, to avoid creation of secondary traveling waves.

OVERVIEW OF THE APPROACH

The project itself is structured to achieve three critical milestones, (1) development of fabrication of DSRD diode stacks by an established semiconductor device manufacturer (in particular Voltage Multiplier Inc of Vaisala CA), (2) development of instrumentation and methods for characterizing the deflection pulses with sufficient accuracy, and (3) development of a reliable and jitter-free source for producing 40-to-50 nanosecond "pump" pulses at the rate of 3 MHz. These are compressed to 2 nanosecond pulses by the DSRD and one-nanosecond delay line - see Figure 2.

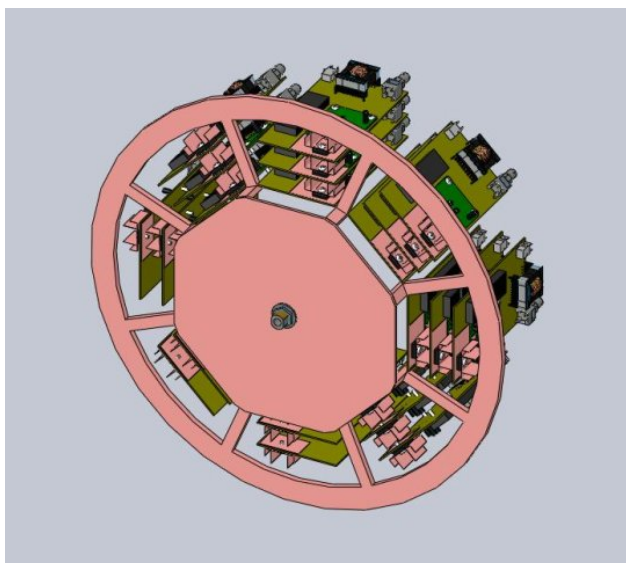

Figure 1: Basic configuration of ILC damping ring pulse generator. Unified 3MHz power/ pulse-synchronization supply and fiber-optic coupled controller are not shown. The one nanosecond delay line emerges from center of plate.

[1] This work supported in part under U.S. Department of Energy SBIR Grant DE-FG02-06ER84459.

DEVELOPMENT OF A NEW HIGHLY BRIGHT X-RAY GENERATOR

Satoshi Ohsawa#, Ikeda Mitsuo, Takashi Sugimura, KEK, Tsukuba, Japan
Noriyoshi Sakabe, KEK, FAIS, Tsukuba, Japan

Abstract

A new type of rotating anticathode X-ray generator has been developed, in which the electron beam irradiates the inner surface of a U-shaped anticathode. We have achieved emission of X-rays 10 times more brilliant than can be attained by a conventional rotating anticathode. The development is still in progress. New results are reported in details.

INTRODUCTION

The U-shaped rotating anticathode X-ray generator has achieved highly brightness by means of using heat of fusion. The electron beams are focused so strong that anticathode material, cupper, is being melted in operation [1]. A high-flux electron beam is focused on the inner surface by optimizing the shape of the bending magnet [2, 3]. In order to minimize the sizes of the X-ray source, the electron beam is focused in a short distance by the bending magnet which is small and is close to the rotating anticathode. The power of the electron beam can be increased over the melting point, because a strong centrifugal force fixes the melting part on the inner surface not to be splashed.

SOUCE SIZE AND RESOLUTION

Electron Beam Focus Size

The electron beam focus size on the U-shaped rotating anticathode was measured using a 10 mm-diameter Au pinhole and a chilled CCD camera with fluorescent film.

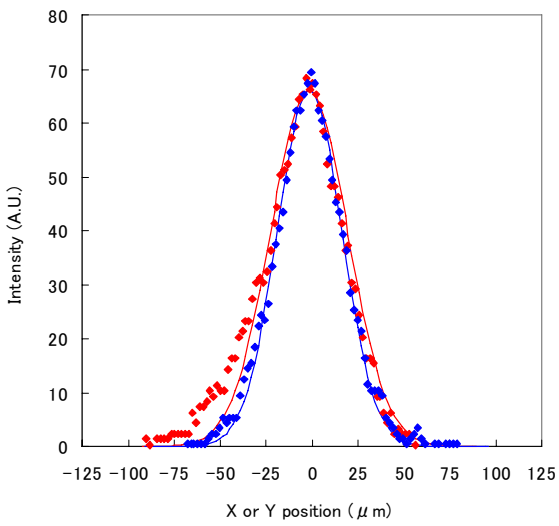

Figure 1: X-ray source distribution on the anticathode.

Figure 1 shows a typical example of the focused electron distribution observed at the takeout angle of 6 degrees from the rotation surface. Each distribution in x and y directions has a FWHM size less than 50μm.

Resolution

In order to estimate resolution, we took an X-ray enlarged picture of a MFT chart, of which line numbers and width are listed in Table 1. Figure 2 shows an example with a magnifying power of 4.7.

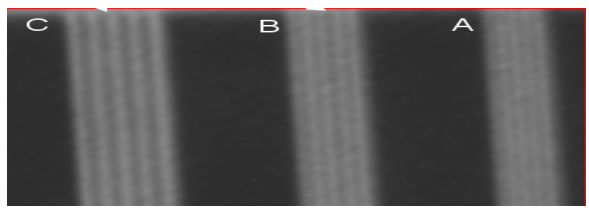

Figure 2: X-ray figure of a MTF chart.

Table 1: MFT chart parameter

Type	Line density	Line width (μm)
A	20 line pairs/mm	25 μm
B	16 line pairs/mm	31 μm
C	12.5 line pairs/mm	40 μm

BRIGHTNESS AND CURRENT

Achieved Brightness

Figure.3 presents examples of the achieved brightness

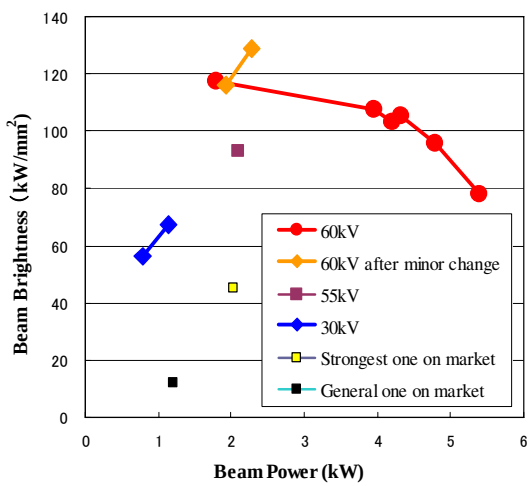

Figure 3: Beam power dependence of brightness.

#satoshi.ohsawa@kek.jp

NUCLEAR REACTION ANALYSIS BY USING QUASI- ELASTIC SCATTERING OF ULTRA LOW INTENSITY ELECTRON BEAMS

Ryoichi Taniguchi, Ryoya Sasaki, Takao Kojima and Shuichi Okuda
Radiation Research Center, Osaka Prefecture University
1- 2 Gakuen- cho, Naka-ku, Sakai, Osaka, Japan

Abstract

High sensitivity nuclear reaction analysis method has been developed by the use of direct nuclear reaction (e,e') with electron bombardment. Huge X-ray burst caused by the bremsstrahlung could be suppressed by the use of ultra low intensity electron beams. Consequently, the neutron emitted by (e,e'n) reaction was measured successfully. The linearity between the neutron count and the concentration of target element was verified experimentally. The method is considered to be useful for the non-destructive analysis of heavy elements such as U and Th.

INTRODUCTION

A beam pulse of an ordinary electron linear accelerator has about 10^{13}electrons. In some cases, the radiation is too intensive. We have attempted to develop an ultra low intensity electron beam system by modifying an electron linear accelerator [(1)]. The minimum beam charge about several aC/pulse has been generated [(2)]. The accelerated electrons are basically mono-energetic, controllable, collimatable and synchronized with the accelerator, which are more favorable features compared with those of β-ray sources. In this study, a new analysis method has been developed by the use of the ultra low intensity electron beam developed.

NUCLEAR REACTION INDUCED BY ELECTRON BOMBARDMENT

Energetic electron beams higher than several MeV occasionally induce direct nuclear reactions with the target nuclei. These processes are attributed to the quasi-elastic scattering of electrons (e,e') with the target nuclei and similar to the photo-nuclear reactions. Theoretically, the reactions are explained that the bremsstrahlung emitted near the nucleus with the electron bombardment (virtual photon) interacts to the same nucleus directly. The experimental results for heavy elements were few, because the reaction becomes to the competitive process with the normal photo-nuclear reaction by the bremsstrahlung emitted from neighboring nuclei. Figure 2 shows an experimental data of electron-disintegration (e,e'n)+(e,e'f) cross section for ^{238}U [(3)] and photo-fission cross section of ^{238}U [(4)]. The figures show that the (e,e') cross section are about one order of magnitude small in comparison with that of the photo-nuclear reaction. However, the following advantages are considered for the purpose of developing a practical nuclear reaction analysis method.

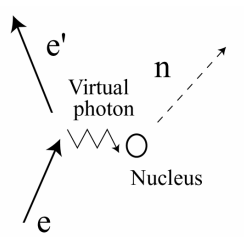

Figure 1: Quasi-elastic scattering of electron

1) The characteristics of the (e,e') reaction are similar to the photo-nuclear reaction. For instance, the both have the same threshold energy. Therefore, the nuclear reaction analysis by using (e,e') reaction has characteristics similar to that of the photo-nuclear reaction analysis. The (e,e') reactions are considered to be effective for analyzing of heavy elements such as U and Th.

2) In the case of the tracer level analysis, the total amount of X-ray burst is far less than that of the photo-nuclear reaction analysis. The X-ray burst is the most harmful phenomenon for the radiation measurement system used in the electron bombardment experiment. In the case of the photo-nuclear reaction analysis, the electron beams are completely transformed to X-rays by a X-ray target, while only partial electrons are transformed to X-rays in the case of the (e,e') analysis.

3) Electron beams are capable of focusing and scanning electrically. The method is considered to be easy of developing to a 2-dimensional analysis method only by the scanning of electron beam.

In the next section, the feasibility of the neutron detection with the electron bombardment are examined experimentally.

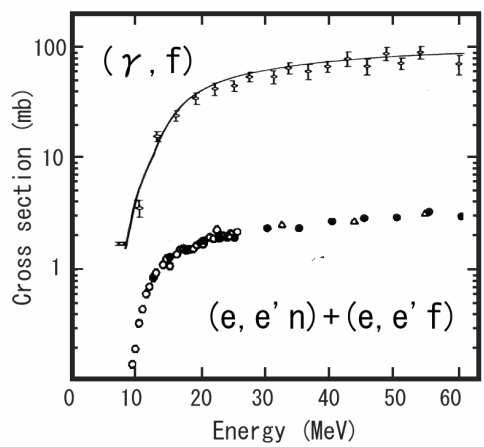

Figure 2: Photo-fission cross section [(4)] and electro disintegration cross section[(3)] of ^{238}U.

DEMONSTRATION OF MULTI-PULSE X-RAY GENERATION VIA LASER-COMPTON SCATTERING USING PULSED-LASER SUPER-CAVITY*

K. Sakaue,† M. Washio, Waseda University, Tokyo, Japan
S. Araki, M. Fukuda, Y. Higashi, Y. Honda, T. Taniguchi, T. Terunuma, J. Urakawa,
KEK, Ibaraki, Japan
N. Sasao, Kyoto University, Kyoto, Japan

Abstract

A compact and high quality x-ray source is required for various field, such as medical diagnosis, drug manifacturing and biological sciences. Laser-Compton based x-ray source that consist of a compact electron storage ring and a pulsed-laser super-cavity is one of the solutions of a compact x-ray source. Pulsed-laser super-cavity has been developed at Waseda university for a compact high brightness x-ray source. The pulsed-laser super-cavity enables to make high peak power and small waist laser at the collision point with the electron beam. 357 MHz mode-locked Nd:VAN laser pulses can be stacked stably in a 420 mm long Fabry-Perot cavity with "burst mode", which means stacking of electron beam synchronized amplified pulses in our R& D. In view of this successful result, we have started an X-ray generation experiment using a super-cavity and a multi-bunch electron beam at KEK-LUCX. Recently, the demonstration experiment between the burst mode pulsed-laser super-cavity and the 100 bunch multi-bunch electron beam is successfully performed. Development of the super-cavity and the experimental results of X-ray generation will be presented at the conference.

INTRODUCTION

Recently, x-rays from synchrotron radiation (SR) is widely used and produced a number of results in various fields, for example, medical diagnosis, biological sciences, material sciences and so on. However, SR x-rays is generated by the huge facility as SPring-8, therefore the use is limited by the operation schedule and the number of users. On these backgrounds, a compact x-ray source has been strongly required and studied in many laboratories. In 1997, Huang and Ruth proposed a compact laser-electron storage ring (LESR) for electron beam cooling or x-ray generation.[1] In this proposal, each electrons and photons storage in storage ring and super-cavity, respectively, and therefore electrons and photons continuously interact and generate a high flux x-rays through the laser-Compton process.

We have developed a laser cavity system as a laser-wire beam profile monitor for measuring the electron-beam emittance at KEK-ATF.[2] We proposed to apply this for pulsed-laser stacking to achieve the high peak power photon target. To use this super-cavity and an electron storage ring, the high peak power laser in super-cavity is scattered by the electron beam continuously, and generate a high quality and high flux x-rays up to 10^{14} photons/sec.[3] On the other hand, to use a multi-bunch electron linac and a "burst mode" super-cavity (see Sec. 3), high peak power laser target can be produced, which synchronized with a multi-bunch electron beam, so that linac based compact x-ray source is also readily achievable.

As the first step, we are performing a proof-of-principle experiment of laser-Compton scattering between pulsed-laser super-cavity and multi-bunch electron beam. We call this linac based x-ray source, "LUCX" (Laser Undulator Compact X-ray source).

LUCX ELECTRON ACCELERATOR

LUCX multi-bunch electron linac is built by the side of the KEK-ATF accelerator. Figure 1 shows the beam line layout of LUCX. As shown in Figure 1, the accelerator

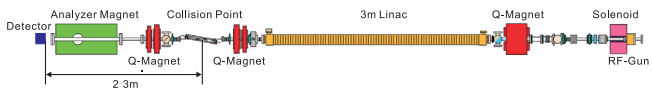

Figure 1: LUCX Electron Beam Line

consists of a photo-cathode RF-Gun and 3 m-long linac to generate and accelerate a multi-bunch electron beam up to 43 MeV. Beam loading effect in the accelerating structure is compensated by adjusting the timing of rf pulse and so the energy difference in a bunch train is compensated less than 1%.[4] The parameters of a multi-bunch electron linac is shown in Table 1.

Table 1: Parameters of Multi-bunch LINAC

Bunch Charge	Energy	Num. Bunch	Rep Rate
0.4 nC	43 MeV	100/Train	12.5 Hz

Laser-electron interaction point is located between the doublet quadrupole magnets to focus at the interaction point and to re-focus a diverging electron beam. At the interaction point, pulsed-laser super-cavity is installed at an angle of 20 deg with beam line, which can produce a high

* Work supported by a Grant-In-Aid for Creative Scientific Research of JSPS (KAKENHI 17GS0210) and a Grant-In-Aid for JSPS Fellows (19·5789)
† kazu-kazu-kazu@suou.waseda.jp

COMMISSIONING OF 10-MEV L-BAND ELECTRON LINAC FOR INDUSTRIAL APPLICATIONS *

S. H. Kim#, H. R. Yang, Y. G. Son, S. D. Jang, S. J. Park, M. Cho, W. Namkung,
POSTECH, Pohang 790-784, Korea

J. S. Oh, NFRI, Daejeon 305-333, Korea

Abstract

An intense L-band electron linear accelerator is now being commissioned for industrial applications in collaboration with POSTECH and KAPRA. It is capable of producing 10-MeV electron beams with the 30-kW average beam power. For a high-power capability, we adopted a traveling-wave structure operated with 2π/3-mode at 1.3 GHz. The structure is powered by the 25-MW pulsed klystron with the 60-kW average RF power. The RF pulse length is 8 μs while the beam pulse length is 7 μs due to the RF filling time into the accelerating structure. The accelerating gradient is 4.2 MeV/m at the beam current of 1.45 A, the fully-beam-loaded condition. In this paper, we present details of the accelerator system and commissioning results.

INTRODUCTION

Recently, there are increase demands on electron linear accelerators for industrial applications [1]. In using electron beams as irradiation sources, the higher beam energy is favorable since the penetration depth is larger. However, the electron beam energy is limited by about 10 MeV due mainly to neutron production. For the clinical X-ray systems, a low current and a low repetition rate are required. The X-ray source for the container inspection requires 5-10 MeV with a few kilowatts of the average beam power [2]. On the other hand, the food or waste sterilization system requires relatively high average beam power to which the process speed is proportional [3].

A high average-power electron accelerator is being developed in the institutional collaboration with PAL/POSTECH and KAPRA. The accelerator is installed at CESC and it will be used for not only for sterilizing foods and medical products, but also reforming materials. The accelerator is required to provide an average beam power of 30 kW at the beam energy of 10 MeV. In order to treat such a high-power, an L-band RF system and accelerating column is adopted due to thermal stability compared with an S-band. A travelling-wave accelerating structure is adopted for industrial purposes due to the following reasons. It needs no circulator necessary for the standing-wave structure. It makes the system simpler and less expensive. Also the RF power coupling is insensitive to the beam-loading effect. It makes the operation of system easier. The design details are presented in table 1 and test results in the following sections.

Table 1: Accelerator Parameters

Accelerator Parameters	
Operating Frequency	1.3 GHz
Pulsed RF Power	25 MW
RF Pulse Length	8 μs
Repetition Rate	300 Hz
Averaged RF Power	60 kW
E-gun High Voltage	- 80 kV
Pulsed E-gun Current	1.6 A
Beam Pulse Length	7 μs
Beam Energy	10 MeV
Output Beam Current	1.45 A
Beam Transmission Rate	90%
Averaged Beam Power	30 kW
Shape of Accelerating Cell	Disk-loaded
Operating Mode of Accelerator	2π/3 mode
RF Filling Time	0.8 μs
Operating Temperature	40°C ± 1°C
Averaged Accelerating Gradients	4.2 MV/m
Beam Loading Factor	- 4.7 MeV/A
Temperature Shift Factor	- 2.3 MeV/1°C

RF MEASUREMENT

The Thales klystron tube (TV2022D) generates 25-MW pulsed RF with 8-μs pulse length and 300-Hz pulse repetition rate. It is powered by a matched pulse modulator, composed of a set of inverter power supplies, a pulse forming network and a thyratron switch.

The inverter power supplies are 8 units in total, each of 45 kV and average 30 kW. The PFN has 15 stages, each with a 50-nF capacitor and a 2.2-μH inductor. The EEV thyratron tube (CX2412X) switches pulsed power of 45 kV and 3 kA. The klystron tube with perveance of 1.6

*Work supported by KAPRA and POSTECH BK21 Program.
#khan777@postech.ac.kr

PROJECT OF A NEUTRON SOURCE BASED ON THE SUB-CRITICAL ASSEMBLY DRIVEN BY ELECTRON LINEAR ACCELERATOR*

V. Azhazha, A. Dovbnya, I. Karnaukhov, A. Kostromin, V. Krasnorutzkiy, I. Neklyudov, S. Perezhogin, S. Soldatov, A. Zelinsky, NSC KIPT, Kharkov, Ukraine
M. Gohar, ANL, Argonne, IL 60439, U.S.A. I. Bolshinsky, INL, Idaho 83403, U.S.A.

Abstract

Today accelerator driven subcritical assembly is candidate for the next generation of energy-generating nuclear facility, which could provide safe energy production, burning of trans uranium elements and transmutation of the radionuclides. Use of the electron beam with particle energy up to 150-200 MeV secures several advantages. Electron linear accelerators are much cheaper compare to hadron accelerators. Homogeneous irradiation of the assembly with neutrons could be provided. NSC KIPT together with ANL develops the project of a neutron source based on the sub-critical assembly driven by electron linear accelerator. Energy of electrons is 100-200 MeV. The target and assembly design is optimized to maximize the neutron source intensity with subcriticality of 0.98. Accelerator on average beam power of 100 kW, with repetition rate up to 300 Hz and pulse duration of 3,2 μs is under development. Transportation line should provide beam transfer with minimal losses of electrons and should form homogeneous distribution of the particle density at the target. Maximal value of a neutron flux is F_m=2.4×10^{13} n/(cm^{2}s), and power of energy release in the result of nuclei fission is P_m≈ 100 kW.

INTRODUCTION

National Science Center "Kharkov Institute of Physics and Technology" (NSC KIPT, Kharkov, Ukraine) together with Argonne National Laboratory (ANL, USA) develops the conceptual project of a neutron source based on the sub-critical assembly driven by electron linear accelerator. The main functions of the subcritical assembly are to support of the nuclear industry and medical researches. Reactor physics and material researchs will be carried out at the facility. The goal of the development is to create in Ukraine the experimental basis for neutron research based on safe intensive sources of neutrons. The main facility components are an electron linear accelerator, a system for electron beam transportation from linear accelerator to the target, neutron production target, subcritical assembly, biological shield, neutron channels and auxiliary supporting systems.

Neutron source is a hybrid facility, which is composed from high-current electron accelerator and subcritical assembly. Photonuclear reactions, induced by hard electromagnetic radiation emerging at retarding of the beam of relativistic electrons in the target from heavy element, are used to generate primary neutrons. Two options of the target are under consideration: tungsten and natural uranium. Energy of electrons in driven beam is 100-200 MeV. The sectioned construction of a neutron-generating target has been selected based on depositing of energy and thermo-hydraulic calculations.

The core of the sub-critical assembly on thermal neutrons is made of fuel elements based on the enriched uranium with level of enrichment of 20% uranium isotope-235. Water is a neutron moderator and coolant. Graphite is used as neutron reflector. The target and subcritical assembly is designed to obtain neutron flux as high as possible with subcriticality of 0.98. Thus, possibility of chain reaction occurrence is excluded in the facilities of such a type. Maximal magnitude of neutron flux F_m, one of the main characteristics of the source, depends on beam parameters of the accelerated particles, efficiency of neutron yield from the neutron-generating target and characteristics of the sub-critical assembly. Magnitude of neutron flux is regulated by beam current and neutron field in the source disappears after shutting down the driving beam.

In the described facility the maximal meaning of middle plane of a neutron flux averaged by time using uranium target and nominal power of electron beam makes F_m=2.4×10^{13} n/(cm^{2}s), and power of energy release in the result of nuclei fission of U^{235} makes P_m≈ 250 kW. Considerable proportion of fast neutrons as well as of neutrons of intermediate energies is in energy spectra together with thermal neutrons.

This pater is the first publication inended to describe the main parameters and status of the facility.

The start of the described project can be marked as 2006. At the moment the conceptual design project of the neutron source are desigen and egieniering development of the facility systems are began.

SUB-CRITICAL ASSEMBLY BUILDING

The arrangement of the neutron source based on the accelerator-driven sub-critical assembly is shown in Fig. 1. The linear accelerator is located in the building of the former linear electron accelerator LUE-2000 (1). The electron beam is transported from the accelerator through the transport channel (2) to the sub-critical assembly (3). The sub-critical assembly is to be installed in the experiment room 24x36 m of a new building adjacent to the accelerator building. The sub-critical assembly building contains all the sub-critical assembly elements, neutron channels, neutron stations, and auxiliary systems. The three-storied part of the sub-critical assembly building (5) will host the control room, express laboratories, and all support systems.

The radial dimension of the heavy-concrete biological shielding with a density of 4.6 g/cm^3 is 1.8 m. The

*Work supported by STCU Project P-233
dovbnya@kipt.kharkov.ua

LOW ENERGY PHOTOEMISSION ELECTRON SOURCE FOR APPLICATIONS IN THZ RADIATION PRODUCTION AND TIME-RESOLVED ELECTRON MICROSCOPY*

N. Vinogradov, P. Piot, C. Prokop, Northern Illinois University, DeKalb, IL 60115, USA
J. Lewellen, J. Noonan, AST DoD Project Office, Argonne National Laboratory, Argonne, IL 60440, USA

Abstract

A simple, inexpensive, and compact low-energy (~20 KeV) photoemission electron source was designed, built and recently commissioned. It uses a commercial ultraviolet photocathode drive laser producing 3 ns (FWHM) pulse. The source will eventually be used to drive a table-top THz radiation source, based on the Smith-Purcell free-electron laser scheme, and could also have potential application to time-resolved electron microcopy. We present experimental measurements of the photoemitted electron beam and numerical simulations of the anticipated parameters. We also discuss the generation of flat beams required to efficiently drive the THz radiation source.

INTRODUCTION

Generation of pulsed electron beams is essential for a variety of applications. In the electron sources based on thermionic and field emission effects it can be obtained by pulsing the extracting voltage, therefore, the temporal beam properties in this case are defined by the performance of the pulsed high voltage power supply. In the case of photoemission-based sources, the electron bunch mirrors the driving laser pulse that dictates the longitudinal and transverse properties of the bunch [1]. Low-energy pulsed electron beam can be generated using a simple, compact structure with dc accelerating field between anode and photocathode. This beam is characterized by very low transverse emittance because the initial transverse energy of the photoelectron is the same as its work function, i.e. a few eV. An additional advantage of photoemission-based sources is a possibility of producing spin-polarized electron beams that can be done, for instance, by impinging a circularly-polarized laser on a strained GaAs photocathode [2]. The time-resolved microscopy and spin-polarized electron microscopy are examples of promising applications for a low-energy photoemission electron gun. Besides, such a source can ideally serve as a driver for compact Smith-Purcell Free-Electron Laser in order to produce THz radiation [3]. In this approach a flat electron beam is propagated over metallic grating thereby producing radiation by periodical motion of the induced surface charge.

Recently we have constructed and commissioned the electron gun to study the physics and operation of a source based on the aforementioned conceptual framework [4]. The source generated >20 keV electron bunches with 1.3±0.1 ns RMS duration and 4±0.2 nC charge that corresponds to a peak current of about 1 A. The experimental results of the source commissioning along with detailed numerical model for the flat beam generation are subjects of this report.

SOURCE DESIGN AND PERFORMANCE

The source structure consists of grounded anode with the beam aperture in the center and biased cathode shaped as a truncated cone for initial focusing of photoelectrons emitted from the central planar area of the electrode. Pure copper was chosen as a cathode material due to simplicity, low cost and modest vacuum requirements. The work function of copper is relatively high (4.65 eV) and requires an ultraviolet (uv) laser as a driver. We used a commercial frequency-quadrupled Nd:YAG laser from Continuum Inc. [5]. The laser operates at 266 nm wavelength (corresponding to a photon energy of 4.66 eV) and is specified to produce 1.3~2.1 ns RMS pulses with energy up to 4 mJ per pulse at repetition rate of 1 to 15 Hz. The quantum efficiency (ratio of number of emitted electrons over the number of photons in the incoming laser pulse) is typically low for pure metals and was reported to be in the range $10^{-6} \div 10^{-4}$ for copper. For the given laser beam energy, the expected total bunch charge of a photoemitted bunch is a few nC. The laser beam is transported using an optical system composed of uv lenses and mirrors to irradiate the cathode through a sapphire window at 45 deg incidence angle. Measurements of the laser pulse energy and duration are performed using a powermeter and a fast photodiode respectively. The transverse distribution of the laser intensity on the cathode is directly monitored using a combination of CCD camera and "virtual cathode" that is one-to-one optical image of the real cathode on a uv-sensitive screen located outside of the vacuum enclosure. The dc bias voltage applied to the cathode can reach 20 kV that corresponds to 0.5 MV/m for axial surface field in the center of cathode and 1.1 MV/m maximum field achieved approximately in the middle of anode-cathode gap. A fast Faraday Cup for bunch charge and length measurements was fabricated and installed on the source axis about 1 cm downstream the anode aperture. All components of the source are mounted inside the vacuum chamber equipped with various ports to connect the vacuum pumps, sapphire window, electrical feedthrough, etc. An overview of the experiment setup appears in the Fig. 1.

Extensive beam measurements have been carried out for a wide range of accelerating voltage, laser pulse energy, and size of the laser spot on the cathode. An

[1] Work supported by the Department of Education under contract P116Z010035 with Northern Illinois University.

THE ISAC-II SC-LINAC OVER CURRENT MONITORING SYSTEM

A.K. Mitra, J. Drozdoff, K. Langton, R.E. Laxdal, M. Marchetto, W.R. Rawnsley, J.E. Richards,
TRIUMF, Vancouver, Canada

Abstract

A personnel protection system is used to monitor the ion beam current into the experimental hall from the ISAC-II SC-linac. Two resonant capacitive pickups in the transfer line operate at 35.36 MHz, the third harmonic of the bunch rate. Ion charge, velocity and bunch width affect the sensitivity so calibration with dc Faraday cups is needed. Each monitor has a single conversion receiver with an active mixer. LO signals are provided by frequency synthesizers locked to the accelerator synthesizer. The 1250 Hz IF signals are amplified, filtered with a 100 Hz bandwidth and amplitude detected. An antenna in each monitor loosely couples a pulsed RF test signal to each pickup. These induced signals are mixed down to 11.875 kHz, filtered, detected and used to provide watchdog signals. The measured currents are displayed through our EPICS control system which allows setting of the gain ranges, trip levels and conversion factors. The signals are also processed independently by dedicated analog comparators and CPLDs to cause the Safety system to trip the beam if the current exceeds a nominal 5 to 10 nA.

INTRODUCTION

A pair of Non-Intercepting beam current Monitors (NIMs) have been installed in the ISAC-II accelerator vault downstream of the SC-linac. Fig. 1 shows a recent calibration using dc Faraday cups downstream of each monitor. The sensitivity of less than 0.1 nA is sufficient for generating beam trips from 5 to 10 nA. The pickups have been described previously [1]. The electronics and Safety system aspects will be described here.

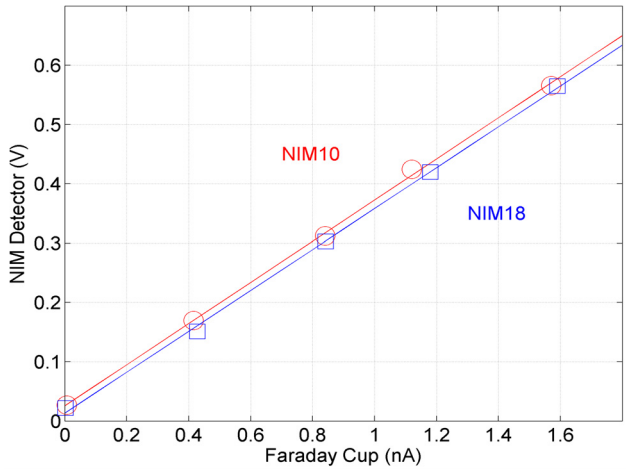

Figure 1: Calibration data using a $^{22}Ne^{+2}$ 2.7 MeV/u ion beam with straight line fits.

SYSTEM

Front End Electronics

The buffered NIM signals are brought out of the vault on Heliax solid shielded coax to the electronics racks, see Fig. 2. Each NIM signal passes through an Analog Devices AD8332 low noise amplifier. The Local Oscillator (LO), an Agilent N5181A frequency synthesizer, is locked to the 10 MHz reference from the accelerator synthesizer to minimize frequency drift. Its frequency is set to be offset from the signal frequency and multiplied by 4 to accommodate the AD8333 I/Q demodulator. The demodulator divides the LO down and

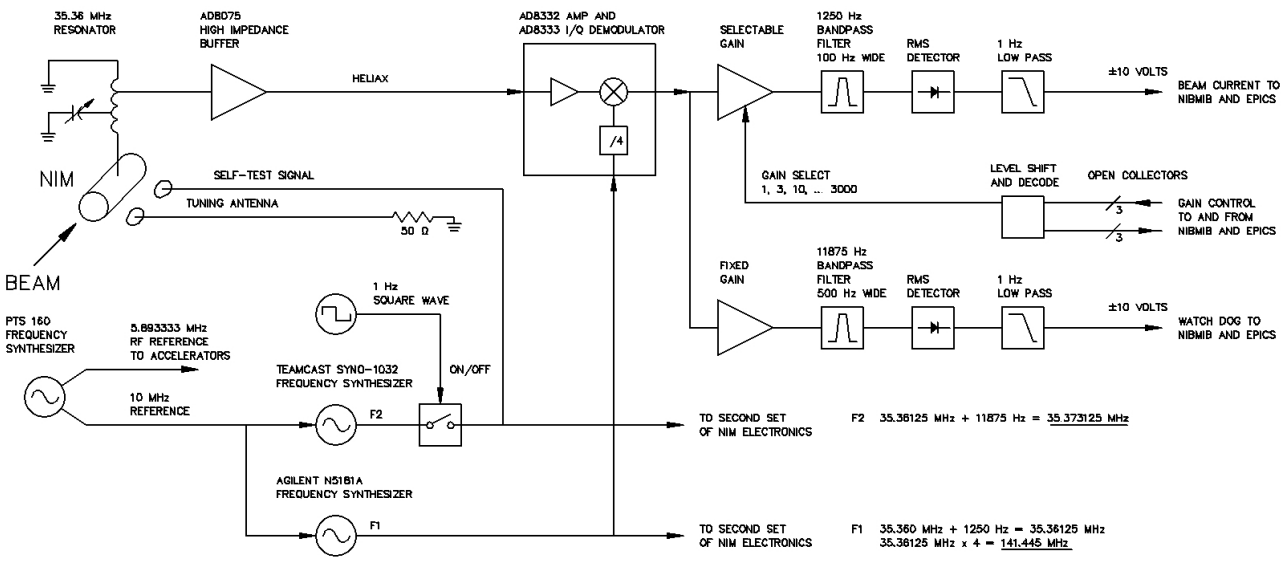

Figure 2: A block diagram of the front end electronics.

AIRIX DIAGNOSTIC DEVICES FOR FOCAL SPOT SIZE AND DOSE MEASUREMENTS

O. Pierret, CEA, Pontfaverger-Moronvilliers

Abstract

AIRIX is a 2 kA, 19 MeV, 60 ns, single shot linear accelerator that produces X-rays from the interaction between relativistic electrons and a Tantalum solid target (Ta). Focal spot size, integrated and temporal dose are the main characteristics that we need for the successful development of flash radiography at hydro test facilities. MTFX is a 12 bit Charge-Coupled Device (CCD) intensified camera which is equipped with a scintillator. It can give focal spot size measurements in two directions using a two dimensional wedge. By another way Mucaddix is a CVD Diamond detector which is integrated nearby the AIRIX X-ray beam source. It gives integrated dose, time resolve dose, temporal characteristics of the X-ray flash and timing of the flash respect to the start of object implosion. These two measurement systems are described and the quantified results are reviewed here.

CONTRIBUTION NOT RECEIVED

TAILORING THE EMITTANCE OF A CHARGED PARTICLE BEAM WITH A TUNNEL EMITTANCE METER

Reinard Becker, Institut für Angewandte Physik der Goethe–Universität Frankfurt, Germany

Abstract

Based on the "tunnel" emittance used for electron beam focusing, a similar procedure is proposed to evaluate fractional emittances for ion beams using two pairs of slits with variable widths. A measurement starts with closing both slits (one after the other) until a specific fraction of the transmitted beam current is cut off. The emittance and brilliance can then be well defined for the transmitted beam. Formulae are given for the emittance as well as for the brilliance as a function of the slit widths and beam current. This emittance measurement technique is free from the background subtraction problem found in the classical density measurement of phase space(s). The measurement device is also at the same time an adjustable emittance/brilliance filter for the transmitted beam. The emittance and/or brilliance of a beam can thus be tailored to any value within the limits of the beam quality at the expense of transmitted beam current**.**

INTRODUCTION

The emittance of ion sources is generally considered an important characteristic value, especially when the ion source will be used in combination with a beam line or the low energy transport (LEBT) section of an accelerator having a well-defined acceptance. Acceptances of beam lines and accelerators usually have the shape of ellipses with uniform density, characterized by the twiss parameters of these elliptical bounded phase spaces. While the matching conditions appear to be well defined by the accelerator expert, the ion source developer has great difficulty in satisfying these requirements for the following reasons:

- Ion source emittances, either measured or calculated, usually are not elliptically bounded but show wings of aberrations caused by the extraction system and the lenses.
- The emittance areas are not uniformly filled.
- Defining an exact value of the emittance is a matter of sophisticated background subtraction [1].

As a solution, we propose here a procedure to not only measure the emittance and brilliance of a beam in a simple and unambiguous way but to also define the beam quality by analysing its fractional emittance. This experimental procedure is based on the well-established experience of electron tube designers in the 1960's who characterized the quality of an electron gun by a "tunnel" emittance device. Recently this procedure has been modified [2,3] by replacing the tunnel with two pairs of slits for the x- and the y-direction.

TUNNEL EMITTANCE

About 50 years ago the microwave industry developed GHz oscillators and rf-amplifiers called travelling wave tubes (TWT). A medium energy electron beam (similar to that of an EBIS) was focused in a strong solenoid (or an alternating permanent magnet structure) of some kilogauss and inside of a helical rf-structure, amplifying the velocity modulation on the beam by bunching. In order to measure the quality (=emittance) of such a gun and beam forming system a very practical experimental procedure has been developed. The beam is injected into a "tunnel" which is a cooled piece of copper with a hole drilled in it for the electron beam to pass through. Then the experiment shows that the smaller the hole and the higher the transmission at high current, the better the gun quality! [4]

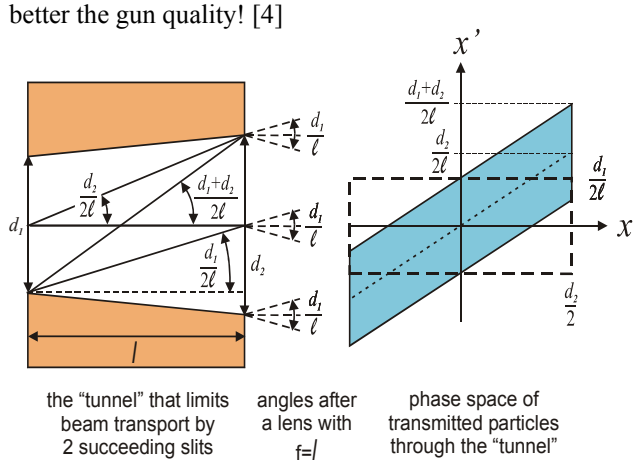

Figure 1: Definition of the tunnel emittance, showing how angles are defined by slit widths and the distance of the two apertures (left panel) and how this translates to the 2D phase space (right panel).

Referring to Fig. 1, assuming that the second aperture with width d_2 is fully illuminated by the beam passing through the first aperture with width d_1 we find the relations for the angles shown on the left characterizing the shaded phase space on the right. By focusing with a thin lens in the position of the second aperture with focal length $f = \lambda$, the shaded parallelogram can be turned into the dashed rectangle. This produces the dashed rays found at the right side of the left panel. By definition the **full** emittance ε_{full} then is calculated as the area of this rectangle with side lengths of d_2 and d_1/λ:

$$\varepsilon_{full} = \frac{d_1 d_2}{\lambda} \quad [m] \qquad (1)$$

COMMISSIONING OF THE HITRAP DECELERATOR USING A SINGLE-SHOT PEPPER POT EMITTANCE METER*

J. Pfister†, R. Nörenberg, U. Ratzinger
Institut für Angewandte Physik, Goethe-Universität Frankfurt, Frankfurt am Main, Germany
W. Barth, L. Dahl, P. Forck, F. Herfurth, O. Kester, T. Stöhlker
GSI, Darmstadt, Germany

Abstract

The Heavy Ion TRAP (HITRAP) project at GSI is in the commissioning phase. Highly charged ions up to U^{92+} provided by the GSI accelerator facility will be decelerated and subsequently injected into a large Penning trap for cooling to the meV/u energy level. A combination of an IH- and an RFQ-structure decelerates the ions from 4MeV/u down to 6keV/u. In front of the decelerator a double drift-buncher-system is provided for phase focusing and a final de-buncher integrated in the RFQ-tank reduces the energy spread in order to improve the efficiency for beam capture in the cooler trap. This contribution concentrates on the beam dynamics simulations and corresponding measurements in the commissioning beam times up to the position of the entrance to the RFQ. Single-shot emittance measurements at higher energies using the GSI pepper pot device and construction of a new device using Micro Channel Plate technology for low energies as well as profile measurements are presented.

HITRAP FACILITY AT GSI

The highly charged ions are accelerated in the heavy ion synchrotron to typically 400MeV/u, almost completely stripped and injected into the experimental storage ring (ESR). Here, they are first treated by stochastic cooling and decelerated to an intermediate energy level of 30 MeV/u. Then they are electron-cooled and further decelerated to 4 MeV/u. After another electron cooling cycle the ions are ejected from the ESR as a bunch of about $10^5 - 10^7$ ions depending on the element and a pulse length of 1-2 µs. Then they enter the linear decelerator of HITRAP. The final goal is the reduction of a deceleration cycle (filling the ESR, cooling, deceleration and ejection) down to 10-20s. Before the ion bunch enters the drift tube structure, the ion pulse is micro bunched by the double-drift buncher (DDB). After deceleration in the IH-structure as well as the RFQ, the ions enter the Cooler (Penning) trap with only 6 keV/u, where they can be confined by a combination of electrostatic and magnetic fields. By sympathetic cooling with cold electrons the trapped highly charged ions will reach a thermal energy corresponding to ~4K. The cold ions are then transported, with kinetic energies of only a few keV*q, to the different setups installed on top of the re-injection channel as a high-quality, low emittance, highly charged ion beam [1].

LINAC COMMISSIONING

After deceleration and cooling of the ions down to 4MeV/u in the ESR, they were ejected via the transport line towards the HITRAP linac (see Fig. 1). The DDB is the first component of the HITRAP linac and is used for phase focussing. It was commissioned during two beam times in 2007 with an uncooled beam of the lighter ion species $^{64}Ni^{28+}$ and $^{20}Ne^{10+}$. The next structure is the IH-structure that decelerates the ions down to 500keV/u. Its initial commissioning took place in August 2008 with a partially cooled heavy $^{197}Au^{79+}$ beam and will be continued in October of this year [2]. For beam diagnostic measurements there are phase probes as well as beam diagnostic stations installed in the beamline. They house Faraday cups, grids and YAG-scintillation targets. Furthermore there were a single-shot pepper pot emittance meter and a diamond detector installed for transversal and longitudinal emittance measurements.

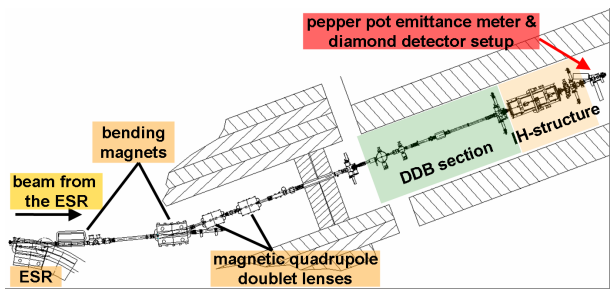

Figure 1: Overview of the transport beam line from ESR towards the position of the pepper pot emittance meter (later: position of the RFQ entrance).

Single-shot Emittance Measurements

Since the HITRAP linac gets a bunch of ions only every 35-60 seconds from the ESR during commissioning the single-shot pepper pot emittance meter is the ideal choice for this task. The GSI pepper pot device has been adapted to the special needs at HITRAP and a new evaluation software has been developed [3].
In 2007 emittance measurements were done at the position of the entrance of the IH-structure whereas in August 2008

* work supported by BMBF under contract 06FY160I
† jpfister@gsi.de

DITANET: A EUROPEAN INITIATIVE IN THE DEVELOPMENT OF BEAM INSTRUMENTATION FOR FUTURE PARTICLE ACCELERATORS

C.P. Welsch
University of Heidelberg, GSI, Darmstadt and MPI-K, Heidelberg, Germany
on behalf of the DITANET consortium

Abstract

Without an adequate set of beam instrumentation, it would not be possible to operate any particle accelerator, let aside optimize its performance. In a joint effort between several research centres, Universities, and partners from industry, DITANET aims for the development of beyond-state-of-the-art diagnostic techniques for future accelerator facilities and for training the next-generation of young scientists in this truly multi-disciplinary field. The wide research program covers the development of beam profile, current, and position measurements, as well as of particle detection techniques and related electronics.

This contribution introduces this new Marie Curie Initial Training Network, presents the DITANET partner institutes, and gives an overview of the various research and training activities.

INTRODUCTION

Marie Curie Initial Training Networks (ITN) are aimed at improving the career perspectives of researchers who are in the first five years of their career by offering structured training in well defined scientific and/or technological areas as well as providing complementary skills and exposing the researchers to other sectors including private companies.

The European Training Network DITANET - "DIagnostic Techniques for particle Accelerators – a Marie Curie initial training NETwork" - covers the development of advanced beam diagnostic methods for a wide range of existing or future accelerators, both for electrons and ions. It is the largest-ever education action for PhD students in the field of beam diagnostic techniques for future particle accelerators and officially started on 1.6.2008 with a total budget of up to 4.2 M€.

DITANET covers the development of advanced beam diagnostic methods for a wide range of existing or future accelerators, both for electrons and ions. DITANET consists of the following network participants:

University of Heidelberg (coordinator, Germany), CEA (France), CERN (Switzerland), DESY (Germany), GSI (Germany), HIT GmbH (Germany), IFIN-HH (Romania), Stockholm University (Sweden), Royal Holloway University of London (UK), and the University of Seville/Centro Nacional de Aceleradores (Spain).

The network is complemented by twelve associated partners from all over the world:

ESRF (France), idQuantique (Switzerland), INFN-LNF (Italy), Instrumentation Technologies (Slovenia), MPI for Nuclear Physics (MPI-K), PSI (Switzerland), THALES (France), Thermo Fisher Scientific (USA), TMD Technologies Limited (UK), TU Prague (Czech Republic), ViALUX (Germany), and WZW Optics (Switzerland).

TRAINING

Beam diagnostics systems are essential constituents of any particle accelerator; they reveal the properties of a beam and how it behaves in a machine. Without an appropriate set of diagnostic elements, it would simply be impossible to operate any accelerator complex let alone optimize its performance. Beam diagnostics is a rich field in which a great variety of physical effects are made use of and consequently provides a wide and solid base for the training of young researchers. Moreover, the principles that are used in any beam monitor or detector enter readily into industrial applications or the medical sector, which guarantees that training of young researchers in this field is of relevance far beyond the pure field of particle accelerators.

Young researchers participating in DITANET will not only get the possibility to perform state-of-the-art research, they will also get a much wider training in the domain of beam diagnostics by interaction with other network participants and close collaboration with associated partners from the industrial sector. This includes regular exchanges of trainees between the partners that will thus get the possibility to participate in ongoing R&D work at linked institutes and universities.

This way, DITANET will provide a cohesive, flexible framework for the training and professional development of researchers in beam diagnostic techniques for particle accelerators, with a strong focus on possible applications of these principles in industry.

In addition, DITANET will organize one week courses on beam diagnostic techniques in spring 2009 at Royal Holloway University of London and in fall 2010 at Stockholm University that will be open to all network participants as well as to external participants. Details on these courses will be published on the DITANET web site [1].

RESEARCH

Future accelerator projects will require innovative approaches in particle detection and imaging techniques to provide a full set of information about the beam characteristics. DITANET covers a wide range of future

DESIGN OF A BEAM HALO MONITOR WITH A HIGH DYNAMIC RANGE

J. Egberts[1], S. Artikova[1], E. Bravin[2], T.Chapman[3], T. Lefèvre[2], M.Pilon[3], C.P. Welsch[1,4,5]
[1]MPI-K, Heidelberg, [4]University of Heidelberg, [5]GSI, Darmstadt, Germany
[2]CERN, Geneva, Switzerland,[3]Thermo Fisher Scientific, Liverpool, NY USA

Abstract

A thorough understanding of halo formation and its possible control is highly desirable for essentially all particle accelerators. Limiting the number of particles in the halo region of a beam would allow for minimizing beam losses and maximizing beam transmission, i.e. the experimental output. Measurements based on either optical transition radiation (OTR) or synchrotron radiation (SR) provide an interesting opportunity for high dynamic range measurements of the transverse beam profile, since the signal is linear with the beam charge over a wide range and is routinely used in many diagnostic applications. In this contribution, first results on beam halo measurements obtained from a flexible core masking technique and an innovative CID camera system are summarized.

INTRODUCTION

The detection and possible control of the beam halo is of utmost importance for high energy accelerators, where unwanted particle losses lead to an activation or even damage of the surrounding vacuum chamber [1], [2]. But also in low-energy machines, like the ultra-low energy storage ring (USR) [3] at the future facility for antiproton and ion research (FLAIR) [4], one is interested in minimizing the number of particles in the tail region of the beam distribution. Since most part of the beam is normally concentrated in the central region, observation techniques with a high dynamic range are required to ensure that halo particles can be monitored with sufficient accuracy. One option to monitor the beam halo is to use light generated by the beam, either through SR, OTR, or luminescent screens. In thus case, a special camera technology is required to allow for high dynamic range measurements.

But also for low energy accelerators and storage rings like the USR such measurements can be envisaged by e.g. exploiting the light from a phosphor screen.

In order to approximate a typical beam distribution as it is found in an accelerator we used a conventional laser beam in our lab. The open angle of the laser of 0.1 corresponds to SR/OTR emitted at some 100 MeV and can be regarded as a realistic approximation of a real particle beam.

CID CAMERA

The charge injection device (CID) derives its name from its unique ability to clear individual pixel sites of photon-generated charge by injecting the charge directly into the substrate. The main features of this imager technology are its distinctive readout capabilities including inherent resistance to ionizing radiation, inherent resistance to charge blooming, true random pixel addressability, non-destructive pixel readout (NDRO), and on-sensor collective pixel readout and clear.

Architecture

The on-sensor collective read feature allows the data acquisition routines to select contiguous pixel regions (e.g., a 3 by 3 pixel region) and interrogate those pixels with a single reading that is the electronic average of the signals on those pixels, thereby improving both readout speed and signal-to-noise ratio. This collective read feature is analogous to the binning that can be performed with certain CCD camera systems. However, unlike the CCD where the charge packets from the individual pixels are physically combined into a single larger charge packet, the CID collective read feature preserves the spatial integrity of the photon-generated charge in the pixels and the read process is non-destructive to that charge. The CID architecture also allows for the clearing of photon-generated charge from contiguous pixel regions with a single inject pulse. Similar to most micro-electronic devices built today, the CID is manufactured with silicon technology. A single crystal silicon wafer forms the substrate of the device. The insulating Si substrate is doped with boron to make it electrically conductive (p-type). Upon the substrate, an n-doped epitaxial layer is grown. As the thickness of the epitaxial layer is increased, the full well capacity and NIR response also increase. The epitaxial layer is slightly doped in such a manner as to cause minority signal carrier diffusion into the bulk silicon. Next, a thick field oxide is grown in a checker board pattern across the surface of the wafer. The field oxide is an isolating layer, a dielectric film, composed of silicon dioxide. A thin gate oxide of about 400 nm of SiO_2, is grown over the remaining exposed epitaxial layer. Conductive poly-silicon is then applied in thin strips that regularly crisscross the entire surface of the imager forming the row and column electrodes. The two orthogonal poly-silicon electrodes are electrically isolated and connect pixels to the processing electronics at the periphery of the

DEVELOPMENT OF SCREEN MONITOR WITH A SPATIAL RESOLUTION OF TEN MICRO-METERS FOR XFEL/SPring-8

K. Yanagida*, H. Tomizawa and A. Yamashita, JASRI, XFEL Joint Project /SPring-8
1-1-1 Kouto, Sayo-cho, Sayo-gun, Hyogo 679-5198
S. Inoue and Y. Otake, RIKEN, XFEL Joint Project /SPring-8
1-1-1 Kouto, Sayo-cho, Sayo-gun, Hyogo 679-5148

Abstract

A screen monitor with a resolution of less than 10 μm was developed for XFEL/SPring-8. It comprises a vacuum chamber with a metal (100 μm, SUS) foil to emit OTR, a lens for focusing and a CCD camera system. In order to realize this resolution, the lens is placed close to the foil, the distance between the lens and the foil is 100 mm, and the lens has a large diameter (2 in.). This optical-geometrical structure contributes much to increase the numerical aperture of a near-field image. Although the range of the observation wavelength is wide, such as from 400 to 800 nm, a resolution of 2.5 μm on the foil surface has been calculated. The experimental data of the developed optics also suggested the same resolution.

INTRODUCTION

At SPring-8, the 8-GeV linac for an X-ray free electron laser (XFEL) is now under construction. In order to realize the XFEL, highly qualified electron beams are required. Especially in the undulator section the beam should have a size of several tens of micro-meters, a peak beam current of several kiro-amperes, a micro-bunch length comparable to the X-ray wavelength, and an emittance of less than 1 πmm·mrad [1].

In order to tune and realize such a beam, beam monitors are very important, and should have a comparable resolution to the beam parameters mentioned above. For a screen monitor (SCM), the required resolution is less than 10 μm. To achieve this resolution we have developed a prototype SCM using OTR and fluorescence radiation, based on the following design concept.

Generally a CCD camera with a ready-made zoom lens is used for SCM measurements. In this case we cannot have a precise parameter of the lens, such as the curvature, broadband property of dispersion, Abbe's number of glass and so on. This means that we cannot evaluate characteristics like aberrations, magnification and effective focal length using an optical design program. Therefore, we decided to know all of the design parameters so that we can evaluate the characteristics of the optical system. Consequently, a lens with published optical parameters was chosen, or a lens produced optimally by using an optical design program was selected. This paper gives a summary of the prototype SCM with the lens developed for transverse spatial structure measurements with a resolution of less than 10 μm.

* E-mail: ken@spring8.or.jp

SYSTEM CONFIGURATION

Mechanical System

The mechanical part of the SCM comprises a vacuum chamber with radiators, motorized stages that change the positions of a lens and a CCD camera.

The vacuum chamber has a shaft that links the upper and lower slide stages, as shown in Fig. 1. There are three holes along the shaft: an aperture of the beam passage and holes for two kinds of radiators.

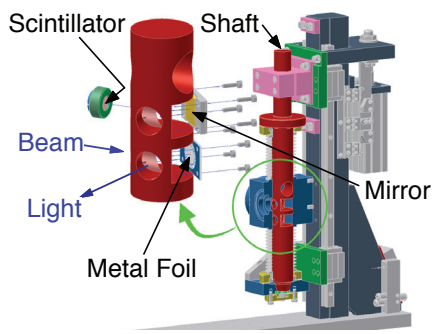

Figure 1: Structure around radiators.

One radiator is metal foil to emit OTR with a thickness of 100 μm. It is placed in the bottom hole where an electron beam hits the foil at an angle of 45°. The foil consists of nine apertured SUS foils (denoted by green foils in Fig. 2) and one SUS mirror foil without an aperture (denoted by the red foil in Fig. 2). The thickness of each foil is 100 μm. These ten foils are bonded by a diffusion bonding process, and form a single plate (see photograph in Fig. 2).

Figure 2: Metal foil.

The other radiator is a scintillator plate with a thickness of 100 μm, which is placed in the center hole where an electron beam hits the plate perpendicularly. The fluorescence from the plate is reflected at a mirror, and then led to the CCD camera.

DEVELOPMENT OF INTEGRATOR CIRCUIT FOR CHARGE MONITORING

K. Yanagida*, S. Suzuki and H. Hanaki
JASRI, Accelerator Division /SPring-8
1-1-1 Kouto, Sayo-cho, Sayo-gun, Hyogo 679-5198

Abstract

At the SPring-8 1-GeV linac, an electric charge of a pulsed electron beam is measured by an integrator circuit. A signal from a current transformer is processed into an integrated voltage. To improve the resolution for future use, a low-noise integrator circuit was developed whose main elements are a gate switch (SW-283-PIN, M/A-COM) and an accumulator (coaxial cable). The resolution is 0.65 pC under conditions of a range of 2 nC and a gate width of 20 ns. The resolution of the developed integrator circuit is 1/12 of the resolution of the present integrator circuit. The nonlinearity of the output voltage is small, 0.14 % rms compared to the output full scale.

INTRODUCTION

At the SPring-8 linac, eighteen current transformers (CTs) have been installed to observe macro longitudinal current structure or the electric charge of a pulsed electron beam by an oscilloscope. Beam charges are not recorded into the database except for two CTs; one is installed in the beam transfer line to the booster synchrotron, and the other is installed in the beam transfer line to the NewSubaru storage ring. These stored data are used to observe the beam charge and to calculate the injection efficiency to the booster synchrotron or the NewSubaru storage ring.

For top-up injection to the SPring-8 storage ring, about every 20 seconds the linac shoots an electron beam whose beam charge is about 1 nC. In the future the beam charge will be decreased due to more frequent beam injection to the storage ring. Presently Fast Gated Integrator and Boxcar Averager Modules (STANFORD RESEARCH SYSTEMS) are equipped as integrator circuits for signal processing. When the beam charge is decreased for the frequent beam injection, the resolution of the present integrator circuit will be worsened, too. To maintain or improve the resolution we developed a new integrator circuit to reduce the noise level to 1/10 of the present integrator circuit. The developed integrator circuits will be installed for all CTs in the linac instead of the present integrator circuits.

PRINCIPLE

The principle of the developed integrator circuit is identical as the principle of the present integrator circuit [1]. The principal elements are a gate switch and an accumulator. The gate switch determines the integration time of the measurement. When the gate is open, the signal voltage is led to an accumulator (1 and 2 in Fig. 1) that is a delay line with a characteristic impedance of 50 Ω. A coaxial cable or a pulse forming network (PFN) is used as an accumulator. The signal voltage led into the accumulator is reflected at the opposite open end and returned to the gate switch (3 in Fig. 1). If the gate is closed before the reflected signal voltage arrives, both ends of the accumulator become open ends, and then the signal voltage is stuck in the accumulator (4 in Fig. 1). The stuck signal voltage is averaged as it goes back and forward (5, 6, and 7 in Fig. 1). This averaged voltage is proportional to the integral of the signal voltage while the gate is open.

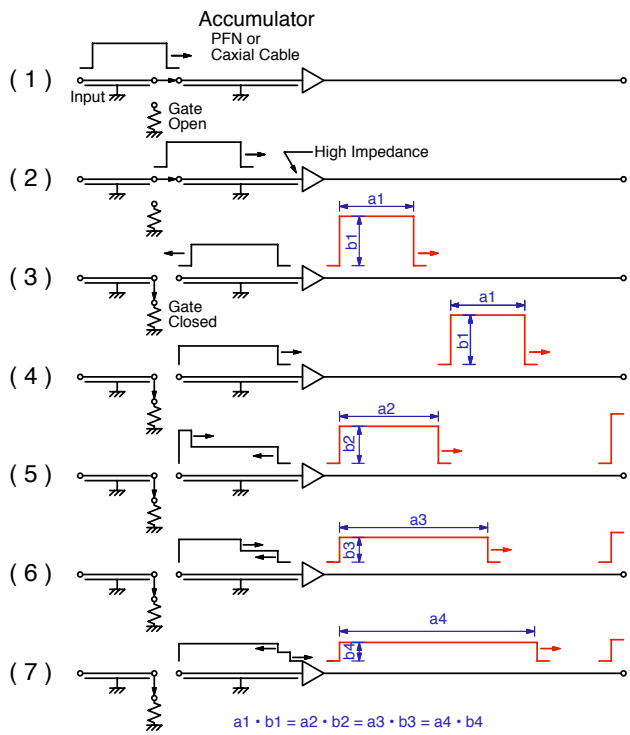

Figure 1: Principle of integrator circuit.

DESIGN

The block diagram and exterior of the developed integrator circuit are shown in Figs. 2 and 3. In Fig. 2 “a:” denotes the parameter for a short (1 ns) pulsed beam measurement,

* E-mail: ken@spring8.or.jp.

OPERATIONAL PERFORMANCE OF A NEW BEAM-CHARGE INTERLOCK SYSTEM FOR RADIATION SAFETY AT THE KEKB INJECTOR LINAC

T. Suwada*, E. Kadokura, M. Satoh, K. Furukawa, KEK, Tsukuba, Ibaraki 305-0801, Japan

Abstract

A new beam-charge interlock system has been developed for radiation safety and machine protection at the KEKB injector linac. Although the previous software-based interlock system was working, it was replaced with the new hardware-based one to improve its operational performance and reliability. The new interlock system restricts the integrated amount of beam charges delivered to four different storage rings (KEKB e^+, KEKB e^-, PF, PF-AR) at six locations along the linac and the beam transport lines. The full-scale operation of the new interlock system has started in 27 March 2008 after elaborate beam tests. In this report we describe the beam tests, the technical improvements, and the operational performance of the new beam-charge interlock system.

INTRODUCTION

A new injection scheme is under development for simultaneous and continuous injection delivered from the KEKB injector linac [1] to both the downstream storage rings (the KEKB electron/positron rings and the PF ring). The technical review was reported elsewhere in detail [2]. The new beam-charge interlock (BCI) system is one of the R&D subjects pertaining to the new injection scheme. The BCI system restricts the integrated amount of the beam intensity passing through the injector linac and the beam transport line to each storage ring. When it exceeds a certain threshold level prescribed at each location, the BCI system directly generates a beam-abort request to the safety control system of the linac for radiation safety and machine protection. Its technical review was reported in detail elsewhere [3-5].

The new BCI system also supplies a proper environment to advance the present accelerator complex towards the future projects. The following four subjects are underway,

(1) to increase of the injection beam intensity towards the next-generation B-factories,
(2) to perform the stable and continuous injection over an hour to the PF-AR,
(3) to enable easy beam tunings for the PF injection with a new beam dump,
(4) and to perform the new injection scheme for both the KEKB and the PF rings.

These subjects are strongly required for improving the stable and fast injection with higher-brightness (or higher-intensity) electron and positron beams into the downstream storage rings. In order to perform them, the instantaneous and integrated beam intensities must be controlled pulse-by-pulse at both the linac and each transport beam line. Therefore, the hardware-based BCI system with a higher reliability must have been developed for these purposes.

The new interlock system enables to relax the restrictions in the beam intensity for each injection mode. Table 1 shows the comparisons of the old and new beam-charge intensities prescribed at each location along the linac and each beam transport line.

Table 1: Comparisons of the Old and New Beam-charge Intensities Prescribed at Each Location

Location	Old		New	
	[nC/s]	[nC/h]	[nC/s]	[nC/h]
R0-01	1250	-	2500	4.50×10^6
22-44	625	-	1250	2.25×10^6
Linac	62.5	-	-	2.25×10^5
KEKB	-	5.76×10^5	-	5.76×10^5
PF	-	-	-	7.80×10^4
PF-AR	-	0.72×10^4	-	2.32×10^4

Based on this modification, the injection beam intensity can be controlled every an hour and every a second. In particular, the instantaneous beam intensity has been relaxed by two times. Thus, this modification has enabled to test high-intensity beam acceleration studies for the next-generation B-factories. On the other hand, the stable injection to the PF-AR over an hour has been realized. For the PF injection, the beam-intensity control has been available with a new beam dump. Thus, the flexible beam-intensity control has started and the highly reliable environment to advance the new injection scheme has been ready.

The development of the new BCI system has been finished after elaborate system tunings with beam tests during two years. The full-scale operation has started without any significant problems.

FURTHER TECHNICAL IMPROVEMENTS

The designs of the new interlock system started in 2006, and the development of both the hardware and software system finished in October 2007. During two months since then, the operational tests were performed to check the technical functions, the reliability, and the stability in the nominal injection operation. We found several faults during the beam tests. Further the technical improvements have been performed step-by-step in order to increase the system reliability and flexibility. For the hardware system, metal doors were installed to shield a system rack to

*E-mail address: tsuyoshi.suwada@kek.jp.

NUMERICAL STUDY OF A NEW BUNCH LENGTH MONITOR UTILIZING A DETECTION OF ELECTROMAGNETIC FIELDS IN MILLIMETER-WAVE REGION

T. Suwada* and M. Satoh, KEK, Tsukuba, Ibaraki 305-0801, Japan

Abstract

A new nondestructive bunch-length monitor has been numerically investigated in high-energy electron/positron linear accelerators. The monitor detects electromagnetic radiation emission generated in wave zone through a gap of a vacuum pipe when a relativistic bunched beam passes across the pipe gap. The frequency spectrum of the radiation emission spreads over microwave to a millimeter-wave region for the bunched beam with a bunch length of a picosecond region. The frequency spectrum strongly depends on the bunch length if the geometrical structure of the pipe gap is suitably fixed. The detection principle of the new bunch-length monitor and some numerical analysis results applied to a single-bunch electron beam at the KEKB injector linac are described in this report.

INTRODUCTION

A bunch-length measurement of a bunched beam is one of important beam diagnostics in linear accelerators. There are several methods to measure the bunch length [1]. One is a standard method with a streak camera. It measures a pulse width of electromagnetic radiations in time domain, such as Cherenkov radiation and optical transition radiation generated through electromagnetic interactions between materials and the bunched beam. This method comes in useful for the bunch-length measurement in a picosecond region. Recently, a fast streak camera can makes the bunch-length measurement possible with a time resolution of sub-picoseconds [2].

These are well-known methods to measure the bunch length in a pico (or sub-pico) second region, and however, they have several drawbacks because they are basically based on destructive diagnostics, and they need expensive instrumentations with complicated systems.

Here, we propose an alternative new method to measure the bunch length in frequency domain by nondestructively detecting electromagnetic radiation emissions. They are shaken off the bunched beam by diffraction (or scattering) at a pipe gap of a beam line. This method requires only a pipe gap normally vacuum-sealed with a ceramic. It does not require any other devices in the beam line.

There are many pipe gaps vacuum-sealed with a conventional ceramic along the beam line of the KEKB injector linac in order to install other beam diagnostic devices. Such pipe gaps are available for the bunch-length measurement based on this new method at any locations of the entire beam line

In this report, the basic principle on this new method are presented. The characteristics of the electromagnetic radiation emitted from the pipe gap are also given, and some numerical results analyzed for a single-bunch electron beam at the KEKB injector linac are summarized.

*E-mail address: tsuyoshi.suwada@kek.jp.

CHARACTERISTICS OF THE RADIATION EMISSION

When a charged particle with a relativistic energy passes through a vacuum pipe in linear accelerators, image charges with the inverse sign are induced on the inner surface of the pipe, and they also flow simultaneously through it. Electromagnetic fields (or self-fields) induced between the charged particle and the image charges are relativistically boosted in the longitudinal direction. When such pancake-like self-fields pass across the pipe gap, a part of the self-fields are emitted out of the pipe gap in wave zone because the self-fields must be met with the electromagnetic boundary conditions under which the charged particle is surrounded with both the pipe gap and the metal pipe.

The characteristics of the electromagnetic radiation emission from the charged particle are determined by depending on the geometrical structure of the pipe gap (see fig. 1(a)) if the charge and the energy of the charged particle are constant.

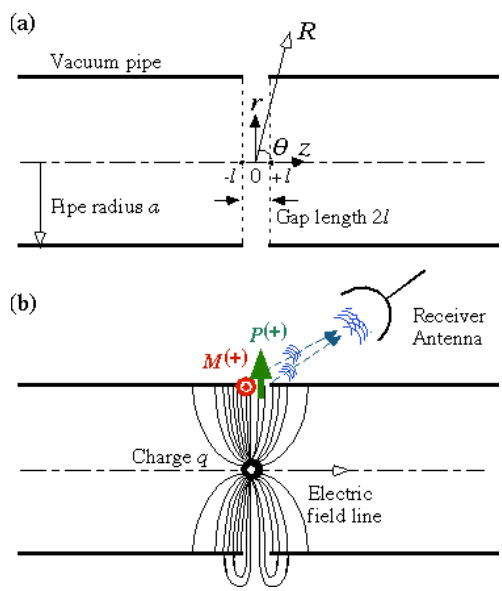

Figure 1: (a) Geometrical structure of the vacuum pipe and the pipe gap and (b) a schematic drawing of the electromagnetic radiation emission through the pipe gap.

On the other hand, when a bunched beam goes across the pipe gap, the characteristics of the electromagnetic

TRANSIENT BEAM LOADING COMPENSATION IN CTF3

A. Dabrowski, S. Bettoni, H. H. Braun, E. Bravin, R. Corsini, S. Doebert, C. Dutriat, T. Lefèvre, M. Olvegård, P. K. Skowronski, F. Tecker
CERN, Geneva, Switzerland

Abstract

In the CLIC Test Facility 3 (CTF3), the strong coupling between the beam and the accelerating cavities (full beam loading) induces transient effects such that the head of the pulse is accelerated almost twice as much as the steady-state part of the pulse. The beam optics in the machine is tailored for the steady-state and not for the higher energy electrons, which are gradually lost. This can lead to inefficiency and contributes to the activation of the machine. A beam loading compensation scheme has been proposed to minimize this effect. By delaying appropriately the arrival time of the rf pulse in accelerating cavities with respect to the beam, the transient energy can be brought close to (within a few percent of) the steady-state one. This paper presents the measurements done on CTF3 using time resolved energy measurements.

INTRODUCTION

In CTF3 an electron pulse of 3.5 A and 1.5 μs is accelerated using fully loaded 3 GHz accelerating structures [1]. The resulting energy spectrum shows a strong time dependency with higher energies in the first 50 nanoseconds of the pulse, followed by the steady state. Time-resolved spectrometry is therefore an essential beam diagnostic tool to correctly set the phase of the accelerating structures. Several spectrometer lines are installed along the CTF3 linac for this purpose. They consist of a bending magnet, which provides horizontal deflection to the electrons, followed by a transverse profile monitor measuring the beam position and its transverse width. The spectrometer lines are equipped with an optical transition radiation (OTR) screen [2] observed by a CCD camera with good spatial resolution and at the end of the line a novel segmented beam dump [3] for time resolved energy measurements.

This paper is devoted to the commissioning and utilization of the segmented beam dump. This device is composed of parallel metallic plates designed to measure a current, proportional to the number of stopped incident particles. By measuring the deposited charge in each segment, the beam energy profile can be reconstructed. The material and the dimension of the segments were chosen based on considerations of the beam parameters, in particular the beam energy and the energy spread, but also on the beam power absorbing efficiency and the radiation hardness requirements. The segments need to be deep enough to stop the particles; on the other hand, the segment thickness must be chosen to optimize the spatial resolution, which is eventually limited due to multiple Coulomb scattering [4]. After simulation studies with the Monte Carlo code FLUKA [5] as described in [3], the design was chosen as consisting of two devices; a passive 4 cm thick multi-slit (400 μm wide vertical slits) collimator made of iron which stops about 75% of the electrons and the active detector, which we refer to as the segmented dump that is installed just behind the collimator. It consists of tungsten plates of 2 mm transverse thickness, 5 cm depth and 5.5 cm height spaced by a 1mm thick radiation hard ceramic insulator as shown in Fig. 1. The role of the collimator is to capture as much beam power as necessary to ensure a good signal in the segmented dump, but to keep the deposited power low enough so that the segmented dump does not require water cooling.

The electronics, used to read the current drawn from each segment, consists of a direct connection to the segment with a 50 Ω impedance to ground. These signals are attenuated by 8 dB, and then digitised by a 100 MSa/s sampling ADC, which limits the time resolution of the post digitised signals to 10 ns, see Fig. 2.

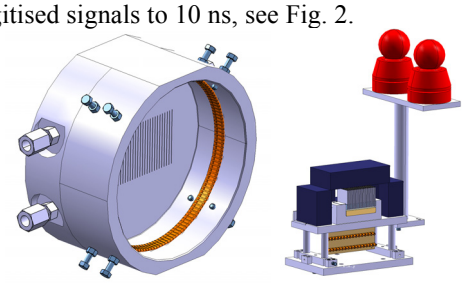

Figure 1: (a) Multi-slit collimator, (b) segmented dump.

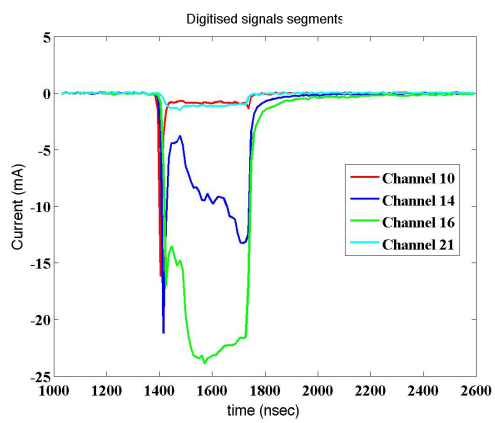

Figure 2: Typical digitised signals from segmented dump.

COMMISSIONING OF THE SEGMENTED DUMP

The first part of the CTF3 drive beam linac is shown in the schematic of Fig. 3. The injector consists of a dc gun followed by a 3GHz bunching system. Two 3 GHz accelerating structures boosts then the beam energy up to

BUNCH LENGTH MEASUREMENTS IN CTF3

A. Dabrowski, S. Bettoni, H. H. Braun, R. Corsini, T. Lefevre, H. Shaker, P. Skowronski,
S. Doebert, F. Tecker, CERN, Geneva, Switzerland
J. J. Jacobson, M. Velasco, Northwestern University, Illinois, USA

Abstract

The CLIC Test Facility CTF3, being built at CERN by an international collaboration, should demonstrate the feasibility of the CLIC two-beam technology by 2010. One of the issues addressed is the control of the electron bunch length in the whole complex. A bunch length measurement system, with a good resolution, is therefore paramount. Two different systems are presently used in CTF3 based on microwave spectroscopy and on transverse rf deflectors, respectively. In the paper we describe the two systems, we discuss the different experimental methods used and present the results of the latest measurement campaigns.

INTRODUCTION

In the framework of the Compact Linear Collider (CLIC) project [1], a test facility named CTF3 [2] is constructed at CERN by an international collaboration. The CTF3 complex shall demonstrate by 2010 the key technological challenges for the construction of a high luminosity 3 TeV e^+-e^- collider. The overall machine starts with a linac delivering a 3.7 A, 1.5 μs long electron beam with an energy of 150 MeV. The bunches are then injected in two consecutives rings [3] where the beam average current and the bunch frequency are multiplied by a factor 8. With a current of 30 A and 2.5 cm distance between bunches, the resulting beam is finally sent to the CLIC experimental area (CLEX) where it will be used to test all key CLIC RF components.

The performances of the accelerator depend directly on the control of the electron bunch length. In the linac the bunches must remain short (about 2 ps r.m.s.) to keep the energy spread as low as possible, but need to be stretched (6 - 10 ps r.m.s.) before the rings to minimize emittance dilution due to coherent synchrotron radiation. Therefore, two magnetic chicanes have been implemented, the first downstream of the injector and the second upstream of the first ring. A sketch of the second magnetic chicane, composed of 4 bending magnets, is presented in Fig. 1. Normally, bunch shortening or lengthening is obtained by changing the phase of the rf in the last accelerating structure. Bunch length measurements can be performed using Optical Transition Radiation screens coupled to a streak camera [4], but the present system limits the time resolution to 2 ps. Shorter bunches are measured with the 1.5 GHz rf deflector [5], normally used to inject the particles in the Delay Loop, but for the purposes of the bunch length measurement, it is used in conjunction with an Optical Transition Radiation screen. Recently, a new detector has been commissioned based on microwave spectrometry, which we commonly refer to as the "rf-pickup" [6]. In this paper, the rf deflector and the rf-pickup bunch length measurement techniques will be presented.

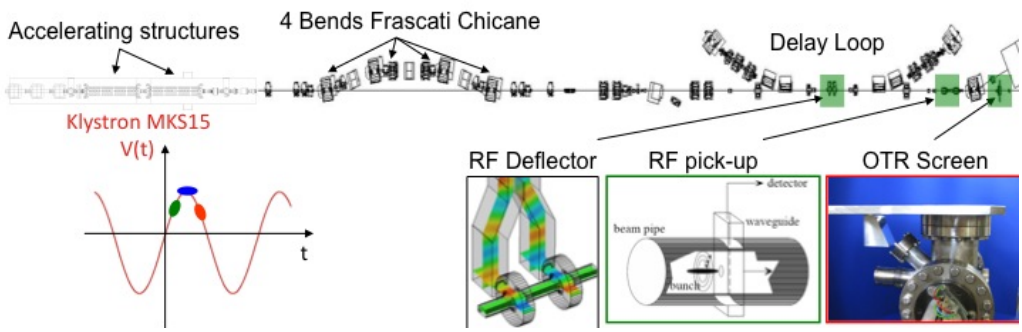

Figure 1: Layout of the Frascati chicane and locations of the bunch length monitors. By changing the Klystron MKS15 phase, the bunch length at the end of the chicane can get shorter (green), longer (red) or just be preserved (blue).

MICROWAVE SPECTROMETER EXPERIMENTAL SETUP

A non-destructive single shot bunch length monitor was commissioned in CTF3 in 2006 [6]. This device, the "rf pick-up", measures the frequency spectrum of the electromagnetic field emitted by the particles and collected by a rectangular K_a waveguide. The rf pickup was installed 50 cm upstream of the OTR screen, and hence cross calibrations can be performed between the rf deflector and the rf pickup monitor. This monitor has a sub-ps time resolution and the calibration is done in a self consistent manner. Moreover, this monitor has the advantage of being non destructive and relatively inexpensive compared to other techniques.

The rf pickup consists of a single WR-28 waveguide connected to the beam pipe as shown in Fig. 1. A 0.5 mm thick CVD diamond window [7] is used to isolate the vacuum in the beam pipe from the atmospheric pressure in the waveguide. Signal frequencies above the cut-off of the WR-28 waveguide (21.1 GHz) are transported in a

DIAGNOSTICS AND MEASUREMENT STRATEGY FOR THE CERN LINAC 4

K. Hanke, G. Bellodi, J.-B. Lallement, A. Lombardi, B. Mikulec, M. Pasini, U. Raich, E. Sargsyan, CERN, Geneva, Switzerland
M. Hori, Max-Planck-Institut für Quantenoptik, Hans-Kopfermann-Str. 1, D-85748 Garching, Germany, and Department of Physics, University of Tokyo, 7-3-1 Hongo, Bunkyo-ku, Tokyo 113-0033, Japan

Abstract

Linac4 is a 160 MeV H^- linac which will become the new injector for CERN's proton accelerator chain. The linac will consist of 4 different RF structures, namely RFQ, DTL, CCDTL and PIMS running at 352.2 MHz with 2 Hz repetition rate and 0.4 ms pulse length. A chopper line ensures clean injection into the PS Booster. The combination of high frequency and a high-current, low-emittance beam calls for a compact design where minimum space is left for diagnostics. On the other hand, diagnostics is needed for setting up and tuning of the machine during both commissioning and operation. A measurement strategy and the corresponding choice of the diagnostic devices and their specific use in Linac4 are discussed in this paper.

INTRODUCTION

Linac4, a 160 MeV H^- linac, is the first step in re-building CERN's proton injector complex. The linac will consist of 4 different RF structures, namely a radio-frequency quadrupole (RFQ), a drift tube linac (DTL), a cell-coupled drift tube linac (CCDTL) and a pi-mode structure (PIMS). Figure 1 shows schematically the different sections of the linac. In a first phase, Linac 4 will inject into the existing CERN PS Booster and deliver beams for fixed-target physics and the LHC through the present accelerator chain. In a second phase, Linac4 will become the front-end of a superconducting linac (SPL), which will inject into a new proton synchrotron (PS2). In the operation of a high-power hadron linac as Linac4, beam loss is a critical issue. The specification of the instrumentation has therefore been driven by beam dynamics calculations. We will discuss in the following paragraphs the diagnostics specified for the commissioning of the different stages of the linac as well as for day-to-day operation.

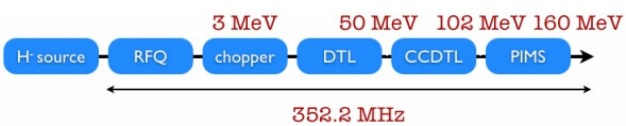

Figure 1: Linac4 layout.

ALIGNMENT, STEERING STRATEGIES AND LOSS CONTROL

After the nominal layout of the machine had been defined, a series of runs (1000-2000) was made in order to evaluate beam losses and emittance growth under the effects of machine and beam errors. The results of these studies are reported in [1]. Starting from these results, a system composed of correctors (dipolar kicks) and diagnostics (beam position monitors) has been integrated in the Linac4 layout in order to minimise losses and to control emittance growth. A procedure has been implemented to find the value of the correctors which minimises orbit excursion at the location of the diagnostics, while maximising transmission. The aim is to have a sufficient number of correctors and monitors to be able to control routine beam loss to less than 1 W/m at the highest possible beam duty cycle (6%, foreseen for future operation of Linac4 as injector for the SPL operated at maximum beam power). These studies show that a correction system made of 15 horizontal and vertical steerers and monitors can correct the effects of quadrupole alignment errors within ±0.1 mm and ± 1 mrad and beam alignment errors of ±0.3 mm and ±0.3 mrad (all values are 1 sigma). The residual losses in the worst case scenario are shown in Figure 2.

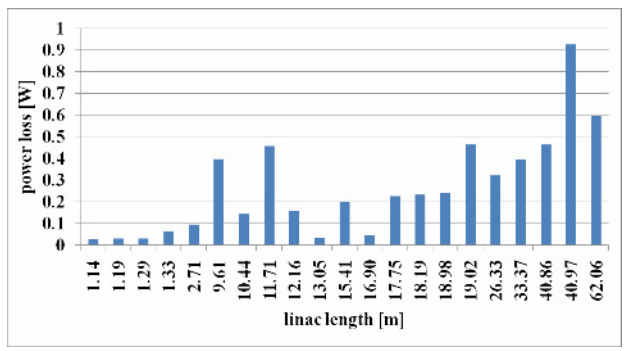

Figure 2: Power loss along Linac4 (40 mA, 6% duty cycle, and worst case out of 2000) for beam and machine alignment errors (quadrupoles 0.1 mm, 1 sigma, beam position ±0.3 mm/0.3 mrad Gaussian) applying the best correction achievable with the given diagnostic and steering system.

DIAGNOSTICS CHOICES

Source and Low-Energy Beam Transport

In order to characterise the H^- source and the 2-solenoid low-energy beam transport (LEBT), measurements of the beam current (transmission), beam profile and emittance are required. During the commissioning phase the source and LEBT will be set up in two different ways: in the spectrometer configuration only one solenoid is used,

EMITTANCE MEASUREMENT INSTRUMENT FOR A HIGH BRILLIANCE H$^-$ ION BEAM*

C. Gabor†[1], C.R. Prior[1], A.P. Letchford[2], J.K. Pozimski[2+3],
[1]STFC, ASTeC, Rutherford Appleton Laboratory (RAL), OX11 0QX, UK,
[2]STFC, ISIS, RAL, [3]Imperial College London, High Energy Physics Department, SW7 2AZ, UK

Abstract

Among present challenges for beam diagnostics and instrumentation are issues presented by high beam intensity, brightness, resolution and the need to avoid inserting mechanical parts into the beam. This very often means applying non–destructive methods, which avoid interaction between ions and mechanical parts and, furthermore, allow on–line measurements during normal beam operation. The preferred technique for H$^-$ beams is the photo–detachment process where (laser) light within the range of 400...1000 nm has a sufficient continuous cross section σ_{PD} to neutralize negative ions. The actual diagnostics are then applied to either the neutrals produced or the electrons. The latter are typically used for beam profiles whereas neutrals are more suitable for emittances, and form the subject of the present paper. This provides an overview of the basic features of the diagnostic technique, followed by discussion about computing the missing second transverse projection view using a method called Maximum Entropy Method (MaxEnt, MEM).

INTRODUCTION

The Front End Test Stand (FETS) project [1] at RAL, UK, makes high demands on the diagnostics because of its beam power (60 mA H$^-$, $\leq$ 3 MeV beam energy, $\leq$ 10 % duty cycle). Using a non–destructive method, i.e. no mechanical parts inside the ion beam, minimizes the influence on the ion beam with the advantage of an on–line diagnostic tool. The experimental set–up uses a Penning source with slit extraction, a solenoid LEBT, a four–vane RFQ who brings the beam from 70 keV up to 3 MeV and a MEBT consisting of quads, rebuncher and a fast/ slow chopper. Particularly the latter and the slit extraction results in a lack of symmetry which makes a 4D emittance measurement highly desirable.

The basic principle of the implemented Photo Detachment Emittance Instrument (PD–EMI) is illustrated in Fig. 1 and widely discussed in [2, 3]. Compared to more common devices like slit–grid/ harp ("slit–slit") and pepperpot ("point–point") instruments the laser acts like a slit whereas the particle detector takes the place of a pepperpot device, therefore the PD–EMI can be described as an instrument with a slit–point transfer function. The yy′ emittance in Fig. 1 can be measured in a direct way by gathering angle profiles for each laser position.

* Work supported by EU/FP6/CARE (HIPPI) RII3-CT-2003-506395
† c.gabor@rl.ac.uk

In principle it would be possible to measure in x–direction similarly to yy′ with a second set of mirrors. But it is technically a challenging problem to place the necessary movable stages inside a dipole. It is also not very attractive in price. A more physical drawback is the separation of the 4D emittance measurement into two projections. But a detector movable longitudinally along the drift length of the neutralized ions could help to overcome the problems: The laser will be moved several times through the ion beam and at each time the z positions of the detector is moved along the drift of the neutrals. It is then possible to add up all detector signals for a given z which results in a $\rho(x,y)_{z(n)}$ density distribution. Each extracted 1D profile is then mapped to the laser position by a drift matrix to calculate the xx′ emittance.

The Maximum Entropy Method MEM

The best candidate to do the xx′ emittance reconstruction utilises a principle called maximum entropy method (MEM). This is a powerful and a extensively used technique for the deconvolution of data and the reconstruction of images (astronomy, tomography, neutron scattering). First applications in accelerator science are published in [5, 4] and a very good but general introduction is given in Sivia's textbook [6].

The strengths of MEM are its generality and ability to deal with *noisy* and *incomplete* positive data. It is based on Bayes' theorem and uses an entropy as described in information theory. The linear transformation between the

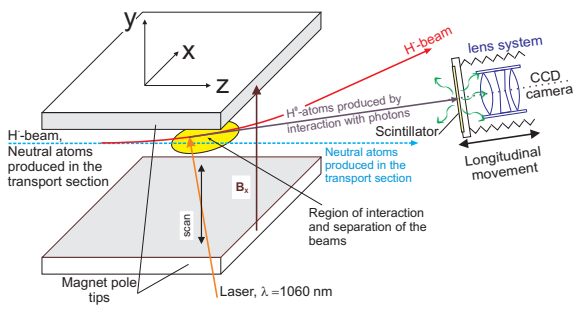

Figure 1: The negative ions penetrate the dipole and after some displacement a laser scans through the beam and neutralize a small amount of ions. The neutrals produced by photo detachment are guided to a detector system (yy′ emittance). The other transverse emittance can then be reconstructed by moving the scintillator and collecting $\rho(x,y)$ profiles along the drift.

FOUR-DIMENSIONAL EMITTANCE METER FOR DC ION BEAMS EXTRACTED FROM AN ECR ION SOURCE*

S. Kondrashev#, A. Barcikowski, B. Mustapha, P. N. Ostroumov, ANL, Argonne, IL 60439, U.S.A.
N. Vinogradov, Northern Illinois University, De Kalb, IL 60115, U.S.A.

Abstract

We have developed a pepper-pot, scintillator-screen probe to measure the emittance of low-energy DC beams extracted from ECR ion sources. Different scintillators have been tested, and CsI (Tl) was chosen due to its high sensitivity, wide dynamic range and long life-time. A fast vacuum shutter with a minimum dwell time of 18 ms has been employed to reduce the scintillator degradation by ion beam irradiation. A CCD camera with shutter speed adjustable from 1 μs to 65 s has been used to acquire pepper pot images. The linearity of both the scintillator and the CCD camera has been studied. On-line emittance measurements are performed by an application code developed on the LabVIEW platform. The sensitivity of the device is sufficient to measure the emittance of DC ion beams with current densities down to about 100 nA/cm^2. The emittance of all ion species extracted from the ECR ion source and post-accelerated to an energy of 75-90 keV/charge have been measured downstream of the LEBT. Because of the two-dimensional array of holes in the pepper-pot, this emittance meter can be used to observe and study four-dimensional emittance correlations in beams from ECR ion sources.

INTRODUCTION

Ion beams extracted from ECR ion sources have a complicated structure in 4-D phase space [1]. The ion motion in the horizontal and vertical planes is strongly coupled due to the magnetic field configuration inside the source and extraction regions. Widely used slits and Alison type emittance scanners only provide 2-D projections of the beam emittance. A pepper pot emittance probe is the most suitable device to study 4-D ion beam emittance. Another significant advantage of the pepper pot probe is its short measurement time. 4-D emittance data can be obtained in less than 1 s on-line, allowing ECR ion source tuning to minimize emittance of the extracted ion beam. Previously, different scintillators were used to measure emittance of intense ion beams extracted from pulsed ion sources [2, 3]. However, there is almost no data on emittance measurements of DC ion beams with moderate intensities, which are typical for ECR ion sources, using a pepper-pot device coupled to a scintillator probe. The main challenge is the choice of a viewing screen that provides high sensitivity, a long life time, good linearity and a wide, dynamic range of measurements.

*This work was supported by the U.S. Department of Energy, Office of Nuclear Physics, under Contract No. DE-AC02-06CH11357.
#kondrashev@anl.gov

Our first tests of the pepper pot coupled to a CsI (Tl) crystal [4] have shown that the sensitivity of the probe is high enough to measure the emittance of DC ion beams with energy 75 keV per charge state for a variety of ion species from protons to heavy ions with current densities below 1 μA/cm^2.

DESIGN OF THE EMITTANCE PROBE

The structure of the pepper pot emittance meter is shown in Fig. 1.

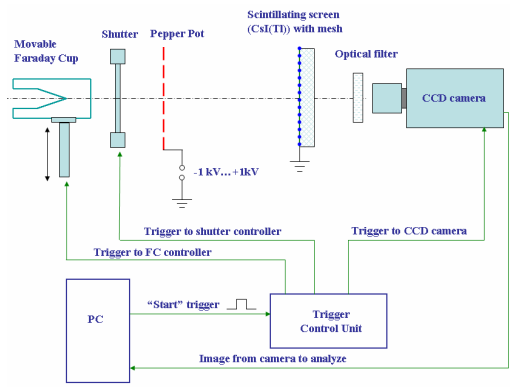

Figure 1: Emittance meter structure.

It consists of a movable Faraday cup (FC) equipped with a negatively biased suppression ring. The diameter of the FC input aperture is 46 mm. A compressed air cylinder drove the FC between two positions: in and out of the beam. The time required to complete the movement in both directions is about 1 s. The FC was used both as a detector of the ion beam current at the input of the emittance meter and as a beam blocker to protect the normally closed iris-type fast shutter from long time irradiation by a DC ion beam with a power of about 10 W. The normally closed iris-type UNIBLITZ-CS65S fast shutter with 65 mm aperture had an adjustable dwell time with a minimum of 18 ms and serves to protect the CsI (Tl) scintillator screen from possible degradation caused by DC ion beam irradiation. The tantalum pepper pot (PP) plate with a diameter of 70 mm and thickness of 380 μm had an aperture array over the whole area with 100 μm diameter holes with 3 mm spacing between them. An optical certification has shown that the diameters of all 415 holes were within the 100 – 104 μm range. The pepper pot plate was isolated from the ground and its potential can be varied in the range of ±1 kV to study the effect of secondary electrons on the emittance measurements. The CsI (Tl) scintillator screen with a diameter of 80 mm and thickness of 3 mm was placed at a distance of 100 mm downstream of the pepper pot plate.

INITIAL COMMISSIONING OF A DUAL-SWEEP STREAK CAMERA ON THE A0 PHOTOINJECTOR*

A.H. Lumpkin, J. Ruan, and T.W. Koeth, Fermilab, Batavia, IL U.S.A. 60510

Abstract

Characterization of the micropulse bunch lengths and phase stability of the drive laser and the electron beam continue to be of interest at the Fermilab A0 Photoinjector facility. Upgrades to the existing Hamamatsu C5680 streak camera were identified, and initially a synchroscan unit tuned to 81.25 MHz was installed to provide a method for synchronous summing of the micropulses from the drive laser and the optical transition radiation (OTR) generated by the e-beam. A phase-locked delay box was also added to the system to provide phase stability of ~1 ps over tens of minutes. Initial e-beam measurements identified a significant space-charge effect on the bunch length and other bunch length measurements supported the A0 emittance exchange experiments. Recent measurements with a re-optimized transverse emittance allowed the reduction of the micropulse number from 50 to 10 with 1 nC each to obtain a useful streak image. Installation of the recently procured dual-sweep module in the mainframe has now been done. Initial commissioning results and sub-macropulse display of the electron beam via OTR will be presented.

INTRODUCTION

The opportunity for a new series of streak camera experiments at the Fermilab A0 photoinjector was recognized in the last year. The first enabling upgrade was adding the synchroscan option to the existing C5680 Hamamatsu streak camera mainframe. By locking this module to the 81.25 MHz subharmonic of the rf system, the synchronous summing of micropulses could be done with trigger jitter of <1.5 ps (FWHM) for both the UV drive laser component at 244 nm and the e-beam via optical transition radiation (OTR) measurements [1,2]. The synchronous summing of the low OTR signal from the 15-MeV electron beam micropulses allowed the needed bandpass filters to be utilized to reduce the chromatic temporal dispersion effects inherent to the broadband OTR source and the transmissive optics components. In addition, the C6768 delay module with phase feedback was also acquired, and this stabilized the streak camera sweep relative to the master oscillator so that camera phase drift was much reduced to the ps level over tens of minutes. This second enabling upgrade allowed a series of experiments to be done on the bandwidth effects and transit-time effects in the respective transport lines[3].

The third enabling upgrade involves our installation and initial commissioning of the horizontal deflection unit which allows dual-sweep streak camera operations. In this case we want to assess the phase jitter and/or slew at the ps level during the macropulse of the drive laser and the electron beam. In synchroscan mode we have synchronously summed over all the micropulses and the jitter and slew effects are included. After characterizing the UV laser bunch length, a series of e-beam experiments on the A0 beamlines was performed [3]. We report measurements of the beam transit time in a double-dogleg transport line as a function of the upstream 9-cell accelerator rf amplitude and the effects of emittance exchange in the x-z phase spaces. We then show our initial dual-sweep streak results on the e-beam.

EXPERIMENTAL BACKGROUND

The tests were performed at the Fermilab A0 photoinjector facility which includes an L-band photocathode (PC) rf gun and a 9-cell SC rf accelerating structure which combine to generate up to 16-MeV electron beams [4]. The drive laser operates at 81.25 MHz although the micropulse structure is usually divided down to 9 MHz. Previous bunch length measurements of the drive laser and e-beam [2] were done with the fast single-sweep module of the Hamamatsu C5680 streak camera with an inherent shot-to-shot trigger jitter of 10 to 20 ps. Such jitter precluded synchronous summing of the short pulses. We have upgraded the camera by acquiring the M5676 synchroscan module tuned to 81.25 MHz with a trigger jitter of less than 1.5 ps (FWHM) and the C6878 phase-locked delay unit which stabilizes the camera phase over 10s of minutes. Due to the low, electron-beam energies and OTR signals, we typically synchronously summed over 50 micropulses with 1 nC per micropulse. The initial sampling station was chosen at Cross #9, and an optical transport system using flat mirrors and a parabolic mirror brought the light to the streak camera as indicated in Fig. 1. A short focal length quartz lens was used to focus the beam image more tightly onto the streak camera entrance slit. The quartz-based UV-Vis input optics barrel transferred the slit image to the Hamamatsu C5680 streak camera's photocathode. Alternatively, the 4-dipoles of the emittance exchange (EEX) line could be powered and experiments done at an OTR station, Cross #24, after the fourth dipole. A second optical transport line brings the OTR to the streak camera. In the EEX line the bunch compression effects were observed, and the shorter bunches were used to help delineate the chromatic temporal dispersion effects for various band pass, long pass, and short pass filters. The OTR converter is

*Work supported by U.S. Department of Energy, Office of Science, Office of High Energy Physics, under Contract No. DE-AC02-06CH11357.

SPECTRAL AND CHARGE-DEPENDENCE ASPECTS OF ENHANCED OTR SIGNALS FROM A COMPRESSED ELECTRON BEAM*

A.H. Lumpkin, Fermilab, Batavia, IL 60510, U.S.A.
N.S. Sereno, W.J. Berg, M. Borland, Y. Li, and S. Pasky,
Argonne National Laboratory, Argonne, IL 60439, U.S.A.

Abstract

Strong enhancements of the optical transition radiation (OTR) signal sampled after bunch compression in the Advanced Photon Source (APS) linac chicane have been observed as has been reported in LCLS injector commissioning. A FIR CTR detector and interferometer were used to monitor the bunch compression process of the PC gun beam down to sub-0.5 ps (FWHM) and correlate the appearance of spatially localized spikes of OTR signal (5 to 10 times brighter than adjacent areas) within the beam image footprint. Spectral-dependence measurements of the enhanced OTR were done initially at the 375-MeV station using a series of band pass filters inserted before the CCD camera. Tests with an Oriel spectrometer with CCD and ICCD readout have now been initiated to extend these studies. We also observed that a beam from a thermionic cathode gun with much lower charge per micropulse (but similar total macropulse charge as the PC gun) showed no enhancement of the OTR signal after compression. Reconstructions of the temporal profiles from the autocorrelations of both beams were performed and will be presented. Based on the available spectral and charge-dependent results, the results are consistent with a microbunching instability which results in broadband coherent OTR (COTR) emissions.

INTRODUCTION

The interest in improved understanding of the strong enhancements in optical transition radiation (OTR) from bright linac beams following bunch compression is rapidly growing as evidenced by recent reports in workshops and conferences in the last year [1-4]. The observed features are attributed to a combination of longitudinal space charge (LSC) effects in a linac, coherent synchrotron radiation (CSR) effects, and a Chicane compression process [4]. There appears to be a microbunching instability such that broadband coherent OTR (COTR) is generated in the visible wavelength regime. During the commissioning of the LCLS injector in 2007, such unexpected enhancements of the signals in the visible light OTR monitors occurred after compression in a chicane [1]. Since the Advanced Photon Source (APS) injector complex includes a flexible chicane bunch compressor that is similar to that at LCLS, we have an option to use an rf photocathode (PC) gun, and we had experience with SASE-induced microbunching [5], a series of experiments was performed to explore the phenomena. We initially performed studies on OTR measured at three screens located after the bunch compressor [3]. We used focus-at-the-object or near-field imaging optics and established that there were clear enhancements of the OTR signals at maximum bunch compression. Such enhancements prevent the normal beam-profiling measurements with OTR monitors at LCLS and APS. On the other hand, it has now been suggested that such microbunching structures are favorable to startup of visible-UV light SASE FELs [6].

We also accelerated the compressed beam to the end of the linac and evaluated the enhancements at 375 MeV. The localized spikes in the beam distribution were still visible at this energy. At this latter station we have the light transported outside of the tunnel to a small optics lab that allowed us to perform additional spectral dependency measurements. Moreover, the use of a thermionic cathode gun pulse train with only 40 pC per micropulse did not show the OTR enhancements when the bunch length was compressed comparably to that of the PC gun beam. Discussions of the possible mechanisms will be presented for the APS case which is similar, but not identical to that of LCLS.

*Work supported by U.S. Department of Energy, Office of Science, Office of High Energy Physics, under Contract No. DE-AC02-06CH11357.

EXPERIMENTAL BACKGROUND

The tests were performed at the APS facility which includes an injector complex with two rf thermionic cathode (TC) guns for injecting an S-band linac that typically accelerates the beam to 325 MeV, the particle accumulator ring (PAR), the booster synchrotron that ramps the energy from 0.325 to 7 GeV in 220 ms, a booster-to-storage-ring transport line (BTS), and the 7-GeV storage ring (SR). In addition, there is an rf photocathode (PC) gun that can also be used to inject into the linac as shown schematically in Fig. 1 of reference [3]. An extensive diagnostics suite is available in the chicane and after the chicane area. The tests were performed in the linac at the three imaging stations after the chicane bunch compressor and at the end of the linac where another beam imaging station is located. A FIR coherent transition radiation (CTR) detector (Golay cell) and Michelson interferometer [7] are located between the three-screen emittance stations. A vertical bend dipole and diagnostics screens in this short beamline allow the monitoring of tranverse x-beam size and energy following compression. The YAG:Ce and OTR were directed by

ELECTRON BEAM TIMING JITTER AND ENERGY MODULATION MEASUREMENTS AT THE JLAB ERL*

P. Evtushenko#, S. Benson, D. Douglas, D. Sexton, Jefferson Lab, Newport News, VA, USA

Abstract

When operating JLab high current ERL a strong reduction of the FEL efficiency was observed with the increase of the average current of the electron beam. Investigating the FEL efficiency drop-off with the electron beam average current we have measured the electron beam phase noise and the fast energy modulations. The phase noise is a variation of the time arrival of the electron bunches to the wiggler. It could be a very effective way of reducing the FEL efficiency especially when the driver accelerator for the FEL is operated with the RMS bunch length of about 150 fs. Under a fast energy modulation we denote a modulation which can not be followed by the FEL due to its time constant, defined by the net FEL gain. Such a modulation also could be a possible cause of the efficiency drop-off. Making the measurements we could rule out the FEL efficiency drop-off due either the fast energy modulation or the phase modulation. We also have learned a lot about instrumentation and techniques necessary for this kind of beam study.

ELECTRON BEAM PHASE NOISE MEASUREMENTS

Investigating the FEL efficiency drop-off with the electron beam average current we have measured the electron beam phase noise and the fast energy modulations. The so-called phase noise is essentially a variation of the time arrival of the electron bunches to the wiggler. That could be a very effective way of reducing the FEL efficiency if one takes in to account that the accelerator is routinely operated with the RMS bunch length of about 150 fs [1]. Under a fast energy modulation we denote a modulation which can not be followed by the FEL due to its time constant, defined by the net FEL gain. Such a modulation also could be a possible cause of the efficiency drop-off. The two effects are strongly connected in the FEL driver accelerator due to the longitudinal phase space transformation, i.e., longitudinal bunch compression. The simplified view of the longitudinal phase space transformation is a rotation of a long and low energy spread beam at the injector by ~90 degrees in the longitudinal phase space so that the bunch length minimum is located at the wiggler [2]. Under such a transformation an energy modulation in the injector would get transferred in to a phase modulation at the wiggler and a phase modulation in the injector would gets transferred in to an energy modulation at the wiggler.

The technique we use for the phase noise characterization of the electron beam was originally developed for noise characterization of ultra fast lasers [3]. It was shown that both phase noise and amplitude noise information can be extracted from the power spectrum measurements of the electron beam intensity. The power spectrum of the electron beam is a comb with spectral lines separated by the frequency of the bunch repetition rate. The envelope of the spectrum is determined by the longitudinal profile of a single bunch. Both the amplitude (AM) and phase modulation (PM) (or noise) of the beam intensity manifest themselves in the power spectrum as the sideband modulations of the spectral lines of the comb spectrum. It was shown in [3] that amplitude of the sideband modulations seen relative to the carrier amplitude changes differently with the harmonic number for AM and PM. The relative amplitude of the sidebands due to the amplitude noise does not change with the harmonic number, whereas the relative amplitude of the phase noise increase as μ^2, where μ is the harmonic number. Thus measurements of the sideband spectrum at the DC contain only the amplitude noise (modulations) and measurements made at very high harmonic number will be dominated by the phase noise (modulations).

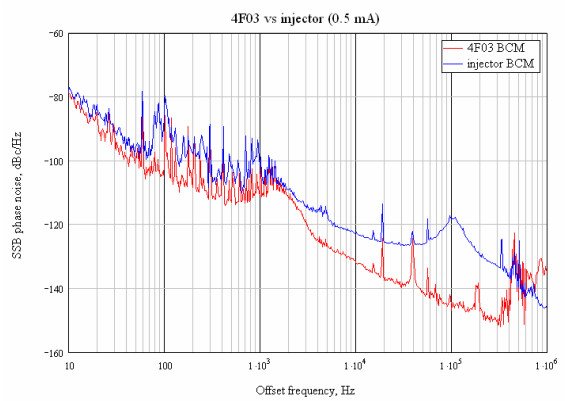

Figure 1a: Single sideband spectrum measured at 0.5 mA.

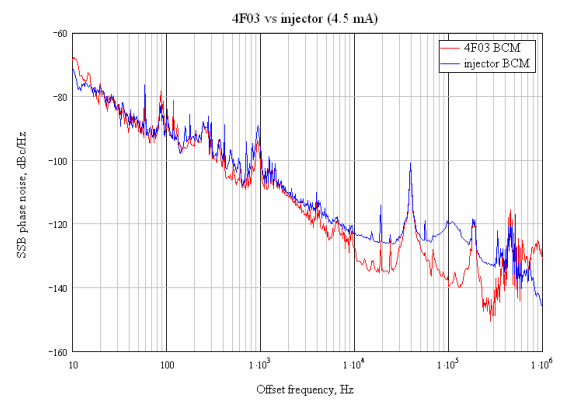

Figure 1b: Single sideband spectrum measured at 4.5 mA.

* Work supported by the U.S. DOE contract # DE-AC05-06OR23177
# Pavel.Evtushenko@jlab.org

OPTICAL DIFFRACTION RADIATION MEASUREMENTS AT CEBAF*

P. Evtushenko#, A. P. Freyberger, C. Y. Liu, Jefferson Lab, Newport News, VA USA
A. Lumpkin, Fermilab, Batavia, IL USA

Abstract

Optical diffraction radiation (ODR) is a promising technique, which could be used for non interceptive beam size measurements. An ODR diagnostic station was designed and installed on a CEBAF transfer beam line. The purpose of the setup is to evaluate experimentally the applicability range for an ODR based non interceptive beam size monitor and to collect data to benchmark numerical modeling. An extensive set of measurements were made at the electron beam energy of 4.5 GeV. The ODR measurements were made for both pulsed and CW electron beam of up to 80 μA. The wavelength dependence and polarization components of the ODR were studied using a set of insertable bandpass filters and polarizers. The typical transverse beam size during the measurements was ~150 microns. Complete ODR data, wavelength and polarization, were recorded for different beam sizes and intensities. The beam size was also measured with an optical transition radiation (OTR) as well as wire scanner located next to the ODR station. In this contribution we describe the experimental setup and present first results of the measurements with the comparison to the numerical simulations.

INTRODUCTION

Optical diffraction radiation is generated when a charged particle passes near a conductor at a distance comparable or smaller than $\gamma \cdot \lambda / 2\pi$, where γ is the relativistic Lorenz factor and λ is the wavelength of the radiation. The theory of the diffraction radiation is well developed [1]. In the case of a highly relativistic particle beam with large γ, a conductor located at a distance bigger than the transverse beam size will generate a significant amount of diffraction radiation in the optical wavelength range. Several ODR based schemes were suggested for non-intercepting beam size measurements [2-6]. Some of them utilize the angular distribution of the ODR whereas others make use of imaging of the radiator surface, i.e., near-field measurements. The near-field ODR was observed experimentally previously [8, 9]. A common condition in such measurements was that the integrated charge used to generate the ODR was several nC.

The Continuous Electron Beam Accelerator Facility (CEBAF) is a multipass superconducting LINAC delivering CW electron beam with an energy up to 6 GeV and average current up to 100 μA for nuclear physics experiments on fixed targets [10]. A typical beam size in CEBAF at high energy is 100 μm. standard video camera uses to integrate one field of a video signal (16.6 ms) and when running 100 μA beam is 1.66 μC. The combination of the these parameters, GeV range energy, 100 μm beam size and μC charge integrated within 16.6 ms, makes CEBAF an ideal facility to study develop and implement an ODR based non-intercepting beam size diagnostic, as was pointed out previously [11]. From the operational point of view it is very desirable to have such a non-intercepting beam size monitor. It can be used to detect drifts leading to a change in the betatron match early and therefore can improve beam availability for the nuclear physics experiments. A set of such beam size monitors positioned properly along a transport beam line could also provide online emittance monitoring as well as emittance measurements.

EXPERIMENTAL SETUP

The optical transition radiation (OTR) was used for reference beam size measurements. We have designed and built a radiator which could be used for both OTR and ODR measurements. The radiator is shown in Fig. 1. The ODR part of the radiator is a 300 μm thin silicon wafer optically polished and aluminized on one side. The thickness of the aluminum layer is about 600 nm. The wafer is mounted on an aluminum holder in such way that its edge does not have any frame underneath. This edge of the wafer was put close to the beam to generate the ODR. Minimizing the beam scattering in the OTR screen and reducing the beam losses downstream of the radiator is always desirable. Therefore next to the ODR radiator we have put a separate OTR radiator. The radiator is a 6 μm thin Kapton foil aluminized on one side and stretched on a frame so that it is flat. Surfaces of both radiators look as an optical mirror. The aluminization of both radiators is done to increase radiation yield.

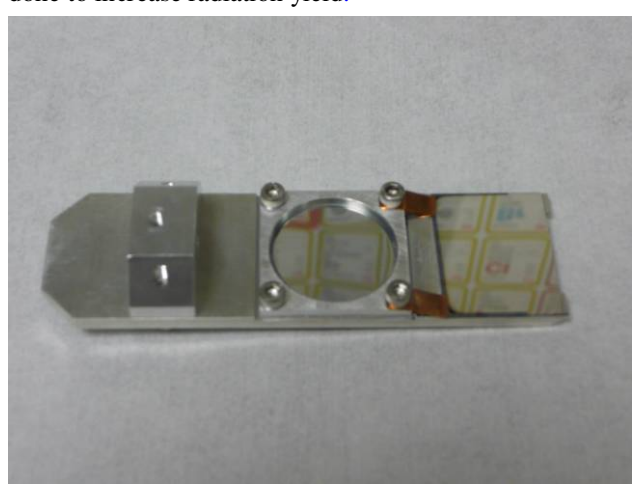

Figure 1: ODR-OTR radiator.

* Work supported by the U.S. DOE contract # DE-AC05-06OR23177
# Pavel.Evtushenko@jlab.org

EXTRACTING INFORMATION CONTENT WITHIN NOISY, SAMPLED PROFILE DATA FROM CHARGED PARTICLE BEAMS*: PART II

C.K. Allen#, W. Blokland, S.M. Cousineau, J.D. Galambos, ORNL, Oak Ridge, TN 38371 USA

Abstract

This is a continuation of work in [1]. The objective is to design a robust procedure for automating the analysis of beam profile data. In particular, we wish to extract accurate values for the beam position and beam size from profile data sets. These values may be then used to estimate additional beam characteristics such as the Courant-Snyder parameters.

INTRODUCTION

Profile data are typically obtained from particle-beam diagnostic devices such as wire scanner, laser strippers, or wire harps. The beam distribution is projected upon various spatial axes the effect being marginalization of the beam distribution with all variables except the projection axis. We provide a model for the data collection process which includes random noise components. The goal is to design a robust, automated procedure for accurate estimation of beam position μ and RMS beam size σ. Additionally, we need a process for automatic identification of bad data sets (typically such a process requires human intervention, a tedious, time consuming, and expensive endeavor). This goal is the first requirement for automated procedures for Twiss parameter estimation, transverse matching, and halo identification and mitigation. To realize our current goal we must make real world considerations. Specifically, we consider information content, noise (randomness), and sampling theory. Information content was covered previously [1]; we briefly review sampling.

Sampling and Measurements

Let $f(x)$ represent the profile distribution where x represents some spatial beam axis. Take the axis sampling locations to be equidistant so that $x_k = kh, k = 0, \ldots, N-1$, where $h > 0$ is the (constant) step length between measurements. Making the definition

$$f_k \triangleq f(x_k)$$

then $\{f_k\}$ is the sampling of the profile f. Now denote the set of profile measurements as $\{m_k\}_{k=0}^{N-1}$. These ordered measurements correspond, respectively, to the set of sampling locations $\{x_k\}_{k=0}^{N-1}$.

Moments

The n^{th} moment $\langle x^n \rangle$ of a distribution f is defined

$$\langle x^n \rangle \triangleq \frac{1}{Q}\int_{-\infty}^{+\infty} x^n f(x)dx, \qquad (1)$$

where the constant $Q \triangleq \int f dx$ is the total beam charge.

* This work supported by SNS through UT-Battelle, LLC, under contract DE-AC05-00OR22725 for the U.S. DOE.
#Corresponding author allenck@ornl.gov

Because we are dealing with sampled data we can only approximate these values. The beam position μ and RMS size σ are the first two moments of the distribution

$$\mu \triangleq \langle x \rangle,$$
$$\sigma \triangleq \langle (x-\mu)^2 \rangle^{\frac{1}{2}}. \qquad (2)$$

Because we are working with sampled data we normalize these quantities by h. Specifically, the continuous approximations to beam position and RMS size are $h\mu$ and $h\sigma$, respectively.

We take two approaches for approximating μ and σ, 1) computing μ and σ directly from the measurements, and 2) fitting a Gaussian approximation for f from the measurements from which μ and σ are determined.

The Measurement Process

Each measurement m_k is composed of both the actual beam profile f_k plus a noise component W_k, where W_k is part of a random process $\{W_k\}$. This noise introduces indeterminacy. Henceforth we can only generalize in terms of probabilities and stochastic (or "random") processes. Denote by E[·] the expectation operator of the random variable W_k, averaging over its ensemble. Then $\Omega_k \triangleq \mathrm{E}[W_k]$ is the mean and the quantity $V_k \triangleq \mathrm{E}[(W_k - \Omega_k)^2]^{1/2}$ is the standard deviation, or variance. Although the values of a random process are not deterministic but their statistics are, specifically, Ω_k and V_k can be measured through a calibration experiment. Most noise processes are modeled as random processes.

Take the process $\{W_k\}$ to be a Gaussian distributed white noise process with mean Ω and variance V, then $W_k = W$ for all k, and W is Gaussian distributed. We have

$$m_k = f_k + W, \qquad k = 0, \ldots, N-1 \qquad (3)$$

where

$$Pr(W = w|\Omega, V) = \frac{1}{\sqrt{2\pi}V} e^{-\frac{(w-\Omega)^2}{2V^2}}. \qquad (4)$$

The notation $\Pr(M_k = m_k|\Omega, V) = \Pr(W = m_k - \Omega - f_k|\Omega, V)$ indicates the probability that the measurement (random variable) M_k at axial position x_k has value m_k, given that the noise has mean Ω and variance V.

DIRECT MOMENT COMPUTATION

Because we are dealing with sampled data we can only approximate the moments $\langle x^n \rangle$. The simplest form of approximation would be to replace the integration in (1) with a finite summation. We begin with a definition to simply the sequel:

LASER-BASED PROFILE AND ENERGY MONITOR FOR H- BEAMS*

R. Connolly, J. Alessi, S. Bellavia, C. Dawson, C. Degen, W. Meng, D. Raparia, T. Russo and N. Tsoupas
Brookhaven National Lab
Upton, NY, USA

Abstract

A beam profile and energy monitor for H- beams based on laser photoneutralization was built at Brookhaven National Laboratory (BNL)* for use on the High Intensity Neutrino Source (HINS) at Fermilab. An H- ion has a first ionization potential of 0.75eV and can be neutralized by light from a Nd:YAG laser (λ=1064nm). To measure beam profiles, a narrow laser beam is stepped across the ion beam, removing electrons from the portion of the H- beam intercepted by the laser. These electrons are channeled into a Faraday cup by a curved axial magnetic field. To measure the energy distribution of the electrons, the laser position is fixed and the voltage on a screen in front of the Faraday cup is raised in small steps. We present a model which reproduces the measured energy spectrum from calculated beam energy and space-charge fields. Measurements are reported from experiments in the BNL linac MEBT at 750keV.

INTRODUCTION

In 2002 we reported on a project at BNL to develop a beam profile monitor for H- beams using photoneutralization by a laser beam directed perpendicular to the ion beam [1]. That effort was in support of the Spallation Neutron Source being built at Oak Ridge National Lab [2]. Recently BNL was contracted by Fermi National Lab to build a laser-based H- beam-profile monitor for use on the HINS [3].

A pulse of electrons is removed from an H- beam by directing a 50mJ, 10ns light pulse from a Q-switched Nd:YAG laser through the ion beam. This electron pulse is channeled into a Faraday cup via a curved axial magnetic field produced by a series of coils. To measure transverse profiles, the trajectory of the focused laser beam is moved across the ion beam in small steps by small rotations of a mirror about 45°. At each mirror angle the electron current is integrated over the full laser pulse. A profile is produced by plotting total charge vs. mirror position.

In addition to transverse ion-beam profiles we measure the energy distribution of the signal electrons by ramping the voltage on a retarding grid in front of the cup. The energy of each electron is the sum of the initial kinetic energy and the energy it receives from the space-charge field as it is transported to the collector [4].

In this paper we describe the detector and the measurements. We present a model which reproduces the measured energy spectrum from the beam current and transverse size, bunch length, and bunching fraction of the H- beam. The energy measurements are motivated by the desire to measure the energy spread of the H- beam. For the test beam energy of 750keV beam energy-spread information is buried in the space-charge effects, but we anticipate being able to measure beam energy spread in the BNL HEBT at 200MeV based on these experiments.

DETECTOR

Figure 1 is a diagram of the detector from the side showing the signal-electron path. The neutralization chamber is a six-way cross with the laser beam passing through viewports either horizontally or vertically. A curved solenoidal magnetic field, generated by a series of coils, channels the signal electrons into the Faraday cup collector. A voltage grid in front of the collector provides secondary-electron suppression for profile scans and retarding voltage for energy scans. The Faraday cup charge signal passes to ground through a 1kΩ resistor. The resulting voltage pulse is digitized by a LeCroy LT584L oscilloscope.

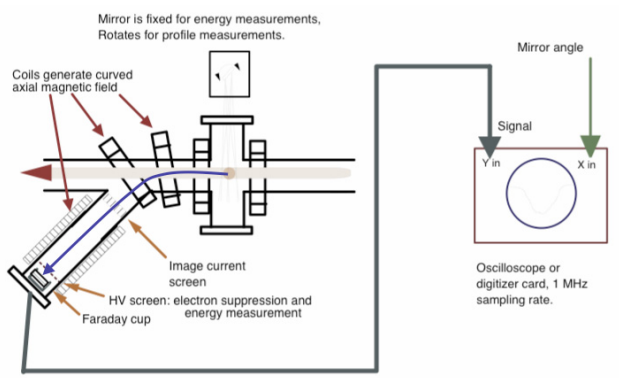

Figure 1: Longitudinal schematic. Electrons from the H- beam are guided by magnetic field through grid into cup.

A transverse diagram of the device is shown in Fig. 2. The 50mJ/pulse laser head [5] is mounted on an optics plate with a linear translation stage [6] to select scanning axis and two galvo-motors [7] to rotate mirrors about 45° to scan the laser beam. The optics platform and the full beamline installation in shown in Fig. 3.

* This work was performed under the auspices of the U.S. Department of Energy.

ACTIVITIES ON HIGH BRIGHTNESS PHOTO-INJECTORS AT THE FRASCATI LABORATORIES, ITALY

R. Boni, D. Alesini, M. Bellaveglia, C. Biscari, M. Boscolo, M. Castellano, E. Chiadroni, A. Clozza, L. Cultrera, G. Di Pirro, A. Drago, A. Esposito, M. Ferrario, L. Ficcadenti, D. Filippetto, V. Fusco, A. Gallo, G. Gatti, A. Ghigo, B. Marchetti, A. Marinelli, C. Marrelli, M. Migliorati, A. Mostacci, E. Pace, L. Palumbo, L. Pellegrino, R. Ricci, U. Rotundo, C. Sanelli, M. Serio, F. Sgamma, B. Spataro, F. Tazzioli, S. Tomassini, C. Vaccarezza, M. Vescovi, C. Vicario,
INFN-LNF, Frascati, RM, Italy
F. Ciocci, G. Dattoli, A. Dipace, A. Doria, M. Del Franco, G. P. Gallerano, L. Giannessi, E. Giovenale, G. Orlandi, S. Pagnutti, A. Petralia, M. Quattromini, A. Lo Bue, C. Ronsivalle, P. Rossi, E. Sabia, I. Spassovsky, V. Surrenti,
ENEA C.R. Frascati, RM, Italy
A. Bacci, I. Boscolo, F.Broggi, F. Castelli, S. Cialdi, C. De Martinis, D. Giove, C. Maroli, V. Petrillo, A.R. Rossi, L. Serafini, INFN-Mi, Milano, Italy
M. Mattioli, M. Petrarca, M. Serluca, INFN-Roma I, Roma, Italy
L. Catani, A. Cianchi, INFN-Roma II, RM, Italy
J. Rosenzweig, UCLA, Los Angeles, CA, USA
M. E. Couprie, SOLEIL, Gif-sur-Yvette, France
M. Bougeard, B. Carré, D. Garzella, M. Labat, G. Lambert, H. Merdji, P. Salières, O. Tchebakoff, CEA Saclay, DSM/DRECAM, France.
J. Rossbach, Hamburg University and DESY

Abstract

An intense activity on high brightness photo-injectors for SASE-FEL experiments and facilities, is being carried out, since 2003, in the Research Site of the INFN Frascati Laboratory, Rome, in collaboration with CNR and ENEA. SPARC is the 150 MeV photo-injector, in advanced phase of commissioning at LNF. The electron beam, which drives a 530 nm FEL experiment, is being characterized in terms of emittance, energy spread, peak current. The matching with the linac confirmed the theoretical prediction of emittance compensation based on the "invariant envelope" matching. The demonstration of the "velocity bunching" technique is in progress too. The SPARC photo-injector is the test facility for the soft-X FEL project named SPARX [1], that is based on the generation of ultra high peak brightness electron beams at the energies of 1.2 and 2.4 GeV generating radiation in the 1.5-13 nm range. SPARX will be realized in the Tor-Vergata University campus. In this paper we report the experimental results obtained so far with SPARC and the design status of the SPARX project.

THE SPARC TEST FACILITY

The INFN Frascati Laboratory (LNF) and the ENEA Frascati Research Center (CRF) are involved since 2003 in the development and the commissioning of the S-band photo-injector SPARC, aimed to generate high brilliance electron beams to drive SASE-FEL experiments in the visible and UV region, with a laser-seeding process. Moreover, SPARC will be the pre-injector of SPARX, the new high brightness electron linac to generate SASE-FEL radiation in the 40 to 0.6 nm wavelength range, that will be built in the campus of the Tor-Vergata (TV) Rome University, 4 km airline from LNF.

The SPARC research program is scheduled in two phases. The first one is concluded and consisted in characterizing the electron beam, photo-emitted at 5.6 MeV by the cathode of a S-band RF gun, illuminated by Ti-Sa Laser beam pulses [2]. The results of the first commissioning phase are reported in [3]. The second phase, still in progress, foresees a detailed analysis of the beam matching with the linac to confirm the emittance compensation theory, based on the "invariant envelope" matching [4] and to verify the emittance compensation with the "velocity bunching" (VB) experiment [5]. SASE and SEEDING experiments are also foreseen by the end of 2008. SPARC will also allow to study ultra-short beams physics, plasma wave-based acceleration, and to generate advanced X-ray beams via Compton back-scattering.

SPARC COMMISSIONING

The installation of the whole machine, including six permanent magnet (pm) undulators and the by-pass diagnostic channel was completed after disassembling the emittance-meter in January 2007. Three S-band sections [6] have been power conditioned in short time and operate at 20-20-10 MV/m respectively, providing a final beam energy of 150 MeV. Digital based, low level RF (LLRF) controls [7] allow to monitor, synchronize and stabilize the accelerating section RF fields and the phase of the laser pulses on the photocathode. The beam energy stability achieved is less than 0.1%. Two solenoids with 0.18 T field, are wrapped around the first two accelerating

DEVELOPMENT OF A PHOTOCATHODE RF GUN FOR AN L-BAND ELECTRON LINAC

S. Kashiwagi , R. Kato, G. Isoyama#, ISIR, Osaka University, Ibaraki, Osaka, 567-0047, Japan
H. Hayano, T. Muto, J. Urakawa, High Energy Accelerator Research Organization, Tsukuba, Ibaraki 305-0801, Japan
M. Kuriki, Graduate School of Advanced Sciences of Matter, Hiroshima University, Higashi-Hiroshima, Hiroshima 739-8511, Japan

Abstract

We have begun development of the L-band photo-cathode RF gun for the L-band linac at ISIR, Osaka University to advance studies with the high-intensity and low emittance electron beam, in collaboration with KEK and Hiroshima University. As the fist step, we plan to develop and commission the L-band RF electron gun for the Superconducting RF Test Facility at the High Energy Accelerator Research Organization. While waiting for delivery of an RF cavity and an input coupler from the Fermi National Accelerator Laboratory, we are preparing for the low lever RF measurement. Some results of the preparatory works are reported, including computer simulation for tuning of RF characteristics of the cavity, design of an input coupler for low level RF measurement, and computer simulation to evaluate characteristics of the accelerated electron beam.

INTRODUCTION

We conduct experiments on radiation chemistry by means of pulse radiolysis and basic study on Self-Amplified Spontaneous Emission (SASE) in the far-infrared region using a high-intensity single-bunch electron beam from the 40 MeV, L-band electron linac at the Institute of Scientific and Industrial Research (ISIR), Osaka University. The linac is equipped with a DC 100 kV thermionic electron gun and can accelerate the single bunch electron beam with charge up to 91 nC.

A project to develop and use an L-band photo-cathode RF gun is being conducted at the Superconducting RF Test Facility (STF) at High Energy Accelerator Research Organization (KEK), which is a facility to develop accelerator technology necessary for construction of the main linac of the International Linear Collider (ILC). The aim of the project is to evaluate performance of superconducting accelerating structures using a multi-bunch electron beam that meets specifications given by ILC. A 1.5 cell L-band RF electron gun to produce such an electron beam is being fabricated currently at Fermi National Accelerator Laboratory (FNAL) in USA for the experiment.

In order to advance the studies at ISIR, Osaka University further in future, we joined the project in 2008 and began development of an L-band photo-cathode RF electron gun, which can produce a high-intensity and low emittance electron beam, in collaboration with KEK and Hiroshima University. We will evaluate RF performance of the cavity to be made at FNAL at a low RF level and then will conduct its high power test. In parallel with the activities, we plan to design an L-band RF electron gun optimized for the L-band linac at Osaka University based on results of the measurement and computer simulation for the FNAL gun.

We currently study how to tune the resonance frequency of the cavity, 1.3 GHz in the π mode, by calculating relations of the frequency and field balance between the half cell and the full cell with variations of the cavity shape and dimensions. We have also begun on design and fabrication of an RF coupler of the coaxial feed type to be used in the low level RF measurement. In this paper, we will report results of electric field calculation for the cavity of the electron gun being made at FNAL, progress of preparation for the low level RF measurement, and results of evaluation of electron beam characteristics calculated with PARMELA.

L-BAND RF GUN

Cavity for Electron Gun

We begin design study of a cavity for the L-band RF electron gun of the resonance frequency 1300 MHz, based on the design of the 1.5 cell RF cavity being fabricated at FNAL. The L-band RF cavity adopts the same design of the cavity used for the XFEL project in Europe, which has been designed by scaling the cavity for the S-band RF electron gun developed at BNL [1] up to the L-band. Cooling water channels of the cavity are reinforced to endure the high duty cycle RF power [2], and a coaxial RF coupler is adopted to make axial symmetry of the

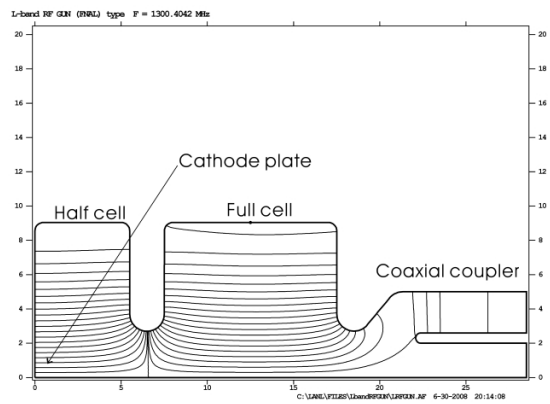

Figure 1: Electric field distribution of the π mode in the L-band RF electron gun.

#isoyama@sanken.osaka-u.ac.jp

DEVELOPMENT OF A CS-TE CATHODE RF GUN AT WASEDA UNIVERSITY

Y. Kato†, K. Sakaue, T. Suzuki, A. Murata, C. Igarashi, A. Masuda, T. Nomoto, A. Fujita, T. Hirose, Y. Hama, M. Washio, RISE, Tokyo, Japan
J. Urakawa, T. Takatomi, N. Terunuma, H. Hayano, KEK, Ibaraki, Japan
S. Kashiwagi, ISIR, Osaka, Japan
R. Kuroda, AIST, Ibaraki, Japan
Y. Kamiya, ICEPP, Tokyo, Japan
M. Kuriki, HU/AdSM, Higashi-Hiroshima, Japan

Abstract

A photo-cathode RF-Gun is one of the good alternatives for the electron source, because of its high gradient on the electron emitter causing small beam emittance, and tenability of initial beam profile especially for electron bunch length. Therefore, we are operating as a high brigh-tness short pulse electron source.

In last year, we have been developing a high quality electron source based on photo-cathode RF-gun which is newly designed RF cavity and has a Cs-Te cathode with high quantum efficiency [1] [2]. Improved RF-Gun cavity has four compact tuners on each half cell and full cell, which can be tuned the resonance frequency to deform the cavity wall. Also removing the Helicoflex seal and tuning holes, reduction of the dark current is expected.

According to these improvements, the Q value and shunt impedance of the new RF-Gun cavity increased 20% compared with the previous RF cavity. In addition, the dark current of cavity was reduced and the good electron beam parameters could be achieved compared with pre-vious RF-Gun with a Cu cathode.

INTRODUCTION

At Waseda University, we have been developing a high quality electron source based on photo-cathode RF-gun and performing the application experiment using high quality electron beam. Until now, we have succeeded the soft X-ray generation via inverse-Compton scattering and pulse radiolysis system for studying the early processes of radiation chemistry using electron beams generated by copper cathode RF-gun as an electron beam application.

Cs-Te RF-gun is expected to generate higher charge electron bunches with a low emittance than a copper cathode because of its high quantum efficiency. Furthermore, its high quantum efficiency enables us to generate a multi-bunch electron beam and to extend the tenability of electron beam parameters for our application experiments [3]. However, a Cs-Te cathode has a relatively short life compared with a copper, so that it has to be exchanged occasionally, thus we have developed a new RF-gun cavity which can be attached the compact cathode load-lock system. Moreover, we improved the design of an existing RF-gun cavity for the reduction of the dark current and the higher electric field.

Figure 1 shows the picture of improved photo-cathode RF-Gun system at Waseda University.

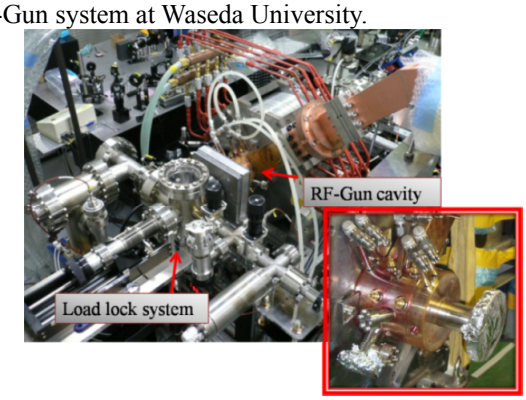

Figure 1: Improved photo-cathode RF-Gun system.

In this conference, the performance of the improved cavity, the results of electron beam generation experiments and the calculated results of beam loading effect of the multi-bunch electron beam generation will be reported.

IMPROVED DESIGN OF PHOTO-CATHODE RF-GUN CAVITY

The design of a new RF-Gun cavity was based on the conventional type operated at Waseda University and KEK-ATF. Figure 2 (a) shows the previously RF-Gun cavity. It consists of the three components such as a half cell, a full cell, and end plate. The wall of end plate was polished as a Cu cathode and attached to the half cell through a SUS plate and a Helicoflex seal, which can be tuned the resonance frequency of the half cell by changing a torque provided to a Helicoflex seal. Concerning the full cell frequency tuning, each cells are brazed so that resonance frequency of the full cell is tuned by conventional tuner with a tuning hole.

However these tuning methods are considered to be the major cause of electrical discharge and dark current source and Q-value decrease. Therefore, as the improvement of RF-Gun cavity end plate is brazed to the half cell for removing the complicated structure around the

*Work supported by MEXT High Tech Research Project HRC707, JSPS Grant-in-Aid for Scientific Research (B) (2) 16340079
#katyu-spring@fuji.waseda.jp

RF GUN DEVELOPMENT WITH IMPROVED PARAMETERS

V. Paramonov *, Yu. Kalinin, INR RAS, Moscow,
M. Krasilnikov, T. Scholz, F. Stephan, DESY, Zeuthen,
K. Floettmann, DESY, Hamburg

Abstract

During development and operation of DESY L-band RF gun cavities, desires for further improvements were formulated. The next step of development is based on the proven advantages of existing cavities, but includes significant changes. The L-band 1.6 cell RF gun cavity is intended for operation in pulse mode with electric fields at the cathode of up to $60\frac{MV}{m}$, RF pulse length of $\sim 1ms$ and average RF power higher than existing gun cavities. In the new design the cell shape is optimized to have the maximal surface electric field at the cathode and lower RF loss power. The cavity cells are equipped with RF probes. Cooling circuits are designed to combine cooling efficiency with operational flexibility. In the report, the main design ideas and simulation results are described.

INTRODUCTION

In the development and optimization of the high brightness electron sources for Free Electron Lasers (FELs) and linear colliders several RF gun cavities, starting from TTF Gun [1] and differing mainly in the cooling circuit design, were constructed and studied. The last results for the Gun cavities developed can be seen in [2]. Experience of operation and results of various Gun cavity parameters study are the basement of desires and ideas for further improvements. In the next step of development more significant changes are required, starting from cavity RF shape. The influence of proposed improvements on different cavity parameters should be considered and analyzed carefully.

RF CAVITY SHAPE

The profile of existing DESY 1.6 cell axial symmetrical RF Gun cavities [1] is shown in Fig. 1a together with electric field distribution. This cavity is considered further as the Reference Cavity (RC) and has the circular iris nose tip. The primary parameter of the RF Gun cavity is the RF electric field strength E_c at the photo cathode surface. The maximal electric field at the cavity surface E_{sm} in RC is at the iris tip and $E_{sm} \approx 1.2E_c$.

In the improved cavity, which is also 1.6 cell, Fig. 1b, the circular iris tip is replaced at the elliptical one. Dimensions are optimized to have $E_{sm} = E_c$. Together with E_{sm} reduction by $\sim 20\%$, the elliptical nose shape results in increasing of the coupling coefficient between cavity cells and related mode separation. The iris nose shape has no influence at the cavity quality factor Q_0 and decreases slightly $\frac{E}{\sqrt{W_0}}$ ratio, where W_0 is the stored energy. More RF power is necessary to get E_c required with the same Q. Cavity Q factor is increased by stronger rounding in the outer cell shapes. Different rounding combinations were considered. From practical reasons we chose the same outer radius for both cells and the same rounding radius in the first cell and in second cell near iris. The cavity operating frequency is adjusted by outer cell radius. The maximal field strength at the axis of the cells is equalized by adjusting the another radius of the second cell rounding. As the result, the cavity Q factor is increased by $\sim 10\%$ and required RF pulse power is less by $\sim 4\%$. Even taking into account effects of RF pulsed heating effects and cavity parameters change during RF pulse, [3], lower RF pulse power is required for improved cavity to get required E_c value.

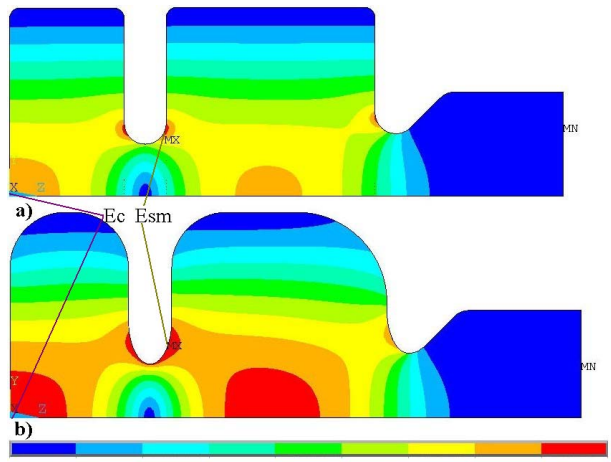

Figure 1: RF shape profile for the reference (a) and improved (f) cavity together with electric field distributions.

BEAM DYNAMIC

The cavity shape change results in small deviations of electric field distribution along the cavity and can change beam parameters. All combinations of shapes, discussed in cavity RF profile definition, were analyzed in simulations with the ASTRA code considering the European XFEL photo injector performance. Simulations revealed no essential difference for various cavity options, including RC and improved option, Fig. 1b. Optimized projected emittance for all cavity types is about the same, within simulations discrepancy. Slice parameters of the electron beam are also very similar. Optimum currents of main solenoid are within several A. Spread of optimum rms sizes of the

* paramono@inr.ru

MEASUREMENTS AND MODELING AT THE PSI-XFEL 500 kV LOW-EMITTANCE ELECTRON SOURCE

T. Schietinger, A. Adelmann, Å. Andersson, M. Dietl, R. Ganter, C. Gough, C.P. Hauri, R. Ischebeck, S. Ivkovic, Y. Kim, F. Le Pimpec, S.C. Leemann, K. Li, P. Ming, A. Oppelt, M. Paraliev, M. Pedrozzi, V. Schlott, B. Steffen, A.F. Wrulich,
Paul Scherrer Institut, CH-5232 Villigen PSI, Switzerland

Abstract

Paul Scherrer Institute (PSI) is presently developing a low-emittance electron source for the PSI-XFEL project. The electron gun consists of an adjustable diode configuration subject to pulses of 250 ns (FWHM) with amplitude up to 500 kV from an air-core transformer-based high-voltage pulser. The facility allows high gradient tests with different cathode configurations and emission processes (pulsed field emission and photo emission). In the first stage, the beamline consists of focusing solenoids followed by an emittance monitor. Selected beam characterization measurements from photo cathode operation driven by a 266 nm UV laser system delivering 4 μJ energy during 6.5 ps (RMS) are presented and compared to the results of 3D particle tracking simulations.

INTRODUCTION AND MOTIVATION

The goal of the PSI-XFEL project is the realization of an X-ray Free Electron Laser (FEL) operating in the wavelength range between 1 and 100 Å and producing up to 10^{12} photons per pulse at a repetition rate of 100 Hz. To keep spatial and financial requirements within reasonable limits, the project foresees a compact design featuring a 6 GeV S-band main linac. This compact layout requires a high-brightness electron beam, which in turn calls for a low-emittance source. The strategy chosen for the PSI-XFEL project consists in utilizing a high-voltage pulsed diode providing fast acceleration with a special cathode optimized for low emittance (photo cathode or field emitter array). To evaluate various configurations and materials, a test stand has been set up at PSI consisting of a pulser, a laser system and a diagnostic beamline [1]. Figure 1 gives an overview of the pulser and beamline assembly.

An important aspect of the test facility, in particular in view of the further advancement of the PSI-XFEL project, is to improve the understanding of the space charge dominated electron beam by way of simulation. Indeed, one of the objectives of the test facility is the validation of our 3D particle tracking code against observations. In this paper we present a set of measurements taken at the test facility and compare it to the result of a 3D particle simulation.

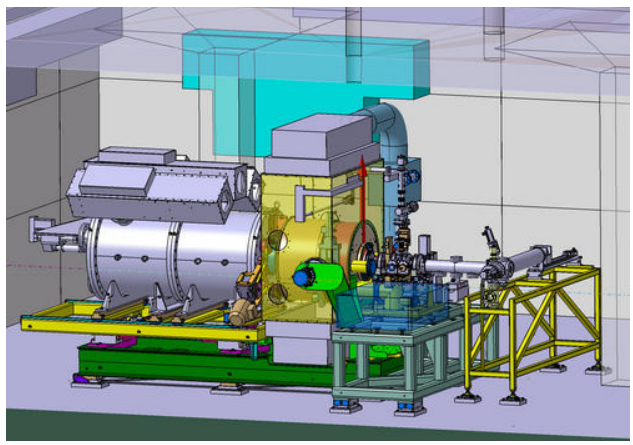

Figure 1: Schematic view of pulser (left) and diagnostic beamline, including the emittance monitor (right).

EXPERIMENTAL SETUP

The air-core transformer-based high-voltage pulser delivers pulses of 250 ns (FWHM) with amplitude up to 500 kV [2]. The diode gap between two mirror-polished electrodes is adjustable between 0 and 30 mm. Electrodes manufactured from stainless steel have been found to withstand the highest gradients and generally to offer the most stable experimental conditions for beam measurements. The measurements described here were performed with hand-polished stainless steel electrodes separated by 7 mm at a voltage of 313 kV, corresponding to a gradient of 44.7 MV/m. The chosen gradient represents a compromise between high accelerating field and stable operation with this particular set of electrodes.

The metallic cathode is illuminated by laser pulses when the applied voltage across the anode-cathode gap is at maximum. The laser light enters the electron beamline from a side viewport and is reflected towards the cathode by a 5 mm × 5 mm mirror. The mirror edge is at least 5 mm away from the electron beam axis. The laser pulses, generated by a Nd:vanadate (Nd:VAN) passively mode locked picosecond system, feature a Gaussian time profile (σ_t = 6.5 ps). The transverse profile is also Gaussian, with spatial dimensions controlled by a two-lens telescope assembly and monitored via a "virtual" cathode: a reflexion from the entrance viewport is monitored on a small optical table beside the beamline, at a distance equal to that between

LIENARD-WIECHERT POTENTIALS AND METHOD OF IMAGES IN RF FREE ELECTRON LASER PHOTOINJECTOR

W. Salah; The Hashemite University, Zarqa 13115, Jordan, R.M. Jones; Cockcroft Institute, Daresbury, WA4 4AD, UK; University of Manchester, Manchester, M13 9PL, UK.

Abstract

Based on Lienard-Weichert retarded potentials and the potential due to the image of charges on the cathode, a rigorous relativistic description of the beam transport inside the RF-photoinjector is presented. The velocity dependent effects are taken into account. Simulations are presented for parameters of the "ELSA" photo-cathode.

INTRODUCTION

RF-photoinjectors are used as a source of low-emittance and ultra-high brightness electron beams. There are a limited number of codes which take wakefield effects into account in computing electron transport in photoemission. Although there are notable exceptions which do include these effects numerically [1]. The electromagnetic wake in a photoinjector is different from the standard case of a coasting ultrarelativistic beam due to the rapidly changing velocity. In this situation the influence of the acceleration-radiation field, or retardation, must be taken in to account in addition to the image charges on the cathode.

The aim of the present paper is to treat the wakefield of an intense electron beam strongly accelerated inside a cylindrical cavity similar to that of a photoinjector. We employ both Lienard-Weichert potentials and the method of images in order to derive an analytical expression for the field driven by the beam. Electromagnetic field expressions are computed for the "ELSA" photoinjector

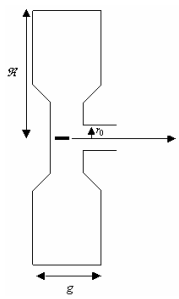

Figure 1: "ELSA" photoinjector (144 MHz cavity).

facility [2] schematized in Fig. 1. Furthermore, by applying the principle of causality we are able to simplify the effects associated with the actual cavity, illustrated in Fig. 1, to an analysis of the electromagnetic fields in a pill-box cavity.

The beam pulse is assumed to be axisymmetric, of radius a, emitted by the cathode from $t = 0$ to $t = \tau$ (where τ is the time at which the photoemission ends), with a constant and uniform current density J. The acceleration RF-electric field $\vec{E}_0$ may be considered as constant and uniform provided, the beam pulse duration $\tau \ll 1/\nu$ (where ν is the RF frequency) and the beam radius a is small compared to the cavity radius $\Re$. For the "ELSA" photoinjector ν = 144 MHz, $\Re$ = 60 cm, πa^2=1 cm^2; the first condition provides the pulse duration τ << 7 ns. Under these conditions, the beam velocity $\vec{\beta}(z,t)$ and acceleration $\vec{\eta}(z,t)$ can be shown [3] to be parallel to $\vec{E}_0$ and independent of time:

$$\vec{\beta}(z,t) = \beta(z)\,\vec{u}_z \tag{1}$$

$$\vec{\eta}(z) = \eta(z)\,\vec{u}_z$$

$$\beta(z) = \frac{\sqrt{(1+Hz(t))^2 - 1}}{1+Hz(t)} \tag{2}$$

$$\eta(z) = 1 + Hz \tag{3}$$

$$z(t) = \frac{1}{H}\left(\sqrt{1+(Hc(t-t_z))^2} - 1\right) \tag{4}$$

$$H^{-1} = \frac{mc^2}{eE_0} \tag{5}$$

where: m and e are the rest mass and charge of the electron, respectively, $z(t)$ is the longitudinal coordinate of an electron at time t, and t_z is the time at which an element z of the beam leaves the photocathode.

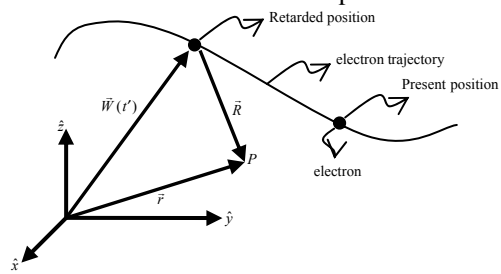

Figure 2: Field driven by an electron.

The electromagnetic fields $(\vec{E},\vec{B})$ generated at time t and point P, by an electron, that is moving on a specified trajectory depend on the position W(t') of the electron at time t' (Fig. 2). These fields are driven from the rebuilt scalar and vector potentials Φ and $\vec{A}$, respectively. Taking into account the boundary condition imposed on the cathode by the equipotential and causality, these fields are given by Lienard-Weichert expression as

$$\vec{E}(P,t|W) = -\frac{A}{c(R - \vec{R}\,.\,\vec{\beta}(t'))^3}\left(c\frac{\left(\vec{R} - \vec{\beta}(t')R\right)}{\gamma(t')} + \vec{R}\times\{(\vec{R} - \vec{\beta}(t')R)\times\frac{\partial\vec{\beta}(t')}{\partial t'}\}\right) \tag{6}$$

DESIGN AND OPTIMIZATION OF AN S-BAND PHOTOINJECTOR

Jang-Hui Han, Diamond Light Source, Oxfordshire, United Kingdom

Abstract

Several X-ray Free Electron Laser (XFEL) projects are under construction or are being proposed over the world. For successful XFEL operations photoinjectors with low transverse emittance are one of the key elements. For the European XFEL and LCLS projects, photoinjectors have been developed to reach their requirements, typically with a normalised emittance of 1 mm mrad for a 1 nC beam. Here, we make a further optimization of an S-band photoinjector to achieve 0.4 mm mrad for a 1 nC bunch in a structure that should permit high repetition rates operation. Optimizations for alternative operation conditions with a 0.2 nC bunch charge for lower emittance and a 10 pC charge for ultrashort pulse ($<$ 100 fs) generation are also shown.

INTRODUCTION

Two kinds of photocathode RF guns are successfully used as injectors for VUV or X-ray FELs. LCLS [1] uses a gun improved from the BNL/SLAC/UCLA guns which operate with a 2.856 GHz resonant frequency. The FLASH gun [2] operates at 1.3 GHz. Both gun cavities are composed of a first half cell and a second full cell. In the LCLS gun, RF power is coupled to the cavity through the side of the second cell and the focusing solenoid is located downstream of the cavity. In the FLASH gun, RF power is coupled coaxially through the exit of the second cell and the solenoid surrounds the cavity. In general, S-band guns provide a shorter pulse length and lower transverse emittance beam thanks to the higher accelerating field compared to L-band guns. Typically, the maximum field is 40 to 60 MV/m in L-band guns but 120 MV/m or higher in S-band guns. With a coaxial RF coupler, the RF field in the cavity is axisymmetric and the focusing solenoid can be located close to the cathode. In addition, the coaxial coupler allows more cooling-water channels around the cavity symmetrically. Here, we show a new design of an S-band photocathode RF gun with a coaxial coupler.

GUN DESIGN AND OPTIMIZATION

In an RF gun cavity, an electron beam is generated by a drive laser pulse illuminated at a photocathode located on the back plane of the first cell. When the photon energy of the laser pulse excites electrons in the cathode so to overcome the potential barrier, the electrons are emitted into the vacuum. Depending on the direction of the RF field the electrons can be accelerated downstream. When the accelerated beam reaches the second cell the direction of the RF field is reversed and therefore the beam can be further accelerated. Since the beam starts at the first cell with almost zero velocity, there exists a large phase slippage. In order for the beam to get accelerated in sequence the beam must start earlier than maximum acceleration phase (90°) at the first cell depending on the first cell length and the accelerating field strength. For example, for a lower field strength or for a longer first cell length, the flight time in the first cell is longer, the phase slippage is higher, and the phase of beam emission for an optimum acceleration is shifted towards 0°. The beam dynamics (emittance and bunch length) of the beam strongly depends on the emission phase.

A new S-band gun was designed adopting the advanced features of the DESY gun [3], like the coaxial RF coupler and the cooling-water channels over the entire cavity surface. The resonant frequency was chosen as 2.998 GHz. Compared to the Eindhoven gun [4], which is another S-band gun with a coaxial coupler, the first cell length has been optimized for smaller emittance and the possibility of further cooling channel installation has been considered here. A focusing solenoid is located around the gun cavity (see Fig. 1). Another solenoid upstream of the gun compensates the magnetic field at the cathode. Even if the resonant frequency of the cavity is fixed as 2.998 GHz, the lengths of the first and second cells are slightly variable while keeping the cavity in resonance. The radii of the cells should be adjusted when the cell lengths are changed. The length of the first cell dramatically influences the beam dynamics while the length of the second cell does not visibly affect the beam dynamics. A shorter first cell length allows a higher acceleration field during beam emission at the cathode and a shorter electron flight time between the cathode and the second cell. A higher acceleration field minimize the beam quality degradation caused by the space charge force. The first cell length was set to 0.54 times a half of the RF wavelength and the second cell set to 0.98 times a half wavelength. The RF field in the cavity were calculated by SUPERFISH [5] (Fig. 2). After scaling down from the DESY L-band gun to the S-band, the iris thickness was changed thicker for allowing cooling channels inside the iris and the diameter of the coupler antenna was enlarged for a weaker interaction with electron beams. The π-mode of the RF is utilized for the beam acceleration. Even if the 0-mode is separated from the π-mode, the tail of the 0-mode peak is still activated at the resonant frequency of the π-mode, 2.998 GHz. When the 0-mode is activated, the electron beam is affected by the unwanted 0-mode field in a wrong phase. If the 0-mode is separated far from the π-mode, the unwanted effect is reduced. In this design, the mode separation is 18.25 MHz, which is larger than those of the other S-band guns [1, 4].

With this gun, the beam dynamics was calculated with ASTRA [6]. Parameters for optimization were the laser beam size and pulse length, the RF gun phase, and the solenoid field distribution and strength and the location.

THE OPTIMIZATION OF A DC INJECTOR FOR THE ENERGY RECOVERY LINAC UPGRADE TO APS*

Yin-e Sun[1,2], Hairong Shang[1], Michael Borland[1], Yuelin Li[1], Katherine Harkay[1]
[1]Advanced Photon Source, Argonne National Lab., Argonne, IL 60439, USA
[2]Accelerator Physics Center, Fermilab, Batavia, IL 60510, USA

Abstract

An energy recovery linac based light source is a potential revolutionary upgrade to the Advanced Photon Source (APS) at Argonne National Laboratory. The concept relies on several key research areas, one of which is the generation of ultra-low emittance, high-average-current electron beams. In this paper, we present our investigation of a dc-gun-based system for ultra-low emittance bunches in the 20 pC range. A parallel multi-objective numerical optimization is performed in multi-parameter space. Parameters varied include experimentally feasible drive-laser shapes, the DC gun voltage, the thermal energy of the emitted photo-electrons and other electric or magnetic field strengths, RF cavity phase etc. Our goal is to deliver a $\sim$10 MeV, 20 pC bunch at the entrance of the linac with an emittance of 0.1 μm or lower, rms bunch length of 2 $\sim$ 3 ps, and energy spread no larger than 140 keV. We present the machine parameters needed to generate such an injector beam, albeit without a merger.

INTRODUCTION

The APS is a storage-ring based light source. Fundamental physics principles governing a storage ring determine the electron beam emittance as well as its fractional energy spread. It is difficult to improve the beam quality dramatically solely by upgrading the storage ring[1], due to the requirement to keep the energy fixed at 7 GeV while accommodating the existing circumference and number of sectors. In contrast, the emittance of the electron beam in a linac is inversely proportionally to the beam energy, as the normalized emittance is constant. Therefore emittance much smaller than the APS storage ring is possible in a linac of the same beam energy. However, high average current (e.g., 100 mA) is needed for a facility to operate as a state-of-art light source. With 7 GeV beam energy, this corresponds to 700 MW beam power. The only feasible way to operate such a linac-based light source is to have the beam energy recovered [2] after it is used to generate light.

One of the most challenging aspects of the ERL design is the injector, as it requires unprecedented average current with extremely small normalized emittance. Currently there are several DC guns in operation for the ERLs, most notably at TJNAF [3]. However, none of these operating guns meets the requirements of the ERL upgrade at APS [4]. Some high performance dc-gun-based system have been investigated for ultra-low emittance beams [5, 6]. None of these analysis delivers the desired charge (20 pC or higher) while including the critical merger between the injector and the linac. In this paper, we present a first step in our efforts, namely, the design of a dc-gun-based injector without a merger system.

OPTIMIZATION METHOD

This injector design is developed using the multi-objective optimization techniques, similar to those employed by Bazarov et al. [5]. At APS, a global parallel optimizer named GeneticOptimizer already existed[7]. Originally it accepted a single penalty function. For the present work, non-dominated sorting was incorporated to perform multi-objective optimization. The current version of GeneticOptimizer is able to do both single object and multi-objective optimization. For single objective optimization, the parents chosen by GeneticOptimizer are those who have the smallest penalty value, while for multi-object optimization, the parents are those with rank 1 after non-dominated sorting. The beam dynamics simulation program used is ASTRA [8], which includes space charge forces.

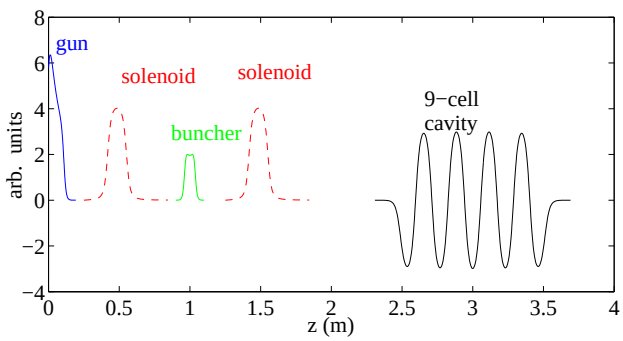

Figure 1: The field maps of the injector elements along the beamline.

INJECTOR AND DRIVE-LASER

The photoinjector we considered is similar to the TJNAF FEL injector [9]. A DC photo emission electron source

*Work supported by the U.S. Department of Energy, Office of Science, Office of Basic Energy Sciences, under Contract No. DE-AC02-06CH11357.

PHOTOCATHODE R&D PROGRAM AT LBNL*

W. Wan#, E. Pedersoli, C. M. R. Greaves, C. Coleman-Smith, A. Polyakov, H. A. Padmore,
ALS, LBNL, Berkeley, CA 94720, USA
S. Pagliara, A. Cartella, F. Lamarca, G. Ferrini, M. Montagnese, S. dal Conte, F. Parmigiani,
Dipartimento di Matematica e Fisica, Università Cattolica, Via Musei 41, I-25121 Brescia, Italia

Abstract

The work of the photocathode R&D program at LBNL is presented. The quantum efficiency (QE) of Cu(111) is measured for different impinging light angles with photon energies just above the work function. We observe that the vectorial photoelectric effect, an enhancement of the quantum efficiency due to illumination of light with an electric vector perpendicular to the sample surface, is stronger in the more surface sensitive regime. This can be explained by a contribution to photoemission due to the variation of the electromagnetic potential at the surface. The contributions of bulk and surface electrons can then be determined. Angle-resolved photoemission data let us obtain the dispersion relation of the surface state, which in turn allows us to determine the thermal emittance of the electrons emitted from the surface.

INTRODUCTION

The advances in diverse fields such as electron microscopy and the free electron laser drive demand for high brightness electron sources [1]. The photocathode R&D program at LBNL was established to explore ways of producing new generation of photocathode that can meet the demand. Our program is designed to study in detail the yield and the energy-momentum dispersion relation of the emitted electrons using angle-resolved photoemission spectroscopy (ARPES), as well as to develop new photocathode using nanotechnology. The capability of fully characterizing the photocathode in the ideal setting allows us to find out the physical limit of the performance of the material, as well as pointing to the direction of making better photocathode. In addition, the gap between the ideal setting and the realistic situation in a gun can be simulated to a certain extent in a controlled manner.

EXPERIMENTS ON CU(111)

The first set of experiments were carried out in Brescia, Italy on Cu(111). New work is carried out using a similar system in the photocathodes lab at the ALS. Although copper has been widely used in RF photoguns [2], there are still a lot of questions remain unanswered, such as the origin of the emitted electrons and the lower bound of the transverse thermal emittance. Furthermore, Cu(111) was chosen as a sample due to its robust nature and its well known and experimentally verified band structure [3].

*Work supported by the U.S. Department of Energy under Contract No. DE-AC02-05CH11231.
#wwan@lbl.gov

An amplified Ti:Sapphire laser was used as the light source in this experiment, providing 150~fs 790~nm pulses with an average light power of 500~mW at 1~kHz repetition rate. The output was split into two beams: the first pumping a parametric amplifier that provided tunability in the near infrared, the second undergoing a process of third harmonic generation obtained with two stages of sum frequency generation in type I BBO crystals. After a delay line that provides temporal coincidence, the beams converge on a third crystal for sum frequency generation providing the desired wavelengths. The sample total current on a picoammeter and the light intensity of a beam reflection on a calibrated photodiode were measured to provide the experimental data.

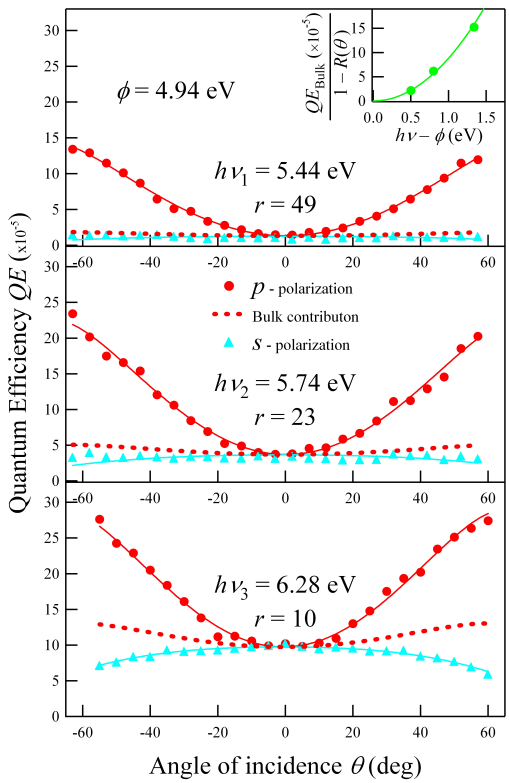

Figure 1: Quantum efficiency data as a function of the incident light angle θ for the three different photon energies are fitted using Eq. (1), (2); the bottom panel shows data from Ref. [4]. The red dotted lines represent the prediction for the bulk contribution, proportional to the absorbed part (1-R(θ)) of light energy. The top right panel shows the bulk quantum efficiency fitted by the Fowler law Eq. (3).

ANALYSIS OF HALO FORMATION IN A DC PHOTOINJECTOR

D. Mihalcea, P. Piot, Northern Illinois University, DeKalb, IL 60115, USA

Abstract

We discovered, by modeling the AES/JLab direct-current photoinjector with several beam-simulation codes, that nominal injector settings would create a large diffuse beam halo as a consequence of the internal space-charge force in the beam. The injector-induced halo is sensitive to the injector settings, but if the settings are judiciously chosen, it can be largely circumvented. We present an exploration of the parameter space for the AES/JLab photoinjector. Measurement of beam halo will be a crucial aspect of commissioning this machine.

INTRODUCTION

The present driving accelerator for the Jefferson Lab 10 kW IR Free-Electron Laser (FEL) provides a 10 mA average current electron beam with energy up to 160 MeV and normalized transverse emittance less than 30 μm [1, 2]. Since the gain of the laser increases with the electron beam current [3], to achieve megawatt-class FELs the injector should be upgraded to increase the average beam current at ampere level.

The normalized transverse emittance scales linearly with the laser wavelength and the relativistic factor γ [4]:

$$\epsilon_N < \frac{\lambda\gamma}{4\pi} \qquad (1)$$

Shorter laser wavelengths and/or more compact driving accelerators (lower energy) can be achieved by decreasing the emittance.

The next generation megawatt-class JLab FEL will require much improved quality of the electron beam. In particular the average beam current must be at ampere level and the transverse emittance not larger than a few microns. The upgraded photoinjector was designed at Advanced Energy Systems (AES) [5] and will be fabricated at Jefferson Lab.

In this paper we present some simulation results for this upgraded AES/JLab photoinjector. Due to the relatively large space charge forces, there is the potential for unwanted halo formation. The goal of our annalysis is to determine what are the photoinjector operating conditions that preclude halo formation and maximize the beam quality.

AES/JLAB PHOTOINJECTOR

This new photoinjector [5] couples a normal-conducting DC gun a section of three 750 MHz superconducting RF single cells and a third harmonic 2250 MHz cavity. The schematic layout of the photoinjector is shown in Fig. 1.

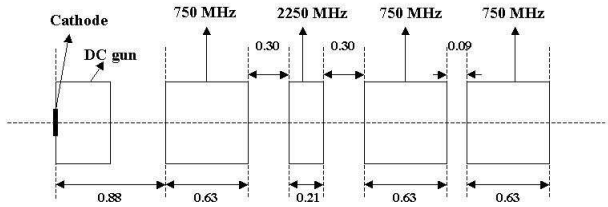

Figure 1: Schematic layout of the AES/JLab photoinjector. Emittance compensation solenoid is not shown. All dimensions are in meters.

Electron bunches of up to 1 nC charge and about 20 ps (rms) long are extracted from a photocathode illuminated with an infrared mode-locked Nd:YLF laser. The maximum accelerating gradient in the DC gun is 6 MV/m and the electron energy at the exit from the gun is about 1 MeV. At the end of the gun there is a solenoid to compensate the emittance growth due to space charge and external fields.

Three 750 MHz superconducting RF single cell cavities raise the energy of the electrons up to 6 MeV. A third harmonic cavity, located between first and second 750 MHz accelerating cavities, is used to linearize the energy dependence on longitudinal spatial coordinate.

BEAM HALO FORMATION

Photoinjector parameters like cavities amplitudes and phases, solenoid magnetic field, gun accelerating voltage are optimized to minimize longitudinal and transverse emittances at the exit from the photoinjector. Fig. 2 shows the most important beam moments when the charge of the electron bunches is 1 nC (750 mA), the initial beam radius at the cathode is 3 mm, and the initial longitudinal bunch profile is gaussian with $\sigma_z = 20$ ps.

The results from Fig. 2 were obtained with Parmela [6] and Impact-T [7]. The most sensitive parameters in the optimization process were the magnetic field in the emittance compensation solenoid and the phase of the third harmonic cavity. The values of the most important beam moments are within the desired limits when the current is 100 mA and about 20% higher for transverse and longitudinal emittances when the current is increased to 750 mA.

Beam halo may develop if the size of the laser spot at cathode is decreased in an attempt to increase the electron bunch charge density. Figure 3 shows the transverse beam distributions at two locations downstream of the cathode when initial distribution has radius 2 and 3 mm respectively, the beam current is 750 mA, and the laser pulse duration is 20 ps. When the initial radius is 2 mm the halo has

A HIGH-BRIGHTNESS LOW-ENERGY PHOTOINJECTOR OPTION FOR THE FERMILAB ELECTRON ACCELERATOR FACILITY

P. Piot, Northern Illinois University, DeKalb, Illinois;
M. Church, Fermilab, Batavia;
D. Mihalcea, Northern Illinois University, DeKalb, Illinois;
S. Nagaitsev, Fermilab, Batavia;
I. V. Pogorelov, LBNL, Berkeley, California;
Y.-E. Sun, Fermilab, Batavia

Abstract

Fermilab is currently constructing a GeV-scale electron accelerator test facility. The accelerator will serve as a backbone for several Fermilab R&D programs, e.g., to test subsystem associated to project-X, ILC and the muon collider program. It is also anticipated that this facility will support beam physics and accelerator R&D programs such as testing of novel acceleration techniques, beam diagnostics and radiation sources concepts. In this paper we describe a possible option for the electron injector based on a photoemission rf gun. Optimization and performance studies of this ~50 MeV photoinjector are performed with various tracking programs (Astra, GPT, Impact-T, Impact-Z). We explore the performances of the magnetic bunch compressor which is extremely challenging at 50 MeV due to strong phase space dilution via collective effects (space charge and coherent synchrotron radiation). We also investigate the generation of flat beams with very high transverse emittance ratio using a round-to-flat beam transformer.

CONTRIBUTION NOT RECEIVED

SIMULATION OF THE UPGRADED PHOTOINJECTOR FOR THE 10 KW JLAB IR-FEL*

P. Piot, Department of Physics, Northern Illinois University, DeKalb, IL 60115, U.S.A.
and Accelerator Physics Center, Fermi National Accelerator Laboratory, Batavia, IL 60510, U.S.A.
D. Mihalcea, Department of Physics, Northern Illinois University, DeKalb, IL 60115, U.S.A.
C. Hernandez-Garcia, S. Zhang, Free-Electron Laser Group,
Thomas Jefferson Accelerator Laboratory, Newport News, VA 23606, U.S.A.

Abstract

The photoinjector of the JLab 10 kW IR FEL was recently upgraded: a new photocathode drive laser was commissioned and the booster section was replaced with new 5-cell cavities. In this paper we present numerical simulation and optimization of the photoinjector performances using ASTRA, IMPACT-T and IMPACT-Z beam dynamics codes. We perform these calculations for the nominal 350 keV operating voltage of the dc gun.

INTRODUCTION

Jefferson Lab is currently operating a high average power infrared free-electron laser [1]. The driver accelerator is an upgraded version of the now decommissioned 1 kW IR-Demo FEL [2]. The facility also serve as a platform to explore beam dynamics phenomena and technologies associated with the realization of very high-average-power free-electron lasers. The driver accelerator comprises a $\sim$ 10 MeV injector followed by a 80-200 MeV energy recovering superconducting RF linac that allows high average current operation with modest klystron power. To reach the 10 kW goal, the charge-per-bunch was increased from 60 pC to 135 pC and the bunch repetition rate from 37.425 MHz to 74.850 MHz. The requirements on beam quality at the wiggler location to lase with a 10 kW average power using 135 pC bunches are gathered in Table 1. The photoemission injector, whose block diagram is shown in Figure 1, is a key element in achieving the required beam quality. It basically consists of a 350 keV line coupled with a high gradient RF structure consisting of two CEBAF-type superconducting cavities that can accelerate the beam up to approximately 10 MeV. The accelerating section is followed by a 10 MeV injection line that includes a diagnostics suite.

BEAM GENERATION & ACCELERATION

The low-energy line consists of a high-voltage DC photoemission gun for electron generation, a room-temperature buncher cavity and two solenoidal lenses (see Fig. 1). The gun uses a GaAs photocathode driven by a Nd:YLF laser [3] . The drive laser is mode locked to

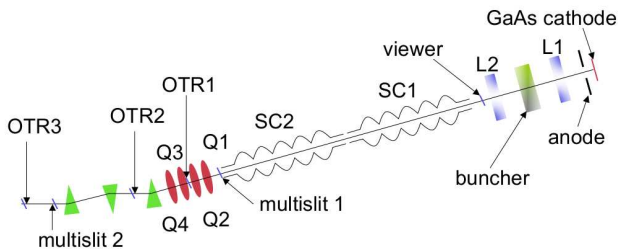

Figure 1: Overview of the Jlab IR-FEL photoinjector. The legend is "L1" "L2": solenoidal magnetic lenses, "SC1" "SC2" superconducting 5-cell CEBAF cavities, "Q1...4" quadrupoles, "OTR1...3" optical transition radiation screen, "multislit" emittance measurement stations. The green triangles indicate the locations of the sector dipoles composing the merger.

Table 1: Beam parameters specifications at the injection point ("multislit 2" in Fig. 1).

parameter	value	units
bunch charge Q	135	pC
transverse emit. $\varepsilon_{x,y}$	≤ 10	μm
$\beta_{x,y}$	10	m
$\alpha_{x,y}$	0	-
bunch duration $\sigma_t = \sigma_z/c$	[1.5,2.5]	ps
longitudinal emit. ε_z	≤ 28	ps-keV
energy spread σ_E	≤ 15	keV

37.425 MHz corresponding to the fortieth subharmonic of the rf fundamental frequency (1497 MHz) of the RF system. It can provide various micropulses shape and durations with a variable repetition rate ranging from 0.245 to 74.850 MHz. The gun is currently operated at 350 kV. Efforts to develop a gun capable of withstanding an accelerating voltage of 500 kV are underway. The beam is then ballistically bunched with a 1.5 GHz single-cell buncher [6] located $\sim$ 1 m upstream of the SCRF accelerating section. The accelerating section incorporate two modified CEBAF 5-cell cavities capable of maximum peak E-field of $\sim$ 20 MV/m.

The performance of the beam generation and acceleration section was investigated with ASTRA [7]. The dc-gun

*Work supported by the Department of Defense under contract N00014-06-1-0587 with Northern Illinois University.

SIMULATION OF FIELD-EMISSION CATHODES FOR HIGH CURRENT ELECTRON INJECTORS

D. Mihalcea, P. Piot, Northern Illinois University, DeKalb, IL 60115, USA

Abstract

From the prospect of the high average current electron injectors, the most important advantage of the field-emission cathodes is their capability to generate very large current densities. Simulation of field-emission cathodes is complicated by the large range of spatial dimensions: from sub-micron scale, for a single field-emission tip, to millimeter scale, for a field-emitter array. To overcome this simulation challenge our numerical model is split in two steps. During the first step, only electrons emitted by a single tip are considered. In the second step, the beams originating from many single emitting tips are merged together to mimic the field-emitter array configuration. We present simulation results of injector based on field array emitters cathodes.

MOTIVATION

Since the gain of a Free Electron Laser (FEL) increases with the electron beam current [1], to achieve megawatt-class FELs the injector should be upgraded to ampere level of average beam current. This can be done with standard photoinjectors but problems related to low quantum efficiency and limited lifetime of the photocathodes still need to be addressed. The upgrade of the Jefferson Lab IR FEL [2], requires a complete replacement of the old photoinjector. The new photoinjector [3] can deliver average beam current at ampere level, but, according to our simulations both transverse and longitudinal emittances exceed the specifications. New electron sources (like field-emitting cathodes) could eventually have better performances than standard photoinjectors. Diamond made field-emitters are mechanically robust, can carry large density currents, and because of the large external fields in the emitting area, the emittance growth due to space charge is diminished.

THEORETICAL MODEL

Quantum tunneling allows extraction of electrons from atoms when large enough external electric field is present. The current density is given by Fowler-Nordheim (FN) equation:

$$j = \frac{K_1 E^2}{\phi} exp(-\frac{K_2 \phi^{1.5}}{E}) \qquad (1)$$

where E is the external electric field, ϕ the work function of the material and K_1, K_2 constants. Throughout this analysis we use the same values of the constants as in [4], $K_1 = 1.54 \times 10^{-6}$ A eV/V^2, $K_2 = 6.83 \times 10^7$ V/ (cm eV$^{3/2}$) and the work function for diamond $\phi = 4.15$ eV. The graph of the current density as a function of external electric field is shown in Fig. 1.

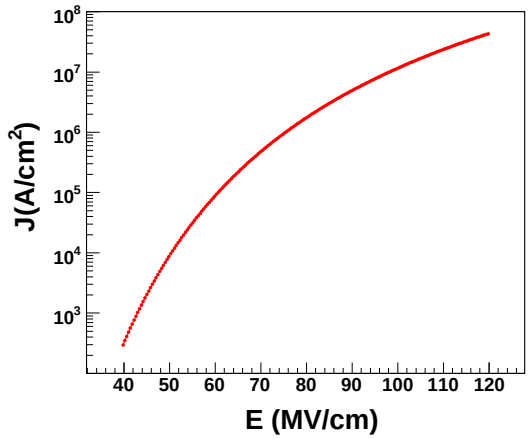

Figure 1: Fowler-Nordheim equation with the values of the constants indicated in the text.

In this paper we consider cylindrically symmetric diamond made field-emitters of conical shape. The tip of the cone is assumed spherical with a small curvature radius to favor a large external field enhancement in the region of the tip. The results shown in this paper are based on the assumption that the curvature radius of the field-emitting tip is 0.1 μm, but smaller tip radii of 0.05 μm and 0.01 μm were also considered. A field-emission cathode consists of an array of diamond made single field-emitters separated by distances of the order of a few tens of microns.

The simulation of electron beams from field-emission arrays is complicated by the large range of spatial dimensions: microns in the region of a single field-emitter and millimeters for the whole cathode. Therefore, as in [6], we split the simulation into two parts: first we simulate the electron beam from a single field-emitter and then in the second part the beamlets are merged together to mimic the beam extracted from the whole array of single field-emitters.

SINGLE FIELD-EMITTERS

A typical single field-emitter consists of a conical shape diamond made cathode, an accelerating control electrode (gate) and at least one focusing layer (Fig. 2). To control

LONGITUDINAL BEAM DIAGNOSTICS FOR THE ILC INJECTORS AND BUNCH COMPRESSORS

P. Piot, Fermilab, Batavia, Illinois;
A. Bracke, Northern Illinois University, DeKalb, Illinois;
C.-J. Jing, Euclid TechLabs, LLC, Solon, Ohio;
T. J. Maxwell, D. Mihalcea, Northern Illinois University, DeKalb, Illinois;
J. G. Power, ANL, Argonne, Illinois;
M. M. Rihaoui, Northern Illinois University, DeKalb, Illinois

Abstract

We present a diagnostics suite and analyze techniques for setting up the longitudinal beam dynamics in ILC electron injectors and bunch compressors. Techniques to measure first order moment and recover the first order longitudinal transfer map of the injector intricate bunching scheme are presented. Coherent transition radiation diagnotics needed to measure and monitor the bunch length downstream of the ~5 GeV bunch compressor are investigated using a vector diffraction model. We finally introduce a new diagnostics capable of measuring time-transverse correlation along a single bunch. Such a diagnostics should be valuable for controlling emittance dilution via transverse wakefield and for properly setting the crab cavities needed for maximizing luminosity for non-zero crossing angle at the interaction point.

CONTRIBUTION NOT RECEIVED

INITIAL RF MEASUREMENTS OF THE CW NORMAL-CONDUCTING RF INJECTOR*

Frank L. Krawczyk#, Nathan A. Moody, Felix A Martinez, Gerald O. Bolme, Karen A. Young, Dinh C. Nguyen, Los Alamos National Laboratory, Los Alamos, NM 87545, USA
Lloyd M. Young, Advanced Energy Systems, Medford, NY 11763, U.S.A.

Abstract

The LANL 2.5-cell, normal-conducting radio-frequency (NCRF) injector has been fabricated [1]. We present initial results of low-power RF measurements (cavity Q, cavity field map, coupling beta, etc.) of the NCRF injector. The measured cavity Q and relative fields are found to be in good agreement with the design calculations and earlier measurements of Glidcop properties [2]. However, the coupling beta of the ridge-loaded waveguides is found to be significantly higher than the design point. The impact of these low-power measurement results on the planned high-power RF and electron beam tests will be discussed.

INTRODUCTION

A 2.5 cell, π-mode, 700 MHz normal conducting RF-photoinjector cavity has been designed and built. It is seen as a crucial building block for low emittance high average current source for a 100 kW CW FEL. The operation at a gradient of 7, 7 and 5 MV/m in the three accelerating cells requires an RF-input in excess of 700 kW. While simulations show that the thermal management of this operation is feasible, the first step is to verify the operation of this prototype cavity without generating any beam. This thermal test is presently under preparation at LANL and is well under way to be started in September and completed by the end of CY2008. The pre-start activities and findings for the test will be reported here. They include vacuum and cooling passage integrity, bakeout and low-power rf-properties.

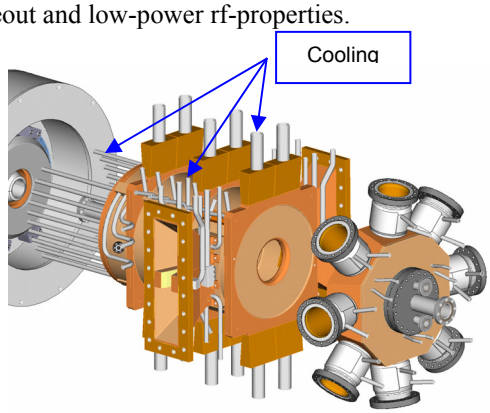

Figure 1: Exploded view of the photoinjector showing the cooling passages.

As the coupling from the ridge loaded waveguides to the cavity was different from the design point, a modification of the test setup for proper operation is provided also.

STRUCTURAL AND VACUUM INTEGRITY

Besides the RF-performance, leak tightness of the cooling channels and proper vacuum sealing were of concern. Tests of all cooling channels indicated proper flow rates and showed no leaks into the cavity volume or to the outside.

The testing of the vacuum sealing required the installation of all vacuum pumps on the unexcited fourth cell, the cathode port in the first cell and the ridge loaded waveguide (RLWG) sections. A total of 9 ion pumps, a non-evaporative getter pump and five turbo pumps have been used. The total pumping speed is 600 l/s. The challenging seal between the waveguide (SST) and the RLWG (Glidcop) has been done with an AL/CU/Ni 90 Alloy Helicoflex seal. The system showed a good vacuum seal with a leak rate of less than 1 10^{-10} Torr l/s.

BAKEOUT INFORMATION

For a first cleaning of the RF-surfaces the cavity and all secondary ports have been baked out in a two-step process. In the first baking step all cavity parts were heated up to 175° C. The cavity was held at this temperature for 2 days. After cool-down the second bakeout period brought all parts of the cavity close to 150° C. For homogeneity the heating was controlled by 12 independent temperature zones. The base pressure after the bakeout was 2-3 10^{-10} Torr. A cavity pressure in the low 10^{-10} Torr is needed for a good lifetime of future photocathodes.

Figure 2: Photoinjector wrapped in heating blankets for a bakeout that resulted in an excellent pre-test vacuum.

fkrawczyk@lanl.gov

* This work is supported by the Office of Naval Research and the High-Energy Laser Joint Technology Office.

MODELING OF A LOW FREQUENCY SRF ELECTRON GUN FOR THE WISCONSIN FEL*

R. Legg#, UW-Madison/SRC, Madison, WI 53589, USA

Abstract

The Wisconsin FEL project is a 2.2 GeV, HHG seeded, FEL designed to provide six individual beamlines with photons from 5 to 900 eV. The FEL requires electron bunches with 1 kA peak bunch current and less than 1 mm-mrad normalized transverse slice emittance. To meet those requirements a low frequency, SRF electron gun is proposed which uses "blow-out" mode bunches [1]. Blow-out mode produces ellipsoidal bunches which are easily emittance compensated [2]. They also have a very smooth density and energy distribution. Results of the modeling of the injector and a diagnostic beamline are presented.

INTRODUCTION

The Wisconsin FEL (WiFEL) project is a 2.2 GeV, HHG seeded, FEL designed to provide six individual beamlines with photons from 5 to 900 eV. The FEL requires electron bunches with 1 kA peak bunch current and less than 1 mm-mrad normalized transverse slice emittance. The injector for the WiFEL must supply the continuous stream of electron bunches which have the necessary transverse and longitudinal properties to support the compression system while minimizing the collective effects in the accelerator to the FEL. The bunch longitudinal profile must be optimized to avoid current spikes at the front and rear of the bunch charge density profile from wakefields [3]. At the same time, it must provide a bunch which reaches the kilo-amp level needed by the FEL for long enough to ensure overlap between the bunch and the seed laser in the undulator. It also must have a very smooth current density profile to prevent CSR or resistive wakefield microbunching in subsequent compressors. The 3D bunch profile which meets this requirement is a uniform ellipsoid [4].

To create an ellipsoidal bunch with uniform charge density, an ultra-short laser pulse with a hemispherical transverse profile is directed onto the photocathode. The charge pancake generated expands dynamically to form an ellipsoidal bunch under space charge forces. The limit on the dynamically formed bunch approach is that the charge density of the bunch is dependant on the peak electric field applied to the cathode. For a greater peak bunch current, either the electric field on the cathode must be increased or the emission radius must be enlarged with a consequent increase in thermal emittance; the limit for the FEL to operate, 1 mm-mrad, is reached at 1 mm rms radius for Cs_2Te [5]. Twenty is about the maximum bunch compression ratio which can be easily achieved with two magnetic chicanes while preserving the beam parameters necessary to lase in a seeded FEL [6]. With that compression ratio 1 kA at the FEL requires 50 A peak from the gun. At the 1 mm rms emission radius the electric field on the cathode necessary to achieve 50 A peak is about 40 MV/m [7]. Such a CW field is too great for either a DC gun (field emission) or a CW normal conducting rf gun (thermal load), but is well within the reach of an SRF electron gun. For this reason, an SRF gun optimized to produce the smoothest maximum field on the cathode was selected.

The gun is to be built as part of the WiFEL R&D program along with a diagnostic beamline which can measure the bunch parameters. ASTRA [8] simulations of the beamline provided guidance in selection and placement of the diagnostic suite.

ELECTRON GUN DESIGN

Table 1: Electron Gun Parameters

Pulse frequency, MHz	10
Charge per bunch, pC	200
Average current, mA	<2
I_{peak} at first bunch compressor, Amps	50
Peak field in gun, MV/m	41
σ_x at 100 MeV, mm	0.34
σ_z at 100 MeV, mm	0.34
Transverse ε at 100 MeV, mm-mrad	0.9
Longitudinal ε at 100 MeV, keV-mm	2.2

The electron gun design [9] uses a 200 MHz SRF half wave cavity with a warm, Cs2Te cathode mounted on a cathode stalk surrounded by a quarter-wave choke joint to

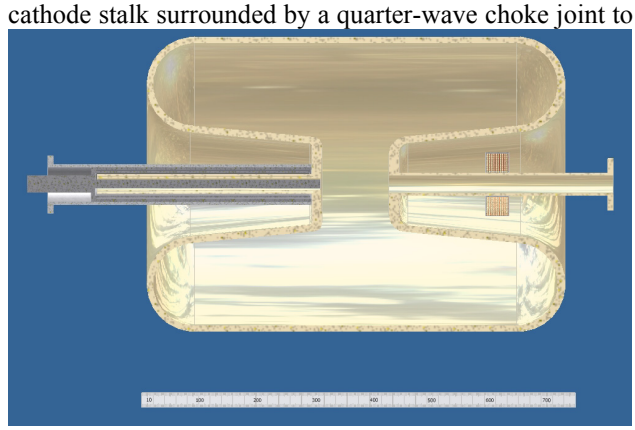

Figure 1: SRF gun cavity w/ cathode and solenoid.

isolate it from the rf in the cavity. The load lock system exploits the required choke joint with its low wall current point to mate the retractable Ti cathode stalk to the SRF

* This work is supported by the University of Wisconsin-Madison and MIT. SRC is funded by the US NSF under award No. DMR-0537588
#rlegg@src.wisc.edu

LONGITUDINAL BUNCH LENGTHENING COMPENSATION IN A HIGH CHARGE RF PHOTOINJECTOR

S. Pei# and C. Adolphsen, Stanford Linear Accelerator Center, Menlo Park, CA 94025, USA

Abstract

In high charge RF photoinjectors for two-beam wakefield accelerators, bunch lengthening between the photocathode and photoinjector exit is a critical issue due to the strong longitudinal space charge forces. We present beam dynamics studies of bunch lengthening in an RF photoinjector for a high charge electron beam and describe methods to compensate the bunch lengthening to various degrees. In particular, the beam dynamics for bunch charge from 1 nC to 30 nC are studied for an S-band (2856 MHz) photoinjector.

INTRODUCTION

RF photoinjector technology [1] is used world-wide in low emittance sources for linac-based free electron lasers [2] and in electron sources for electron storage rings [3]. It has been demonstrated that photoinjectors can produce high brightness and low emittance electron beams [4-6]. A particular challenge for high charge electron photoinjectors for two-beam wakefield accelerators is the longitudinal bunch lengthening that occurs due to strong space charge forces [7].

The longitudinal evolution of electrons in an RF injector can be divided into four steps as discussed in Ref. [8]: 1) initial launching and expansion; 2) RF compression inside the gun cavity; 3) drift space bunch compression or expansion; 4) longitudinal emittance compensation through the booster linac. To reduce the bunch lengthening in the first step, the laser pulse length can be reduced and beam radius increased, which usually results in transverse emittance growth. In the second step, one wants to accelerate the electron beam with as high a gradient as possible [9], which is constrained by the available klystron power and the maximum sustainable surface electric fields in the gun cavity. For the third step, appropriate tuning of the emittance compensation solenoid is needed to reduce the bunch lengthening. The fourth step, which ultimately determines whether the bunch is lengthened, preserved or shortened, appropriate phasing (off-crest acceleration to create an energy chirp along the bunch) is done in part of the booster linac and the electron beam focusing is adjusted along the entire injector.

Here we present two studies of longitudinal bunch lengthening compensation. In the first, we consider only increasing the RF gun acceleration gradient while optimizing the initial phase of the electron beam with the booster linac operated on-crest. The second study focuses on phasing both the RF gun and the first half booster linac for gun acceleration gradients ranging from 120 MV/m to 200 MV/m.

PHOTOINJECTOR DESIGN

Fig. 1 shows the schematic layout of the photoinjector. Due to the strong space charge effect of a high charge beam (10 nC - 30 nC), the RF gun is immersed in the magnetic field of an integrated cathode solenoid. This magnet is composed of two symmetric solenoid coils whose symmetry plane is the cathode plane. The two coils are powered by separate supplies with opposite current flows so the magnetic field at the cathode surface can be easily adjusted to be near zero. The solenoid and the drift space just after the gun are used to compensate the linear space charge induced emittance growth in the gun region. For high charge, the combined axial magnetic field profiles of the cathode solenoid and the emittance compensation solenoid are shown in Fig. 2 (left) for a typical case. For low charge, only the emittance compensation solenoid is used, and a field profile example is shown in Fig. 2 (right, the two lines coincide with each other).

The basic parameters of the RF gun are listed in Table 1. The RF gun operates in π-mode, and Fig. 3 shows the 0-mode and π-mode electric field profiles for the geometry with a balanced π-mode at 2856 MHz.

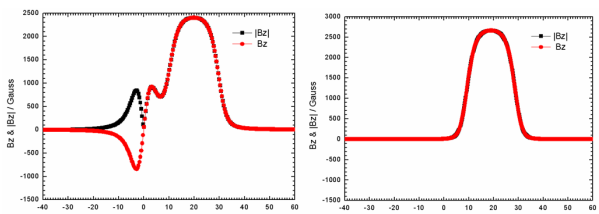

Fig. 2: Typical axial magnetic field profiles in the gun region for high charge (left) and low charge (right).

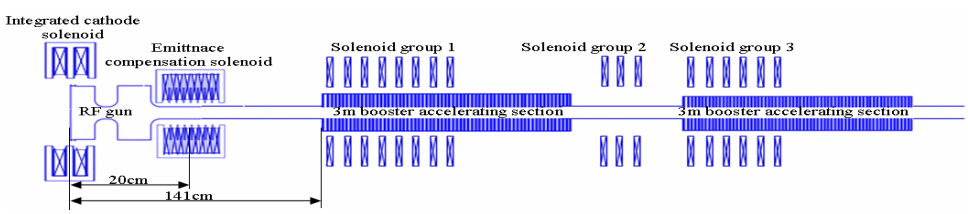

Fig. 1: Schematic layout of the photoinjector.

*Work supported by the DOE under contract DE-AC02-76SF00515.
#slpei@slac.stanford.edu

LASER TIMING JITTER MEASUREMENTS AT THE FERMILAB A0 PHOTOINJECTOR

Justin Kien Keung*, University of Pennsylvania, Philadelphia, PA, 19104, USA
Jinhao Ruan, Sergei Nagaitsev, FNAL, Batavia, IL, 60510, USA

Abstract

The Fermilab A0 Photoinjector is a 16 MeV high-intensity, low emittance electron linac used for advanced accelerator R&D. To achieve a high quality beam here it is important to maintain a stable laser in terms of both intensity and timing. This paper presents our measurement of the laser timing jitter, which is the random late or early arrival of the laser pulse. The seed laser timing jitter has been measured to be less than 200 fs, by examining the power spectrum of the signal of a fast photodiode illuminated by it. The pulsed and pumped laser timing jitter has been measured with limited resolution to be less than 1.4 ps, by examining the phase of a cavity impulsively excited by the signal from a fast photodiode illuminated by the laser pulse.

INTRODUCTION

Photoinjectors are widely used in particle accelerators. They have uses from nuclear and high energy physics research in collider experiments (e.g. ILC), to biology and condensed matter research in light source experiments (e.g. XFEL).

The A0 Photoinjector [1] consists of a 1.3 GHz copper RF gun and a TESLA type RF cavity, and is a 16 MeV high-intensity, low emittance electron linac used for advanced accelerator R&D at Fermilab.

To achieve a high quality beam for advanced accelerator R&D it is important to maintain a stable laser in terms of both intensity and timing. Timing jitter of the laser is the unwanted random variation of the pulse arrival time. Low beam timing jitter is good because it increases collider luminosity (e.g. ILC nominal: 0.5ps RMS), and is necessary for Lasing in FEL (e.g. XFEL: 0.1ps RMS).

The laser timing jitter has been measured by examining the power spectrum of the seed laser at the 12th harmonic, and by examining the phase of a cavity impulsively excited by the signal of a fast photodiode illuminated by the pulsed laser shot. Our aim is to have a pulsed laser timing jitter measurement resolution of less than 200 fs.

A0 LASER SYSTEM OVERVIEW

The A0 Laser System (Fig. 1) [2] consists of a seed laser, pumps, and two sets of doubling crystals. The laser begins as a continuous train having 5.5 nJ per FWHM 5 ps long infrared (1054 nm) laser pulses at 81.25 MHz. Some pulses (10 to 10000 out of 81.25 million) are allowed to pass through every second, to be pumped by a series of amplifiers. The amplified laser then passes through two sets of doubling crystals to become first green, then ultraviolet (UV). This UV laser having 5 μJ per FWHM 5 ps long pulse is directed with only three turning corners to hit the Cs_2Te photocathode to generate 10 nC of electrons per pulse to be accelerated to 16 MeV.

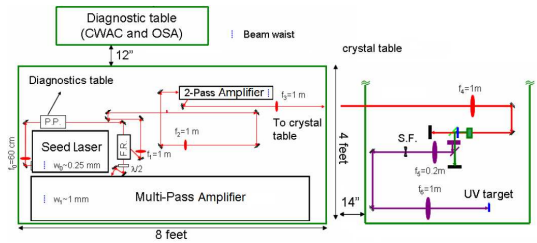

Figure 1: Layout of the A0 Laser System.

SEED LASER TIMING JITTER

To study the laser timing jitter we begin at the seed laser (Time Bandwidth Products GE-100), which gives a continuous train having 5.5 nJ per FWHM 5 ps long infrared (1054 nm) laser pulses at 81.25 MHz. A high-speed photodiode with a rise/fall time of 12 ps (Fermionics Lasertech HSD-30) is illuminated by the seed laser, and the electrical output signal from the photodiode is analysed by a microwave spectrum analyzer (Agilent E4445A).

The power spectrum of the photodiode signal contains information both on the amplitude and timing jitter. The technique of calculating the timing jitter from the power spectrum is called the Power Spectral Density Technique. Amplitude jitter and timing jitter both show up as shoulders beside the spectral lines (Fig. 2). The RMS jitter is given by an integral of the power in the shoulders (Eq. (1)):

$$\text{RMS Jitter}_{\ f_1 to f_2} = \frac{1}{2\pi f_c}\sqrt{2\int_{f_1}^{f_2} 10^{\frac{L(f)}{10}} df} \qquad (1)$$

Where the factor of 2 inside the square root uses the fact that the spectral shoulders are symmetric.

To separate the amplitude and timing jitter, we make use of the fact that amplitude jitter shoulder is constant, whereas the timing jitter shoulder is proportional to the square of the frequency [3], and measure the power spectrum of the 12th harmonic of the 81.25 MHz pulse rep rate. The timing jitter is measured to be 184 fs at 10 Hz to 10 kHz (Fig. 3).

* keungj@hep.upenn.edu

EMITTANCE EXCHANGE AT THE FERMILAB A0 PHOTOINJECTOR*

Timothy W. Koeth#, Rutgers University, Piscataway, New Jersey, USA

Helen Edwards, Raymond P. Fliller III†, Leo Bellantoni, Jinhao Ruan, Alex H. Lumpkin,Randy Thurman-Keup, Amber S. Johnson, Fermilab, Batavia, Illinois, USA

Abstract

An experiment to exchange the longitudinal emittance with the horizontal emittance has been installed at the Fermilab A0 Photoinjector. The exchange apparatus consists of a TM_{110} deflecting mode cavity positioned between two magnetic doglegs as proposed by Kim & Sessler [1]. We report on the measurement of the emittance exchange beamline matrix elements and a direct measurement of emittance exchange.

INTRODUCTION

A transverse to longitudinal emittance exchange (EEX) has been installed at the Fermilab A0 Photoinjector for a proof-of-principle demonstration through the exchange of a larger normalized longitudinal emittance, 30 mm.mrad, with that of a smaller normalized horizontal emittance, 10 mm.mrad, of a 14.3 MeV electron beam. In this paper we report on measurements of the emittance exchange beamline matrix elements as well as a preliminary measurement of an emittance exchange.

EEX BEAMLINE & OPTICS

It is the goal of our emittance exchange experiment to exchange horizontal and longitudinal emittances of an electron beam. The apparatus that we have developed, which is a variant of Kim and Sessler's proposal, can be easily described through a linear optics treatment of the exchange beamline [1]. We describe the entire exchange apparatus by a typical 4x4 matrix relating the horizontal and longitudinal parameters, Δx, $\Delta x'$, Δz, $\Delta\delta$ ($\delta = \Delta p/p$) :

$$M_{EEX} = \begin{pmatrix} A_{11} & A_{12} & B_{11} & B_{12} \\ A_{21} & A_{22} & B_{21} & B_{22} \\ C_{11} & C_{12} & D_{11} & D_{12} \\ C_{21} & C_{22} & D_{21} & D_{22} \end{pmatrix}$$

A complete exchange matrix would be one in which the elements of the ***A*** and ***D*** sub-blocks become zero and the ***B*** and ***C*** sub-blocks become populated.

The A0 Photoinjector EEX apparatus, outlined in Fig. 1, consists of a 3.9 GHz TM_{110} deflecting mode cavity located between two 'dogleg' magnetic channels. The TM_{110} deflecting mode cavity is a lN_2 cooled, normal conducting, variant of a superconducting version previously developed at Fermilab [2]. The longitudinal electric field of the TM_{110} mode is zero on axis and grows linearly off axis, the vertical magnetic field produces a time dependent transverse kick with respect to the synchronous particle. The TM_{110} deflecting mode cavity's strength, k, is given by:

$$k = \frac{eV_{\perp}\omega}{Ec},$$

where $V_{\perp}$ is the peak deflecting field normalized to the beam energy, E, and ω is the resonant frequency.

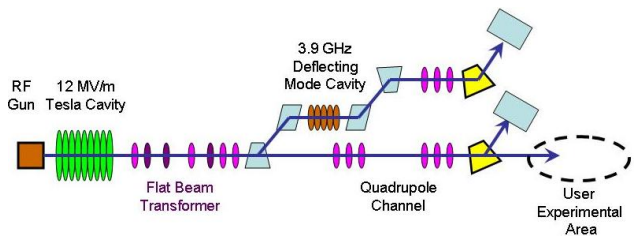

Figure 1: Layout of the A0 Photoinjector with straight ahead and EEX beamline sections.

Using a thin lens approximation of a cavity immediately between two magnetic doglegs, we can analytically express our EEX beamline matrix as:

$$\begin{pmatrix} 1+Dk & L+Dk+(1+Dk)L & kL & D+D(1+Dk)+\alpha DkL \\ 0 & 1+Dk & k & \alpha Dk \\ \alpha Dk & D+D(1+Dk)+\alpha DkL & 1+Dk & \alpha D+\alpha D^2k+\alpha D(1+Dk) \\ k & kL & 0 & 1+Dk \end{pmatrix}$$

where L is the drift between two magnetic dipoles that form a magnetic dogleg and D is the dispersion generated by one dogleg, and α is the magnitude of the bend angle.

It can easily be seen that in the special case where the TM_{110} cavity strength, k, (defined 100% at 3.03 m^{-1} in our case) equals the negative reciprocal of the dispersion, D, (0.33 m in our case) the diagonal sub-blocks of the matrix become zero while the off-diagonal sub-blocks become populated. Our bending angle is 22.5º.

$$M_{EEX} = \begin{pmatrix} 0 & 0 & \frac{-1}{\alpha} & 0 \\ 0 & 0 & \frac{-1}{D} & -\alpha \\ -\alpha & 0 & 0 & 0 \\ \frac{-1}{D} & -\frac{1}{\alpha} & 0 & 0 \end{pmatrix}$$

In practice, due to the finite length of our TM_{110} deflecting mode cavity, several of the on-diagonal block elements are left non zero [3]. This, in addition to other higher order effects, such as space charge and CSR, will lead to an imperfect exchange and a coupling of the final emittances [4].

* This manuscript has been authored by Fermi Research Alliance, LLC under Contract No. DE-AC02-07CH11359 with the U.S. Department of Energy.

#koeth@physics.rutgers.edu

†Present address: NSLS II Project, Brookhaven National Laboratory, Upton, NY, 11973-5000NY

BEAM TRANSPORT EFFECTS FOR ECRIS

P. Spädtke, R. Lang, J. Mäder, J. Roßbach, K. Tinschert, GSI Darmstadt, Germany

ION BEAM EXTRACTION

Experimental results from ion beams, extracted from an Electron Cyclotron Resonance Ion Source (ECRIS) are compared with the model used for simulation, which has to taken into account that the energy of ions within the magnetically confined plasma in a trap of several T is in the eV-range. Electrons do have a different energy distribution: there are hot electrons up to MeV range, but also low energy electrons, responsible for charge neutrality within the plasma. Because the gyration radius of ions is within the sub-mm range, ions can be extracted only if they are located on a magnetic field line which goes through the extraction aperture. Ion-ion collisions are not important for the path of the ion. Because of the gradient dBz/dz of the mirror field only these ions can be extracted, which have enough energy in direction of the field line. These conditions are fulfilled for ions which are going to be lost through the loss cones created by the hexapole. The extracted beam shows a typical behavior for any ECRIS: when the beam is focused by a lens (here a solenoid) directly behind extraction, the initial round and hollow beam develops wings with a 120-degree symmetry. Because of these considerations, the magnetic flux density in the plane of extraction is a good approximation for the minimum required flux density from which ions can be extracted. This surface is shown in 2D-cuts for two different ECRIS types (see Fig. 2 to Fig. 6). It is assumed that the plasma generator is able to produce particles in the required charge state at these locations. The model has been tested for different existing ion sources, and for ion sources which are still under design or under construction.

CAPRICE

This source, routinely in operation at GSI, has been used together with the technique of viewing targets, to proof our model for ion beam extraction. The ion source has two normal conducting coils for the mirror trap and a hexapolar device created by permanent magnets. Using different materials for these permanent magnets, we have had tested three differently strong hexapolar fields: 0.8 T, 1.0 T, and 1.2 T measured always at the plasma chamber. Whereas the transverse magnetic flux density is fixed when the hexapole has been installed, the mirror field for both mirror coils is variable up to 1.2 T on axis. By changing the current in the mirror field coils on injection side and extraction side, the location of extraction can be changed from the back side of the source to the radial location of the loss lines, starting at injection side and going to about the center between both coils. Because the allowed starting conditions are different for different magnetic settings, it is important for ECRIS extraction simulation to use the actual used magnetic fields. An example is shown in Fig. 9 for the 1 T hexapole.

SUPERNANOGAN

This commercial available source[1] is much easier to simulate, because the magnetic flux density is frozen, which might be a disadvantage on the other side. The magnetic flux density has been calculated using the PANDIRA code[2]. This program calculates the cylinder symmetric mirror field, created by permanent magnets only. The hexapolar field has been added in the 3D-map required for the KOBRA3[3] simulation analytically. Because of the permanent magnets, the longitudinal flux density component changes sign within the extraction.

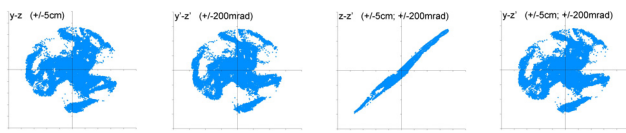

Figure 1: Different projections of the 6D phase space from left to right: beam cross section, momentum space, emittance, mixed phase space. Total current for the simulation 3 mA, shown is one charge state only.

ARC-ECRIS

This is an already old idea from plasma-fusion science [4], using a curved coil to produce the required magnetic configuration. Because of this simple design, the idea has been re-invented [5] to check the performance of such a source. This device creates a minimum $|\vec{B}|$ structure with a quadrupole like loss cones, shown in Fig. 2. If the plasma generator provides a comparable charge state distribution as regular ECRIS it would be a promising alternative, see Fig. 3.

MS-ECRIS

This source has been designed within a European collaboration[6]. It consists out of three solenoidal coils to produce the mirror field and a set of coils for the hexapole, designed to be 2.7 T at the plasma chamber. Depending on

DEVELOPMENT OF VERY SMALL ECR ION SOURCE WITH PULSE GAS VALVE

M. Ichikawa#, H. Fujisawa, Y. Iwashita, T. Sugimoto, H. Tongu and M. Yamada, Kyoto University, Uji, Kyoto, Japan

Abstract

Neutrons are very interesting for scientists as new probes used for investigating inner structure of materials. But, there are few neutron science facilities available in the world for such purposes. To remedy a situation, we started to develop linear accelerator base small neutron source.

At present, we are working on a small H^+ ion source as the first step of development of a small neutron source. We have selected a type of ECR ion source with permanent magnets as a small and high intensity ion source.

A pulse gas valve made of a piezoelectric element was built-in in the ion source plasma chamber to reduce the loading of evacuation systems.

We have obtained in our test stand a beam current of 1.13 mA at RF frequency of 5.74 GHz and 25 W RF power. The ratio of H^+ to other ion species was also measured with an analyzing magnet.

INTRODUCTION

We aim to develop a small and high intensity proton source for a compact accelerator based neutron source. Because this proton source shall be located close to RFQ for compactness, the ratio of H^+ to molecular ions such as H_2^+ or H_3^+ must be large. Therefore we have selected a type of ECR ion source with permanent magnet as a small and high intensity ion source. The ECR ion sources can provide high H^+ ratio because of their high plasma temperature. Using permanent magnets makes the ion source small and running cost low. Because there is no hot cathode, longer MTBF is also expected.

Usually, gas is fed into ion sources continuously, even if ion sources run in pulse operation mode. But, continuous gas flow becomes a load to the vacuum system. So, we decided to install a pulse gas valve directly to the plasma chamber. Feeding the gas only when RF power is enabled reduces the gas load to the evacuation system and the vacuum level can be kept high.

PULSE GAS VALVE

We developed pulse gas valve with commercial piezoelectric element (Kyocera Co. KBS-20DA-7A) [1]. Fig. 1 shows the piezoelectric element, which is used for developing a pulse gas valve. Table 1 shows the specifications of the element. This valve utilize the piezoelectricity such that the elements warps by internal mechanical stress when a voltage is applied. As shown in Fig. 2, the application of a voltage opens a path under the element and the gas flow into the chamber.

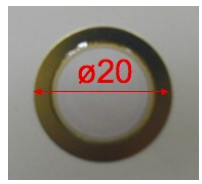

Figure 1: Piezoelectric element.

Table 1: Specifications of the piezoelectric element.

Diameter of metal base	20.0±0.1mm
Diameter of piezoelectric element	14.2±0.1mm
Total thickness	0.45±0.1mm
Thickness of metal base	0.20±0.03mm
Resonance frequency	6.6±1.0kHz
Capacitance	10±0.3nF
Electric strength(catalogue spec.)	$30V_{p\text{-}p}$

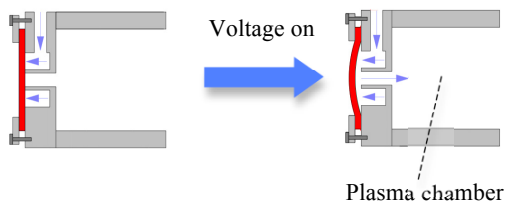

Figure 2: Operating principal of the valve .

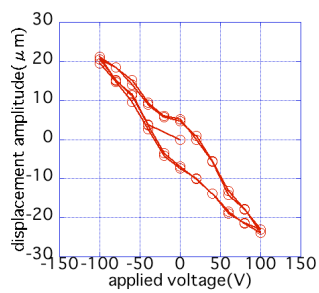

Figure 3: Hysteresis curve.

This piezoelectric element has a hysteresis characteristic like Fig. 3. When negative voltage is applied the valve opens and gas can flow. But because of hysteresis, applying only negative voltage reduce the displacement of the element or its warpage. Therefore, a bipolar voltage pulse generator was prepared for driving

#ichikawa@kyticr.kuicr.kyoto-u.ac.jp

DEVELOPMENT OF ULTRA-LOW EMITTANCE INJECTOR FOR FUTURE X-RAY FEL OSCILLATOR*

P.N. Ostroumov#, K.-J. Kim, ANL, Argonne, IL 60439, U.S.A
Ph. Piot, Northern Illinois University, DeKalb, IL, U.S.A.

Abstract

An XFELO proposed recently [1] requires a continuous sequence of electron bunches with ultra-low transverse emittance of less than 0.1 μm, a bunch charge of 40 pC, an rms energy spread of 1.4 MeV, repeating at a rate between 1 MHz to 100 MHz. The bunches are to be compressed to rms lengths less than 2 ps at the final energy of 7 GeV. Following the successful commissioning of the pulsed injector based on a thermionic gun [2] we discuss a concept for ultra-low emittance injector to produce 100 MHz CW electron bunches. The electron beam is extracted by ~ 1MV RF voltage using low frequency ~100 MHz room temperature RF cavity [3]. The injector also includes a chicane and slits to form a short ~0.5 nsec bunch, a buncher to form low longitudinal emittance of the bunched beam, an accelerating section to ~20 MeV using higher harmonic cavities, and an RF cosine-wave chopper to form any required bunch repetition rate between 1 MHz and 100 MHz. The results of initial optimizations of the beam dynamics with the focus on extracting and preserving ultra-low emittance will be presented.

GENERAL LAYOUT

The 7 GeV electron beam must be delivered with the parameters listed in Table 1. We propose 7 GeV CW SC linac which includes Ultra-Low Emittance Injector (ULEI) based on a thermionic RF-gun as a solution to deliver an electron beam as specified in Table 1.

The proposed electron linac includes the following main systems:

- An RF-gun with a small diameter thermionic cathode to extract ultra-low emittance beam. The latter is possible primarily due to the low equivalent DC current which is ~80 mA for 0.5 nsec bunches and high extraction voltage.
- A low-frequency RF cavity capable to provide ~ 1.0 MV extracting voltage. The highest possible extraction voltage should suppress beam space charge in the following sections of the injector.
- An energy filter which includes a magnetic chicane and slits to form a short, ~ 0.5 nsec bunch.
- A 6th harmonic RF cavity (600 MHz) as a monochromator to minimize momentum spread of the electron beam.
- A velocity buncher (300 MHz) to form low longitudinal emittance of the bunched beam.
- A booster acceleration up to ~20 MeV using higher harmonic cavities (400 MHz).
- An RF cosine-wave chopper to form any required bunch repetition rate between 1 MHz and 100 MHz.
- Two chicanes along the linac for bunch compression.
- A final acceleration using SC ILC cavities (1300 MHz) with 20 MV/m accelerating field.

Table 1: Main Beam Parameters.

Parameter	Value	Unit
Transverse rms emittance	<0.1	μm*
Bunch charge	40	pC
Bunch rms time width	2	psec
Bunch rms energy spread	1.4	MeV
Bunch repetition rate	1-100	MHz

*The emittance defined as the area must be multiplied by π.

The layout of the injector and the 1.6 GeV section of the linac is shown in Fig. 1.

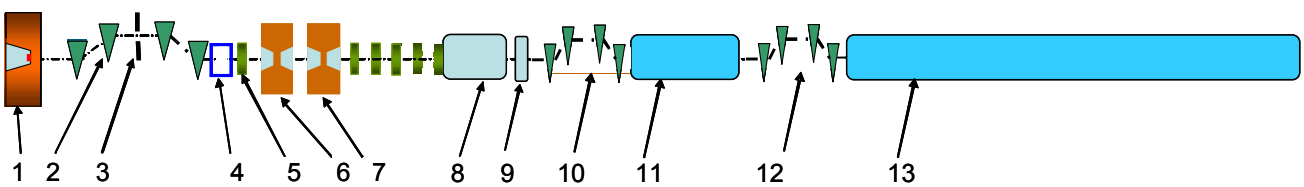

Figure 1: General layout of the linac for XFELO. 1 – RF cavity with thermionic cathode, 100 MHz, 1 MV; 2 – chicane and slits (3) as an energy filter; 4 – quadrupole triplet; 5 – focusing solenoid; 6 – monochromator of the beam energy, f=600 MHz; 7 –buncher, f=300 MHz; 8 – booster linac section, f=400 MHz; 9 –RF cosine-chopper to form rep. rate 1 MHz to 100 MHz; 10 – bunch compressor – I; 11 –SC linac section, 460 MeV, f=1300 MHz; 12 – bunch compressor – II; 13 – initial section of the SC linac, f=1300 MHz.

* This work was supported by the U.S. Department of Energy, Office of Nuclear Physics and Basic Energy Sciences, under Contract No. DE-AC02-06CH11357 . P.P is supported by U.S. Department of Education, under contract P116Z010035 with Northern Illinois University
#ostroumov@anl.gov

EXTRACTION FROM ECR AND RECOMBINATION OF MULTIPLE-CHARGE STATE HEAVY-ION BEAMS IN LEBT*

P.N. Ostroumov#, A. Barcikowski, S.A. Kondrashev, B. Mustapha, R.H. Scott, and S.I. Sharamentov, ANL, Argonne, IL 60439, U.S.A.
N.E. Vinogradov, Northern Illinois University, DeKalb, IL 60115, USA

Abstract

A prototype injector capable to produce multiple-charge-state heavy-ion beams has been developed and constructed at ANL. The injector consists of an ECR ion source, a 100 kV platform and a Low Energy Beam Transport (LEBT). The latter comprises two 60-degree bending magnets, electrostatic triplets and beam diagnostics stations. Several charge states of bismuth ions from the ECR have been extracted, accelerated to the energy of 1.8 MeV, separated and then recombined into a high quality beam ready for further acceleration. This technique allows us to double heavy-ion beam intensity in high-power driver linac for future radioactive beam facility. The other application is the post-accelerators of radioactive ions based on charge breeders. The intensity of rare isotope beams can be doubled or even tripled by the extraction and acceleration of multiple charge state beams.

INTRODUCTION

Ion accelerators worldwide use only single-charge state beams from the ion source. ECR Ion Sources (ECRIS) are widely used as injectors of highly charged ions. Current state of the art ECRIS built using superconducting (SC) magnets has recently demonstrated ~6 pμA of uranium ions with charge state 33+ or 34+ [1]. Taking into account the acceleration and stripping efficiencies, the ion source intensity must be doubled to meet the power requirements for the proposed Facility for Rare Isotope Beams (FRIB) [2] and other nuclear physics applications based on high-intensity ion linacs. Obviously, the intensity of single-charge state beams cannot be doubled in the near future and the appropriate solution is to simultaneously extract and accelerate multiple-charge states of the desired heavy-ions. This solution is not appropriate for light ions due to larger charge states separation in the phase space (large q/A separation, where q is the ion charge state and A is the mass number). Fortunately, ion sources produce enough single-charge state intensity for light ions. In addition to future facilities, existing facilities could benefit from the concept of multiple-charge state acceleration as well.

We have designed and built a prototype multiple-charge state injector system to demonstrate the possibility of extracting, analyzing and combining several charge states of a heavy-ion beam from the ion source to the point of injection to an RF accelerator. The injector consists of an ECRIS placed on a High-Voltage (HV) platform and an achromatic LEBT. The system was successfully tested for a two-charge state bismuth beam. This technique can be applied for both the driver and post accelerator in radioactive beam facilities. It is well recognized that the ECRIS and the Electron Beam Ion Source (EBIS) are effective charge breeders for radioactive beams [3]. The intensity of radioactive ions extracted either from an ECRIS or EBIS can be increased by combining several neighboring charge states into the same phase space area for further acceleration. This is especially important for rare isotope beams where doubling or tripling the intensity is critical for certain measurements.

EXPERIMENTAL SET-UP

A 3D model of the injector is shown in Fig. 1. It consists of an ECR ion source, a 100-kV platform and an achromatic LEBT system based on two 60° bending magnets. The stand-alone ECR ion source is built using all permanent magnets, it is described in more detail elsewhere [4]. The HV platform was designed and constructed to accelerate all ion species extracted from the ECR source to higher energy to suppress space charge effects in the LEBT. The focusing is provided by electrostatic Einzel lenses and quadrupole triplets. Rotating wires are used for beam profile measurements. The beam emittance is measured by a specially developed scintillator-based pepper-pot emittance probe described in

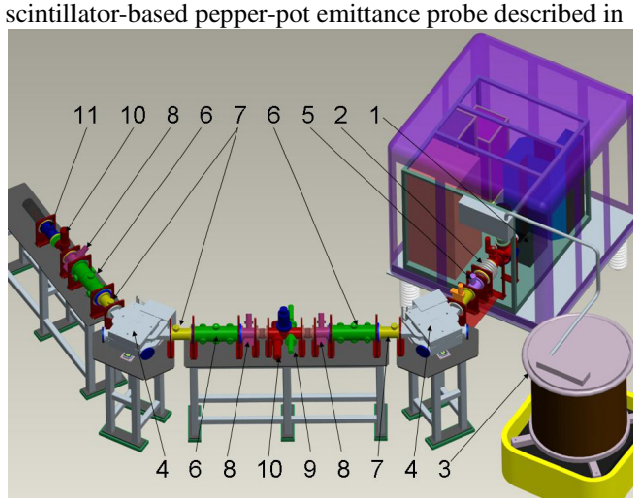

Figure 1: General view of the injector. 1 - ECRIS installed on HV platform, 2 - 75-kV accelerating tube, 3 - isolation transformer, 4 - 60° bending magnet, 5 - Einzel lens, 6 - electrostatic triplet, 7 - electrostatic steering plates, 8 - rotating wire scanner, 9 - horizontal jaw slits, 10 - Faraday cup, 11 - emittance probe.

* This work was supported by the U.S. Department of Energy, Office of Nuclear Physics Contract No. DE-AC02-06CH11357 . N.E.V. is supported by U.S. Department of Education, under contract P116Z010035 with Northern Illinois University
#ostroumov@anl.gov

RAMPING UP THE SNS BEAM CURRENT WITH THE LBNL BASELINE H⁻ SOURCE

Martin P. Stockli, B. Han, S. N. Murray, D. Newland, T. R. Pennisi, M. Santana, R. F. Welton,
Spallation Neutron Source, Oak Ridge National Laboratory, Oak Ridge, TN 37831, U.S.A..

Abstract

Over the last two years the Spallation Neutron Source (SNS) has ramped up the repetition rate, pulse length, and the beam current to reach 540 kW, which has challenged many subsystems including the H- source designed and built by Lawrence Berkeley National Laboratory (LBNL). This paper discusses the major modifications of the H⁻ source implemented to consistently and routinely output the beam current required by the SNS beam power ramp up plan. At this time, 32 mA LINAC beam current are routinely produced, which meets the requirement for 690 kW planned for end of 2008. In June 2008, a 14-day production run used 37 mA, which is close to the 38 mA required for 1.44 MW. A medium energy beam transport (MEBT) beam current of 46 mA was demonstrated on September 2, 2008.

INTRODUCTION

LBNL designed and built the SNS baseline H⁻ source, a mulicusp RF ion source [1]. Typically 250 W from a 600 W 13.56 MHz generator are matched into a 2.5 turn antenna loop inside the plasma chamber where it generates continuous, low-power hydrogen plasma. An additional 6%-duty-factor, 80-kW 2 MHz supply superimposes 40-70 kW for ≤1.23 ms at 60 Hz to boost the plasma density for beam production. As shown in Fig. 1, a transverse ~300 G filter field cools the plasma, which drifts towards the outlet aperture. The Cesium collar contains less than 30 mg of Cs in Cs_2CrO_4 cartridges [2]. Most of the negative ions form when bouncing from the Cs collar outlet aperture that is next to the source outlet.

A 1.6-kG dipole field, peaking 7 mm outside the source outlet, steers the co-extracted electrons toward one side of the e-dump, which is kept between +2 and +7 kV with respect to the -65 kV source potential. A fraction of the electrons impacts on the e-dump, while the other fraction ends on the extractor, where they generate thermal and radiation problems, especially when the extractor uses some of its +20 kV potential.

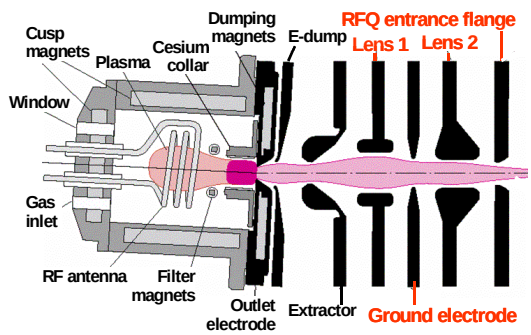

Figure 1: Schematic of the SNS H- source and LEBT.

Table 1: Duty factor, pulse length, unchopped MEBT beam current requirement and achievements, and the source and LEBT availability for neutron production runs. Run numbers reflect the calendar year.

Production Run	Duty fator	Pulse length	mA required	mA in MEBT	%Availability
Run 2006-1		~.1 ms	20	20-28	99.9
Run 2006-2	0.2	~.25ms	20	14-30	99.98
Run 2007-1	0.8	~0.4ms	20	10-20	70.6
Run 2007-2	1.8	~0.5ms	20	11-20	97.2
Run 2007-3	3.0	~0.6ms	25	25-30	99.65
Run 2008-1	3.6	~0.6ms	25/30	25-37	94.9
Run 2008-2	4.0	0.67ms	32	32-35	

The extractor accelerates the beam into the 12-cm long, two-lens electrostatic low-energy beam transport (LEBT), which focuses the beam into the radio frequency quadrupole (RFQ). The compactness of the LEBT prohibits any characterization of the beam before it is accelerated to 2.5 MeV by the RFQ. The first beam current measurement is obtained from the first MEBT beam current monitor near the exit of the RFQ (BCM02).

This paper discusses the failures and successes in meeting MEBT beam current requirements as outlined in the SNS power ramp up plan [3] and listed in Table 1.

LOW POWER PERFORMANCE

At the beginning of the SNS beam power ramp up, the short pulse length allowed the H⁻ source to exceed the required 20 mA as seen in Fig. 2a. When the pulse length was increased to ~0.25 ms for the 2nd 2006 run, the source was at times unable to match the 20 mA requirement as seen in Fig. 2b.

Short beam pulses (<<0.2 ms) yield high beam currents when the matching network is matched without plasma. When the pulse length of short pulses is extended, a significant reduction in beam current is found, as seen in Fig. 3.

Long pulses yield the highest beam current when the matching network is tuned with the presence of plasma,

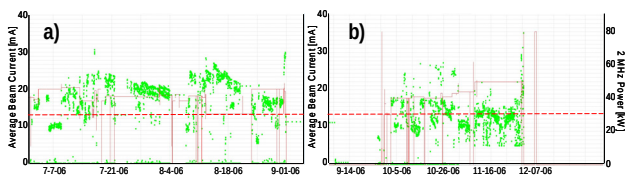

Figure 2: Requested 2 MHz peak power (solid line) and average chopped MEBT beam current (dots) compared with the required 13 mA (dashed line) for 2006.

EBIS PREINJECTOR CONSTRUCTION STATUS*

J. Alessi#, D. Barton, E. Beebe, S. Bellavia, O. Gould, A. Kponou, R. Lambiase, E. Lessard, R. Lockey, V. LoDestro, M. Mapes, D. McCafferty, A. McNerney, M. Okamura, A. Pendzick, D. Phillips, A.I. Pikin, D. Raparia, J. Ritter, J. Scaduto, L. Snydstrup, M. Wilinski, A. Zaltsman, BNL, Upton, Long Island, New York
U. Ratzinger, A. Schempp, IAP, Frankfurt am Main

Abstract

A new heavy ion preinjector is presently under construction at Brookhaven National Laboratory. This preinjector uses an Electron Beam Ion Source (EBIS), and an RFQ and IH Linac, both operating at 100.625 MHz, to produce 2 MeV/u ions of any species for use, after further acceleration, at the Relativistic Heavy Ion Collider, and the NASA Space Radiation Laboratory. Among the increased capabilities provided by this preinjector are the ability to produce ions of any species, and the ability to switch between multiple species in 1 second, to simultaneously meet the needs of both physics programs. Fabrication of all major components for this preinjector is in process, with testing of the EBIS and RFQ starting this year. The status of this construction is presented.

INTRODUCTION

The layout for the new EBIS-based heavy ion preinjector is shown in Fig. 1. This preinjector, will be located at the high energy end of the existing 200 MeV H-linac building. Not shown in this figure is an additional 37 m long beamline which connects the preinjector to the heavy ion injection point of the Booster Synchrotron. This preinjector will replace two existing Tandem Van de Graaff accelerator and an 800 m transport line, as the heavy ion preinjector for both the Relativistic Heavy Ion Collider (RHIC) and NASA Space Radiation Laboratory (NSRL). It is designed to deliver milliampere currents of any ion species in short pulses, to allow single-turn injection into the Booster. With any of several external ion sources able to inject pulses of 1+ ions into the EBIS trap, species from EBIS can be changed on a pulse-to-pulse basis. The switching time for the magnets in the HEBT line will be 1 second. Some key parameters are given in Table 1. More details on the EBIS source and preinjector can be found in [1] and [2].

Table 1: Preinjector Parameters

Ions	He - U
Q / m	≥1/6
Current	> 1.5 emA
Pulse length	10 μs (for 1-turn injection)
Rep rate	5 Hz
Output energy	2 MeV / u
Time to switch species	1 second

EBIS SOURCE

The design of the EBIS source is based on the very successful performance of the prototype Test EBIS at Brookhaven [1]. The primary changes in the present EBIS, relative to the prototype, is the increase of the source trap length from 0.7 to 1.5 m, which requires a superconducting solenoid with a length of 2m. Other changes relative to the Test EBIS are intended to allow operation at higher repetition rates, and improve reliability and maintainability. The source is shown schematically in Fig. 2. A brief status of some of the key components follows.

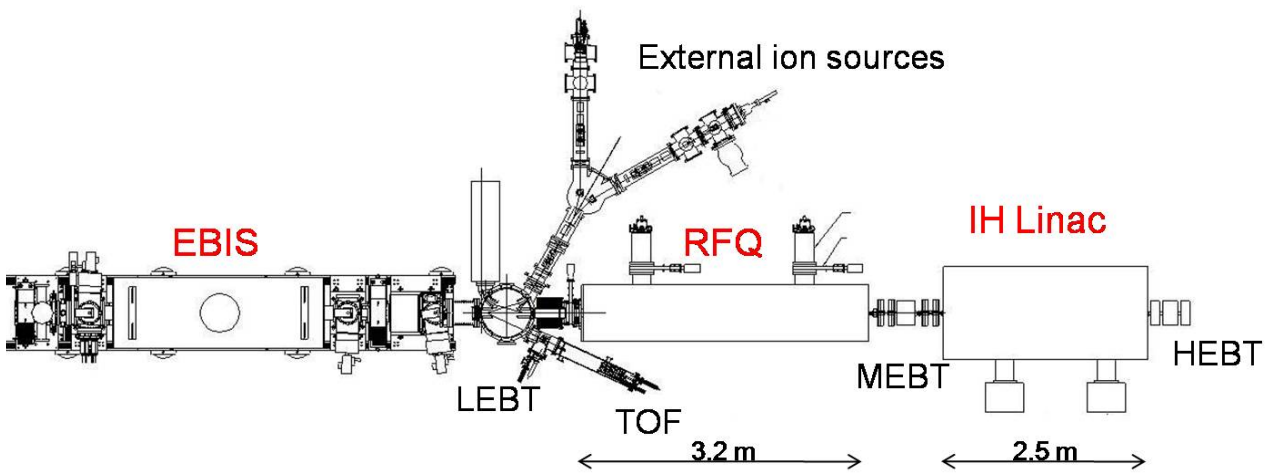

Figure 1: Layout of the EBIS-based heavy ion preinjector

*Work supported under the auspices of the US Department of Energy and the National Aeronautics and Space Administration.
#alessi@bnl.gov

ENERGY RECOVERED LINACS*

G. A. Krafft#, Jefferson Lab, Newport News, VA 23606, U.S.A.

Abstract

In the last decade, stimulated by the success of the energy recovered free electron lasers, many projects have been initiated exploring the applications and limitations of beam energy recovery in recirculated linear accelerators (linacs). In this talk the performance of many existing energy recovered linacs is briefly reviewed. Looking forward, potential applications of energy recovered linacs such as recirculated linac light sources, high energy beam electron cooling devices, and electron beam sources for high energy colliders have been pursued with varying degrees of effort. The types of new technology that must be developed for applications, and more broadly, some of the open issues regarding this technology, are discussed.

RECIRCULATED AND ENERGY RECOVERED LINACS

Over the course of the last decade, there has been a growing interest in developing accelerators using the idea of beam energy recovery. This paper presents a review of the work done on energy recovery to date. In brief, applying the technique of beam energy recovery allows the construction of electron linear accelerators that can accelerate average beam currents similar to those provided by storage rings, but with the superior beam quality typical of linacs. Such an ability to simultaneously provide both high current and high beam quality can be broadly utilized. For example, high average power free electron laser sources may be built yielding unprecedented optical beam power, light sources extending the available photon brilliance beyond the limits imposed by present day synchrotron light sources may be designed, electron cooling devices may be possible which would benefit from both high average current and good beam quality to ensure a high cooling rate of the circulating particles in a storage ring collider, or, as a final theoretical possibility, the electron accelerator in an electron-ion collider intended to achieve operating luminosity beyond that provided by existing, storage-ring-based colliders may be based on an energy recovered linac (ERL).

In the following, we compare recirculating linacs to two more common types of accelerators: single pass linear accelerators and storage rings. We then discuss energy recovery conceptually, and review the work to date on this technique, primarily in the energy recovered free electron lasers. Most of this introductory material is a condensed paraphrase of material in an earlier review of energy recovered linacs [1]. Please consult this reference for a more detailed discussion.

In the past, two types of particle accelerators (Fig. 1) have been used. Among the electron accelerators, the first class of accelerators consists of the high-energy electron linacs. In such accelerators, the electron beam has a definite beginning and a definite end. Usually, the beam propagates along a nearly straight line, and there is a substantial length of RF beam-acceleration devices.

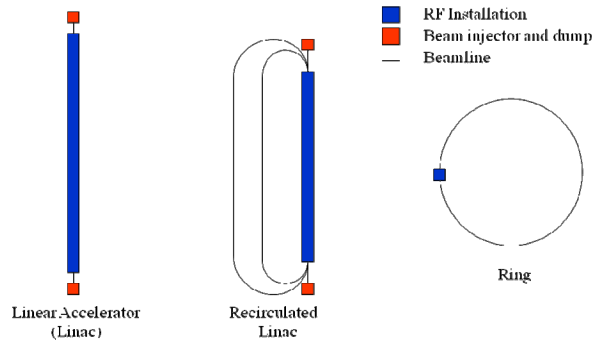

Figure 1: Main accelerator types.

Some main features of an electron linac are: first, an individual electron resides in the accelerator only briefly, certainly for times that are short compared to any relevant radiation damping times. Second, if a laser-driven photocathode gun is used as the electron source, it is relatively easy to load, or program, the beam current or beam polarization delivered to users by controlling the duration and polarization of the lasers that stimulate electron production at the gun. Third, the emittance, of the electrons in a typical beam tends to be set by phenomena in the low-energy electron source region, and this emittance may be well preserved during the acceleration to high energy. Fourth, the pulse duration, and more generally the longitudinal phase space distribution, is relatively easily manipulated by using standard beam-rf and electron beam optical techniques. Having long distance between the end of the linac and the beam dump is easy to arrange in a linear geometry.

The second class of high-energy electron accelerators is the synchrotron-like storage ring. In an electron storage ring, the electrons are bent on a roughly circular orbit. Because transversely accelerated electrons radiate copious amounts of electromagnetic radiation, to achieve a long-term equilibrium it is necessary to supply energy to the circulating electrons. Energy is supplied, as in linacs, with RF cavities but they subtend a small portion of the total machine circumference. After the beam is injected into the ring, the electrons rapidly settle into an equilibrium where the synchrotron radiation losses are made up by the energy transferred from RF to beam. The equilibrium characteristics point to the main limitations of storage rings. The equilibrium beam emittance, and hence the

*Authored by Jefferson Science Associates, LLC under U.S. DOE Contract No. DE-AC05-06OR23177. The U.S. Government retains a non-exclusive, paid-up, irrevocable, world-wide license to publish or reproduce this manuscript for U.S. Government purposes.
#krafft@jlab.org

HIGH AVERAGE CURRENT SRF CAVITIES

T. Furuya, KEK, Ibaraki

Abstract

Higher-order-mode (HOM) free superconducting (SC) single cell cavities were developed for the rf system of high luminosity storage ring colliders. Because of the successful results of these cavities under ampere-class beams, the components and technology of the SC cavities have immediately been applied to the middle sized storage rings upgrading the beam intensity by using a few SC cavities. Beside the storage ring rf, a SC based high intensity proton linac was commissioned for neutron physics. Recently, the feasibility study of energy recovery linacs has been carried at various laboratories aiming for the 4th generation light source. Status of these developments will be described.

CONTRIBUTION NOT RECEIVED

FIRST RESULTS FROM THE ERL PROTOTYPE (ALICE) AT DARESBURY

D.J.Holder#, on behalf of the ALICE team at STFC Daresbury Laboratory, Warrington, UK.

Abstract

The energy recovery linac prototype at Daresbury is now called ALICE (Accelerators and Lasers In Combined Experiments). This paper presents the results obtained in the past year, including the fourth period of gun commissioning. Following the completion of gun commissioning in November 2007, the dedicated gun diagnostic line was removed and the electron gun attached to the booster cavity and hence the rest of the machine.

The paper outlines some of the challenges experienced during the commissioning of both the photoinjector system and the superconducting cavities and presents the current status of the project as well as the very latest results from commissioning during the summer of 2008.

INTRODUCTION

Following the outcome of a review of synchrotron light sources in the UK, the proposed 4th Generation Light Source (4GLS) project was cancelled. The Energy Recovery Linac Prototype (ERLP), which was originally conceived as a prototype test-bed for the key concepts and technologies expected to feature in 4GLS, now has a broader role as an accelerator physics and technology test facility and for developing fourth generation light source science. Renamed ALICE (Accelerators and Lasers In Combined Experiments), the facility is being commissioned at present. The past year has been a frustrating combination of both progress and setbacks. A short productive period of gun commissioning has been book-ended with several vacuum problems with the gun. However in parallel to the commissioning work with beam, progress has also been made with the cryogenic and RF systems.

ALICE is based on a combination of a DC photocathode electron gun, a superconducting injector linac and a main linac intended to operate in energy recovery mode. These drive an IR-FEL, an inverse Compton Back-Scattering (CBS) x-ray source [1] and a terahertz beamline.

In addition, next year sees the start of construction the world's first non-scaling, Fixed-Field Alternating Gradient (FFAG) accelerator called EMMA, for which ALICE will act as an injector [2]. Fig. 1 shows the layout of both ALICE and EMMA.

PROGRAMME

At the end of 2007, the dedicated gun diagnostic beamline, with which the gun was commissioned and characterised, was removed as the rest of the machine was ready to accept its first beam. It was expected that operation in energy-recovery mode (initially without the beam-disrupting effects of the FEL) would have been achieved, followed by installation of the FEL components and progress with the CBS source and terahertz beamline made. Unfortunately at the time of writing ALICE is still on the brink of this step. This paper will record both the successes and the lessons learnt during this sometimes painful period.

OVERVIEW OF GUN COMMISSIONING

The first electron beam was obtained from the gun at 250 keV into a dedicated gun diagnostic beamline [3] in August 2006. Further operation of the electron gun was disrupted by various issues before the final (successful) period of operation at 350 keV towards the end of 2007.

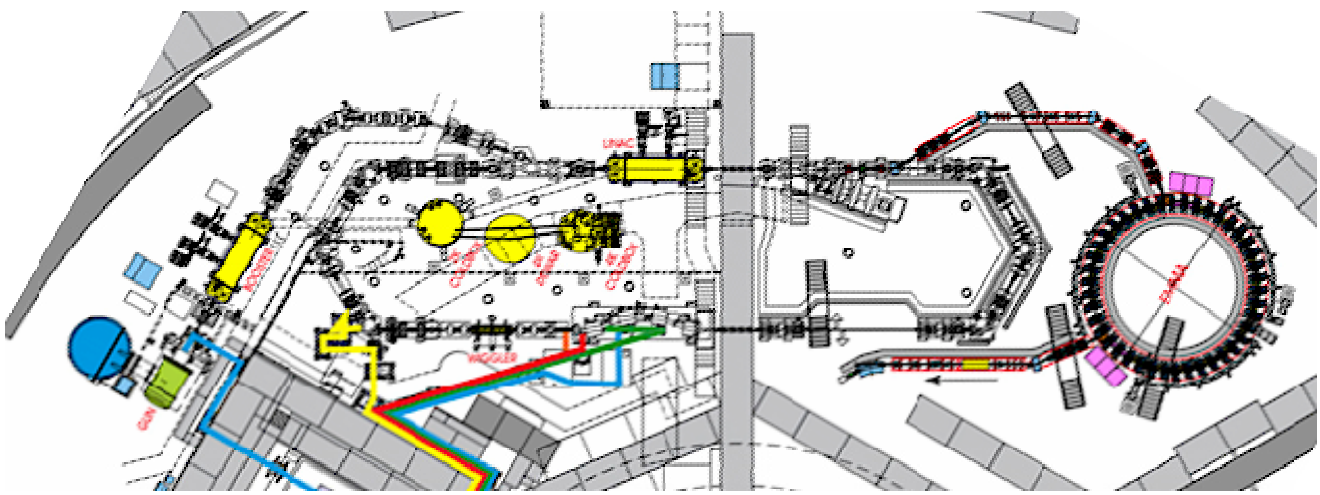

Figure 1: Layout of ALICE and EMMA.

#david.holder@stfc.ac.uk

FIRST TESTS OF THE CORNELL UNIVERSITY ERL INJECTOR*

B. Dunham#, I. Bazarov, S. Belomestnykh, M. Billing, E. Chojnacki, Z. Conway, J. Dobbins, R. Ehrlich, M. Forster, S. Gruner, G. Hoffstaetter, V. Kostroun, M. Liepe, Y. Li, X. Liu, D. Ouzounov, H. Padamsee, D. Rice, V. Shemelin, C. Sinclair, E. Smith, K. Smolenski, S. Temnykh, M. Tigner, V. Veshcherevich, T. Wilksen, CLASSE, Cornell University, Ithaca, NY 14853, U.S.A.

Abstract

Cornell University is planning to build an Energy Recovery Linac (ERL) X-ray facility. For an ERL, it is well known that the x-ray beam brightness for the users is mainly determined by the initial electron beam emittance provided by the injector. To address technical challenges of producing very low emittance beams at high average current as required for an ERL, Cornell University has proposed a prototype injector with 5-15 MeV beam energy, 100 mA maximum average current and 77 pC/bunch. In this article, we describe the design, construction and initial results for an ERL injector prototype now under operation.

INTRODUCTION

An electron injector for an ERL has many challenges. To provide the x-ray beam quality that users demand for the future, the injector needs to meet the requirements show in Table 1 [1].

Table 1: Injector Requirements (values in ( ) are goals for the prototype system of this paper)

Beam Energy	10-15 (5-15) MeV
Charge per bunch	77 (77) pC
Average Current	100 (100) mA
Bunch Length	2-3 (2-3) ps
Transverse Emittance	0.3 (2) μm
Operating Frequency	1.3 (1.3) GHz

At Cornell University, we have undertaken a program to develop and test such an injector (see Fig. 1) towards realization of this difficult set of requirements. The design was based on detailed simulations using genetic algorithms to find the optimum solutions to the multi-parameter design space [2]. The electron source is a DC photoemission gun using a GaAs cathode, providing a 1.3 GHz bunch train of 77 pC/bunch with a 20-40 ps 'beer can' distribution. This is followed by a short section for emittance compensation solenoids and a normal conducting buncher cavity [3]. The beam is then accelerated through a cryomodule containing five 2-cell niobium superconducting RF (SRF) cavities, each with individual control of phase and gradient. The cavities have two opposing 50 kW input couplers to feed in 100 kW per cavity. The available RF power allows for either 100 mA at 5 MeV or 33 mA at 15 MeV. After the SRF cavities, an extensive suite of diagnostics allows for a complete characterization of the transverse and longitudinal phase space of the beam. The beam is terminated in an aluminum dump with a capacity for disposing 600 kW of average power.

Each section of the injector will be described in detail, along with the current status of commissioning and beam tests.

DC PHOTOEMISSION GUN

Based on the experience of other labs [4] and of the authors, DC photoemission guns provide the best chance of producing the low emittance, high average power beam to meet the needs of an ERL. The present record for average current belongs to the Boeing normal conducting RF (NCRF) gun [5] at 32 mA (25% duty factor), and while other projects continue to push for higher current with NCRF guns, no improvements have been realized. Work on SRF guns has made excellent progress recently [5], but the prospect of obtaining 100 mA average current is still many years away. The DC gun used for the Jefferson Lab FEL project [4] has reliably provided 135 pC bunches at an average current of ~9 mA, and an extension of that technology is the most likely path to meet the needs of an ERL injector in the near future.

High Voltage Gun

Common sense dictates that high initial beam energy and high electric field at the cathode are necessary to overcome the space charge forces in bunched beams and obtain the best possible emittance. Simulations [2] show that higher gun voltage is important for obtaining low emittance up to a certain point, after which the improvement is relatively small. Thus, a DC gun operating in the range of 500-600 kV should meet the emittance goals with the appropriate cathode. To minimize dark current at the operating voltage, the gun must be processed to roughly 25% above the operating value, consequently the Cornell gun has been designed to withstand 750 kV maximum voltage.

A schematic cutaway of the Cornell DC photoemission gun is shown in Fig. 2, and was designed to meet the requirements in Table 2. The gun was operated for over a year using a test beamline to measure the performance of the gun and cathode before mating it to the rest of the injector. Details of these measurements have been published elsewhere [7, 8], with the main result that the emittance measurements at 77 pC/bunch and 250 kV beam energy match the simulations very closely, giving confidence that the simulations for the entire system are valid. Two difficulties observed involved the laser profile and laser stability. Tails in the phase space distribution were traced (through simulation) to non-uniformities

RF CONTROL OF HIGH Q_L SUPERCONDUCTING CAVITIES*

Curt Hovater#
Jefferson Lab, Newport News VA, USA

Abstract

In the last 20 years the requirements for RF Control have increased as the target use has broadened from electron/ion accelerators for Nuclear and Particle Physics to light sources such as Free Electron Lasers. The increasing requirement of cavity field control to meet the spectral and jitter performance specifications for light sources has led system designers to a more rigorous approach in designing the RF controls. Design attention must be applied not only to the hardware and control algorithms but also to the overall accelerating system to meet performance and cost requirements. As an example, cavity Q_L in Energy Recovery Linacs (ERL) must be optimized such that the RF controls can accommodate the lowest possible RF power given the background cavity microphonics. This paper presents the status and future directions of high Q_L superconducting RF control systems.

INTRODUCTION

Recent proposals for energy recovering linacs (ERLs) at Cornell, Daresbury and Argonne have challenged the RF community to meet the field control requirements of the higher Q_L cavities. It should be noted the operation of high Q_L cavities is not new. Superconducting (sc) accelerating structures such as the types used in proton and ion accelerators have always operated with $Q_L > 10^7$. The difference is that beam requirements to meet the optical frequencies and line widths require them to be on the order of $< 0.1^o$ and 10^{-4} amplitude stability. Some of the techniques (Self Excited Loop) for operating these cavities can be applied to the ERLs. In addition to field control sc cavities can have large Lorentz coefficients making turn on or cavity recovery difficult. Fortunately, advances in electronics have made developing and designing RF control systems easier, where the designs have shifted from fairly rigid analog-centric hardware 20 years ago to a more flexible digital-centric software design.

RF control design starts at the beginning of the accelerator design. Depending on the application, energy spread and jitter specifications will directly correlate to the required cavity field control. Once this is known, the designer can begin modeling the receiver and feedback necessary to meet the field control requirement. Next, one must optimize the cavity Q_L for the application. If the Linac is pulsed, some form of Lorentz detuning compensation must be considered.

* Notice: Authored by Jefferson Science Associates, LLC under U.S. DOE Contract No. DE-AC05-06OR23177. The U.S. Government retains a non-exclusive, paid-up, irrevocable, world-wide license to publish or reproduce this manuscript for U.S. Government purposes.
# hovater@jlab.org

Other control considerations include: multiple cavity control (i.e. vector sum) vs. single cavity control and Generator Driven Resonator (GDR) vs. Self Excited Loop (SEL).

OPTIMIZING CAVITY Q_L

The RF system must be optimized for minimum power which ultimately sets the cavities loaded Q. The optimum coupling (β_{opt}) to a cavity can be derived from the steady state cavity equations and is given by

$$\beta_{opt} = \sqrt{(b+1)^2 + \left[\frac{2\delta f}{\Delta f_o}\right]^2} \qquad (1)$$
$$\text{where} \quad b = \frac{I_o (R/Q) Q_o}{V} \cos\phi$$

V is the cavity voltage, I_o is beam current, R/Q is the shunt impedance, Q_o is the cavity quality factor, ϕ is the beam phase, f_o is the cavity frequency, δf is the cavity detuning, and Δf_o is the cavity bandwidth [1]. In the limit where the $Q_o >> Q_L$, one can make the approximation that $\beta \sim Q_o/Q_L$. In the case of a heavy beam loaded cavity such as one might find in an injector, the optimized loaded Q is driven by beam loading (i.e. $b >> 1$) and eq. (1) reduces to

$$Q_{Lopt} \cong V / I_o (R/Q) \qquad (2)$$

In the case of an ERL where the vector sum of the two beams results in a net current that is less than a few tens of micro-amps, there is an incentive to increase the Q_L [2]. Q_L is limited by the amount of microphonic detuning the cavity exhibits under normal operating conditions (i.e. $2\delta f/\Delta f_o >> b+1$). In this case Q_{Lopt} is given by

$$Q_{Lopt} \cong f_o / 2\delta f \qquad (3)$$

Figure 1 shows the optimizations on generator power for different beam loads.

If the cavity power requirement is driven by the microphonics, some consideration to cavity stiffening is necessary. At Jefferson Lab, we have operated both stiffened and un-stiffened cavities. The stiffening rings can have an effect on roughly similar cell shapes. Table 1 shows the microphonic detuning of elliptical cavities with and without stiffening. Included in the table is the klystron power required for the Q_{Lopt} given the 6σ microphonic detuning.

RF SYSTEMS FOR CW SRF LINACS

S. A. Belomestnykh, CLASSE, Ithaca, New York

Abstract

The talk will provide an overview of the latest developments in rf systems for cw operated SRF linacs, such as CEBAF (in particular, 12 GeV Upgrade), Cornell ERL injector, ELBE, and ERLP at Daresbury.

CONTRIBUTION NOT RECEIVED

OPERATIONAL EXPERIENCE WITH HIGH POWER BEAMS AT THE SNS SUPERCONDUCTING LINAC*

J. Galambos, on behalf of the SNS team, ORNL, Oak Ridge, TN, 37830, U.S.A.

Abstract

The Spallation Neutron Source (SNS) accelerator is in a period of rapid beam power ramp-up, with operation of over 0.5 MW achieved to date. SNS is the first high power proton pulsed superconducting linac (SCL), and has unique challenges. Beam tuning methods have been developed for setting the many independently powered SCL cavities, and recover from faults. The challenges and experience of minimizing beam loss at the high operational powers are also presented.

INTRODUCTION

The Spallation Neutron Source provides a high power source of protons to drive a short pulsed spallation neutron source [1-5]. The beam acceleration is accomplished in a linac, with copper structures providing acceleration up to 186 MeV and superconducting RF structure providing acceleration to 1000 MeV. The linac design goal is a 1 msec long pulse of 26 mA average current provided at 60 Hz (~ 1.5 MW). This beam is injected into an accumulator ring and the pulse length compressed to ~ 1 μsec to provide a short pulse source of spallation neutrons. Many of the details of the power ramp-up over the last two years are provided in Ref [1-5]. Here we concentrate on the operational experience with beam of the Superconducting linac (SCL). Details of the operational experiences with the equipment are provided in Refs [6-7].

POWER RAMPUP PROGRESS

To date the beam SCL has provided over 550 kW of production beam. Typical beam operating conditions at this power level are 60 Hz repetition rate, 18 (32) mA average (peak) current, 600 μsec pulse length and 890 MeV. For neutron production conditions, the beam energy is reduced to 890 MeV because of the SCL equipment issues discussed in Ref. 6, pulse length is limited by availability concerns for the High Voltage RF support systems, and peak current is limited by Ion Source capability and availability concerns. Figure 1 shows the history of the beam on Target power ramp-up (We note that the SCL beam power is ~ 5% higher than that provided on the neutron producing Target, because ~5% of the beam is lost at the Ring Injection.

* SNS is managed by UT-Battelle, LLC, under contract DE-AC05-00OR22725 for the U.S. Department of Energy

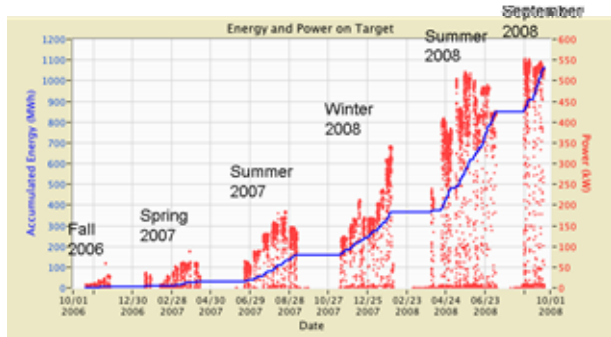

Figure 1. The beam on target power ramp-up progress since the start of neutron production at SNS.

SCL RF SET-UP

One of the most striking features we have come to realize regarding the SCL operation with beam is its flexibility. The copper structures tend to be large, high power cavities (> 1 MW klystron power level), with many (~ 100) individual RF-gaps. For these large structures there is a significant change in the beam β, as well as significant phase advance of the beam bunch in longitudinal phase space. The copper cavity geometries are manufactured to match the expected energy gain and provide appropriate longitudinal focusing. Only one klystron RF phase and amplitude setting is correct. If one varies the phase and amplitude setting about the nominal set-point in the warm linac cavities, the resulting effect on the beam is complicated and each warm cavity has a unique output beam "response signature" [7]. Figure 2 shows the measured response of the beam Time-of-flight (TOF) downstream of the first Drift Tube Linac (DTL) tank in SNS, to perturbations in its phase and amplitude.

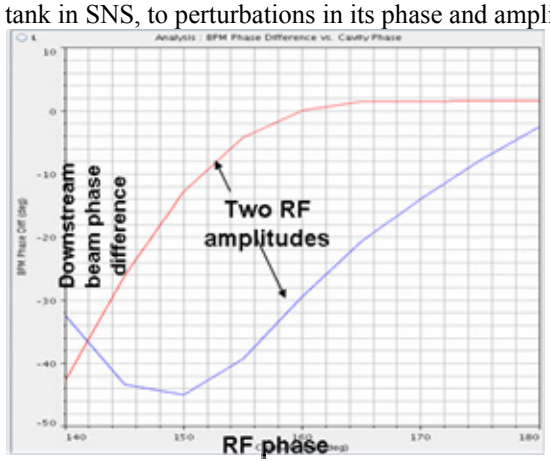

Figure 2. Measured change in the downstream beam velocity with changes to the RF phase and amplitude in the first DTL tank (Red is ~ 2 % below nominal amplitude; blue is ~ 2 % above).

FERMILAB'S PROJECT X

S. Nagaitsev, Fermilab, Batavia

Abstract

The present status and plans for Fermilab's Project X will be reviewed.

CONTRIBUTION NOT RECEIVED

IH-DTL AS A COMPACT INJECTOR FOR A HEAVY-ION MEDICAL SYNCHROTRON

Y. Iwata*, T. Fujisawa, S. Hojo, N. Miyahara, T. Murakami, M. Muramatsu,
H. Ogawa, Y. Sakamoto, S. Yamada, and K. Yamamoto,
NIRS, 4-9-1 Anagawa, Inage, Chiba 263-8555, Japan
T. Fujimoto and T. Takeuchi, AEC, 2-13-1 Konakadai, Inage, Chiba 263-0043, Japan.
T. Mitsumoto, H. Tsutsui, T. Ueda, and T. Watanabe, Sumitomo Heavy Industries (SHI), Ltd.,
1-1, Osaki 2-Chome, Shinagawa, Tokyo 141-6025, Japan

Abstract

Compact linacs, consisted of a Radio-Frequency-Quadrupole (RFQ) linac and an Interdigital H-mode Drift-Tube-Linac (IH-DTL) having the same operating frequency of 200 MHz, were designed for an injector of heavy-ion medical synchrotrons. For beam focusing of IH-DTL, the method of Alternating-Phase-Focusing (APF) was applied. The total length of the RFQ linac and the IH-DTL is as short as 6 m. With the two linacs, carbon ions of $^{12}C^{4+}$, produced by an ECR Ion-Source (ECRIS), are accelerated to 4.0 MeV/*u* with the beam intensity of 380 eμA. The compact linacs were constructed and installed in NIRS. We have succeeded to accelerate carbon ions with the APF linac for the first time.

INTRODUCTION

With development of accelerator physics and technology, number of compact linear accelerators as well as cyclotrons has been constructed around the world, and is utilized for medical and industrial applications. At the National Institute of Radiological Sciences (NIRS), cancer therapy using energetic carbon ions, as provided by the Heavy Ion Medical Accelerator in Chiba (HIMAC), has been carried out since June 1994 [1], and more than 4,000 patients have been treated until now. With the successful clinical results, projects of constructing these accelerator complexes, dedicated to the cancer therapy, are initiated over the world. To construct such the complex, construction costs as well as a size of the complex itself are issue, because existing complexes are costly and large in size. Therefore, the development of cost-effective and compact accelerators for a hospital-based complex is needed for the increased use of the heavy-ion therapy.

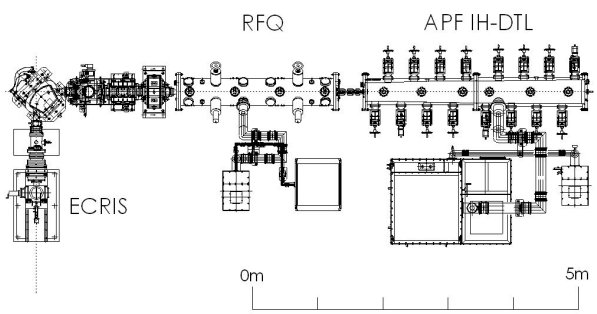

Figure 1: A schematic drawing of the compact injector.

* y_iwata@nirs.go.jp

In the development of the hospital-based accelerator complex, the design of an injector plays a key role, because the existing heavy-ion linacs such as Alvarez linacs are quite large. The size of the injector would affect the total size of the complex as well as total costs of construction. Therefore, we developed the compact injector for the heavy-ion medical synchrotrons.

The compact injector consists of the ECRIS and two linacs, which are the RFQ linac and the IH-DTL having the same operating frequency of 200 MHz. A schematic drawing and major parameters of the compact injector are shown in Figure 1 and Table 1, respectively. In this paper, design as well as performance of the compact injector is described.

Table 1: Major Parameters of the Compact Linacs

Parameters	RFQ	IH-DTL	Units
Injection energy	0.01	0.61	MeV/*u*
Extraction energy	0.61	4.0	MeV/*u*
Operating frequency	200	200	MHz
q/m	1/3	1/3	-
Cavity length	2.5	3.4	m
Cavity outer diameter	0.42	0.44	m

DESIGN OF LINACS

Beam Dynamics

Beam optics of the RFQ linac was designed by using the PARMTEQ code. By optimizing cell parameters for acceleration of $^{12}C^{4+}$, and using the rather high operating-frequency of 200 MHz, we could design the compact cavity; length and outer diameter of the cavity are 2.5 m and 0.42 m, respectively. The RFQ linac can accelerate carbon ions of $^{12}C^{4+}$ having 10 keV/*u*, as produced with the ECRIS, up to 608 keV/*u*. The normalized emittance of the extracted beam from the RFQ linac was calculated to be 0.68 π•mm•mrad.

Carbon ions, as extracted from the RFQ linac, are then accelerated with the IH-DTL up to 4.0 MeV/u. For beam focusing of the IH-DTL, the method of APF was applied [2]. This method utilizes the focusing and defocusing strengths as provided by the rf acceleration field by choosing the positive and negative synchronous phases alternately at each gap. By analogy with the principle of strong focusing, both longitudinal and transverse stability of beam motion could be obtained just with the rf acceleration field. By using this method, no additional

COMMISSIONING AND OPERATION OF THE INJECTOR LINACS FOR HIT AND CNAO

B. Schlitt, GSI, Darmstadt, Germany

Abstract

The Heidelberg Ion-Beam Therapy Centre (HIT) is the first dedicated clinical synchrotron facility for cancer therapy using high energy proton and ion beams (C, He, and O) in Europe. The accelerator consists of a 7 MeV/u, 217 MHz injector linac and of a 430 MeV/u synchrotron. Installation and commissioning of the linac were performed in three phases for ion sources and LEBT, 400 keV/u RFQ, and 20 MV IH-type drift tube linac. The initial commissioning of the linac was finished successfully in December 2006, the commissioning of the synchrotron and the high energy beam lines was finished for both fixed-beam treatment places in December 2007. HIT intends to be ready for patient treatments by the end of 2008. The results of the linac commissioning are reported as well as the experience of more than one year of operation. To provide optimum conditions for patient treatment, an intensity upgrade program has been initiated for the linac. A copy of the HIT linac is presently being installed at the Centro Nazionale di Adroterapia Oncologica (CNAO) in Pavia, Italy. The status of the CNAO linac is also reported.

INTRODUCTION

The number of accelerator facilities dedicated to radiation therapy using high energy proton and heavy-ion beams – also called hadrontherapy – is remarkably growing during the last years [1]. Since the first dedicated clinical centres started operation in Loma Linda, California, and at HIMAC / NIRS in Chiba, Japan, a number of technical improvements have been developed, namely raster-scanning techniques as well as compact synchrotron facilities for heavy-ion treatment and heavy-ion gantries. Also the role of industry has changed and turn-key hadrontherapy facilities are now offered by a number of commercial companies, e.g. IBA, HITACHI [2], ACCEL / VARIAN, or SIEMENS / DANFYSIK [3]. In particular for heavy-ion synchrotron facilities, size and availability of suitable injector linacs are of major technical and economical interests. Whereas compact injector linacs are commercially available for proton synchrotron facilities [2], new compact heavy-ion injectors based on IH linacs have been developed at NIRS [4][5] and at GSI (in close collaboration with the Institute of Applied Physics (IAP) at Frankfurt University) [6][7][8] during the last ten years.

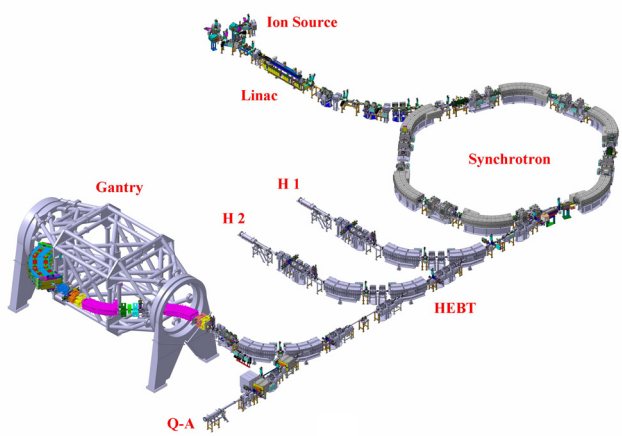

Figure 1: Layout of the HIT accelerator facility.

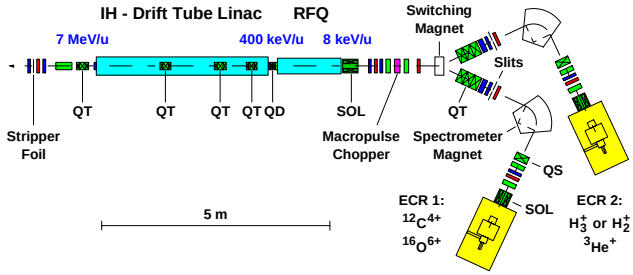

Figure 2: Layout of the HIT injector linac. QS, QD, and QT means quadrupole singulet, doublet and triplet, respectively, SOL means solenoid magnet; focusing and steering magnets (green), profile grids and viewing screens (red), and beam current monitors (blue).

Table 1: Main design parameters at the HIT linac exit

Design ion	$^{12}C^{4+}$
Operating frequency	216.816 MHz
Final beam energy	7 MeV/u
Beam pulse length	≤ 300 µs
Beam repetition rate	≤ 5 Hz
Pulse current after stripping	100 µA ($^{12}C^{6+}$)
Transv. norm. emittances (95 %) [1]	0.8 π mm mrad
Exit energy spread [1]	±0.3 %
Total injector length [2]	≈ 13 m

[1] straggling effects in the stripper foil not included
[2] including ECRIS, LEBT and foil stripper

In Europe, two clinical heavy-ion facilities are currently being commissioned: the Heidelberg Ion-Beam Therapy Centre (HIT) [9][10] in Germany and the Centro Nazionale di Adroterapia Oncologica (CNAO) [11][12] in Pavia, Italy. An additional centre is being constructed by SIEMENS / DANFYSIK [3] in Marburg, Germany. All three centres will use the GSI linac design.

The HIT accelerator facility is shown in Fig. 1. It consists of two all permanent magnet ECR ion sources (ECRIS) of the SUPERNANOGAN type, a 7 MeV/u linac injector, and a compact synchrotron of about 65 m circumference to accelerate ions to final energies of 48 – 430 MeV/u. The beam is distributed by the high energy beam transport lines (HEBT) either to two fixed horizontal beam treatment places (H1, H2), to the isocentric heavy-ion gantry, or to a fixed horizontal beam quality-assurance place (QA) for dosimetry as well as

SUPERCONDUCTING RF R&D TOWARD HIGH GRADIENT*

C.M. Ginsburg#, Fermilab, Batavia, IL 60510, U.S.A.

Abstract

High-beta superconducting RF elliptical cavities are being developed in large numbers for several accelerator projects including the International Linear Collider (ILC). In recent years, the understanding of cavity performance limitations has improved significantly, leading to better than 40 MV/m in some cavities. However, further improvement is needed to reach reliably the 31.5 MV/m operating gradient proposed for the ILC Main Linac cavities. World-wide R&D on the cavity gradient frontier includes improved surface cleaning and smoothing treatments, development of alternative cavity shapes and materials, and novel cavity manufacturing techniques. Substantial progress has been made with diagnostic instrumentation to understand cavity performance limitations. Some highlights of the efforts in superconducting RF R&D toward achieving higher gradients in high-beta elliptical cavities are reviewed.

INTRODUCTION

High-gradient superconducting radiofrequency (SRF) cavity technology is being advanced on many fronts because many cavities are needed for current and proposed projects: (1) the test/user facilities STF (KEK), NML (Fermilab), and FLASH (DESY), (2) the European XFEL currently under construction, (3) Project X at Fermilab, and (4) the International Linear Collider (ILC). The common requirements or choices for the high-gradient cavities in these projects are gradients of at least 23 MV/m, beta=1, elliptical shape and an accelerating mode frequency of 1.3 GHz. Recent studies intended to improve gradients in these cavities are reviewed.

First, the requirements for achieving high gradient and current standard cavity treatments are described. Second, some highlights of studies are shown: surface treatments to reduce field emission, alternative shapes to improve average performance, and new fabrication techniques and materials to reduce cost or improve performance. Third, one fundamental study into the cause of poor cavity quality factor (Q_0) at high gradients is shown. Finally, the cavity diagnostic instrumentation which has been used and/or developed within the last year to study cavity performance and sources of premature quenches is described.

ACHIEVING HIGH GRADIENT

Because RF fields occupy the first ~40 nm of the inner cavity surface for these cavities, the quality of the innermost surface is critical and must be carefully controlled. For the niobium sheets which are used to make cavities, RRR of at least 300 is specified for the ILC[1]. Eddy current scanning (ECS) of all sheets is now done before cavity fabrication. ECS has proven to be a very useful technique to provide feedback to material vendors which has resulted in an overall improvement in the delivered material in recent years. The cavity inner surface has to be very smooth, with no inclusions of foreign particles, or topological defects such as bumps or pits or sharp grain boundaries. No dust or other microscopic contaminants may be introduced after the final surface preparation which could contribute to field emission.

Cavity cell shapes have been optimized for low peak surface magnetic field (H_{peak}) and low peak surface electric field (E_{peak}) relative to the gradient (E_{acc}), as well as ease of surface processing and fabrication.

Many cavities have reached 35 MV/m or more in the last decade, particularly single-cell cavities of varying elliptical shapes and 9-cell Tesla-shape cavities [2].

SURFACE PROCESSING

The surface treatment intended to maximize cavity performance which was developed for the ILC [3] includes initial preparation steps to remove ~150 μm from the inner surface using electropolishing (EP). This initial removal step is also done with centrifugal barrel polishing (CBP) or buffered chemical polishing (BCP) at some labs, though the maximum gradients reached with BCP as the initial preparation step are lower than those achieved using the other methods. Cavities then undergo an 800°C annealing step, to drive hydrogen from the surface. The final preparation steps include degreasing with detergent, another light electropolishing (~20 μm), a high pressure rinse (HPR) with ultrapure water, drying in a class-10 cleanroom, and then evacuation and low-temperature baking (120°C) for about 48 hours after the final assembly with couplers. Additional treatments after the final EP are being studied to reduce field emission, and will be described later.

The primary methods for material removal during surface preparation are CBP, EP and BCP. CBP is a standard technique developed for cavities at KEK in which abrasive small stones are placed into a cavity with water to form a slurry and the cavity is rotated. As a centrifugal process, the material is preferentially removed from the equator region. Since standard cavities have an equator weld, CBP is very effective in smoothing the weld. EP is an electrolytic current-supported material removal, and has been developed for use on cavities by KEK in collaboration with industrial partners and adopted

#ginsburg@fnal.gov

SRF DEVELOPMENTS FOR ION ACCELERATION

G. Olry#, CNRS/IN2P3, IPN Orsay, France

Abstract

This paper gives an overview of the recent Superconducting Radio Frequency developments on low and medium beta resonators, including Quarter-Wave Resonator, Half-Wave Resonator, Spoke and CH-type cavities, for ion accelerators.

We will describe the work done for the upgrade of some existing facilities, as well as the on-going developments on cavities for new projects.

INTRODUCTION

SRF cavities (mainly low beta QWRs) are operating for many years in heavy-ions boosters [1-2]. Their successful operation leads to their integration into most of the new developments for ion acceleration: on existing facilities, such as ISAC-II, ATLAS or PIAVE-ALPI, and new facilities under construction like SARAF and SPIRAL2. Moreover, each driver of the future large-scale accelerators (HINS, FRIB in USA and EURISOL, EUROTRANS in Europe, for example) includes SRF low and medium beta cavities.

QWRs (and HWRS in a lesser extent) are mainly used for existing facilities upgrades and new facilities because of the need of a wide velocity acceptance in order to boost various ion species. Typical range of betas is from 0.001 to 0.15 and voltage gain per cavity around 1 MV.

Spoke resonators and CH-type cavities are studied in the frame of larger SC linacs for which, their multi-gap structure is a real advantage.

UPGRADE OF EXISTING ION ACCELERATORS – UNDER CONSTRUCTION

TRIUMF/ISAC-II

The ISAC-II superconducting linac is currently delivering beams since 2007. It boosts ion energy by 20 MV, thanks to 20 bulk Niobium QWRs housed in 5 cryomodules. The extension of that linac (called "Phase 2") has started since one year and should end up, by the end of 2009, to the addition of twenty new 141 MHz, "high beta 0.11", QWRs [3]. One can note that, besides the beta and frequency values, the inner conductor geometry has been modified (i.e. new "donut" shape) [SRF2007].

A local company, PAVAC, was chosen for the prototyping development and the series production. They built, at first, two copper models to test fabrication, assembly sequence and frequency tuning procedure then, two bulk Niobium prototypes (see photograph in Fig. 1). Final frequency of both cavities was well within 10 kHz of goal, demonstrating a good reproducibility of the fabrication.

Buffered Chemical Polishing (BCP) and High Pressure Water Rinsing (HPWR) were done in-house, at Triumf. Both resonators exceeded the ISAC-II specifications (Fig. 1) [4].

The 6 first cavities should be delivered at the end of October 2008.

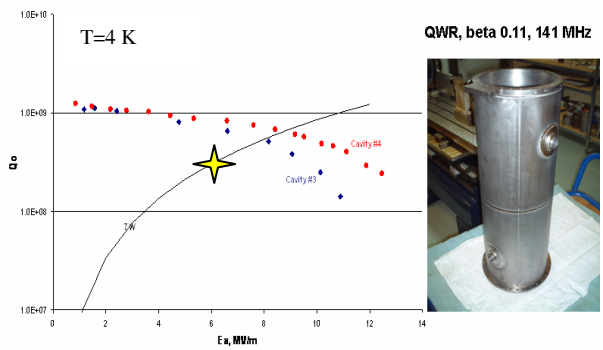

Figure 1: Vertical cold test results of the two first QWR prototypes. Yellow star: ISAC-II, phase 2 specifications.

ANL/ATLAS

This upgrade calls for a total voltage boost between 12 and 14 MV (depending on ion species) thanks to the replacement of an "old" cryomodule by a new one. It will house seven 109 MHz, beta 0.14, QWRs made of bulk Niobium [5]. Cavities have been already qualified in vertical cold tests, giving a 25% higher average accelerating gradient than the design goal (Fig. 2). Details about the cavities' fabrication and preparation can be found in [6].

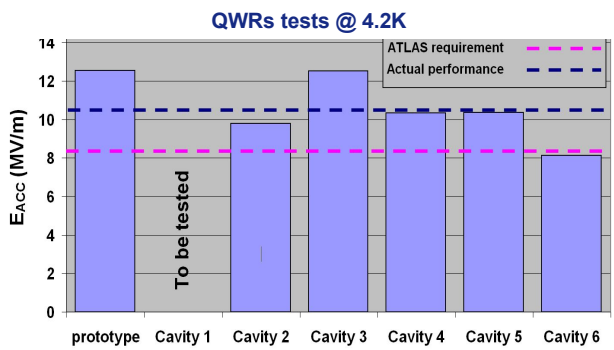

Figure 2: Vertical cold test results of the QWRs composing the new cryomodule for the ATLAS upgrade.

The cryomodule is currently under assembly in the ANL clean room. Its completion is foreseen by the end of 2008 and then, it shall be moved into the ATLAS tunnel.

#olry@ipno.in2p3.fr

DEVELOPING FACILITIES FOR SNS CRYOMODULE PERFORMANCE IMPROVEMENTS*

J. Mammosser,# SNS/ORNL, Oak Ridge, TN, U.S.A.

Abstract

Superconducting RF cavity facilities are currently being developed at SNS, aimed at addressing the limitations and availability of installed cavities and the direct support of the future power upgrade plans. Current efforts are directed towards development of in-situ repairs and developing processing techniques to increase available linac gradients. Procedures have been developed and implemented and the results will be presented for the repair of four cryomodules in the last year. Cryomodule testing facilities are being developed to further understand the collective limitations of installed cavities and spare cryomodule production is underway to develop and fabricate two high beta and one medium beta cryomodules. The direction and status of SRF facilities will be presented.

SUPERCONDUCTING CRYOMODULE FACILITIES AT SNS

During the construction of the SNS accelerator, 11 medium beta (0.61) and 12 high beta (0.81) cryomodules were fabricated at Thomas Jefferson National Accelerator Facility, shipped to SNS and installed in the linac section of the accelerator. At this time there was no urgent need for SRF facilities with the exception of some clean work areas, portable cleanrooms, and limited utilities which were used for the installation effort. During this time the RF Test facility was installed but was not functional and the main focus was on commissioning and developing cryomodule operational experience as quickly as possible. Once the Superconducting Linac (SCL) was commissioned and operating, several limitations to cavity operating performance became known and further understanding of the operational limits was needed. The main concern was unusual higher order mode (HOM) signals, excessive fundamental power coupling out HOM couplers and breakdowns in cavities due to field emission and multipacting. Individual cavities operate to high gradients but must be turned down due to collective effects from electron heating [1]. Significant effort was spent understanding these problems and this knowledge was critical to setting optimal operating parameters. Today the SCL is one of the most stable operating systems in the accelerator [2].

Table 1: SRF Facilities at SNS

SRF Facility	Classification	Details
Cleanroom		
Small part cleaning/degreasing	ISO 7 (M 5.5)	58m^2
Cleanroom- String assembly	ISO 5 (M 3.5)	58m^2
Cleanroom – Cavity assembly	ISO 4 (M 2.5)	2.5m^2
Cryomodule Test Facility		
Horizontal Test Facility		
	Space	11m x 4m
	Cryogenic Connections	Supply transfer line
		Shield transfer line
		**Return transfer line
	**Test Facility Refrigerator	200W 2K
		200W Shield
***Vertical Test Facility**		Standard dewar/pit design
	Dewar	Depth -3.35m
		Diameter – 71.1cm
	Cryogenic source	Separate helium refrigerator
***DI water Plant**	E-1	2268 liter storage, 38 liter makeup
***High Pressure Rinse Station**		Cavity remains stationary
	Wand	Rotates and translates
	Nozzles	Water Fanjets
		2 opposed
		Nitrogen gas Fanjets 2 opposed
	Pump	LEWA Teflon diaphragm -15 lpm

Today there is the need to expand the SCL facilities to support linac maintenance on cryomodules, qualify subcomponents for repairs and for the development of spare cryomodules. Spare cryomodules will allow for the

*SNS is managed by UT-Battelle, LLC, under contract DE-AC05-00OR22725 for the U.S. Department of Energy.
#mammosserj@ornl.gov.

AN OVERVIEW OF LINAC ION SOURCES*

R. Keller,# LANL, Los Alamos, NM 87545, U.S.A.

Abstract

This paper discusses ion sources used in high-duty-factor proton and H^- Linacs as well as in accelerators utilizing multi-charged heavy ions, mostly for nuclear physics applications. The included types are Electron Cyclotron Resonance (ECR) sources as well as filament and rf driven multicusp sources. The paper does not strive to attain encyclopedic character but rather to highlight major lines of development, peak performance parameters and type-specific limitations and problems of these sources. The main technical aspects being discussed are particle feed, plasma generation and ion production by discharges, and plasma confinement.

INTRODUCTION

For the purpose of this presentation, the term Linac is narrowed down to include rf structures that accelerate ion beams with duty factors between about 5% and continuous operation. This group of Linacs includes high-current proton and H^- machines as well as accelerators utilizing low- or moderate-current beams of multi-charged heavy ions, mostly for nuclear physics applications. Main types of ion sources serving these Linacs include Electron Cyclotron Resonance (ECR) sources, filament and rf driven multi-cusp sources, Penning (PIG) sources, duoplasmatrons and duopigatrons. However, the latter three source types have been in use for more than 50 years by now with more or less stagnant operational features, and for that reason they will not be discussed in the following even though they continue to produce beams for a number of Linac facilities.

This overview does not at all strive to attain encyclopedic character in terms of source varieties and performance results but rather to highlight the dominant design features, evolving performance parameters, major lines of development and general, as well as type-specific, limitations and problems. The main technical aspects being discussed are particle feeding methods, plasma generation and ion production by discharges, and plasma confinement.

PARTICLE FEEDING METHODS

The simplest way of feeding particles into an ion source consists of letting gas flow into the discharge vessel, but sometimes a user needs to limit the overall gas flow into the subsequent Low-Energy Beam Transport (LEBT) structure of an injector and is forced to use a fast-pulsed valve, typically piezo-electrical driven [1].

The use of gaseous or liquid compounds with high-enough vapor pressure is the next best choice, with one note of caution: many of these substances contain a chemically aggressive component, and in the discharge plasma the reaction rates are typically much faster than at normal atmosphere. Erosion of source body and extraction electrodes and a significant increase of the sparking rate in the extraction system are typical consequences. A survey on this subject is given in Ref. 2; it is certainly a very good starting point to obtain information on specific feeding techniques and substance properties.

Many substances have sufficient vapor pressure at elevated temperatures to be fed into an ion source, but this option comes with its own design constraints: Once vapor of the desired pressure has been produced it should not be lost to condensation on any surface part of the conduit to the discharge vessel or that vessel itself. In other words, the oven where the solid feeding material is heated should be the coldest part of all internal ion source components. This condition suggests the installation of hot liners in the discharge vessel or even the use of dual heating elements for oven proper and conduit. A design example where the conduit is heated by the cathode filaments is given in Fig. 1. In many cases, the ion production will be much more stable when small amounts of an auxiliary gas such as argon are added into the discharge vessel.

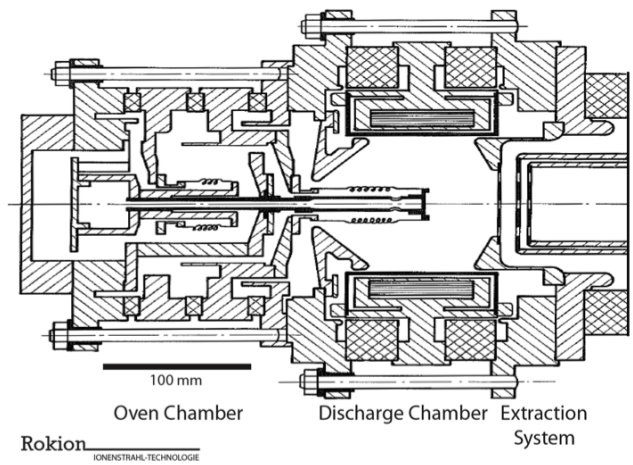

Figure 1. Hot-running multicusp ion source CHORDIS with oven and 18 cusp magnets [3]. Heat shields around the oven filaments are left out for the sake of clarity.

High-melting elements that cannot conveniently be fed into a source as part of a volatile compound can be released using the sputtering technique, adding an auxiliary gas such as argon. A dedicated sputter electrode may be inserted into the discharge vessel at a convenient location, or an existing electrode can be biased positively [3]. As with oven-equipped sources, use of sputtering benefits from the installation of hot-running liners or thinned-out electrodes to avoid re-condensation of the sputtered particles. Shares of the desired ion species typically do not exceed 10-20% of the entire extracted beam current.

Work supported by the US Department of Energy under Contract Number DE-AC52-06NA25396
#roderich@lanl.gov

CHARGE STATE BOOSTERS FOR RADIOACTIVE ION ACCELERATION

F. Ames, TRIUMF, 4004 Wesbrook Mall, Vancouver, BC V6T 2A3, Canada

Abstract

For the post acceleration of radioactive ions produced at ISOL facilities the increase of the charge state is essential to fulfill the A/q requirements of the accelerators. Many of those existing or proposed facilities are relying on the performance of charge state boosters of EBIS or ECRIS type. Although, in principle both types of sources can be used in pulsed or continuous mode operation an EBIS is better suited for pulsed beams whereas an ECRIS is most efficient in a continuous mode. The first charge state booster of the EBIS type had been installed at CERN/ ISOLDE and is working in a routine way since several years. It has been constantly optimized and reaches efficiencies in the order of 10% for a single charge state. More recently ECRIS type devices with similar efficiencies for noble gas ions are being set up and put into on line operation at KEK and TRIUMF. The paper will discuss the present state of the art with respect to existing data of both sources and potential future developments.

INTRODUCTION

At an ISOL type facility radioactive species are produced by the impact of an energetic beam of protons, heavy ions, electrons or photons on a solid or liquid target. The target is operated at high temperature to allow the products to diffuse out and into an ion source where an ion beam can be extracted. As those conditions, high radiation fields, high outgassing rates, are not very favorable for the operation of sophisticated ion sources normally only singly charged ions are produced. The isotope of interest can be selected by its mass and transported directly to the experiment or to an accelerator to boost its energy. In the later case increasing the charge state of the ions is essential. Transferring singly charged ions into highly charged ones can be achieved via collisions with electrons with total interaction energy higher than the ionization energy for the desired ionization state.

The simplest method to achieve this is accelerating the singly charged ions to a velocity higher than 100 keV/u and directing them through a thin stripper foil. For light ions this can lead to very high efficiency of about 25% in the maximum of the charge state distribution. As this distribution broadens for heavier elements and the cross sections for high charge states decrease the efficiency decreases. Furthermore, at those energies only low or moderate charge states can be reached and a second or third stripping at higher energy will become necessary, thus, reducing the total efficiency even more. Stripping is used at the ISAC I facility after a first acceleration to 150 keV/u. This is achieved with an RFQ accelerator capable of handling ions with a mass to charge ratio of A/q < 30.

So far all other facilities are using or are proposing an active system, where the charge state is increased before acceleration. The ions are injected into an ion source for highly charged ions where they interact with high energy electrons and their charge state is increased before they are extracted again. Two sources are being used for this: an electron beam ion source (or trap) EBIS/T and an electron cyclotron resonance ion source ECRIS. The charge state evolution in both systems can be described by a system of rate equations

$$\frac{dn_i}{dt} = n_e v_e \left[\sigma^{ion}_{i-1\to i} n_{i-1} - \left(\sigma^{ion}_{i\to i+1} + \sigma^{RR}_{i\to i-1}\right) n_i + \sigma^{RR}_{i+1\to i}\right] - n_0 v_i \left[\sigma^{chex}_{i\to i-1} n_i - \sigma^{chex}_{i+1\to i} n_{i+1}\right] - f_i^{coll} \frac{exp\left\{-\frac{ieU_w}{kT_{ion}}\right\}}{-\frac{ieU_w}{kT_{ion}}} n_i$$

with n_i, n_e, n_0 being the density of ions with charge q=i, electron and neutrals, v_i and v_e the velocity of ions and electrons, σ^{ion}, σ^{RR}, σ^{chex}, the cross sections for ionization, radiative recombination and charge exchange, f_i^{coll} the coulomb collision frequency, T_{ion} the ion temperature and U_w the trapping potential. Only charge changes by +/- 1 are considered here. Especially at high electron energies or high charge states this may not be true, but there is only very little knowledge of charge changing cross sections in those cases. In principal the charge state distribution after a limited confinement time or in the equilibrium state can be calculated. As the cross section for ionization strongly depends on the electron energy the electron energy distribution function has to be known.

Charge breeding with both sources will be described in more detail in the following sections.

EBIS

In an EBIS a high intensity electron beam with an energy up to several 10 keV is compressed within a strong magnetic field of usually several T in order to reach current densities of several hundred A/cm^2 or in some modern EBIT devices several 10 kA/cm^2. Ions injected can be confined radially inside the space charge potential of this beam and longitudinally by a superimposed electrostatic potential. They will be ionized to high charge states via collisions with the high energy electrons. The difference between EBIS and EBIT is mainly the length of the trapping region, which is much shorter in case of an EBIT allowing for a higher compression of the electron beam.

HEAVY ION LINAC BOOSTER AT IUAC, NEW DELHI

Amit Roy

Inter-University Accelerator Centre, Aruna Asaf Ali Marg, New Delhi – 110067, India

Abstract

The first module of the booster superconducting linear accelerator that will have a total of three modules, each having 8 quarter wave coaxial line bulk Nb resonators, has been commissioned at IUAC. During initial operation of the first linac module, energy gain was found to be much lower due to various problems which are now identified and solved. After acceleration through the linac module and subsequent re-bunching using superconducting Rebuncher, 158 MeV Silicon beam having pulse width of 400 ps was delivered to conduct nuclear physics experiments. The other two linac cryostats and the required 16 resonators to be installed in those two cryostats are in the final stage of fabrication. Work has also progressed on a high current injector that would act as an alternate source of heavy ions for the super conducting Linac.

INTRODUCTION

Currently the programmes for addition of superconducting linac boosters for increasing the energy of heavy ions from the Pelletron accelerator at Inter-University Accelerator Centre (IUAC), New Delhi is nearing completion. The accelerating structures for the linac is a quarter wave cavity resonators (QWR) made of bulk Niobium operating at 97 MHz and optimised for β = 0.08 [1]. One module with eight cavities have been operated for beam acceleration and several problems faced with the drive coupler, slow tuner have been sorted out. A very novel method was found to reduce the microphonic noise in the cavity, which reduced the power required to amplitude and phase lock the cavities. Fields of the resonators obtained in the linac cryostat are in the range of 3 –5 MV/m at 6 watts of dissipated power at critically coupled condition of the power coupler. Fabrication of 15 more resonators for the next two modules is progressing according to schedule in the in-house resonator fabrication facility. In addition to the resonator production, several ANL built resonators have been repaired. It is also planned to design, develop and prototype a suitable low beta resonator around β = 0.045 for the high current injector.

IUAC has also agreed to build two β = 0.22, 325 MHz Single Spoke Resonators for the proton driver linac project of Fermi National Accelerator Lab (FNAL), USA. The resonators will be built at IUAC, and the final processing and testing will be carried out at FNAL.

QUARTER WAVE RESONATOR

The Quarter Wave resonator is a coaxial structure operating in the TEM mode with beam accelerating gaps in a direction perpendicular to the symmetry axis. The QWR incorporates a few distinctive features viz., a pneumatic slow-tuner in the form of a niobium bellow provides a tuning range of approximately 100 kHz, substantially larger than in any working quarter wave resonators; the Nb cavity being jacketed by a stainless steel shell joined to the Nb cavity through explosively bonded Nb-SS transition flanges. A picture of completed QWR along with the Nb slow tuner bellows is given in Fig. 1.

Figure 1: Indigenously built niobium quarter wave resonator with slow tuner bellows at IUAC.

The prototype QWR and twelve more resonators were fabricated in ANL and out of these, 8 resonators are used in the first linac module.

In order to fabricate the resonators in house, a Superconducting Resonator Fabrication Facility (SuRFF) has been set up and is fully functional. It consists of a 15 kW Electron Beam Welding machine, an automated Surface Preparation Laboratory for electro-polishing the cavities, a High Vacuum Furnace, and a dedicated test cryostat set-up.

Production of the superconducting niobium quarter wave resonators for the second and third linac modules has progressed sufficiently and nearing completion. There have been some problems faced in completing the (technically difficult) closure welds (the weld joining the top flange with the niobium housing as shown in Fig. 3) although several bare niobium resonators have been successfully welded and are ready for the stainless steel outer jacketing. After all the electropolishing was over, welding of the major sub-assemblies began for

BEAM COMPRESSION IN HEAVY-ION INDUCTION LINACS*

P.A. Seidl[1#], A. Anders[1], F.M. Bieniosek[1], J.J. Barnard[2], J. Calanog[1],3, A.X. Chen[1,3], R.H. Cohen[2], J.E. Coleman[1,3], M. Dorf[4], E.P. Gilson[4], D.P. Grote[2], J.Y. Jung[1], M. Leitner[1], S.M. Lidia[1], B.G. Logan[1], P. Ni[1], P.K. Roy[1], K. Van den Bogert[1], W.L. Waldron[1], D.R. Welch[5],
[1]Lawrence Berkeley National Laboratory, Berkeley, CA 94720, USA
[2]Lawrence Livermore National laboratory, Livermore, CA 94550, USA
[3]University of California, Berkeley, CA 94720, USA
[4]Princeton Plasma Physics Laboratory, Princeton, NJ 08543-0451, USA
[5]Voss Scientific, Albuquerque, NM 87108, USA

Abstract

The Heavy-Ion Fusion Sciences Virtual National Laboratory is pursuing an approach to target heating experiments in the Warm Dense Matter regime, using space-charge-dominated ion beams that are simultaneously longitudinally bunched and transversely focused. Longitudinal beam compression by large factors has been demonstrated in the LBNL Neutralized Drift Compression Experiment (NDCX) experiment with controlled ramps and forced neutralization. The achieved peak beam current and energy can be used in experiments to heat targets and create warm dense matter. Using an injected 30 mA K^+ ion beam with initial kinetic energy 0.3 MeV, axial compression leading to ≈50x current amplification and simultaneous radial focusing to beam radii of a few mm have led to encouraging energy deposition approaching the intensities required for eV-range target heating experiments. We discuss experiments that are under development to reach the necessary higher beam intensities and the associated beam diagnostics.

INTRODUCTION

To create a short (~ ns) pulse with duration suitable for the study of warm dense matter [1], our approach has been to modulate the energy of an initially much-longer non-relativistic beam. To achieve target temperatures around ~ 1 eV, the required beam intensity calls for space charge neutralization, which has been achieved with a background plasma through which the beam passes while it is focusing transversely and bunching longitudinally.

We are approaching the required beam intensities for heating targets toward warm dense matter conditions, and have arrived at this stage through a sequence of experiments over the past several years. The scaled final focusing experiment demonstrated the successful neutralization of an initially space-charge-dominated beam by a background source of electrons in order to achieve an emittance-limited focal spot [2]. The experiment was scaled from a design of a final focusing system for a heavy ion fusion driver using quadrupole magnets for beam transport (driver parameters: 10 GeV Bi^+ at 1.25 kA/beam). Following initial experiments with an emittance-limited 95 μA, 160 keV Cs^+ beam, the beam current was then increased to 400 μA with a perveance of 5 x 10^{-5}; space-charge limited near the focal plane for an un-neutralized beam. The spot radius with neutralization was ~2X smaller, in agreement with models assuming 80% and 0% neutralization, respectively. LSP simulations [3] showed good agreement with the experiments.

Next, the Neutralized Transport Experiment, used a higher current (~25 mA) and higher energy (250-350 keV) K^+ beam. The beam perveance (~10^{-3}) was effectively neutralized with RF and cathodic-arc plasma sources [4]. This demonstrated the feasibility of neutralization of higher perveance beams, a precursor to the additional feature of axial bunching of the ion beam.

The axial compression is achieved with an induction bunching module (IBM) inserted after the matching section. Operating at ±80 kV, a ±12.5% velocity ramp is imparted to 150-200 ns subset of the several-microsecond beam pulse. The beam then drifts through a neutralizing plasma in a drift compression section a few meters in length (L). To establish a neutralizing plasma along most of the length of the drift compression section, the RF plasma used in NTX was replaced with a ferro-electric plasma source [5], and cathodic arc plasma sources injected a high-density plasma near the focal plane where the beam density is greatest. Current amplification of ≈ 50 was demonstrated in the first NDCX experiments [6].

A fundamental limit to the current amplification and pulse duration is the longitudinal energy spread (longitudinal phase space and emittance) of the injected beam, as shown in Eq. 1:

$$t_{\min} = \frac{L}{v^2}\sqrt{\frac{2kT}{M}} \qquad (1)$$

where v is the average ion velocity, T is the effective longitudinal beam temperature and M is the ion mass.

The energy spread was measured with an electrostatic energy analyzer. The measured energy spread is adequate for achieving nanosecond-duration bunches (see below). Other limits are set by the uniformity and density of the background neutralizing plasma, and imperfections of the bunching module waveform. In general, simulations have shown that if the background plasma density is greater than the local beam density, then the effectiveness of the neutralization is independent of the details of the plasma density distribution [7]. For near-term warm dense matter experiments, the beam density increases steeply and

* This work supported by the U.S. Dept. of Energy contracts W-7405-ENG-48, DE-AC02-05CH11231 and DE-AC02-76CH-O3073.
#PASeidl@lbl.gov

STUDENT PRIZE WINNER TALK

TWISTED STRUCTURES AND THEIR APPLICATION AS ACCELERATING STRUCTURES

J. L. Wilson, ORNL, Oak Ridge, Tennessee

Abstract

Normally, reactive loading is employed to construct accelerating cavities in order to slow the phase velocity of the electromagnetic wave. However, due to their non-uniform cross section, they tend to be difficult to machine, requiring complicated welding or brazing processes which increase the total cost. Although empty straight waveguides can only support faster-than-light propagation, empty twisted waveguides can support propagation at or below c. Because twisted structures have a uniform cross section in the transverse plane, they offer several potential advantages over dielectric loaded structures or other types of periodic structures. Of particular interest are twisted structures whose longitudinal cross section has been selected to resemble well-known accelerating structures, such as the iris-loaded accelerating structure and the TESLA type elliptical cavity. Comparisons are drawn between these conventional cavities and their twisted counterparts. Specifically, the phase velocity and dispersion relationship are discussed, the accelerating mode is found and analyzed, and R/Q is calculated. Design guidelines for the design of twisted structures are given.

SEE THE SLIDES OF THIS TALK AND PAPER THP045

BEAM DYNAMICS STUDIES OF THE 8 GeV LINAC AT FNAL*

P.N. Ostroumov†, B. Mustapha, ANL, Argonne, IL 60439 USA
J.-P. Carneiro‡, FNAL, Batavia, IL 60510, U.S.A.

Abstract

The proposed 8-GeV proton driver (PD) linac at FNAL includes a front end up to ~420 MeV operating at 325 MHz and a high energy section at 1300 MHz. A normal conducting RFQ and short CH type resonators are being developed for the initial acceleration of the H-minus or proton beam up to 10 MeV. From 10 MeV to ~420 MeV, the voltage gain is provided by superconducting (SC) spoke-loaded cavities. In the high-energy section, the acceleration will be provided by the International Linear Collider (ILC)-style SC elliptical cell cavities. To employ existing, readily available klystrons, an RF power fan out from high-power klystrons to multiple cavities is being developed. The beam dynamics simulation code TRACK, available in both serial and parallel versions, has been updated to include all known H-minus stripping mechanisms to predict the exact location of beam losses. An iterative simulation procedure is being developed to interact with a transient beam loading model taking into account RF feedback and feedforward systems.

INTRODUCTION

Fermilab is developing the design for a high intensity proton driver 8 GeV superconducting (SC) H^- linac. The principal mission of this proton driver (PD) linac is to increase the intensity of the Fermilab Main Injector for the production of neutrino superbeams. There are many other possible applications such as fixed target programs or acceleration of other species (e-, p, μ, etc…) as discussed in ref. [1] and [2].

To make the overall project cost-effective, the general approach was to adopt designs from existing accelerator or proposals. In particular we propose [3]:

- To directly apply the International Linear Collider (ILC) RF system (cavities, cryomodules and klystrons) operating at 1.3 GHz to accelerate the beam from 1.2 GeV to 8 GeV.
- To use Squeezed ILC (S-ILC) cavities operating at 1.3 GHz and designed for β_G=0.81 to accelerate the beam from ~420 MeV to 1.2 GeV.
- To operate the whole linac with only 2 frequencies in order to simplify the RF system. The front-end of the linac provides acceleration up to ~420 MeV operating at 325 MHz, the 4th sub-harmonic of the ILC frequency.

The front-end of this linac, up to 60 MeV, is currently being built by the High Intensity Neutrino Source (HINS) R&D Program to demonstrate some of the novel design concepts [4]. In the paper we discuss the beam dynamics design of the PD linac.

LAYOUT OF THE FNAL PD LINAC

Based on the design published in 2006 [3], the proposed linac has the characteristics listed in Table 1. A schematic layout of the accelerator is shown in Fig. 1 together with the transport line to the Main Injector.

Table 1: Basic Parameters of the Linac

Parameters	Value
Particle type (baseline mission)	H^-
Beam kinetic energy	8 GeV
Beam current avg. over the pulse	25 mA
Beam current upstream of the chopper	43 mA
Pulse repetition rate	10 Hz
Pulse length	1 msec
Number of protons per pulse	$1.56 \cdot 10^{14}$
Beam pulsed power	200 MW
Beam average power	2 MW
Wall power (estimate)	12.5 MW
Total length	~678 m

Choice of Accelerating Structure

As depicted in Fig. 1, the H^- beam from the Ion Source is bunched and accelerated to 2.5 MeV by a Radio-Frequency Quadrupole (RFQ, [5]) operating at 325 MHz. At that energy, a Medium Energy Beam Transport (MEBT) provides the space for a fast beam chopper (<2 ns) that eliminates unwanted bunches and forms an optimal beam time structure for injection into the Main Injector. This chopping decreases the beam average current over the 1 msec pulse from ~45 mA to ~25 mA. Acceleration to ~100 MeV could be provided by Room temperature DTL cavities; however, a different approach was selected. Taking advantage of the development and excellent performance of SC Spoke cavities [6], it was decided to accelerate the beam from ~10 MeV to ~420 MeV using SC Single and Triple Spoke resonators (SSR and TSR). The Spoke resonators not only present the advantages of higher accelerating gradients and cost-effective operation but also allow one single klystron to power several cavities with the use of high-power ferrite vector modulators [7]. With this outstanding feature of the FNAL PD, only five J-PARC type 2.5 MW klystrons

* Work supported by the U.S. Department of Energy, under Contracts No. DE-AC-02-06CH11357 and DE-AC02-07CH11359.
† ostroumov@anl.gov
‡ carneiro@fnal.gov

TRANSPORT LIMITS IN PERIODIC FOCUSING CHANNELS

S. M. Lund, LLNL, Livermore, California

Abstract

It has been empirically observed in both experiments and particle-in-cell simulations that space-charge-dominated beams suffer strong growth in emittance and particle losses in alternating gradient quadrupole transport channels when the undepressed phase advance increases beyond about 85 degrees per lattice period. Although this criterion has been used extensively in practical designs of strong focusing intense beam transport lattices, the origin of the limit has not been understood. We propose a mechanism for the transport limit resulting from strongly chaotic classes of halo particle resonances near the core of the beam that allow near-edge particles to rapidly increase in oscillation amplitude when the space-charge intensity and the flutter of the matched beam envelope are both sufficiently large. A core particle model is applied to parametrically analyze this process and the results are compared with extensive particle simulations.

CONTRIBUTION NOT RECEIVED

TOWARDS A MODEL DRIVEN ACCELERATOR WITH PETASCALE COMPUTING*

B. Mustapha#, P.N. Ostroumov and J. Xu
Argonne National Laboratory, 9700 S. Cass Ave, IL 60439, U.S.A.

Abstract

Accelerator simulations still do not provide everything designers and operators need to deploy a new facility with confidence. This is mainly because of limitations preventing realistic end-to-end simulations of the beam from the source all the way through to a final interaction point and because of limitations in on-line monitoring that prevent a full characterization of the actual beam line. As a result, once a machine is built there can be a gap between the expected behavior of the machine and the actual behavior. This gap often corresponds to enormous work and significant delays in commissioning a new machine. To address the shortcomings of the existing beam dynamics simulation codes, and to fulfill the requirements of future hadron and heavy-ion machines, a starting point for a realistic simulation tool is being developed at ANL that will support detailed design evaluation and also fast turnaround simulations to support commissioning and operations. The proposed simulations will be performed on the fast growing computing facility at ANL with peta-scale capability.

MODEL DRIVEN ACCELERATOR: CONCEPT & MOTIVATIONS

Presently, no accelerator in the world could fully rely on a computer model for its operations. The main reason is a discontinuity between the design and operation phases. Many factors contribute to this discontinuity: 1- Simulations in the design phase assume almost perfect conditions and cannot reproduce the real machine, 2- Actual elements specification and performance are usually different from their original design and in most cases 3- Not enough diagnostic devices to characterize the machine. The lack of a realistic model to support the commissioning and operations results in significant delay in the deployment of a new machine and a lot of time spent on machine tuning during operations. This usually leads to low availability and high operating cost of the machine. For example, a complex project such as the proposed FRIB facility [1], where primary beams from proton to uranium up to 600 MeV/u are used to produce beams of rare isotopes all over the map, cannot afford not to have a computer model to support its operations.

We here propose to bridge the gap between the design and operation phases and develop a realistic model of the machine. Among the benefits of such a model is fast tuning for the desired beam conditions and fast retuning to restore the beam after a failure. This should significantly improve the availability of the machine and reduce its operating cost. The requirements for the development of such a model and the realization of the concept of the model driven accelerator are discussed in the next sections.

*This work was supported by the U.S. Department of Energy, Office of Nuclear Physics, under Contract No. DE-AC02-06CH11357.
mustapha@phy.anl.gov

REQUIREMENTS TO REALIZE THE MODEL DRIVEN ACCELERATOR

The main requirements for the realization of the model driven accelerator could be summarized in the development of a 3D beam dynamics code with the appropriate set of optimization tools and large scale computing capabilities. A multi-particle beam dynamics code is more realistic than matrix-based and single-particle codes because it supports 3D fields, includes fringe fields and appropriate space charge calculations. It also allows more detailed simulations necessary to study eventual beam loss and produce data similar to the measured data. Such a code should also include a large set of optimization tools. Optimization tools are needed not only for design optimization but also to tailor the computer model to the actual machine to be useful for real-time operations. Multi-particle optimizations usually involve tracking a large number of particles for large number of iterations which is very time consuming and requires large scale parallel computing. Therefore the beam dynamics code should have parallel computing capabilities.

The beam dynamics code TRACK [2] is being developed at Argonne to meet these requirements. TRACK and a selected set of applications will be presented in the next section.

A REALISTIC BEAM DYNAMICS CODE

The beam dynamics code TRACK is being developed over the last few years at the Physics Division of Argonne National Laboratory. Among the main features of TRACK are:

- A wide range of E-M elements with 3D fields
- End-to-end simulations from source to target
- Tracking multiple charge states heavy ion beams
- Interaction of heavy ion beams with strippers
- Automatic transverse and longitudinal beam tuning
- Error simulations: Static and dynamic errors
- Realistic transverse correction procedure
- Large number of particles for large number of seeds
- Beam loss analysis with exact location of the losses

And more recently:

- Possibility of fitting experimental data (profiles,…)
- H- Stripping: Black body, Residual gas and Lorentz

Nb-RRR SHEET INSPECTION BY MEANS OF ULTRASONIC MICROSCOPY

R. Grill, H. Traxler, L.S. Sigl, H. Kestler
PLANSEE SE, 6600 Reutte, Austria

Abstract

Nb-RRR sheet material is one of the key components of super-conducting linear particle accelerator projects (e.g. XFEL, ILC). The high quality requirements led to sophisticated quality systems in the manufacturing line. A major aspect is the development of non-destructive inspection methods for the detection of surface defects, delaminations, pores, inclusions and impurities. Up to now the standard inspection technologies for quality assurance of Nb-RRR sheet material are based on electromagnetic techniques, e.g. SQUID and eddy current. For these methods the detection limit is in the range of 0.1 mm.

Ultrasonic microscopy (USM) is a well established and economic technique for non-destructive surface inspection. For such applications strongly focused ultrasonic waves are applied. For volume inspection of sheet material the focal length of the ultrasonic transducer needs to be increased in order to enable constant defect resolution throughout the whole cross section of the material under inspection. For Nb-RRR sheets with typical thickness of 2.8 mm a detection limit of 0.1 mm is expected. First results of USM on Nb-RRR sheet material are presented.

INTRODUCTION

Sheet material made of ultra-high-purity Niobium (so called Nb-RRR grade) is the key component for future linear accelerators, based on the superconducting RF technology. One is the XFEL (X-ray Free Electron Laser) whose construction started in 2007 at the German Electron Synchrotron in Hamburg. Based on the same technology is the ILC (International Linear Collider) which is currently in the design phase and will be the next major accelerator project in particle physics after XFEL realization.

Since 2004 Plansee SE (A) worked on the qualification as material supplier for the XFEL project. In co-operation with W. C. Heraeus (DE), which covers the raw material competence, Plansee SE established the industrial production of products made of Nb-RRR in various geometries and sizes. In December 2007 the qualification procedure at DESY could be successfully finished and Plansee SE was qualified as supplier for Nb-RRR 300 sheet material.

To be prepared for large production scale quantities for the XFEL project, activities for the installation of a Quality Assurance (QA) management system are ongoing. A major quality criterion for Nb-RRR sheets is the surface quality. For inspection of surface quality visual inspection and eddy current testing (ET) are established for pre-series production and future project realization as baseline. Both methods are commonly used for detection of defects and inclusions at the surface. For volumetric inspection SQUID (Superconducting Quantum Interference Device) was investigated during the last years and activities for establishment of a test standard are in work [1-4].

With ultrasonic microscopy (USM) an equivalent test procedure is available which allows a standardized surface inspection on industrial scale. For USM an automized visualization of surface defects and establishment of standardized test records is possible [5]. With adaptation of test setup the possibility of volumetric testing was assessed and first results will be presented.

ULTRASONIC MICROSCOPY

Ultrasonic microscopy (USM) is established for the inspection of thin films in various industrial applications, e.g. electronics [6]. USM uses ultrasonic frequencies from 50 MHz to 2 GHz which is much higher compared to conventional ultrasonic NDT operating frequencies using about 1 to 20 MHz. This leads to enhanced defect resolution since the wavelength is reduced to the µm regime. An additional feature is the strong focussing of the ultrasonic wave which leads to lateral resolution in the magnitude of microns in the focused plane. For high resolution inspection in the volume the focus of the transducer is moved below the surface [7]. For inspection of the whole sample volume several scans need to be performed.

For the application described a device of the type Krämer Scientific Instruments, Vario III B is used. The inspection is performed in water immersion applying the pulse echo technique. A scanning mechanism moves the transducer and enables the generation of a C scan image. A sketch of the setup is given in Fig. 1.

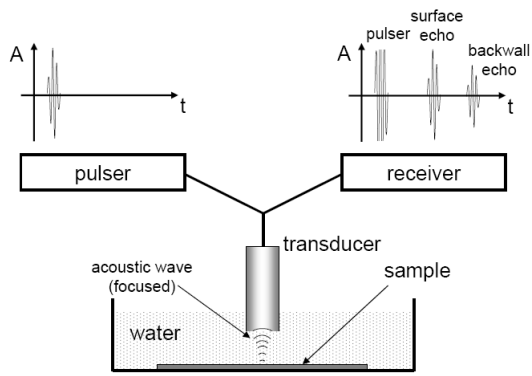

Figure 1: Sketch of the measurement chain of the USM.

THE 1.3 GHz SUPERCONDUCTING RF PROGRAM AT TRIUMF

R.E. Laxdal, K. Fong, A. Grassellino, A.K. Mitra, I. Sekachev, V. Zvyagintsev,
TRIUMF*, Vancouver, BC, Canada,
R.S. Orr, W. Trischuk, U. of Toronto, Toronto, Ont., Canada

Abstract

TRIUMF is proposing to build a 50 MeV electron Linac as a driver to produce radioactive ion beams through photofission. The present design calls for the use of nine-cell 1.3 GHz Tesla type cavities. A 1.3 GHz Superconducting RF (SRF) program has been initiated with the goal to produce and test one nine cell cavity by the end of 2009. The program will use the existing clean room and SRF test facilities that support the ISAC-II heavy ion superconducting Linac. A vertical cryostat has been modified with a new insert to allow single cell testing. A single cell fabrication program is being initiated with a Vancouver company. A RRR measurement program is on-going to test cavity welds. The goal of the 1.3 GHz upgrade is to produce cavities for the 'in house' project as well as broaden TRIUMF's technical base for future potential collaborations.

INTRODUCTION

Existing Program at 100 MHz

A cavity testing program was initiated at TRIUMF in 2002 in support of the construction of a superconducting heavy ion Linac.[1] A test cryostat was used for single cavity characterizations, LLRF controls and RF ancillary development. Since then over 40 vertical cold tests have been completed to characterize a production series of twenty 106 MHz quarter wave bulk niobium cavities. In addition five full cryomodules have been assembled and ten cryomodule cold tests have been completed prior to installation of the modules in the Linac vault. TRIUMF has built a core competency in 100 MHz SRF technology while producing the ISAC-II heavy ion Linac. Due to the incorporation of modern processing techniques and clean room assembly, largely developed in the $\beta = 1$ community, the accelerating gradients achieved in the TRIUMF Linac are significantly higher than those found at other existing heavy ion machines. Presently a new series of cavities at 141 MHz is in production at PAVAC Industries of Richmond BC after a successful prototyping of two cavities.[2] Twenty cavities will be assembled in cryomodules for installation by the end of 2009.[3]

e-Linac Project

The aim of the ISAC-III (ARIEL) proposal[4] is to generate additional radioactive ion beams (RIBs) on target to produce more physics. Presently a 500 MeV proton beam from the cyclotron at 100μA produces radioactive isotopes through fission and spallation from a thick target. It is proposed to increase the RIBs available by adding an independent and complimentary driver: a high-power 50 MeV electron Linac.[5] The electron linac would operate at 1.3 GHz and use, where possible, existing ILC technology to reduce development time.

EXISTING FACILITIES

The existing ISAC SRF facilities consist of the following areas as shown in Fig. 1:

- Preparation area: A staging area for receiving parts intended for use or assembly in the clean room. The room contains two large tanks one for ultrasound cleaning and one for rinsing. These tanks are used for cleaning of parts before sending to the assembly area.

- Clean room: This is divided up into sections depending on the level of particulate control required. The eastern area including the HPWR and assembly areas are cleanest (Class III). The cavity test area with an overhead crane has the next level of particulate control and protocol (Class II) and the RF measurement area is the third isolated area with a third protocol (Class I). The clean rooms are not commercial installations but home-made with large HEPA filter installations in the ceiling and return air ducts near the floor located around the room. Air pressure control is maintained to force HEPA filtered air to flow from the cleanest areas to the less clean areas. Particle counts are typically below 100 in Class III and below 1000 in Class II.

  - HPWR Rinse Area: Houses a fume hood for light chemical cleaning and a horizontal rinse stand to allow semi-automatic rinsing of quarter wave cavities. Filtered 18 MOhm water is delivered at high pressure as the cavities are rotated.
  - Assembly Area: Single cavities and whole cryomodules are assembled in clean conditions in preparation for cold tests.
  - RF measurement area: Houses the LLRF control racks and RF measurement equipment for cavity characterizations during vertical tests.
  - Cavity Test Area: Equipped with a test pit for x-ray shielding during RF tests. It is sufficient to contain both the single cavity test cryostat and the medium beta cryomodule, with dimensions 4m long x 2 m wide x 2.5m deep. An overhead crane is available for lifting the cold mass into

* TRIUMF receives funding via a contribution agreement through the National Research Council of Canada

PRODUCTION AND TESTING OF TWO 141 MHz PROTOTYPE QUARTER WAVE CAVITIES FOR ISAC-II

R.E. Laxdal, R.J. Dawson, K. Fong, A. Grassellino, M. Marchetto, A. K. Mitra, T. Ries, V. Zvyagintsev, TRIUMF*, Vancouver, BC, Canada,
R. Edinger, PAVAC Industries, Inc., Richmond, BC, Canada

Abstract

The medium beta section of the ISAC-II superconducting linac (β=5.7% and 7.1%) has been operational since April 2006 providing 20 MV of accelerating potential at 106 MHz. The 'high beta' extension to the linac, in progress, will see the addition of twenty 141 MHz quarter wave cavities at $\beta = 11\%$. The design specification calls for cw operation at a voltage gain of at least 1.1 MV/cavity for no more than 7 W of power dissipated in the cavity. This operation point corresponds to challenging peak surface fields of 30 MV/m and 60 mT. The cavity design is similar in concept to the medium beta cavities except for the addition of a drift tube to render symmetric the accelerating fields. A prototyping and qualification program was initiated with PAVAC Industries Inc. of Richmond, B.C. Two full size models in copper and two in niobium have been completed. The cold performance of both cavities exceeds the specification and the final frequency is within tuning range. The design, fabrication details and test results will be presented.

INTRODUCTION

The high beta section will double the voltage gain of the ISAC-II superconducting accelerator by means of an additional twenty cavities[1]. These cavities will be housed in three cryomodules with common isolation and cavity vacuum. Two cryomodules will contain six cavities and the last one will contain eight cavities. The plan is to install the completed and tested cryomodules during an extended shutdown of ISAC-II starting in September 2009. The medium beta section is in operation since April 2006 and is reliably operating at an average acceleration gradient of 7 MV/m at 7 W cavity power, corresponding to peak electric and magnetic fields of 35 MV/m and 70 mT[2] and represent the highest values for an operating cw heavy ion linac. The medium beta design was accepted as a basis for the design of the high beta section.

CAVITY DESIGN

The design of the new ISAC-II superconducting high beta cavity is presented in Fig. 1 and it is similar in structure to the medium beta 106 MHz cavities design[3]. The operational frequency is 141.44 MHz and $\beta_0 = 0.11$. It is a bulk niobium double wall structure ~25% shorter than the medium beta cavity. The main difference is the donut shaped inner drift tube to provide higher geometric β and transit time factor (TTF), and improved field symmetry. The acceleration gap is reduced from 40 to 35 mm and the grounded beam ports diameter is also reduced from 60 to 50 mm to achieve a 115 mm gap to gap distance with the 180/60 mm coaxial arrangement. The position of RF ports was optimized for coupler operation. A mechanical dissipator is inserted inside of the inner conductor of the cavity to dampen vibrations. The bottom plate of the cavity is modulated and slotted to provide a deformation of at least 3 mm for cavity tuning.

Figure 1: ISAC-II high beta cavity design.

CST 2008 Microwave Studio model and cavity parameters are shown in Fig.2. Virtual volumes in the model were used in the simulation to avoid errors from meshing. The models include a virtual cylinder around the beam tube donut and a virtual coaxial in the high magnetic field stem region. The peak electric field, E_p, is calculated from a donut geometry parameterization. B_p is calculated assuming a cosine longitudinal, hyperbolic radial magnetic field distribution in the virtual coaxial and the value of magnetic field stored in this volume. Frequency sensitivity for beam ports and top and bottom flange displacements are calculated from surface densities of electric and magnetic fields by using the Slater theorem. The acceleration gradient definition is $E_a = V_a/D$ where V_a is an acceleration voltage gain of the cavity at optimum velocity β_0 (including a transit time factor TTF_0), D is a conventional cavity length chosen as the cavity outer conductor diameter. The design goal is $E_a = 6$ MV/m and corresponds to $V_a = 1.08$ MV. The steering effect due to the electric and magnetic transverse rf fields can be largely compen-

* TRIUMF receives funding via a contribution agreement through the National Research Council of Canada

PERFORMANCE OF THE ISAC-II 141 MHZ SOLID STATE AMPLIFIER

Amiya Kumar Mitra, Iouri Bylinskii, Ken Fong, Robert Edward Laxdal, Joseph Lu,
Richard Shanks, Vladimir Zvyagintsev, TRIUMF, Vancouver, Canada

Abstract

The ISAC-II linac extension requires an additional 20 rf amplifiers to power twenty 141 MHz quarter wave superconducting cavities. Solid state amplifiers will be used for this extension as compared to tube amplifiers which have been employed for the existing ISAC-II linac section, operational since 2006. These solid state amplifiers are rated to an output power of 600 W. A prototype amplifier of the production series has been tested for gain and phase linearity. Phase noise of this amplifier has been measured on a 141 MHz superconducting cavity and compared with phase noise measured with a tube amplifier. The test results and general rf interlock and interface requirements are verified against tendered specification before series production of the remaining amplifiers can proceed. Benchmarking tests of the prototype amplifier will be reported.

INTRODUCTION

An upgrade of the ISAC-II superconducting linac, operational since April 2006, is in progress. Additional 20 MV accelerating potential will be added to the ISAC Radioactive Ion Beam (RIB) facility by the end of 2009 [1]. The new installation consists of twenty 141 MHz quarter wave cavities at a design beta of 11%. The cavities will be housed in three cryomodules with six cavities in the first two cryomodules and eight cavities in the last. These additional 20 cavities will be powered by 20 solid state amplifiers which have been purchased from QEI Corporation, NJ, USA. The first amplifier of the production series is tested rigorously before production of final amplifiers can proceed. The medium beta linac which employs 20 quarter wave cavities operating at 106 MHz uses 20 triode tube amplifiers to power the cavities [2,3]. The limited tube life and marginal phase noise led to the option of using solid state amplifiers. Also, the tube amplifiers were rated for 1 kW however, only 600 watts was used for conditioning the cavities and around 200 watts was used for regular beam operation. The solid state amplifiers were therefore specified for maximum 600 watts output along with gain and phase linearity and phase noise requirements.

GAIN AND PHASE MEASUREMENT

The amplifier output is terminated into a 50 ohms dummy load in order to measure the gain and phase characteristics and other basic functions. Figure 1 shows the gain and the phase characteristics which satisfy the specification outlined in table 1. Amplifier gain is measured to be 65 ± 0.75 dB (specified 55 ± 2 dB). Higher gain is acceptable since it can be lowered by addition of external 10 dB attenuator. The 1dB bandwidth is 8 MHz which is much higher than the specified 1 MHz bandwidth.

Table 1: Gain and Phase Linearity Requirement

Parameter	value
Gain Linearity from 1 to 250 Watts	< ± 0.5 dB
Gain Linearity from 250 to 600 Watts	< ± 2.0 dB
Phase Linearity from 1 to 250 Watts	< ± 5°
Phase Linearity from 250 to 600 Watts	< ± 20°
Phase noise in 2 – 200 Hz range	< 0.3° rms.

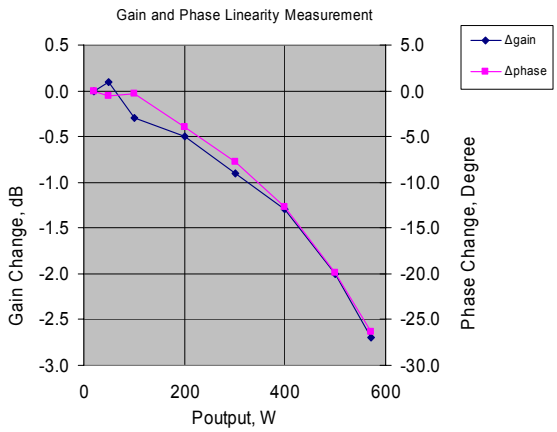

Figure 1: Gain and phase linearity measurement

PROTECTION AND INTERFACE

The amplifiers are housed in the power supply room which is above the linac vault. These amplifiers are remotely operated from the control room via EPICS interface. These amplifiers are also interlocked with TRIUMF safety system which enables operation of the amplifiers when all safety requirements to operate the linac are satisfied. Table 2 outlines the alarm indications that are displayed on the front panel of the amplifier and are also sent to EPICS interface. Amplifier status and some of the rf parameters are also read by the EPICS system and are available at the EPICS page of the ISAC control system. This will help to debug the problems in the event of amplifier fault. This interface is similar to the existing 106 MHz amplifier. As an added new feature, these solid state amplifiers are protected for input over drive up to 10 dBm for a short period of time. If the maximum input power is exceeded a threshold

TESTS OF WIRE SUBLIMATIONS VERY CLOSE TO SPIRAL 2 SUPERCONDUCTING CAVITY

R. Ferdinand, J-L. Vignet, P. Robillard, E. Gueroult, GANIL, Caen, France
P. Ausset, H. Saugnac, G. Olry, D. Longuevergne, P. Szott, CNRS/IN2P3, IPN-Orsay, France.

Abstract

The construction of the new Spiral 2 facility has started in Caen (France) at the National Heavy Ions Accelerator Center (GANIL). The SPIRAL 2 project is based on a multi-beam Superconducting Linac Driver delivering 5 mA deuterons up to 40 MeV and 1 mA heavy ions up to 14.5 MeV/u delivering different Radioactive Isotope Beams (RIB). The LINAC is composed of 2 cryomodule families. The low energy family (cryomodules A) is composed of 12 cryomodules housing a single superconducting cavity at beta=0.07. The "high" energy family (cryomodules B) is composed of 7 cryomodules housing 2 cavities at beta=0.12. In between cryomodules are located the focalisation quadrupoles and the diagnostic boxes. Their multiplication may lead to cavity pollution. Strong believes forbid the use of interceptives diagnostics around superconducting cavities. We simulated the use of wires for diagnostics in the linac, sublimating 14 wires of tungsten, niobium and carbon while operating the cavity B at full performances. The results describe in this paper looks promising.

DESCRIPTION

The objective for SPIRAL2 is to produce light ions (deutons, protons) up to 5 mA and a large diversity of heavy ions with intensities up to 1mA, including noble gases like Ar^{12+} and metallic ions like Cr, Ni and Ca. The Injector, dedicated to protons, deuterons and ions of q/A=1/3, is mainly composed of two ECR ion sources with their associated LEBT lines, a warm RFQ and the MEBT line connected to the LINAC.

The LINAC is based on superconducting independently-phased resonators [1,2]. It is composed of 2 families of quarter-wave resonators (QWR) at 88 MHz, developed respectively by the CEA/DAPNIA and the IN2P3/IPNO teams: 12 resonators with β=0.07 (1 cavity/cryomodule) [3], and 14 resonators at β=0.12 (2 cavities/cryomodule) [4] (see Figure 1). The transverse focusing is ensured by means of room temperature quadrupole doublets located between each cryomodule. Additional dipolar coils are installed into the quadrupoles in order to compensate the steering effect of QWR cavities and eventually adjust the optimum beam position. These 20 “warm” sections (Figure 2), as opposed to the superconducting cavities, include also beam diagnostic boxes with different sensors types. The specifications require 20 Beam Monitors, 10 TOF and 6 phase length measurement devices and 20 vacuum pumping systems.

The multiplication of warm sections in such superconducting accelerator may lead to pollution problems and degradation of cavities performances.

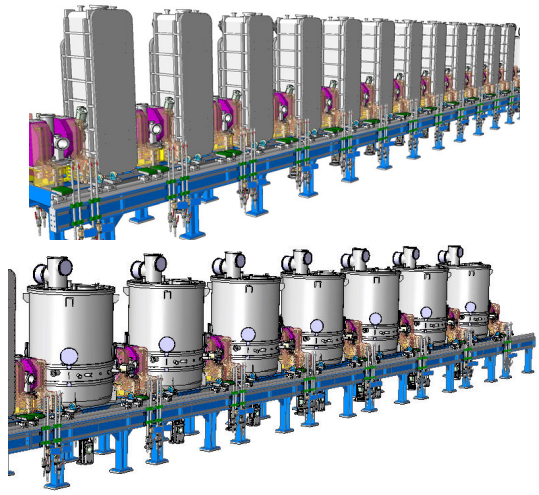

Figure 1: SPIRAL2 superconducting cryomodules (top: β=0.07, bottom: β=0.12).

One of the main beam diagnostic devices is the Beam Monitor (BM) which will measure more than the classical position of the centroid of the beam in the beam pipe of the accelerator. It plays a role of prime importance for the accelerator tuning and control. These capacitive sensors BM are located in the LINAC between the LINAC’s cryomodules and are mechanically integrated to the beam pipes into the quadrupole bore. The BMs give the classical beam positions, beam time of flight and possible phase information and current. Because of the non-cylindrical symmetry of the beam at this location, the signals return also information on quadratic moment related to the beam size. We expect CW operation as well as low duty factor pulsed mode operation. A ± 0.1mm resolution is foreseen and this criterion must be strongly taken in account for the mechanics and the electronics.

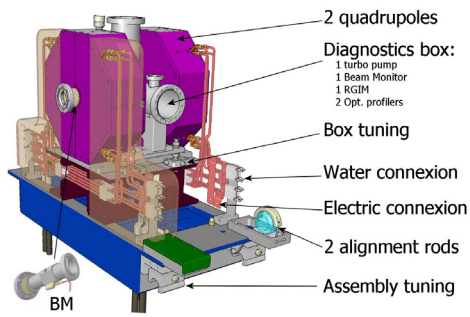

Figure 2 : Schematic of the “warm” section in between cryomodules.

The reference longitudinal diagnostics is the GANIL Residual Gas Ionization Monitor (RGIM) profiler [5] based on electron production resulting of the beam interaction with the residual gas (resolution 100 ps for a

704 MHz HIGH POWER COUPLER AND CAVITY DEVELOPMENT FOR HIGH POWER PULSED PROTON LINACS

J. –P. Charrier, S. Chel, M. Desmons, G. Devanz, Y. Gasser, A. Hamdi,
P. Hardy, J. Plouin, D. Roudier, CEA, IRFU, F-91191 Gif-sur-Yvette, France

Abstract

In the framework of the European CARE-HIPPI program we develop components for superconducting high pulsed power proton linacs at 704 MHz. We have designed, fabricated and tested a beta 0.47 5-cell elliptical cavity with an optimized stiffening to reduce its sensitivity to Lorentz forces. A fast piezo tuner has been developed in order to be able to operate the cavity in pulsed mode in our horizontal test cryostat CryHoLab. We also have carried out the development of a fundamental power coupler. It is designed to transmit a power up to 1 MW at a 10 % duty cycle. A high power test area has been setup consisting of a 1 MW klystron, a pulsed high voltage power supply and a coupler test stand.

INTRODUCTION

Elliptical superconducting (SC) cavities will be used in future high intensity proton linacs like SPL[1] for relative velocities β above 0.6. One goal of the CARE-HIPPI program is to build and test SC cavities for the lower energy section of pulsed proton accelerators. We have built and tested in vertical cryostat a 704 MHz 5-cell cavity optimised for pulsed operation at 2 K with a geometrical beta of 0.47, with a reduced sensitivity to Lorentz detuning [2]. The results of the vertical test are shown on figure 1. The measured static Lorentz coefficient K_L is -3.8 Hz/(MV/m)^2.

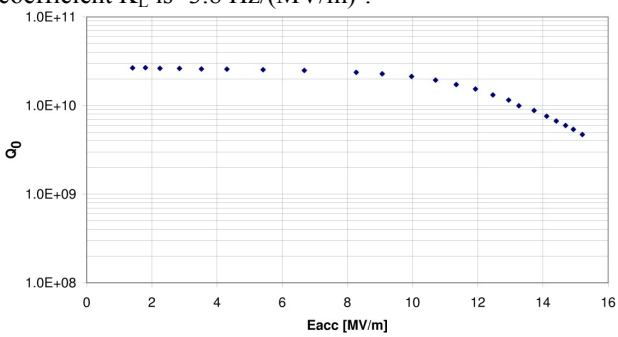

Figure 1: $Q_0(E_{acc})$ curve at 1.8 K.

The full test in pulsed mode in vertical cryostat requires developing of a fundamental power coupler (FPC) and setting up a pulsed power RF installation. Although the power needed for this type of cavity is limited to several hundreds of kW, the goal was to establish a 704 MHz test area enabling future developments demanding a higher power. In the higher energy section of SPL, a peak power of 1 MW must be transferred to the beam, this sets the target of our power coupler developments. The RF source has been commissioned reaching nominal parameters, 1 MW peak power, 2 ms RF pulse length at 50 Hz repetition rate [3]. The peak power can exceed 1.2 MW when the repetition rate is reduced. The circulator has been tested on a matched load at full power, filled with dry nitrogen. Tests have been performed in full reflection at all phases on a movable short, at nominal peak power and pulse length, but at the reduced repetition rate of 10 Hz. This limitation was due to a breakdown problem that occurred in the pulsed high voltage power supply which is being corrected.

Our horizontal test cryostat CryHoLab is being modified to accept the beta 0.47 cavity equipped with a FPC. The main changes are the larger FPC port, the LN2 copper thermal shield and the supporting systems for the cavities. Fig. 2 shows the new configuration with the cavity (mostly hidden by the magnetic shield) prepared for the low power measurements.

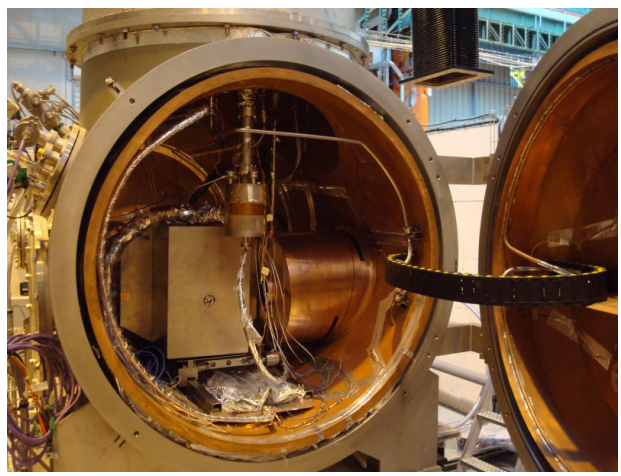

Figure 2: The new CryHoLab configuration.

PIEZO TUNER

We have developed a fast piezo tuner based on the Saclay-II tuner design [4] built and qualified on a 1.3 GHz 9-cell Tesla type cavity. The main difference is the size of the system, and the piezo support which consists of a stainless steel elastic frame holding a single 30 mm piezo stack. It is designed in order to apply an adjustable preload on the piezo, limiting the influence of the spring constant of the cavity. The slow tuning range is +/-2.5 MHz. The tuner is attached between the He tank and the beam tube flange opposite to the power coupler side. With our optimized design, the tuner does not increase the overall length of the cavity (fig. 3).

A NOVEL FREQUENCY TUNING SYSTEM BASED ON MOVABLE PLUNGER FOR SPIRAL2 HIGH-BETA SUPERCONDUCTING QUARTER-WAVE RESONATOR

D. Longuevergne, S. Blivet, G. Martinet, G. Olry, H. Saugnac,
CNRS/IN2P3, Institut de Physique Nucléaire, France

Abstract

SPIRAL2 aims at building a multi-purpose facility dedicated to nuclear physics studies, including the production of rich-neutrons isotopes. The multi-beam linear accelerator is composed of superconducting accelerating modules and warm focusing magnets. IPN Orsay is in charge of the high energy accelerating modules, each hosting two superconducting 88 MHz quarter-wave resonators operating at an accelerating field of 6.5 MV/m (β = 0.12). The static and dynamic frequency tuning is achieved by the insertion and displacement of a niobium plunger into the magnetic field area. The efficiency of the tuning (1 kHz/mm) has been validated during the tests of the cryomodule. In this paper we discuss the impact of such a tuning system, based on experimental results on SPIRAL2 cavities, on the different aspects: maximum accelerating field, Qo slopes, quench, multipacting and microphonics.

INTRODUCTION

The multi-purpose linear accelerator for SPIRAL2 has entered the construction phase since April 2006 [1]. Niobium quarter-wave resonators, composing the high energy part of the linac, have already been prototyped and qualified thanks to the construction of 2 cavities. These high-beta (β = 0.12) cavities resonating at 88 MHz, contrary to the low-beta ones (β = 0.07), are not tuned with a classical wall-deformation system due to the too low frequency shift versus the force applied [2]. The solution retained is the frequency tuning with a niobium movable plunger inserted into the magnetic field part of the cavity. This paper will present the full mechanism in the first part and then discuss the different results obtained with electromagnetic simulations and tests.

DESCRIPTION

The Plunger

The plunger, consists in a tube made of niobium (RRR = 250) with a length of 250 mm, a diameter between 30 and 20 mm (not yet defined) and a wall-thickness of 3 mm (see Fig. 1). It is totally filled with liquid helium when the cavity is operating. The plunger is maintained on the top cavity port through a stainless steel bellow stiffened by 3 guiding rods. A stainless steel bell, linking the rod coming from the motor and the plunger, closes the liquid helium circuit (See left Fig. 2). The bellows permit a total translation of about 5 mm. This kind of plunger achieves the static tuning as the plunger penetrates into the cavity of about 50 mm and the dynamic tuning thanks to its motion on a total range of about 4 mm.

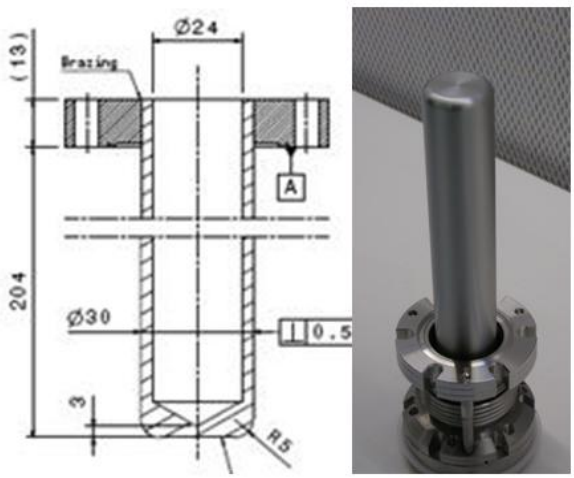

Figure 1: Picture and sketch of the plunger.

The Motion Controller

The plunger is controlled by a stepping motor, installed on the top of the cryomodule. The stepping motor controller and the gear box provide a total reduction of about 0.125 µm/step. The motion is transmitted to the plunger through a rod fixed on the closing bell (See right Fig. 2).

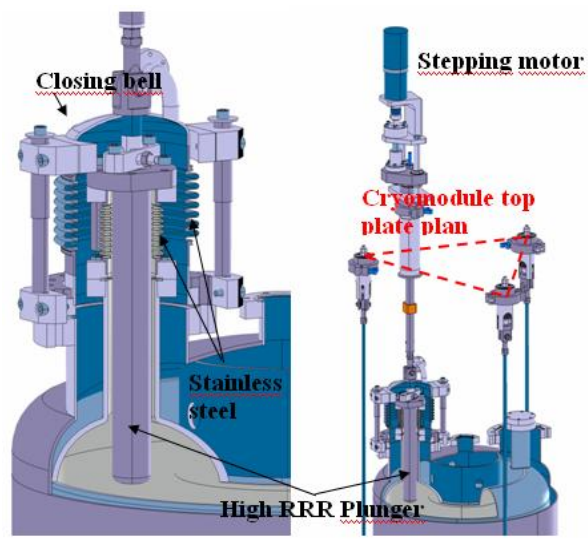

Figure 2: The system in its entirety.

RF AND CRYOGENIC TESTS OF THE FIRST BETA 0.12 SPIRAL2 CRYOMODULE

H. Saugnac, C. Commeaux, C. Joly, J. Lesrel, D. Longuevergne, F. Lutton, G. Martinet, G. Olry
IPNO, Orsay, France

Y. Gomez Martinez, F. Vezzu LPSC, Grenoble, France

R. Ferdinand, R. Beunard, M. Souli GANIL, Caen, France

Abstract

The SPIRAL 2 project, installed in GANIL for Radioactive Ion Beam physics purposes requires the manufacturing of a multi beam driver. This driver is based on a superconducting LINAC [1] featuring two 88 MHz Quarter Wave Resonator (QWR) families. IPN Orsay is in charge of the study and the assembly of the 7 high energy (beta = 0.12) cryomodules. Each cryomodule is composed of two QWRs, specified to operate at 4.2 K at a nominal accelerating gradient of 6.5 MV/m. A first "qualifying" cryomodule has been manufactured and tested at the beginning of 2008 in order to validate the resonator and the cryostat design before launching the serial production of the 6 remaining cryomodules. The paper presents the main results of this test and the cryomodule design in its final version.

INTRODUCTION

A first beta = 0.12 Cryomodule was manufactured [2] in order to qualify and validate the design of its different sub components: QWR resonator, Cold Tuning System (CTS), cryogenic circuits, power coupler, alignment procedure…. For this first test the cryomodule was not in its final configuration. Only one resonator was equipped with a power coupler and a cold tuning system and the cryomodule was not shielded against Earth's magnetic field. The cryogenic feeding valves box, the power coupler as well as the solid state 10 kW RF amplifier are also "qualifying" units of the Spiral 2 superconducting LINAC components. The different results, concerning the cryogenic, mechanical and RF performances of the cryomodule are summarized below.

CRYOGENIC PERFORMANCES

Cool Down Times

For the test, the 60 K thermal shield was cooled with Liquid Nitrogen and the 4.2 K volume with Liquid Helium at around 1.3 bars. The thermal shield was first cooled during 9 hours and reached a temperature of about 80 K. Then the cavities were cooled from the bottom. Liquid appeared on the helium buffer situated on the top of the cavities after 4 hours. However the cool down time in the temperature range from 200 K to 20 K was below 1 hour which is fast enough to prevent from Q-disease. Both cavities were cooled in parallel with only one feeding valve. We noticed a small cooling time difference in the 70K/4K range of only 15 minutes between the two cavities.

Figure 1: Spiral 2 cryomodule test stand at IPN Orsay.

Cryogenic Static Losses

Static losses (without RF) at 4 K are summarized in the Table 1. We note that for this test the cryomodule was not optimised in term of cryogenic losses and was not in the final configuration. For the cryomodule there are around 3 W more losses than expected. A part of these losses, 2 W, is explained by a lack of thermal interception sinks. For the final configuration the evaluated losses are 8.5 W.

INFLUENCE OF PIEZO-HYSTERESIS AND RESOLUTION ON CAVITY TUNING*

O. Kugeler†, W. Anders, J. Knobloch, A. Neumann, BESSY, Berlin, Germany

Abstract

All mechanical tuning systems are subject to hysteresis effects: For coarse tuning with a stepper motor, the exercised forces lead to a visco-elastic deformation of the tuner body. In piezo-based fine tuning, even if the smaller deformations of tuner and cavity can be regarded as fully elastic, the piezo-actuators themselves suffer from remanent polarisation effects. The extent of these nonlinearities has been measured in three different tuning systems (Saclay I, Saclay II and Blade Tuner) utilizing high-voltage as well as low-voltage piezo actuators. An estimate of the resulting tuner-resolution and performance degradation with respect to microphonics compensation is given. Experiments were performed at the HoBiCaT facility at BESSY.

BACKGROUND

Future CW-LINAC driven light sources like the BESSY-FEL or ERL require an RF-phase stability better than 0.02°. At an external quality factor of 3.2×10^7 and an LLRF feedback gain of 100 this corresponds to a maximum allowable detuning of 0.7 Hz. RF control systems are limited in gain or by phase noise of the RF reference system. Thus, it is a viable option to minimize the main error source, i.e. microphonic detuning. Microphonics compensation in cw-operated narrow-bandwidth (20-40 Hz FWHM) superconducting cavities has been demonstrated [1] with various different tuning systems [2, 3]. The maximum achievable compensation is limited by the resolution of the tuner system and hysteresis issues. The microphonics spectrum may be composed of a variety of small scaled detuning amplitudes. In order to compensate such a detuning, a piezo based system needs to resolve down to the centi-hertz regime, see Figure 1.

PIEZO HYSTERESIS MEASUREMENT

Cavities were operated in a closed loop PLL, see Figure 2. In order to measure the dynamic hysteresis a piezo voltage history was imposed with a function generator (carrier signal). For simplicity, a periodic sawtooth wave with a small frequency was used. This signal was added to a low amplitude, high frequency sine-wave from a lock-in amplifier (modulator signal). The phase error signal from the cavity was measured with the lock-in amplifier yielding the true momentary piezo-voltage-history-dependent value of the transfer function at the modulator frequency.

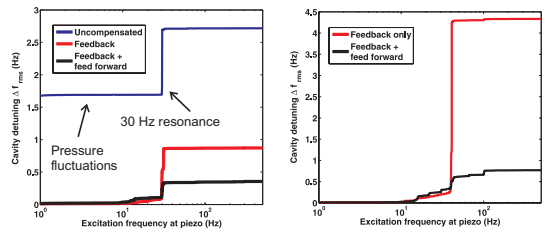

Figure 1: Microphonics compensation results: Integrated microphonics spectra of Saclay I (left) and Saclay II (right). By comparing feedback-only compensation with feedback/feedforward compensation, a resolution limit can be extracted: 0.1±0.05 Hz for the Saclay I tuner, and 0.2±0.05 Hz for the Saclay II tuner.

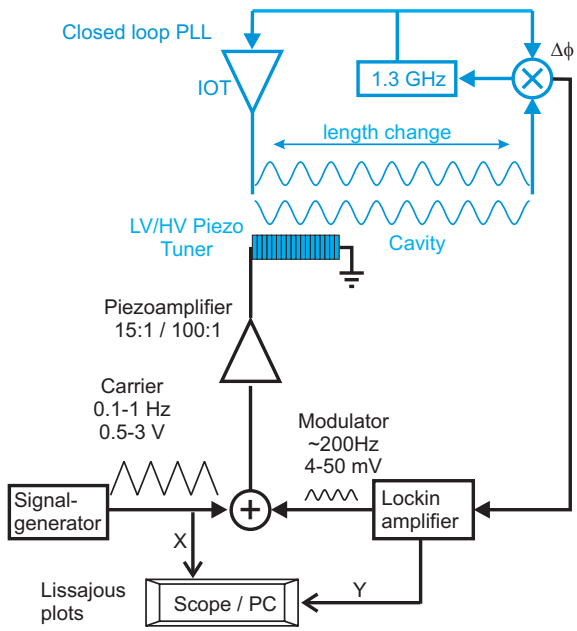

Figure 2: Experimental setup of the hysteresis measurements.

The dynamic response of the piezo to the controlling voltage is dependent on the history of the voltages, see Figure 3. The hysteresis effect can change the transfer function of the system: All resonances, or their Q-factors, respectively, are varied within an amplitude range defined by the maximum difference between the expanding and the contracting piezo. However, this viscoelastic nonlinearity of the piezo response is strongly deterministic, as can be seen from the shape of the hysteresis curves. With all the tuner modes mapped out properly, it can be incorporated into a feed forward based tuning algorithm.

* Work partly funded by the BMBF and the Land Berlin and the European Commission in the Sixth Framework Program, contract no. 011935 EuroFEL

† kugeler@bessy.de

RECENT DEVELOPMENTS ON SUPERCONDUCTING CH-STRUCTURES AND FUTURE PERSPECTIVES

H. Podlech, M. Amberg, A. Bechtold, M. Busch, F. Dziuba, Ratzinger, C. Zhang
Institut für Angewandte Physik (IAP), Goethe Universität, Frankfurt am Main, Germany

Abstract

Worldwide there is an increasing interest in new high intensity proton and ion driver linacs with beam powers up to several MW. A very challenging part of these accelerators is the low and medium energy section up to 100 MeV. Depending on the duty cycle room temperature or superconducting options are favoured. In both cases the Crossbar-H-mode (CH)-structure developed at the IAP in Frankfurt is an excellent candidate. Room temperature as well as superconducting prototype cavities have been developed and tested successfully. A superconducting 19 cell low energy CH-cavity at 360 MHz reached effective gradients of 7 MV/m corresponding to an accelerating voltage of 5.6 MV. This cavity could be used for high intensity, cw operated linacs like accelerator driven systems (ADS, EUROTRANS) or the international fusion material irradiation facility (IFMIF). Recent developments of this new type of a multi-cell drift tube cavity, tests of the prototypes and future plans will be presented.

INTRODUCTION

The CH-cavity is operated in the H_{21}-mode and belongs to the family of H-mode cavities like the IH drift tube cavity and the 4-vane RFQ. Due to the mechanical rigidity of the CH-cavity room temperature (r.t.) as well as superconducting (s.c.) versions can be realized [1]. For higher duty cycles or even cw operation superconducting solutions become more favourable because of a lower plug power consumption and higher achievable gradients [2]. In many cases the rf linac efficiency and compactness can be increased significantly by the use of multi-cell cavities.

360 MHZ PROTOTYPE CAVITY

The superconducting CH-protoype cavity (f=360 MHz, β=0.1, 19 cells) has been tested successfully in Frankfurt. After a second chemical surface preparation gradients of 7 MV/m corresponding to an effective voltage of 5.6 MV have been achieved (Fig. 1). Presently the cavity is being prepared for tests in a horizontal cryostat which is equipped with a slow and a piezo based tuner system. The basic principle of the tuner is an elastic deformation of the cavity by applying an external force at the end flanges of the tank [3]. This changes the width Δx of the end gaps and the gap capacitance. Tests at room temperature have been

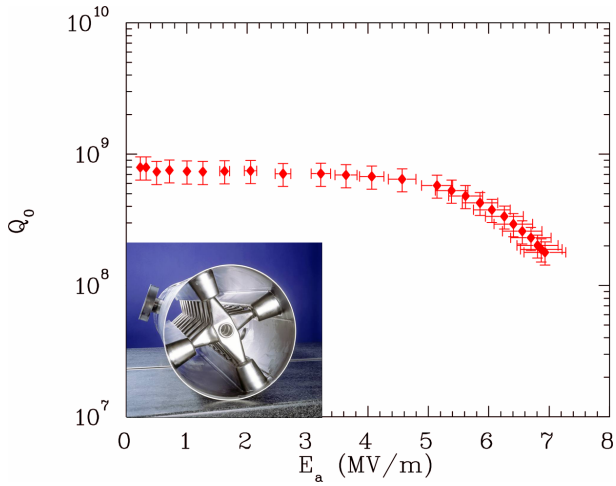

Figure 1: Measured Q-value of the superconducting CH-prototype cavity. Effecitve gradients of 7 MV/m have been achieved.

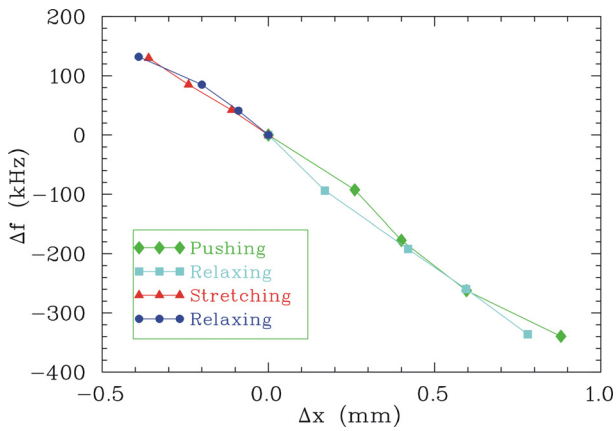

Figure 2: Measured frequency shift as function of the cavity deformation.

performed. The measured frequency tune shift is $\Delta f/\Delta x$ = 400 kHz/mm (see fig. 2). The change of field distribution according to the deformation of the tank has been measured by using the bead pull method. The experimental results are in good agreement with MWS simulations. The effect is mainly concentrated on the end cells of the structure, where a maintainable maximum field variation of 10% within the tuning range was observed [1]. The fast tuner will be used to operate the cavity at constant frequency. It

NONDESTRUCTIVE TESTING OF NIOBIUM SHEETS FOR SRF CAVITIES USING EDDY-CURRENT AND SQUID FLAW DETECTION

A. Brinkmann#, W. Singer, DESY, D-22607 Hamburg, Germany

Abstract

For more than 10 years DESY has been operating a high resolution Eddy Current scanning installation with rotating table for non destructive flaw detection on niobium sheets for SRF Cavities. About 2500 sheets have been examined up to now. Several types of defects have been detected and identified using different supplementary methods such as EDX, X-ray fluorescence, neutron activation analysis etc. In order to scan Niobium sheets needed for XFEL Cavity production, new scanning devices have to be built. One improvement of the Eddy Current installations could be the use of a more sensitive superconducting SQUID sensor. A SQUID based scanner system was built and is in evaluation at DESY. A status report will be given.

INTRODUCTION

In 1996 the cavity D6 showed a strong temperature increasing during a RF test. The hotspot was located with a T-map system. Analysis with X-Ray radiograph, Synchrotron Radiation Fluorescence (SYRFA) and Neutron Activation Analysis (NAA) detected a tantalum inclusion 0.2 mm in diameter (Fig. 1). Due to this experience a non destructive testing device for niobium sheet inspection was designed.

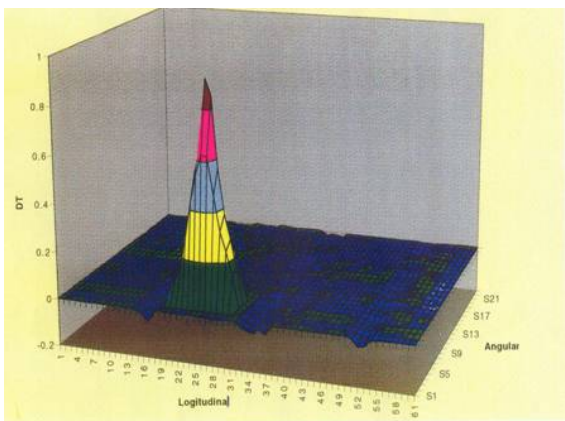

Figure 1: Hotspot found with T-Map.

EDDY CURRENT INSPECTION SYSTEM

DESY and BAM (Bundesanstalt für Materialforschung und – prüfung, Berlin, Germany) developed an Eddy Current Inspection System. About 2500 Nb sheets were inspected up to now [1] (Fig.2).

Figure 2: Eddy current inspection system.

Several kinds of flaws and imperfections were found with this system and could be analyzed with either EDX or SYRFA. For example: Fe inclusions (Fig.3-1), Si and Mg in small pits caused by grinding (Fig.3-2), imprints from rolling components (Fig.3-3), etching pits (Fig.3-4). Recently an image of the support frame in the 800° C furnace was found on a Nb sheet coming from evaporation or abrasion (Fig.3-5). On this niobium sheet Cr, Ni and W (1 %) could be detected on the surface using EDX.

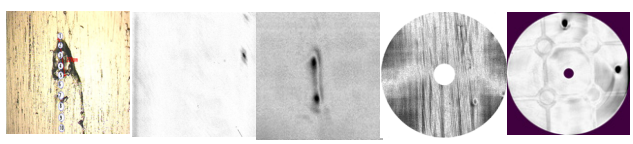

Figure 3: Several imperfections found with the Eddy Current Inspection System (explanation see text).

SQUID SCANNER

New scanning devices are required for the XFEL cavity production. One option is to replace the pick up coil of the conventional device by a superconducting SQUID element. This sensor promises a much higher sensitivity [2]. Therefore a SQUID scanner was developed and built in collaboration between DESY and the Company WSK. An excitation coil induces eddy currents in the sample. But in the case of a SQUID scanner a superconducting SQUID detects the related magnetic field. A compensation coil close to the SQUID cancels the primary excitation field (Fig.4).

arne.brinkmann@desy.de

VARIOUS APPLICATIONS OF DRY-ICE CLEANING IN THE FIELD OF ACCELERATOR COMPONENTS AT DESY

A. Brinkmann#, D. Reschke, J. Ziegler DESY, D-22603 Hamburg, Germany

Abstract

Dry-Ice cleaning offers a dry and waterless cleaning option removing hydrocarbons and particles without residues. Complex excavations like Cu RF gun cavities and Nb multicell cavities in horizontal installation position can be cleaned in an effective way. In the recent past RF gun cathodes and cathode transport boxes could be cleaned satisfactory. A status report will be given.

INTRODUCTION

Since recent 1-cell cavity RF-Tests showed acceptable behavior such as Eacc > 35 MV/m and promising results after RF conditioning a CO_2-cleaned RF gun cavity for the photo injector at PITZ (Photo Injector Test Facility Zeuthen) could be presented, the idea is to apply this cleaning method to other RF components and multicell Cavities.

A description of the cleaning process and the experimental setup for cleaning 1-cell niobium cavities has been given in [1, 2, 3].

Basic mechanical and chemical essentials for the cleaning effect are:

- Due to shock-freezing the contaminations become brittle.
- High pressure and a high momentum of snow crystals remove the contaminations. Particles down to 100 nm can be removed.
- Hitting the surface snow particles partially melt at the point of impact. Liquid CO_2 is a good solvent for hydrocarbons and silicones.

The major advantage of this cleaning method is the absence of water or other liquids which not evaporate in short time. Figure 1 illustrates the basic design of the device.

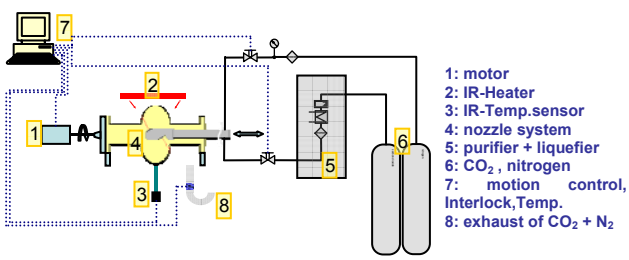

Figure 1: Basic design.

For cleaning gun cavities a cleaning apparatus with a vertical nozzle exists. The principle setup is similar to the horizontal one shown in Figure 1.
The difference is the new rod with a gas supply and movable CO_2 nozzle, delivered from Fraunhofer Institute IPA, Stuttgart/Germany [4].

CLEANED PARTS

2-Cell Cavity 2AC1 and 3-Cell Cavity 3AC1

These two cavities were cleaned with the horizontal setup with additional heating from the IR-heater (Fig. 2).

Figure. 2: 3-cell cavity assembled to the horizontal cleaning setup with IR-heater above the cavity

The 2-cell cavity shows no field emission up to the thermal breakdown at ca. 23 MV/m (Fig. 3). The 3-cell cavity will be tested soon.

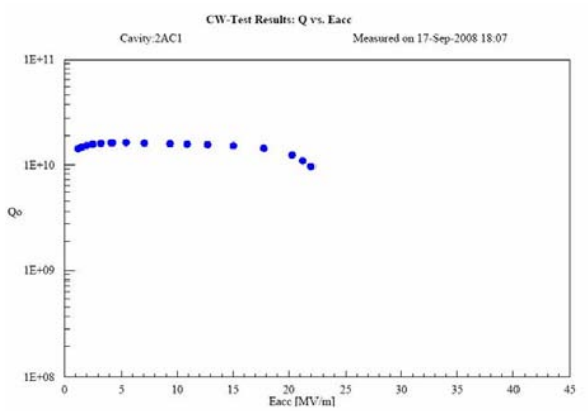

Figure 3: (Q/E)-Performance of cavity 2AC1.

#arne.brinkmann@desy.de

RECENT RESULTS ON 1.3 GHz NINE-CELL SUPERCONDUCTING CAVITIES FOR THE EUROPEAN XFEL

L. Lilje#, D. Reschke, DESY, 22607 Hamburg Germany.

Abstract

The most recent production of superconducting nine-cell cavities of the TESLA [1] shape in preparation for the European XFEL [2, 3] is currently under test at DESY. The goals are training of companies in cavity preparation, streamlining the cavity preparation process and a better comparison of final treatments. The current measurements are compared to the previous production cycles.

GOALS OF THE ONGOING XFEL NINE-CELL PROGRAMM

Training of Industry

The main goal is the training of industry. In previous production runs for the TTF at DESY, companies have fabricated the cavities. Additional quality control steps were introduced in the fabrication process. Most recently, a high resolution optical inspection system has been obtained from Kyoto University and KEK. This will be put into operation in the near future to further improve weld quality.

In the recent production run, the damage layer removal after fabrication was done by industrial companies. The process planned to be used in the XFEL production run is electropolishing (EP). So far, industrial electropolishing of multi-cell cavities was only available in Japan.

The final surface preparation (see below) for this production cycle was done at DESY. For the XFEL pre-series this process will also be transferred to industry.

Streamlining Procedures for XFEL

More efficient processes a desirable for the XFEL project in order to save cost. Several changes were introduced into the cavity preparation and assembly cycle.

Although the final treatment for the XFEL cavities has not yet been decided, tank welding at an early stage of the cavity process was considered a potential cost saving. The tank welding process was introduced after the furnace treatment and before the vertical test (For a detailed sequence of the assembly steps see next section).

The serious disadvantage of putting the tank on at such an early stage is that temperature mapping of the cavity is not possible anymore. In addition, a repair using EP is not viable either.

A second idea following along the same lines is to mount the HOM antennas already after the tank welding. The reason for this is, that a final cleaning. process i.e. high pressure rinsing with ultra-pure water can be done after the potentially particle-generating assembly processes.

It is a disadvantage, that assembled HOM antennas do not allow full passband mode measurements due to the narrow-band nature of the filter in the TESLA HOM couplers.

During vertical low-power continuous wave RF tests in some cavities Q-switches were observed. The effect disappears, when the HOM couplers are not equipped with antennas. During pulsed operation with HOMs these effects have never been observed. The nature of these effects is not fully understood yet, but is likely related to a temperature effect either at the feed-through or the antenna tip.

Comparison of Final Surface Treatment

The final surface treatment critically affects the cavity performance. The last treatment step is still under discussion for the XFEL. In the previous production run it turned out, that both a short final etch (10 µm) or a short EP (40 µm) followed by an ethanol rinse had good performance in terms of a reduction of field emission. The maximum gradient of the electropolished set of cavities seemed to be higher. To get a larger data set it was decided to test 10 cavities with each of the two choices of treatment.

CAVITY PREPARATION

The 30 fine-grain niobium cavities in the recent program have been subjected to the following processes::

- Damage layer removal: 150µm EP inside
- 10µm etching (BCP) outside,
- Degassing: 800 C firing
- Frequency and field flatness tuning
- Tank-welding
- followed by either
  - final EP 50 µm, ethanol rinse
- or
  - final BCP (“EP+”) of 10µm
- HPR (High-pressure rinsing with ultra-pure water)
- Antenna assembly,
- HPR
- 130 °C bake
- Low-power Test

For simplification several additional cleaning steps like ultrasonic cleaning are not listed here.

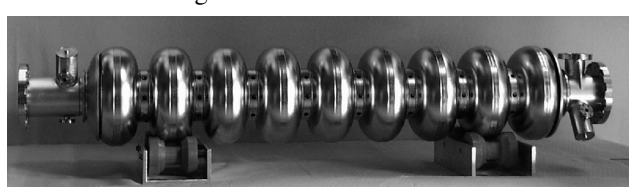

Figure 1: A TESLA 9-cell cavity with a length of about 1m.

OPEN 120°C BAKE IN ARGON ATMOSPHERE: A SIMPLIFIED APPROACH FOR Q-DROP REMOVAL

D. Reschke#, J. Ziegler, Deutsches Elektronen-Synchrotron DESY, 22603 Hamburg, Germany

Abstract

The removal of the Q-drop without field emission by a low temperature bake procedure (app. 120°C) is essential in order to achieve the full performance in both electropolished (EP) and chemically etched (BCP) high gradient SCRF Nb cavities. A simplified procedure applying an open 120°C bake in an Argon atmosphere is presented. The first successful cavity results are compared to the well-established bake procedure under ultra-high vacuum (UHV) conditions.

INTRODUCTION

The low temperature annealing ("bake") at 100°C – 130°C is an essential preparation step following a chemical or electrochemical surface treatment in order to achieve high gradients (> 30 MV/m) at high Q-values [1, 2]. The standard bake procedure in UHV conditions is applied to the fully assembled cavity ready for its rf test (Fig. 1). The cavity itself is kept under vacuum during the bake, while the outside is an inert gas atmosphere in order to prevent oxidation (Fig. 1 shows the bake stand without its outer hood, which can be partially seen at the right-most of the picture). Typical parameters applied at DESY are (120 – 129)°C for 48 h. On single-cell cavities a modified process with (130 – 138)°C for 12 h has been applied successfully.

Figure 1: DESY bake stand for UHV bake.

In order to adapt the bake procedure for a large scale cavity production two alternatives have been proposed:

- a higher temperature (130 – 160)°C , but shorter time of (1 – 12) h [3, 4, 5]
- open bake in inert gas atmosphere or air with 110 – 120 °C for 12 h – 60 h or 145°C for 3 h

The latter using an inert gas atmosphere has been developed also at CEA Saclay [6].

NEW BAKE PROCEDURE

Single-Cell Apparatus+ Procedure

For the single-cell tests described below a commercial lab vacuum drying cabinet was used successfully (Fig. 2). The vacuum drying cabinet has a programmable temperature control unit with a stability of ± 3°C and excess temperature protection. The vacuum and venting installation is integrated, which allows an adjustable, permanent Argon flow with overpressure protection. A dry, oil-free diaphragm pump is used for the initial pump-and-purge cycles. Applied parameters are a temperature of 120°C for 24 h with an Ar flow of app. 250 l/h. The purity of the Ar gas is better than 99,999%. Typically, warm-up takes 2 h; cool-down takes 16 h.

Figure 2: Vacuum drying cabinet for single-cell cavities.

detlef.reschke@desy.de

ANALYSIS OF QUENCHES USING TEMPERATURE MAPPING IN 1.3 GHz SCRF CAVITIES AT DESY*

D. Reschke#, Deutsches Elektronen-Synchrotron DESY, 22603 Hamburg, Germany.

Abstract

The local thermal breakdown (quench) behavior of one- and nine-cell SCRF Nb accelerator cavities is investigated systematically. For more than 50 cavities, in addition to the rf test results, temperature mapping data have been analyzed with respect to surface preparation, Nb material etc.. Results on rf properties, quench location and characteristic correlations are presented.

T-MAPPING SYSTEMS AT DESY

Presently, three different T-mapping systems for superfluid Helium are in use at DESY.

- Fixed, high sensitivity T-mapping system for single-cell cavities with 768 sensors on 48 boards (= 7.5 ° angle spacing) (Fig. 1a) [1]
- Rotating nine-cell T-mapping system with 128 sensors for quench detection (Fig. 1b) [2]
- "Quick" fixed T-mapping with 72 sensors at 24 angle positions for equator region (Fig. 1c).

All sensors are based on carbon resistors [3]. The block diagram of the multiplexed data acquisition is shown in Fig. 1d. The off-line analysis is based on in-house programming using LINUX PC applications.

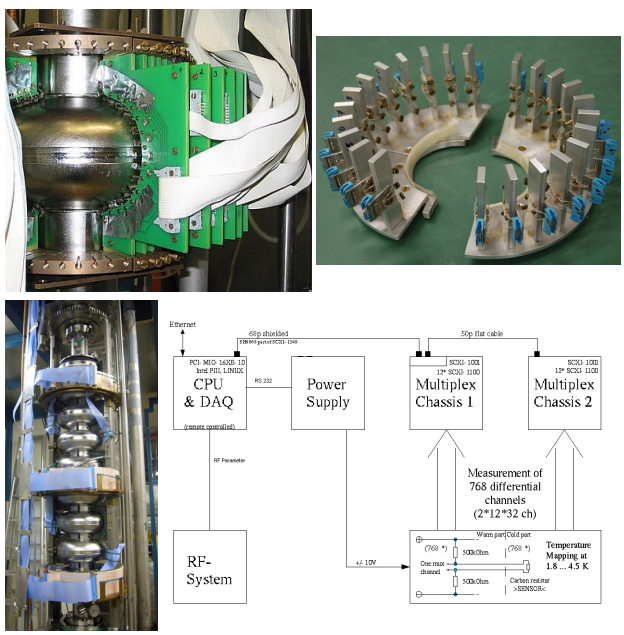

Figure 1: a) Single-cell T-map system (top left); b) rotating nine-cell T-map system (bottom left); c) "quick fixed" T-map (top right); d) data acquisition scheme (bottom right).

* We acknowledge the support of the European Community Research Infrastructure Activity FP6 "Structering the European Research Activity" program (CARE) contract number RII-CT_2003-506395
#detlef.reschke@desy.de

LARGE GRAIN CAVITIES: ELECTRO-POLISHING vs. CHEMICAL ETCH

Cavities and Surface Treatment

Three nine-cell cavities (AC112 – AC114) [4] and five single-cell cavities [5] of TESLA shape were fabricated of two ingots of Large Grain (LG) Nb by W.C. Heraeus Co.. The cavities "AC" were machined and electron beam welded at Accel Instruments Co.; the cavities "DE" are DESY in-house production. Before the first cold rf test at least 120 µm of the surface have been removed by electropolishing (EP) or chemical etch (BCP) on all cavities. Also all cavities have been 800 °C vacuum annealed. After the final surface treatment by final EP or BCP, all cavities were assembled in a cl. 10/100 cleanroom and rinsed with ultrapure high pressure water of > 100 bar. Typical parameters of the low temperature bake procedure were (120 – 125) °C for 48 h for the nine-cells and (130 – 138) °C for 12 h for the single-cells. Both processes show comparable results. In Table 1 only the major preparations steps are shown; the full preparation and test summary can be found in [6].

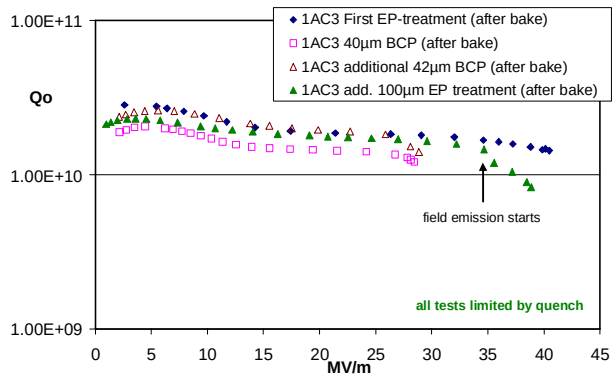

Figure 2: Q(E)-performance of an EP - BCP - BCP - EP preparation cycle of single-cell cavity 1AC3.

Preparation Dependency of Quench Gradient

As shown in Table 1 the influence of the final surface preparation of either > 40 µm removal by BCP or > 48 µm removal by EP on the Q(E)-performance has been investigated systematically. All test results of all 8 LG Nb cavities are given for $T_B = 2K$. Especially, the single-cells 1AC3 and 1AC4 went through full cycles of successive EP - BCP - EP treatments (Fig. 2). For both cavities a reproducible gradient gain of > 10 MV/m after EP compared to BCP is observed. A final BCP treatment applied on 6 cavities results in reproducible gradients of (25 – 30) MV/m limited by quench for all cavities. A final EP gives quench fields between (33 – 43) MV/m in 6 of 8 cavities. Two nine-cell cavities show low gradients

USE OF PIEZOELECTRIC ACTUATOR TO FREQUENCY LOCK SUPERCONDUCTING QUARTER WAVE RESONATOR

B.K.Sahu, S.Ghosh, R.Mehta, G.K.Chowdhury, A.Rai, P.Patra, A.Pandey, D.S.Mathuria, K. Singh, D.Kanjilal and A.Roy , Inter University Accelerator Centre (IUAC), Aruna Asaf Ali Marg, New Delhi – 110067, India

Abstract

The frequency control of the superconducting quarter wave resonator at Inter University Accelerator Centre (IUAC) is currently accomplished by mechanical and electronic tuners which are operated in the time scale in the range of a few seconds to a few microseconds. During operation, input RF power ≤ 100 W was required to control the resonator for a typical field of 3-5 MV/m for 6 watts of power dissipated in liquid helium. Though resonators are working fine at this power level, investigations are going on whether more reliable operation of the resonators is possible using a piezoelectric actuator to control the amplitude and phase of the accelerating fields. The piezoelectric tuner working in ~ milliseconds range with the dynamic phase control scheme will share a substantial load from the electronic tuner. In addition, in this new scheme, the resonator's phase lock loop will operate with lesser RF power than presently required. The test results of the piezoelectric tuner are presented in this paper.

INTRODUCTION

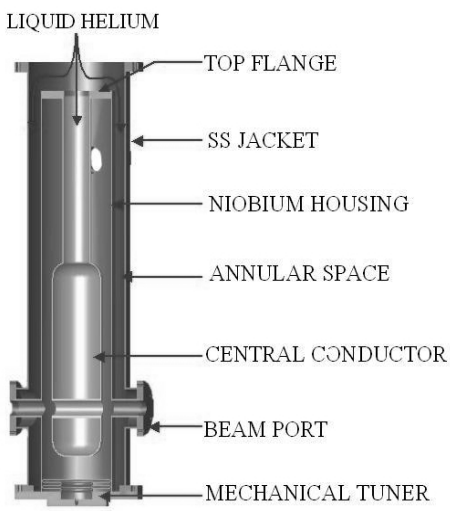

Figure 1: The schematic of the resonator and its mechanical tuner.

Presently, at IUAC, the commissioning of a superconducting (SC) linear accelerator (linac) based on niobium quarter wave coaxial resonator (QWR) is approaching completion [1,2]. The schematic of the resonator is shown in figure 1. The 15 UD Pelletron accelerator producing dc and bunched ion beam covering almost the entire periodic table, is used as the injector of the linac. Silicon and Oxygen beam from Pelletron accelerator has already been accelerated by the first accelerating module of linac and beam was delivered to conduct experiment.

The QWR of IUAC, is made from bulk niobium sheet and enclosed in a SS-jacket. Near the high voltage end of the central conductor, a pneumatically operated niobium bellows is placed to tune the resonator frequency. The complete resonator and the niobium bellow tuner are shown in figure 2 and 3.

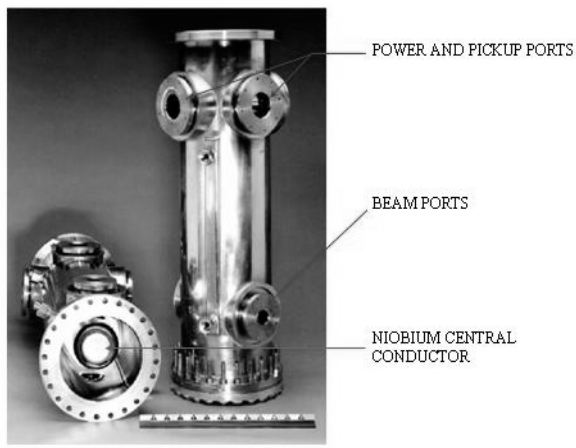

Figure 2: The photograph of two complete QWR.

The superconducting bulk niobium resonators have Quality factor in the range of 10^9. For IUAC QWR with resonance frequency of 97 MHz, the bandwidth of resonator is around 0.1 Hz. Vibration induced fluctuations of the frequency are of the order of a few tens of Hz in these resonators. The frequency fluctuations have got two components – one happens in slow time scale (seconds) and the other happens in faster (a few tens to hundreds of μsec) time scale.

To arrest the fast drifts of frequency, the effective bandwidth is increased by overcoupling the resonator with respect to the RF amplifier and the resonator is supplied with the additional reactive power. By flexing the niobium bellows acting as the mechanical tuner, the slow drift of the frequency is controlled. This helps to reduce the overall power requirement of the fast tuner to control the frequency jitter.

The two tuning mechanisms working simultaneously are able to lock the phase and amplitude of the resonators with respect to master oscillator and beam was

SUCCESSFUL QUALIFICATION OF THE COAXIAL BLADE TUNER

Angelo Bosotti, Carlo Pagani, Nicola Panzeri, Rocco Paparella, INFN/LASA, Segrate (MI)
Clemens Albrecht, Rolf Lange, Lutz Lilje, DESY, Hamburg
Jens Knobloch, Oliver Kugeler, Axel Neumann, BESSY GmbH, Berlin

Abstract

Cavity tuners are needed to precisely tune the narrow-band resonant frequency of superconducting cavities. The Blade Tuner is installed coaxially to the cavity and changes the resonator frequency by varying its length. Piezoceramic actuators add dynamic tuning capabilities, allowing fast compensation of main dynamic instabilities as Lorentz Forces, under pulsed operations, and microphonic noise. A prototype piezo Blade Tuner has been assembled on a TESLA cavity and extensively cold tested inside the horizontal cryostats CHECHIA (DESY) and HoBiCaT (BESSY). Then, as suggested by test results, few modifications have been implemented thus achieving the current Blade Tuner design. The introduction of thicker blades re-distributed along the circumference allows increasing its stiffness and fulfilling European and American pressure vessel codes, while ensuring the requested performances at the same cost. The paper will present the successful characterization tests performed on the prototype, the extensive mechanical analyses made to validate the final model and the results from qualification tests of first revised Blade Tuner produced, to be installed in the second module of ILCTA at FNAL.

PROTOTYPE TESTS

The blade tuner working principle is to transfer azimuthal rotation, provided by a stepper motor into longitudinal motion by means of bending blades [1]. The device that has been tested inside CHECHIA and HoBiCaT is an enhancement of the TTF superstructures tuner, where the design has been simplified in view of the ILC requests, and completed with the insertion of the piezo for dynamic tuning operations.

Two prototypes of this device have been realized, one made from Titanium and the other from Stainless Steel (SS) with Inconel blades. The two new tuners where first tested at LASA at room temperature to check mechanical properties: after these tests we decided to use the SS – Inconel tuner for cold tests [2,3].

The first cold test inside horizontal cryostats has been performed, inside CHECHIA, at DESY, in pulsed RF regime. Then two other test sessions with CW RF have been done inside HoBiCaT, at BESSY. The tuner has been installed at DESY on the Zanon n°86 cavity (Z86), using a modified He tank, with the insertion of a central bellow, to allow for coaxial tuning operation. For the CHECHIA test, a stepper motor from Sanyo inc. has been installed, equipped with an harmonic drive component set. Two low-voltage, multilayer piezo from Noliac, 40 mm long and with 10x10 mm^2 cross section, have been installed as active elements.

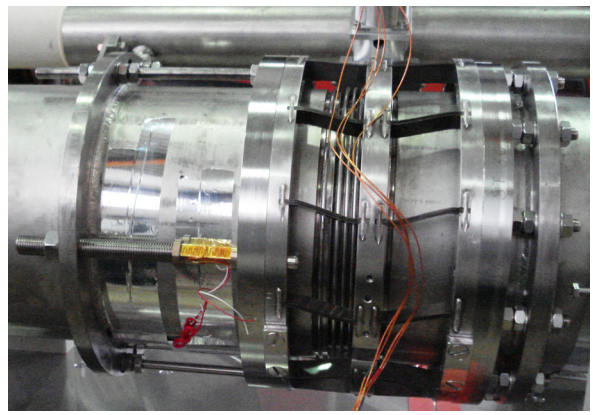

Figure 1: The Blade Tuner completely installed before cold test at BESSY; piezo actuators are in place and preloaded. The central bellow is also visible.

The correct preload to the piezo is given using the screws connected to the piezo supports. The goal pre-load value, about 1.5 kN on each piezo, is reached when the cavity is cooled at 2 K, taking into account all the cavity length changes, due to thermal contractions and pressure gradient sustained during the cooldown operation. During CHECHIA tests on September 2007, the entire Lorentz force detuning (LFD) shown by Z86 cavity at full gradient, about 300 Hz, has been successfully compensated in different load conditions. This was achieved using just one piezo, fed with one third of the nominal maximum driving voltage.

After the test in pulsed regime at DESY, the tuner was transferred to BESSY, to be tested from February to April 2008, inside the CW facility HoBiCaT. A Phytron stepper motor, provided with a planetary gear box, has been used in place of the former Sanyo stepper motor with harmonic drive gear (40000 half-steps per complete spindle turn instead of 35200). It must be remarked that this configuration was used for the first time for this application.

Among several other parameters (working point tuning range, piezo actuator DC tuning range, transfer functions and loading effect analyses), the whole tuning range has been extensively measured [2,3]. All the measurements are summarized in Figure 2, proving that the slow tuning performances meet expectations.

The cold tests inside CHECHIA and HoBiCaT facilities certified that the coaxial Blade Tuner has successfully overcome the prototype phase, providing a lot of useful information to optimize its design.

More than the required 600 kHz of tuning range has been achieved (Figure 2), with a tuning sensitivity of 1.5 Hz/half-step. The hysteresis of the first load cycle in

THIRD HARMONIC SUPERCONDUCTING CAVITY PROTOTYPES FOR THE XFEL

P. Pierini*, A. Bosotti, N. Panzeri, D. Sertore, INFN LASA
H. Edwards, M. Foley, E. Harms, D. Mitchell, FNAL
J. Iversen, W. Singer, E. Vogel, DESY

Abstract

The third harmonic cavities that will be used at the injector stage in the XFEL to linearize the bunch rf curvature distortions and minimize beam tails in the bunch compressor are based on the rf structures developed at FNAL for the DESY FLASH linac. The design and fabrication procedures have been modified in order to match the slightly different interfaces of XFEL linac modules and the procedures followed by the industrial production of the main (1.3 GHz) XFEL cavities. A revision of the helium vessel design has been required to match the layout of the cryomodule strings, and a lighter version of the tuner has been designed (derived from the 1.3 GHz ILC blade tuner activities). The main changes introduced in the design of the XFEL cavities and the preliminary experience of the fabrication of three industrially produced and processed third harmonic rf structures are described here.

INTRODUCTION

The RF cavity design for the 3.9 GHz structures [1] has been performed by FNAL for the design of the FLASH 3rd harmonic section (ACC39) [2,3]. Several cavities have been fabricated and tested [4] with accelerating gradients up to 24 MV/m, well above the design value of 14 MV/m needed for the FLASH operation.

The design of the European XFEL project [6] foresees a third harmonic section in the injector linac, at the beam energy of 500 MeV, before a bunch compression stage.

Three modules of 8 cavities are currently envisaged in the XFEL TDR to provide a sufficient linearization of the RF field seen by the bunch [3].

In the context of the XFEL activities the production of three prototypical cavities of the FNAL design has been tendered to one of the qualified producers of the main linac RF structures, including the responsibilities for the subsequent processing needed before the vertical testing (BCP chemical etching and high pressure rinsing stages). Fabrication is ongoing and, although no changes have been performed to the RF characteristics of the cavities as designed by FNAL, a few interfaces have been modified in order to either profit from existing components developed for the 1.3 GHz cavities (HOM pickup antennas, RF pickups, slim blade tuner design) or to reflect the different physical layout of the cross section of the XFEL cryomodules. In addition, the production process has been revised and adapted to the consolidated vendor experience based on the production of the 1.3 GHz cavities.

* paolo.pierini@mi.infn.it

XFEL CRYOMODULE LAYOUT

Type II and Type III Cryomodules vs XFEL

The FLASH linac, previously known as the TESLA Test Facility, TTF, is currently composed of cryomodules of two types, with different cryogenic piping locations within cross-sections of different sizes. The changes were performed in “generations” after successive iterations aimed at design simplification and cost reduction [7]. Currently Type II and Type III cryomodules are located in the linac tunnel. The first accelerating section of the FLASH linac (ACC1), after which ACC39 will be placed, is of Type II, meaning a large vacuum vessel (1.2 m diameter) and an internal piping distribution different than in the standardized 38” vessel of the Type III. Since ACC39 is cryogenically connected to the ACC1, the transverse cross section of the FNAL module has been designed to match that of a Type II.

However, the XFEL module design has been derived from the Type III, in particular concerning the relative location of the He Gas Return Pipe (HeGRP, acting as a structural backbone for the entire cold mass), the 2-phase He pipe and the cavity string.

The XFEL third harmonic cryomodules, which are in the early design stage, need to reflect this change in the cross-section and, in particular, the ACC39 design of the dressed cavity package (cavity+He tank and 2 phase pipe) needs to be revised to account for these different interfaces.

Main Couplers Orientation

Beam dynamics simulations of the entire XFEL linac suggests that, in order to obtain an on-axis cancellation of the RF coupler kicks, an alternating scheme for the coupler direction different from ACC39 needs to be used to limit emittance growth effects [8, 9]. This again has implications on the module design and requires the use of two types of dressed cavity assemblies, according to the coupler direction.

Slim Blade Tuner

The coaxial tuner used on the FNAL ACC39 module has been derived from the INFN blade tuner originally proposed for the TESLA collider [10], scaled to the smaller size of the 3.9 GHz RF structures. Recent progresses at INFN on the blade tuner concept for ILC led to the development of a simpler, lighter and cheaper device, that has been extensively characterized [11]. Slim tuners of this kind will be installed in the second FNAL ILCTA cryomodule currently under construction.

DEVELOPMENT OF INSPECTION SYSTEMS FOR SUPERCONDUCTING CAVITIES

Yoshihisa Iwashita, Kyoto ICR, Uji, Kyoto
Hitoshi Hayano, Ken Watanabe, KEK, Ibaraki, Japan

Abstract

Development of inspection systems including high resolution camera for inner cavity surface, thermometry system for a cavity outer surface, and Eddy current scan for bare Nb plates are described. The cavity camera system revealed undiscovered defects at the inner sides of the locations predicted by passband-mode and thermometry measurements. A thermometry measurement system and an eddy current scan system are under development.

INTRODUCTION

Inspections of superconducting (SC) RF cavities seem essential in achieving high accelerating gradient. The inspection of the interior surface with high enough resolution to find defects more than several tens microns is achieved by our high-resolution camera system. This system revealed undiscovered defects at the inner sides of the locations predicted by passband-mode and thermometry measurements (see Fig. 1)[1]. This system will help to improve cavity fabrication processes and their yield. We are planning to widen our activity in this field: developments of a new thermometry system with easy installation and less cabling, and high sensitivity eddy current surface inspection system for bare Nb sheets. The detailed systems and some preliminary data obtained from the systems are presented.

HIGH RESOLUTION CAMERA

This high-resolution camera system is developed to search the defects and measure the shape of them for better yield of accelerating gradient of SC 9-cell cavities. As shown in Fig. 2, a black cylinder with EL (ElectroLuminescence) sheet as an illuminator on it having a camera inside is inserted into a cavity. The camera directs to the cylinder head and looks a reflected image of the cavity wall on a mirror installed in front of the camera [1]. The improvement of this system has been performed for the industrialization toward worldwide delivery. Figures 2-6

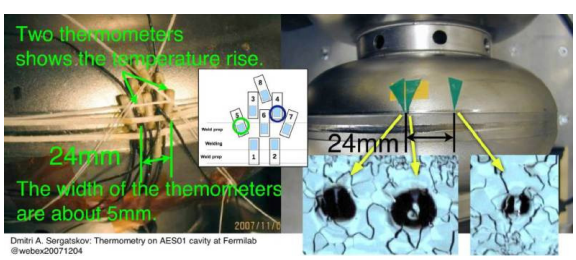

Figure 1: Positions of the two hot spots found at FNAL (left) and those found at Kyoto (right). The inset of left figure shows the location of the thermometers. The two thermometers (#4 and #5) that showed abnormal temperature rise are marked. (Courtesy of FNAL/JLAB.)

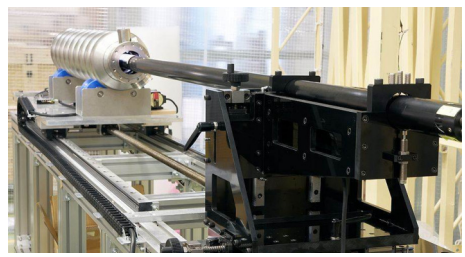

Figure 2: Production model of the inspection system.

show the production model of our inspection system. The improvement points are listed as follows:

1) The width of EL strip illumination is reduced from 10 mm to 7 mm for a better resolution in the shape measurement (see Fig. 3).
2) The EL illuminator is separated from the pipe unit, and all the electric wirings from the module are though two connectors for an easy replacement; its life may be up to a few thousand hours.
3) The EL illuminator unit slides with the mirror angle to keep the peephole on the sight line of the camera (see Fig. 4).
4) The half mirror for the coaxially illuminating LED is located before the tilting mirror to keep the illuminating direction and the sight line of the camera the same at any tilting angle.
5) The head assembly including the EL illuminator and mirror units is demountable from the camera cylinder. This modular structure also helps its maintenance. (see Fig. 5)
6) The camera lens is accessible by removing the head assembly and sending the camera all the way out. The magnification or even the lens itself can be changed at this position.
7) The damper against the vibration of the camera cylinder is installed on the cylinder support.
8) Better interface for the lighting control: each EL strip can be independently turned on/off. Any lighting pattern can be rotated right and left at a rate of about 2 Hz (see Fig.6).
9) The cavity table is retractable for easy shipping.

Figure 3: New EL stripe illuminator. The strip width is reduced from 10 mm to 7 mm; hence, the number of strips increases from 14 to 20. The camera looks through a peephole located at the center of strips.

SC Nb SPUTTERED QWRs FOR THE REX-ISOLDE ACCELERATOR AT CERN: PROTOTYPE DESIGN AND MANUFACTURING

M. Pasini*, S. Calatroni, L. M. A. Ferreira, D. Ramos, T. Tardy, F. Thierry, P. Trilhe
CERN, Geneva, Switzerland

Abstract

The HIE-ISOLDE activity aims to construct a superconducting linac based on 101.28MHz niobium sputtered Quarter Wave Resonators (QWRs), which will be installed downstream of the present REX-ISOLDE linac. The current design considers two basic cavity geometries (geometric β_0 = 6.3% and 10.3%) for which a mechanical and a chemical treatment and niobium coating design study has been performed. We report here on the status of the high β prototype cavity and sputtering chamber.

INTRODUCTION

In the framework of a general upgrade activity, named HIE-ISOLDE [1], of the Radioactive Ion Beams (RIBs) facility ISOLDE at CERN, a new superconducting linac based on QWRs (see Fig. 1) is planned [2]. Presently, the REX linac is delivering beams with mass to charge ratio of $3 \leq A/q \leq 4.5$ at a final energy of 3 MeV/u by means of a combination of several normal conducting structures. The energy upgrade will happen in two stages; in a first stage the final energy will be limited to 5.5 MeV/u while for the second stage the required final energy will be 10 MeV/u. The superconducting linac will also replace part of the normal conducting one so the energy span covered by the SC cavities will be between 1.2 and 10 MeV/u. In order to efficiently accelerate the beams in this velocity range two cavity geometries have been studied, one with a geometrical $\beta_0 = 6.3\%$ and the other with a geometrical $\beta_0 = 10.3\%$ (units are in % with respect of the speed of light). These values were optimized in order to allow an optimum acceleration efficiency for the heaviest A/q ratio (A/q=4.5).

CAVITY RF DESIGN

For the electromagnetic simulation of the two cavity geometries the `MWS` [3] code was used. The design aims at minimizing the peak surface electric field to accelerating field ratio ($E_{\mathrm{pk}}/E_{\mathrm{acc}}$), and the peak magnetic field to accelerating field ratio ($H_{\mathrm{pk}}/E_{\mathrm{acc}}$). The actual optimization is a trade-off between the RF performances and a simple shape that is better suited for the Nb sputtering. Another important aspect for this type of cavity is the magnetic steering effect due to a non-negligible magnetic field component at the beam axis. A special race-track shape, of the beam port (see Fig. 2) has been designed in order to minimize this effect. The beam axis position is in fact not centered vertically but shifted upwards by 4 mm. The vertical component of the electric field can in fact compensate the effect of the magnetic field on the beam so that the remnant steering kick is less then 0.1 mrad. The nominal gradient required is 6 MV/m over an active length of 195 and 300 mm respectively for the low and high β cavity. A residual resistance R_s of 50 nΩ is considered as a normally achievable value [4]. All the main cavity parameters are listed in Table 1

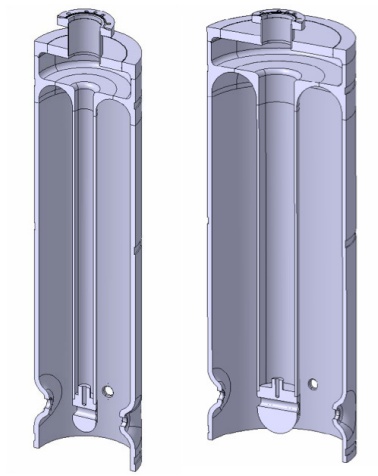

Figure 1: Low and high β cavities.

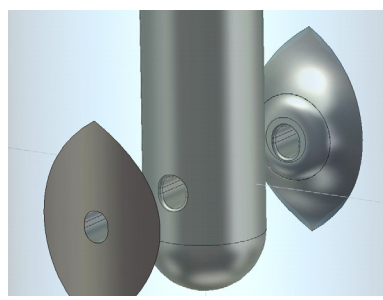

Figure 2: Details of beam port.

CAVITY MECHANICAL DESIGN

The basic technological choice for the HIE-ISOLDE cavities lies in the use of the Nb/Cu sputtering technology [5] and [6]. Compared to bulk niobium cavities, copper ones can easily be made massive and stiff in order to reduce microphonics effects, and to prevent the deformations due to the mechanical actions of the tuning system,

* matteo.pasini@cern.ch

CRAB CAVITIES FOR LINEAR COLLIDERS

G. Burt, P. Ambattu, R. Carter, A. Dexter, I. Tahir, Cockcroft Institute, Lancaster University, Lancaster, UK, LA1 4YR
C. Beard, M. Dykes, P. Goudket, A. Kalinin, L. Ma, P. McIntosh, ASTeC, Daresbury Laboratory, Warrington, Cheshire, WA4 4AD, UK
D. Shulte, CERN, Geneva, Switzerland
R. Jones, Cockcroft Institute, Manchester University, Warrington, UK, WA4 4AD
L. Bellantoni, B. Chase, M. Church, T. Khabouline, A. Latina, FNAL, Batavia, Illinois, 60501
C. Adolphsen, Z. Li, A. Seryei, L. Xiao, SLAC, Menlo Park, California

Abstract

Crab cavities have been proposed for a wide number of accelerators and interest in crab cavities has recently increased after the successful operation of a pair of crab cavities in KEK-B. In particular crab cavities are required for both the ILC and CLIC linear colliders for bunch alignment. Consideration of bunch structure and size constraints favour a 3.9 GHz superconducting, multi-cell cavity as the solution for ILC, whilst bunch structure and beam-loading considerations suggest an X-band copper travelling wave structure for CLIC. These two cavity solutions are very different in design but share complex design issues. Phase stabilisation, beam loading, wakefields and mode damping are fundamental issues for these crab cavities. Requirements and potential design solutions will be discussed for both colliders.

INTRODUCTION

Most linear collider concepts envision a crossing angle at the IP to aid the extraction of spent beams. This crossing angle will however reduce the luminosity of the collisions as the beam presents a larger effective transverse size. This loss in luminosity can be recovered by rotating the bunches prior to collision using the time dependant transverse kick of a crab cavity. In particular crab cavities are required for both the CLIC [1] and ILC [2] machines. The proposed solutions for these two colliders are very different and a comparison of the cavities will be the focus of this paper.

A crab cavity is a type of transverse deflecting cavity in which the RF is phased such that the centre of the bunch does not receive a net kick, and the head and tail of the bunch receive equal and opposite kicks [3]. Both travelling and standing wave solutions exist and the cavity can be either normal or superconducting depending on the bunch structure. As the cavity is typically positioned close to the IP before the final doublet their performance can be very sensitive to wakefields. Additionally as the separation between the incoming and extraction beam-lines are very close at this position, the cavities have to be transversely compact.

The voltage, V_{cav}, required to cancel the crossing angle of a bunch of energy, E_0, is given by equation 1,

$$V_{cav} = \frac{cE_0\theta_c}{2\omega R_{12}} \quad (1)$$

where θ_c is the crossing angle, ω is the cavity frequency and R_{12} is the ratio of the bunch displacement at the IP to the divergence created by the crab cavity. The crab cavity is positioned at a location with a high R_{12} to reduce the required voltage. The ILC has a crossing angle of 14 mrad and an R_{12} of 16.2 m at the crab cavities location. This means a 3.9 GHz system requires a peak deflecting voltage of 2.64 MV at 1 TeV CoM. The CLIC has a crossing angle of 20 mrad and an R_{12} of 25 m; hence a 12 GHz cavity will require a similar voltage of 2.39 MV at 3 TeV CoM.

PHASE AND AMPLITUDE STABILITY

As both the ILC and CLIC machines have very small transverse bunch sizes at the IP, the phase and amplitude of the crab cavities have to be very stable, as the primary action of a crab cavity is to displace the head and tail of the bunch at the IP. The displacement of a bunch at the IP, Δx, due to a timing error Δt is given by,

$$\Delta x(\Delta t) = R_{12}\frac{V_{cav}}{E_o}\sin(\omega\Delta t) \quad (2)$$

and the luminosity reduction factor, S, is given by

$$S = \exp\left(-\frac{\Delta x^2}{4\sigma_x^2}\right) \quad (3)$$

The horizontal beam size in the ILC is around 500 nm giving a positron-to-electron arm phase tolerance of 80 fs which is around the state of the art level [4]. For the CLIC beam size of 60 nm the timing stability is much smaller at 5 fs which is a major challenge to be overcome and will certainly require all cavities to be driven by a single amplifier.

The amplitude tolerance of a crab cavity is set by the luminosity loss associated with beams colliding with crossing angles. The incorrect amplitude on a crab cavity will cause incorrectly bunch rotation for the crossing angle and the bunches will collide with a small

INITIAL STUDY ON THE SHAPE OPTIMISATION OF THE CLIC CRAB CAVITY

P. K. Ambattu, G. Burt, R. G. Carter, A. C. Dexter, Cockcroft Institute, Lancaster University, Lancaster, UK, LA1 4YR
R. Jones, Cockcroft Institute, Manchester University, Warrington, UK, WA4 4AD
P. McIntosh, STFC, Daresbury Laboratory, Warrington, Cheshire, WA4 4AD, UK

Abstract

The compact linear collider (CLIC) requires a crab cavity to align bunches prior to collision. The bunch structure demands tight amplitude and phase tolerances of the RF fields inside the cavity, for the minimal luminosity loss. Beam loading effects require special attention as it is one potential sources of field errors in the cavity. In order to assist the amplitude and phase control, we propose a travelling wave (TW) structure with a high group velocity allowing rapid propagation of errors out of the system. Such a design makes the cavity structure significantly different from previous ones. This paper will look at the implications of this on other cavity parameters and the optimisation of the cavity geometry.

INTRODUCTION

Deflection cavities were first proposed in 1988 for the rotation of particle bunches prior to the interaction point (IP) in the presence of a finite crossing angle. Efficient design of the crab cavity will lead to a flexible design of the interaction region. Unlike an accelerating cavity, a crab cavity is operated in the lowest dipole mode, which is TM_{110}-like in nature, as it has the highest transverse geometric shunt impedance defined as

$$\left(\frac{R}{Q}\right)_{\perp} = \frac{|V_z|^2}{\omega U}\left(\frac{c}{\omega r}\right)^2 \qquad (1)$$

where U is the stored energy and V_z is the longitudinal voltage measured at the radial offset of r from the cavity axis at the angular frequency of ω [1]. For a crossing angle of θ_c, the peak transverse kick voltage required is given by

$$V_{\perp} = \frac{\theta_c E_{beam} c}{2 \omega R_{12}} \qquad (2)$$

where E_{beam} is the beam energy and R_{12} is the transfer matrix element representing the final focussing system, given by,

$$\Delta x_{ip} = R_{12} x_c' \qquad (3)$$

where Δx_{ip} is the vertical displacement of the bunch at the IP and x_c' is the angular direction of the bunch when leaving the cavity [2]. Eq. (2) shows that higher frequency operation of the cavity reduces the kick required to produce a given deflection angle. For 1.5 TeV beams crossing at 20 mrad and for $R_{12} = 25$ m, the maximum kick voltage required is 2.4 MV. For a transverse gradient of 20 MV/m, a structure length of 120 mm would be required to achieve the above kick. For a phase advance of $2\pi/3$ per cell, this requires about 15 cells. In addition to providing a kick at the operating frequency, the cavity should also suppress the wakefields that include monopole and higher order dipole modes in the cavity. However this aspect is not discussed here.

CAVITY CELL SHAPE

The cavity cell shape is shown in Fig. 1. This is adopted from the basic disc-loaded waveguide structure, where the coupling between adjacent cells is achieved through a common iris. In the figure, L, R and C stands for the length, radius and curvature respectively and suffixes c, e and i stand for the cell, equator and iris respectively. The cell length (cavity + iris), is set by the phase advance per cell, $\Phi = k_{rf}(2L_c)$, where k_{rf} is the free space phase constant in rad./meter. The iris edges are curved to avoid surface field enhancement and consequent field emission.

We studied the eigenmode characteristics of the single cell of an infinitely periodic copper structure as it can be used to infer the performance of a multi-cell structure. A $\Phi = 2\pi/3$ per cell structure, for which $2L_c = 8.337$ mm is modelled in Microwave Studio™ [3] as a first step.

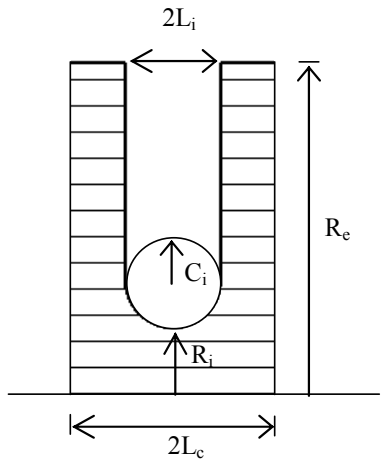

Figure 1: Cavity cell shape with dimensions.

Various cell shapes are simulated for the fixed operating frequency and the important figures of merit such as the transverse R/Q, group velocity and maximum surface fields are calculated.

SUPERCONDUCTING QUARTER-WAVE RESONATORS FOR THE ATLAS ENERGY UPGRADE

M. P. Kelly, J. D. Fuerst, S. Gerbick, M. Kedzie, K. W. Shepard, G. P. Zinkann, P. N. Ostroumov
Argonne National Laboratory, Argonne, IL 60439, U.S.A

Abstract

A set of six new 109 MHz β=0.15 superconducting (SC) quarter-wave resonators (QWR) has been built at ANL as part of an upgrade to the ATLAS superconducting heavy-ion linac at Argonne National Laboratory. The final cavity string assembly will use most of the techniques needed for the next generation of large high-performance ion linacs such as the U.S. Department of Energy's FRIB project. Single-cavity cold tests at T=4.5 K have been performed for 5 of 6 cavities. Tests were performed with a moveable coupler, rf pickup, and VCX fast tuner as required for the full 5-meter cryomodule assembly. The average maximum accelerating gradient of 6 cavities (5 new + 1 prototype), is E_{ACC}=10.6 MV/m (B_{PEAK}=62 mT). Assembly of the clean cavity string has just begun using techniques which are fairly well developed based on many single cavity clean assemblies and one assembly of the entire string performed under non-clean conditions. Details on single cavity performance including high-field cw operation, microphonics and fast tuning are presented.

INTRODUCTION

Advances in the last decade in SC cavity performance achieved using clean processing and assembly techniques at KEK, DESY and JLab for elliptical cavities have been adapted for TEM-cavities at Argonne and elsewhere. TEM cavity field performance with B_{PEAK}~100 mT or higher in single cavity tests is often achieved and is comparable to surface magnetic fields found in today's state-of-the-art elliptical cell cavity linacs. The ANL 7-cavity cryomodule, shown partially assembled in Figure 1, will be the first section of TEM-cavity linac incorporating all of the essential features found in clean elliptical cavity string assemblies. Features include electropolished high RRR bulk niobium cavities cleaned using high-pressure water rinsing and assembled in a clean room into a single sealed cavity string assembly. Isolation of the cavity rf volume from the cryomodule insulating volume greatly reduces the number of components assembled in the clean room and should help maintain cavity cleanliness.

CAVITIES AND CRYOMODULE

Specifications

Primary specifications for the upgrade cryomodule are shown in Figure 2. Initially the module was to hold seven β=0.15 quarter-wave resonators and one β=0.24 half-wave resonator, however, the half-wave requires additional work and will not be included in the initial assembly. This cw SC cryomodule is designed for a "real estate gradient" 3 MV/m which is now higher than achieved in pulsed normal conducting linacs for this velocity range.

Fabrication

The quarter-wave prototype and six production cavities were fabricated from RRR~250 3-mm thick niobium sheet purchased from Wah Chang. Parts were die hydroformed at Advanced Energy Systems and then electropolished at ANL to remove at least 100 μm of niobium from the rf surface. To perform the initial rough tuning of the cavity, the niobium subassemblies were clamped together and the frequency was measured. The cavity housing and center conductor were then trimmed along the length using a wire EDM. Ref. [1] contains many additional details on fabrication and tuning. The niobium subassemblies were then electron beam welded together at Sciaky Inc. and the complete niobium cavity was enclosed in an integral stainless steel helium vessel. Details of the critical niobium-to-stainless steel braze transition have been presented [2]. In order to remove residues from electron beam welding, a final five minute

Figure 1: Partial assembly of the quarter-wave cavity string in the clean room.

physical length	4.62 meters
# cavities	7
L_{EFF}/cavity	0.25 cm
required gradient	8.4 MV/m
total voltage	14.7 MV
static load (4.5 K)	15 Watts
rf load/cavity (4.5 K)	12 Watts
total heat load (4.5 K)	100 Watts

Figure 2: Primary specifications for the ATLAS upgrade cryomodule.

SURFACE PROCESSING FACILITIES FOR SUPERCONDUCTING RF CAVITIES AT ANL

M.P. Kelly, S.M. Gerbick, ANL, Argonne, IL 60439
D. Olis, A. Rowe, FNAL, Batavia, Illinois, 60510

Abstract

New SRF cavity processing systems at ANL, including those for electropolishing (EP), high-pressure water rinsing (HPR), and single-cavity clean room assembly have been developed and operated at ANL for use with cavities for a range of electron and ion linac applications. Jointly with FNAL, systems for 1.3 GHz single- and multi-cell elliptical cavities for the linear collider effort have been developed. New systems for use with low-beta TEM-class cavities have also been built and used to process a set of six quarter-wave resonators as part of an upgrade to the ATLAS heavy-ion accelerator at ANL. All of the new hardware is located in a 200 m^2 joint ANL/FNAL Superconducting Cavity Surface Processing Facility (SCSPF) consisting of two separate chemical processing rooms, a clean anteroom, and a pair of class 10 and 100 clean rooms for HPR and cavity assembly. First cold tests results for elliptical cavities processed in these facilities are discussed.

INTRODUCTION

A facility for processing superconducting (SC) niobium RF cavities has been built at Argonne National Laboratory (ANL) as part of an accelerator physics collaboration between ANL and Fermi National Accelerator Laboratory (FNAL). The facility will house in one location all hardware required to receive fabricated cavities as delivered from industry and, at the end of the process, yield a sealed cavity/coupler assembly ready for installation into a cold test cryostat. Overall costs and effort for construction of the facility are being shared approximately equally by ANL and FNAL. In addition to supporting upgrades for the ATLAS SC linacs at Argonne and linear collider R&D, the facility may also support development for the next-generation light source and proposed hadron linacs.

FACILITY DESCRIPTION

The 200 m^2 surface processing facility contains two types of work areas: chemical processing rooms (see *e.g.* Fig. 1), and clean rooms for high pressure rinsing (see *e.g.* Fig. 2) and clean assembly. Details of the facility layout were presented previously [1]. Other major supporting hardware includes a 3000 scfm large air scrubber to remove hazardous airborne fumes from chemistry operations, a deionized water system with 4500 liter storage capacity for supplying up to 40 liter/minute of clean water to any of the work areas, and a high-pressure Teflon diaphragm pump from LEWA supplying 13 liter/minute of water for performing HPR.

Chemical Processing Rooms

Two separate large chemical processing rooms, one administered by each laboratory is located at one end of the facility. The ANL administered chemistry room is presently configured for electropolishing of 1.3 GHz elliptical cell cavities. A nine-cell cavity, as positioned during electropolishing, is shown in Fig. 1. Previously, the same room has been used to perform electropolishing on six new production quarter-wave cavities for the ATLAS energy upgrade.

The FNAL administered chemistry room holds a buffered chemical polishing apparatus and automated

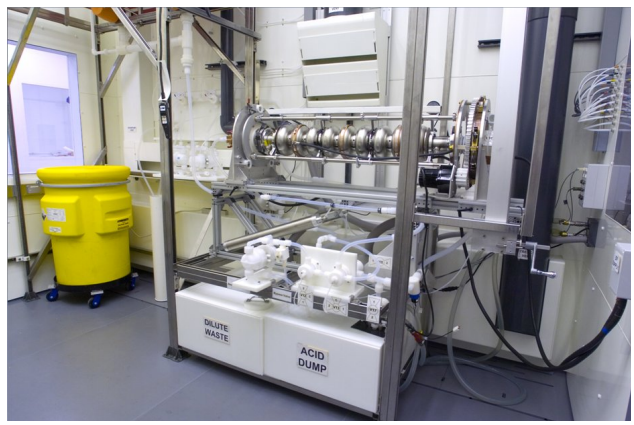

Figure 1: An electropolishing system for single- and multi-cell 1.3 GHz elliptical cavities at ANL

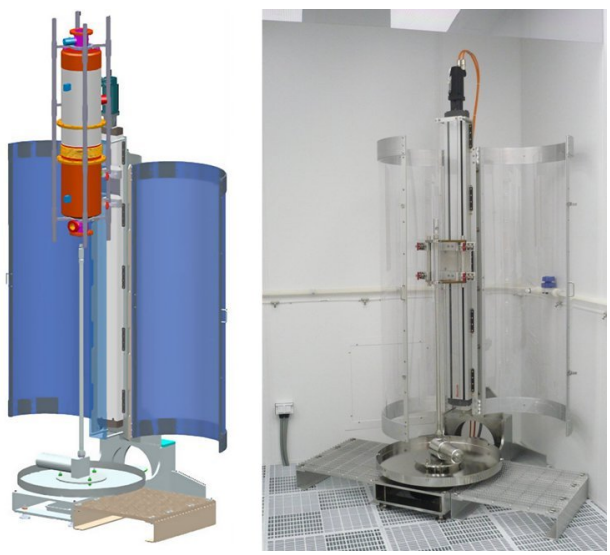

Figure 2: High-pressure rinsing system installed by Fermilab at the joint ANL/FNAL facility.

WELDING HELIUM VESSELS TO THE 3.9 GHz SUPERCONDUCTING THIRD HARMONIC CAVITIES*

M. Foley, T. Arkan, H. Carter, H. Edwards, G. Galasso, C. Grimm, E. Harms, T. Khabiboulline, D. Mitchell, D. Olis, T. Peterson, P. Pfund, N. Solyak, D. Watkins, M. Wong
Fermilab, Batavia, IL 60510, U.S.A.

Abstract

The 3.9 GHz 3rd harmonic cavities are designed to serve as compensation devices for improving the longitudinal emittance of the free-electron laser FLASH at DESY. These cavities operate in the TM010 mode, and will be located between the injector and the accelerating cavities. Fermilab is obligated to provide DESY with a cryomodule containing four 3rd harmonic cavities. In this paper we discuss the process of welding helium vessels to these cavities. Included will be a description of the joint designs and weld preparations, development of the weld parameters, and the procedure for monitoring the frequency spectrum during TIG welding to prevent the cavity from undergoing plastic deformation. Also discussed will be issues related to qualifying the dressed cavities as exceptional vessels (relative to the ASME Boiler and Pressure Vessel Code) for horizontal testing and eventual installation at DESY, due to the necessary use of non-ASME code materials and non-full penetration electron beam welds.

INTRODUCTION

The procedure for dressing a 3.9 GHz 3rd harmonic cavity with a helium vessel entails three welds in the following sequence: (1) Electron-beam (EB) weld of the helium vessel titanium shell to the large Nb55Ti conical disk, (2) EB weld of the titanium spacer ring to the small Nb55Ti conical disk, and (3) TIG fillet weld joining the titanium spacer ring to the titanium shell of the helium vessel. The weld joint geometry is shown in Figure 1. Full penetration EB welds are not allowed due to the possibility of vapor or weld debris deposition on the exterior surface of the cavity cells, thus potentially degrading the heat transfer rate from the cavity to the surrounding helium bath. The objective was to attain sufficient penetration to insure structural integrity and operational safety.

WELD PARAMETERS

Weld samples were developed to generate final welding parameters. Each sample was cut, polished and etched. Figure 2 shows a final sample of the EB weld joining the helium vessel shell to the large conical disk. Penetration depth achieved is approximately 3 mm. Figure 2 also shows a final sample of the EB weld joining the titanium spacer ring to the small conical disk. Penetration depth is approximately 2.25 mm. Before TIG welding, a titanium filler ring will be inserted to span the gap between the

* Operated by Fermi Research Alliance, LLC under Contract No. DE-AC02-07CH11359.

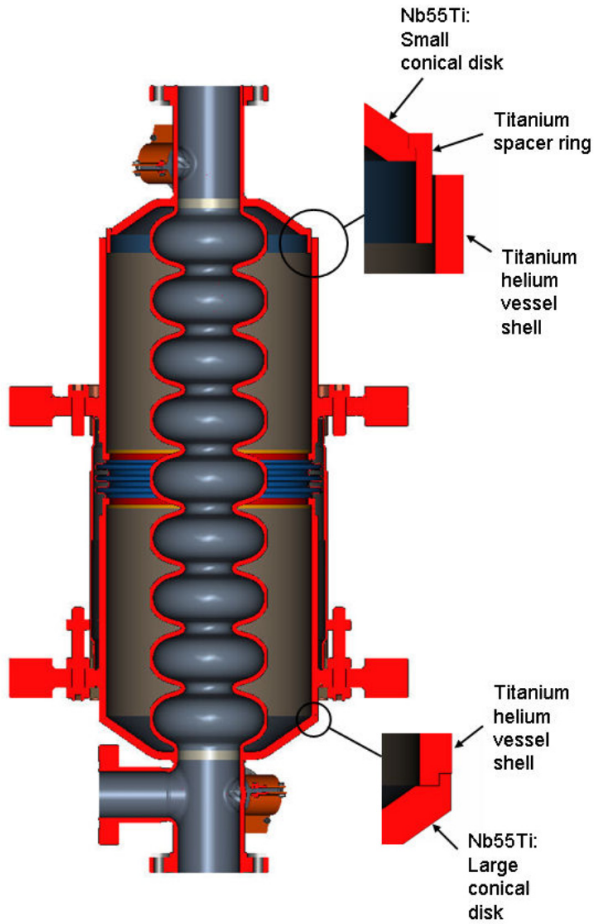

Figure 1: Breakaway view of dressed cavity showing the weld joint geometry.

spacer ring and the inner wall of the helium vessel shell. This is shown in Figure 3. The filler ring helps align the cavity and the helium vessel, and supplies material to augment the TIG fillet weld. The filler ring is fusion welded to the spacer ring on the cavity and the helium vessel shell, thus closing the entire circumferential gap between the helium vessel and the cavity. A TIG fillet weld will complete the process. Figure 3 shows the final sample for the TIG fillet weld.

WELDING PROCEDURE

After all components are properly cleaned and no more than twenty-four hours before EB welding, the cavity and helium vessel are assembled in a specially designed welding fixture in a clean room environment as shown in Figure 4. The entire assembly is enclosed in a

STATUS OF 3.9 GHz SUPERCONDUCTING RF CAVITY TECHNOLOGY AT FERMILAB*

E. Harms, T. Arkan, V. Bocean, H. Carter, H. Edwards, M. Foley, T. Khabiboulline, M. McGee, D. Mitchell, D. Olis, A. Rowe, N. Solyak, FNAL, Batavia, IL 60510, U.S.A.

Abstract

Fermilab is involved in an effort to design, build, test and deliver four 3.9 GHz superconducting rf cavities within a single cryomodule to be delivered to DESY as a 'third harmonic' structure for the FLASH facility to improve the longitudinal emittance. In addition to an overall status update we will present recent results from single 'dressed' cavity horizontal tests and shipping and alignment measurements.

INTRODUCTION

Fermilab is constructing a cryomodule containing four superconducting radio frequency (SRF) cavities operating at 3.9 GHz for the Free electron LASer in Hamburg (FLASH) facility at the Deutsches Elektronen-SYnchrotron (DESY) laboratory. This cryomodule was proposed to linearize the energy distribution along a bunch upstream of the bunch compressor. The four 9-cell cavities were designed to operate at 2 K in the TM_{010} π-mode at an accelerating gradient E_{acc} = 14 MV/m. Table 1 contains a list of parameters.

Table 1: Cryomodule Parameters

Number of Cavities	4
Active Length	0.346 meter
Gradient	14 MV/m
Phase	-179°
R/Q [$=U^2/(\omega W)$]	750 Ω
E_{peak}/E_{acc}	2.26
B_{peak} (E_{acc} = 14 MV/m)	68 mT
Q_{ext}	1.3 X 10^6
BBU Limit for HOM, Q	<1 X 10^5
Total Energy	20 MeV
Beam Current	9 mA
Forward Power, per cavity	9 kW
Coupler Power, per coupler	45 kW

CAVITY FABRICATION AND TESTING

Eight cavities have now been fabricated and undergone various levels of testing. A summary of test results and status of each is found in table 2. Details as to cavity performance can be found elsewhere [1] and at this conference [2].

*Operated by Fermi Research Alliance, LLC under Contract No. DE-AC02-07CH11359 with the United States Department of Energy.

Table 2: Cavity Fabrication and Testing Status

Cavity	Assembled by	Completion date	Test results and status
#1: 2-leg HOM	Fermilab	January 2006	- Never tested: HOM membrane break during cleaning - Used as horizontal test prototype
#2: 2-leg HOM	Fermilab	February 2006	- Best vertical test: 12 MV/m limited by HOM heating - Fractured Formteils - Awaiting repair
#3: 2-leg trimmed HOM	Fermilab JLab	August 2006	- Best Vertical test: 24.5 MV/m, achieved after HOM trimming - Welded into Helium vessel - Dressed for Horizontal testing
#4: 2-leg trimmed HOM	Fermilab JLab	March 2007	- Best Vertical test: 23 MV/m - Final vertical test with HOM feedthroughs
#5: 2-leg trimmed HOM	Fermilab JLab	May 2007	- Best Vertical test: 24 MV/m - Welded into Helium vessel - Horizontal testing complete: 22.5 MV/m - Ready for string assembly
#6: 2-leg trimmed HOM	Fermilab JLab	May 2007	- Best Vertical test: 22 MV/m - Faulty welds repaired - Awaiting final vertical test with HOM feedthroughs
#7 single-post HOM	Fermilab JLab DESY	November 2007	- Best Vertical test: 24.5 MV/m - Welded into Helium Vessel - Awaiting dressing and horizontal test
#8 single-post HOM	Fermilab DESY	October 2007	- Vertical test: 24 MV/m - Welded into Helium vessel - Awaiting dressing and horizontal test

Fabrication

Cavity fabrication has been reported previously [3]. Recently, Jefferson Lab expertise was called upon to repair broken welds found on cavity #6 ends during vertical testing. Cavity #2, which failed early in the test process, is now being fitted with replacement HOM bodies. At this time, weld samples are being evaluated prior to attempting this novel repair.

PERFORMANCE OF 3.9-GHZ SUPERCONDUCTING CAVITIES*

E. Harms, H. Edwards, A. Hocker, T. Khabiboulline, N. Solyak,
Fermilab, Batavia, Illinois, 60510 USA

Abstract

We report on the performance of 3.9 GHz SRF cavities built and tested at Fermilab for use in the DESY FLASH facility. Comparisons of performance in various test scenarios are presented. We also report on analysis of expected maximum performance.

INTRODUCTION

Four 3rd harmonic nine-cell 3.9 GHz superconducting cavities will operate at a gradient of 14 MV/m in the TM_{010} mode and will be placed in TTF/FLASH. These cavities are designed to linearize the accelerating gradient of the accelerator, providing improved longitudinal emittance.

TESTING SEQUENCE

Once fabricated, each 3.9 GHz cavity goes through a sequence of processing steps prior to high power RF being introduced to the cavity. This has been described previously [1]. Following initial processing, all cavities are tested vertically in the Fermilab's A0 North cave test area. This test area consists of a shielded enclosure, cryogenic system, LLRF, and traveling wave Tube amplifier capable of providing up to 150 watts CW. A basic controls system allows for Labview™ applications, electronic logbook, and file archival.

Vertical Tests

More than fifty cold vertical tests have been conducted to date. Figure 2 shows the Q vs E slope for all such tests. Recently, cavities have been operated at the default operating temperature of 1.8K as well as the operating FLASH temperature, 2K. One can note that with few exceptions, cavities are able to achieve gradients well in excess of the goal of 14 MV/m. Several factors limit ultimate cavity performance in this stage. In best cases the limit is the available RF power. Excessive x-ray emission suggesting a need to re-rinse or, in isolated cases, repeat a BCP is not uncommon. Performance of cavities fitted with HOM feedthoughs tend to be limited by heating or quenching of one or both HOM's.

The number of tests per cavity have ranged from as few as 3 (for #7) to 14 (for #6) in the case of poor-performing cavities. All cavities destined for the next step in processing must achieve the cavity performance parameters and gradients at least 20% better than the goal of 14 MV/m. Figure 1 shows the Q vs E result for the four cavities passing the vertical test and welded into helium vessels.

Operated by Fermi Research Alliance, LLC under Contract No. DE-AC02-07CH11359 with the United States Department of Energy.

Table 2: Summary of Best Performance in Vertical Tests

Cavity	# of tests	Emax (MV/m)	Status
#1	n/a	n/a	Prototype; used as test bed
#2	6	12	Fractured HOM formteils; to be repaired
#3	10	24.5 @ 1.8K 20.27@ 2K	Welded into helium vessel; dressed; being prepared for horizontal testing
#4	10	24.27 @ 1.8K	Final vertical testing in progress
#5	4	24 @ 1.8K Horizontal test: 22.5 @ 2K	Welded into helium vessel; Horizontal testing completed; awaiting string assembly
#6	14	22.5 @ 1.8K	Weld repair, plasma processing attempted to improve vertical test performance
#7	3	24.5 @ 1.8K 19.17 @ 2K	Welded into helium vessel; awaiting dressing & horizontal testing
#8	5	24.5 @ 1.8K	Welded into helium vessel; awaiting dressing & horizontal testing

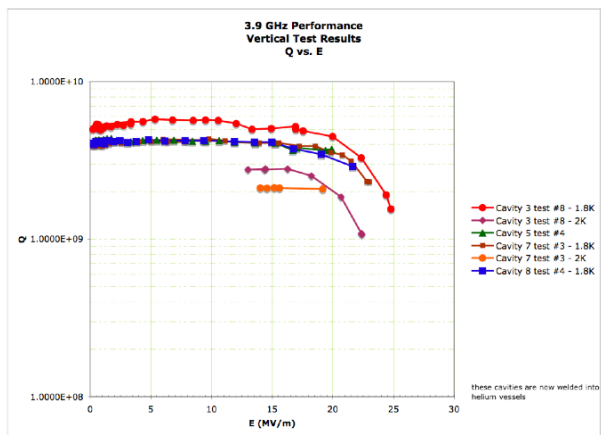

Figure 1: Q vs. E slope for 3.9 GHz cavities welded into Helium Vessels.

Recently, one cavity, #3, has undergone a final vertical test after being welded into a helium vessel, but prior to dressing. As the schedule permits, additional cavities may be subjected to this intermediate step.

Two production cavities, #4 and #6, remain to complete vertical testing owing to recent problems with vacuum system contamination and High Pressure Rinse system failures.

HIGH GRADIENT TESTS RESULTS OF 325 MHz SINGLE SPOKE CAVITY AT FERMILAB

I. Gonin, T. Khabibouline, G. Lanfranco, A. Mukherjee, J. Ozelis, L. Ristori, G. Romanov, D.A. Sergatskov, R. Wagner, R. Webber, G. Apollinari - FNAL, Batavia, IL 60510, U.S.A.
J. Fuerst, M. Kelley, K. Shepard - ANL, Argonne, IL 60439, U.S.A.

Abstract

Eighteen β = 0.21 superconducting single spoke resonators comprise the first stage in the cold section of the 8-GeV H^- Linac for Fermilab's proposed Project X. After Buffered Chemical Polishing and High Pressure Rinse, one resonator has undergone high gradient RF testing at 2.0 – 4.5 K in the Vertical Test Stand at Fermilab. We present measurements of the surface resistance as a function of temperature and the quality factor as a function of accelerating field. The resonator reached an accelerating field of 18.0 MV/m.

SUPERCONDUCTING SPOKE RESONATORS IN PROJECT X AND HINS

Fermilab recently proposed Project X, a high intensity, 8-Gev, H^- Linac based on independently phased superconducting resonators [1] to explore the Intensity Frontier. The High Intensity Neutrino Source (HINS) program is aimed at the demonstration of critical technologies for the low-energy front-end of the Linac.

Three superconducting spoke resonators comprise the low energy portion of the Linac cold section and operate at 325 MHz, one quarter of the frequency of the ILC type cavities that make up the high energy end. Two Single Spoke Resonators, SSR1 with β = 0.21 [2] and SSR2 with β = 0.4, will be built and operated as part of HINS.

Two SSR1 prototypes, SSR1-01 at Zanon [3] and SSR1-02 at Roark [4], have been fabricated. Figure 1, an exploded-view schematic of SSR1, shows the main features. The spoke spans the inner diameter of the shell, and two accelerating gaps are formed between the spoke and the endwalls. Liquid helium flows around the outer surfaces of the shell and endwalls and through the spoke.

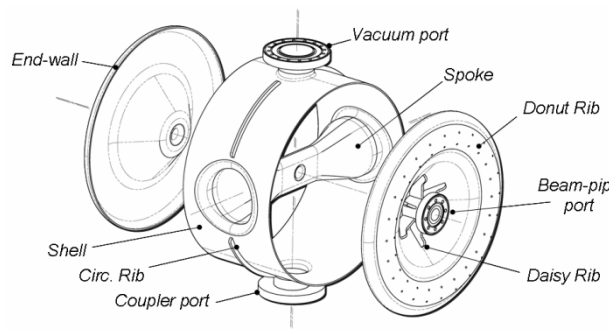

Figure 1: Exploded-view schematic of SSR1.

The cavity operates at a temperature T = 4.4 K, a nominal accelerating gradient E_{acc} = 10 MV/m, and an intrinsic quality factor $Q_0 > 0.5 \times 10^9$ at the accelerating gradient of 10 Mv/m.

After the first prototype, SSR1-01, arrived at Fermilab from Zanon, low gradient RF measurements, including bead pulls, were made to check the resonant frequency and compare the field profile with the calculation of Microwave Studio (MWS) [5]. The agreement was very good, with a field flatness of 99.7%.

BUFFERED CHEMICAL POLISHING AND HIGH PRESSURE RINSE

The interior surface of SSR1-01 was then prepared for testing at high gradient. The cavity was immersed in a bath of Ultra-Pure Water (UPW) with a degreasing agent and ultrasonically cleaned. It was then taken to the ANL G150 facility for Buffered Chemical Polishing (BCP), followed by a High Pressure Rinse (HPR).

The BCP used the standard $HF:HNO_3:H_3PO_4$(1:1:2) acid mixture. During BCP, acid flow and temperature were controlled in the following manner. The cavity was immersed in a bath of UPW that was initially cooled to 7.5 ºC by a continuously operating chiller. The cavity interior, sealed from the water bath, was connected to a pump for acid circulation. The cavity was oriented with the power coupler port and the vacuum port along the vertical axis and the beam pipes along the horizontal axis. In order to begin etching, acid (earlier chilled to 14 ºC) was pumped up through the bottom port to fill the interior of the cavity plus an "overflow bucket" connected to the top port. After shutting off the source of acid, the closed loop circulation pump drew acid from the overflow bucket and sent it back to the cavity through flanges on both beam pipes. Heat generated by the etching was dissipated through the cavity walls (including the spoke walls) to the continuously cooled water bath.

In order to obtain a total etching of ~120 µm and keep the niobium content in the acid below 10 g/l, spent acid was replaced with fresh acid about half way through the etching. Given the asymmetry in the acid flow pattern, the cavity was flipped top to bottom between the two etching sessions. The reduction in wall thickness was monitored at 20 locations using an ultrasonic thickness gauge.

The wall thickness reduction averaged 119 µm after a total etching time of 160 minutes. The acid temperature averaged 15.9 ºC and ranged between 14.9 ºC and 17.0 ºC during the etching. The thickness reduction was not as uniform as hoped, and we have plans to distribute the acid flow more uniformly in the future.

After BCP, the SSR1-01 was moved to the G150 class

SUPERCONDUCTING QUARTER-WAVE RESONATOR CAVITY AND CRYOMODULE DEVELOPMENT FOR A HEAVY ION RE-ACCELERATOR*

W. Hartung, J. Bierwagen, S. Bricker, C. Compton, J. DeLauter, P. Glennon, M. Hodek, M. Johnson, F. Marti, P. Miller, D. Norton, J. Popielarski, L. Popielarski, D. Sanderson, J. Wlodarczak, R. C. York, National Superconducting Cyclotron Laboratory, Michigan State University, East Lansing, Michigan, USA
A. Facco, Istituto Nazionale di Fisica Nucleare, Laboratori Nazionali di Legnaro, Legnaro, Italy
E. Zaplatin, Forschungszentrum Jülich, Jülich, Germany

Abstract

A superconducting linac is being planned for re-acceleration of exotic ions at the National Superconducting Cyclotron Laboratory. The linac will include two types of superconducting quarter-wave resonators (QWRs). The QWRs (80.5 MHz, optimum $\beta \equiv \beta_m = 0.041$ and 0.085, made from bulk niobium) are similar to existing cavities presently used at INFN-Legnaro. The re-accelerator's cryomodules will accommodate up to 8 cavities, along with superconducting solenoids for focussing. Active and passive shielding is required to ensure that the solenoids' field does not degrade the cavity performance. First prototypes of both QWR types have been fabricated and tested. A prototype solenoid has been procured and tested. A test cryomodule has been fabricated, containing one QWR, one solenoid, and two other beam-line elements. The QWR and solenoid have been operated successfully inside the cryomodule.

INTRODUCTION

The National Superconducting Cyclotron Laboratory (NSCL) is building a re-accelerator for exotic ion beams [1, 2]. Stable ions are produced in an ion source and accelerated in the NSCL coupled cyclotron facility. The primary beam produces a secondary beam of exotic ions by particle fragmentation.

The re-accelerator will consist of a gas stopper to slow down the secondary ion beam, a charge breeder to increase the charge of the ions by removing electrons, a multi-harmonic buncher, a radio frequency quadrupole for initial acceleration and focussing, and a superconducting linac to accelerate the beam to a final energy of 3 MeV per nucleon. Additional cryomodules can be added to increase the energy to 12 MeV per nucleon.

The superconducting linac will consist of quarter-wave resonators (QWRs) optimised for $\beta = 0.041$ [3] and $\beta = 0.085$ [4]. The cavities will be housed in a rectangular box cryomodule. A test cryomodule [5] has been designed, assembled, and tested. This paper covers design and prototyping work on the $\beta_m = 0.041$ QWR, $\beta_m = 0.085$ QWR, and cryomodules for the re-accelerator.

*Work supported by Michigan State University.

CAVITY DESIGN

The QWRs developed by Legnaro for ALPI and PIAVE [6] are the basis for the design of the QWRs for the re-accelerator (see Fig. 1). Some design modifications have been implemented. A larger aperture (30 mm) is used. Separation of cavity vacuum from insulation vacuum is implemented to reduce particulate contamination of cavity surfaces. Probe couplers [7] are used instead of loop couplers.

The cavity design has undergone some evolution since the first prototype cavity was fabricated and tested. For the second and third generation of QWRs, the shorting plate is formed from sheet niobium (3 mm thick) instead of being machined and the tuning plate (1.25 mm thick) is slotted to reduce the tuning force [7]. The shorting plate design is similar to designs used by Argonne [8] and SPIRAL 2 [9].

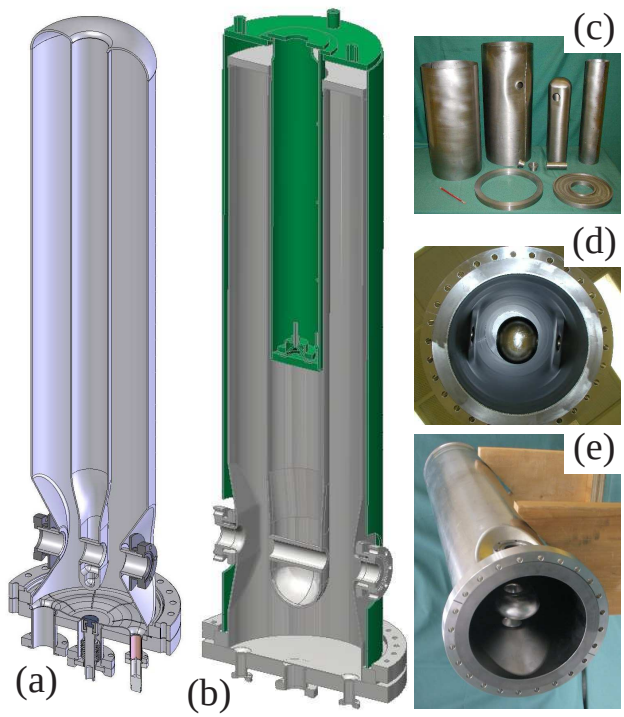

Figure 1: Drawings: (a) second generation $\beta_m = 0.041$ QWR; (b) first generation $\beta_m = 0.085$ QWR with damper and He vessel, shown in green. Photographs: (c) parts for first generation $\beta_m = 0.085$ QWR and (d) completed cavity; (e) completed second generation $\beta_m = 0.041$ QWR.

CW RF SYSTEMS OF THE CORNELL ERL INJECTOR*

S. Belomestnykh#, Z. Conway, J. Dobbins, R. Kaplan, M. Liepe, P. Quigley, J. Reilly, J. Sikora, C. Strohman, V. Veshcherevich, CLASSE, Cornell University, Ithaca, NY 14853, U.S.A.

Abstract

Two high power 1300 MHz RF systems have been developed for the Cornell University ERL Injector. The first system, based on a 16 kWCW IOT transmitter, is to provide RF power to a buncher cavity. The second system employs five 120 kWCW klystrons to feed 2-cell superconducting cavities of the injector cryomodule. The sixth, spare klystron is used to power a deflecting cavity in a pulsed mode for beam diagnostics. A digital LLRF control stem was designed and implemented for precise regulation of the cavities' field amplitudes and phases. All components of these systems have been recently installed and commissioned. The first operational experience with the systems is discussed.

INTRODUCTION

A prototype of the ERL injector [1], under commissioning at Cornell University's Laboratory for Accelerator based Sciences and Education (CLASSE), is the first step toward the future X-ray light source based on the Energy Recovery Linac (ERL) [2]. The injector faces a challenging task of producing high-current, ultra-low-emittance beam. This, in turn, imposes very stringent requirements on its RF systems [3]. There are three different types of cavities, all operating at 1300 MHz: buncher cavity [4], five 2-cell superconducting (SC) cavities [5], and deflecting cavity [6]. Due to different power requirements for buncher and SC cavities, two different RF systems have been developed. The buncher RF is based on a 16 kWCW IOT transmitter. The injector cryomodule (ICM) RF system employs five 120 kWCW klystrons. The sixth, spare klystron is used to power a deflecting cavity in a pulsed mode for beam diagnostics. A new generation of the Cornell low level RF (LLRF) controls is used for precise cavity field regulation. All components of the RF systems have been recently installed and commissioned.

RF FOR BUNCHER CAVITY

Specifications of the buncher RF system are listed in Table 1. As power requirements for this system are quite moderate, an IOT-based high power amplifier (HPA) was chosen. The HPA was manufactured by Thomson-BM. The system includes a 16 kWCW tube TH 713 (manufactured by Thales-ED) incorporated into a modified version of the DCX SIIA broadcast transmitter system. The high voltage power supply is manufactured by NWL. The block diagram of this system is shown in Figure 1. The HPA was tested at the factory and then at Cornell upon delivery [7].

A very small vacuum leaks were found in the buncher cavity tuners after the cavity installation. Vacuum dams were implemented to allow the injector operation while replacement tuners are being manufactured. After that the buncher was powered and commissioned up to 160 kV. A rather strong multipacting (MP) was observed during cavity processing. The multipactor exists at cavity voltages above 49 kV with the highest out-gassing between 60 and 70 kV. While the cavity body and input coupler are not susceptible to multipacting, it was found that the electric field in a small gap between the tuner plunger and the port is high enough to bring this area into the first order MP zone. It requires many hours to process this multipactor.

Table 1: Buncher RF Specifications

Number of cavities	1
Nominal accelerating voltage	120 kV
Maximum accelerating voltage	200 kV
Shunt impedance, $R = V^2/2P$	2.1 MOhm
Maximum dissipating power	9.6 kW
Maximum transmitter output power	16 kW
Amplitude stability	8×10^{-3} (rms)
Phase stability	0.1° (rms)

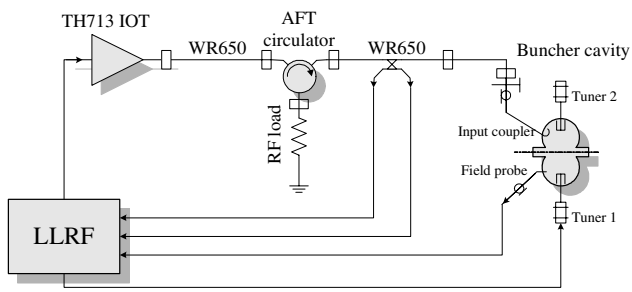

Figure 1: Block diagram of the buncher cavity RF system.

INJECTOR CRYOMODULE RF SYSTEM

ICM houses five two-cell SC cavities, each delivering up to 100 kW of RF power to beam. As each cavity operates independently, the system consists of five identical channels. RF power is delivered to cavities via twin input couplers [8], each carrying up to 50 kWCW. Main parameters of this system are given in Table 2 and its block diagram is presented in Figure 2.

* Work is supported by the NSF grant PHY 0131508.
#s.belomestnykh@cornell.edu

MULTIPACTOR IN MINIMUM ELECTRIC FIELD REGIONS OF TRANSMISSION LINES AND SUPERCONDUCTING RF CAVITIES*

S. Belomestnykh# and V. Shemelin, CLASSE, Cornell University, Ithaca, NY 14853, U.S.A.

Abstract

Multipactor in beam-pipe transitions of superconducting RF cavities can be explained using RF potential well theory [1]. In this paper we present simulation results supporting this explanation for both RF cavities and transmission lines.

INTRODUCTION

Curved-shaped transition regions between a cavity and a beam pipe were thought to be multipactor-free. Thus recent experimental observations of multipactor (MP) in two such transitions in Cornell ERL injector cavity [2] and KEK Ichiro cavity [3] surprised experimenters. The possibility of multipacting in those geometries was later confirmed in computer simulations. Analyzing these cases we have noticed that the electric field along the cavity profile has a minimum at the locations of MP. We proposed an explanation based on the Gaponov-Miller theory [4]. According to the theory an electric field minimum is associated with the local potential well, thus attracting electrons. This creates conditions favorable for multipacting. More details can be found elsewhere [1]. To check this explanation, we performed MP simulations for cavity geometries with different transition shapes, which confirmed that multipactor is suppressed for transitions with no electric field minimum.

The potential well theory can be applied to transmission lines too. For example, Miller force was used in [5] to derive an analytic solution of electron motion in a coaxial line and also was invoked in discussion of MP in a waveguide iris [6]. This force can also explain drift of multipacting electrons from the waveguide midline to sidewalls, that was observed in computer simulations [7] and, in case of partial or full standing wave in a transmission line, migration of electrons toward the standing wave minimum. We explore electron migration in the latter case for coaxial line and rectangular waveguide later in this paper.

Simulation results presented here were obtained with computer codes MultiPac [8] (for cavity-to-beam-pipe transitions and a coaxial line) and XingRK4 [9, 10] (for a rectangular waveguide.)

MP IN CAVITY-TO-BEAM-PIPE TRANSITIONS

Figure 1 shows MP trajectories at the electric field minimum in the transition form the Cornell ERL injector cavity end cell to a beam pipe. The contour line of the geometry, shown in Figure 2, consists of elliptic arcs connected with tangential straight segments. *Ae, Be, Ai, Bi* and so on are half-axes of the ellipses, *i* refers to the inner half of the cell, *e* refers to the outer half, *R* is the radius of the circle smoothening the transition; *Req* is the equatorial radius, *Rbp* is the radius of the beam-pipe.

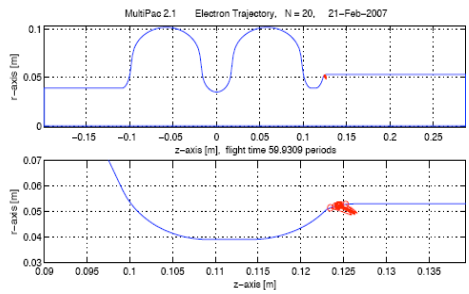

Figure 1: MP in the ERL injector cavity [2].

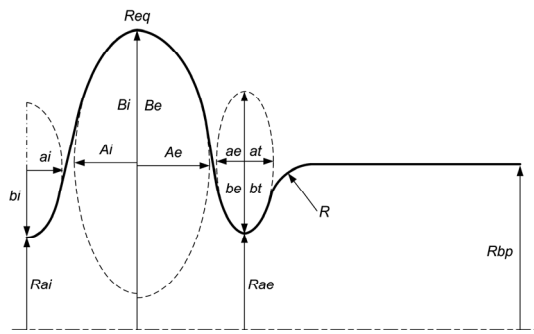

Figure 2: Geometry of the cavity-to-beam-pipe transition.

We have examined a transition from the end iris aperture *Rae* = 37 mm to the beam-pipe radius *Rbp* = 55 mm with different radii *R*. Half-axes of the end iris ellipses were *ae* = *at* = 12.53 and *bt* = *be* = 20.95 mm. Other dimensions of the cavity are chosen to tune its frequency to 1300 MHz and the ratio of the peak electric field to the accelerating field to $E_{pk}/E_{acc} = 2.0$.

Figures 3 and 4 show dependence of the maxima of the enhanced counter function *A* on the radius *R* and corresponding values of the peak electric field *E*. Three sets of points correspond to three different MP bands. Analyzed values of field levels were in the range from 25 to 35 MV/m as it has the most distinct maximum of the function *A*. Two points from Figures 3 and 4 corresponding to *R* = 12 mm are further looked at in Figure 5. Two maxima of the normalized enhanced function e_{20}/c_0 and corresponding impact energies and trajectories are presented. These trajectories can be related to two kinds of MP: three-periodic for 25 MV/m, and two-periodic MP for 33.5 MV/m (with some deviations from exact periodicity). Both are located in the flat minimum of the electric field.

* Work is supported by the NSF grant PHY 0131508.
#s.belomestnykh@cornell.edu

OSCILLATING SUPERLEAK TRANSDUCERS FOR QUENCH DETECTION IN SUPERCONDUCTING ILC CAVITIES COOLED WITH HE-II*

Z. A. Conway#, D. L. Hartill, H. S. Padamsee, and E. N. Smith
CLASSE, Cornell University, Ithaca, New York, USA

Abstract

Quench detection for 9-cell ILC cavities is presently a cumbersome procedure requiring two or more cold tests. One cold test identifies the cell-pair involved via quench field measurements in several 1.3 GHz TM_{010} pass-band modes. A second test follows with numerous fixed thermometers attached to the culprit cell-pair to identify the particular cell. A third measurement with many localized fixed thermometers is necessary to zoom in on the quench spot. We report here on a far more efficient alternative method which utilizes a few (e.g. 8) oscillating superleak transducers to detect the He-II second sound wave driven by the defect induced quench. Using a 9-cell reentrant cavity we identified the quench location in one cold test by powering several modes of the fundamental pass-band. Results characterizing the defect location with He-II second sound detection and corroborating measurements with carbon thermometers will be presented.

INTRODUCTION

Due to major R&D efforts by many laboratories within the TESLA Technology Collaboration (TTC) DESY has now successfully tested more than 12 cavities over 35 MV/m [1]. Nevertheless the means for reliably producing cavities which achieve accelerating gradients >35 MV/m with a high yield remains to be demonstrated as one of the ILC highest priority R&D goals. Frequently, the cavity gradients are limited by defects on the RF surface which quench at field levels well below 35 MV/m. Such quench limited cavities may be repairable but the process of locating defects in 9-cell cavities remains a lengthy and cumbersome process.

Many laboratories are developing large scale thermometry systems to pin-point the quench locations. Here, we present a cost-effective and simple method to determine quench locations. By testing a superconducting cavity in a superfluid helium bath it is possible to observe second-sound temperature waves driven by the conversion of stored RF energy to thermal energy at the defect [2, 3]. By measuring the time-of-arrival of the second sound wave at three or more detectors the defect location can be determined. Here, we use oscillating superleak transducers (OST), which measure the fluctuating counterflow velocity [4, 5, 6], to detect the time of arrival of second sound waves.

The remainder of this paper is split into four parts. First, we briefly discuss the RF performance history of the 9-cell reentrant cavity used in the experimental work. Next, we present the second-sound time-of-flight results used to locate the defect. Third, we show results of direct thermometric measurements of the cavity outer surface which corroborate the second sound defect location. Finally, we conclude with a few closing comments.

RESONATOR TESTING

Resonator Processing and RF Performance

After fabrication at AES (Medford, NY) the initial chemical processing of the 9-cell reentrant cavity was performed in early 2007 [7]. This included a final vertical EP of 25 µm and a bake at 110^{0}C for 48 hours. After cooling the cavity to 2 K, the RF performance shown in figure 1 was measured (July 2007 curve). The cavity operated cw at accelerating gradients up to 14.6 MV/m where the cavity quenched. This accelerating gradient corresponds to a peak surface magnetic field of 549 Oe and a peak surface electric field of 35 MV/m [8].

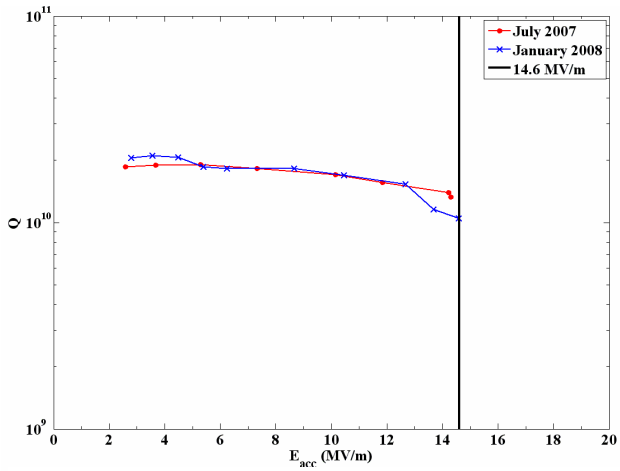

Figure 1: 9-cell reentrant cavity test results.

Immediately following the initial test which found the cavity RF field amplitude to be quench limited, two programs were implemented: 1) perform a heavy EP, to remove enough material to repair the cavity and 2) locate the defect should the EP repair prove ineffective.

First, the cavity received a series of heavy vertical electropolish procedures to remove 125 µm of material from the RF surface. The EP procedures were followed with a 48 hour 600^{0}C bake at FNAL. After another light EP etch (20 µm), HPR cleaning and 110^{0}C bake the cavity was again cooled to 2 K and tested. It was found that the cavity RF performance was unchanged (figure 1), requiring the determination of the defect location.

*Work supported by NSF and DOE
zac22@cornell.edu

RF DESIGN OF A SPOKE RESONATOR FOR HIGH POWER FREE-ELECTRON LASERS

F. L. Krawczyk, LANL, Los Alamos, New Mexico;
S. J. Cooke, NRL, Washington, DC;
D. C. Nguyen, LANL, Los Alamos, New Mexico;
B. Rusnak, LLNL, Livermore, California;
T. I. Smith, Stanford University, Stanford, Califormia;
E. L. Wright, Beam-Wave Research, Inc., Union City

Abstract

We are investigating spoke resonators that originally were proposed for moderate energy proton acceleration for application in high-average-current free-electron lasers (FEL). This structure holds the promise of alleviating the BBU limitations of conventional rf structures. Spoke resonator have several advantages: 1) strong coupling simplifies the access to higher order modes (HOM), 2) at the same frequency a spoke resonator is about half the size of an elliptical resonator, 3) the spokes provide additional mechanical stability and stiffening , 4) the power and HOM couplers can be attached to the cavity body and do not take up additional space along the length of the accelerator, 5) the presence of the spokes limits the polarizations of the HOMs to two orientations which facilitates the selection of HOM coupler positions. The rf performance of a spoke resonator specifically designed for high-current electron applications (beta=1.0) will be presented and compared with the expected performance of elliptical resonators designed for such applications. Besides the structure's effectiveness for acceleration also HOM properties will be presented.

CONTRIBUTION NOT RECEIVED

A NEW SRF CAVITY SHAPE WITH MINIMIZED SURFACE ELECTRIC AND MAGNETIC FIELDS FOR THE ILC*

Zenghai Li and Chris Adolphsen, SLAC, Menlo Park, CA 94025, U.S.A.

Abstract

The TESLA TDR cavity has been chosen as the baseline design for the International Linear Collider (ILC) main linacs. There are continuous SRF R&D efforts to develop alternative cavity designs that can produce higher gradient which in turn could lead to significant cost savings in machine construction and operation. It is believed that the maximum gradient achievable in a superconducting cavity is limited by the critical magnetic flux Bc of the niobium, which is approximately 180 mT. Most of the new designs were focused on minimizing the surface magnetic field (Bs) while the requirement on electric field (Es) was relaxed. The Low Loss design was one of the optimized designs with a Bs reduction of more than 10% over the baseline design which could support a gradient as high as 50MV/m. The Es field in this design is however about 15% higher than the baseline design. Though it is not clear what undesirable effects the high Es field may induce at high gradient, it is advantageous in a design with both Bs and Es surface fields minimized. In this paper, we will present an optimized cavity shape that minimizes both the Bs and Es fields. The design of the HOM couplers for damping the wakefields will also be presented.

INTRODUCTION

The TESLA TDR cavity shape [1], was proposed as the baseline design for the International Linear Collider (ILC) [2]. The cavity shape was optimized mainly with respect to Es/Ea, the ratio of maximum surface electric field to the accelerating gradient, and a ratio less than 2 was achieved. This low surface field ratio was considered advantageous in suppressing electron field emission at high gradients. Remarkable progresses have been made in understanding the limitations of field gradient in a superconducting cavity since the TDR was developed. It is believed that the maximum gradient achievable in a superconducting cavity is limited by the critical magnetic flux B_c of the niobium which is approximately 180 mT [3]. The later works on the ILC cavity optimization were then aimed towards a lower Bs/Ea ratio. The Low Loss (LL) [4,5,6] cavity shape was then developed as an alternative design for the ILC. The geometry of the LL cavity is optimized to have a lower Bs/Ea ratio and a higher shunt R/Q by reducing the size of the iris and increasing the cavity volume in the high magnetic field region. As a comparison to the TDR shape, the iris radius of the LL cell is 30-mm, 5-mm smaller than TDR, and the side wall of the LL cell is more upright. These modifications resulted in more than 10% lower in Bs/Ea and 15% higher in R/Q and geometric factor G which make the cavity more efficient in acceleration and less cryogenics loss. However, the Es/Ea of the LL design is about 15% high than the TDR cavity. If the B field limitation is the dominant factor for reaching high gradient, the new LL shape could support an ultimate gradient of over 50 MV/m because of low Bs/Ea ratio. There are concerted efforts in various labs to fabricate and test the LL shape cavities [7,8] to realize such a gradient goal. Significant progresses have been made in high gradient testing of the LL 9-cell cavities in the past years. These efforts are on going to explore the gradient reach of such a design. Although it is not clear what undesirable effects the high surface electric field may induce at high gradients, it would be advantageous to have a cavity design that has both the Es/Ea and Bs/Ea minimized to alienate potential side effects of high surface fields. We have recently developed a Low Surface Field (LSF) cavity shape for the ILC. This shape could potentially improve the cavity performance since both the Bs and Es fields are lower. In this paper, we present the optimization results of the LSF shape, and the HOM coupler design to damp the harmful dipole modes.

* Work supported by DOE contract DE-AC02-76SF00515.

CELL SHAPE OPTIMIZATION

Choice of Iris Aperture

A small iris opening increases the shunt impedance thus reduces the stored energy in the cell for a given gradient, and in turn lowers the surface fields. It was found however that the cell-cell coupling quickly becomes undesirably small as the iris radius becomes much smaller than 30-mm as shown in Table 1. At a lower cell-cell coupling, the field imbalance becomes more sensitive to cell dimension errors as the figure of merit for the sensitivity is N^2/k_{cc}, where N is the number of cells and k_{cc} is the cell-cell coupling. In addition, a smaller iris opening will result in higher wakefields which would tighten the alignment tolerances. So the 30-mm iris radius is chosen for the LSF design.

Table 1: Monopole bandwidth versus iris opening

iris radius (mm)	Bandwidth (MHz)
25.0	9.6
27.5	13.0
30.0 (LL & LSF)	19.2
35.0 (TDR)	24.2

Cell Profile

The new shape profile is similar to the LL shape except that the disk wall is straight up without a tilt angle. The cell contour is composed of an elliptical iris (*an, bn*) and

SRF CAVITY IMPERFECTION STUDIES USING ADVANCED SHAPE UNCERTAINTY QUANTIFICATION TOOLS*

V. Akcelik, L-Q. Lee, Z. Li, C-K Ng, L. Xiao and K. Ko, SLAC, Menlo Park, CA 94536, USA

Abstract

The deviations of a SRF cavity from the design shape may results in significant impact on cavity performance and wakefields that could lead to unexpected effects in beam dynamics. Yet, most of these deviations are unknown in the final cavity installation because of the complicated process of assembly and tuning. It is desirable to be able to infer for such distortions using measurable RF quantities. With these data, the cavity performance can be analyzed and realistic tolerance criteria may be implemented in the cavity design and manufacture for quality assurance. To perform such analyses, SLAC has developed advanced Shape Determination Tools, under the SciDAC support for high performance computing, that recover the real cavity shape by solving an inverse problem. These tools have been successfully applied to analyze shape deviations of many SRF cavities, and identified the cause of unexpected cavity behavior. The capabilities and applications of these tools are presented.

INTRODUCTION

The SRF cavities differ from original shape due to manufacture error and the tuning for the accelerating mode to achieve the right frequency and flat field. The deformation of the cavity leads to changes in higher-order mode frequencies, field distribution and wakefield damping, and may result in beam instabilities. It is important to understand the shape deviations of the real cavity from the design shape so that undesirable side effects due to shape deviation can be minimized in the manufacture of new cavities. Although direct measurements of the cavity shape are not feasible after the cavity is installed in the cryomodule and tuned, some of the RF quantities can be measured and can be used to evaluate the cavity shape deviations. SLAC has developed a set of shape uncertainty quantification tools based on SLAC's parallel finite element software that can recover the real cavity shape by solving an inverse problem using measurable RF quantities as input data.

We formulate the shape determination problem as a PDE constraint optimization problem, where the constraint is the Maxwell eigenvalue problem, the objective function is the weighted summation of the least squares difference of the modeled and measured RF quantities, and the inversion variables are the unknown shape deviations.

We present capabilities of the shape uncertainty quantification tools on two real applications: 1) the shape determination of the TDR cavity; and 2) identifying the cause of the BBU in one of the CEBAF 12-GeV upgrade prototype cavities.

METHODS

We pose the shape determination problem as a nonlinear least squares optimization problem

$$\begin{aligned} \underset{\mathbf{e}_j,k_j,\mathbf{d}}{\text{minimize}} \quad & \sum_i \alpha \left(f_i - \bar{f}_i\right)^2 + \sum_i \beta \left(Q_i - \bar{Q}_i\right)^2 \\ \text{subject to} \quad & \mathbf{K}\mathbf{e}_j + ik_j\mathbf{W}\mathbf{e}_j - k_j^2\mathbf{M}\mathbf{e}_j = \mathbf{0} \\ & \mathbf{e}_j^T\mathbf{M}\mathbf{e}_j = 1 \end{aligned}$$

where α and β are weighting constants, $\mathbf{e}_j$ eigenvector, and k_j eigenvalue for the jth mode, f_i are mode frequencies, and Q_i are external Q value for the ith mode, and $\mathbf{d}$ the represents the unknown shape parameters.

To solve the optimization problem, we follow a gradient based approach. The resulted nonlinear problem is solved using Gauss-Newton method, in which the required eigenvalue and eigenvector sensitivities are computed with a discrete adjoint approach. Inverse shape determination problem is generally ill-posed and rank deficient. To remedy this we use regularization methods such as truncated singular value decomposition (T-SVD), and Tikhonov regularization. The nonlinear optimization algorithm typically converges within a handful of nonlinear iteration. Each nonlinear iteration requires solutions of the forward eigenvalue problem, the adjoint problems, and evaluations of inversion equations. The forward eigenvalue problem is solved using Omega3P, and adjoint problems are solved using direct solvers such as MUMPS.

SHAPE DETERMINATION OF TDR CAVITY

The shape determination tool is used to infer for the unknown cavity deviations of a TDR cavity (Fig. 1). The following RF quantities are used as input in the objective function: 9 monopole frequency value, 36 dipole frequency values, and normalized field values measured at the center of each cell for the 9 monopole modes. These input data were obtained from the TFF-III measurements [1].

* Work supported by the U.S. DOE ASCR, BES, and HEP Divisions under contract No. DE-AC02-76SF00515. The work used the resources of NCCS at ORNL which is supported by the Office of Science of the U.S. DOE under Contract No. DE-AC05-00OR22725, and the resources of NERSC at LBNL which is supported by the Office of Science of the U.S. DOE under Contract No. DE- AC03-76SF00098. Work used resources of NCCS/ORNL supported under US DOE Contract No. DE-AC05-00OR22725, and NERSC/LBNL supported under US DOE Contract No. DE-AC03-76SF00098.

A NEW TEM-TYPE DEFLECTING AND CRABBING RF STRUCTURE*

J. R. Delayen[1,2#] and H. Wang[1]
[1]Thomas Jefferson National Accelerator Facility, Newport News, VA 23606, U.S.A
[2]Old Dominion University, Norfolk, VA 23529, USA

Abstract

A new type of rf structure for the deflection and crabbing of particle bunches is introduced. It is comprised of a number of parallel TEM-resonant lines operating in opposite phase from each other. One of its main advantages is its compactness compared to conventional crabbing cavities operating in the TM_{110} mode, thus allowing low frequency designs. The properties and characteristics of this type of structure are presented.

INTRODUCTION

Rf cavities for the deflection or crabbing of particle beams have been developed for many years. Most of them are comprised of superconducting cavities operating in the TM_{110} mode [1-4] although some are room temperature structures operating in a $\lambda/4$ mode [5] or are of *H*-type [6]. Crabbing rf structures have been of interest for the increase of luminosity in colliders [7,8], and more recently for the generation of sub-picosecond x-ray pulses [9,10].

The concept of the parallel-bar deflecting structure introduced here is shown in Fig. 1. It consists of 2 parallel $\lambda/2$ TEM resonant lines operating in opposite phase. The voltages generated are maximum and of opposite sign in the middle of the rods and generate a transverse electric field as shown in Fig. 2. The magnetic field is null in the mid-plane containing the beam line and is maximum where the bars meet the shorting planes, as shown in Fig. 3. Thus, unlike TM_{110} structures where the deflection is produced by interaction with the magnetic field, in the parallel-bar structure, the deflection is produced by interaction with the electric field.

Figure 1: Concept of the parallel-bar deflecting structure.

* Authored by Jefferson Science Associates, LLC under U.S. DOE Contract No. DE-AC05-06OR23177. The U.S. Government retains a non-exclusive, paid-up, irrevocable, world-wide license to publish or reproduce this manuscript for U.S. Government purposes.
#delayen@jlab.org

In the absence of beam pipe apertures, and if the outer wall were made of flat planes, the deflecting π-mode would be degenerate with the accelerating 0-mode where the 2 bars are oscillating in phase. Because the π-mode has no electric or magnetic field where the beam line meets the entrance and exit walls, while the 0-mode has an electric field, the beam pipe apertures remove the degeneracy. The mode splitting is further increased by rounding all the corners as shown in Fig. 1.

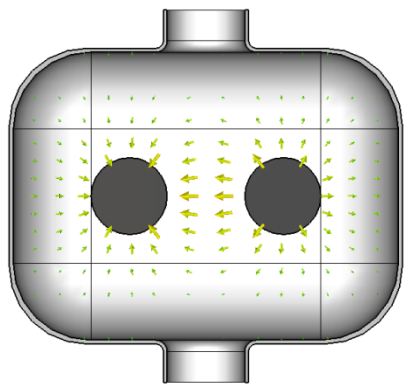

Figure 2: Electric field in the mid-plane of the parallel-bar structure operating in the π-mode.

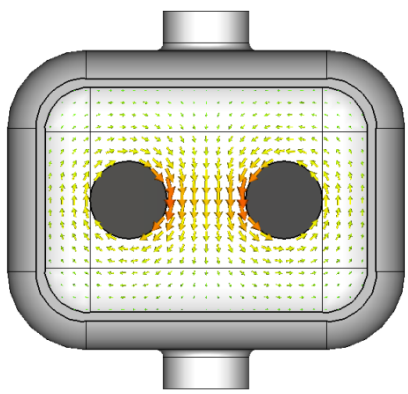

Figure 3: Magnetic field in the top-plate of the parallel-bar structure operating in the π-mode.

ANALYTICAL MODEL

If the distance between the side walls and the rods is substantially larger than the distance between the rods and the vertical symmetry plane, then the walls' contributions to the electromagnetic properties will be small and the fundamental cell can be modeled by two parallel infinite planes separated by $\lambda/2$ and joined by two parallel

ANALYSIS OF ELECTRONIC DAMPING OF MICROPHONICS IN SUPERCONDUCTING CAVITIES*

S. U. De Silva#1 and J. R. Delayen†1,2
[1]Old Dominion University, Norfolk, VA 23529, U.S.A.
[2]Thomas Jefferson National Accelerator Facility, Newport News, VA 23606, U.S.A.

Abstract

In low current applications superconducting cavities have a high susceptibility to microphonics induced by external vibrations and pressure fluctuations. Due to the narrow bandwidth of the cavities, the amount of rf power required to stabilize the phase and amplitude of the cavity field is dictated by the amount of microphonics that need to be compensated. Electronic damping of microphonics is investigated as a method to reduce the level of microphonics and of the amount of rf power required. The current work presents a detailed analysis of electronic damping and of the residual cavity field amplitude and phase errors due to the fluctuations of cavity frequency and beam current.

INTRODUCTION

In superconducting cavities microphonics and ponderomotive effects are the major causes of the fluctuations in the cavity fields [1]. Microphonics are the changes in the cavity frequency caused by the connections to the external world, such as external vibrations, pressure fluctuations, etc., and the ponderomotive effects are changes in the cavity frequency caused by the electromagnetic field (radiation pressure). The amount of rf power required in controlling the cavity field–to maintain the amplitude and phase stabilized–is dominated in low-current superconducting cavities by the presence of microphonics.

Electronic damping may be an effective way of reducing microphonics; it requires an active modulation of the cavity field to induce ponderomotive effects that counteract the effects of external sources. The model developed to control the cavity field is to operate the superconducting cavity in a self excited loop with amplitude and phase feedback. This paper analyses the method of electronic damping of microphonics and presents a generalized analytical solution for the residual changes of the cavity field amplitude and phase with and without the presence of beam.

MODEL AND EQUATIONS

The model, described in detail in [2-4], operates the cavity in a self excited loop. The transfer function diagram for the model described in [2-4] is given in Figure 1.

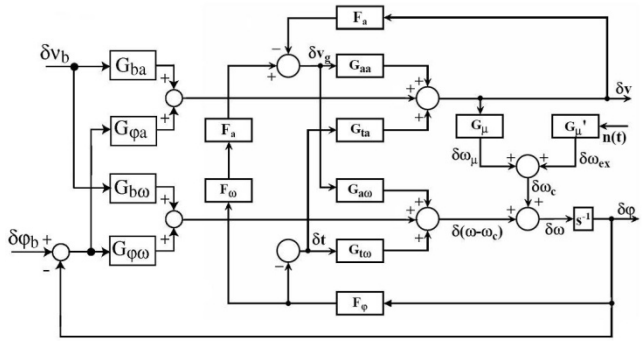

Figure 1: Transfer function representation of the system.

The corresponding transfer functions are as follows.

$$G_{aa}=\frac{\cos(\theta_l+\theta_f)}{\cos\theta_l}\frac{1}{1+\tau s},\ G_{ta}=-\frac{\sin(\theta_l+\theta_f)}{\cos\theta_l}\frac{1}{1+\tau s},$$

$$G_{a\omega}=\frac{1}{\tau}\frac{\cos(\theta_l+\theta_f)}{\cos\theta_l}\left[y-\frac{y_r}{1+\tau s}\right],\ G'_{\mu}=\frac{\Omega_{\mu}^2}{s^2+\frac{2}{\tau_{\mu}}s+\Omega_{\mu}^2},$$

$$G_{t\omega}=\frac{1}{\tau}\frac{\cos(\theta_l+\theta_f)}{\cos\theta_l}\left[1+\frac{y\,y_r}{1+\tau s}\right],\ G_{\mu}=-\frac{2\Omega_{\mu}^2\ \ k_{\mu}V_0^2}{s^2+\frac{2}{\tau_{\mu}}s+\Omega_{\mu}^2},$$

$$G_{ba}=-\frac{m}{1+\tau s},\qquad G_{\varphi a}=-\frac{m\,y_0}{1+\tau s},$$

$$G_{b\omega}=\frac{m}{\tau}\left[-y_0+\frac{y_r}{1+\tau s}\right],\qquad G_{\varphi\omega}=-\frac{m}{\tau}\left[1+\frac{y_0 y_r}{1+\tau s}\right],$$

$$y=\tan(\theta_l+\theta_f),\ y_r=\frac{\tau_0(\omega_r-\omega_c)}{(1+\beta)}=\tau(\omega_r-\omega_c),\ y_0=\tan\theta_0,$$

$F_a, F_{\varphi}, F_{\omega}$: Amplitude, Phase and Frequency feedbacks,

$\tau=\frac{\tau_0}{1+\beta}$: Loaded amplitude decay time,

$b=\frac{V_b\cos\varphi_0}{V_0}$: Ratio of power absorbed by the beam to power dissipated in the cavity,

$m=\frac{b}{1+\beta}$: Beam matching coefficient,

φ_0 : Nominal phase between the beam and the rf field,

τ_0 : Intrinsic amplitude decay time,

β : Coupling coefficient,

Ω_{μ} : Frequency of the mechanical mode of the cavity,

*Authored by Jefferson Science Associates, LLC under U.S. DOE Contract No. DE-AC05-06OR23177. The U.S. Government retains a non-exclusive, paid-up, irrevocable, world-wide license to publish or reproduce this manuscript for U.S. Government purposes.
#pdesilva@odu.edu, †delayen@jlab.org

HIGH-GRADIENT SRF R&D FOR ILC AT JEFFERSON LAB*

R.L. Geng#, A.C. Crawford, G. Ciovati, Jefferson Lab, Newport News, VA 23606, U.S.A.
M.S. Champion, D.A. Sergatskov, FNAL, Batavia, IL 60510, U.S.A.
F. Furuta, K. Saito, KEK, Tsukuba, Japan

Abstract

Jefferson Lab plays an active role in high-gradient SRF R&D in the frame work of the internationally coordinated International Linea Collider (ILC) S0 program. The S0 aim is to push the yield at 35 MV/m in 9-cell cavities. So far, twelve cavities have been electropolishing (EP) processed and RF tested by using the state-of-the-art recipes at JLab, in close collaboration with FNAL and KEK. Seven of them reached a best gradient of over 31.5 MV/m. Understanding gradient limiting mechanisms in real 9-cell cavities is an important component of our studies. Thermometry and high-resolution optical inspection are used to locate and understand the source of gradient limits. Experimenting with selective cavities is still a necessary method for process optimization. One example is the first demonstration of 35 MV/m without detectable Bremsstrahlung X-ray after a light EP is applied to a previously heavy chemical etched 7-cell cavity. Some new understanding has been gained with regard to quench behaviors, field emission behaviors as well as optimized processing. Progress has been made as a result, exemplified by the recent achievement of ≥ 35 MV/m in two cavities, each after the first light EP. Several exploratory studies are under way at JLab, aiming to covert the new understandings into further improved cavity gradient results.

INTRODUCTION

A summary of our earlier high-gradient cavity R&D work for ILC was reported at SRF2007 and can be found in Ref. [1]. Seven 9-cell cavities (A6, A7, A8, AES1, AES2, AES3 and AES4) were reported therein. The present report focuses on the new results obtained after the 2007 SRF Workshop. These include continued studies of four old (AES2, AES3, AES4 and A8) cavities and new studies of ***five new cavities*** (I5, A11, A12, A15 and J2). Till the present time, twelve 9-cell cavities have been EP processed and tested. In addition, a previously chemically etched 7-cell cavity was electropolished for 30 micron surface removal and reached an excellent result. Over 100 hours of active EP time has been accumulated.

Improvements in many areas have been made toward optimized processing. Initial acid mixing is made using a volume ratio of 1:10 (HF(49%):H_2SO_4(96%)). Nominal voltage across the cavity and cathode is 14-15 V. Acid supplying holes in the cathode face upward. The optimal EP is done in the continuous current oscillation mode [2][3]. More active temperature control is accomplished by steering the cooling water in the heat exchanging loop. The minimum purging N_2 gas flow reduces HF loss. Sealing openings around the acid sump prevents water (moisture) addition into acid and also reduces HF loss. High pressure water rinsing (HPR) after bulk EP and before 600°C furnace heat treatment improves cleaning and avoids burning chemical residuals into surface.

A major enhancement of our cavity gradient studies is added instrumentation of T-mapping and high-resolution optical inspection (Fig. 1). We will give some examples of understanding cavity quench and field emission behaviors by using these new capabilities.

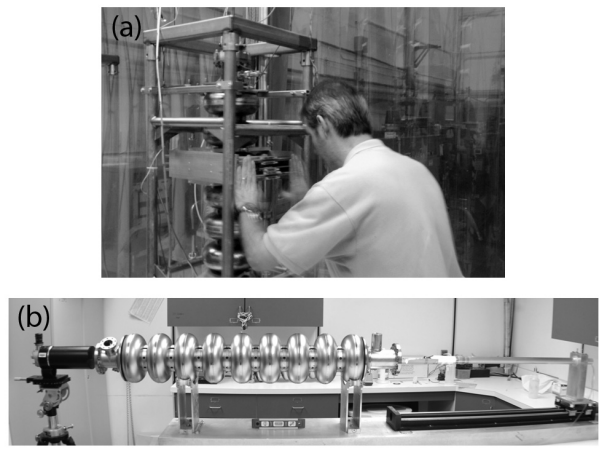

Figure 1: 9-cell cavity T-mapping (a) and high-resolution optical inspection (b) instruments used at Jefferson Lab.

9-CELL CAVITY RESULTS

Four (AES2, AES3, AES4 and A8) of the nine studied cavities were previously reported in Ref. [1]. Their further study results are reported herein. AES2 reached a best gradient of 32.8 MV/m. A8 reached a best gradient of 31.7 MV/m. AES3 was previously found [1] quench limited at 17-19 MV/m with the rough location of the quench origin determined. Finally, with 16 thermometers attached to the suspected region, the quench location was pinpointed by using FNAL's fast thermometry system. AES4 remained field emission limited at the gradient level of 27-29 MV/m despite further re-processing efforts.

Five of the nine cavities reported here are *new cavities*: three (A11, A12 and A15) are from the new batch of ACCEL procurement; one (I5) from KEK; one (J2) from the two new 9-cell cavities fabricated at Jefferson Lab.

A complete summary of all RF tests and associated surface processing histories is given in Table 1.

The best $Q(E_{acc})$ of cavities manufactured by "qualified" vendor (A8, A11, A12 & A15) and new

* Work supported by DOE and US-Japan Collaboration. Authored by Jefferson Science Associates, LLC under U.S. DOE Contract No. DE-AC05-06OR23177. The U.S. Government retains a non-exclusive, paid-up, irrevocable, world-wide license to publish or reproduce this manuscript for U.S. Government purposes.
#geng@jlab.org

PRELIMINARY RESULTS FROM MULTI-CELL SEAMLESS NIOBIUM CAVITIES FABRICATED BY HYDROFORMING *

W. Singer, I. Jelezov, X. Singer, A. Matheisen, DESY, Hamburg, Germany
P. Kneisel#, G. Ciovati, M. Morrone, TJNAF, Newport News, VA 23606, USA

Abstract

The technology of forming multi-cell seamless niobium cavities has been developed at DESY within the European CARE (Coordinated Accelerator Research in Europe) program. Three-cell units have been manufactured successfully and a 9-cell cavity has recently been completed from three sub-sections and has been successfully tested at DESY.

Additionally, we have equipped two 3-cell units – one center unit of a 9-cell cavity and one end-unit – with niobium beam pipes, have tuned these units and carried out cryogenic radio-frequency (RF) tests after standard BCP surface treatments had been applied to these cavities.

In addition, we have taken temperature maps with JLab's two-cell thermometry system to compare with standard electron-beam welded cavities.

This contribution will report about the preliminary cryogenic test results and the T-mapping – this is an ongoing investigation.

INTRODUCTION

Traditionally, rotational symmetric (elliptical) niobium accelerating cavities are fabricated by deep drawing of half-cells and, after machining to the length dimension, they are completed by electron beam welding (EBW) at the irises and the equators. Improved quality control procedures during the mechanical fabrication and the EBW resulted in cavity performances which, in some cases, came close to the fundamental limits of the high purity niobium. However, more recently improved inspection methods revealed that features in the weld and heat affected zone in a multi-cell cavity can and have contributed to limitations in cavity performance [1]. Therefore, electron beam welds have come again under scrutiny worldwide, mainly because the performance goals for cavities for the International Linear Collider (ILC) are quite close to the fundamental limitations of the material and any fabrication defects override the material properties.

Contrary to this experience, seamless cavities have no equator welds (the high magnetic field region in an "elliptical" cavity) and therefore an improved reliability could be expected. Additionally, cavity fabrication costs could be reduced, especially, if the end-groups of an accelerating cavity (these are the parts of the cavity, which are outside the cell structure and provide input coupling capability and higher order mode damping capability) can be flanged onto the cell structure [2]. Seamless cavity fabrication techniques have been pursued in the last years mainly at INFN Legnaro [3] – the chosen method was spinning – and at DESY (hydroforming) [4]. Both methods have produced single-cell cavities with high performance [5]. This contribution reports about an extension of the single-cell work to multi-cell cavities, 3-cell and 9-cell.

CAVITY FABRICATION TECHNIQUE

The hydroforming technique, developed at DESY over several years, has been described in details in previous publications [4-6]. Here we will only summarize the essential steps in the process and describe the extension from the single-cell to the multi-cell hydroforming.

For hydroforming, one starts with a seamless tube of a diameter intermediate between iris and equator. During the computer controlled forming, a two-stage process takes place, namely a reduction of the tube diameter in the iris region and an expansion of the tube in the equator area. Considerations of surface roughness at the iris region for too much diameter reduction and work hardening at the equator for too much expansion determined a tube diameter of 130 mm to 150 mm to be the optimum for 1300 MHz TESLA/ILC type cavities.

The tube diameter reduction at the iris was optimized – after research into different methods such as hydraulic necking, electromagnetic strike necking and spinning – by using a specially profiled ring being moved in radial and axial directions. For this purpose a computer controlled hydraulic machine has been built, which is useable for up to 3-cell cavities.

During hydraulic expansion of the equator region an internal pressure is applied to the tube and simultaneously an axial displacement, forming the tube into an external mold. The hydraulic expansion relies on the use of the correct relationship between applied internal pressure and axial displacement under the assumption that the plastic limit of the material is not exceeded, which would result in rupture. Material uniformity of the tubing and the experimentally determined stress-strain characteristics as well as simulation calculations are essential and have led to a successful development of the hydroforming technology. A hydroforming machine was specially built for the tube expansion. Since no tubing with uniform material properties were commercially available, much effort was invested in researching – in collaboration with industrial partners and scientific institutions – several tube

* This manuscript has been authored by Jefferson Science Associates, LLC under U.S. DOE Contract No. DE-AC05-06OR23177. The U.S. Government retains a non-exclusive, paid-up, irrevocable, world-wide license to publish or reproduce this manuscript for U.S. Government purposes. We acknowledge the support of the European Community Research Infrastructure Activity under FP6 "Structuring the European Research Area" program (CARE, contract number RII-CT-2003-506395).
#kneisel@jlab.org

COAXIAL COUPLING SCHEME FOR FUNDAMENTAL AND HIGHER ORDER MODES IN SUPERCONDUCTING CAVITIES*

J. Sekutowicz, P. Kneisel, G. Ciovati, TJNAF, Newport News, 23606 Virginia, USA
L. Xiao, SLAC, Menlo Park, 94025 California, USA

Abstract

Higher Order Modes generated by a particle beam passing through a superconducting accelerating cavity have to be damped to avoid beam instabilities. A coaxial coupler located in the beam pipes of the cavities provides for better propagation of HOMs and strong damping in appropriate HOM dampers. The whole damping device can be designed as a detachable system. If appropriately dimensioned, the RF currents can be minimized at the flange position. Additionally, the coaxial system also provides efficient coupling of fundamental mode RF power into the superconducting cavity. Compared to presently available solutions for HOM damping, this scheme provides for several advantages: stronger HOM damping, attachable solution, and exchangeability of the HOM damping device on a cavity, less complexity of the superconducting cavity, possible cost advantages.

This contribution discusses modeling, which lead to an optimized layout of a cavity-coupler system and describes* results from the room temperature and first cryogenic temperature measurements .

INTRODUCTION

The coaxial HOM couplers were originally developed for the 500 MHz HERA cavities in 1985 and later in the early 90's they were scaled to 1300 MHz and adapted for the TESLA cavities [1]. The scheme fulfills also the specification for the ILC project, which is the TESLA successor, and can be used for the superconducting cavities in the main accelerator. The coupling device we propose here (Fig. 1) takes advantage of the TESLA HOM damping scheme and combines it with the coaxial fundamental power coupler (FPC) used for the superconducting TESLA (ILC) cavities. In this scheme, all couplers are screened by the inner tube, which is supported by the Nb "donut" (disk) welded to it and to the beam tube. The "donut" is an electric short in the coaxial line, which is formed by the inner and outer tubes, and thus separates electrically two mirrored coupling devices and neighboring cavities. The pair of mirrored coupling devices can be placed between two cavities.

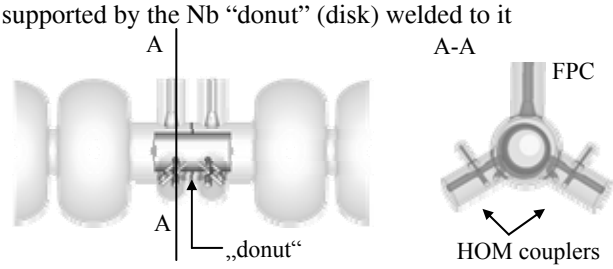

Figure 1: FPC and HOM couplers in two mirrored coaxial coupling devices placed between two cavities (left) and cross-section of the coupling device (right).

Motivation

This coaxial coupling scheme has the following advantages as compares to the standard TESLA scheme:

1. Field asymmetries and kicks from all couplers are minimized
2. The distance between two cavities can be shorter (higher real estate gradient); for the ILC, the difference is 9 cm.
3. The body of the cavity stays cylindrically symmetric, which enables its fabrication by hydro-forming as seamless device.
4. The interior of the coupling assembly and the cavities can be better cleaned before the final assembly.

MODELING AND BENCH RF MEASUREMENTS

Modeling

HOM damping and coupling to the fundamental mode have been modeled by the ACD team at SLAC. The RF model and HOM damping result for the 9-cell TESLA cavity is shown in Fig.2. For the accelerating mode, the computed Q_{ext} for the FP coupler vs. its penetration depth, covered a wide range of values beginning at a lowest value of 10^5.

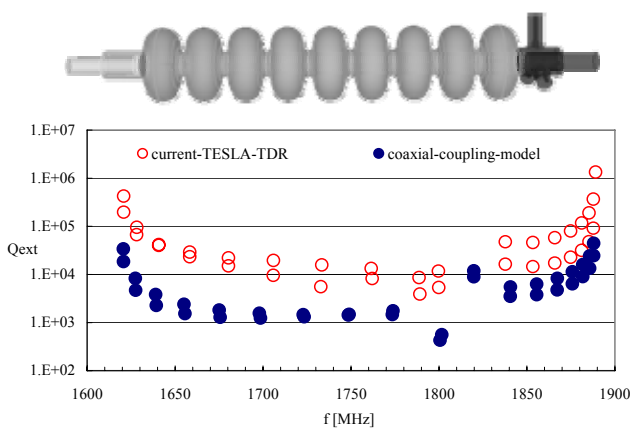

Figure 2: RF-model and damping (Q_{ext}) for the first two dipole passbands for the TESLA structure. The diagram compares the standard TESLA-TDR damping scheme with the scheme discussed in this paper.

Bench Measurements

The second step in the verification of the concept was the HOM damping and FM coupling measurements for

* This manuscript has been authored by Jefferson Science Associates, LLC under U.S. DOE Contract No. DE-AC05-06OR23177. The U.S. Government retains a non-exclusive, paid-up, irrevocable, world-wide license to publish or reproduce this manuscript for U.S. Government purposes.

TWISTED STRUCTURES AND THEIR APPLICATION AS ACCELERATING STRUCTURES*

J. Wilson, Y. Kang, SNS, Oak Ridge, TN, USA
A.E. Fathy, EECS Department, University of Tennessee, Knoxville, TN, USA

Abstract

Normally, reactive loading is employed to construct slow-wave accelerating cavities. However, their non-uniform cross section, difficult machining, and complicated welding or brazing processes increase the total cost. Although straight hollow waveguides can only support faster-than-light propagation, twisted waveguides can support propagation at or below c. Because twisted structures have a uniform cross section in the transverse plane, they offer several potential advantages over dielectric loaded structures or other types of periodic structures. Of particular interest are twisted structures whose longitudinal cross section has been selected to resemble well-known accelerating structures, such as the disk-loaded accelerating structure and the TESLA type elliptical cavity. Comparisons are drawn between these conventional cavities and their twisted counterparts in terms of the phase velocity and dispersion relationship. The accelerating modes are found and analyzed, and R/Q's are calculated.

INTRODUCTION

One very important consideration in the effective acceleration of particle beams is matching the velocity of an electromagnetic wave to the velocity of the particles traveling slower than c.

A conventional method for slowing the wave that is more well-suited for superconducting accelerators is to use a corrugated structure with nonuniform cross section. However, such corrugated structures have drawbacks. First, manufacturing is difficult due to the necessecity of very difficult machining and welding to create the smooth finish necessary. Secondly, trapped modes can exist in the structure because of the presence of stop bands in the dispersion characteristics. Finally, such corrugated structures tend to have zero group velocity when operating at $\pi-$mode, which causes problems for mode separation.

Therefore, we consider a uniformly twisted waveguide as a potential accelerating structure, consisting of a uniform cross section twisted about the beam axis. It has long been known that such a twisted structure can be a slow wave structure, and a preliminary investigation into the feasibility of twisted guides as accelerating structures was undertaken by Kang [1]. In this paper, we show that a twisted waveguide accelerating structure can be used to circumvent problems relating to trapped modes and mode separation. Also, tuning for a twisted structure could be done for the whole structure at once.

Any non-circular cross section will generate a nontrivial shape when twisted along the center axis, which has the potential to produce slow-wave effects. However, this paper concentrates on a few simple representative cross sectional shapes in order to describe the general nature of the slow-wave accelerating characteristics: a twisted structure whose longitudinal cross section is identical to that of a disk-loaded accelerating cavity, and a twisted structure with an elliptical cavity-like longitudinal cross section.

PROPAGATION CHARACTERISTICS OF TWISTED STRUCTURES

When selecting a cross sectional shape for a twisted waveguide, an interesting choice would be one that would produce a structure with similar longitudinal cross section to an existing accelerating structure. The first structure we considered has the shape shown in Fig. 1. This figure shows that when this particular cross section is twisted, the shape of the longitudinal cross section is identical to a disk loaded structure. Table 1 gives relevant information for this structure based on simulation results.

Fig. 2 shows a CST Microwave Studio [2] simulation of the electric field in such a twisted structure subject to a periodic boundary condition. The simulation results clearly indicate a TM mode which could be useful for particle acceleration. Such a twisted analog can also be considered for the medium β SNS superconducting cavity. Although the details are not given here, Fig. 2 shows the electric fields for such a structure. A clear similarity is seen between the fields of these twisted structures and the fields typically seen in rotationally symmetric (non-twisted) corrugated accelerating cavities.

Table 1: Parameters for twisted analog of disk-loaded accelerating cavity

Parameter	Value	Unit
Frequency	2.84	GHz
Inner radius	4.13	cm
Outer radius	5.493	cm
Twist rate	89.76	Radians/m
Notch angle	1.048	Radians
Phase advance per cell	$\frac{2\pi}{3}$	Radians
Phase velocity	2.98×10^8	m/s

* This work has been sponsored by ORNL-SNS. The Spallation Neutron Source is managed by UT-Battelle, LLC, under contract DE-AC05-00OR22725 for the U.S. Department of Energy.

PRELIMINARY DESIGN OF THE SLOW CHOPPER FOR THE SPIRAL 2 PROJECT

A. Caruso, A. Longhitano, D. Rifuggiato, G. Gallo, T. Spartà, E. Zappalà INFN/LNS, Catania, Italy
M. Di Giacomo, CEA/GANIL, Caen, France

Abstract

The Spiral 2 LEBT line uses a single chopper situated in the line section common to protons, deuterons and A/Q=3 ions. The paper describes the design and the test of the power circuits, based on standard components and working up to 10 kV, at a 1 kHz repetition rate.

THE LOW ENERGY LINE

The low energy (LEBT) line of the Spiral 2 driver is designed to transport CW, high intensity, beams of protons (5mA), deuterons (5mA) and ions (1mA) with m/q=3 to the radiofrequency quadrupole (RFQ). The RFQ input energy is 20 keV/A and source voltages of 20, 40 and 60 kV are used for the 3 kind of particles. As shown in Figure 1, the chopper is located at the beginning of the common section just before the beam stop.

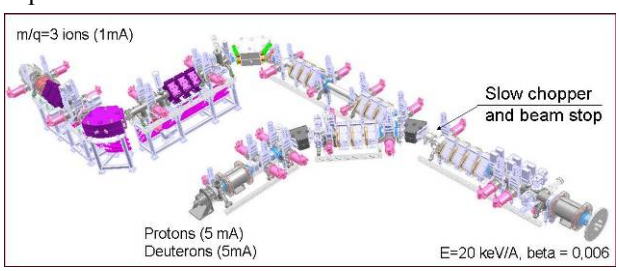

Figure 1: The injector low energy lines and the slow chopper position.

The chopper will be used to progressively increase the beam power during accelerator tuning, to rapidly remove the beam in case of failure detection, to avoid hitting the wheel spokes of rotating targets similar to the one shown in Figure 2 (FULIS or S3 experiences).

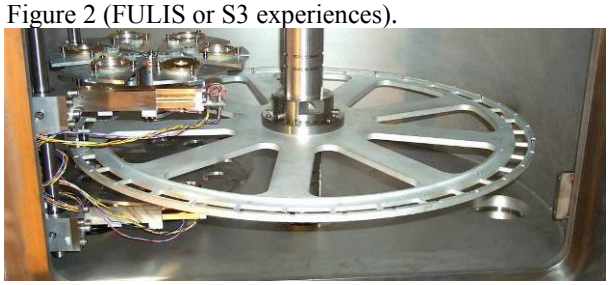

Figure 2: FULIS rotating target wheel (courtesy of C. Stodel).

CHOPPER REQUIREMENTS

Accelerator tuning is performed at quite low frequency. Due to the high beam power: 200 kW, a very large range of duty cycles will be used, starting from very low fractions (10^{-4}). The rotating target asks for pulse repetition rates around 1 kHz. In both cases rapid transition times are required to avoid fractions of beam neither accelerated nor deviated to be lost through the linac.

The chopper voltage depends on the ion source voltage on the distance and length of the plates and on the beam stop location. Due to the LEBT line architecture and to the current intensity, the beam transversal section at the chopper location is quite large and relevant voltages have to be applied to the electrodes to compensate their distance.

In our case, the beam section has a diameter of 76 mm, the electrode hard-edge length considered in the beam dynamics simulations is of 160 mm, deflection at the end of the plates is of 10 mm. and a total deviating voltage of 17 kV has to be applied. Transient times for the pulse have to be shorter than 100 ns, and an amplitude stability of few percents is required.

High reliability and easy maintenance are also strong requirements of the devise.

ELECTRODE GEOMETRY

The preliminary geometry shown in Figure 3 was designed to have a flat transversal field and to produce field maps for beam dynamic simulations. Two cases where simulated: a) one plate positively biased and one grounded and b) both plates biased with opposite voltages but no differences where observed.

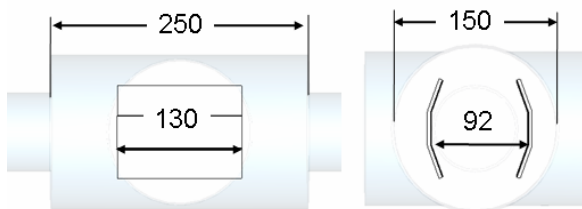

Figure 3: The simulated geometry, plate bending angle is 20°.

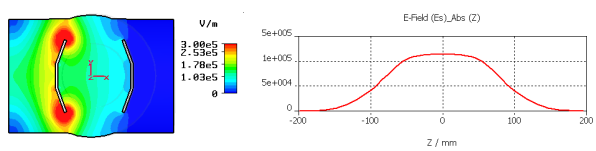

Figure 4: Electric field on the transversal plane and on the beam axis.

The first case, with positive voltage, was chosen, because it would let easier water cooling of the ground electrode if some beam was eventually lost. The deflection plane is horizontal because the beam section is

DESIGN OF THE MEBT REBUNCHERS FOR THE SPIRAL2 DRIVER

M. Di Giacomo, JF Leyge, M. Michel, P. Toussaint, GANIL, Caen, France

Abstract

The SPIRAL2 project uses room temperature RFQ and rebunchers and a superconducting linac to accelerate high intensity beams of protons, deuterons and heavier ions. All cavities work at 88 MHz, the beta after the RFQ is 0.04 and 3 rebunchers are located in the MEBT line, which accepts ions with A/q up to 6. The paper describes the RF design and the technological solutions proposed for an original 3-gap cavity, characterised by very large beam holes (60mm) and providing up to 120 kV of effective voltage.

INTRODUCTION

The SPIRAL2 [1] driver presents a quite long medium energy beam transport line (Figure 1) to insert a second beam line from a future RFQ for heavier ions: q/a=1/6, a single bunch selector and the corresponding beam dump. The line is seven and a half meters long and is equipped with three rebunchers to keep the beam longitudinal phase dimension.

Room requirements for all the devices are very tight and the cavities have to be compact on the beam axis direction. Moreover, the beam transverse section can be quite large in the line, then the beam aperture in the cavity drift tubes is much longer than the tube length and the gap electric fields interact with each other. The Transit Time Factor (TTF) is consequently quite low and voltages higher than usual have to be applied on the electrodes to obtain the required effective voltage.

REBUNCHER REQUIREMENTS

The first and the last cavities will work at an effective voltage of 120 kV with the heaviest ions while the second one will work at 60 kV CW only. For the RFQ initial commissioning, only the first cavity will be installed before the diagnostic test bench and pulsed voltages up to 190 kV will be used for emittance measurements.

The line beta is 0.04 which is a reasonable figure with respect to the injector working frequency of 88,0525 MHz.

RF DESIGN

To keep the longitudinal length of the cavity as small as possible and to handle reasonable values of RF power and electric field, a 3-gap structure has been chosen. The double quarter wave resonator of Figure 2 has been preferred to the more usual split ring, to have right stems with more homogeneous loss, easier cooling opportunities and better alignment guarantees. The central part of the tank has a square section to host the beam ports and the tuner (trimmer) while the rest of the tank is cylindrical. The stems are conical to progressively increase the diameter from the drift tube end (where it couldn't be bigger) to the short circuit. The drift tubes are spaced in order to obtain the required beta value and to limit the maximum electric field.

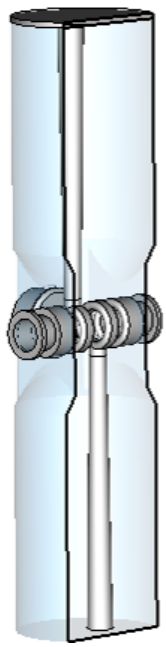

Figure 2: The RF structure.

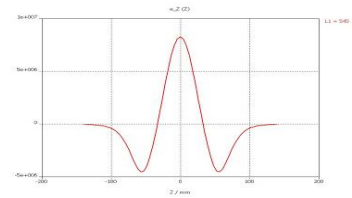

Electric field on the beam axis (@1 joule of stored energy)

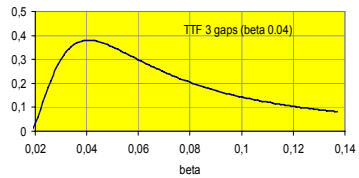

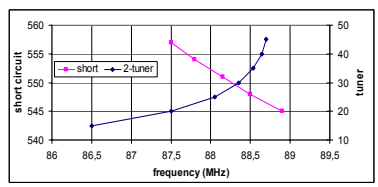

Tuner and shorting plate responses

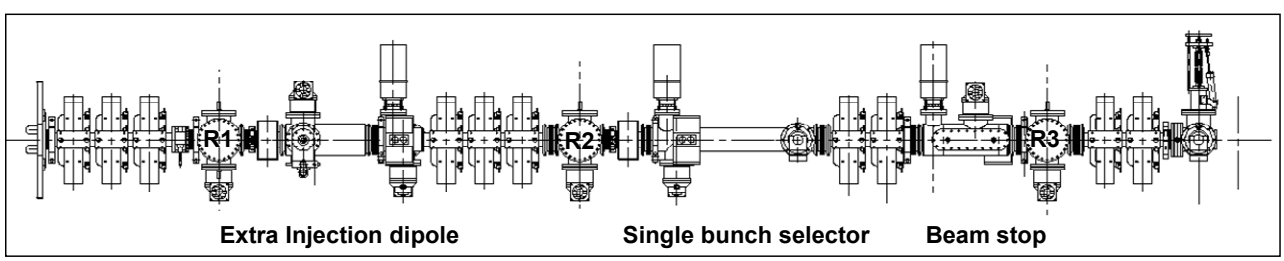

Figure 1: The medium energy beam transport line.

RF POWER AMPLIFIERS FOR THE SPIRAL 2 DRIVER: REQUIREMENTS AND STATUS

Marco Di Giacomo, Bernard Ducoudret, GANIL, Caen, France

Abstract

The Spiral 2 project [1] uses a RFQ, normal conducting rebunchers and a superconducting linac to accelerate high intensity beams of protons, deuterons and heavier ions. All cavities work at 88 MHz, are independently phased and powered by amplifiers whose power ranges from few kilowatts to 250kW. The paper describes the amplifier requirements, the proposed solutions and their status.

INTRODUCTION

The search of cost effective solutions has been one of the major aims of the project and studies about the RF power systems have begun since the very beginning phases. Concerning the linac frequency, the possibility of taking advantage of all developments from the FM market in the low level and power electronics, and the amount of RF power required by RFQ cavities at higher frequencies were among the major issues that lead to the choice of 88.0525 MHz.

Once the driver frequency was defined, two ranges of amplifiers were required: above 150 kW for the RFQ cavity and up to 20 kW for the linac cavities and the rebunchers of the medium energy line.

The solid state technology was investigated and definitely chosen for the second range. Security issues, modularity, quick trouble shooting, life time, have been privileged as already done in other accelerator projects and commercial fields.

Industrially available power at competitive cost being increasing quickly, the hope to have the same technology for the RFQ amplifiers too was kept for a while, but recently abandoned due to the amount of power finally required by the cavity.

RFQ AMPLIFIER

Cavity Requirements

Power loss in the RFQ cavity has been continuously upgraded as the contribution of different elements was calculated. Design study simulations, based on a 3D model of a 1-meter section including extremities, and 2D simulations of the other sections with changing beam aperture, had given some 130 kW. Power test on the prototype cavity (corresponding to the 3D model) revealed a Q factor 10% lower than expected which implies a correspondent increase of power loss. More recently, in the framework of the study for tuning procedure, manufacturing and positioning tolerances of the poles have been simulated and losses due to extreme tuner positions have been calculated. According to latest estimation, total loss in the cavity could reach some 180 kW [2].

Another important request from the RFQ team was to respect the quadrupolar symmetry of the RF structure. It was then decided to drive the cavity through four coupling loops, placed in the four quadrants of the same section as shown in Figure 1b.

Choice of the Amplifier Architecture

Manufacturing considerations, as the cost of the power tube and the number of potential manufacturers, influenced the decision of using four different amplifiers too.

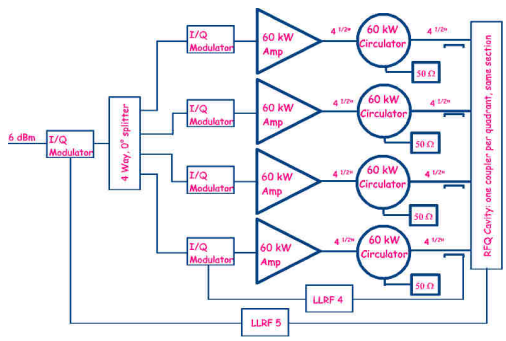

Figure 1a: Four amps and circulators scheme. The scheme shows the fast I/Q RFQ feedback loop (LLRF5) and one of the four local slower loops (LLRF4) to control the combining efficiency.

Up to several tens of kW, commercial, robust and non expensive power triodes working in the FM bandwidth are available and several broadcast companies are equipped with the ancillary systems for power tests. Behind the 30-40 kW threshold, the number of either power devices and potential manufacturers quickly decreases.

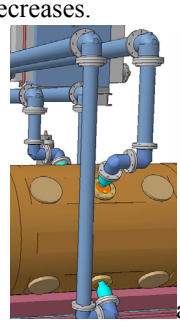
a)


b

Figure 2: The four lines combined into the cavity and a 60 kW circulator.

Driving a cavity with more than one amplifier can easily be source of oscillation problems, unless they are isolated by circulators. Circulators present some percent of RF loss but match the amplifier load and handle the reflected power. The total balance is then highly positive as one doesn't need to oversize the amplifier power stage (tube and power supply) to work in mismatched conditions, like usual in accelerator applications.

OPTIMIZATION OF SPIRAL-LOADED CAVITIES USING THE 3D CODE OPERA/SOPRANO*

M. Schuh[1,2], K.U. Kühnel[2], C.P. Welsch[2−4]
[1]CERN, Geneva, Switzerland
[2]MPI for Nuclear Physics, Heidelberg, [3]GSI, Darmstadt, and [4]University of Heidelberg, Germany

Abstract

Rebunching cavities are today routinely used for matching a beam of charged particles between different accelerator structures, and thus optimizing the overall transmission and beam quality. At low resonance frequencies, unnecessary large dimensions of these cavities can be avoided by using spiral-loaded cavities. The optimization of these structures is a complicated process in which a wide range of different parameters have to be modified essentially in parallel. In this contribution, we investigate in detail the characteristics of a model structure with the 3D code OPERA/SOPRANO. This includes the optimization of the structure in terms of the spiral geometry for a given resonance frequency, the investigation of power losses on the inner surfaces, and the possibility of cavity tuning by means of a tuning cylinder.

INTRODUCTION

Spiral-loaded cavities are today routinely used in many accelerator facilities around the world [1], [2]. Mainly as buncher and post accelerator elements to vary the temporal profile and the final energy of the beam [3]. The big advantage of this structure is its compact size as compared to quarter-wave resonators. These small structures allow changing the energy as well as the velocity distribution in a beam very efficiently and thus providing an efficient matching between different sections of an accelerator or shaping of the longitudinal beam profile in front of an experiment. Different types of spiral-loaded cavities have already been realized in the past, differing in number of accelerating gaps and in the winding of the spiral arms.

In this contribution, we consider a single arm normal conducting structures as it was already built up [4]. It consists of a cylindrical external tank and three drift tubes on the symmetry axis. The middle drift tube is attached to the spiral arm. A model of this structure is shown in Fig.1 and the design parameters for the initial model are found in Tab.1. A particularity of this type of structure is the ratio of the radii, where the small radius equals half of the large radius. In order to efficiently accelerate charged particles in such a structure, the distance between the midgaps needs to be an integer multiple of half an RF period. The geometry of this structure can be described by the following equation

$$L = \frac{n\beta\lambda}{2} \qquad (1)$$

* Work supported by GSI and the Helmholtz Association of National Research Centers (HGF) under contract number VH-NG-328

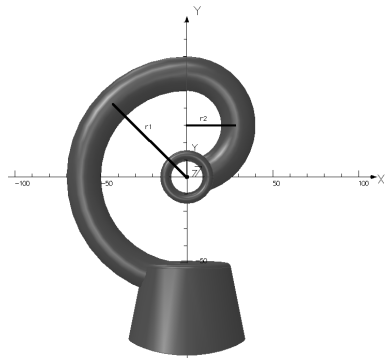

Figure 1: Model of the spiral arm with hidden tank walls and marked spiral radii.

where $\beta = \frac{v}{c}$, λ the wavelength and L is the distance between the middle of two gaps which is also referred to as the cell length.

Table 1: Design values of cavity tank and spiral arm

Design Parameter	Size [mm]
Cavity length	150
Cavity radius	100
Cavity wall thickness	5
Drift tube length	60
Drift tube thickness	10
Gap width	15
Aperture radius	10
Blend radius	2.5
Spiral radius r1	60
Spiral radius r2	30
Spiral thickness	20

In the frame of this study, we built up a model of a well-known cavity, which was then simulated and analyzed by using the different modules of OPERA [5]. This allowed us to benchmark the results of this code with previous data and results from other simulation codes. In our investigations, we used the eigenvalue solver SOPRANO to determine the relevant resonance frequencies. The solver can be used to find the different resonance modes of a cavity structure with either perfect conducting boundaries or realistic metal surfaces by solving the Helmholtz equation via the Galerkin method and subsequently solve the sparse generalized eigenvalue problem.

DEVELOPMENT OF A HIGH-PRESSURE CHEMICAL ETCHING METHOD AS A SURFACE TREATMENT FOR HIGH-FIELD ACCELERATING STRUCTURES MADE OF COPPER

Hiromitsu Tomizawa, Tsutomu Taniuchi, Hideki Dewa, Akihiko Mizuno, Hirofumi Hanaki,
Accelerator Division, Japan Synchrotron Radiation Research Institute (JASRI/SPring-8),
Kouto, Sayo-cho, Sayo-gun, Hyogo 679-5198, Japan

Abstract

The acceleration gradient is limited by rf breakdown in accelerating rf structures, as well as by the surface condition of the inner wall. Surface treatment is an important technique for achieving the maximal acceleration gradient of accelerating rf structures. We chose chemical etching as a surface treatment method for accelerating rf structures made of copper (OFC). A maximum cathode surface field of 183 MV/m was achieved for an S-band (2856 MHz) pillbox-type single-cell rf gun cavity with this surface treatment under an rf-conditioning elapsed time of 1.9×10^7 shots (21 days) in 2004. Furthermore, we developed a high-pressure chemical etching method for complex inner structures in 2006. The results showed that the higher the pressure, the higher the cathode surface field (162 MV/m; 6 atm).

INTRODUCTION

We have been developing a surface treatment method for optimizing the surface condition of the inner wall in order to achieve a maximum cathode surface field of ~200 MV/m. The acceleration gradient is limited by the rf breakdown in accelerating rf structures, as well as by the surface condition of the inner wall. Surface treatment is an important technique for achieving the maximal acceleration gradient in accelerating rf structures. It is necessary to realize chemically noncontaminated and physically smooth surfaces. In accelerator fields, oxygen-free copper (OFC) is widely used as a base material for normal conducting accelerators. Previously, we chose chemical etching as a surface treatment method for accelerating rf structures made of copper after several failed attempts involving high-pressure pure water rinsing [1]. In order to study rf breakdown and the effects of surface treatment [2], we used an S-band (2856 MHz) pillbox-type single-cell rf gun cavity. The highest cathode surface field (183 MV/m) of the rf gun cavity was achieved with this surface treatment under an rf-conditioning elapsed time of 1.9×10^7 shots (21 days) in 2004 [3]. The SPring-8 rf gun has been operating with the world's highest gradient of 190 MV/m [4]. This indicates that our treatment is remarkably effective in improving the properties of the inner cavity surfaces, which are made of copper (OFC). Furthermore, we developed a high-pressure chemical etching method for achieving more complex inner structures in 2006 [5]. Using a cartridge-type revolver photocathode rf gun [6], high-field experiments were performed with cathode plugs subjected to chemical etching at different pressure conditions. We found that the higher the pressure, the higher the cathode surface field. Here, we report these novel results regarding the highest gradient, which were obtained by using test copper (OFC) samples treated with high-pressure chemical etching.

CHEMICAL ETCHING AND ITS OPTIMUM CONDITIONS

Chemical Etching

Chemical etching entails a chemical reaction between an acid and a metal. We used an etching solution composed of sulfuric acid (H_2SO_4) and hydrogen peroxide (H_2O_2), each at 2 wt% standard concentration, in order to make the processing time loss negligible in relation to the etching rate at room temperature.

Investigation of Optimum Conditions for Etching

Before etching, a copper test piece was dipped in Neos CM200C (5 wt%) solution at 40°C for 1.5 h as a degreasing preprocess. After rinsing in tap water for 5 min at room temperature, the copper test piece was etched with shaking to remove hydrogen bubbles from its surface. The etched copper test piece was then rinsed in pure water and then in ultrapure water for 1 min each at room temperature.

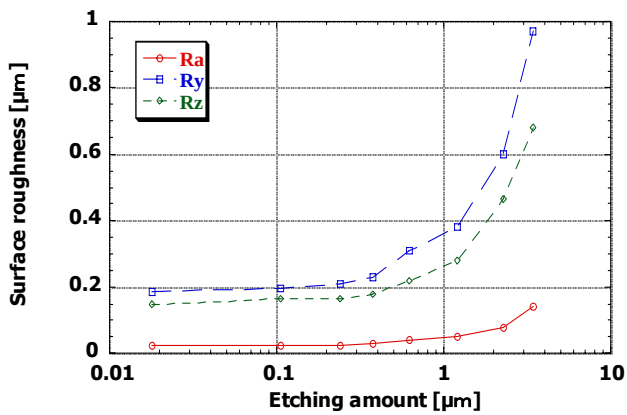

Figure 1: Dependence of the surface roughness on the etching amount in oxygen-free copper (OFC): After degreasing, Ra: 0.02 μm, Ry: 0.19 μm, Rz: 0.17 μm.

THE STATUS OF NEXTEF: THE X-BAND TEST FACILITY IN KEK

S. Matsumoto*, M. Akemoto, S. Fukuda, T. Higo, N. Kudoh, H. Matsushita, H. Nakajima,
T. Shidara, K. Yokoyama, M. Yoshida, Accelerator Lab, KEK, Tsukuba, Ibaraki 305-0801, Japan

Abstract

Nextef is the 100MW-class X-band (11.424GHz) RF test facility in KEK. By combining the power from two klystrons, 100MW RF power is produced. While the facility was originally planned to conduct fundamental research programs of RF breakdown issues, it will be used as the one of the high power station for new international research collaboration on the study of future high gradient linear accelerators. A series of high gradient test structures are being tested at the facility. The gradient is as high as 100MV/m.

INTRODUCTION

XTF (X-band Test Facility) was the test facility for X-band accelerator structures in KEK which had run during 2003~2007. It was eventually evacuated in May 2007 due to the termination of R&D program of normal conducting linear collider (LC) project. Most of the key equipments and essential components of XTF were selected and moved into the "new place", KEKB Injector test area, to be reassembled them as Nextef (stands for NEw X-band TEst Facility), based on the plan originally proposed to use this new facility for small size fundamental research programs for the development of high gradient normal conducting linear accelerator and its applications. The new place for Nextef is chosen since the facility can be jointly operated with KEKB Injector. This enables 6,000 hrs of annual operation of this facility.

In December 2006, a decision was made on Compact Linear Collider (CLIC). They optimized the operating frequency of the main linac from 30GHz to 12 GHz and relaxed the accelerating gradient from 150MV/m to 100MV/m [1]. In order to establish the feasibility of this parameter choice, we organized new international research collaboration with CERN and SLAC on the X-band accelerator structures in June 2007 [2].

To demonstrate such a high gradient (~100MV/*m*) accelerator structure, at least several tens MW RF power is necessary and Nextef meets this requirement. Although the construction of Nextef was still ongoing when the collaboration started, KEK has agreed to run this new facility for testing a series of X-band structures (T18 series) newly developed and prepared in this collaboration. There have been some active X-band test facilities at SLAC and Nextef plays a role of their new counterpart in this collaboration research.

The commissioning of Nextef has been done and the facility currently runs for its first testing of the structure, named T18_vg2.4_Disk #2 shown in Fig.1. As we will see below, we will conduct the tests of T18 structures at this facility for next two years. Our fundamental research program originally supposed to be done here, such as the study of high gradient RF breakdowns in narrow waveguides [3], is now being done at another X-band test station (Klystron Test stand). It is an individual 50MW RF station driven by a single klystron, located adjacent to Nextef, originally prepared for the X-band klystron tests. Although the available power is half to that of Nextef, this station is usable for small size experiment.

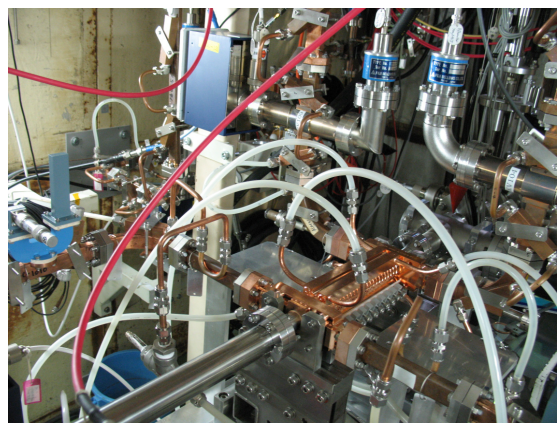

Figure 1: T18_vg2.4_Disk installed in Nextef.

FACILITY

The configuration of Nextef is shown in Fig.2. The modulator drives two klystrons simultaneously. By combining the power from two klystrons, the maximum RF power of 100MW for 400ns can be produced. We employ twin PPM (Periodic Permanent Magnet) klystrons. The structures to be tested are installed in the bunker. The distance from the klystrons to the test area is about 16*m* [4]. About half of the distance, a circular waveguide is used to reduce the power loss. Two SLAC mode converters are mounted at both ends of the circular waveguide to transform rectangular WR90 TE10 mode ↔ circular TE01 mode. Measurement shows there is about 25% power loss in the power transmission. The specification of the facility is given in Table.1. For the details of each component, refer to [5].

Table 1: Nextef Nominal Specifications

Frequency	11.424GHz
Max power production	100MW
Max power for test*	75MW
Pulse width	400ns
Repetition rate	50pps

* 25% power loss in the waveguide.

*shuji.matsumoto@kek.jp

STATUS OF RF SOURCES IN SUPER-CONDUCTING RF TEST FACILITY(STF) AT KEK

S. Fukuda#, M. Akemoto, H. Hayano, H. Honma, H. Katagiri, S. Kazakov, S. Matsumoto, T. Matsumoto, S. Michizono, H. Nakajima, K. Nakao, T. Shidara, T. Takenaka, Y. Yano, M. Yoshida, KEK, Ibaraki, 305-0801, Japan.

Abstract

The super-conducting RF test facility (STF) at KEK has been functional since 2005, and the STF phase-I, which involves the testing of a cryomodule with four superconducting cavities, is now under way. Furthermore, KEK will conduct the S1-global test and the STF-II project in the future. The S1-global test aims at evaluating the performance of the superconducting cavities provided by Japan and the international collaborators, USA and Europe. The phase-II project aims at testing RF unit of the proposed ILC. In this paper, we describe the current status of the RF sources in the STF phase-I and the development of RF source for future projects.

INTRODUCTION

The superconducting RF test facility (STF) at KEK comprises two phases, as shown in figure 1, and has been operational since 2005 [1]. The STF Phase-I consists of a cryomodule with a four-cavity structure having a gradient of 35 MV/m and is being tested. In Phase-I, the high level RF (HLRF) team is planning to install two types of power distribution systems (PDSs) and conduct the associated R&D. The low level RF (LLRF) team is planning to test the digital feedback with vector sum control. The STF Phase-II employs one RF unit, which is similar to the ILC baseline configuration design (BCD) layout. Phase-II employs beam acceleration to evaluate the entire linac system. The construction of STF-II is delaying and it is scheduled from 2012 to 2015. Recently, an S1-global phase was proposed; this phase will be completed before Phase-II of the STF. The S1-global phase will include two cryomodules with eight super-conducting cavities provided by Japan and international collaborators, USA and Europe. A different RF PDS scheme is tried to be used for evaluating the performance of the cavities, and currently, our efforts are focused on meeting the requirement to optimized operation of the cavities. In this paper, we describe the current status of the RF sources in the STF-I phase and the preparation of RF sources for future projects.

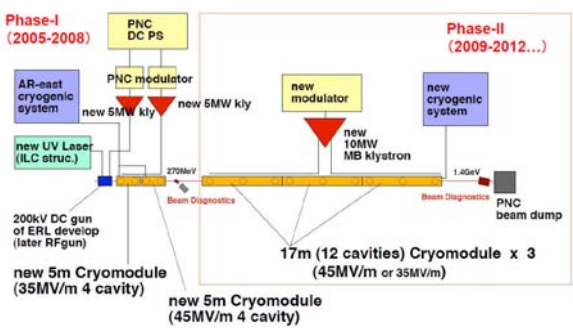

Figure 1: STF layout.

#Shigeki.fukuda@kek.jp

HLRF

Modulator and Klystron

The current STF RF sources comprise two stations. In the first station, a bouncer-type insulated gate bipolar transistor (IGBT) modulator is used along with a pulse transformer with a step-up ratio of 1:6. A 5-MW Thomson klystron, TH2104C, is used in this station; this klystron was previously used in the JAPAN HADRON PROJECT (JHP). The maximum available power of this station is 3.0 MW [1]. The power limitation is come from fast over-voltage protection for the IGBT switch which comprises 36 IGBT devices connected in series. The maximum voltage applied to a IGBT in the switch comes when the switch is turned off for a klystron gun spark, and must not exceed the maximum rating of 1200 V. The maximum IGBT switch operating voltage is 21.5 kV at the primary of the pulse transformer, which corresponds to a klystron voltage of 120 kV[2]. The RF source used in station no. 1 is utilized for conducting coupler processing tests and the STF-I experiment. Station no. 2 uses another bouncer-type IGBT modulator with a pulse transformer having a step-up ratio of 1:15 [3]. A 5-MW Thales klystron, TH2104A, is used in this station. The performance of the bouncer circuit in both modulators was excellent and a flat-top of less than ±0.8% was achieved in both modulators. A breakdown failure of the IGBT modulator in station no. 2 occurred due to a water leak in the pulse transformer; therefore, we have been checking the protection system for the shorting the undesired load ever since. The layout of the STF is shown in figure 1. We will introduce a third modulator and a 10-MW multi-beam klystron in the STF phase-II. We will select this modulator from two candidate modulators—the bouncer-type modulator and a Marx modulator.

PDS for STF-I

Figure 2: Tree type PDS connected to cryomodule.

CHARACTERISTICS OF DIFFERENT MATERIALS ON HIGH-GRADIENT EXPERIMENTS

K. Yokoyama#, T. Higo, S. Fukuda, S. Matsumoto, Y. Higashi, N. Kudoh, Y. Watanabe,
KEK, Ibaraki, Japan

Abstract

RF breakdown is one of the major problems encountered in the development of accelerating structures that operate at high fields since the acceleration field is limited by the damage caused to metal surfaces. We examine electrical discharge characteristics such as breakdown rates and conduct surface observations of various materials in order to investigate the possibility of the stable operation of accelerating structures for high-field accelerations; a similar fundamental research has also been conducted at CERN and SLAC [1, 2,]. High-gradient RF breakdown studies have been in progress at Nextef (New X-band Test Facility at KEK) since 2006 [3, 4, 5]. In order to investigate the characteristics of various materials at high-gradient RF breakdown, we have performed high-gradient experiments by using narrow waveguides having a field of around 200 MV/m at a power of 100 MW. Copper (OFC) and stainless-steel (AISI-316L) waveguides were tested in order to perform high-gradient experiments at Nextef. The result of the experiment conducted at XTF (Old X-band Test Facility at KEK) suggested that the stainless-steel waveguide had a better performance than the copper waveguide, and it exhibited a lesser number of RF breakdowns at a higher electric field. This paper reports the results of breakdown rates and observations of the surface of stainless-steel waveguide subjected to high-gradient experiments.

HIGH-GRADIENT EXPERIENTS

Narrow Waveguide

A narrow waveguide was designed to obtain a group velocity of around 0.3 c, which is used to drive an LC accelerating structure, and a field gradient of approximately 200 MV/m at an RF power of 100 MW at the centre, as shown in Fig. 1. The geometry was transformed from the X-band rectangular waveguide (WR90). The height and the width were reduced from 10.16 mm to 1 mm and from 22.86 mm (λ_g ~ 32.15 mm) to 14 mm (λ_g ~ 76.59 mm), respectively. A narrow waveguide was constructed from four parts in the manufacture. After annealing in a hydrogen furnace, the narrow waveguide was processed by milling. The parts were chemically polished in an acid solution by 10 μm, following which they were brazed in a hydrogen furnace. A narrow waveguide having a voltage standing wave ratio (VSWR) of less than 1.1 is required for our experiments.

#kazue.yokoyama@kek.jp

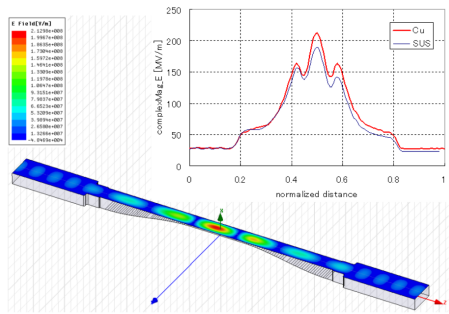

Figure 1: Electric field in a narrow waveguide at an input power of 100 MW obtained by the HFSS calculation.

Experimental Setup

The setup for the high-gradient experiment is shown in Fig. 2. RF power is supplied to the narrow waveguide from a PPM-focused klystron that is operated at 11.424 GHz with a pulse width of 400 ns, pulse repetition rate of 50 Hz, and peak output power of approximately 50 MW. Transmitted and reflected RF waveforms are observed for breakdown events. An RF pulse is detected by using a crystal diode and a digital oscilloscope is used to calculate the power, VSWR, and power loss. All RF pulses are measured, and the digital data for 10 successive pulses is saved in order to analyze the RF waveforms when some interlock controls such as HV, Trig, and RF are tripped. In order to distinguish a breakdown in the narrow waveguide from one that occurs at another location, photomultipliers (PMTs) and acoustic sensors are placed along the waveguide.

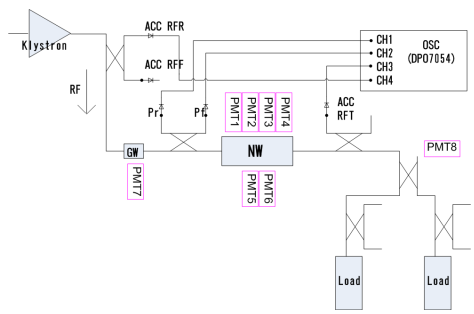

Figure 2: Setup of a high-gradient experiment conducted at Nextef.

During waveguide processing, the RF pulse width is increased from 50 ns to 400 ns, and an RF power of up to 50 MW at a repetition rate of 50 pps is supplied. The increase in the output power and the duration of incremented power are controlled by a computer in accordance with the past processing history depending on the experienced power and the pressure. When the pressure in the waveguide increases, the processing power

IMPROVEMENT IN THE ACS CAVITY DESIGN FOR THE J-PARC LINAC ENERGY UPGRADE

H. Ao*, K. Hirano, H. Asano, T. Morishita, A. Ueno, K. Hasegawa, J-PARC, JAEA, Ibaraki, Japan
F. Naito, M. Ikegami, Y. Yamazaki, J-PARC, KEK, Japan, V. Varamonov, INR, Moscow, Russia

Abstract

The ACS is the accelerating structure for the J-PARC Linac from 190-MeV to 400-MeV. The mass production of the ACS with a tight time schedule is now an issue. This paper mentions two main issues. The first one is that the coupling slot machining especially needed much long time on the fabrication process. We simplify the finishing of the coupling slot, comparing the surface roughness and the machining time. From the low-level measurements with the test cells, the simplified slot machining is judged to be acceptable for the practical cavity. The second one is that the coupling mode frequency has about 0.5 MHz error after the final brazing, because that the frequency shifts by the brazing are not stable. Thus, we consider the coupling mode frequency tuning by the fixed tuner after the final brazing. The equivalent circuit analysis shows that the -0.5 MHz accelerating mode error and +1 MHz coupling mode error brings the 3.7 % electric field error under the correction with the 12 coupling cells.

INTRODUCTION

The ACS (Annular-ring Coupled Structure) cavities were under development for the J- PARC Linac [1, 2] from 190-MeV to 400-MeV. We have fixed the cavity specification, taking into account the results of the high-power conditioning [3] and the fabrication experience.

The mass production of the ACS with a tight time schedule is now an issue, since the user community strongly requests the beam power upgrade as early as possible. Therefore, the design and the fabrication process of the ACS cavity have been reexamined on the basis of the experience, stored during the course of the fabrication and the tuning of the prototype ACS tanks.

Here, we also discussed about the key issues on the mass production with a manufacturer. The cavity shape, that required complicated machining, was simplified to some extent, while the frequency tuning strategy was reconsidered to reduce the production period.

The present paper mentions two main issues about the recent progress of the ACS developments. The first one is the simplification of the coupling slot machining, and the other is the coupling mode frequency tuning after the final brazing. The following sections describe these results in detail with the background of these issues.

* hiroyuki.ao@j-parc.jp

SIMPLIFY COUPLING SLOTS

Background

The ACS cavity consists of many half-cell parts (cell), and vacuum brazing connects these cells. The 1300 cells are required for mass production (18.5 modules×2 tanks×17 cells×2 parts/cell=1258), so that it is very important to reduce the machining time of the cell.

On the cell machining process through the several R&D modules, the coupling slot machining especially needed much long time. Although the modules brought good results through the high-power conditioning, one slot machining required 3 hours 20 minutes with a 5-axis processing machine, thus one cell (4 slots) needed more than 13 hours only for the slot machining.

We, therefore, simplify the finishing of the coupling slot, comparing the surface roughness and the machining time for each machining step.

The four test cells are machined with the reexamined process. And then, the RF properties are measured to compare frequencies and Q-values before and after the simplification.

Machining Process

The new slot machining (See Fig.1) takes only 46 minutes that is much shorter than the original of 3 hours 20 minutes. The total machining time with a 5-axis processing machine will be reduced from 1.5 day/cell to 1 day/cell. It means that, at a rough estimate, the 1300 cells require two years and two months. It seems that it is the acceptable period for the mass production.

In this new machining process, we also restrict the movement of the tool within XYZ-axes and a rotation around the beam-axis. This restriction for the 5-axis “simultaneous” processing allows the machining process without the input programs that have been developed more than one month. It also makes very easy for an operator to input and change parameters, even though we use a 5-axis processing machine.

It is another great advantage to skip the programming process other than the machining time. The main reason for the long time development is not only the complicated structure of the ACS, but also the inefficient machining as, for example, it takes much more time for the surface finishing in a very small area.

Continuously, we are interested in simplifying the machining process for the other parts to optimize the balance between the machining time and the cavity properties.

DEVELOPMENT OF RF CAVITIES FOR THE SHB SYSTEM OF THE L-BAND ELECTRON LINAC AT OSAKA UNIVERSITY

R. Kato, S. Kashiwagi, Y. Morio, S. Suemine, G. Isoyama#
Institute of Scientific and Industrial Research, Osaka University, Ibaraki, Osaka 567-0047, Japan

Abstract

Two 108 MHz and one 216 MHz RF cavities are developed for the subharmonic buncher system of the L-band electron linac at Osaka University. They are quarter-wavelength coaxial RF cavities made only of oxygen-free copper. Special care is taken to make their operation stable by keeping their temperature constant with cooling water. The cavities are successfully fabricated and commissioned.

INTRODUCTION

A sub-harmonic buncher (SHB), which operates at a sub-harmonic of the RF frequency of a linac, is used to produce a single-bunch electron beam by preliminary bunching of electrons. The 40 MeV L-band linac at Osaka University operating at a 1.3 GHz frequency in the L-band is equipped with a three-stage SHB system and it is optimized to produce a high-intensity single-bunch electron beam. When constructed in 1978, it was equipped with a single 216 MHz quarter-wavelength coaxial RF cavity, frequency of which is a sixth sub-harmonic of 1.3 GHz, and afterward two 108 MHz, or 12th sub-harmonic RF cavities of the same type were added between the electron gun and the 216 MHz cavity, comprising a three-stage SHB system. The charge in a single bunch beam is higher than 30 nC/bunch in ordinary operation and the maximum charge so far realized reaches 91 nC/bunch with the SHB system.

The SHB system is turned on in the single bunch mode and the multi-bunch mode of operation of the L-band linac. The single bunch mode is used for laser-synchronized pulse radiolysis experiments in the time range down to femto-seconds and for basic study on Self-Amplified Spontaneous Emission (SASE) in the far-infrared region, and the multi-bunch mode is used for free electron laser experiments in the same wavelength region. These experiments require stable operation of the linac. Problems of the linac in these experiments were that it took three to four hours to warm up the linac after start-up in the morning and that a beam condition suddenly and sometimes changed, and their causes are found to be due to the SHB system. The RF cavities of the SHB system are made of clad plates of copper on stainless steel and they are cooled with water flowing through a copper pipe wound on the outside wall of the cavity, which is the stainless steel side of the outer conductor. The area of heat generation and the cooling part are away and cooling is made only by heat conductivity through a thin clad plate of copper and stainless steel, which makes the warm-up time longer, and when temperature of the clad plate varies, the cavities slightly change their shapes and sizes due to difference in thermal expansion coefficients of the two metals, which produces sudden changes of the beam condition. To solve these problems, we have fabricated new RF cavities for the SHB system that have higher temperature stability; two 108 MHz cavities and one 216 MHz cavities, which are designated from the upstream side as cavity #1 through #3. We will report design, fabrication, and commissioning of the RF cavities.

DESIGN

Basic design concept of the new RF cavities is as follows. The new cavities will be substituted for the present ones, so that physical sizes must fit with the present environments. Longitudinal lengths of the cavities between the entrance and the exit flanges should be same as the present values and transverse sizes should be smaller than the inner size of the Helmholtz coils, 253 mm. The physical aperture for the beam should not be smaller than the present value, 50 mm in diameter. The new cavities should be made of pure copper to realize higher temperature stability. The cavities will be cooled with water, temperature of which is precisely controlled to be 38 ± 0.03°C, so that water channels should be equally distributed over bodies of the cavities, including the outer and the inner conductors, in order to make the temperature of the cavities uniform and constant and not to rely on thermal conductivity of copper too much. Routes of the water channels should be designed so that heat is taken away by water at the place it is generated.

The mechanical design of the cavities are made by referring to a similar SHB cavity used for the electron and positron linac at KEK, which is a quarter wavelength coaxial cavity of a resonance frequency of 114 MHz made of copper. The physical design is made using the computer code, SUPERFISH. The main parameters calculated for the cavities #1 and #2, and the cavity #3 are listed in Table 1.

Table 1: Calculated Main Parameters of the Cavities

	Cavity#1, #2	Cavity#3
Resonance freq. (MHz)	108.4	216.8
Unloaded Q-value Q_0	8765	11642
Shunt impedance R (MΩ)	1.45	2.07
RT^2 (MΩ)	0.844	0.871
RT^2/Q (Ω)	96.3	74.8
Transit time factor (β=0.55)	0.764	0.649

#isoyama@sanken.osaka-u.ac.jp

ACCELERATING STRUCTURE FOR C-BAND ELECTRON LINEAR ACCELERATOR OPTIMIZATION

S.V. Kutsaev, N.P. Sobenin, A.A. Anisimov, Moscow Engineering-Physics Institute (State University), Moscow, Russian Federation
M. Ferderer, A.A. Zavadtsev, A.A. Krasnov, Identification Beam Systems LLC, Atlanta, USA

Abstract

This paper presents the results of a survey study that analyzed and compared several linear accelerator designs operating in the range of 5 to 20 MeV for use in advanced cargo inspection systems. These designs were based on klystron generated RF power input of 3.2 and 4.5 MW at 5712 MHz. Several different accelerating structures were considered including standing wave (SW) and travelling wave (TW) structures. In addition several hybrid structures, composed of a SW buncher sections and TW accelerator sections, were included in the study. Cells geometries and beam dynamics parameters, for these accelerating structures, were calculated using advanced numerical simulation methods. Accelerating structures and input couplers for SW and hybrid structures were designed.

INTRODUCTION

Cargo inspection systems should be simple, compact and highly reliable. Historically S-band liner accelerators have been used for this application. By using a higher frequency structure we can significantly increase the shunt impedance and therefore provide necessary energy gain with a shorter structure length. The effective shunt impedance of a 5712 MHz biperiodic structure is 30% greater than a 2856 MHz structure while the external diameter is approximately half the diameter. In addition to the cavity being significantly smaller waveguides and other RF components are as well. To facilitate large capture coefficients, without using an external focusing magnet, SW biperiodic structure bunchers were used. Along with the SW biperiodic structures, hybrid structures are of particular interest for this type of application.

Modern cargo systems need to generate more than a black and white image to be effective in solving the cargo security problem that the world is facing. To be effective the systems must also generate material based information. In particular, Z-function and density information needs to be presented to the operators. To obtain Z-function and density information the accelerator must be able to vary output energy from pulse to pulse.

SW STRUCTURE

In designing SW biperiodic accelerating structures it is important to ensure that the necessary beam parameters are met without requiring unrealistic manufacturing tolerances. To satisfy this requirement the coupling coefficient (k_c) was increased to 11 percent from the more traditional range of 4 to 5 percent.

Cell tuning to the required frequency and field distribution was performed using the resonant models. In Figure 1 a resonant model for the regular cell and the distribution of longitudinal component of electric field on axis are illustrated.

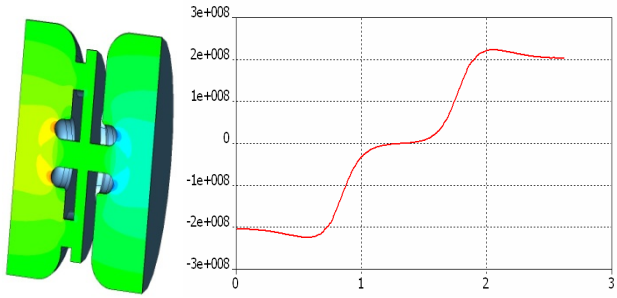

Figure 1: Resonant model of the regular cell and the distribution of electric field in it.

For constructional convenience the RF power is input into the first cell. Two WR187 waveguides are connected to the first cell symmetrically to provide symmetry of the field in this cell. One of these waveguides is short-circuited by the metal pin and is used for vacuum pumping. Figure 2 shows the model of this coupler as well as electric field intensity.

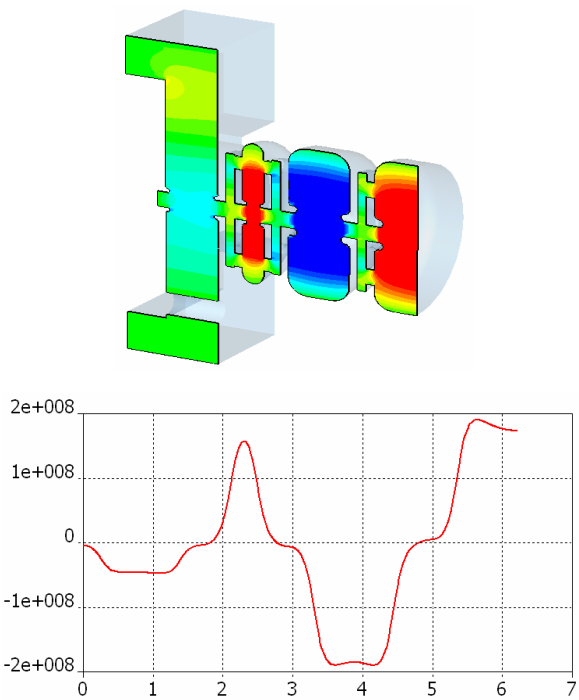

Figure 2: Distribution of electric field in SW buncher.

THE CUT DISK STRUCTURE PARAMETERS FOR MEDIUM PROTON ENERGY RANGE

V. Paramonov *, INR RAS, 117312 Moscow, Russia

Abstract

For intense proton beam acceleration the structure aperture diameter should be $\approx 30mm$. With such aperture room temperature coupled cell accelerating structures have the maximal effective shunt impedance Z_e value at operating frequency $\approx 650MHz$. For this frequency well known Side Coupled Stricture (SCS), Disk and Washer Structure (DAW), Annular Coupled Structure (ACS) have large transversal dimensions, leading to essential technological problems. The Cut Disk Structure (CDS) has been proposed to join both high Z_e and coupling coefficient k_c values, but preferably for high energy linacs. In this report parameters of the four windows CDS option are considered at operating frequency $\approx 700MHz$ for proton energy range $80MeV \div 200MeV$. The outer diameter $\approx 30cm$ and $kc \approx 0.12$ result naturally, but Z_e value is of $(0.7 \div 0.9)$ from Z_e value for SCS ($k_c = 0.03$). Small cells diameter opens possibility of CDS applications for twice lower frequency and structure parameters at operating frequency $\approx 350MHz$ are estimated too. Cooling conditions for heavy duty cycle operation are considered.

INTRODUCTION

The scaling relation for effective shunt impedance of a structure $Z_e \sim \sqrt{f}$, where f is an operating frequency, is widely known and is frequently used for fast Z_e estimations at different f values. It means, that we simultaneously scale all dimensions of the structure. It is not perfectly correct for practical case.

Let us consider typical Ω-shaped accelerating cell geometries, shown in Fig. 1 for structures with External Coupling Cells (ESS), such as SCS, ACS, Fig. 1a, and for Internal Coupling Cells (ISS), for example, On-Axis Coupled Structure (OSC), Fig. 1b. The aperture diameter of the structure $2r_a$, Fig. 1a, is defined by a transverse beam size and safety margins. These parameters are not related directly with operating frequency. We can not reduce $2r_a$ for high operating frequency, but there are no reasons for $2r_a$ increasing for lower f. As it is known well, Z_e value increases with r_a decreasing. A septum thickness t_1, Fig. 1a, for ESS, is defined by cooling channels placing and rigidity requirements. From these requirements a reasonable t_1 value is $(10 \div 15mm)$. We also can not reduce t_1 at higher f values and there are no reasons for t_1 increasing for lower operating frequency. And Z_e increases with relative $\frac{t_1}{L}$ increasing, where $L_p = \frac{\beta\lambda}{2}$ is the period length, β, λ are the relative particle velocity and the operating wavelength, respectively. For the ICC case we should have two septa with the thickness t_1 and coupling cell with the length l_{cc} in between with effective septum thickness $t_2 \approx 2 \cdot t_1 + l_{cc}$.

To find a frequency for the maximal Z_e value we have the contradiction - for higher frequencies skin effect leads to RF losses reduction, but we have to increase ratio $\frac{r}{\lambda}$ and $\frac{t_1}{\lambda}$. For lower frequencies it are conversely.

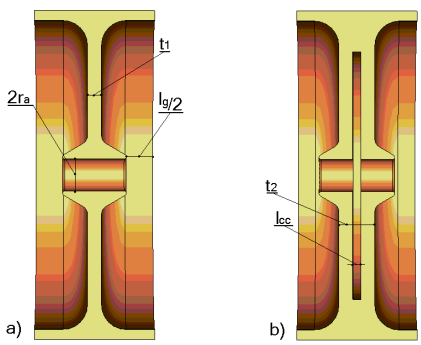

Figure 1: Typical cells geometries for structures with ECC (a) and ICC (b).

CDS ADVANTAGES

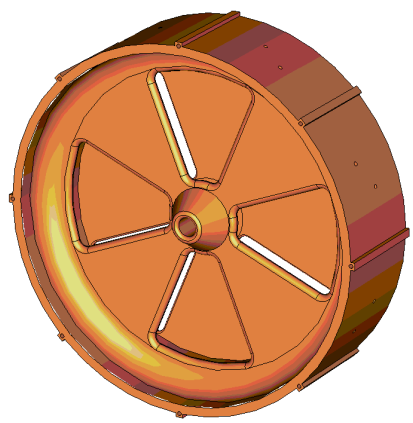

Figure 2: Four windows CDS option.

The CDS was proposed for high energy linacs $\beta \approx 1$ and L-band operating frequency [1]. CDS is topologically similar to OCS, but realizes quite different coupling concept - coupling mode has no own space for magnetic field, which should penetrate strongly through coupling windows (slots) in an accelerating cell, resulting in the high coupling coefficient value $k_c \sim 0.12 \div 0.25$. Coupling windows in CDS have not so strong magnetic field enhancement at windows ends, as compared to coupling slots in OCS, ACS, SCS and a high coupling coefficient is not connected with Z_e

* paramono@inr.ru

ROOM TEMPERATURE ACCELERATING STRUCTURE FOR HEAVY ION LINACS

V. Paramonov *, V. Moiseev, INR RAS, Moscow, Russia,
Yu. Bylinskii, TRIUMF, Vancouver, Canada

Abstract

In this report we consider room temperature DTL structure for heavy ions acceleration from $150\frac{keV}{u}$ to $400\frac{keV}{u}$. The structure design is based on known and proven solutions. The structure has no end wall problem. It allows flexible segmentation in RF cavities to place transverse focusing elements between cavities. As compared to well known IH DTL, considered structure has smaller transverse dimensions and is designated for lower operating frequency. The structure promises high RF efficiency: calculated effective shunt impedance value is higher than $1.0\frac{GOm}{m}$ for operating frequency $\sim 70MHz$ and particle energy $E \sim 150\frac{keV}{u}$.

INTRODUCTION

Interdigital H-type Drift Tube (IH DT) structure, see, for example [1], [2] and related references, is now well developed and widely used for heavy ion acceleration. Idea of Interigital Structure (IS) is in two steps. First one is to generate RF voltage between two conductors, placed along the beam line, providing a transverse electric field. At the second step with drift tubes, connected in turn to opposite conductors, transverse field transforms into longitudinal accelerating one. Efficiency of such structure depends on number of drift tubes per unit length and a zero order estimation for effective shunt impedance Z_e is $Z_e \sim \frac{1}{\beta^2}$, where β is the relative particle velocity.

Similarly we can consider another classical device - Radio Frequency Quadrupole (RFQ). With some RF geometry one should provide RF voltage between four conductors, placed along the beam line. Every RF circuit for quadruple RF voltage distribution can be adopted for dipole one to be the IS basement. Basing on this approach, several RF circuit, used for RFQ, were considered in [3] for IS at operating frequency $f = 105MHz$. The Split Ring (SR) RF circuit, applied in TRIUMF RFQ [4] at $f = 35MHz$ and adopted in [3] for IDS with $f = 105MHz$, Fig. 1, have shown attractive properties - the small cavity outer diameter and calculated $Z_e \sim 1.0\frac{GOm}{m}$ for $\beta = 0.015$.

The lower operating frequency for DTL part of the heavy ion linac [5] results in the higher linac acceptance. In this report we consider the parameters of Split Ring Drift Tube (SR DT) structure for operating frequency $f = 70MHz$.

* paramono@inr.ru

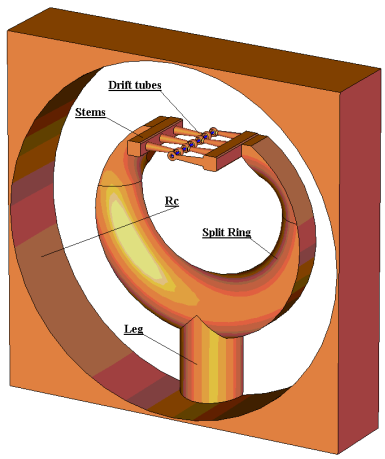

Figure 1: Proposed structure with Split Ring RF circuit and Drift Tubes. Half of the structure period.

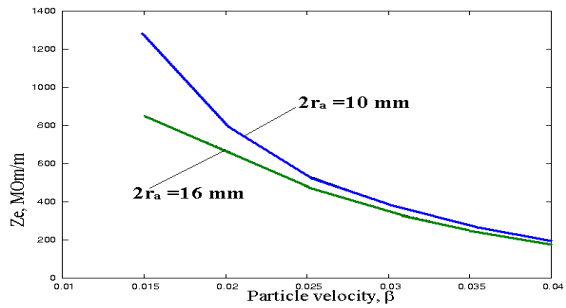

Figure 2: Z_e dependence on β for aperture diameters $2r_a = 10mm$ and $2r_a = 16mm$, $\alpha = 0.5$.

PERIODICAL STRUCTURE

RF parameters of the proposed structure at operating frequency $70MHz$ can be estimated in consideration of one half of ideal periodical structure shown in Fig. 1. For $Z_e(\beta)$ dependence estimation the gap ratio $\alpha = \frac{l}{L} = \frac{2l}{\beta\lambda}$, where l_g is the accelerating gap length, L_p is the period length, λ is the operating wavelength, was fixed to $\alpha = 0.5$. Effective shunt impedance Z_e is defined as:

$$Z_e = \frac{(E_0 T)^2 N_p L_p}{P_s}, \quad \text{MOm/m} \qquad (1)$$

where E_0 is the average electric field along the structure axis, T is the transit time factor, $N_p = 6$ is the number of accelerating periods in the half structure, P_s is the RF loss power in the half structure.

HIGH POWER TEST OF A LOW GROUP VELOCITY X-BAND ACCELERATOR STRUCTURE FOR CLIC

S. Döbert, A. Grudiev, G. Riddone,M. Taborelli, W. Wuensch, R. Zennaro,
CERN, Geneva, Switzerland
S. Fukuda, Y. Higashi, T. Higo, S. Matsumoto, K. Ueno, K. Yokoyama, KEK, Tsukuba, Japan
C. Adolphsen, V. Dolgashev, L. Laurent, J. Lewandowski, S. Tantawi, F. Wang, J. W. Wang,
SLAC, Menlo Park, USA

Abstract

In recent years evidence has been found that the maximum sustainable gradient in an accelerating structure depends on the rf power flow through the structure. The CLIC study group has consequently designed a new prototype structure for CLIC with a very low group velocity, input power and average aperture (<a/λ> = 0.13). The 18 cell structure has a group velocity of 2.6 % at the entrance and 1 % at the last cell. Several of these structures have been made in a collaboration between KEK, SLAC and CERN. A total of five brazed-disk structures and two quadrant structures have been made. The high power results of the first KEK/SLAC built structure is presented which reached an unloaded gradient in excess of 100 MV/m at a pulse length of 230 ns with a breakdown rate below 10^{-6} per meter active length. The high-power testing was done using the NLCTA facility at SLAC.

INTRODUCTION

The CLIC study [1] aims to demonstrate a prototype accelerating structure suitable for a linear collider with an average loaded gradient of 100 MV/m at 12 GHz. To reach a sufficient luminosity for the collider a bunch train of 312 bunches with 3.7 10^9 electrons each has to be accelerated with a reasonable rf-to-beam efficiency. Therefore the structure needs to be equipped with heavy higher order mode damping and the gradient should be sustainable for 230 ns. The present structure is the result of a sophisticated optimization procedure to maximize the overall collider luminosity taking into account rf constraints like surface fields, input power, pulse length dependence and pulse heating as well as beam dynamics constraints for short and long range wake fields [2]. The rf constraints used in the optimization are the result of a comprehensive analysis of the available data mostly from the NLC/GLC program [3] and from 30 GHz tests at CERN. The rf power flow characterized by $P/C*\tau^{1/3}$ (P= input power, C= circumference of the first iris, τ = pulse length) was identified in this analysis as a possible limitation [4] and is therefore limited to previously demonstrated values in the optimization. The structure obtained is strongly tapered resulting in a quasi constant gradient with beam loading and a constant ratio of power over circumference along the structure. The unloaded gradient rises linearly towards the end of the structure due to this design. The structure needs only 55 MW for an average unloaded gradient of 100 MV/m due to its low group velocity- starting at 2.6 % and reaching 1% in the last cell. The detailed parameters of this structure can be found in table 1 and [5].

Table 1: Design and Measured Parameters of T18_vg2.6_disk (1)

Frequency:	11.424 GHz
Cells:	18+2 matching cells
Filling Time:	36 ns
Length: active acceleration	18 cm
Iris Dia. a/λ	0.155~0.10
Group Velocity: vg/c	2.6-1.0 %
S11/ S21	0.035/0.8
Phase Advace Per Cell	2π/3
Power for <Ea>=100MV/m	55.5MW
Unloaded Ea(out)/Ea(in)	1.55
Es/Ea	2
Pulse Heating ΔT: (75.4MW@200ns)	16 - 25 K

Four of these structures have been made in collaboration between KEK and SLAC using the NLC/GLC fabrication technique which comprises single crystal diamond turning of the cells, high temperature bonding (1000 C°) in a hydrogen furnace followed by extensive vacuum baking at 650 C° . CERN has made one more of this structure out of disks but using a vacuum furnace just above 800 C° for the bonding. In addition two structures with HOM damping are being prepared made out of clamped quadrants, one by CERN in OFC Copper and one by KEK in CuZr. More information about structures made out of clamped quadrant can be found in [6]. The aim is to compare different fabrication technologies and preparation techniques. A photo of the first structure tested made by KEK/SLAC is shown in figure 1. The high-power prototypes made out of disks do not include high order damping which will be added in subsequent versions. The higher order mode damping for this structures consists out of four damping waveguides in each cell which change the rf parameters slightly but in particular enhances the pulsed heating temperature rise by about a factor 2.

DESIGN OF AN X-BAND ACCELERATING STRUCTURE FOR THE CLIC MAIN LINAC

A. Grudiev, W. Wuensch, CERN, Geneva, Switzerland

Abstract

The rf design of an accelerating structure for the CLIC main linac is presented. The 12 GHz structure is designed to provide 100 MV/m average accelerating gradient with an rf-to-beam efficiency as high as 27.7 %. The design takes into account both aperture limitations and HOM-suppression requirements coming from beam dynamics as well as constraints related to rf breakdown and pulsed surface heating.

INTRODUCTION

Recently the CLIC study has changed the operating frequency and accelerating gradient of the main linac from 30 GHz and 150 MV/m to 12 GHz and 100 MV/m respectively. This major change of parameters has been driven by the results of a main linac cost and performance optimization [1]. A new set of overall CLIC parameters is under preparation [2]. In this report, the rf design of the new X-band accelerating structure for the CLIC main linac is presented.

RF DESIGN AND OPTIMIZATION

Frequency and gradient are the key parameters for any accelerating structure. Following their major change fundamental issues ranging from the basic rf design of the cell to the structure rf design and optimization procedure have been revisited.

Basic Cell Geometry and HOM Damping

The basic cell geometry and heavy damping developed for 30 GHz CLIC structures have been carried over into the X-band CLIC structures. However the reduction in frequency by factor 2.5 and, even more importantly, the gradient reduction by factor 1.5 results in an overall reduction of the pulsed surface heating temperature rise ΔT^{max} of $1.5^2 \cdot 2.5^{1/2} \approx 3.6$ in a scaled structure at the same pulse length. Because of this the old structure design, which was based on hybrid slotted iris plus waveguide damping, was not simply scaled [3] to the new frequency keeping pulse length the same. Instead the decrease in the pulsed surface heating was used to eliminating the iris slots, and compensating by opening the damping waveguide coupling aperture. The first measure reduces the maximum surface fields on the iris and consequently increases the high gradient potential, on one hand, but degrades the HOM damping because of the absence of slots, on the other hand. The second measure improves the waveguide damping to the required level but reduces the surface of the outer cell wall and thus increases the temperature rise which, nevertheless, still remains acceptable. The basic cell geometry after these modifications is shown in Fig. 1. The wakefield damping waveguides result in a lowest dipole-band Q of below ten. The cell has an elliptical cross section iris and convex elliptical cross-section outer walls in order to minimize surface fields. The four damping waveguides are terminated with broadband loads which are not shown in Fig. 1. This geometry is very close to the one which has been already proposed as the nominal CLIC accelerating structure design [4].

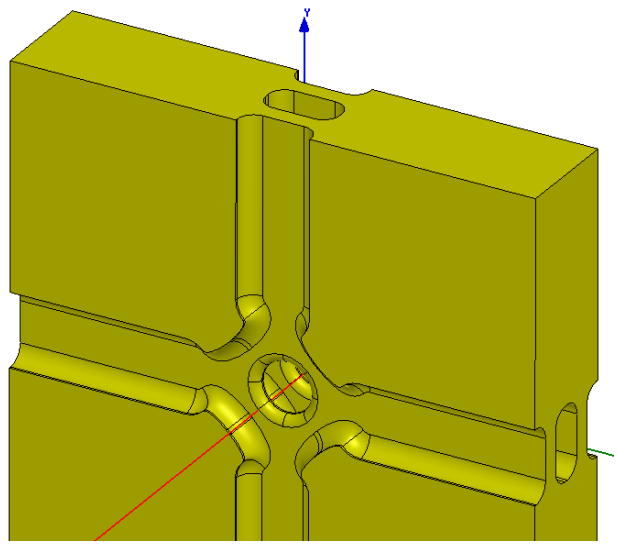

Figure 1: Basic cell geometry of the accelerating structure with strong waveguide HOM damping.

RF Constraints for X-band Copper Structures

A significant effort has been made to collect as many additional X-band experimental data points as possible beyond those that have been used in [1] in order to refine the rf constraints for copper structures. Based mainly on the NLC/JLC X-band program [5] many new unpublished data points have been collected via private communications with SLAC colleagues [6]. All the collected data is summarized in [7]. Based on the high gradient performance of X-band travelling-wave accelerating structures with rf phase advance per cell of 120 and 150 degree the two rf constraints (1) and (3) used in [1] have been updated to:

1. Surface electric field: $E_{surf}^{max} < 260$ MV/m
2. Pulsed surface heating: $\Delta T^{max} < 56$ K
3. Power: $P_{in}/C \cdot \tau_p^{1/3} < 18$ MW/mm· ns$^{1/3}$

Here E_{surf}^{max} refers to maximum surface electric field in the structure, P_{in} refers to input power and τ_p refers to pulse length. C is the circumference of the first regular iris. This set of rf constraints has been used in the rf design and optimization of the CLIC X-band accelerating structure which is described in the next section.

A NEW LOCAL FIELD QUANTITY DESCRIBING THE HIGH GRADIENT LIMIT OF ACCELERATING STRUCTURES

A. Grudiev, W. Wuensch, CERN, Geneva, Switzerland

Abstract

A new local field quantity is presented which gives the high-gradient performance limit of accelerating structures in the presence of vacuum rf breakdown. The new field quantity, a modified Poynting vector S_c, is derived from a model of the breakdown trigger in which field emission currents from potential breakdown sites cause local pulsed heating. The field quantity S_c takes into account both active and reactive power flow on the structure surface. This new quantity has been evaluated for many X-band and 30 GHz rf tests, both travelling wave and standing wave, and the value of S_c achieved in the experiments agrees well with analytical estimates.

INTRODUCTION

Limitations coming from the rf breakdown in vacuum strongly influence the design of a high gradient accelerating structures. Rf breakdown is a very complicated phenomenon involving effects which are described in different fields of applied physics such as surface physics, material science, plasma physics and electromagnetism. No quantitative theory to date satisfactorily explains and predicts rf breakdown levels in vacuum. In the framework of CLIC study [1] a significant effort has been made to derive the high-gradient limit due to rf breakdown and to collect all available experimental data both at X-band and at 30 GHz to use to check the validity of the limiting quantity. The quantity has been used to guide high gradient accelerating structure design and to make quantitative performance predictions for structures in the CLIC high power testing program [2].

EXPERIMENTAL DATA

The quest to accumulate high-gradient data in a coherent and quantitatively comparable way focused on two frequencies: 30 GHz, the old CLIC frequency, and 11.4 GHz which is the former NLC/JLC frequency and is very close to the new CLIC frequency of 12 GHz. To our knowledge only at these two frequencies has a systematic study been done where the structure accelerating gradient was pushed up to the limit imposed by the rf breakdown and where relevant parameters were measured. In particular all available data where the breakdown rate (BDR), the probability of a breakdown during a pulse, was measured at certain gradient and pulse length was collected. Data from structures where the performance was limited by an identified defect or by some other area of the structure such as the power couplers which are not directly related to the regular cell performance were not included. The main parameters of the structures are summarized in the Table 1 which shows the rather large variation in group velocity (from 0 up to ~40 % of the speed of light), rf phase advance (from 60 to 180 degree per cell) and iris geometry which is available for analysis. The experimentally achieved value of the gradient scaled to pulse length of 200 ns and breakdown rate of 10^{-6} per pulse as described below is presented together with the corresponding references.

In a typical high-gradient experiment, the BDR is measured at fixed value of accelerating gradient and pulse length. On the other hand, it is most convenient to compare performance with the achieved gradient at a fixed value of the pulse length and BDR. To do this the measured data has had to be scaled. This involves two steps - first scaling the gradient versus pulse length and then scaling the gradient versus BDR. Both of these scaling behaviours have been measured in a number of structures but not systematically in all cases. In order to scale the data for the structures where these scaling laws have not been measured a general scaling law which us consistent with all measured data has been applied.

The dependence of gradient on pulse length at a fixed BDR has well established scaling law observed in many experiments (see for example [3]):

$$E_{acc} t_p^{1/6} = const \qquad (1)$$

where E_{acc} denotes the gradient and t_p the pulse length. It was also confirmed by fitting the data for the structure numbers 3, 4, 8, 9, 10, 12, 13, 18, 20 in Table 1.

For the gradient versus BDR dependence at a fixed pulse length the different scaling laws which have been used are exponential (see for example [3]) and a power law. In this paper, we have used a power law:

$$E_{acc}^{30} / BDR = const \qquad (2)$$

It was also confirmed by fitting the data for the structure numbers 3, 8, 10, 12, 13, 18, 20, 21 in Table 1.

Finally, (1) and (2) can be combined into,

$$E_{acc}^{30} t_p^5 / BDR = const \qquad (3)$$

This general scaling law has been used to scale the collected experimental data to the pulse length of 200 ns and BDR of 10^{-6} per pulse. The results are presented in the last column of Table 1.

RF BREAKDOWN CONSTRAINTS

For a long time, the surface electric field was considered to be the main quantity which limits accelerating gradient because of its direct role in field

DEVELOPMENT STATUS OF THE PI-MODE ACCELERATING STRUCTURE (PIMS) FOR LINAC4

P. Bourquin, R. De Morais Amaral, G. Favre, F. Gerigk, J-M. Lacroix, T. Tardy, M. Vretenar, R. Wegner, CERN, Geneva, Switzerland

Abstract

The high-energy section of Linac4, between 100 and 160 MeV, will be made of a sequence of 12 seven-cell accelerating cavities of the Pi-Mode Structure (PIMS) type, resonating at 352 MHz. The cell length is the same within a cavity, but changes from cavity to cavity according to the beam velocity profile. Compared to other structures used in this energy range, π-mode cavities with a low number of cells have the advantage of simplified construction and tuning, compensating for the fact that the shunt impedance is about 10% lower because of the lower frequency. Field stability in steady state and in presence of transients is assured by the low number of cells and by the relatively high coupling factor of 5%. Standardising the linac RF system to a single frequency is considered as an additional economical and operational advantage.

The mechanical design of the PIMS will be very similar to that of the 352 MHz normal conducting 5-cell LEP (Large Electron Proton collider at CERN) accelerating cavities, which have been successfully operated at CERN for 15 years. After reviewing the basic design principles, the paper will focus on the tuning strategy, on the field stability calculations and on the mechanical design. It will also report the results of measurement on a cold model and the design of a full-scale prototype.

RF DESIGN

The PIMS replaces a Side Coupled Linac (SCL), which was originally foreseen in the high energy section of Linac4 [1]. The SCL was using a total of 468 cells (220 accelerating cells plus coupling cells) operating at 704 MHz to accelerate beam from 90 to 160 MeV, while the PIMS now covers 102 to 160 MeV using only 84 cells (12 cavities of 7 cells). Since the construction and tuning of π-mode cavities is already well known at CERN, and since the SCL entails the use of 2 different RF frequencies in Linac4 it was decided to give preference to the PIMS [2] despite the $\approx 12\%$ lower shunt impedance (see Fig. 1).

The basic design is a scaled (in geometrical β) version of the normal conducting LEP accelerating structure [3], which was then modified for higher cell-to-cell coupling. The accelerating gradient in the first 10 cavities has been adjusted to a relatively high value of 4 MV/m, resulting in a maximum power of $\approx$ 1 MW per cavity. Using a high gradient limits the number of cells per cavity to 7, and thus makes it easier to obtain a flat field distribution. The last 2 cavities are used not only for acceleration but also for energy painting for injection into the subsequent Proton Synchrotron Booster (PSB). In order to achieve a high ramping speed in these cavities ($\approx$ 2 MeV/10 μs), the nominal accelerating gradient was lowered to 3.1 MV/m. An overview of the main parameters is given in Table 1. The basic design was made with Superfish and the 3D calculations to determine the coupling coefficients, shunt impedance degradation (due to coupling, tuners, etc), end-cell tuning were made with GdfidL [4] (see Fig. 2).

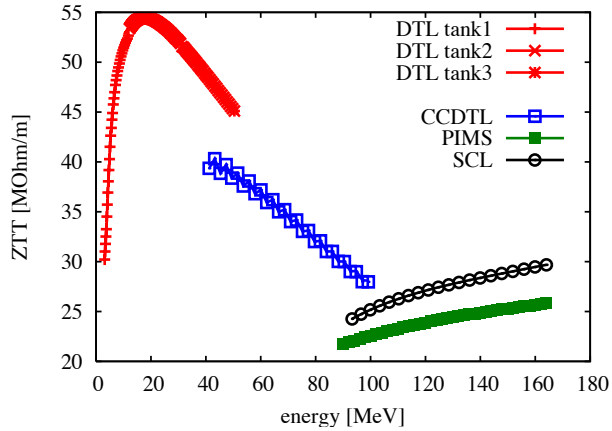

Figure 1: Shunt impdance (ZT^2) for the Linac4 accelerating structures (80% of simulated values, including additional losses on stems, coupling holes, tuning rings).

Table 1: Main Parameters

parameter		value
frequency	MHz	352.2
input energy	MeV	102
output energy	MeV	160
electric gradient	MV/m	4
peak power/cav.*	MW	1
max. surface field	kilpatrick	1.8
design duty cycle	%	10
max. expected d.c.	%	6
Linac4 d.c.	%	0.1
cells/cavity		7
number of cavities		12
beam aperture	mm	40

* including beam loading

Using a coupled circuit model one can evaluate the voltage error due to the exptected spread in cell frequencies, which is linked to the production tolerances and the tuning precision. Assuming the same frequency scatter ($\pm$25 kHz)

SHUNT IMPEDANCE STUDIES IN THE ISIS LINAC

C. Plostinar, STFC/RAL/ASTeC, Harwell, Didcot, Oxfordshire, UK
A. Letchford, STFC/RAL/ISIS, Harwell, Didcot, Oxfordshire, UK

Abstract

The ISIS linac consists of four DTL tanks that accelerate a 50 pps, 20 mA H^- beam up to 70 MeV before injecting it into an 800 MeV synchrotron. Over the last decades, the linac has proved to be a stable and reliable injector for ISIS, which is a significant achievement considering that two of the tanks are more than 50 years old. At the time the machine was designed, the limited computing power available and the absence of 3D electromagnetic (EM) simulation codes, made the creation of a linac optimized for power efficiency almost impossible, so from this point of view, the ISIS linac is quite simple by today's standards. In this paper, we make a shunt impedance comparison study using the power consumption data collected from ISIS and the results obtained when simulating each of the four DTL tanks with 2D and 3D EM codes. The comparison will allow us to check the accuracy of our simulation codes and models and to assess their relative performance. It is particularly important to benchmark these codes against real data, in preparation for their use in the design of a proposed new linac, which will replace the currently aging ISIS injector [1].

THE ISIS INJECTOR

The ISIS facility at Rutherford Appleton Laboratory (RAL), has been the world leading pulsed neutron source for over two decades, delivering neutrons for users from all over the world and proving to be a very stable and reliable machine. It consists of a 70 MeV H^- injector, an 800 MeV synchrotron and two target stations [2]. The injector starts with an H^- ion source, followed by a low energy beam transport line and a 665 keV RFQ operating at 202.5 MHz. The energy is then raised to 70 MeV by four Drift Tube Linac (DTL) tanks. Tanks 2 and 3 were built in the 1950s for the RAL Proton Linear Accelerator [3] and have been in operation ever since, while tanks 1 and 4 were built in the 1970s originally intended for the Nimrod accelerator, but first used in ISIS. A layout of the DTL section of the linac can be seen in Figure 1 and a list of parameters is given in Table 1.

Table 1: ISIS Linac Parameters

Energy	70.4	MeV
Frequency	202.5	MHz
Pulse Length	200 – 250	μs
Peak Current	25	mA
Repetition Rate	50	Hz
Total Length	55	m
Duty Cycle	1 – 1.25	%

ELECTROMAGNETIC MODELLING

The choice of accelerating structures is essential for every linac. In ISIS, the DTL structure is used for the entire length of the linac with small geometry variations between the tanks. The synchronous phase is kept constant at -30° in the four tanks, while the accelerating gradient varies: 1.6 – 2.2 MV/m in tank 1, 2.45 – 2. 55 MV/m in tank 2, 2.3 – 2.4 MV/m in tank 3 and 2.6 MV/m in tank 4. The geometry of a single DTL cell is very simple and it is not fully optimised for power efficiency resulting in a longer linac structure. In modern linac designs, the overall length of every tank is reduced by choosing a higher accelerating gradient and synchronous phase, optimising the cell geometry and by increasing the transit time factor by shortening the cell gap lengths [4].

The figure of merit which will be used to characterize the accelerating cavities is the effective shunt impedance per unit length, ZT^2, which is a measure of the effectiveness of producing an axial voltage V_0 for a given power dissipated, P [5]:

$$ZT^2 = \frac{(E_0 T)^2}{P/L}$$

T – transit time factor
$E_0 = V_0/L$ – average axial electric field
L – cell length

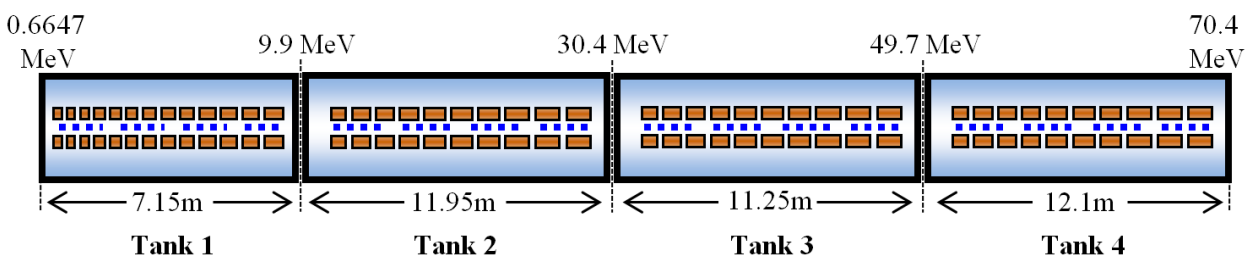

Figure 1: Layout of the DTL section of the ISIS Linac.

BREAKDOWN IN PRESSURIZED RF CAVITIES*

R. Sah#, M. Alsharo'a, M. Neubauer, R. P. Johnson, Muons Inc., Batavia, IL, USA
D. Li, J. Byrd, LBNL, Berkeley, CA, USA
M. BastaniNejad, A. Elmustafa, G. Wang, ODU, Norfolk, VA, USA
D. V. Rose, C. Thoma, and D. R. Welch, Voss Scientific, LLC, Albuquerque, NM, USA

Abstract

The performance of many particle accelerators is limited by the maximum electric gradient that can be realized in RF cavities. Recent studies have shown that high gradients can be achieved quickly in 805-MHz cavities pressurized with dense hydrogen gas, because the gas can suppress, or essentially eliminate, dark currents and multipacting. In this project, two new test cells operating at 500 MHz and 1.3 GHz will be built and tested, and the high pressure technique will be used to suppress the vacuum effects of evacuated RF cavities, so that the role of metallic surfaces in RF cavity breakdown can be isolated and studied as a function of external magnetic field, frequency, and surface preparation. Previous studies have indicated that the breakdown probability is proportional to a high power of the surface electromagnetic field, in accordance with the Fowler-Nordheim description of electron emission from a cold cathode. The experiments will be compared with computer simulations of the RF breakdown process.

INTRODUCTION

RF cavities pressurized with hydrogen gas are being developed to produce low emittance, high intensity muon beams for muon colliders, neutrino factories, and other applications. The high-pressure gas suppresses dark currents, multipacting, and other effects that are complicating factors in the study of breakdown in usual RF cavities that operate in vacuum. In the studies reported here, various metals were tested in a pressurized cavity where RF breakdown is expected to be due only to the interaction of the metallic surfaces with the electromagnetic fields. After exposure to the RF fields, metallic Be, Mo, Cu, and W samples were examined using a Hirox microscope and a scanning electron microscope (SEM) to measure the distribution of breakdown events on the electrode surfaces [1].

Apparatus

A schematic of the 805 MHz Test Cell (TC) geometry is shown in Figure 1. The TC is a cylindrical stainless steel pressure vessel. RF power is fed into the chamber via a coaxial line. A solenoid magnet (not shown in the figure) provides an axial magnetic field of up to 3 T, which is used in some of the data sets. Replaceable hemispherical electrodes of various materials (Cu, Mo, Be, W) are separated by a 2 cm gap.

*Supported in part by the US DOE under grants DE-FG02-08ER86350, -08ER86352, and -05ER86252
#rol@muonsinc.com

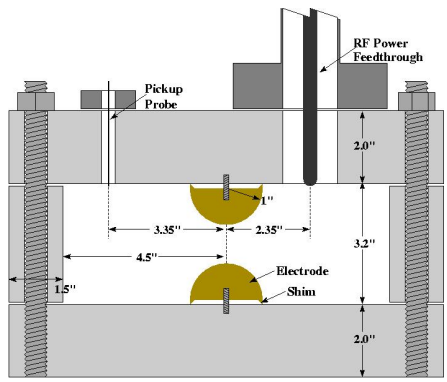

Figure 1: Cross section of the 805-MHz test cell showing the replaceable one inch radius Cu, Be, Mo, or W, hemispherical electrodes. The top and bottom plates and the cylinder are copper-plated stainless steel (the gas input/exhaust port is not shown in the figure).

EXPERIMENTAL RESULTS

RF Breakdown

Increasing gas density reduces the mean free collision path for ions giving them less chance to accelerate to energies sufficient to initiate showers and avalanches. As shown in Figure 2, it is found that Cu and Be electrodes operated stably with surface gradients near 50 MV/m, Mo near 63 MV/m, and W near 72 MV/m [2].

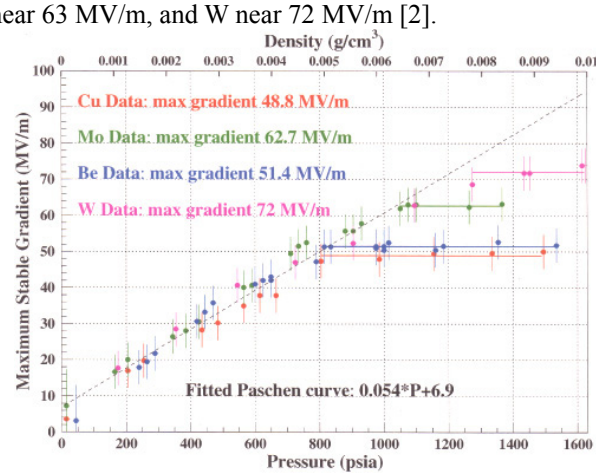

Figure 2: Maximum stable TC gradient as a function of hydrogen gas density or pressure for Cu, Be, Mo, and W with no external magnetic field.

EXPERIMENTAL DATA ANALYSIS

To investigate the correlation of breakdown and the electric field, the local surface density of breakdown

DESIGN AND TEST OF THE TRIPLE-HARMONIC BUNCHER FOR THE NSCL REACCELERATOR*

Q. Zhao†, V. Andreev, J. Brandon, G. Machicoane, F. Marti, J. Oliva, J. Ottarson, J. Vincent
NSCL, East Lansing, MI 48823, U.S.A.

Abstract

A unique triple-harmonic buncher operating at the fundamental frequency of 80.5 MHz upstream the Radio Frequency Quadrupole (RFQ) linac has been designed, manufactured and tested at the National Superconducting Cyclotron Laboratory (NSCL) to meet the requirement of a small output longitudinal beam emittance from the reaccelerator. The buncher consists of two coaxial resonators with a single gridded gap. One cavity provides both the fundamental and the third harmonic simultaneously with λ/4 and 3λ/4 modes respectively, while the other provides the second harmonic in λ/4 mode. This buncher combines the advantages of using high quality factor resonator and only a pair of grids. Details on design considerations, electromagnetic simulations, and primary test results are presented.

INTRODUCTION

The National Superconducting Cyclotron Laboratory (NSCL) at Michigan State University is developing a facility named ReA3 to demonstrate the technical feasibility and performance characteristics for stopping and reaccelerating rare-isotope beams, as an important step towards a next-generation rare-isotope facility in the United States [1]. Beams of rare isotopes will be produced and separated in-flight at the NSCL Coupled Cyclotron Facility and subsequently stopped by a novel gas stopper, breeded by a state-of-the-art electron beam ion trap based charge-breeder, and reaccelerated by a modern linear accelerator. The linac consists of a low energy beam transport line, a cw radio-frequency quadrupole, a quarter wave resonator based superconducting linac, and a high energy beam transport line [2]. ReA3 will delivery various exotic beams with charge-to-mass ratios (Q/A) of 0.2 – 0.4 and variable energies of about 0.3 to 3 MeV/u.

Nuclear experimental programs require a beam on target with an energy spread of ~1 keV/u and a bunch length of ~1 ns simultaneously. Therefore, a longitudinal beam emittance of less than 0.3 π·ns·keV/u from ReA3 is demanded. Since the intensities of the rare-isotope beams will be low, the scheme of using an external multi-harmonic buncher upstream of the RFQ has been adopted to produce a small longitudinal emittance beam from RFQ with high bunching efficiency [3-6]. A unique triple harmonic buncher using two high quality factor resonators with one pair of grids has been designed, fabricated and tested at NSCL for this application.

DESIGN CONSIDERATIONS

The buncher is designed to operate with three harmonics, a fundamental frequency of 80.5 MHz and two additional harmonics of 161 and 241.5 MHz, respectively. The fundamental frequency, same as that of the downstream RFQ and superconducting cavities, is mainly determined by the small longitudinal beam emittance requirement. Since beams from the charge breeder will have a larger intrinsic energy spread (e.g. ΔE ~ ±25eV/u for Q/A = 0.25), the beam micro-bunch frequency should not be lower than ~80 MHz, otherwise the longitudinal emittance of the bunched beam will be too large to achieve the required time and energy resolution on target. Considering the higher bunching efficiency and lower output longitudinal emittance needed, a total of three harmonics are chosen for the operation of the buncher [6]. A high quality factor resonator was proposed, which needs a lower power amplifier to drive it. This buncher consists of two coaxial cavities, as shown in Fig. 1. One cavity provides both the fundamental and the third harmonics. The other cavity provides the second harmonic with a λ/4 mode. The dual frequency cavity will operate simultaneously at the λ/4 and 3λ/4 modes, as was done at PIAVE in Legnaro [5]. The buncher bunches beams with a nominal relativistic velocity β = 0.00507 (beam energy of 12keV/u), so the βλ is small especially for harmonics. For example, βλ = 9.4 mm for second harmonic. On the other hand, the beam diameter is about 30mm at the buncher position in order to match it into RFQ. Therefore gridded electrode tubes are necessary to achieve uniform field distributions and thus satisfactory transit time factors. We proposed to design the buncher in such a way that all three harmonics are applied in one single gridded gap. This configuration with only one pair of grids minimizes the beam losses on grids and makes the buncher longitudinally more compact as well.

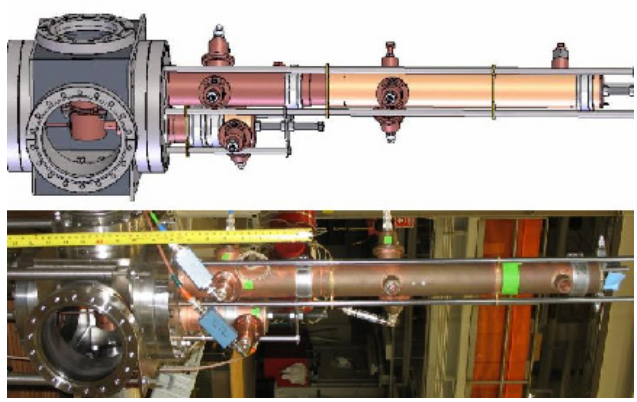

Figure 1: Triple harmonic buncher with two coaxial resonators and a single gridded gap: design drawing (top), photograph (bottom).

*Work supported by Michigan State University.
†zhao@nscl.msu.edu

SURFACE-LOSS POWER CALCULATIONS FOR THE LANSCE DTL

Sergey S. Kurennoy, LANL, Los Alamos, NM 87545, U.S.A.

Abstract

The surface losses in the drift-tube linac (DTL) tanks 3 and 4 of the LANSCE linear accelerator are calculated using 3-D electromagnetic modeling with the CST MicroWave Studio (MWS). The results are used to provide more realistic power estimates for the 201.25-MHz RF upgrade design within the LANSCE-R project. We compared 3-D MWS results with those from traditional 2-D Superfish computations for DTL cells and their simplified models and found differences on the level of a few percent. The differences are traced to a 3-D effect consisting in a redistribution of the surface currents on the drift tubes (DT) produced by the DT stem. The dependence of MWS results on the mesh size used in computations is also discussed.

INTRODUCTION

There are some disagreements between the existing results on the surface-loss power in the LANSCE DTL tanks 3 and 4 [1]. In particular, the power values cited in the book [2], respectively 2.745 and 2.674 MW, are noticeably higher than the historical maxima in 1994-1998, 2.090 and 2.493 MW, as well as the values found in old design reports, 2.33 and 2.33 MW [1].

More accurate values of the power loss in the DTL tanks 3 and 4 are important for finalizing a design of the 201.25-MHz RF system upgrade within the LANSCE-R project. The surface losses in the DTL tanks 3 and 4 were recalculated using both 3-D electromagnetic modeling with MicroWave Studio (MWS) [3] and the traditional approach with Superfish (DTLfish) [4]. This paper summarizes our results.

CALCULATION METHOD AND RESULTS

We used a piece-wise approach to calculate the surface losses in the DTL tanks, performing MWS computations separately for a few selected cells in the tank, with electric boundary conditions on the cell end walls. The standard DTLfish approach is essentially the same: 2-D Superfish (SF) computations are performed for a few selected half-cells and the results are interpolated [4]. The parameters of the DTL tank cells were taken from the LANSCE online database and post-coupler tuning tables. Figure 1 shows the MWS model of the DTL cell DT98, the first cell in the tank 3. The cell is about 43 cm long and has 44-cm radius. The MWS model includes a drift tube (DT), stem with bellows, and post-coupler. The picture inset shows the post-coupler with two tab rotations, at 22.5 and 45°. These two virtual tab shapes are vacuum-filled and not used in this particular calculation; however, their presence influences the MWS mesh.

Figure 2 shows the surface currents calculated by MWS in the model of the DTL cell DT165, the last cell in the tank 4. Its length is 55.6 cm, and the DT is almost 35 cm long. The highest current density is on the DT stem near its connection to the DT.

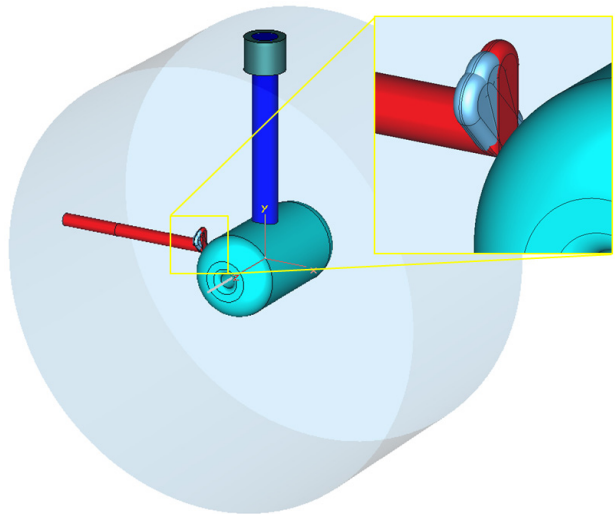

Figure 1: MWS model of DTL cell: drift tube (cyan), stem (dark-blue), bellows (sea-green), and post-coupler (red).

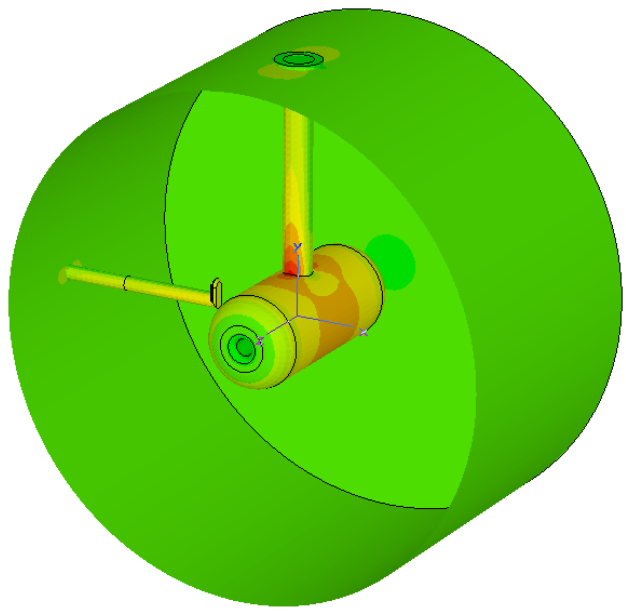

Figure 2: Surface-current magnitude in DT165 cell (red corresponds to the highest value, dark-green to zero).

In the Superfish approach, 2-D computations are performed for an axisymmetric model of the (half-)cell that includes only the cavity and DT. After that a theoretical perturbation correction is added to include the DT stem effect [4], but post-couplers are usually not taken into account. In the MWS 3-D models with post-couplers, we impose the electric boundary conditions on the side walls and find the modes with the MWS eigensolver. Such an approach is justified when the post-couplers are

EFFICIENT LOW-BETA H-MODE ACCELERATING STRUCTURES WITH PMQ FOCUSING

S.S. Kurennoy, J.F. O'Hara, E.R. Olivas, L.J. Rybarcyk, LANL, Los Alamos, NM 87545, U.S.A.

Abstract

We are developing high-efficiency room-temperature RF accelerating structures for beam velocities in the range of a few percent of the speed of light by merging two well-known ideas: H-mode cavities and the transverse beam focusing with permanent-magnet quadrupoles (PMQ). Combining electromagnetic 3-D modeling with beam dynamics simulations and thermal-stress analysis, we have found that the H-mode structures with PMQ focusing provide a very efficient and practical accelerator for light-ion beams of considerable currents. Such accelerating structures following a short RFQ can be used in the front end of ion linacs or in stand-alone applications such as a compact deuteron-beam accelerator up to the energy of a few MeV.

INTRODUCTION

Room-temperature H-mode resonators – inter-digital (IH) or cross-bar (CH) – provide effective acceleration at low beam velocities, $\beta=v/c<0.3$-0.4, e.g. [1]. IH structures are especially efficient at very low velocities, $\beta<0.1$. Transverse focusing options used in H-structures include electric RF quadrupoles in RFQ at very low β and magnetic focusing by quadrupole triplets inserted into the structure [1]. The triplet insertions interrupt the structure reducing its acceleration efficiency. On the other hand, small sizes of the drift tubes (DTs) required to achieve high shunt impedances in H-structures prevent placing usual electromagnetic quadrupoles inside DTs. Using permanent-magnet quadrupoles (PMQs) placed inside H-structure small DTs was suggested [2], which promises both efficient beam acceleration and beam focusing.

Here we focus on a particular application: using IH structures with PMQ beam focusing for a compact deuteron-beam accelerator from 1 to 4 MeV at the RF frequency around 200 MHz, with the peak current up to 50 mA and duty factor of 10%. Such an accelerator can serve in a mobile intense neutron and gamma source for interrogation of special nuclear materials for homeland defense. Requirements of the system mobility and ease of use favor the room-temperature (RT) option. For higher energies and/or higher RF frequencies using CH-PMQ structures can be beneficial.

PMQ FOCUSING IN IH STRUCTURES

Deuteron kinetic energies from 1 to 4 MeV correspond to the beam velocity range of $\beta=0.033$-0.065. The cell length $L_c=\beta\lambda/2$ – equal to a half-period in IH structures – is very short at the low-energy end, only about 2.5 cm. To keep the DT length L_{DT} as long as possible, we consider first the IH structure with narrow gaps g between DTs by fixing the ratio $g/L_c=0.15$. A 2-cm long PMQ with the bore radius 5 mm can readily provide the field gradient $G=200$ T/m, even if the PMQ outer radius is only 11 mm. Such PMQs fit into DTs even at the lower end of the IH accelerating structure, with geometrical value $\beta_g=0.034$, where the DT length is $L_{DT}=2.16$ cm. In Ref. [3, 4] we explored the beam transverse focusing structure FnODnO, where the focusing period consists of one focusing (F) and one defocusing (D) PMQ separated and followed by n empty DTs, n=0,1,2,… We denote such structures as IH 1-(n+1), with one PMQ per (n+1) cells. Initial beam dynamics calculations were performed with the envelope code TRACE-3D; the results for the beam sizes and phase advances are summarized in [3, 4]. Long focusing periods are excluded because of large phase advances $\sigma_{0x/y}$ per focusing period, above 90°. All configurations IH1-2 to IH1-4 were found acceptable, and the differences between them were not very significant. Overall, IH1-3 (n=2), cf. Fig. 1, where PMQs are inserted in every third DT, provided the smallest beam size.

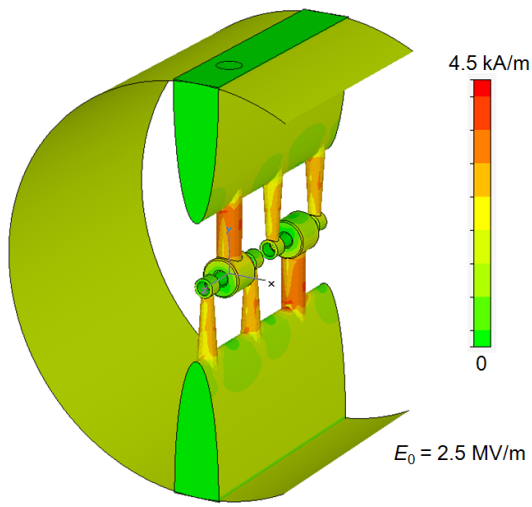

Figure 1: Surface current magnitude in the modified IH1-3 structure for β_g = 0.04 (the cavity wall is partially cut).

Still, the beam size was rather large in all the cases, which can lead to undesirable beam losses. We plan to perform multi-particle beam-dynamics simulations next. Should they indicate significant beam losses, we will apply stronger transverse focusing using PMQ pairing, e.g. FFODDO (IH2-3); the structure is illustrated in Fig. 2. Such focusing schemes make the matched beam size smaller and reduce losses. TRACE-3D envelope calculations were performed also for the high energy end, $\beta_g=0.065$. There are more options there since the DT lengths are longer. For example, using longer PMQ while simultaneously increasing the PMQ and DT apertures to prevent beam losses gives good results [3]. Preventing beam losses is especially important at the high-energy end of the deuteron linac.

PERFORMANCE OF A 1.3 GHZ NORMAL-CONDUCTING 5-CELL STANDING-WAVE CAVITY*

Faya Wang, Chris Adolphsen and Juwen Wang, SLAC, Menlo Park, CA 94025, U.S.A

Abstract

A 5-cell, normal-conducting, 1.3 GHz, standing-wave (SW) cavity was built as a prototype capture accelerator for the ILC positron source. Although the ILC uses predominately superconducting cavities, the capture cavity location in both a high radiation environment and a solenoidal magnetic field requires it to be normal conducting. With the relatively high duty ILC beam pulses (1 msec at 5 Hz) and the high gradient required for efficient positron capture (15 MV/m), achieving adequate cavity cooling to prevent significant detuning is challenging. This paper presents the operational performance of this cavity including the processing history, characteristics of the breakdown events and the acceleration gradient witnessed by a single bunch at different injection times for different rf pulse lengths.

INTRODUCTION

Due to high radiation levels and the need of a solenoidal magnetic field for focusing, the 1.3 GHz pre-accelerator that follows the ILC positron target will be normal conducting. A half-length (5-cell) prototype standing-wave (SW), cavity was built at SLAC to verify that the gradient (15 MV/m in 1.0 ms pulses) can be achieved stably and without significant detuning from the RF heat load (4 kW per cell). Details of the design can be found in [1, 2], and the cavity cross-section is shown in Fig. 1 [3].

Fig. 2 is a plot of the cold test measurement of the mode frequencies (dots); the solid line is the fitted dispersion curve, expressed as,

$$f_n^2 = \frac{f_0^2}{1 + k_1 \cos(\phi)}$$

with f_0= 1291.8 MHz and k_1= 0.01249. The unloaded Q of the cavity is ~ 29000 and the operating frequency (at π phase advance) is 1299.7 MHz. The time constant of this critically-coupled cavity ($0.5Q_o/\omega$) is 1.8 us.

So far, the cavity has been rf processed at the π-mode for about 530 hrs and it has incurred about 6200 breakdowns. The gradient goal of 15 MV/m with 1 ms pulses has been achieved. Fig. 3 shows the breakdown rate history during processing. For these data, the pulse repetition rate was 5 Hz except for 1 ms pulses where it was lowered to 1 Hz to reduce the detuning as the reflected power was causing waveguide breakdowns (the source of these breakdowns has since been eliminated and 5 Hz operation is expected to be possible in the future).

The goal when designing the cavity cooling system was to have about 25% reflected power when the cavity was turned on 'cold' that then dropped to zero in steady state with full rf power dissipation (20 kW at 15 MV/m). In this way, a cavity temperature control system is not needed (at least for testing). However, the flow rate that was achieved (due to a limited supply of temperature-regulated water) was 86 gpm compared to the 140 gpm desired, which increased the cavity temperature by about 50% (to 0.13 degC per kW dissipated). Also, the detuning (-2.7 kHz/kW) was about 25% larger than expected from simulations using the actual temperature rise and led to an overall reflection of about 50% when cold with the appropriate choice of rf frequency to minimize the reflection at full power in steady state.

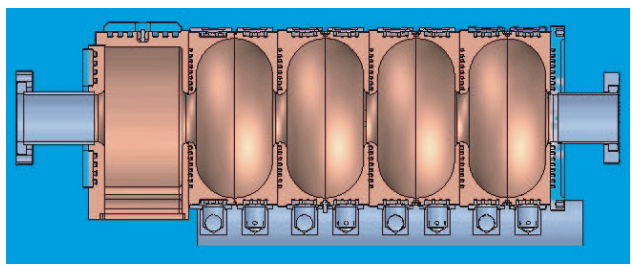

Figure. 1: Cross sectional view of the 5-cell cavity where the coupler cell is on the left. Water circulates through rectangular grooves in the irises and outer cavity walls.

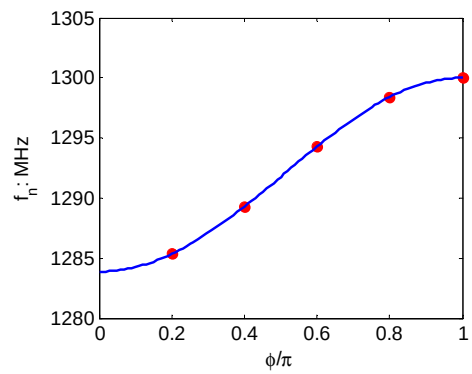

Figure 2: The 5-cell SW cavity dispersion curve.

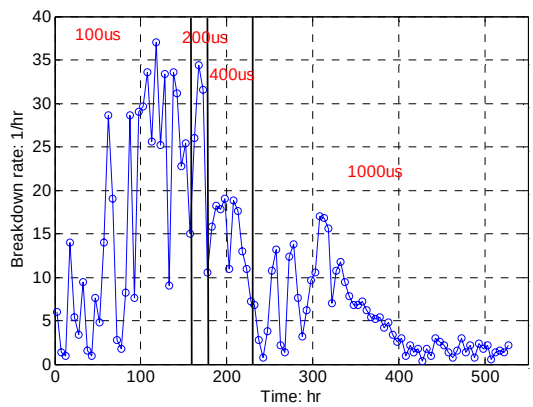

Figure 3: Breakdown rate history of the cavity for various pulse lengths (in red).

* Work Supported by DOE Contract DE-AC03-76F00515.

PROGRESS IN L-BAND POWER DISTRIBUTION SYSTEM R&D AT SLAC*

Christopher Nantista, Chris Adolphsen and Faya Wang, SLAC, Menlo Park, CA 94025, U.S.A.

Abstract

We report on the L-band RF power distribution system (PDS) developed at SLAC for Fermilab's NML superconducting test accelerator facility. The makeup of the system, which allows tailoring of the power distribution to cavities by pairs, is briefly described. Cold test measurements of the system and the results of high power processing are presented. We also investigate the feasibility of eliminating the expensive, lossy circulators from the PDS by pair-feeding cavities through custom 3-dB hybrids. A computational model is used to simulate the impact on cavity field stability due to the reduced cavity-to-cavity isolation.

INTRODUCTION

In high energy particle accelerators, particularly in high-gradient linear collider designs, there is generally a significant mismatch between the peak power and pulse length in which RF can be efficiently produced and that in which they can be efficiently used for acceleration. The waveguide network connecting the sources to the structures, or power distribution system (PDS), is thus often less straight-forward than might be thought. Sources might be combined for convenient transport, sometimes compression techniques are used to trade pulse width for peak power, and power division at the accelerator for feeding multiple structures is usually required.

For L-band (1.3 GHz) superconducting linacs, state-of-art klystrons can produce 10 MW in 1.6 ms pulses, and state-of-the-art cavities can sustain gradients corresponding to about 300 kW of input power. Thus one source can drive quite a few cavities, 26 in current ILC plans, with allowance for losses and overhead for low-level RF control. The most direct approach to implementing this, adopted at DESY's TTF, is to use a set of hybrid directional couplers connected in series, each with a different coupling. Another approach, less compact, would be to use successive splitting in a branching arrangement.

In an inter-lab R&D collaboration, SLAC is providing RF system components for the test accelerator under construction in Fermilab's NML building, eventually a full system including couplers, but initially a PDS for the first cryomodule. The layout we chose [1] uses two levels of splitting (as does that chosen for the European XFEL), so that an appropriate portion of the power flowing in a main waveguide line is tapped off and then evenly split for each successive pair of cavities.

The two unique features of our PDS are the use of a novel variable tap-off (VTO), a four-port directional coupler with mechanically adjustable coupling [2], and the use of a four-port hybrid rather than a simple "T" for the binary split. The former allows uniform fabrication of the main line tap-offs as well as the ability to better optimize the overall gradient by tailoring the power distribution to accommodate a spread in sustainable gradient among the cavities [3]. The use of a 3-dB hybrid, standard for feeding standing-wave normal conducting accelerator structures, for the final split allows the reflected power from each cavity pair to be directed to a load. We hope thus to eliminate the need for an expensive and lossy circulator for each cavity.

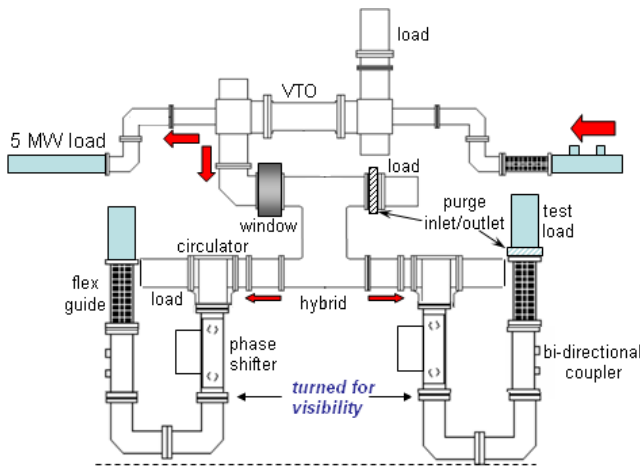

Figure 1: A two-feed sub-unit of the power distribution system. Blue components belong to the test setup, not the unit. The U-bends at the bottom are actually perpendicular to the page.

THE PDS UNIT

The pair-wise feeding in our approach is well suited to standard 8-cavity cryomodules. The local PDS along such a cryomodule consists of four, two-feed modular units connected in series. Fig. 1 shows a diagram of one such unit as built for FNAL. The VTO and the hybrid are SLAC designs, machined from aluminum and dip-brazed. The WR650 waveguide bends, spool pieces and semi-flexible sections are supplied commercially with custom lengths, many thick-walled for pressurizability. The remaining components were developed for DESY's L-band program by commercial vendors. They include a modified pillbox window to separate pressurized and non-pressurized regions, 1 MW loads, circulators (isolators), phase shifters and diagnostic directional couplers. Most flange connections employ aluminum gaskets combining knurled contact surfaces with rubber pressure seals.

The assembly is supported for testing and shipping in an aluminum box frame as shown in Fig. 2. Only one wall of this frame will remain after anchoring it in the accelerator enclosure. The upper waveguide, which would

*Work supported by the U.S. Department of Energy under contract DE-AC02-76SF00515.

A NEW ACCELERATOR STRUCTURE CONCEPT: THE ZIPPER STRUCTURE*

Christopher Nantista, SLAC, Menlo Park, CA 94025, U.S.A.

Abstract

I introduce a novel normal-conducting accelerator structure combining standing wave and traveling wave characteristics, with relatively open cells. I describe the concept and geometry, optimize parameters, and discuss the advantages and limitations this new structure presents.

INTRODUCTION

A number of different geometries have been employed over the years in accelerating structures. Currently, efforts continue toward finding the optimal design for use in a normal conducting TeV-scale electron-positron linear collider. The key general structure parameters of shunt impedance and quality factor relate to the RF-to-beam power transfer efficiency. Also rising to prime importance for a linear collider are the sustainable accelerating gradient, which drives the overall linac length, and the HOM wakefields, which impact beam dynamics and emittance preservation. To maximize the former, generally limited by RF breakdown or pulsed heating, variation of geometrical parameters has been tried, including group velocity, phase advance per cell, and iris tip shape, as well as different materials, surface preparations, and frequencies. Standing-wave structures have also been considered as perhaps offering advantages over traveling-wave structures in regard to breakdown. The deleterious effects of wakefields have been addressed by techniques such as damping into external manifolds, radiating out through chokes or channeling through slots into absorbers.

I present below an idea for a radically different structure with features that may recommend it over perturbations of more conventional geometries. It has not yet been tested, but is currently in the design stage. I will attempt to motivate its conception, describe its features, and suggest reasonable parameters for an X-band prototype.

MOTIVATING CONSIDERATIONS

Large iris apertures, for large group velocity (traveling-wave structures) or mode spacing (standing wave structures), seem to exacerbate breakdown problems. They tend to increase the ratio of the peak surface electric field to the accelerating gradient and reduce shunt impedance. If we decouple power flow/cell coupling from the beam irises, we can keep the latter as small as short-range wakefield considerations allow.

Coupler cells (and those near them) have proven to be particularly prone to gradient limiting RF breakdown. Even if pulsed heating of the waveguide coupling iris is minimized, squeezing the full structure power through such cells seems inadvisable. We can eliminate the bottleneck presented by coupler cells if we couple to all cells identically.

Long range wakefields must be suppressed by removing HOM power deposited by the bunch train. What if all the cells were heavily coupled, with a fairly wide-open geometry, into an easily damped volume? One might then avoid pulsed heating and high electric field problems associated with slots and chokes.

A $\pi/2$ phase advance per cell might offer improved R/Q, though perhaps lower Q, compared to larger phase advances, since the cell transit time factor can be significantly larger (0.90 *vs.* 0.64 for a π mode in a simple pillbox). For traveling-wave structures, variations from the $2\pi/3$ traditional SLAC choice that have been tried range from $\pi/3$–$5\pi/6$. For a standing-wave structure, a $\pi/2$ mode leaves every other cell empty, thus killing the effective shunt impedance. This problem is often dealt with by employing a bi-periodic structure with the empty cells either collapsed in length or moved off axis (side-coupled).

What if, instead, we excited the set of empty cells in their own independent resonance $\pi/2$ out of phase with the first set, so that the beam is synchronously accelerated throughout?

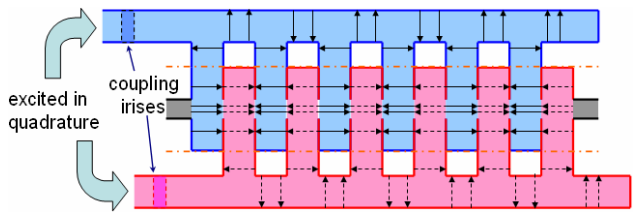

Figure 1: Basic waveguide circuit and field pattern of the zipper structure with degenerate orthogonal resonances driven $\pi/2$ out of phase.

THE ZIPPER CONCEPT

Consideration of the above issues eventually led to the zipper-like structure geometry suggested by Fig.1. With normal, axial cell coupling, the tuning of the end cells would determine whether one, the other, or neither $\pi/2$ mode was a resonance in the fundamental mode passband of the structure. If the cells are decoupled on axis, or such coupling is overwhelmed by heavy side coupling between sets of every other cell through a waveguide, as shown, one might imagine driving both degenerate resonances.

The structure is essentially a pair of interleaved combs of stubbed waveguide. The regions comprising the actual cells are, as envisioned here, square, rather than axially symmetric. One wall of each cell is removed, perfectly substituted for by a null in the standing-wave field pattern

*Work supported by the U.S. Department of Energy under contract DE-AC02-76SF00515.

X-BAND TRAVELING WAVE RF DEFLECTOR STRUCTURES *

J. W. Wang# and S. Tantawi., SLAC, Menlo Park, CA 94025, USA

Abstract

Design studies on the X-Band transverse RF deflectors operating at HEM_{11} mode have been made for two different applications. One is for beam measurement of time-sliced emittance and slice energy spread for the upgraded LCLS project, its optimization in RF efficiency and system design are carefully considered. Another is to design an ultra-fast RF kicker in order to pick up single bunches from the bunch-train of the B-factory storage ring. The challenges are to obtain very short structure filling time with high RF group velocity and good RF efficiency with reasonable transverse shunt impedance. Its RF system will be discussed.

INTRODUCTION

The RF deflectors were developed from 1960's for high energy particles separation using the interaction with a transversely deflecting mode. As a measure of the deflecting efficiency, the transverse shunt impedance $r_\perp$ is defined as:

$$r_\perp = \frac{\left(\frac{c}{\omega}\frac{\partial E_z}{\partial r}\right)^2}{\partial P/\partial z} \quad , \qquad (1)$$

where z and r is structure longitudinal and transverse axis respectively, E_z is the electrical field amplitude for the dipole mode with angular frequency ω and P is the RF power as function of z. Using the simulation codes for electromagnetic field in RF structures, the transverse shunt impedance can be calculated from:

$$r_\perp = \frac{QV_\perp^{\,2}}{\omega UL} = \frac{c^2 QV_z^{\,2}}{\omega^3 r_0^2 UL} \quad , \qquad (2)$$

where Q is quality factor, $V_\perp$ and V_z are integrated potential change in r and z direction for a particle traversing through structure along a trajectory with $r=r_0$ and length of L, U is stored energy within the structure with the length of L.

Traveling wave X-Band deflector structures have many advantages: their RF systems are simpler without the requirement of circulators for standing wave structures and their shunt impedances (proportional to the square root of frequency) are higher than structures working at lower frequencies. In addition, SLAC is well advanced in the art of high power X-Band RF source [1] including klystrons and pulse compression systems. In recent years, many new applications of RF deflectors have been developed. Here we will mainly discussion the deflector applications for measurement of bunch length as well as longitudinal phase space and super fast RF kicker for future light sources, which could not be realized by conventional charged particle deflecting devices.

DEFLECTOR FOR BEAM MEASUREMENT

If a charged particle beam is at the zero-crossing phase of the deflecting mode, the bunch is given a strong correlation between longitudinal coordinate and transverse position due to RF kick.

Recently at SLAC, a 2.4 m long S-Band deflector built in 1960's was used in LCLS beam line for commissioning. [2] The bunch length in the order of 100 fs was successfully measured and the tuning of the bunch compressor was performed based on the bunch measurement data.

In the future, in order to characterize the extremely short bunch of the LCLS project, we need to extend the time-resolved electron bunch diagnostics to the scale of 10-20 fs. We have to consider a new RF deflector with much powerful deflecting capability. The peak deflecting voltage necessary to produce a temporal bunch resolution of Δt is: [3],[4]

$$eV_\perp \approx n\frac{\lambda}{2\pi c\Delta t}\sqrt{\frac{\varepsilon_N Emc^2}{\beta_d}} \, , \qquad (3)$$

where E is the electron energy and the transverse momentum of the electron at time Δt (with respect to the zero-crossing phase of the RF) is $p_y = eV_\perp/c$, n is the kick amplitude in the unit of nominal rms beam size, λ is the RF wavelength, ε_N is the normalized rms vertical emittance, c is the speed of light, and β_d is the vertical beta function at the deflector. This is for an RF deflector, which is $\pi/2$ in betatron phase advance from a downstream screen.

As a practical estimation, in order to create an offset of roughly double rms beam size with 10 fs temporal separation, for the LCLS beam parameters with full beam energy of 13.6 GeV and vertical normalized rms emittance of 1 μm, the necessary peak vertically deflecting voltage for a X-band (11424 MHz) deflector is 33 MV.

For the accelerator structure design, we have to consider to use the available peak power from an X-Band klystron and to obtain higher RF efficiency and reliability at acceptable maximum electric field for RF breakdown and maximum magnetic field for RF pulse heating. Making effort in optimization, the designed deflector is a single section $2\pi/3$ mode backward wave structure with length of 1.5 m. Its main parameters are listed in the Table 1.

*Work supported by U.S. Department of Energy, contract DE-AC02-76SF00515.

jywap@slac.stanford.edu

LAST SPIRAL 2 10 KW CW RF COUPLER DESIGN

Y. Gómez Martínez, T. Cabanel, J. Giraud, D. Marchand, R. Micoud, F.Vezzu,
LPSC (UJF-CNRS/IN2P3-INPG), Grenoble, France.

Abstract

RF tests of the SPIRAL 2 coupler were done successfully in the cryomodules of the LINAC. Weakness during the transport has led to an updated mechanical design. We present here the results of the RF tests as well as the new design.

INTRODUCTION

SPIRAL 2 is a 40 MeV-5mA deuterons and a 14.5MeV/u-1mA heavy ions superconducting LINAC under construction at GANIL. The SPIRAL 2 superconducting LINAC consists of 19 cryomodules, 12 of them called A (including 1 Quarter-Wave Resonator (QWR) at beta=0.07) and the other 7 cryomodules called B (including 2 QWR at beta = 0.12).

The coupler transfers the power into the two types of cavities and keeps the vacuum into the accelerator. The RF couplers have to provide 10 kW Continuous Wave (CW) nominal power to the cavities at 88.05 MHz for an accelerating field of 6.5 MV/m. The coupler must handle 100% reflected power at maximum incident power.

The Laboratory of Subatomic Physics and Cosmology (LPSC) realized the design, the simulation and the test of the disc shape ceramic coupler. [1].

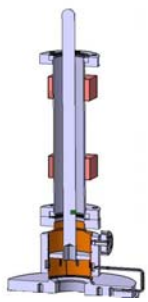

Figure 1: The RF coupler prototype.

Four coupler prototypes were manufactured and conditioned [2] and two of them were mounted in each cryomodule type. For the B-cryomodule, high power tests are finished and they were done successfully.

Figure 2: Coupler prototype.

TESTS OF THE COUPLER PROTOTYPE IN THE B-CRYOMODULE

Figure 3: Coupler in the B-cryomodule.

We measured a reflected coefficient S_{11} = -50 dB, and a quality factor $Q_{ext} = 1.1*10^6$ (beam dynamic quality factor choice).

At the resonance frequency of the cavity, the maximal accelerating field has been reached; the cleanness of the coupler is confirmed.

Outside the resonance, the coupler has been conditioned till 10 kW CW at room temperature and also at 4.2 K. During this test, weak multipactor (0.2mA) has been found only at low power (less than 300W).

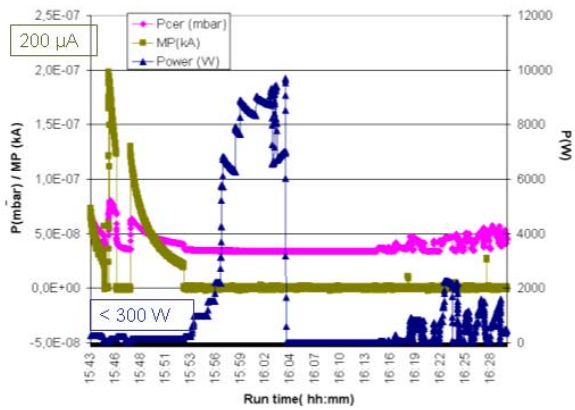

Figure 4: First conditioning at 4.2K (out of the resonance).

After those tests the RF design of the coupler was validated.

MAIN DESIGN CHANGES

The reasons of the mechanical changes were to obtain a more robust coupler especially during the transports.

The Antenna

To minimise the risks of deviation of the antenna during the transport we designed a hollow antenna. For this purpose we also have chosen a long internal support of the antenna.

STUDIES ON INPUT COUPLERS FOR SUPERCONDUCTING CAVITIES *

H. Jenhani#, A. Variola, L. Grandsire, T. Garvey, M. Lacroix, W. Kaabi, B. Mercier, C. Prevost, S. Cavalier, LAL, Univ Paris-Sud, CNRS/IN2P3, Orsay, France.

Abstract

We have recently demonstrated a dramatic reduction in conditioning time for TTF-III couplers [1]. This was carried out by a systematic study of the different parameters that play a role in the conditioning process. In addition, many investigations have been made in order to have a better understanding of the couplers' behaviour. These activities represent some aspects of a larger technology program that we are developing to study power couplers and their multipacting. This paper will give an overview of some of these studies, our future experiments on couplers and the development of the associated technology program.

INTRODUCTION

An ambitious R&D program on power couplers for superconducting cavities has been established at LAL. The LAL-DESY collaboration, which aims to study the behaviour of the TTF-III prototype couplers for the European XFEL and the reduction of their conditioning time, was at the origin of these activities. In this context, successful results, with a dramatic reduction in conditioning time, were achieved and good experience was acquired concerning the behaviour of these couplers under RF power [1]. However, much R&D effort has still to be made in order to face many other challenges. The TTF-III couplers have a very complex geometry and are composed of many sub-parts. To understand the influence of some of these parts on the coupler behaviour, multipacting (MP) simulations are being performed. This allows some correlation between the simulation results and the measured signals during the coupler power tests. Furthermore, many difficult industrial processes are needed for coupler manufacturing. Thin layer deposition of Titanium-Nitrogen (TiN) on ceramic windows is one of the processes which needs to be mastered and optimized. The TiN sputtering deposition processes is currently studied at LAL using a reactive DC magnetron sputtering bench [2]. This device will also strongly contribute to experimental MP studies. Technological solutions have also to be found for the power couplers that would be needed for the ILC in order to increase their operating RF power, while decreasing their cost. We have designed, built and tested two coupler prototypes, TTF-V and TW60, for this purpose.

A short overview on our coupler activities, including realisation of our proto-types and their test results will be presented in this paper.

* We acknowledge the support of the European Community-Research Infrastructure Activity under the FP6 "Structuring the European Research Area" programme (CARE, contract number RII3-CT-2003-506395)

Corresponding author: jenhani@lal.in2p3.fr

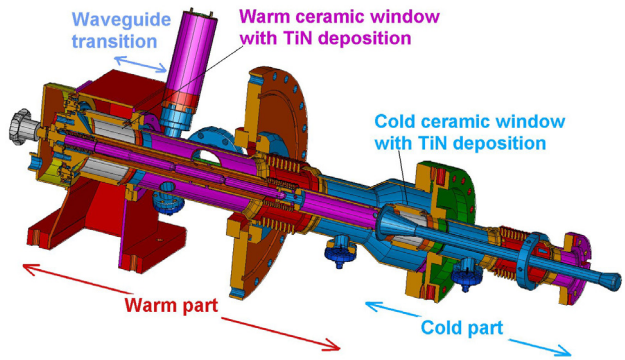

Figure 1: TTF-III power coupler (DESY design).

MULTIPACTING CALCULATION

Much effort is needed in order to understand the coupler behaviour during processing. Therefore, we have tried to find a correlation between e^- currents measured during standard TTF-III coupler conditioning and the calculation results using the 2D MP simulation program for axi-symmetric geometries named MultiPac 2.1 [3].

During TTF-III coupler conditioning, we observe that the power levels corresponding to e^- current enhancement in the cold parts are generally the same for most of the couplers. However, these similarities were not noticeable for the warm coupler parts. This may be due to the higher geometrical complexity of this part (figure 1). To perform MP simulations, we initially considered a model for the cold part that was composed of the RF window geometry and a simple coaxial line geometry. The effect of the bellows on MP levels was neglected in this approach. Consequently, simulation shows that, for a pure RF travelling wave, there is no MP on the cold ceramic window. Nevertheless, the presence of many MP levels in the coaxial line geometry was confirmed. Some incoherence between the calculated MP levels and the measured e^- currents during conditioning was noticed. In fact, we usually measure a relatively high e- current in the cold part for a forward RF power of about 700 kW. Our simulations show complete absence of a MP threshold in this power range. In order, to see if the bellows are at the origin of this MP we integrated them into the model and made new calculations. The new results show a good correlation between the calculated MP levels and the measured e^- currents from several conditioning tests (figure 2). As a consequence, the bellows appear to be the origin of the MP power level taking place at 700 kW. Nevertheless, electron trajectory calculations show that this MP level is not built up within the bellow undulations but rather in their neighbourhood.

HIGH POWER RF SUPPLIES FOR THE FAIR INJECTOR LINACS

W. Vinzenz, G. Schreiber, L. Groening, W. Barth, M. Hoerr, H.-L. Dambowy
GSI, Darmstadt, Germany

Abstract

The operating frequency of the FAIR proton linac was fixed to 325.224 MHz two years ago. Even though the six coupled CH-structures need slightly different RF levels, the proton linac will be equipped with identical RF power sources. That applies also for the RFQ structure.

To supply the FAIR accelerators with a good beam quality by the UNILAC as the high current heavy ion injector for FAIR as well as a high duty factor accelerator for nuclear physics experiments, different upgrades and modifications have to be made at the RF components.

The provision of an excellent RF operation for the next years postulates some general renewals. This paper describes the actual status of the proton linac RF system and the future requirements for the existing UNILAC RF systems.

INTRODUCTION

In the context of the dedicated proton linac within the FAIR project seven high power RF amplifiers up to 2.5 MW at 325 MHz have to be installed. The Toshiba E3740A klystrons selected meanwhile can provide enough power for the overall RF pulse length of 200 µs at a repetition rate of 4 Hz with sufficient margin.

For the UNILAC altogether eight high power RF tube amplifiers at 36 MHz (3 up to 2 MW) and at 108 MHz (5 up to 1.6 MW) will be involved in the future beam operation for high current beams (up to 800 kW beam load in addition at HSI) and a so-called long pulse mode (up to 50% beam duty cycle for a/q ~ 6). The FAIR requirements will meet or exceed the present capabilities in maximum power and duty factor. This leads to detailed improvements of the existing amplifiers and power supplies involved.

FAIR PROTON LINAC

Choosing an operating frequency of 325,224 MHz was triggered by an existing prototype of a coupled CCH-Structure [1] and the presence of high power klystrons used at the J-PARC facility. Following these facts, the number of RF power sources for the DTL could be reduced to six. Even though the RFQ needs less than half the RF power with respect to one CH-structure we decided to stay at the same amplifier type. This makes sense due to spare part storage and reduces the diversity of amplifier types. Two more identical amplifiers will supply the bunching cavities at the same frequency with an expected RF power of 15 and 50 kW, respectively.

Test Bench

For tests with all infrastructure components of one klystron section a test bench is mandatory. Also the first CCH-Structure has to be tested in an X-ray shielded cave. In February 2008 the first Toshiba klystron was successfully tested at manufacturer's site in Japan and delivered to GSI in April. A 100 W driver amplifier was ordered and delivered by RES Ingenium (Italy) in 2007. At present a test bench [Fig. 1] is under construction, offers for additional technical equipment are available. All power supplies will be developed by the GSI power supply group. Because of the very low duty factor a crowbar-less solution has been developed [2]. The prototyping of the LLRF is made by GSI, based on a system that will be installed at the GSI/FAIR synchrotrons using IQ detection and digital control FPGA/DAC solutions. After some technical revision the measurement and data acquisition system used at the High Current Injector (HSI) RF section will be also implemented at the proton linac.

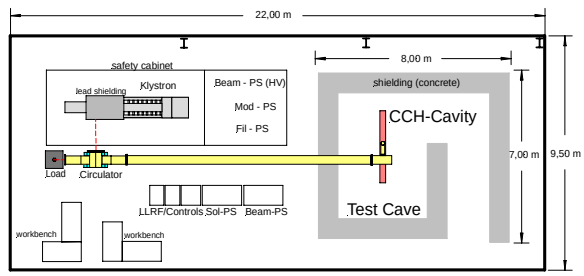

Figure 1: Layout of the test bench.

Some special features on behalf of pulse forming and tube protection purposes will be updated from the UNILAC LLRF system and functionally included in the new digital control system. There are established and approved methods for pulsed RF operation at high power levels reducing faults and off-times as well as enormous time savings during cavity conditioning. Due to the higher demands for the proton linac, the existing analogue value measurement was meanwhile improved. The standard LLRF layout is shown in [Fig. 3]; an overview of the special functions is shown in [Fig. 6].

Proton LINAC RF System

The layout of a klystron driven high power RF system has been sufficiently described in conference proceedings. Building restrictions e.g. the maximum length of the klystron gallery as well as the cost optimised infrastructure of the building has to be taken into account, however. As [Fig. 3] shows seven klystrons will be installed inside the RF-Gallery at ground level. Each klystron is feeding one cavity, which makes the variation of the linac output energy very simple. Further more all electronic devices and supply units are arranged in the

OPERATION EXPERIENCE WITH THE FLASH RF WAVEGUIDE DISTRIBUTION SYSTEM AT DESY

S. Choroba, F. Eints, T. Froelich, A. Gamp, T. Grevsmühl, V. Katalev, DESY, Hamburg, Germany

Abstract

The RF stations for the FLASH linear accelerator at DESY provide RF up to 10MW for 1.3ms and 10Hz at 1.3GHz for forty-eight superconducting cavities grouped into six cryogenic modules and for one normal conducting RF gun. A WR650 waveguide distribution system distributes the power generated by five RF stations using 5MW single beam and a 10MW multibeam klystron to the cavities and the gun. Since FLASH is based on the Tesla Test Facility, TTF, a number of different distribution layouts for the different modules and the gun have been developed and used over the years in terms of type of components and distribution scheme. This paper presents the layout and summarizes the experience with the existing waveguide distribution system.

INTRODUCTION

FLASH bases upon the TESLA Test Facility at DESY which has been constructed since the early 1990 in order to test all components required to construct a linear collider using superconducting cavity technology. Over the years the test facility has undergone many changes in order to meet the demands of different test options and operation conditions. Today FLASH serves as a user facility for synchrotron radiation research as well as a test facility for the European XFEL and for ILC studies.

FLASH accelerates an electron beam of 1nC bunches up to 1GeV which is used to generate laser light in the VUV regime. The electrons are produced in a RF gun and are accelerated in forty-eight superconducting nine-cell niobium cavities which are grouped in six cryogenic modules. The cavities are operated in a range between 12MV/m and 32MV/m. The RF power required by the RF gun and the cavities is generated by three 5MW klystrons and one 10MW multibeam klystron. The RF power distribution based on WR650 type waveguide distributes the power between the RF sources and the RF gun or the superconducting cavities. Due to different requirements and state of the art at a certain point of time a number of waveguide components and layouts have been developed, installed and operated over the years.

RF STATION LAYOUT

Each FLASH RF station consists of a HV pulse modulator with pulse transformer, a high power klystron, which generates the power required by the RF gun and the cavities, and a number of additional components. The HV pulses modulator converts AC line voltage to pulsed high voltage up to 130kV at a pulse duration of 1.5ms and 10Hz repetition rate. The klystrons convert pulsed power into pulsed RF power by amplifying an input RF drive power of 200W to the 5MW or 10MW output level with pulse durations up to 1.3ms of which 500µs required to fill the cavities with RF power and 800µs to accelerate the beam. More detailed information of the RF station layout can be found in [1].

RF DISTRIBUTION LAYOUTS

General Distribution Layout

Six RF stations have been installed at TTF and are labelled by #1 to #6. Station #1 is not in regular use for FLASH. It serves as power source for superconducting cavity tests but could be used as spare for FLASH which has not been required during the years. Station #3 provides RF power to the RF gun of FLASH, #2 to the first cryogenic module ACC1 with eight cavities, #5 supplies RF power for the modules ACC2 and ACC3 with sixteen cavities in total. Station #4 supplies power to the three modules ACC4, 5 and 6 with twenty-four cavities in total. Station #6 serves as spare for the other stations and, in case this is not required, is used for experiments and tests of waveguide elements. Figure 1 shows the actual RF distribution.

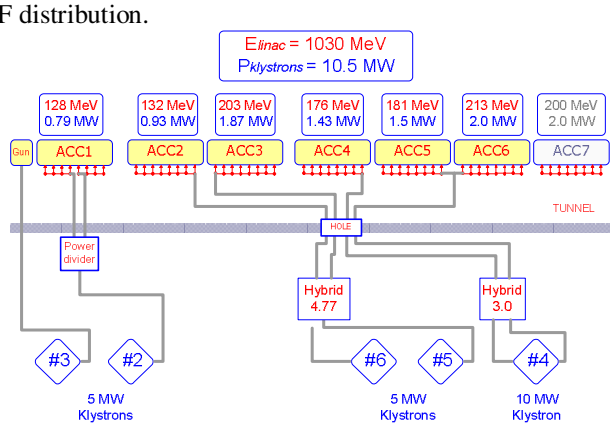

Figure 1: FLASH RF System.

All waveguide distributions between the klystrons and the superconducting cavities comprise the following sections. A section of typical 2m between the klystron window and an additional window with circulator in between filled with SF6 of typical 1.2bar, a module distribution for eight cavities at the cryogenic module either of linear or of combined (tree like and linear) type, and several meters of WR650 waveguide filled with air between these two sections. The module distributions with the exception of the distribution for ACC6 are of linear type. Equal amounts of power are branched off by

ELIMINATION OF PARASITIC OSCILLATIONS IN RF TUBE AMPLIFIER FOR HIGH POWER APPLICATION

E. Feldmeier, Heidelberg Ion Beam Therapy Center, Universitätsklinik Heidelberg, Germany
G. Hutter, W. Vinzenz, B. Schlitt, GSI, Darmstadt, Germany

Abstract

For the heavy ion therapy center HIT in Heidelberg a 1.6 MW power amplifier for 217 MHz was built to supply the 7 MeV/u IH cavity. The inherent parasitic oscillations of the RF tube increases rapidly the anode current until the system switches off. For the elimination of those parasitic oscillations ferrite material is used. The electro magnetic fields are simulated to find an optimal positioning of the ferrite material in the anode cavity such that only the parasitic oscillations are attenuated without affecting the fundamental mode.

INTRODUCTION

A dedicated clinical cancer therapy center designed by GSI was built at the Universitätsklinik in Heidelberg, Germany [1,2]. The facility is designed to treat about 1200 patients per year using the intensity controlled raster scan method developed by GSI. Since 1997 more than 400 patients have been successfully treated with carbon ions at GSI.

During the last two years the HIT accelerator and its subsystems were commissioned [3]. In December 2007 the carbon beam reached therapy quality in the treatment rooms. The start of the clinical operation is planned for December 2008.

The facility consists of the 7 MeV/u injector linac, a 430 MeV/u synchrotron, an experimental area, two treatment rooms with horizontally fixed beam lines and one treatment room with an isocentric gantry.

The injector linac consists of a 400 keV/u RFQ and a 7 MeV/u IH drift tube linac with an effective acceleration length of 5.5 m.

The RF system of the compact injector operates at 216.816 MHz. It consists of three RF tube amplifier working in pulsed operation at 200 kW (RFQ) and 120 kW/1.4 MW (IH) with a pulse length of 500 µs and a duty cycle of 0.5%. The 200 kW tube amplifier and the preamplifier for the 1.6 MW final stage was built commercially by THALES/THOMSON. The final stage of the 1.6 MW amplifier was designed and manufactured by BERTRONIX, Munich. This stage was mechanically assembled in Munich and delivered to GSI for the commissioning and RF tests. For the clinical application a very stable and reliable operation is mandatory. To get more options the stage is constructed for two different tube types, the THALES TH 526 and the EIMAC E 8973. In the beginning of the project it was not decided which tube would be used for standard operation. During the commissioning the TH 526 was chosen.

PARASITIC OSCILLATIONS

One of the main problems during the commissioning was the parasitic oscillations of the TH526 which appear with different strengths at 478 MHz, 818 MHz, 875 MHz, 1024 MHz, 1240 MHz, 1468 MHz and 1680 MHz.

Parasitic oscillations occur even without RF when the tube is pulsed to the A-working point. Using the control grid voltage the tube should be set to a working point with an anode current of 6 A. When increasing the anode current to more than 2 A the parasitic oscillations set in and lead to an uncontrollable operation in which the tube cannot be locked by the control grid anymore. The problems occur mainly with the parasitic oscillations at 875 MHz and 1240 MHz.

It was shown earlier [4] that oscillations can be suppressed successfully by using ferrite material in the anode circuit and between grid 1 and grid 2. This paper proposes a new method find an optimal position for the ferrite material.

FIELD SIMULATIONS

The ferrites have to be positioned at locations where the H-field of the parasitic mode is large in order to suppress these modes most effectively. To find the optimal position for the ferrite rods and slabs the electro magnetic field distribution within the cavity is numerically calculated using CST Microwave Studio. It is sufficient to calculate the fields in the anode cavity of the amplifier. One part of the anode cavity is the amplifier tube which however is an active component that cannot be simulated within the used FIT method [5].

The electron flux in the tube represents a conductive area in the active system of the tube. In the simulation this area is represented by a conductive material with a conductivity σ which can be calculated as

$$\sigma = \frac{1}{2\pi \cdot L} \cdot \frac{I_A}{U_A} \cdot \ln \frac{R_2}{R_1}.$$

L denotes the length of the active system, R_2 and R_1 are the outer and inner radii of the cylindrical cavity, respesctively. The anode current I_A and voltage U_A are measured.

First one has to verify that one gets the correct frequency of 216.816 MHz for the fundamental mode. To correct for uncertainties in the geometrical dimensions and inaccuracies in the mapping of the active tube system, for example the leakage of the field through the grid, one may move the position of the cavity bottom slightly.

The next step is to verify that besides the fundamental mode also the higher eigenmodes coincide with the

DEVELOPMENT OF ALL SOLID STATE BOUNCER COMPENSATED LONG PULSE MODULATORS FOR LEP 1MW KLYSTRONS TO BE USED FOR LINAC4 PROJECT AT CERN*

Purushottam Shrivastava#, J. Mulchandani, V.C. Sahni
Raja Ramanna Centre for Advanced Technology, Indore, India
Carlos A. Martins, Carlo Rossi, Frédérick Bordry, CERN, Switzerland.

Abstract

CERN is building a 352.21 MHz 3 MeV RFQ based test stand as first part of LINAC4. Extending its earlier collaboration with RRCAT, India, CERN had approached it to design and develop a high voltage pulsed modulator for 1 MW LEP klystrons, planning their reuse. RRCAT proposed three design schemes out of which an all solid state bouncer compensated modulator was chosen for follow up development work. The main considerations for the design were to avoid gas tube crowbar on the HV side, to have low rise and fall times and to realize high voltage stability of the flat top. The output voltage and current are rated up to 110 kV/24 A, with pulse duration 800 µs, repetition rate of 2 Hz, <1% droop and <0.1% ripple on pulse top with energy restricted to 10 J in case of klystron arc. Based on these principles, a modulator has been developed and constructed at CERN and is currently undergoing tests with a klystron while another one with similar development is in the final stages of integration/evaluation at RRCAT. The present paper describes the topology, simulation results, protection strategy and briefly summarizes the results achieved.

INTRODUCTION

The 3 MeV test stand will enable to explore the beam dynamics issues at the low energy end and comprises of 352.21 MHz, 3 MeV, 3-meter long RFQ, (part of SPL Front End) as the first part of the LINAC4 [1], a new PS Booster injector proposed to improve the proton beam quality and availability for CERN users in the LHC era.

LEP 352.21 MHZ, 1 MW CW klystrons will be operated in pulsed mode with maximum average power up to 2 kW, to feed the RF sections of the linear accelerators. This requirement necessitated the development of new high voltage pulsed modulators tailored for operation at duty cycle of 0.1%.

Design Considerations

The following issues were considered in the design:

- Crow-bar-less (no ignitron or thyratron) protection of klystron against arcing. The protection is assured by a) switching-off the main series switch very swiftly b) absorbing and dissipating the maximum of energy stored in the parasitic elements (stray capacitances, inductances, etc) inside the damping networks
- Low rise and fall time to limit the amount of wasted power
- High voltage stability of the flat top to assure the necessary phase stability of the RF output
- High reliability, minimum maintenance efforts and high lifetime due to solid-state construction.
- Modular structure to facilitate higher repetition rate up to 15 % duty at a later stage.
- The power supply interlock system able to be integrated into the CERN control and interlock system

#purushri@rrcat.gov.in
*work supported by DAE of India under aegis of DAE CERN NAT Protocol

TECHNICAL SPECIFICATIONS

The major requirements are listed in Table 1.

Table 1: List of modulator main parameters

Parameter	Design Targets
Klystron modulator type	Bouncer
High Voltage pulse amplitude	-10 kV to -110 kV
High Voltage pulse width measured at 70% to 70 % of peak.	800 µsec
Minimum Flat top available	600 µsec
Maximum current during pulse	24 A
Pulse repetition rate	2 Hz
Acceptable voltage drop	≤ 1.0%
Allowed ripple on flat top (≥ 10 kHz)	≤ 0.1%
Rise time/fall time	<100 µsec
Energy dissipated in klystron during klystron arc	<10 J

TOPOLOGIES CONSIDERED

At RRCAT we have designed and commissioned several modulators for klystrons based on the PFN topologies with step up pulse transformers, which have peak pulse power up to 15 MW and mean power up to 90 kW[2]. Few solid state switched modulators were also developed using RRCAT built stacked MOSFET/IGBT solid state switches, operating at 5 kV/0.5 A@10 µsec/ 1 Hz and 50kV/2A@10µsec/300Hz for pulsing driver klystrons and LINAC electron guns respectively. Looking into large reservoir of experience gathered on various topologies RRCAT took up the present project for CERN. Out of several schemes three options were found to be suitable and therefore an initial evaluation was restricted to: 1) Hard switched klystron modulator with high voltage programmable power supply for droop correction (active

COOLING SYSTEM DESIGN OF COMPACT KLYSTRON MODULATOR POWER SUPPLY IN THE XFEL PROJECT AT SPring-8

Chikara Kondo, Takahiro Inagaki, Katsutoshi Shiarasawa, Tatsuyuki Sakurai, Tsumoru Shintake,
RIKEN SPring-8, 1-1-1 Koto, Sayo, Hyogo, Japan

Abstract

XFEL project at SPring-8 requests the high performance modulator power supply for klystron i.e., low pulse-to-pulse fluctuation, low parameter drift, low noise, compact size, and easy maintenance [1]. To meet these requirements, we developed the compact klystron modulator power supply which stores the high voltage components in single steel tank. In order to obtain the practical heat transfer efficiency, we measured the heat transfer efficiency for various cooling panels in the model tank. Based on the results, we designed the optimum cooling system for the actual modulator power supply. We installed the cooling system to the modulator power supply, and confirmed the cooling efficiency was as expecting, and the oil temperature was under 45 °C.

THE KLYSTRON MODULATOR POWER SUPPRY AT XFEL/SPRING-8

In the XFEL/SPring-8 project, the electron beams are accelerated by 128 of C-band accelerating structures. Since the accelerator is compact thanks to the acceleration gradient as high as 35 MV/m, the interval lengths of the modulator power supply for klystron become narrow. Therefore, the size of the modulator should be more compact than traditional one. Consequently, we developed the compact modulator power supply for klystron, which stored the PFN condensers, a thyratron, and a pulse transformer in an oil-filled tank. The specification of the modulator is listed in table 1.

The insulation oil enabled the tank to be compact, and isolate the performance from dust and humidity. Otherwise, the cooling system of the oil is one of the most important points for the requirement of stable operation and maintenance-free. The modulator dissipates the heat mainly coming from a thyratron cathode heater, a klystron cathode heater, a pulse transformer, and electrical resistors. The excessive increase of the oil temperature by the heat generation leads the problems as written blow;

- The drifts of the electrical properties of the components.
- The drift of the air temperature by the heat dissipation from the modulator to the air.
- The deterioration of the insulation oil and the heat dissipation to the air.

To avoid the problems, we need the efficient cooling system which transfers the heat from the oil to the cooling water. We aimed for the cooling system not only efficient but also compact and maintenance-free. We chose the natural convection cooling, i.e. fan-less cooling.

In this paper, we described the review of the oil cooling, the efficiency of the fan-less cooling system, and the results of the oil temperature of the modulator in our prototype modulator.

Table1: Klystron modulator specifications

PFN charging voltage	45 kV
Output voltage	350 kV
Output current	316 A
Transformer step up ratio	1 : 16
Pulse width (at 70% of the voltage peak)	4.2 μsec
Peak output power	110 MW
Maximum repetition rate	60 pps

HEAT TRANSFER IN NATURAL CONVECTION

The oil flows by natural convection which occurs due to the heat transfer between oil and object. Around the heat sources, such as electric resistors or cathode heaters, the oil is heated and starts to rise. When the hot oil reaches to the cooling material, such as a water pipe or panel, the heat moves to the water and the oil sinks down.

The heat transfer rate q between the oil and the object can be written as,

$$q = hA(T_h - T_c) \quad (1)$$

where h is the heat transfer coefficient, A is area of the cooling material, T_h and T_c are the temperature of the hot object and the cold object, respectively. The heat transfer coefficient represents the cooling efficiency. The practical value of the coefficient is difficult to be calculated analytically, because it depends on not only the property of the oil but also the geometry of the panel and the detail flow around the object [2].

There are a few reports for the heat transfer coefficient for the insulation oil [3]. But, the conditions of the report differ from our condition in the oil type and the cooling panel geometry. Therefore, we performed the experiment to measure the coefficients.

COLD CATHODE ELECTRON TUBE TOWARD PLENTY MULTI BEAM TUBE

M. Yoshida, KEK, Ibaraki, Japan
T. Hioka, K. Someya, Tokyo University of Science, Chiba, Japan
K. Utsunomiya, University of Tokyo, Tokyo, Japan

Abstract

The multi beam electron tube with a lot of beam pipes is required for the lower applied voltage and the higher frequency because the efficiency has a limit according to the perveance. However, the total heater power consumption becomes too high if many thermal cathodes are used. Thus the cold cathode such as the carbon nano tube (CNT) is suitable for such a multi beam electron tube. Further the cold cathode has the advantage to work as a switching device since the metal grid close to the cathode can be used. The design and the fundamental test of the partial model will be presented.

ELECTRON TUBE USING COLD CATHODE

If we attempt to design the hundred or thousand multi beam electron tube, the following problems were occurred:

- Huge power consumption of thermal cathodes.
- Complicated gain cavity system using higher mode.
- Huge solenoid magnet.
- Parallel switching device adopting higher current is required for the pulse operation.

To avoid them, the grid triode [1] like the inductive output tube (IOT) using the field emission cathode has a possibility as a solution of such a plenty multi beam electron tube.

The advantages using the field emission cathode compared with the thermal cathode are as followings:

- No power consumption for the cathode.
- Very thin metal wire grid can be used and long life time is expected since the life time described in reference [1] is mostly caused by the high temperature of the thermal cathode.
- No resonant frequency change is occurred.
- Shorter grid gap and higher surface field makes to operate at higher frequency.
- Shorter bunch caused by the E-I curve of the field emitter can operate as the frequency doubler as shown in Fig. 1. Fig. 1 (left) shows the expected emission current according to the E-I curve of the carbon nano tube (CNT). Fig. 1 (right) shows the comparison of the frequency component between the CNT cathode and the thermal cathode

Further the grid tube has many advantages as followings:

- Huge solenoid magnet is not required since the beam trajectory is shorter.
- No switching device is required for the pulse operation.
- Simple cavity system

The disadvantages using the field emission cathode are as followings:

- Much higher surface field is required for the emission.
- Since it causes the lower gain, multi stage tube has to be considered to get higher gain.
- Proper ageing process is required for the field emission cathode.
- Special treatment is required to reduce the ununiformity of the cathode emission. One candidate for this is that the field emitter is arranged on the high resistance plate.

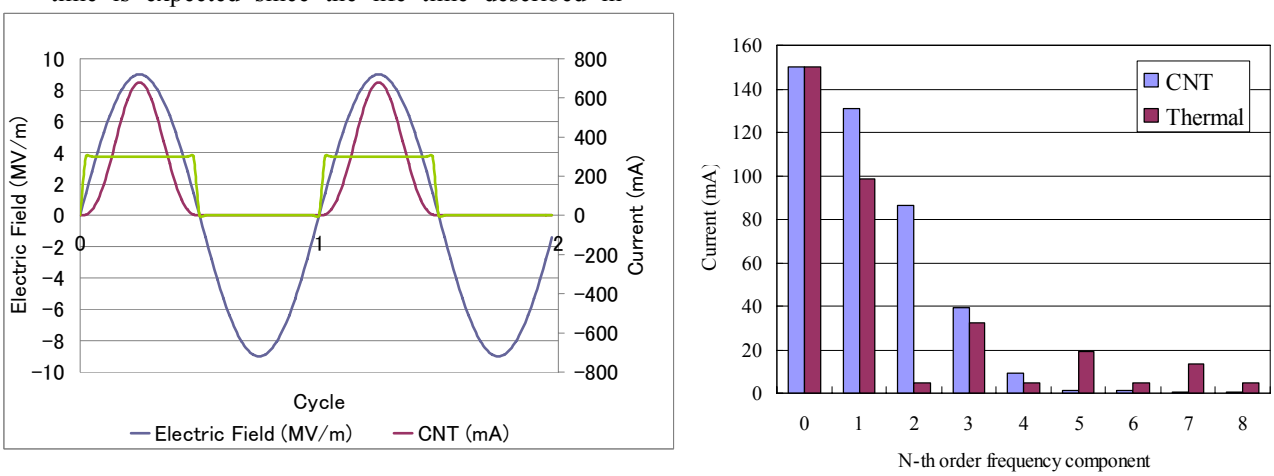

Figure 1: The emission current and its frequency component.

QUARTER-WAVE-STUB RESONANT COUPLER

Donald A. Swenson, Linac Systems, LLC, Albuquerque, NM

Abstract

Most small proton and other ion linacs involve two different linac structures, namely an RFQ linac section and some other, more efficient, linac structure, such as the Drift Tube Linac (DTL), the interdigital (Wideröe) linac, or the Rf Focused Interdigital (RFI) linac. Such linacs can benefit a lot by being resonantly coupled into a single resonant unit. The resonantly coupled structures can be driven by a single rf power system, through single rf drive loop, at a single rf frequency. The relative phase and relative amplitude of the fields in the two structures are locked by the resonant coupler. Such systems require no control of phase of the rf power. By designing the rf power system to track the resonant frequency of the combined structures, the control of the resonant frequencies of the two structures is greatly simplified. A simple, compact, resonant coupler, based on a quarter-wave-stub, will be described. Models of this resonant couple have been tuned and adjusted, and are scheduled to be tested at operating powers in the fourth quarter of 2008.

BACKGROUND

Resonantly coupled linac structures have been around for 50 years. In the mid-60s, the Side Coupled Linac (SCL) structure was developed at Los Alamos for use in the Los Alamos Meson Physics Facility (LAMPF), and subsequently in thousands of today's electron linacs. Later in that decade, the post coupled Drift Tube Linac (DTL) was developed, which stabilized the amplitude and phase of the fields in these structures. Resonant coupling and operation in the $\pi/2$ mode are essential to modern linac technology.

The same technology that stabilizes linac structures can be used to couple any two resonant structures that operate at the same frequency. The bridge couplers of LAMPF are prime examples. They are not resonant couplers themselves, but rather resonant structures that are resonantly coupled to adjacent linac structures. The first 8 modules of LAMPF are built as 4 SCL linac tanks and 3 bridge couplers. The last 36 modules of LAMPF are built as two SCL linac tanks and one bridge coupler. In all cases, the SCL tanks are resonantly coupled to the bridge coupler by a minor modification of the side coupling cell. The "bridge coupler" name comes from the fact that these devices bridge the resonant properties of the structure around the required beam focusing quadrupoles.

For proton and ion linac applications, where the relative amplitude and phase of the fields are so important, the resonant coupling of the resonant units in a linac system is very important. The resonant couplers operate in the $\pi/2$ mode. They are nominally unexcited while the units that they couple are excited. The $\pi/2$ mode is unique in that it is the only mode in the mode spectrum where no changes are required in the amplitude or phase of the excited cells to accommodate changes in power flow through the structure. The resonant couplers lock the relative amplitude and phase of the fields in the excited cell of the structures. They stand by to support power flow in whichever direction is required to keep the fields in the excited structure at their design value.

For the theory of resonant coupling go to the Nagle, Knapp, and Knapp[1] or the Knapp, Knapp, and Potter[2] papers of the late 60's.

INTRODUCTION

Particle accelerators employ electromagnetic resonators to produce high electric fields that can be used to accelerate charged particles to higher energies. Particle accelerators involving a single resonator have a requirement that the amplitude and distribution of the fields in the resonator be appropriate for the acceleration process. Particle accelerators involving two or more resonators have an additional requirement that the relative phase of the fields in adjacent resonators be controlled. Control of the relative phase of the fields requires that the frequency of the electromagnetic excitations in the all resonators be the same or harmonically related.

The conventional solution to these requirements is to control the resonant frequency of all resonators to the required accuracy, to control the amplitude of the fields in all resonators to the required accuracy, and to control the phase of rf fields in all cavities to some phase reference to the required accuracy.

The use of a resonant coupler greatly simplifies the controls problem for two-resonator particle accelerators. The resonant coupler provides a single frequency at which the pair of resonators can be excited, even when the resonant frequencies of the individual resonators are slightly different. The resonant coupler locks the relative amplitudes and relative phases of the field in the two resonators. Consequently, the resonant coupler reduces the controls problem for two-resonator accelerators to that of controlling the frequency of the drive power to the single frequency offered by the resonant coupler and controlling the amplitude of either resonator to the required accuracy.

Two-resonator accelerators are common in low energy range of ion accelerators, where the first resonator is a radio frequency quadrupole (RFQ) linac structure, with its superb very low energy capabilities, followed by some other low energy linac structure with better acceleration properties. This resonant coupler offers significant advantages to this important class of low energy ion accelerator.

A block diagram of two generic resonators that are resonantly coupled by a generic coupling resonator is shown in Fig. 1.

HIGH POWER 325 MHZ VECTOR MODULATORS FOR THE FERMILAB HIGH INTENSITY NEUTRINO SOURCE (HINS)*

Robyn Leigh Madrak and David Wildman
Fermilab, Batavia, IL 60510, U.S.A.

Abstract

One of the goals of the low energy 60 MeV section of the HINS H^- linac [1] is to demonstrate that a total of ~40 RF cavities can be powered by a single 2.5 MW, 325 MHz klystron. This requires individual vector modulators at the input of each RF cavity to independently adjust the amplitude and phase of the RF input signal during the 3.5 ms RF pulse. Two versions of vector modulators have been developed; a 500 kW device for the radiofrequency quadrupole (RFQ) and a 75 kW modulator for the RF cavities. High power tests showing the vector modulator phase and amplitude responses will be presented.

INTRODUCTION

The first high power microwave phase shifters using ferrite-loaded coaxial structures were first described more than forty-five years ago [2,3]. Recently, there has been renewed interest in the field with advances in technology and materials. The possibility of powering multiple RF cavities from a single RF source has become a viable alternative to the traditional single RF source per cavity [4,5]. At Fermilab we are in the process of building a 60 MeV H^- linac to be used as the front end of a future High Intensity Neutrino Source (HINS). The linac is designed to accelerate 20 mA of beam current in either 1 ms pulses at a 10 Hz rate or 3 ms pulses at a 2.5 Hz rate. The first 30 MeV section of this new linac will have a 2.5 MeV RFQ, two bunching cavities, 16 room temperature CH type (3 & 4 spoke) cavities, and 18 superconducting single spoke cavities all being driven by a single 2.5 MW, 325 MHz klystron (Toshiba E3740AFermi.) Here there will be one vector modulator between the klystron and each cavity to independently control the phase and amplitude of the RF drive signal to its coupling loop. For the room temperature cavities these vector modulators will serve two purposes. First, they will be used to correct for cavity tuning errors caused by cavity heating and cooling water temperature fluctuations. Second, they will provide a means of compensating the effects of beam loading. To meet these goals we have developed two versions of high power vector modulators using fast ferrite loaded coaxial phase shifters. A 75 kW version will be used for all of the room temperature RF cavities. The RFQ which requires a larger 500 kW model.

VECTOR MODULATORS

A photograph of one of the 75 kW vector modulators is shown in Figure 1. The 325 MHz signal from the klystron enters port 1 of a –3 dB quad hybrid (Dielectric Communications) where it is equally split with a 90° phase difference between ports 2 and 3. Two shorted 1.625″ OD coaxial, ferrite-loaded phase shifters, described below, are attached to ports 2 and 3 and provide full reflections with phase shifts φ2 and φ3 respectively. The desired phase shift is produced by a variable solenoidal magnetic field along the axis of the coaxial line which is used to adjust the permeability, μ, of the ferrite. These reflected signals are recombined at the output (port 4) of the quad hybrid with a resulting output phase of (φ2 + φ3)/2 and power proportional to $\cos^2$ (φ2 - φ3)/2. A 3 port 75 kW circulator (D & M Co. Ferrit-Quasar) with a 5 kW water cooled RF load (Altronic) is connected between the quad hybrid output and the RF cavity to isolate the phase shifters from any power being reflected from the cavity during the cavity filling time or under cavity detuning conditions.

The higher power vector modulator to be used with the RFQ is similar to the one described above except that the components are physically larger. The –3 dB quad hybrid (Micro Communications) has a coaxial design with 6″ EIA flanges and is filled with SF_6 to prevent sparking. The two phase shifters are 3.125″ OD, ferrite-loaded, shorted coaxial lines and are also filled with SF_6. A high power 3 port coaxial/stripline circulator (D & M Co. Ferrit-Quasar) is used to prevent the reflection of power back to the phase shifters.

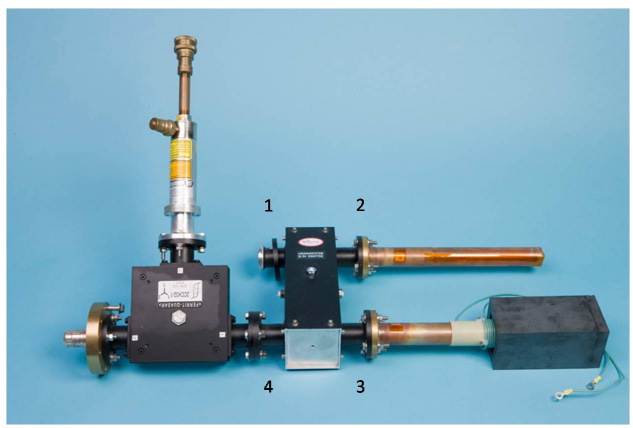

Figure1: Photograph of a 75 kW vector modulator.

* Operated by Fermi Research Alliance, LLC under contract with the U.S. Department of Energy

HIGH POWER L-BAND FAST PHASE SHIFTER*

I. Terechkine#, T. Khabiboulline, N. Solyak, FNAL, Batavia, IL 60510, U.S.A.

Abstract

A design of a waveguide-based, L-band, fast, high-power phase shifter is proposed. The shifter uses two magnetically biased blocks of Yttrium Iron Garnet (YIG) positioned in contact with the side walls of a rectangular waveguide. The cross-section of the waveguide is chosen to suppress unwanted RF modes that could otherwise compromise performance of the phase shifter. Static bias field in the YIG blocks is created by permanent magnets. Low inductance coils in the same magnetic circuit excite changing component of the bias field. Design of the device ensures effective heat extraction from the YIG blocks and penetration of the fast magnetic field inside the waveguide with minimum delay. This paper summarizes main steps in this development and gives brief description of the phase shifter.

INTRODUCTION

The attractiveness of using devices that control phase and amplitude of input RF power of superconducting accelerating cavities of a high-power linac is widely recognized [1]. Once implemented, this approach will result in significant savings in number of klystrons. This motivates multiple efforts towards building a high-power, fast phase and amplitude modulator, also known as vector modulator [2], [3]. At Fermilab, a prototype of a waveguide-based phase shifter was built and tested to demonstrate high power handling capability: up to 2 MW at 1300 MHz [4]. The phase shift range of this device was limited by the onset of sparking in the ferrite-loaded waveguide. Understanding the nature of the this effect was considered crucial for improvement of the performance, and a study was conducted that connected the sparking with the excitation of one of several resonant modes in the ferrite-loaded part of the waveguide [5]. The resonant modes could exist due to imperfections in positioning of the YIG blocks inside the waveguide or due to some difference in the levels of the bias field in the blocks. Variations in the magnetic properties of the YIG blocks can also result in resonances. Following this phase shifter performance study, a way to design a resonance-free system was proposed [6].

In the end, the answer to the question of whether the use of vector modulators in RF distribution system of a linac is advantageous in comparison with the "one transmitter per cavity" approach is in the complexity of a power system needed to activate the device. An impact of possible design solutions on requirements for the power supply must be closely watched.

This paper summarizes results of the phase shifter prototype performance study and presents a design concept of a fast, high-power phase shifter. The operating frequency (1.3 GHz) and the transmitted power requirement (~125 kW per one phase shifter) were chosen having in mind an elliptical (TESLA-type), nine-cell superconducting cavity.

*Work supported by the U.S. Department of Energy under contract No. DE-AC02-07CH11359.

#terechki@fnal.gov

PHASE SHIFTER PERFORMANCE

Dynamic range of the phase shifter prototype described in [4] depended on the input power. It was ~90° at 100 kW and reduced to ~30° at 1500 kW due to onset of sparking in the gaps between the YIG blocks and the walls of the waveguide. The sparking could be stopped by partial filling the waveguide with SF_6. The sparking was the result of RF electric field increase when one of trapped RF modes in the ferrite-loaded waveguide was close to resonance and got coupled with the main TE_{10} mode.

In the regular section of the prototype's waveguide (165.1 mm x 50.8 mm), the modes TE_{11}, TM_{11}, TE_{20}, TE_{21}, etc. have critical frequencies higher than 1300 MHz. Only TE_{10} mode can propagate along the waveguide – the critical wavelength of this mode is 330.2 mm versus the free space wavelength at 1.3 GHz of 230.8 mm. In the ferrite-loaded section of the waveguide, critical frequencies for all modes shift to lower values; as a result, these modes can propagate in this section. Each high-order mode can be excited if there is a coupling with the main TE_{10} mode. If the coupling is small, corresponding mode can have a quality factor high enough for the electric field to exceed the breakdown threshold setting off the sparks.

The following subsections show which high order modes exist in the ferrite-loaded section and how they are coupled with the main mode.

TE_{20} Modes

If the two YIG blocks of the phase shifter are identical, positioned in the same longitudinal space, and have equal magnetic bias, TE_{20} mode is not coupled with the main mode: coupling with one of the blocks is cancelled by coupling with another one. By introducing bias asymmetry, or moving one of the blocks longitudinally, the coupling through electric and magnetic field is made possible. As a result, trapped resonance condition can exist for TE_{202} or TE_{203} mode. To ensure the absence of the coupling, the bias field in the blocks must be equal.

TE_{11} Modes

The presence of the YIG blocks makes it possible for the RF modes with variations along the short side of the waveguide to exist. In this case, the section of the waveguide between the YIG blocks is impassible for the modes. Each block supports its own oscillation mode, and these modes can be excited independently. It means that we will observe not a pure TE_{11} mode, but two separate

MARX BANK TECHNOLOGY FOR ACCELERATORS AND COLLIDERS

J. Casey, R. Ciprian, I. Roth, M. Kempkes, M. P.J. Gaudreau, F. Arntz
Diversified Technologies, Inc., 35 Wiggins Avenue, Bedford, MA 01730 USA

Abstract

Diversified Technologies, Inc. (DTI) has developed high power, solid-state Marx Bank modulators for a range of accelerator and collider designs. We estimate the Marx topology can deliver equivalent performance to conventional solid state modulator designs, while reducing system acquisition costs by 25-50%.

In this paper DTI will describe the application of Marx based technology to two different designs, built under two separate DOE Phase II SBIR grants: a long-pulse ILC focused design (140 kV, 160 A, 1.5 ms), and a short-pulse design (500 kV, 265 A, 3 µs). These designs span the known requirements for future accelerator modulators. For the ILC design, the primary challenge is minimizing the overall size and cost of the storage capacitors in the modulator. For the short-pulse design, the primary challenge is high speed operation, to limit the energy lost in the pulse rise-time while providing a very tight (+/- 3%) voltage flattop. Each design demands unique choices in components and controls, including the use of electrolytic capacitors in the ILC Marx design.

INTRODUCTION

In the last decade, advances in high voltage, solid state switches have enabled a new class of Marx modulators, using "opening switch" technology for the basic building blocks. Three key advances are enabled by using this class of switches. First, the switches may open under fault conditions with sub-microsecond response, minimizing the energy discharged into a load arc, and the need for arc protection crowbars. Second, the capacitors may be sized for an arbitrarily small droop during the pulse duration, eliminating the need for pulse forming circuitry. Last, the triggering of the individual stages may be staggered, with the non-triggered stages bypassed via a diode, allowing programmable waveform synthesis within a single high voltage pulse.

We are nearing completion of two Marx development projects funded under the U.S. Dept. of Energy SBIR program. Although both of these projects are inspired by advanced accelerator requirements, the detailed engineering requirements of each are quite different.

COMMONALITIES TO MARX MODULATORS

The Marx cell is fundamentally composed of an energy storage capacitor and a pulse switch, with a bypass diode spanning them both (Figure 1). When the pulse switch is closed, the capacitor is added in series to the circuit, erecting the high voltage pulse. If the switch remains open, but other cells are closed (and pulse current is flowing), the bypass diode is pulled into conduction and the cell contributes nothing to the series voltage.

This choice – to fire or not to fire the pulse switch – is the key to synthesizing a desired waveform during the pulse. The usual application is to compensate for capacitor droop by firing additional cells as the voltage falls. We can also use such waveform synthesis to actively compensate for transient effects, such as leading edge ringing due to parasitic capacitance.

Between pulses, the energy storage capacitors must be recharged. At very low repetition rates, this charge can be dribbled in with high impedance resistance or high inductance daisy-chain wiring, which carries little current during the erection of the pulse. For short pulse durations, a common-mode choke topology can be used, with differential leads to recharge the capacitors at low impedance, while providing common-mode impedance during the pulse. This technique becomes impractical for long pulse durations, however, as the choke core becomes prohibitively large to avoid saturation. Instead, the technique of choice for long pulses is to use a second string of high voltage switches to supply a charging chain, firing these switches with gating complementary to the pulse switches (Figure 1).

Diversified Technologies has over a decade of experience building series arrays of IGBTs that act as single high voltage switching elements, and are sufficiently robust to use as hard switches in systems over 100 kV. These arrays are ideal for sizing the individual cells of a Marx modulator to optimize the overall system performance. The use of such series arrays can yield further advantage – since IGBTs generally fail short, a properly sized system can lose a single IGBT and

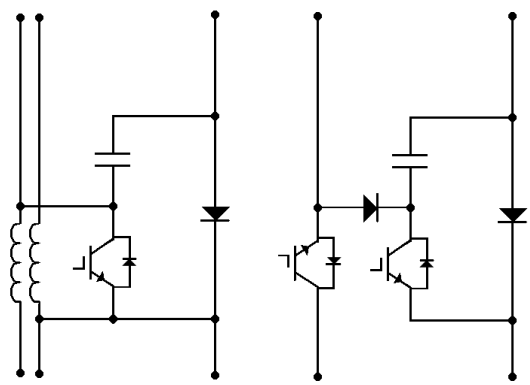

Figure 1: (left) A single Marx cell, recharged via common mode choke, is suitable for short pulses. (right) Long pulses require prohibitively large choke cores, thus recharge is better served via a second switch.

POWER COUPLER AND TUNER DEVELOPMENT FOR SUPERCONDUCTING QUARTER-WAVE RESONATORS*

J. Wlodarczak#, P. Glennon, W. Hartung, M. Hodek, M. J. Johnson, D. Norton, J. Popielarski,
National Superconducting Cyclotron Laboratory, Michigan State University, East Lansing, Michigan, USA

Abstract

The construction of a re-accelerator for secondary ion beams is currently underway at the National Superconducting Cyclotron Laboratory (NSCL). The re-accelerator linac will use superconducting quarter-wave resonators (QWR) operating at 80.5 MHz with $\beta = 0.041$ and $\beta = 0.085$. A coaxial probe-type RF fundamental power coupler (FPC) will be used for both QWR types. The power coupler makes use of a commercially available feedthrough to minimize the cost. The FPC has been simulated and optimized for operation at 80.5 MHz using a finite element electromagnetics code. Prototype FPCs have been fabricated and conditioned with traveling wave and standing wave power using a 1 kW amplifier. A niobium tuning plate is incorporated into the bottom flange of the QWR. The tuner is actuated by a stepping motor for slow (coarse) tuning and a stacked piezoelectric element in series for fast (fine) tuning. A prototype tuner for the $\beta = 0.041$ QWR has been tested on the cavity at room temperature.

INTRODUCTION

NSCL is building a re-accelerator, currently titled ReA3, which will create rare isotope beams (RIBs) for experiments in nuclear science [1]. Stable ions will be produced in an ion source and accelerated by the NSCL Coupled Cyclotron Facility. Particle fragmentation will be used to create a secondary beam. The secondary beam will then be stopped and re-accelerated. This will allow measurements on the exotic beams to be done with higher precision than other techniques.

The first phase of the re-accelerator will accelerate the RIBs up to 3 MeV per nucleon. The superconducting linac will consist of three cryomodules, containing a total of 15 QWRs for either $\beta = 0.041$ or $\beta = 0.085$ [2-4]. Both QWR cavities will utilize similar methods for frequency tuning and RF coupling. Tuning will be done using a slotted tuning plate made from sheet niobium, similar to the designs used at TRIUMF and Legnaro [5,6]. One feature of the NSCL QWRs is the use of separate cavity and insulation vacuum, as opposed to common vacuum, which affects the design of the tuning plate assembly. This plate will provide approximately 20 kHz of tuning for the $\beta = 0.041$ cavities. A fixed probe-type power coupler will penetrate through the tuning plate to transmit power to the cavity. This differs from the adjustable loop-type couplers used at Legnaro and TRIUMF.

This paper will cover the design, prototyping, and testing of both the fundamental power coupler and the tuner for the ReA3 QWRs.

COUPLER DESIGN

The FPCs for ReA3 will be coaxial, operating at 80.5 MHz, with fixed coupling and continuous wave (CW) power, with 400 to 800 watts of forward power, depending on the cavity type [7]. A key component of the power coupler is the RF power feedthrough, which will isolate the cavity vacuum and allow cavity pressures of less than 10^{-8} torr. The feedthrough is based on a power feedthrough readily available in industry, which helps reduce cost and production time.

A prototype low-β cryomodule [8] has been built and tested. The coupler used for the prototype cryomodule test has a small diameter inner conductor and a thin ceramic window [9]. This coupler was designed for lower forward power than needed for ReA3. The updated design incorporates a larger diameter center conductor, thicker alumina window, and less obtrusive air side geometry. These improvements increase the durability, especially during assembly, and power handling capacity of the coupler. The addition of diagnostic ports on the coupler allows the condition of the ceramic window to be monitored. The diagnostic devices consist of a vacuum gauge, current probe, and spark detector. Additionally, a sealed adapter flange is used on the air side, which will be filled with argon gas. In the event of a window failure, the cavity vacuum will be less vulnerable, and the increase in argon can be detected using a residual gas analyzer (RGA).

Several iterations of feedthrough configurations were modeled using Analyst[1], a finite element solver, until an acceptable geometry was found. The S-parameters were also modeled. The final design utilizes a semi-custom feedthrough to allow a more compact size.

After the feedthrough configuration was chosen, an analysis of the mechanical modes of the copper inner conductor was performed. Fundamental modes were found near 30 Hz, and were verified experimentally. Several inner conductors with various lengths of stainless steel liners were modeled, in an attempt to increase this frequency. With an 11 inch (279.4 mm) liner, the frequency was shifted up approximately 7 Hz. Other methods are being investigated to increase the fundamental frequency above 100 Hz.

The heat load to liquid helium from the coupler is a major concern. The total load of the coupler can be

*Work supported by Michigan State University
#wlodarcz@nscl.msu.edu

[1] Simulation Technology & Applied Research, Inc., Mequon, Wisconsin, USA.

LEVERAGING THE LEDA HIGH VOLTAGE POWER SUPPLY SYSTEMS FOR THE LANSCE REFURBISHMENT PROJECT*

J. Bradley III, D. Rees, W. Roybal, K. A. Young, LANL, Los Alamos, NM 87545, U.S.A.

Abstract

The LANSCE Refurbishment Project (LANSCE-R) will revitalize the LANSCE accelerator infrastructure. Much of the equipment has been in use for over 39 years and is approaching the end of its design lifetime. As obsolescence issues make like-for-like replacements increasingly more expensive, modern systems with lower costs become a reasonable alternative. As part of the LANSCE-R project, four of the seven HV power supplies for the 805 MHz RF klystrons will be replaced. The present and future requirements for these power supplies influence the selection of replacement options. Details of the HV power supply replacement requirements and the different replacement options will be discussed. One option is to use four 95 kV, 21 A DC power supplies originally installed nearby as part of the Low Energy Demonstration Accelerator (LEDA) project. Significant material and labor cost savings can be achieved by leaving these supplies installed where they are and building a HV transport system to bring high voltage power from the existing LEDA facility to the LANSCE facility. The different replacement options will be compared based on material and labor costs as offset by long-term energy savings.

OVERVIEW OF THE EXISTING LANSCE HVPS SYSTEMS

The LANSCE facility uses seven sectors of 805 MHz klystrons to drive a side coupled 800-MeV proton linac capable of delivering up to 800 kW of beam power. The klystrons require pulsed High Voltage (HV) DC power to operate. The High Voltage Power Supply (HVPS) systems regulate the incoming AC power and convert it to regulated HV DC power. Each sector has a HVPS located just outside the north wall of the klystron gallery and a capacitor room located within the klystron gallery. Underground HV cables transmit the power from the HVPS system to the capacitor room. All of the klystron modulators in a sector draw pulsed HV DC power from that sector's capacitor room.

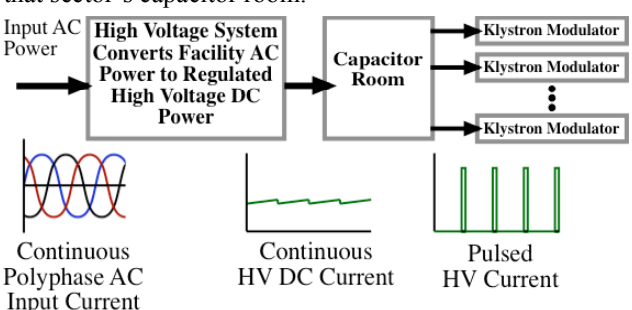

Figure 1: HV System Overview.

*Work supported by the NNSA, U. S. Department of Energy under contract DE-AC52-06NA25396.

Fig 1 diagrams the power flow in the HV system. When the klystron modulators are pulsed on, the peak klystron beam current is provided by the charge stored within the capacitor bank. During the interpulse period when the klystrons are off, the HVPS system recharges the capacitor bank to the nominal 85 kV level.

The existing LANSCE HVPS systems consist of two sub units: an Inductrol® Voltage Regulator (IVR) and a HV step-up Transformer/Rectifier (T/R). The IVR can vary the three phase 4160VAC input power by ±33%. The output of the IVR feeds T/R. Adjustment of the IVR varies the T/R output voltage from 47 to 90 kV. The standard IVR and T/R sub units are both oil filled devices and are shown in Fig 2 . The existing HVPS systems for the seven sectors (B-H) at LANSCE were installed during the late 1960s and early 1970s.

Figure 2: IVR and T/R sub units in the existing LANSCE HVPS systems.

NEED FOR HVPS REPLACEMENT

The LANSCE HVPS systems are in excess of 30 years old and it is well known in the literature that systems of this age are approaching end of life [1]. Dissolved gas analysis has been adopted as a tool for assessing the status of the LANSCE HVPS systems. The transformer oil is typically sampled on a yearly prior to any reprocessing (cleaning). Because the level of dissolved gases in the oil and the gas evolution within the transformers varies with hours of operation and operating parameters, we use the level of dissolved gas not as an absolute quantitative indicator of health but as a qualitative indicator of which units are experiencing the highest level of age related degradation. The status of the LANSCE HVPS systems is inferred from the dissolved gases within the oil in accordance with the following list [2]:

- Methane, Ethane, Ethylene, and Hydrogen are produced from high temperature thermal heating of oil.

PROGRESS TOWARDS THE LANSCE RF SYSTEM REFURBISHMENT

D. Rees, J. T. Bradley III, S. Kwon, J. T.M. Lyles, M. T. Lynch, M. S. Prokop, W. Reass, K. A. Young,
LANL, Los Alamos, New Mexico

Abstract

The Los Alamos Neutron Science Center (LANSCE) is in the conceptual design phase of a refurbishment project that will sustain reliable facility operations well into the next decade. The LANSCE accelerator was constructed in the late 1960s and early 1970s and is a national user facility that provides pulsed protons and spallation neutrons for defense and civilian research and applications. The refurbishment will focus on systems that are approaching "end of life" and systems where modern upgrades hold the promise for significant operating cost savings. The current baseline consist of replacing all the 201 MHz rf amplifiers, replacing greater than 75% of the 805 MHz rf systems with a combination of high efficiency klystrons and new klystrons of the existing style, replacing four high voltage systems, and replacing all the low level rf cavity field control systems along the accelerator. System designs and requirements will be presented and the project plan will be discussed.

CONTRIBUTION NOT RECEIVED

NEXT GENERATION IGBT SWITCH PLATE DEVELOPMENT FOR THE SNS HIGH VOLTAGE CONVERTER MODULATOR*

Mark A. Kemp, Craig Burkhart, Minh N. Nguyen, SLAC, Menlo Park, CA, U.S.A.
David E. Anderson, ORNL, Oak Ridge, TN, U.S.A.

Abstract

The RF source High Voltage Converter Modulator (HVCM) systems installed on the Spallation Neutron Source (SNS) have operated well in excess of 200,000 hours, during which time numerous failures have occurred. An improved Insulated Gate Bipolar Transistor (IGBT) switch plate is under development to help mitigate these failures. The new design incorporates two significant improvements. The IGBTs are upgraded to 4500 V, 1200 A, press-pack devices, which increase the voltage margin, facilitate better cooling, and eliminate explosive disassembly of the package in the event of device failure. The upgrade to an advanced IGBT gate drive circuit decreases switching losses and improves fault-condition response. The upgrade design and development status will be presented.

BACKGROUND

SNS HVCM

The topology of the SNS HVCM is shown in Fig. 1 [1]. There have been numerous upgrades to the original design which have greatly improved the reliability [2]. However, to further improve reliability and to provide voltage regulation of the output pulses at full average power, additional improvements are required. Work is underway at SLAC to develop a new H-bridge switchplate, a part of the modulator which has caused many of the modulator failures. The new design incorporates higher power IGBTs, improved fault current control and an advanced fault-detecting IGBT gate drive.

Press-Pack IGBTs

The press-pack IGBTs selected to replace the flat-pack devices used in the present switchplate, offer several advantages. First, the new IGBTs will have an increased voltage margin (3.3 kV vs 4.5 kV). Second, these IGBTs can be cooled on two sides, which will aid in heat removal. Third, press-pack IGBTs have been shown to have increased reliability in pulsed-power applications [3]. Lastly, unlike the flat-pack devices, the press-pack will not explosively disassemble in the event of an IGBT failure.

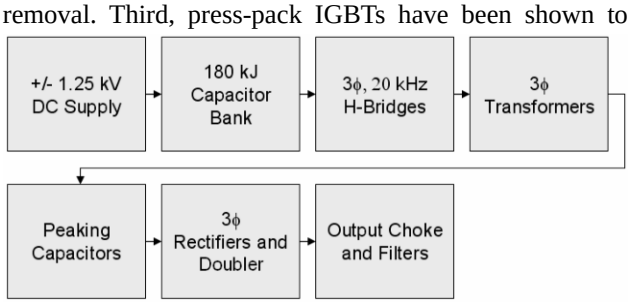

Figure 1: Simplified diagram of the SNS HVCM.

*Work supported by the U.S. Department of Energy under contract DE-AC05-00OR22725. SLAC-PUB-13385
e-mail: mkemp@slac.stanford.edu

DESIGN

Press-Pack Switchplate

A photograph of the current switchplate is shown in Fig. 2 and the simplified circuit schematic is shown in Fig. 3. The flat-pack IGBTs utilized in the present switchplate design have an advantage in being relatively straightforward to implement mechanically. The anti-parallel diode is in the same package as the IGBT, further simplifying the assembly.

A drawing of the SLAC press-pack switchplate is shown in Fig. 4. Compared to the current design, the press-pack based design has several key advantages in addition to those mentioned above:

- The bottom heat-sink is at the same potential as the

Figure 2: Photograph of one SNS H-bridge card on the SLAC single phase test stand.

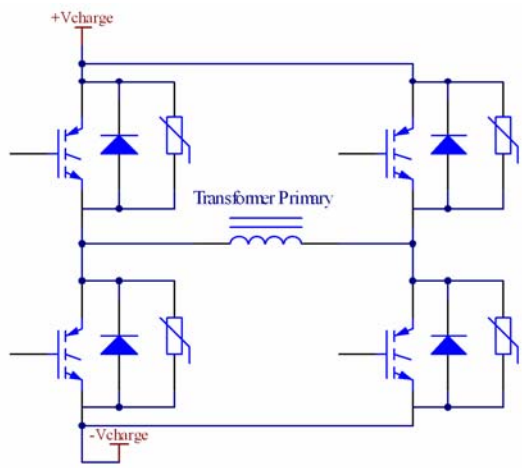

Figure 3: Simplified circuit model of the SNS H-bridge. In the original design, the IGBTs and diodes are in one, flat-pack package and there is no parallel MOV.

ILC MARX MODULATOR DEVELOPMENT PROGRAM STATUS*

C. Burkhart#, T. Beukers, R. Larsen, K. Macken, M. Nguyen, J. Olsen, T. Tang,
SLAC, Menlo Park, CA 94025 USA, U.S.A.

Abstract

Development of a first generation prototype (P1) Marx-topology klystron modulator for the International Linear Collider is nearing completion at the Stanford Linear Accelerator Center. It is envisioned as a smaller, lower cost, and higher reliability alternative to the present, bouncer-topology, "Baseline Conceptual Design." The Marx presents several advantages over conventional klystron modulator designs. It is physically smaller; there is no pulse transformer (quite massive at ILC parameters) and the energy storage capacitor bank is quite small, owing to the active droop compensation. It is oil-free; voltage hold-off is achieved using air insulation. It is air cooled; the secondary air-water heat exchanger is physically isolated from the electronic components. The P1-Marx employs all solid state elements; IGBTs and diodes, to control the charge, discharge and isolation of the cells. A general overview of the modulator design and the program status are presented.

INTRODUCTION

The International Linear Collider (ILC) will require 576 RF stations. Each 10 MW L-band klystron will require a modulator capable of; 120 kV, 140 A, 1.6 ms (27 kJ) at 5 Hz repetition rate. The existing Baseline Conceptual Design (BCD) is a transformer-based topology. The large size, weight, and cost of this transformer, owing to the long pulse length, have motivated research into alternative topologies that do not employ power magnetics.

The P1-Marx [1] modulator uses solid-state switches and isolation elements to connect capacitors in parallel while charging but in series during discharge to generate high voltage output without the use of a transformer.

DESIGN OVERVIEW

The topology is illustrated in Fig. 1. A diode string provides a path for charging the 50 μF capacitor of each of the 16 Marx cells to 11 kV and isolation between the cells during erection. Likewise, a second diode string provides a path for auxiliary power to each cell. A charge switch in each cell provides a common return path for both power sources.

Closure of a fire switch will produce a -11 kV output pulse from the cell; closure of additional switches will increase the output by -11 kV for each cell that is fired. The by-pass diode provides a conduction path to the load through the cells that have not been fired. The series inductor limits dI/dt of the output current.

*Work supported by the U.S. Department of Energy under contract DE-AC02-76SF00515
#burkhart@slac.stanford.edu

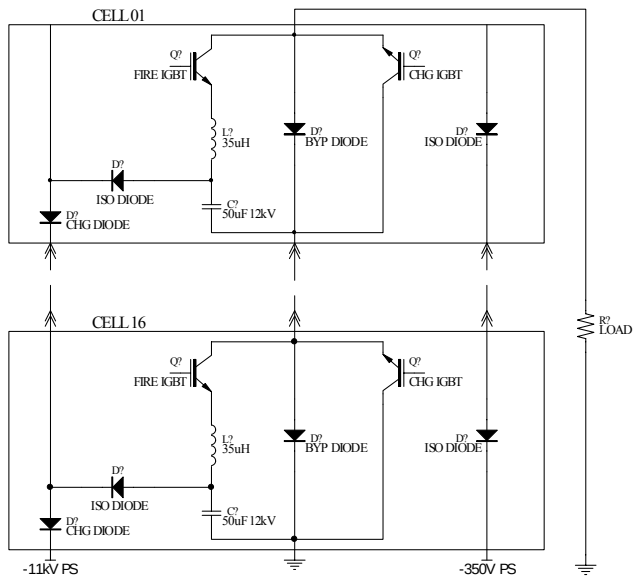

Figure 1: Simplified schematic diagram of the SLAC Marx.

Eleven cells are triggered to produce the required output voltage. As the energy storage capacitors discharge, the output voltage drops. Once it has decreased by 11 kV, in ~0.35 ms, an additional cell is triggered to bring the output back to 120 kV. This proceeds sequentially through the remaining five cells to provide coarse, ±5%, pulse flattening.

The output will be further regulated to ±0.5% by a second Marx, the vernier regulator, in series with the main Marx. The topology of the vernier is similar to the main Marx, however each of the 16 cells is charged to 1.2 kV. These are fired sequentially to generate a stair-step waveform, which is added to the main Marx to maintain an approximately constant output voltage.

Marx Structure

Fig. 2 is a photo of the P1-Marx modulator. A steel structure supports the modulator components and the control system (not visible, outside the enclosure in the front of the support structure). A hollow, cantilevered beam supports the individual Marx cells, forms a duct to direct the forced air coolant, and houses the control system fiber optic cables. It also supports a PCB backplane that provides the electrical interconnections between cells. When a cell is installed, it hangs from the beam, plugs into connectors on the backplane, and aligns the fiber optic lenses with those in the beam to transmit and receive optical control and diagnostic information.

RF VECTOR CONTROL FOR EFFICIENT FAN-OUT POWER DISTRIBUTION *

Y. W. Kang, Oak Ridge National Laboratory, Oak Ridge, TN, USA

Abstract

Distributing RF power of a generator to many cavity loads is often considered in RF linacs for possible cost reduction and simplification of system. If the amplitude and phase of the power delivered to individual cavity have to be controlled precisely, using fixed power splitting system may not be satisfactory. An approach for fan-out RF power distribution using transmission line circuit parameters for achieving full vector control and maximum power efficiency is considered. This fan-out distribution approach can provide required RF power to the cavities by adjusting the transmission line phase delays between the cavities and reactive loads at the cavity inputs. In this approach, the phase delays and the reactive loads become the RF control parameters for delivering a set of required cavity RF voltages for an entire system.

INTRODUCTION

Many high power RF accelerators may have to drive one cavity with one RF generator if independent and accurate RF vector control is required. Fan-out power distribution system feeding many cavities with a high powered generator can be useful for large scale high powered systems, especially for SRF ion accelerators, to reduce construction costs and save on operating costs. Various RF power distribution systems have been used and proposed in [1] and often pulse compression is combined for short pulse systems. Mechanically variable directional couplers are employed for an adjustable distribution [2]. RF distribution systems using high power vector modulators have been considered for fast control [3]. Using a vector modulator at a cavity input with a fixed power splitting requires more power than the power required in the cavity to enable adequate RF control.

A fan-out distribution presented in this paper can use only the power required to maintain right RF voltages in the cavities with a transmission line network. This approach can maximize the RF power to beam efficiency of a fan-out system. The multi-cavity system is controlled as a whole for various operation condition of the accelerator. The vector control is done by adjusting phase delays between the load cavities and reactive loads at cavity inputs. The reactive loads and transmission line phase delays can be realized using high power RF phase shifters.

Figure 1(a) shows an arbitrary fan-out power distribution system for a particle accelerator with N cavities. There can be various ways to construct a fan-out power distribution system using a transmission line network: one approach is shown in Figures 1(b) with the loads connected in parallel to the transmission line and 1(c) with the loads connected in series. The two types of connections may be mixed if construction and operation can benefit.

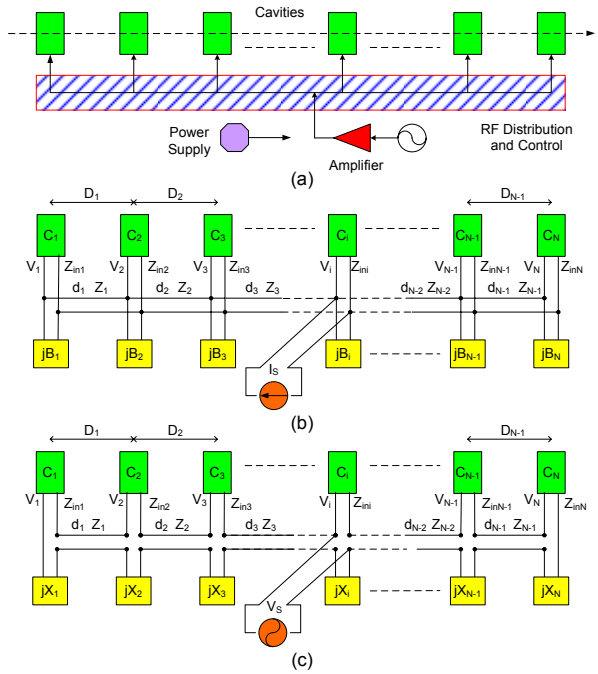

Figure 1: (a) Generalized high power RF distribution in a multi-cavity accelerator, (b) using transmission line network with loads and control elements connected in parallel, (c) using transmission line network with loads and control elements connected in series.

DEVELOPMENT

The transmission line network shown in Figure 1(b) can be synthesized and analyzed using short-circuit admittance parameters and the network in Figure 1(c) can be treated using open-circuit impedance parameters similarly [4]. Although either one of the approaches can be used, it seems the parallel connection can be more practical in using various transmission lines. The design in Figure 1(b) using the short-circuit admittance parameters is discussed in the following.

Generally, in an accelerator, the cavity input impedances and the required load voltages are known for an operating condition. Therefore, in a network shown in Figure 1(b), any two of the three unknown parameters, transmission line characteristic impedance, Z_i, electrical length between the two neighboring loads, d_i, and the reactive loads, B_i can be varied for having the required

* SNS is managed by UT-Battelle, LLC, under contract DE-AC05-00OR22725 for the U.S. Department of Energy.

SPALLATION NEUTRON SOURCE SUPERCONDUCTING LINAC KLYSTRON TO CAVITY MISMATCH EFFECTS AND COMPENSATION*

M. McCarthy, M. Crofford, S. Kim ORNL, Oak Ridge, TN 37831, USA

Abstract

Observations of several of the 81 klystron output waveforms into their respective superconducting cavities do not correspond with their rectangular klystron inputs in open loop mode. This can't be completely explained by a drooping high voltage power supply especially when the waveform is parabolic. Some possible causes and effects of these anomalies are presented.

DISTORTED WAVEFORMS

While optimizing the superconducting linac (SCL) cavity fields of the SNS linac [1] we noted that some of the 81 cavity input power waveforms were not linearly tracking the shape of the input signal (Figure 1). This caused concern that this would be an additional error source that the low level RF (LLRF) control system must compensate.

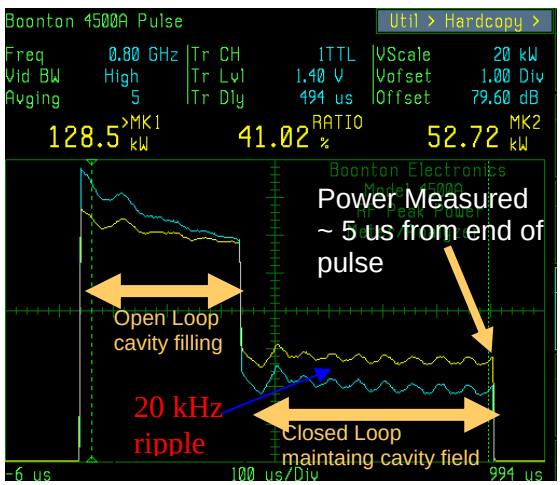

Figure 1: SCL Klystron RF Out and Cavity RF In.

Other sources of error include the phase and amplitude changes that occur during the 1ms RF pulse caused by drooping klystron cathode voltage and the resulting increased delay of the electron beam through the klystron. Also contributing are 20 kHz ripple, cavity resonance drift, beam loading and cable tolerances. Typical cathode voltage droop is ~3%. Klystron power follows cathode voltage to the 5/2 power so we expect an 8% power droop without LLRF feedback (open loop). However, some droops were as high as 32% (Figure 2).

Possible causes of the distortion were:

1) Non-linear measurement device or mis-calibration.
2) Solid State Amplifier (SSA) distortion.

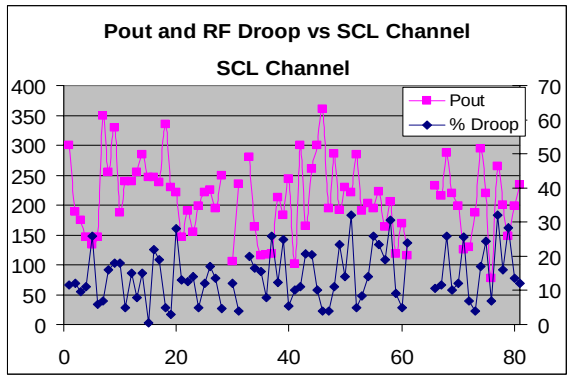

Figure 2: Klystron power and droop by SCL cavity.

3) Impedance mismatch between klystron and circulator caused by:
   a) Bad water-load match.
   b) Harmonics from klystron.
   c) Misadjusted TCU (circulator Temperature Compensating Unit)
   d) Waveguide discontinuity (bent).
   e) Bad circulator matching during full reflected power from cavity.
   f) Heating of the circulator ferrites changing their H-field during the pulse.

These possible causes were investigated; the measuring instrumentation was in calibration and two of the directional couplers were checked on the bench, the SSA met its <1% droop specification, and the waster load had a good 1.05 VSWR. A calculation of the estimated heat deposited in the circulator ferrites over the time of an RF pulse indicated insignificant temperature change. A mismatch between the circulator and the klystron appeared to be the primary candidate for the distortion.

Each TCU is factory matched to a circulator with specific internal look-up tables that compensate for changes in ferrite characteristics as a function of temperature. Over the past five years of SNS commissioning and operation, seven TCUs and two circulators have failed. Because the circulator weighs 250 lbs and hangs 13 feet above the floor, it was not changed when its matching TCU failed. The replacement TCU was tuned in-situ with a factory (AFT: Advanced Ferrite Technologies) proprietary program using a laptop. Because we couldn't vary water temperature while monitoring reflected power, the circulator was optimized for minimum reflected power to the klystron at the nominal temperature and cavity operating field.

*SNS is managed by UT-Battelle, LLC, under contract DE-AC05-00OR22725 for the U.S. Department of Energy

SELF-TUNING REGULATOR FOR ISAC 2 SUPERCONDUCTING RF CAVITY TUNER CONTROL

K. Fong, M. Laverty and Q.W. Zheng, TRIUMF, Vancouver, Canada

Abstract

The ISAC 2 superconducting RF cavities use the self-excited, phase-locked mode of operation. As such the microphonics are sensitive to the alignment of the phase control loop. Although initial alignment can minimize the effect of microphonics, amplitude-dependent phase shift and long term drift, particularly in the power amplifiers, can cause the control loop misalignment and an increase in sensitivity to microphonics. The ISAC 2 control system monitors several points in the control loop to determine the phase alignment of the power amplifiers as well as the RF resonant cavities. Online adaptive feedback using Self-Tuning Regulator is employed to bring the different components back into alignment.

INTRODUCTION

Figure 1 shows the block diagram of a self-excited system. In this type of system amplitude control is achieved by feedback regulation of the In-phase channel, while frequency and phase control are achieved by feedback regulation of the Quadrature-phase channel.

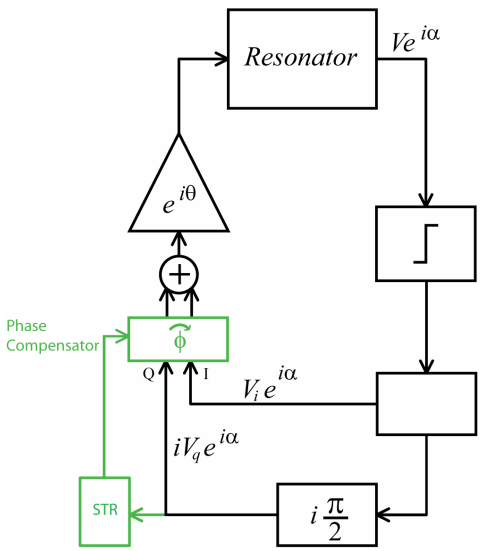

Figure 1: Phase-locked Self-excited loop with Self-Tuning phase compensator.

The feedback signal is derived by comparing the phase of the self-excited signal with an external reference frequency. In ISAC 2, the I/Q feedback controller functions are performed by a single digital signal processor[1], while the phase comparison is done by a FPGA[2]. Proper phase-locked operation and the amount of residual microphonics in the feedback system depends on its alignment[3]. This includes the phase delays of the cables, the amplifier system as well as the resonant cavity. Phase delay changes in all these components can be caused by cryogenic helium pressure, thermal effects and long term deterioration such as power tube emissivity. To counter act these changes a digital phase shifter, coloured in green in Figure 1, is incorporated into the feedback controller DSP. This phase shifter is essentially a rotation matrix operating on the In-phase and the Quadrature-phase channel outputs of the DSP. The phase sifter is controlled by a self-tuning regulator for automatic phase noise reduction. The self-tuning regulator monitors the original Q channel output, then calculates the optimum drive to modify the rotation angle.

THEORY

The equation for the voltage of the cavity is [1]

$$\ddot{v} + 2\frac{1}{\tau}\dot{v} + \omega_c^2 v = 2\frac{\gamma}{\tau}\dot{V}_g \qquad (1)$$

Using the I and Q components of the input voltage V_g as the independent variables and the amplitude and phase of the output voltage v as the dependent variables for a phase-locked self-excited system, the equation of state is

$$\begin{bmatrix}\delta V\\ \delta\omega\end{bmatrix} = \gamma\cos\theta\begin{bmatrix}\frac{1}{s\tau+1} & -\frac{\tan\theta}{s\tau+1}\\ \frac{1}{\tau V_0}\left(\tan\theta - \frac{\tan\phi}{s\tau+1}\right) & \frac{1}{\tau V_0}\left(1 - \frac{\tan\phi\tan\theta}{s\tau+1}\right)\end{bmatrix}\begin{bmatrix}\delta v_i\\ \delta v_q\end{bmatrix} \qquad (2)$$

The phase shift ϕ of the RF cavity is given by

$$\phi = \tan^{-1}(\omega_c - \omega)\tau \qquad (3)$$

and the I/Q modulator produces a phase shift ρ given by

$$\rho = \tan^{-1}\frac{V_q}{V_i} \qquad (4)$$

The phase relation in a self-excited loop must obey

$$\theta + \rho + \phi = 2n\pi \qquad (5)$$

In order to minimize the power requirement, ϕ should be set to zero. While ϕ can be measured directly from the phase difference between the input and the output of the cavity, θ is a dynamic variable, namely the amplifier phase shift. In self-excited mode θ and ϕ are not independent variables since they must obey Equation 5. Therefore when ϕ is set to zero by the tuner, and when $\theta = 0$, $q \equiv V_q = 0$. This is operationally desirable since it eliminates cross-talk between the I and the Q channels. Another important reason for $\theta = 0$ is that when this condition is not met, the cross-talk between the I and Q channel outputs can in some cases trip the built-in limiters

AM-PM CONVERSION INDUCED INSTABILITY IN AN I/Q FEEDBACK CONTROL LOOP

K. Fong, M. Laverty and Q.W. Zheng, TRIUMF, Vancouver, Canada

Abstract

Most RF feedback control systems today use the I/Q demodulation and modulation scheme because of its simplicity. Its performance, however, depends on the alignment of the feedback loops. If the loop contains elements that have a high AM-PM conversion factor such as a class C amplifier or a high power klystron, then the misalignment is dynamic and power dependent. In most systems the phase noise is increased, and in some cases the I/Q loops become unstable and the system settles into a limit-cycle oscillation.

INTRODUCTION

The 92MHz RF Booster has been in operation in the TRIUMF cyclotron for more than 15 years[1]. The original system was an analogue system that used amplitude/phase modulation. When the control system was replaced in 2005 with a digital signal processor system, the control algorithm was converted into I/Q modulation. After the conversion the feedback system would operate satisfactory at 90% nominal power, but at 100% nominal power, on some occasions, the I/Q loops and the tuner loop would jump into limit cycle oscillations. It was also determined that the booster RF amplifier chain has a large phase shift that is power dependent. In an I/Q system, detuning of the resonant cavity will introduce cross-talk between the I and the Q channels. Normally the detuning will be suppressed by the tuning feedback loop but in the TRIUMF RF Booster the tuning motor movement is relatively slow and is unable to correct the detuning within a few seconds. During this crucial time the cross-talk is enhanced by the dynamic phase shift of the amplifier chain. Its growth rate, depending on the initial detuning, can sometimes exceed the damping rate provided by the tuner loop and cause the collapse of this RF system.

BOOSTER RF POWER AMPLIFIER

The Booster RF power amplifier chain consists of a three-stage amplifier: a 10W solid state driver amplifier, a 10kW tube pre-amplifier and a 100kW final tube power amplifier. The final stage amplifier is a grounded grid power amplifier for the booster cavity of the TRIUMF cyclotron, operating at the frequency 92MHz. The configuration is shown in Figure 1.

A huge phase shift in the Booster PA was detected which was dependent on RF output power, possibly due to a thermal effect. Phase changes from 0 to -15 degrees with power going from 0 to 15 kW and then from -15 to 40 degrees when output ramping up to full power (40kW) as indicated in Figure 2. Bipolar phase shift response is most likely caused by alternate behaviour of the FM transmitter and final PA, and is difficult to suppress with a phase compensation circuit inside the Booster RF power amplifier.

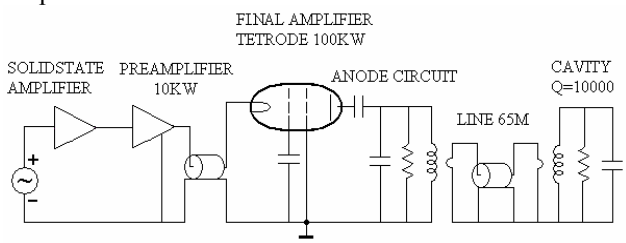

Figure 1: TRIUMF RF booster amplifiers.

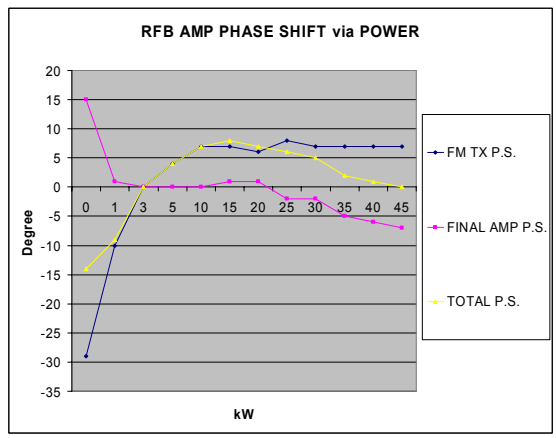

Figure 2: Phase shift vs. power.

This high AM-PM conversion phase shift enhances I/Q loop cross-talk, eventually making the Booster RF system operation unstable.

THE BOOSTER RF TUNING SYSTEM

The automatic frequency tuning system keeps the RF cavity at its resonant frequency. This achieves the desired RF voltage with minimum RF power input and minimum reflected RF power. The TRIUMF booster tuning unit uses two DC motors to move the upper and lower shorting plates in the root region of the cavity to accomplish the Booster cavity frequency tuning. To prevent wearing out of mechanical contacts due to constant movement of the tuner, a bang-bang controller is used for the booster tuning control. The motors are also heavily geared down in order to have enough force to move the tuning plate. All these factors contribute to the slow response of the tuning control system.

EVALUATION OF FAST ADCS FOR DIRECT SAMPLING RF FIELD DETECTION FOR THE EUROPEAN XFEL AND ILC

Z. Geng#, S. N. Simrock, DESY, Hamburg, Germany

Abstract

For the LLRF system of superconducting Linacs, precision measurements of the RF phase and amplitude are critical for the achievable field stability. In this paper, a fast ADC (ADS5474) was employed to measure the 1.3 GHz RF signal directly without frequency down conversion. In the laboratory, the Signal to Noise Ratio (SNR) of the ADC was studied for different RF input levels, and the temperature sensitivity of the ADC has been determined. A full bandwidth phase jitter of 0.2 degree (RMS) and amplitude jitter of 0.2% (RMS) was measured. For field control of superconducting cavities with a closed loop bandwidth up to 50 kHz, one can expect to achieve a phase stability close to 0.01 degree. The main limitation will be the jitter of the external clock. We represent measurements of the cavity fields at FLASH and compare the result with the existing system with down converter.

INTRODUCTION

The superconducting Linacs in facilities such as European XFEL and ILC, require significant RF field stability up to 0.01 degree in phase and 0.02% in amplitude [1], which are guaranteed by the LLRF system. Precision measurements of the RF phase and amplitude are critical for the achievable field stability for the LLRF system.

Most of the superconducting cavities of European XFEL and ILC work on the frequency of 1.3 GHz, which until recently could not be directly measured by commercially available ADCs. The most widely used way for measurement is to convert the 1.3 GHz RF signal to an intermediate frequency and then sample by ADCs.

Though ADCs with a bandwidth of a few GHz are available since a few years, their resolution was limited to 8 or maximum 10 bits. Recently, ADCs with 12 or even 14 bits are available, making it possible to measure the RF signal directly without frequency down conversion. Direct sampling ADC gets rid of the down converter and makes the RF measurement circuit much simpler and smaller, but will be sensitive to the clock jitter. The ADS5474 is an ADC with 14-bit resolution, 400 MSPS and 1.4 GHz bandwidth, which is suitable to sample the 1.3 GHz signal directly with under sampling scheme. This ADC was evaluated both in the laboratory and for the injector RF system at FLASH.

#zheqiao.geng@desy.de

RF FIELD DETECTION

The ADC sampling frequency (400 MSPS) is much smaller than the RF frequency (1.3 GHz), so under sampling is used, and the RF signal is measured in a higher Nyquist band. In order to derive the phase and amplitude directly from the sampling, the clock frequency should be synchronized with the RF frequency and chosen based on the non-IQ sampling scheme [2]. The possible sampling frequency f_s is

$$f_s = \frac{f_0}{k + \frac{m}{n}}, \quad k = 0,1,2... \tag{1}$$

where f_0 is the RF frequency, m and n represent the phase difference between two adjacent samples

$$\Delta\varphi = \frac{m}{n} \cdot 2\pi \tag{2}$$

The I and Q baseband components can be calculated by the ADC sampling according to the formula below

$$I = \frac{2}{n}\sum_{i=0}^{n-1} x_i \sin(i\Delta\varphi)$$
$$Q = \frac{2}{n}\sum_{i=0}^{n-1} x_i \cos(i\Delta\varphi) \tag{3}$$

where x_i is the ADC sampling data.

The non-IQ demodulation by equation (3) can separate and suppress the harmonics of the carrier frequency.

During testing, the sampling frequency is chosen to be 178.8990825 MHz (m = 4 and n = 15), and the RF frequency is mapped to 47.7064225 MHz.

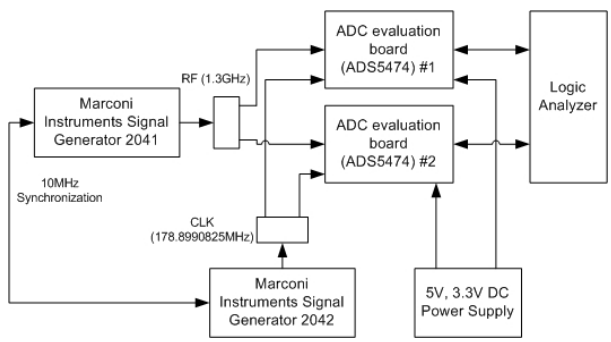

Figure 1: ADC testing stand in laboratory.

NOISE CHARACTERISTICS

The ADC evaluation board is measured in laboratory for estimating the noise characteristics. The testing stand is shown in Fig. 1. Two synchronized low noise signal generators are used for clock and RF signals. The ADC sampling data are recorded by a logic analyzer. The

LLRF SYSTEM REQUIREMENT ENGINEERING FOR THE EUROPEAN XFEL

S.N. Simrock#, G. Ayvazyan, Z. Geng, M. Grecki, DESY, Hamburg, Germany
B.Aminov, CRE, Wuppertal

Abstract

The LLRF system of the European XFEL must fulfill the requirements of various stakeholders: Photon beam users, accelerator operators, rf experts, controls system, beam diagnostics and many others. Besides stabilizing the accelerating fields the system must be easy to operate, to maintain, and to upgrade. Furthermore it must guarantee high availability and it must be well understood. The development, construction, commissioning and operation with an international team requires excellent documentation of the requirements, designs and acceptance test. For the RF control system of the XFEL the new system modelling language SySML has been chosen to facilitate the system engineering and to document the system. SysML uses 9 diagram types to describe the structure and behavior of the system. The hierarchy of the diagrams allows individual task managers to develop detailed subsystem descriptions in a consistent framework.

We present the description of functional and non-functional requirements, the system design and the test cases.

CONCEPT OF SYSTEM ENGINEERING

Systems Engineering signifies both an approach and, more recently, as a discipline in engineering. The aim of education in Systems Engineering is to simply formalize the approach and in doing so, identify new methods and research opportunities similar to the way it occurs in other fields of engineering. As an approach, Systems Engineering is holistic and interdisciplinary in flavor.

Systems engineering is a robust approach to the design, creation, and operation of systems. In simple terms, the approach consists of identification and quantification of system goals, creation of alternative system design concepts, performance of design trades, selection and implementation of the best design, verification that the design is properly built and integrated, and post-implementation assessment of how well the system meets (or met) the goals.

- Understand the whole problem before you try to solve it.
- Translate the problem into measurable requirements
- Examine all feasible alternatives before selecting a solution.
- Make sure you consider the total system life cycle. The birth to death concept extends to maintenance, replacement and decommission. If these are not considered in the other tasks, major life cycle costs can be ignored.
- Make sure to test the total system before delivering it.
- Document everything.

#stefan.simrock@desy.de

The seven-task process defined above is an excellent representation of systems engineering as is presently practiced and should serve to avoid most of the problems that have plagued the development of large, complex systems in the past.

SYSML LANGUAGE

The Systems Modeling Language (SysML), is a Domain-Specific Modeling language for systems engineering. It supports the specification, analysis, design, verification and validation of a broad range of systems and systems-of-systems. SysML was originally developed by an open source specification project, and includes an open source license for distribution and use. SysML is defined as an extension of a subset of the Unified Modeling Language (UML) using UML's profile mechanism. SysML uses seven of UML 2.0's thirteen diagrams, and adds two diagrams (requirements and parametric diagrams) for a total of nine diagram types. SysML also supports allocation tables, a tabular format that can be dynamically derived from SysML allocation relationships.

Table 2: Diagram Types

SysML Diagram	Purpose
Activity	Show system behavior as control and data flows. Useful for functional analysis.
Block Definition diagram	Show system structure as components along with their properties, operations and relationships. Useful for system analysis and design.
Internal Block diagram	Show the internal structures of components, including their parts and connectors. Useful for system analysis and design.
Parametric diagram	Show parametric constraints between structural elements. Useful for performance and quantitative analysis.
Requirement diagram	Show system requirements and their relationships with other elements. Useful for requirements engineering.
Sequence diagram	Show system behavior as interactions between system components. Useful for system analysis and design.
State Machine diagram	Show system behavior as sequences of states that a component or interaction experience in response to events. Useful for system design and simulation/code generation.
Use case diagram	Show system functional requirements as transactions that are meaningful to system users. Useful for specifying functional requirements. (Note potential overlap with Requirement diagrams.)

LOW LEVL RF AND TIMING SYSTEM FOR XFEL/SPRING-8

T. Ohshima[a,#], N. Hosoda[a], H. Maesaka[a], K. Tamasaku[a], M. Musha[b], Y. Otake[a]
[a]RIKEN, XFEL project/SPring-8, 1-1-1 Kouto, Sayo, Hyogo, 679-5148, Japan
[b]Institute of Laser Science, Univ. Electro-communications, 1-5-1 Chofugaoka, Chofu, Tokyo, 182-8585, Japan

Abstract

The construction of XFEL/SPring-8 is progressing. In this accelerator, it is needed to obtain stabilities of 50 fs and 1E-4 in time and amplitude of the acceleration voltage. To satisfy these requirements, rf components, such as a reference rf oscillator with low phase noise, IQ modulators and so on, were developed. These modules were installed to an SCSS test accelerator. Their performance was confirmed by monitoring the beam arrival timing compared with the reference rf signal. The measured time jitter of the arrival timing was 46 fs, which implies that the rf modules have a potential to control the timing of the accelerator within several 10 fs. Using these modules, the SCSS test accelerator is operated stably and offers EUV light to user experiments. The compression factor of the XFEL is about 10-times larger than that of the test accelerator. Thus special care is taken for the XFEL to keep the temperature of rf modules constant. For delivery of the reference rf signals, an optical system is adopted instead of coaxial cables, because signal transmission loss with coaxial cable is not allowed for the long distance for the XFEL..

INTRODUCTION

Construction of the XFEL/SPring-8, Japan is in progress. Fig. 1 shows a schematic view of the rf components of the XFEL. An electron beam with an energy of 500 keV and a current of 1A is extracted from a thermionic gun. Velocity bunching is done by using 238 MHz, 476 MHz, and 1428 MHz (L-band) sub harmonic cavities, which increase the beam energy and compress the bunch length. Then, the beam is passed through cavities with frequencies of 2856 MHz (S-band) and 5712 MHz (C-band) and three magnetic bunch compressors (BC 1 ~ 3). Two correction cavities are used to compensate for the non-linearity of the sine wave, and to give a linear energy chirp to the beam. The peak current is increased very carefully as the beam energy is increased.

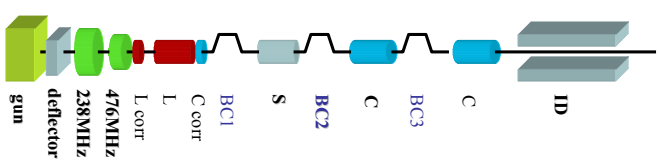

Figure 1: Schematic view of the rf components in the XFEL.

#ohshima@spring8.or.jp

This is because the beam emittance is easily blown up by a strong space charge force. Thus the allowable amplitude and phase fluctuations of the accelerating cavity voltages at the bunch compressor section are very severer: 50 fs and 1E-4 [1]. At the crest acceleration section the requirement to the rf phase stability is relaxed: 240 fs because dV/dt is nearly zero. Finally, the expected peak current at the insertion device is 3 kA with a beam energy of 8 GeV. To obtain saturated self-amplified spontaneous emission (SASE) light, it is important to maintain a very high peak current, i.e., a very high bunch compression ratio. The phases and amplitudes of the rf cavities should be stable within their tolerances, as mentioned above.

To satisfy these requirements, the rf components, such as a reference rf oscillator with low phase noise and an IQ (In-phase and Quadrature) modulator / demodulator have been developed [2]. Their performances measured at a test accelerator, issues concerning temperature stabilization of the rf modules, and the delivery system of the reference signal for the XFEL are shown in the following.

PERFORMANCE OF THE LLRF SYSTEM AT THE SCSS TEST ACCELERATOR

The SCSS test accelerator was constructed in 2005. Its beam energy is 250 MeV. The machine length is about 70 m. Components shown in Fig.1 with bold face are installed in the test accelerator. To drive all of the high power rf sources of the test accelerator, and to realize stable SASE generation, a low-noise reference signal oscillator was developed. The phase noise of 5712 MHz signal is -140dBc/Hz at an offset frequency of 1 MHz to the carrier signal. The sub-harmonic signals for velocity bunching are generated by dividing the 5712MHz signal. The reference signals are transmitted to 19" racks located along the klystron gallery of the test accelerator through coaxial cables. There, the reference signal is modulated by an IQ modulator controlled by a high-speed 14-bits DAC, and fed to a high-power klystron. It excites the accelerating cavity. The phase and the amplitude of the accelerating voltages are monitored by an IQ demodulator and high-speed 12-bits ADCs.

As described in the previous section, the phase and amplitude of the 238MHz sub-harmonic cavity voltage are sensitive to the lasing stability. Thus, a feedback process to stabilize the rf phase and amplitude of the cavity voltage is introduced. Fig. 2 shows the set and measured values of (a) the phase and (b) the amplitude of the pickup signal of the 238MHz cavity. The setting

LLRF CONTROL SYSTEM OF THE J-PARC LINAC

Z. Fang, S. Anami, S. Michizono, S. Yamaguchi, KEK
T. Kobayashi, H. Suzuki, JAEA

Abstract

In the J-PARC proton LINAC, each klystron drives two RF cavities. The RF amplitude and phase of the cavities are controlled by an FPGA-based digital feedback control system. The test results show that the variations in the cavity amplitude and phase are less than 0.1% and 0.1° without beam loading, or 0.3% and 0.2° with beam loading. The tuning of each cavity is also controlled by a DSP of this control system. The cavity auto-tuning is successfully controlled to keep the detuned phase within ±1 degree. In our RF system, the tuning information including detuned frequency and phase, and Q-value of each cavity are measured in real-time and displayed in the PLC touch panel of the control system.

INTRODUCTION

The RF sources of the J-PARC 181-MeV proton LINAC consist of 4 solid-state amplifiers and 20 klystrons with operation frequency of 324 MHz. The RF fields of each RF source are controlled by an FPGA-based digital RF feedback system installed in a compact PCI, which consists of the CPU, IO, DSP with FPGA, Mixer & IQ modulator, and RF & CLK boards [1-5]. Besides, the tuning of each accelerator cavity including 3 DTLs and 15 SDTLs is also controlled by this feedback system through a cavity tuner.

FEEDBACK PERFORMANCE

High-power tests were performed for the 24 RF systems of the J-PARC LINAC. A very good stability of the accelerating fields has been successfully achieved about ±0.1% in amplitude and ±0.1° in phase without beam loading, or ±0.3% in amplitude and ±0.2° in phase with beam loading, much better than the requirements of ±1% in amplitude and ±1° in phase. Fig. 1 shows an example of the cavity outputs with FB ON at SDTL7 with full power operation, when the RF amplitude is set to 4000 and the phase is set to 0°.

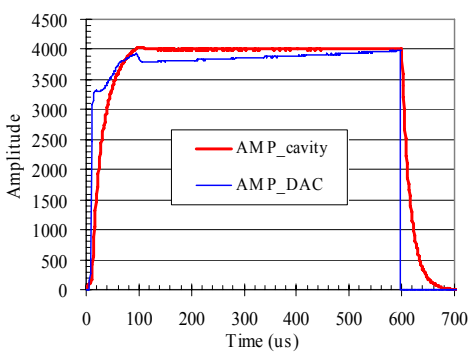

a) full scale of cavity and DAC amplitude waveform.

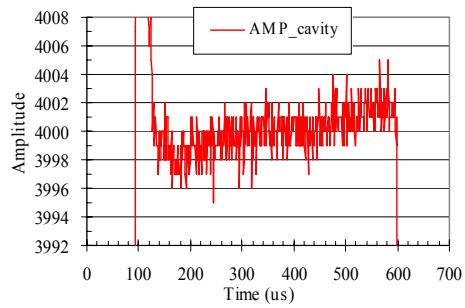

b) expansion of flat top of cavity amplitude.

Figure 1: Amplitudes of cavity and DAC outputs with FB ON at SDTL7.

THREE METHODS OF F_0 SETTING

By adjusting the tuner position, we tune the RF cavity with a resonant frequency of 324 MHz, and register the phase difference between picked-up signal from cavity and cavity input signal, which will be used in the auto-tuning control of the RF cavity. This process is called as f_0 setting of RF cavity.

We have investigated three methods of f_0 setting of RF cavity with FB OFF. With the cavity tuner moved, we take data of 1) cavity amplitude, 2) reflection from cavity, and 3) phase slope during field decay. Then the tuner positions for 1) the maximum cavity amplitude, 2) the minimum reflection, and 3) the flat cavity-phase decay, are obtained, which correspond to the positions for f_0 setting of the three methods.

Figure 2 shows an example of f_0 setting data by the three methods at S1A; cavity amplitude normalized by input signal (red curve), reflection amplitude from cavity (green curve), and cavity phase slope during field decay (blue curve), as function of tuner position. We can see that, the f_0 setting tuner positions of the three methods are different from each other.

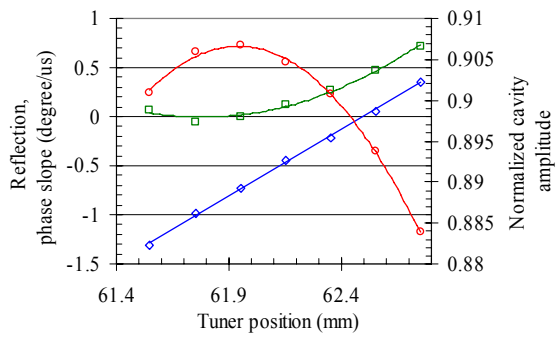

Figure 2: Cavity amplitude (red curve), reflection from cavity (green curve), and cavity phase slope during field decay (blue curve), as function of tuner position for S1A.

HIGH SPEED DATA ACQUISITION SYSTEM USING FPGA FOR LLRF MEASUREMENT AND CONTROL

H. Katagiri, S. Fukuda, T. Matsumoto, T. Miura, S. Michizono, Y. Yano, M. Yoshida
High Energy Accelerator Research Organization
1-1 Oho, Tsukuba, Ibaraki 305-0801, Japan

Abstract

Currently, FPGA (Field Programmable Gate Array) technology is being widely used for accelerator control owing to its fast digital processing capability. We have recently developed a high-speed data acquisition system that combines a commercial FPGA board (ML555) with a fast ADC (ADS5474; 14 bit; maximum sampling rate: 400 MS/s; bandwidth: 1.4 GHz). This system enables direct measurements of 1.3-GHz RF signals at a sampling frequency 270 MHz. This direct sampling method does not require a down-converter, and hence, the calibration step can be avoided. These results are analyzed and compared with those obtained with the conventional measurement method.

INTRODUCTION

Plans for the construction of an STF (Superconducting RF Test Facility) for the ILC (International Linear Collider) are currently in progress [1,2]. An LLRF (Low Level RF) control system based on a compact PCI has been installed in the STF at KEK in order to achieve the required amplitude and phase stability (0.3% and 0.3°) during RF pulse (1300 MHz, 1.5 ms) generation [3]. A customized FPGA board, which is built into the PCI crate, conducts feedback and feedforward control. The amplitude and phase, measured using the intermediate frequency (IF) conversion method, have been adopted in the LLRF control system. An RF signal is converted into a 10-MHz IF signal using a down-converter. The FPGA board (equips 10 16-bit ADCs) samples the IF signal at a 40-MHz clock signal and calculates IQ elements for the collection of amplitude and phase data. Recently, a high-speed and wideband ADC, which that can sample RF signal directly, 1300 MHz RF signal is available. A high-speed data acquisition system using a fast ADC has been utilized for evaluating the efficiency of the direct sampling method.

CONSTRUCTION OF HIGH-SPEED DATA ACQUISITION SYSTEM

The high-speed data acquiring system is composed of an ADC board (ADS5474EVM) and an FPGA board (ML555). The FPGA board stores the raw data acquired by the ADC board in its internal memory. This data is then transmitted and analyzed by the host PC (Fig.1). Figure 2 shows the ML555 installed in a PCI-Express slot on the host PC. ML555 and ADS5474EVM are connected by LVDS cables via adaptors, as shown in Fig.3.

ADS5474

ADS5474EVM is an evaluation board equipped with an ADS5474 ADC manufactured by Texas Instruments. Its features are as follows:

- Resolution: 14 bit
- Maximum sampling rate: 400MSPS
- Analog bandwidth: 1.4 GHz
- Data output: LVDS compatible

ML555

ML555 is a commercial FPGA board manufactured by Xilinx and is equipped with a Virtex-5 (XC5VLX50T).

Its features are as follows:

- PCI-Express/PCI/PCI-X card-edge connector
- DDR2-SDRAM
- LVDS interface with SAMTEC connector

USB port

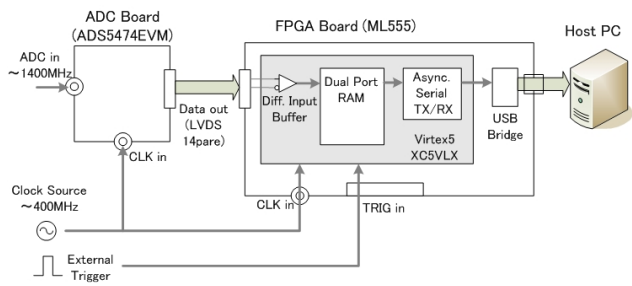

Figure 1: Block diagram of the high-speed data acquisition system.

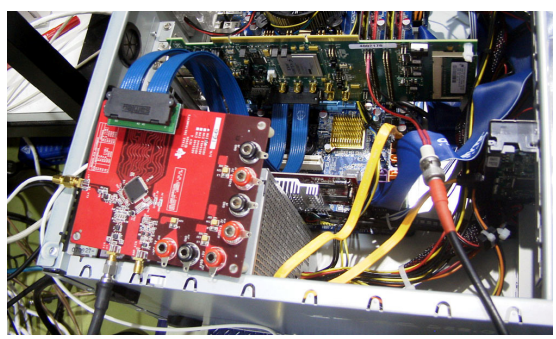

Figure 2: ML555 and ADS5474EVM on host PC.

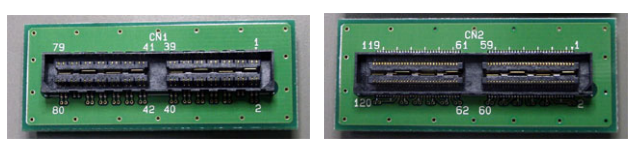

Figure 3: SAMTEC connector adaptor.

PERFORMANCE OF DIGITAL LOW-LEVEL RF CONTROL SYSTEM WITH FOUR INTERMEDIATE FREQUENCIES

T. Matsumoto*, S. Fukuda, H. Katagiri, S. Michizono, T. Miura, Y. Yano, KEK, Tsukuba, Japan

Abstract

In superconducting accelerators, an FPGA-based low-level RF (LLRF) system is employed with a digital feedback control system to satisfy the stability requirement of the accelerating field. In the digital LLRF systems, an RF signal picked up from a cavity is down-converted into an intermediate frequency (IF) signal to estimate the I and Q components of the RF signal. A new digital LLRF system that uses four different IFs has been developed to decrease the number of analog-to-digital converters (ADC) required during the feedback operation of the RF sources.

In this study, the digital LLRF system with four different frequencies is examined and the feedback operation using a superconducting cavity is performed at the Superconducting RF Test Facility (STF) at KEK. The performance of the digital LLRF system is reported by measuring the stabilities of the accelerating fields.

INTRODUCTION

A single RF system of the International Linear Collider (ILC) consists of three accelerating cryomodules (two of these are composed of nine superconducting cavities each and one is composed of eight cavities) and a klystron that generates RF power [1]. In the ILC, an accelerating field stability of 0.07% in amplitude and 0.24° in phase is required for its operation. In order to meet this requirement, the RF field is controlled with vector-sum feedback (FB) and feedforward (FF) mechanism using a digital low-level RF (LLRF) system based on an FPGA/DSP board.

In the digital LLRF system, the RF signal picked up from a cavity is down-converted into an intermediate frequency (IF) signal while retaining the amplitude and phase information of the RF signal. The IF signals are sampled by analog-to-digital converters (ADCs) with a constant sampling rate (SR) and the amplitude and phase information (or I and Q components) of the RF signal are determined by digital signal processing.

In the case of vector-sum FB control, the number of ADCs required for field detection is equal to the number of cavities, as shown in Figure 1(a). In the case of the ILC, one RF station requires 26 ADCs to operate the RF field with FB control. It is difficult to construct an FPGA board that can hold such a large number of ADCs because the number of lines between the FPGA and the ADCs increases as the number of ADCs increases.

Currently, a digital LLRF control system using a new IF-mixture technique is being developed in order to decrease the number of ADCs required for field detection. In this technique, the RF signals from different cavities

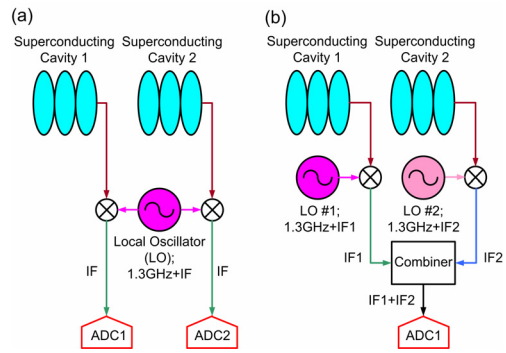

Figure 1: Schematic diagram of the digital LLRF system: a) conventional and (b) IF-mixture technique.

are down-converted into different IF signals and these IF signals are then combined using a combiner, as shown in Figure 1(b). The I and Q components of each IF signal are evaluated from the combined IF signal sampled by ADC. By employing two IFs in the digital LLRF system, the number of ADCs can be reduced to half the original value.

A digital LLRF system employing the IF-mixture technique on two IF signals has been developed and the performance of FB operation has been evaluated by using two cavity simulators [2]. In this study, we developed a digital LLRF system with four IF signals that operated a superconducting cavity [3] at the Superconducting RF Test Facility (STF) at KEK.

IF-MIXTURE TECHNIQUE

The down-converted IF signal is expressed as follows:

$$x(t) = I(t)\cdot\cos(\omega_{IF}t+\varphi) + iQ(t)\cdot\sin(\omega_{IF}t+\varphi)$$

where $I(t)$, $Q(t)$, and φ are the I and Q components and the loop phase of the cavity, respectively, and $\omega_{IF} = 2\pi\cdot IF$. When the sampling rate of the ADC and the frequency of the IF signal satisfy the condition $M \cdot IF = N \cdot SR$ (N is an integer and M is an integer greater than 3), the I and Q components of the IF signals can be numerically calculated using the following equations for averaging consecutive signal samples [4, 5].

$$I = \frac{2}{M}\sum_{n=1}^{M} x_i(n)\cdot\cos\left(\frac{2\pi\cdot N}{M}\cdot n\right)$$
$$Q = \frac{2}{M}\sum_{n=1}^{M} x_i(n)\cdot\sin\left(\frac{2\pi\cdot N}{M}\cdot n\right) \qquad (1)$$

It is expected that the influence of noise and jitter caused by the ADC sampling can be reduced by averaging the signal samples.

#toshihiro.matsumoto@kek.jp

PERFORMANCE OF DIGITAL LLRF SYSTEM FOR STF IN KEK

S. Michizono#, H. Katagiri, T. Matsumoto, T. Miura, Y. Yano and S. Fukuda, KEK, Tsukuba, Japan

Abstract

RF operations were carried out at the STF (Superconducting RF Test Facility) in KEK. The digital feedback system was installed in order to satisfy the strict rf-field requirements. The rf field stabilities under various feedback parameters are presented in this report. Cavity detuning measurements (microphonics, quench detection, etc.) were among the various studies that were conducted. Results of these studies are also summarized.

INTRODUCTION

The STF is a test facility for pulsed superconducting cavities aiming for ILC (International Linear Collider). An amplitude of 0.07% and a 0.24° phase are required for rf stability in the ILC in order to satisfy the collision luminosity [1]. In order to satisfy these requirements, a digital llrf (low-level radio frequency) system has been developed.

The STF started its operation in July 2007 [2], and several llrf studies have been carried out. Some of the topics studied are as follows:

(1) Study of cavity field stability

(2) IF mixture method: This method enables us to reduce the number of ADCs by combining intermediate frequency (IF) signals. This method has been validated by using electrical cavity simulators. This is the first time a study has been conducted using a real super-conducting cavity [3].

(3) Instability evaluation: An evaluation of the feedback performance under all fundamental modes such as the 8/9π mode was performed. This evaluation was carried out by eliminating the analog low-pass filter that was inserted between the IQ modulator and the DACs [4].

(4) Direct rf detection using a fast 14-bit ADC: In order to develop next-generation future rf detection systems, we examine a 14–bit fast ADC with a bandwidth of more than 1.3 GHz. This method allows the detection of the rf signal without the use of a downconverter [5].

(5) Analysis of the rf monitor: llrf monitors are used for the evaluation of cavity characteristics such as microphonics and for quench detection.

In this report, we summarize the results of the above studies.

DIGITAL LLRF SYSTEM

The digital llrf system comprises an rf signal generator (RF & CLK), downconverters, and a DSP/FPGA board having ten 16-bit ADCs and two 14-bit DACs. The

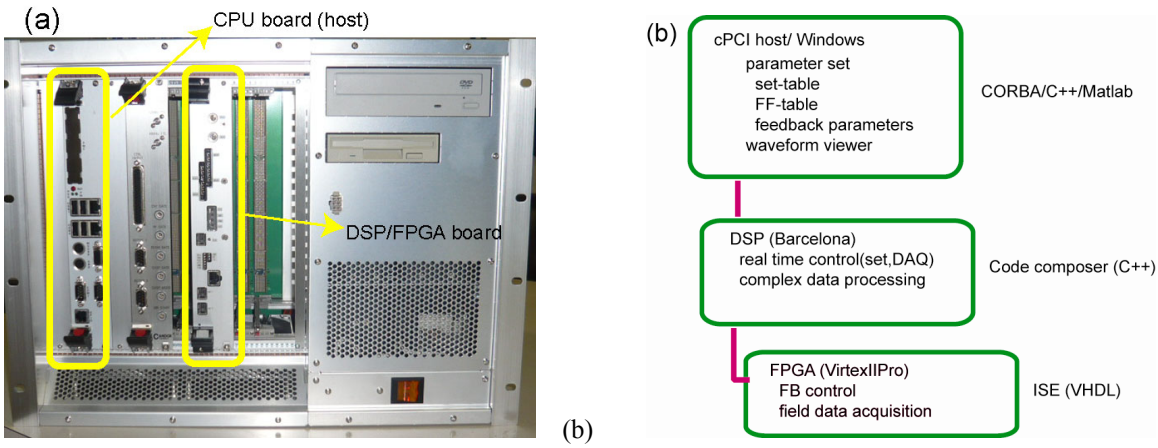

Figure 1: Photograph of cPCI system (a), and system layers inside cPCI (b).

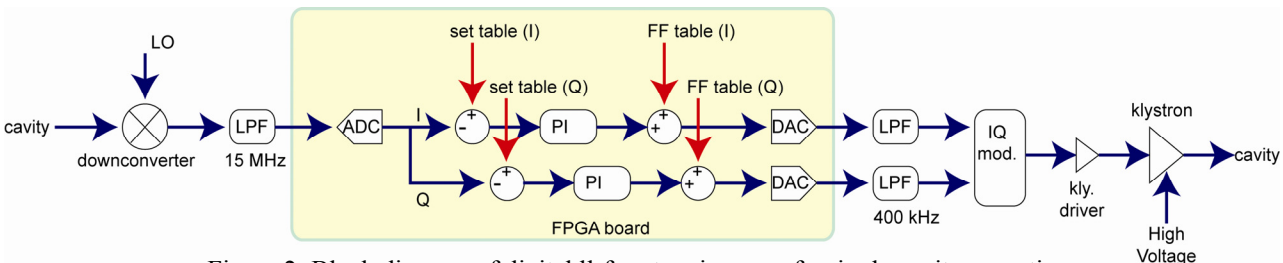

Figure 2: Block diagram of digital llrf system in case of a single cavity operation.

#shinichiro.michizono@kek.jp

MEASUREMENTS OF FEEDBACK-INSTABILITY DUE TO 8/9π AND 7/9π MODES AT KEK-STF

T. Miura#, H. Katagiri, T. Matsumoto, S. Michizono, Y. Yano, S. Fukuda, KEK, Ibaraki, Japan

Abstract

At the superconducting RF test facility (STF) at KEK, high-power tests of the superconducting nine-cell cavity for the International Linear Collider (ILC) have been performed. The cavity was driven by an RF of 1.3GHz which corresponds to the π mode with zero beam acceleration. Feedback instabilities due to the 8/9π and 7/9π modes were observed when the other modes were not filtered. The intensities of the 8/9π and 7/9π modes were measured by varying the feedback loop delay, and the stable/unstable regions appeared at regular intervals as expected.

INTRODUCTION

The superconducting RF test facility (STF) at KEK is the research and development facility of the International Linear Collider (ILC). At the STF, high-power tests of the superconducting nine-cell cavity have been performed. The cavity is driven by an RF of 1.3 GHz with a pulse duration of 1.5 ms and a repetition rate of 5 Hz. A stability of 0.3% amplitude and 0.3° phase is required at the flat-top region where beam acceleration is performed. To achieve this stability, we adopt a high-speed digital feedback control system using a field programmable gate array (FPGA) in the low-level RF (LLRF) system [1,2]. The cavity is operated in the π mode which has the highest efficiency for beam acceleration. However, Vogel [3] has pointed out the occurrence of the feedback control instability due to the passband of TM_{010} mode except for the π mode. Therefore, we measured the instability in the STF.

MODE FREQUENCIES

Table 1: Frequency differences the π mode and other modes for each cavity

	cav#1@2K *f-f*π (MHz)	cav#2@2K *f-f*π (MHz)	cav#3@2K *f-f*π (MHz)	cav#4@RT* *f-f*π (MHz)
8/9π	−0.70	−1.11	−0.88	−0.83
7/9π	−3.53	−3.45	−3.39	−3.04
6/9π	−7.31	−6.98	−7.08	−6.27
5/9π	−11.69	−11.62	−11.50	−10.00
4/9π	−16.47	−16.37	−16.31	−14.05
3/9π	−20.83	−20.94	−20.63	−17.86
2/9π	−24.54	−24.52	−24.20	−21.14
1/9π	−27.25	−26.68	−26.64	no−data

*RT: Room Temperature

Table 1 shows the frequency differences between the π mode and other modes for each cavity in the STF. For a given mode, the frequency is different for different cavities due to fabrication error. When performing vector-sum control, we have to pay attention to many frequency components in comparison with the control for only one cavity. Figure 1 shows the band-pass characteristics of a TH2104A klystron used at the STF. The peak is observed at 1294 MHz. Therefore, it is easier for frequencies of modes in the range 6/9π - 8/9π to pass through the klystron as compared to π mode.

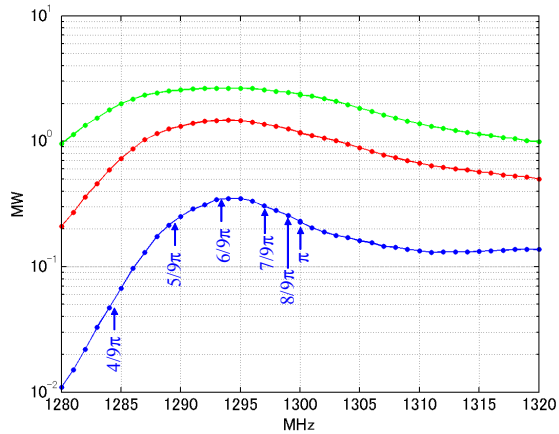

Figure 1: Band-pass characteristics of klystron (TH2104A).

ESTIMATION OF GAIN MARGIN

In order to estimate the feedback instability, the gain margin of each mode, except the π mode, was calculated. A more detailed description of the calculation is presented by Vogel [3]. The open-loop transfer function (TF) of the system is represented as follows:

$$H(s) = Gp\, H_{delay}(s)\, H_{cav}(s)\, H_{kly}(s), \qquad (1)$$

where Gp is the proportional gain of the feedback, $H_{delay}(s)$ is the TF of the feedback loop delay, $H_{cav}(s)$ is the TF of the cavity, and $H_{kly}(s)$ is the TF of the klystron. In this calculation, $H_{kly}(s)$ is approximated by a low-pass filter with a 3 dB bandwidth of 3 MHz in a manner similar to that employed by Vogel [3]. $H(s)$ is converted to a discrete system of 40 MHz, which is the sampling frequency in analog-to-digital converter (ADC), and the gain margin is calculated from the Nyquist stability criterion. The gain margins for different feedback loop delays are shown in Fig. 2. In the figure, the area shaded grey indicates a stable region, while that shaded white denotes an unstable region. Even when Gp is small, the feedback system becomes unstable for modes in the range of 8/9π – 5/9π. The stable and unstable regions appear at regular intervals with the intervals depending on the difference between their frequencies and the frequency of the π mode. On the other hand, low-order modes such as the 2/9π and 1/9π modes are stable for large values of Gp.

#takako.miura@kek.jp

PULSE-BY-PULSE SWITCHING OF BEAM LOADING COMPENSATION IN J-PARC LINAC RF CONTROL

T. Kobayashi#, E. Chishiro, H. Suzuki, JAEA, Tokai, Naka, Ibaraki, Japan
S. Anami, Z. Fang, S. Michizono, S. Yamaguchi, KEK, Tsukuba, Ibaraki, Japan

Abstract

For the J-PARC linac low level RF system, a new function that switches the feed-forward control parameters in every pulse was installed into the digital accelerating-field control system, in order to compensate beam-loading change by pulses in the operation of 25-Hz repetition.

The linac provides a 50-mA peak current proton beam to a 3-GeV rapid-cycling synchrotron (RCS). Then the RCS distributes the 3-GeV beam into a following 50-GeV synchrotron (main ring, MR) and the Materials and Life Science Facility (MLF), which is one of the experimental facilities in the J-PARC. The 500-us long macro pulses from the ion source of the linac should be chopped into medium pulses for injection into the RCS. The duty (width or repetition) of the medium pulse depends on which facility the RCS provides the beam to the MR or MLF. Therefore the beam loading compensation needs to be corrected for the change of the medium pulse duty in the 25-Hz operation.

INTRODUCTION

J-PARC will be one of the highest intensity proton accelerators, which consists of a 181 or 400-MeV Linac, a 3-GeV rapid-cycling synchrotron (RCS) and a 50-GeV synchrotron (main ring, MR) [1]. The beam is applied to several experimental facilities, for example, the Materials and Life Science Facility (MLF), the Hadron Physics Facility and the Neutrino Facility (See Fig. 1). The MLF is aimed at promoting materials science and life science using the world highest intensity pulsed neutron and muon beams which are produced using 3-GeV protons with a current of 333micro-amps and a repetition rate of 25 Hz.

The beam commissioning has progressed steadily, since the linac beam commissioning was started in October 2006. Then the first neutron production was succeeded at the MLF, and in the MR the 3-GeV beam was captured by RF and extracted to the beam dump after 1000 turns in this year. Now more detail beam sturdy is in progress.

As described in above, the RCS has to distribute the beam to the MLF and the MR. This switching of the beam destination (MLF or MR) influences the beam intensity of the linac. Therefore the parameters of the beam-loading compensation need to be switched due to the destination of the beam in the 25-Hz pulse operation. Accordingly, a new function that switches the feed-forward control parameters in every pulse was installed into the digital accelerating-field control system.

For high quality and high intensity beam acceleration, the stability of the accelerating field is one of the most important issue. Because the momentum spread ($\Delta p/p$) of the RCS injection beam is required to be within 0.1%, the accelerating field error of the linac must maintained within ±1% in amplitude and ±1 degree in phase. To realize this stability, a digital feedback (FB) control is used in the low level RF (LLRF) control system, and a feed-forward (FF) technique is combined with the FB control for the beam loading compensation [2]. In the 181-MeV acceleration of the linac, the 24 LLRF systems are operated in a frequency of 324 MHz and the stability of ±0.2% in amplitude and ±0.2 degree in phase is achieved including the beam loading [3]. This RF stability makes high reproducibility of the injection beam and then contributes to the steady commissioning progress of the J-PARC.

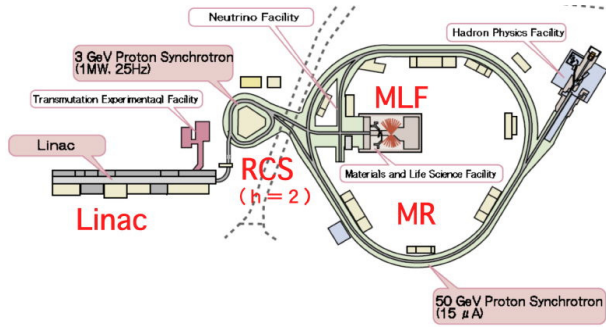

Figure 1: Layout of J-PARC accelerator.

BEAM STRUCTURE AND RF SYSTEM

The beam structure of the J-PARC linac is shown in Fig. 2. Maximum peak current will be 50 mA. Macro-pulses of 500-μs widths are accelerated in 25-Hz repetition. The macro-pulse is chopped by a RF-chopper into medium pulses as synchronized with the RCS RF

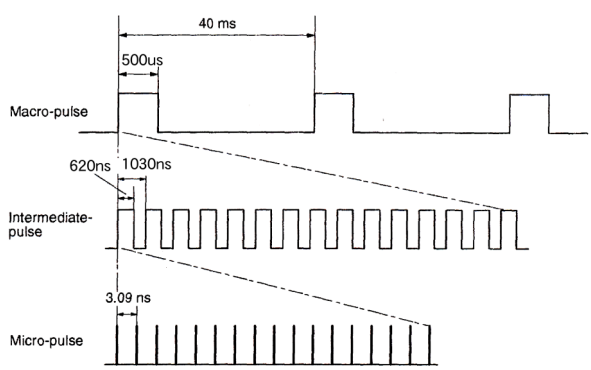

Figure 2: Beam Structure of the J-PARC linac.

tetsuya.kobayashi@j-parc.jp

LLRF CONTROL SYSTEM USING A COMMERCIAL BOARD*

Han-Sung Kim#, Hyeok-Jung Kwon, Kyung-Tae Seol, and Yong-Sub Cho
Korea Atomic Energy Research Institute, Daejeon 305-353, Korea

Abstract

The requirements for the field amplitude and phase stability of the PEFP linac are 1% and 1 degree, respectively. To achieve the requirements, a digital LLRF control system has been developed using a commercial digital board for general purpose (FPGA). The feedback with PI control and feedforward are implemented in the FPGA. The LLRF control systems are currently used for the linac test. In this paper, test results and discussion on the advantage and disadvantage of the LLRF system based on a commercial board are presented.

INTRODUCTION

In the 100 MeV proton linear accelerator for PEFP (Proton Engineering Frontier Project), the RF source will power an RFQ cavity and DTL tanks operated at a frequency of 350 MHz [1]. The low level RF(LLRF) system for 100 MeV proton linear accelerator provides field control including an RFQ and DTL tanks at 350 MHz. In our system, an accelerating field stability of ±1% in amplitude and ±1 deg. in phase is required for the RF system. The digital RF feedback control system using the FPGAs and PowerPC Embedded Processor is adopted in order to accomplish these requirements and flexibility of the feedback and feed-forward algorithm [2]. The analog front-end also developed which contains the IQ modulator, RF mixer, attenuators etc. To check the performance of the digital feedback control system, low power test with a dummy cavity has been performed with an intentional perturbation and has shown that the feedback system rejected the perturbation as expected. High power RF test with 3 MeV RFQ and 20 MeV DTL has been performed and the accelerating field profiles were measured and the pulse-to-pulse stability was checked by pulse operation with 0.1 Hz repetition rate. In addition, the LLRF system can be used for resonant frequency observer. Measured frequency offset from resonance condition is converted to analog voltage signal, which can be used as an error input signal for RCCS (Resonance Control Cooling System).

LLRF SYSTEM DESCRIPTIONS

The main hardware components of the digital RF feedback system are ADC for sampling of the RF signal, FPGA for the signal processing and DAC for driving the IQ modulator. A ICS-572B commercial board which is shown in figure 1 is adopted for the ADC/DAC and FPGA board. ICS-572B is a PMC module with 2-channel 105 MHz ADC, 2-channel 200 MHz DAC and with 4 million gate onboard Xilinx FPGA.

The board uses two 14-bit ADCs (Analog Devices AD6645) with a maximum sampling rate of 105 MHz. The sampling clock can be either internally or externally generated. The minimum ADC sample rate is 30 MHz. Both input channels are simultaneously sampled and transformer-coupled with turn rato of 4:1.

The outputs of the ADCs are connected to a Xilinx FPGA for direct processing of the ADC data. The ICS-572B includes a Xilinx Virtex-II FPGA (XC2V4000) that can be programmed by the user via a JTAG port or PCI communication.

On the output side, the ICS-572B uses two 14-bit high speed DACs (Analog Devices AD9857). The maximum simultaneous conversion rate is 200 MHz. The DAC has a built-in quadrature up-converter that allows the user to provide complex baseband input which is up-converted to a programmable IF (up to 100 MHz). The DAC also provides a programmable clock multiplier.

The communication between the ICS-572B board and host system is made using PCI bus. The QL5064 QuickPCI chip from QuickLogic is used for PCI interface solution. The performance of the QL5064 is 64 bit/66 MHz and automatically backwards compatible to 33 MHz or 32 bit

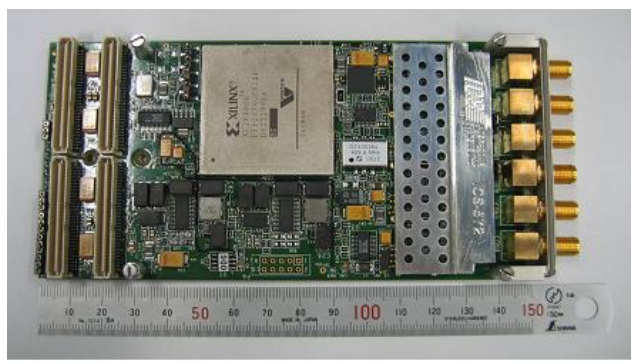

Figure 1: ICS-572B PMC Board.

For the host system of the ICS-572B FPGA board, a Motorola VME processor module, MVME5100, is adopted. The main roles of the host system are the configuration of the FPGA board and the data acquisition.

The feedback logic based on the PI control is implemented in the FPGA by using VHDL. The I and Q component of the cavity field signal is fed into the FPGA using the ADC, which samples the RF signal four times during one period. The sampled I and Q components of the cavity signals are compared with the set value, which generates the error signal. The calculated proportional and integral control values are added then converted to an analogue signal by using DAC.

* This work is supported by the Ministry of Education, Science and Technology of the Korean government.
#kimhs@kaeri.re.kr

NUMERICAL SIMULATION OF THE INR DTL A/P CONTROL SYSTEM

A.I.Kvasha, Institute for Nuclear Research, RAS, Moscow, Russia

Abstract.

Stabilization of amplitude and phase in linear accelerator cavities can be realized by means of control systems, operating both in polar (A/P) and rectangular (I/Q) coordinate. In analyzing of linear control systems, as a rule, transfer functions are used, which, in turn, are the symbolic representation of the linear differential equation, connecting the input and output variables. It's well known that generally in A/P coordinate it is impossible to get two separate linear differential equations for amplitude and phase of RF voltage in a cavity except for estimating of the control system stability "in the small" near steady state values of variables [1]. Nevertheless, there is a possibility of numerical simulation of nonlinear A/P control system using up-to-date programs. Some results of the simulation are presented.

INTRODUCTION

In contrast to A/P, in I/Q coordinates it is succeeded in separating of both variables in two linear differential equations even for detuned cavity. That is why I/Q control systems became so popular last years, particularly, in connection with successful development of digital feedback systems. Despite obvious advantages of I/Q control system, its real application in pulse DTL RF system, operating at frequencies below 300 MHz, meets some difficulties. In this case RF amplifiers, as a rule, are based on application of vacuum tubes. The vacuum tube RF amplifiers construction inevitably contains bypass capacitors, which always are sources of RF parasitic radiation. Since I/Q control systems basically use standard integrated circuits: mixers, I/Q modulators and demodulators, working at low RF power level, its operation due to interferences from vacuum tube RF amplifiers, can be disturbed. That is why application of I/Q control systems is preferable for stabilization of accelerating field in cavities with klystron RF supply or with the low gain vacuum tube amplifiers in a case of CW accelerators.

Since at INR linear accelerator output RF power amplifier (PA) is connected with the DTL cavity (tank) by means of coaxial transmitting line (CTL) without circulator, the PA and the tank can be considered as a common high quality oscillating system [1]. At that, processes in the system are described by the first order linear differential equation with complex coefficients, which appear in result of two admissions:

- Transients in the high quality cavity are so slow that changing of amplitude and phase for the RF period can be not taken into account.
- Transients in the output RF power amplifier circuits and CTL are so fast in comparison with transients in the accelerator high quality cavity that steady-states are available in these circuits (including CTL) at every instant of amplitude and phase transients in the cavity.

These admissions allow simplifying not only the calculation of transients in the high quality tank, but also estimating parameters of control systems, stabilizing amplitude and phase of RF voltage in the DTL tank. As it was shown in [1] the first order - linear at complex variable plane, Differential Equation (DE) for a "complex envelope" of RF voltage in a high quality accelerator cavity can be presented in the following way:

$$T_n \frac{d\bar{U}_c(t)}{dt} + (1 - j\xi_c)\bar{U}_c(t) = \frac{T_n}{T_0} R_S(\bar{I}_g - \bar{I}_b), \qquad (1)$$

where $\bar{U}_C$ is a complex amplitude of accelerating voltage in the high-quality cavity; $\xi_c = (\Delta\omega_g + \Delta\omega_0)T_n$; $\Delta\omega_0, T_0, R_s$ are the own cavity detuning, cavity time constant and cavity shunt impedance; $\Delta\omega_g, T_n$ are the cavity "detuning" and "time constant" of the cavity, determined by the RF system parameters, such as internal resistance of the PA vacuum tube, coupling with CTL both from the side of the output RF power and from the cavity, length of the CTL [1,2]; $\bar{I}_g$ is a complicated function of RF supply parameters, listed above; $\bar{I}_b$ is a complex amplitude of the beam current resonance harmonic. So, one could say that Eq. (1) determines transient in common "PA-cavity" oscillating system. Moreover, as evident from Eq. (1), application of the complex envelope of RF in the cavity notably simplifies an analysis of control systems since both RF channel with the cavity and the feedback circuits are arranged in the same low-frequency domain. In polar A/P coordinates the complex amplitude $\bar{U}_c(t) = a_c(t)\exp(j\varphi_c(t))$. Substituting this expression in Eq. (1) and taking into account that $\bar{I}_g = I_g e^{j\varphi_g}$, $\bar{I}_b = I_b e^{j\varphi_b}$ it is easy to get from Eq. (1) the next system of the nonlinear differential equations for the real and imaginary parts of the Eq. (1):

$$\begin{aligned} T_n \frac{d\varphi_c}{dt} - \xi_c &= \frac{T_n R_s}{a_c T_0}(I_g \sin(\varphi_g - \varphi_c) - I_b \sin(\varphi_b - \varphi_c)) \\ T_n \frac{da_c}{dt} + a_c &= \frac{T_n}{T_0} R_s (I_g \cos(\varphi_g - \varphi_c) - I_b \cos(\varphi_b - \varphi_c)) \end{aligned} \qquad (2)$$

OPTIMAL COUPLER AND POWER SETTINGS FOR SUPERCONDUCTIVE LINEAR ACCELERATORS*

J. Branlard†, B. Chase, S. Nagaitsev, O. Nezhevenko, J. Reid
Fermi National Accelerator Laboratory, Batavia, IL, U.S.A.

Abstract

The modeling analysis presented in this paper addresses the question of how to achieve the highest vector sum gradient for all beam currents when individual cavities operate at different gradients due to their inherent quenching limitations. The analytical method explained here constitutes a step forward toward the operability of the International Linear Collider (ILC), Project X [8], or XFEL [7]. Unlike previously proposed methods [1, 2], this approach prevents cavities from quenching should the beam current be lower than its maximum value.

INTRODUCTION

Ideally, all superconducting cavities of a linear accelerator RF station operate at the target gradient (31.5 MV/m for the ILC). Practically however, cavities show a certain disparity in their gradient performance. Based on the experience acquired at DESY XFEL [6], we know that some cavities quench or exhibit a Q drop behavior when operating above 22 MV/m while others will sustain an accelerating gradient of 34 MV/m. This disparity among cavities raises challenging issues related to conditioning and operations of linear accelerators using one klystron per RF station. More precisely, this paper presents an analytical solution to the following question: for N cavities with a given maximum gradient distribution (i.e. quenching limits), what is the highest vector sum gradient that can be maintained for the entire flat top duration with beam or in the absence of beam, while ensuring that no cavity quenches? Currently, one approach has been proposed [1, 2] to address this issue but it only guaranties maximum gradient operability when the beam current is maximum. A second approach implemented at DESY for XFEL [7] only guaranties maximum gradient without beam current. In contrast, the method presented here predicts the maximum vector sum gradient that can be reached for a given cavity distribution, independently of the beam loading.

Q_L AND P_K SETTINGS

The present model consists of a low level RF (LLRF) controller driving a single klystron, providing the RF forward power to multiple cavities. The amplitude and phase of the klystron drive signal can be adjusted from the LLRF controller, the proportion of forward RF power delivered to individual cavities can be adjusted at the wave guide level by tuning the wave guide couplers, (referred to as P_k setting) and at the cavity level by changing the loaded Q of each cavity's input coupler, (referred to as Q_L settings). Several techniques have been suggested to adjust the forward power distributed to a pair of cavities: variable tap off splitters [5], or phase shifters [9]. Either of these techniques requires hardware replacement and interrupting accelerator operations for an extended period of time. Hence, this tuning is considered to be set once and not changed again. Setting the external Q at the cavity input coupler is an operation which does not require shutting down the RF station. It is nonetheless a time consuming procedure and is not practical for large scale machines. Finally, the LLRF drive signal can dynamically (i.e. during the RF pulse) control and adjust the amplitude and phase of the klystron drive signal. The goal of this study is to find the optimal configuration of these parameters to achieve the highest vector sum gradient, while respecting the operational and security constrains listed above.

The approach described in [4] consists of choosing Q_L and P_k settings specific to each cavity so as to match every cavity with maximum beam loading. One major issue associated with this scheme is that the individual Q_L and P_k need to be readjusted every time the beam loading is less than maximum which can become a real operation bottleneck for large scale accelerators. Alternatively, lowering the klystron forward power for less than maximum beam current operations can prevent cavities from quenching but will significantly degrade the vector sum gradient. In the DESY approach [7], all cavities are set to the same Q_L but some cavities will quench when the beam is on unless the vector sum gradient is lowered. The approach presented here addresses these issues.

ANALYTICAL INSIGHT

Flat Top without Beam

The voltage inside a superconducting cavity, on resonance and with on-crest beam loading can be modeled as follows [3]:

$$V_C(t) = 2R_L \left[I_{g0}(1 - e^{-\frac{t}{\tau}}) - I_{b0}(1 - e^{-\frac{t-t_0}{\tau}}) \right] \quad (1)$$

where R_L is the loaded resistance of the cavity, I_{b0} is the nominal DC beam current, $\tau = \frac{2Q_L}{\omega_0}$ is the cavity time constant and t_0 is the duration of the fill time of the cavity, after which the forward power is dropped by four when no beam is present. Achieving a flat top in the absence of beam

* work supported by Fermi Research Alliance, LLC under Contract No. DE-AC02-07CH11359 with the United States Department of Energy
† branlard@fnal.gov

NEW LLRF SYSTEM FOR FERMILAB 201.25 MHZ LINAC

Trevor A. Butler, Lawrence J. Allen, Julien Branlard, Brian Chase, Ed Cullerton, Paul W. Joireman, Michael Kucera, Vitali Tupikov, Philip Varghese, Fermilab, Batavia, IL 60510, U.S.A.

Abstract

The Fermilab Proton Plan, tasked to increase the intensity and reliability of the Proton Source, has identified the Low Level Radio Frequency (LLRF) system as the critical component to be upgraded in the Linac. The current 201.25 MHz Drift Tube Linac LLRF system was designed and built over 35 years ago and does not meet the higher beam quality requirements under the new Proton Plan. A new VXI based LLRF system has been designed to improve cavity vector regulation and reduce beam losses. The upgrade includes an adaptive feedforward system for beam loading compensation, a new phase feedback system, and a digital phase comparator for cavity tuning. The new LLRF system is phase locked to the 805 MHz reference line, currently used as frequency standard in the higher energy accelerating section of the Linac. This paper will address the current status of the project, present the advancements in both amplitude and phase stability over the old LLRF system, and discuss commissioning plans.

INTRODUCTION

The RF control system that is presently implemented in low energy (LE) Linac was first commissioned in the late sixties. Although it received minor modifications in 1994, it does not meet the present amplitude and phase stability requirements. During the last seven years, the types and number of beam pulses that are being accelerated in the Linac have risen tenfold, resulting in an increase in activation of the Linac enclosure. As a result, the Proton Plan was developed to fund projects that could either improve beam quality or reduce enclosure activation due to beam loss [1]. In order to meet these demands, a new LLRF for the LE Linac system has been designed and prototyped. The design goal for the new LLRF system is to reduce amplitude variations to < 0.2% and to reduce the beam setting time to < 2 μs. The current LLRF system (see Fig. 1) is only able to achieve 2% amplitude stability. During the first 10 μs of beam, both the RF amplitude and phase errors have the largest excursion. These errors cause momentum drift in the beam, which in turn, creates matching problems into the downstream Booster accelerator. A beam drift of 2 mm, both vertically and horizontally was measured at the downstream end of Linac. In order to reduce this mismatch into Booster, the first 10 μs of beam is presently chopped off and sent to a dump line. With the increased repetition rate of the Linac, this wasted beam has steadily increased the activation of both the dump line and the accelerating structure. By reducing the beam settling time from 10 μs to less than 2 μs, and by improving beam loading compensation and regulation, the beam loss and resulting activation can be greatly reduced [2].

LINAC LLRF SYSTEM

In order accomplish the goals of the Proton Plan, a new LLRF system has been designed and implemented to replace the present LLRF system (see Fig. 1). The new system consists of three parts, a slot 0 controller, a multi-channel field control (MFC) module, and an analog RF module (see Fig. 2). The slot 0 controller is used to connect the Fermilab controls network (ACNET) with the

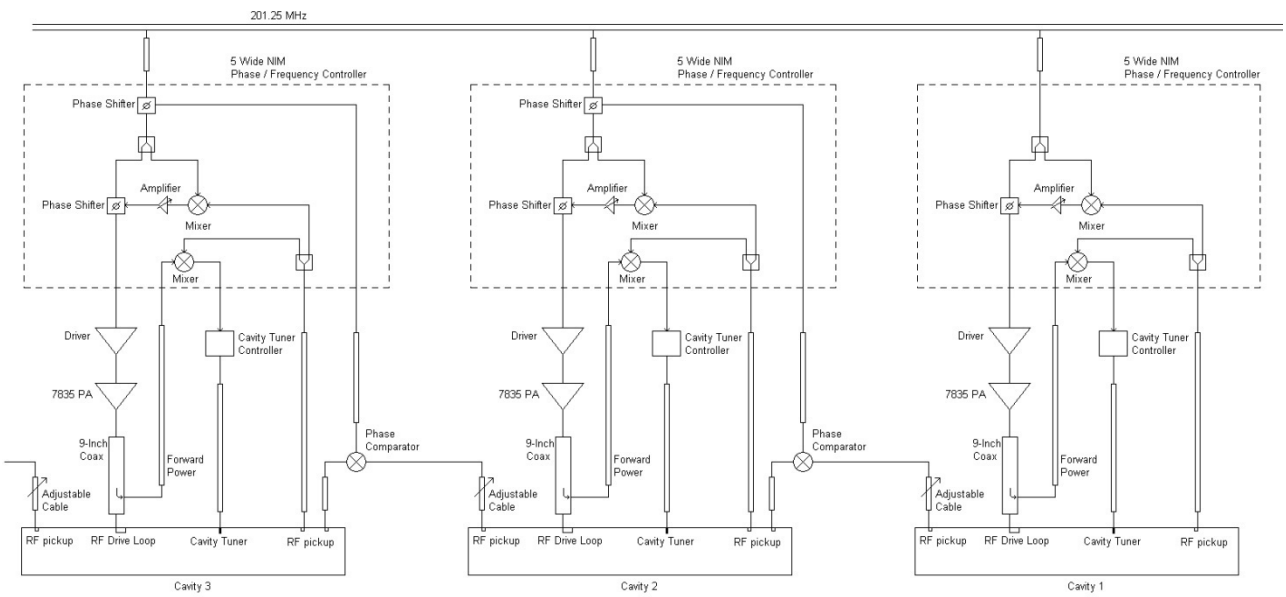

Figure 1: Simplified low energy (LE) linac RF block diagram of the present LLRF control system.

OPTIMIZING CAVITY GRADIENTS IN PULSED LINACS USING THE CAVITY TRANSIENT RESPONSE*

G. Cancelo#, A. Vignoni, Fermi National Accelerator Laboratory, Batavia, IL 60510, U.S.A.

Abstract

In order to achieve beam intensity and luminosity requirements, pulsed LINAC accelerators have stringent requirements on the amplitude and phase of RF cavity gradients. The amplitude and phase of the RF cavity gradients under heavy beam loading must be kept constant within a fraction of a % and a fraction of a degree respectively. The current paper develops a theoretical method to calculate RF parameters that optimize cavity gradients in multi cavity RF units under heavy beam loading. The theory is tested with a simulation example.

INTRODUCTION

Modern pulsed LINAC accelerators are being designed taking advantage of the cost reduction that can be achieved powering a string of cavities from one klystron. At 70% peak power utilization a 10 MW klystron can power 24 superconducting cavities at an average gradient of 31.5MV/m and a beam current of 9 mA. The XFEL main LINAC klystrons at DESY will power 32 cavities at 23.6MV/m and an average beam current of 5mA. As multiple cavities are connected to a single klystron the RF system parameters and control become more complex. A typical low level RF (LLRF) control loop controls the amplitude and the phase of the klystron's RF power, however, the loop cannot dynamically control individual cavity amplitude and phases. Typically, the control is done over the vector sum of all cavity gradients within the RF unit. The problem is further complicated by the need to obtain the maximum possible acceleration from the RF unit, pushing cavity gradients up close to their quenching limits. These cavity maximum gradients are different within a certain spread. Proton LINACs such as HINS [5] and Project X [6] add extra complexity to the RF system. A RF unit may need cavities operating at different synchronous phases (Φs). Secondly, particles travel cavities at increasing (non-relativistic) velocities, which implies different beam loading conditions from cavity to cavity.

Most of the literature available on cavity field dynamics follows a steady state approach [1-4]. The cavity is modeled by a 2nd order ODE (ordinary differential equation) and later approximated by a 1st order ODE model due to the high loaded Q of the cavity. The steady state approach determines optimality conditions for minimum generator power as a function of the cavity coupling parameter βopt and cavity tuning angle φopt. The steady state analysis works well for continuous

*Work supported by Fermi Research Alliance, LLC. under Contract No. DE-AC02-07CH11359 with the United States Department of Energy.
#cancelo@fnal.gov

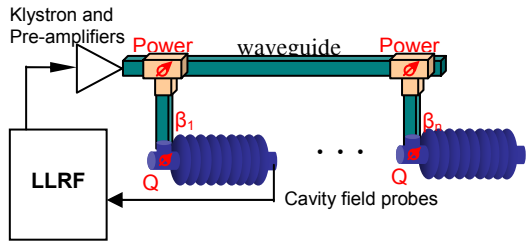

Figure 1: RF system block diagram.

waveform (CW) machines. A similar steady state assumption is assumed about the beam, and these models use the average beam current.

The steady state analysis applied to pulsed RF Linacs does not provide optimum operation parameters for all cases. For cavities operating "on crest" (Φs=0) under heavy beam loading and strong RF coupling an exact calculation of the forward power and beam injection time can set constant cavity gradients (flattops) and minimize or zero out the reflected power. For "on crest" operation, gradient flattops can still be maintained for cavities operating at different gradients with one time optimization of the coupling parameter. Unfortunately, this is not longer valid when cavities in the same RF unit need to be operated at different synchronous phases. Moreover, as is the case for pulsed RF proton beam Linacs such as HINS [5] and Project X [6], cavities have different beam loading conditions. To exemplify the theory that will be developed in this paper we use one RF unit from the Project X proposal. The RF unit has 3 cryomodules with a total of 21 cavities operating with synchronous phases and beam loadings as described in Table 1. A typical ±10% Vcav spread is assumed.

Table 1: Example Using a Project X RF Unit

Cavity Number	Beam Beta In	Beam Beta Out	Cavity Phase (degrees)	Cavity voltage (MV/m)
182	0.9196	0.9208	-20	23.22
183	0.9208	0.9220	-20	25.62
184	0.9220	0.9232	-20	24.90
185	0.9232	0.9243	-20	27.30
186	0.9243	0.9255	-20	23.46
187	0.9255	0.9266	-19	26.34
188	0.9266	0.9277	-19	24.66
189	0.9277	0.9288	-19	24.18
190	0.9288	0.9299	-19	26.58
191	0.9299	0.9309	-19	22.74
192	0.9309	0.9320	-18	27.54
193	0.9320	0.9330	-18	25.38
194	0.9330	0.9340	-18	24.42
195	0.9340	0.9350	-18	26.82
196	0.9350	0.9360	-18	25.86
197	0.9360	0.9370	-17	22.98
198	0.9370	0.9380	-17	23.94
199	0.9380	0.9389	-17	25.14
200	0.9389	0.9398	-17	23.70
201	0.9398	0.9407	-17	26.10
202	0.9407	0.9416	-16	27.06

REAL TIME RF SIMULATOR (RTS) AND CONTROL*

G. Cancelo#, C. Armiento, K. Treptow, A. Vignoni, T. Zmuda, FNAL, Batavia, IL 60510, U.S.A.

Abstract

The multi-cavity RTS allows LLRF algorithm development and lab testing prior to commissioning with real cavities and cryomodules. The RTS is a valuable tool since it models the functions, errors and disturbances of real RF systems. The advantage of a RTS over an off-line simulator is that it can be implemented on the actual LLRF hardware, on the same FPGA and processor, and run at the same speed of the LLRF control loop.

Additionally the RTS can be shared by collaborators who do not have access to RF systems or when the systems are not available to LLRF engineers. The RTS simulator incorporates hardware, firmware and software errors and limitations of a real implementation, which would be hard to identify and time consuming to model in off-line simulations.

RTS ARCHITECTURE

The RTS simulates the amplitude and phase dynamics of the RF carrier in the RF system. It does not simulate the RF behavior of RF components such as up and down converters, klystron, waveguides and cavities. However, since the LLRF control is performed over the RF envelope, most errors and disturbances are incorporated. As shown in Figure 1 the multi-cavity simulator and the LLRF control are connected in a loop. The RTS can be operated in any combination of feedforward (FF) and feedback (FB) modes.

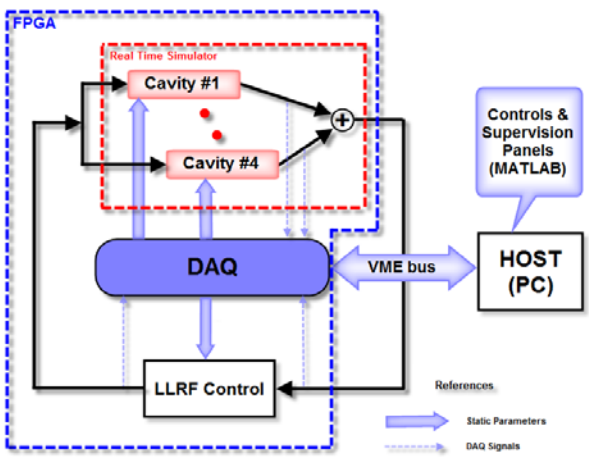

Figure 1: RTS and LLRF control basic scheme.

The RTS and the LLRF control interface to a host computer via a real-time DAQ. The computer server hosts the control software and applications so as perform the RTS and LLRF control initialization, acquire statistics and perform data analysis. The DAQ acquires data during the simulation/control pulse. The data is locally stored into a memory which is readout by the Control server in between RF pulses.

*Work supported by Fermi Research Alliance, LLC. under Contract No. DE-AC02-07CH11359 with the United States Department of Energy.
#cancelo@fnal.gov

RTS MODELS

Cavity Models

The RTS models some of the electrical and mechanical fundamental cavity modes. The electrical model is a 1st order approximation of the cavity's Π mode in the complex plane (1) [1,3]. The mechanical mode, models the Lorentz force detuning [3]. The total detuning from the mechanical model is the linear sum of three mechanical resonances (2). The differential equations for such behaviours are:

$$\begin{bmatrix}\dot{V}_r(t)\\ \dot{V}_i(t)\end{bmatrix} = \begin{bmatrix}-\omega_{1/2} & -\Delta\omega(t)\\ \Delta\omega(t) & -\omega_{1/2}\end{bmatrix}\begin{bmatrix}V_r(t)\\ V_i(t)\end{bmatrix} + \begin{bmatrix}\omega_{1/2}R_L\\ \omega_{1/2}R_L\end{bmatrix}\begin{bmatrix}I_r(t)\\ I_i(t)\end{bmatrix} \quad (1)$$

$$\frac{d^2(\Delta\omega_m)}{dt^2} + \frac{\omega_m}{Q_m}\frac{d(\Delta\omega_m)}{dt} + (\omega_m)^2\,\Delta\omega_m = (\omega_m)^2\,2\pi K_m V^2(t)$$

$$\Delta\omega_m = \sum_{m=1}^{3}\Delta\omega_m \qquad m = 1,2,3 \quad (2)$$

The electrical and mechanical cavity models combined behave as a linear time variant system. The detuning coefficient in the electrical model's transition matrix is a function of the mechanical model's dynamics, which has the cavity gradient as an input. The RTS can also simulate the cavity's 8/9Π mode whose response is added to the Π mode response.

BEAM LOADING

The beam loading is implemented by a table, which is preloaded by the Control server before run time. Each cavity has its own table allowing individual cavity beam loading conditions. This feature is particularly important when the RTS simulates a beam traveling at non relativistic velocities, with β changing at each cavity or when the synchronous phase between the cavity and the beam changes along the simulated cavities.

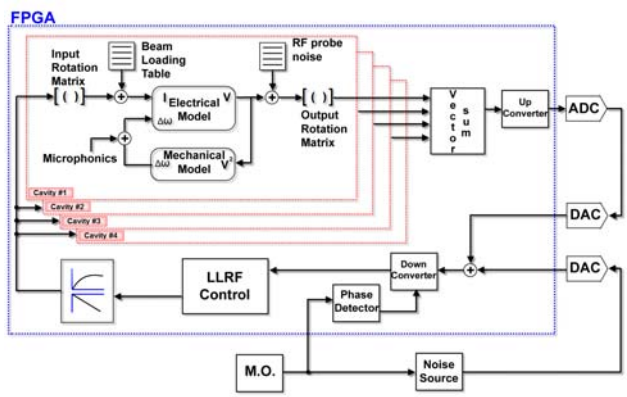

Figure 2: Real time simulator.

KLYSTRON AND RF COUPLERS

Klystron characteristics have a nonlinear behavior in amplitude and phase as a function of the input drive. The RTS models the klystron's nonlinear behavior with amplitude and phase tables. Since a typical klystron bandwidth is on the order of 5 MHz, at least an order of

DESIGN AND EVALUATION OF THE LOW-LEVEL RF ELECTRONICS FOR THE ILC MAIN LINAC*

U. Mavric#, B. Chase, J. Branlard, V. Tupikov, B. Barnes, D. Klepec, Fermilab, Batavia, IL 60510

Abstract

The proposed 30 km long ILC electron/positron collider is pushing the limits not only in basic physics research but also in engineering. For the two main LINACs, the pulsed RF power that is feeding the high number of SC RF cavities (~ 17 000) must be regulated to app. 0.1% for amplitude and 0.2° for phase. This guarantees the required energy spread (0.1%) at the interaction point in the detector. The regulation of phase and amplitude is carried out by the analog/digital electronics also denoted as the low-level RF control system. Besides meeting the regulation specifications, the low-level RF must be reliable, robust and low cost. In the paper we present a possible hardware solution that addresses these issues. The system is evaluated on a cavity emulator implemented on the FPGA. We also present measurement carried out at AØ photo injector.

INTRODUCTION

The two main LINACs for the proposed ILC, will accelerate electrons and positron from 15 MeV up to 250 GeV with the goal luminosity of 2 · 1034 cm $^{-2}$s $^{-1}$. The energy spread of the beam, introduced by the RF system will be mitigated by the low-level RF (LLRF) control system. The lowest achievable energy spread is ultimately defined by the disturbances introduced by the electronics that is controlling it. Besides regulation requirements, the LLRF electronics for the ILC main LINACs must address also reliability, price, low power consumption, mechanical robustness and ease of automation. It is worth noting that the LLRF will have to process over 50 000 RF channels (pick-up probes, reference signals, reflected power, forward power, beam signals, interlocks etc.) coming from both LINACs.

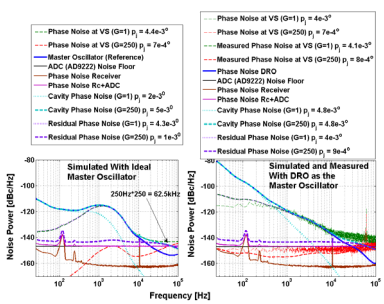

Figure 1: Analysis of close-in noise at various loop gains (>250). The analysis is done at the vector sum, at the output of the cavity and as a relative measurement of the beam compared to the cavity phase uncertainty.

Regulation Requirements

According to [1], the correlated error at the interaction point should be lower than 0.5\% for amplitude and 0.24° for phase. The unanswered question at this point is what is the allowed contribution of the LLRF system to this error budget? Ultimately, the measurement of the residual phase (meaning the relative fluctuation of beam compared to the cavity field) is limited by the noise added in the receiver. After various measurements on-the-bench we proved that a 12 bit (-147dBc/Hz noise floor, AD9222) ADC meets the regulation requirements for the ILC main LINACs. Fig.1 shows a theoretical analysis of the expected regulation at very high gains.

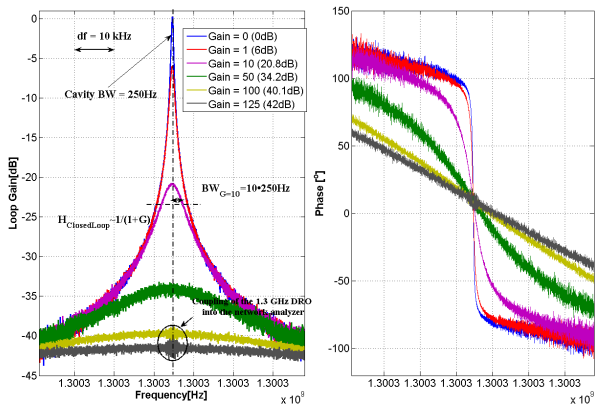

Figure 2: Transfer function of disturbance injected before the cavity to the output of the cavity.

Further on we will present the practical implementation of the LLRF and the evaluation of the system by using a cavity simulator and on an operating machine (AØ photo injector at Fermilab).

THE LLRF SYSTEM FOR THE ILC MAIN LINACS

The system presented in this paper is composed of the 33 channel digital board (Multichannel Field Controller - MFC) and the nine channel analog receiver/transmitter board. The 1.3GHz RF signal is first downconverted by mixing with the LO at 1.313GHz to get the IF at 13MHz. The LO is generated in a separate chassis. The processing of the signal in digital domain is shown in Fig.3. The analog downconversion is done by using the 8 channel receiver/transmitter presented in [2].

*Work supported by …
mavric@fnal.gov

A FEMTOSECOND-LEVEL FIBER-OPTICS TIMING DISTRIBUTION SYSTEM USING FREQUENCY-OFFSET INTERFEROMETRY*

J. W. Staples, J. Byrd, L. Doolittle, G. Huang and R. Wilcox, LBNL, Berkeley, California, USA

Abstract

An optical fiber-based frequency and timing distribution system based on the principle of heterodyne interferometry has been in development at LBNL for several years. The fiber drift corrector has evolved from an RF-based to an optical-based system, from mechanical correctors (piezo and optical trombone) to fully electronic, and the electronics from analog to fully digital, all using inexpensive off-the-shelf commodity fiber components. Short-term optical phase jitter and long-term phase drift are both in the femtosecond range over distribution paths of 2 km or more.

Future Accelerator Timing Requirements

The next generation of accelerators, spread over an area measured in kilometers, will require femtosecond-level synchronization of RF cavities, lasers, photoinjectors and diagnostic devices. Phase-stabilized optical fiber is well-suited for this, along with its immunity to electrical interference, gigaHertz bandwidth, low loss and easy installation in wireways.

Commodity-level single-mode glass fiber, such as Corning SMF-28, optimized for 1300-1550 nm wavelength, exhibits about the same phase velocity dependence on temperature as copper, although the mechanism is temperature dependence of the glass dielectric constant. All fiber components used are inexpensive off-the-shelf devices developed for the telecommunications industry.

The stabilization system developed at LBNL uses the technique of frequency-offset interferometry.

As shown in Figure 1, the optical output of a 1550 nm CW laser is split between the short arm of a Michaelson interferometer and the long fiber to a remote receiver. The short arm of the interferometer is temperature-controlled to a variation of less than 0.01 C. At the end of the long fiber arm, an acousto-optical modulator (AOM) excited at 50 MHz up-shifts the 195 THz laser frequency by 50 MHz, where it is then reflected by a 50% Faraday rotator mirror. The shift of the laser frequency is phase coherent with the 50 MHz RF drive of the AOM. The reflected laser signal is again upshifted by 50 MHz by its return passage through the AOM, resulting in a 100 MHz total frequency shift where it returns along the long fiber, and combines with a sample of the original laser frequency from the interferometer short arm in the splitter.

The variation of the phase length of the fiber is phase coherent to the phase variation of the 100 MHz upshifted return signal. The original laser frequency, from the short arm and the upshifted laser frequency are transmitted along a second fiber, the error signal fiber, to a photodiode at the stabilizer where they produce a 100 MHz beat note which is compared to the 100 MHz reference oscillator. Any change in the phase length of the long fiber is reflected in a phase shift of the 50 MHz signal to the AOM, derived from the 100 MHz reference oscillator, which adds or subtracts the same number of optical cycles in the AOM. The resulting error signal is integrated, the integral representing the change of phase length of the fiber, which shifts the phase of the 50 MHz drive signal to the AOM. All these function are combined in a single chip field-programmable gate array (FPGA) controller.

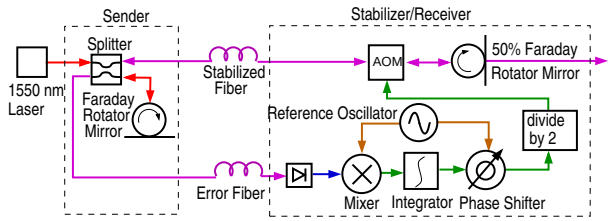

Figure 1: Frequency-offset stabilizer configuration.

The fiber that carries the error signal to the stabilizer needs no stabilization itself, as it is providing optical phase information down-converted to 100 MHz. The 100 MHz beat note is phase-coherent with changes in optical phase in the stabilized fiber, but the frequency ratio of 195 THz (1550 nm wavelength) and 100 MHz is 2×10^6, so a 1 nanosecond change in the error signal fiber produces an error of only 0.5 femtosecond to the correction.

In previous implementations of the stabilizer, the AOM phase was fixed, and mechanical phase shifters (piezo and motor-driven optical trombone) were placed in series with the stabilized fiber. These suffered from a finite range of correction and the usual problems with devices using moving parts. The transition to an all-electronic system significantly simplified the system with a smaller parts count, essentially unlimited range of correction, and increased reliability.

The frequency reference for the system is the 195 THz laser frequency itself, which must be stabilized to 1 part in 10^9 for the system to provide 1 femtosecond stability with with variations of the long fiber of 1 nanosecond. The CW laser is stabilized by taking a sample of the laser, doubling its frequency, and locking it to a saturated absorption line in a Rubidium cell using a Pound-Drever-Hall (PDH) [2]

* This work is supported by the Director, Office of Science, U.S. Dept. of Energy under Contract No. DE-AC02-05CH11231

CONCEPT DESIGN STUDIES OF THE REX-ISOLDE CRYOMODULES AT CERN

V. Parma, S. Calatroni, N. Delruelle, C. Maglioni, M. Modena, M. Pasini, P. Trilhe, J.Hansen,
CERN, Geneva, Switzerland
S. Pattalwar, STFC, Daresbury Laboratory, UK

Abstract

The High Intensity and Energy (HIE) proposal plans a major upgrade of the existing ISOLDE and REX-ISOLDE facilities at CERN [1], with the objective of substantially increasing the energy and the intensity of the delivered radioactive ion beams. In the frame of this upgrade activity, a superconducting linac, based on Nb sputtered Quarter Wave Resonators (QWRs) is proposed to be installed downstream the existing normal conducting machine. The present design of the accelerator lattice features housing of five high-beta cavities (β=10.3%) and a superconducting solenoid in a common cryomodule. In most of the existing low-energy heavy-ion installations worldwide, insulation and beam vacuum are in common, with the risk of cavity surface contamination in case of accidental leak of the cryostat vessel. Following a concept study, we report in this paper on three design options, namely cryo-modules with *single* vacuum, with *separate* or with *hybrid* vacuum systems (the latter having a low conductance between insulation and beam vacuum) and compare them in terms of technical complexity, performance, reliability and maintainability.

INTRODUCTION

QWRs are commonly used in linacs for the acceleration of heavy ion beams in the range of 5-10 MeV/u, due to their high velocity acceptance allowing the coverage of a wide variety of nuclei and beam energies. Examples of heavy ion accelerators based on similar superconducting resonators are the ISAC-II at TRIUMF (Vancouver, Canada) [2], in operation since 2007, the ALPI at LNL (Legnaro, Italy) [3], in operation since several years, ATLAS at Argonne national laboratory [4], in operation since 1992 (Argonne, Illinois, US), the QWR superconducting linac for the 15 UD Pelletron at IUAC (New Delhi, India) [5], and the SPIRAL II at Ganil (Caen, France) [6], now in the construction phase.

In most of the projects, a single vacuum system was chosen both for beam and thermal insulation of the cryo-modules, essentially because it leads to simpler mechanical design and assembly of the cryo-modules; despite the required cleanliness, the number of components is generally smaller and complex flanged connections in the usually compact inter-cavity spacing can be avoided. But, as a consequence, in order to preserve the superconducting surface from contamination, a high level of cleanliness of all internal surfaces is needed, and the use of Multilayer Insulation protection (MLI) and of volatiles like lubricants and brazing fluxes is precluded.

The choice of single vacuum carries a number of drawbacks, the main one being the risk of contamination in case of accidental break of the insulation vacuum leading to particulate contamination of the cavity surface at any stage of the preparation of the cryo-modules outside clean-room or during machine operation. Similar events have been reported and discussed on existing linacs [7], and in some cases the disassembly of the cavities for reconditioning was the only alternative to recover performance. A failure in one of the cryo-module would also propagate through the adjacent units affecting an entire SC linac, unless a sound protection system with fast-closing interlocked vacuum valves is capable of isolating the leak.

Single-vacuum cryo-module is also subject to higher radiation heat loads due to the absence of MLI protection, only in part compensated by low-emissivity surface plating of cold surfaces, and therefore lead to larger cryo-plants, capital and cryogenic operating costs.

Spiral II has made the choice of cryo-modules with separate vacuum, despite the higher complexity of the design, considering contamination of the cavities a major risk for reliability and the heaviness of repair interventions would hinder the machine availability.

THE REX-ISOLDE SC LINAC

In the present REX-ISOLDE facility the radioactive ion beams are accelerated to higher energies with a compact normal conducting linac where, with a complex scheme of several acceleration stages and re-bunching, the energy at extraction is of 3 MeV/u. For the increase in energy, a SC linac is proposed, designed to achieve a final energy of at least 10 MeV/u, delivering an effective accelerating voltage of at least 39.6 MV.

The linac requires a total of 20 high β and 12 low β cavities, and 8 SC solenoids, cooled by boiling helium at 4.5 K.

Cryoplant and Cryogenic Distribution

The possibility of making use of an existing refrigerator at CERN, formerly used for the ALEPH experiment during the LEP operation, would allow substantial cost saving in the HIE upgrade; keeping the heat load budgets well below the refrigeration capacity of 630 W at 4.5 K and 2700 W at 55-75 K (measured capacities during commissioning in 1998), is mandatory to leave

OVERVIEW OF THE FIRST FIVE REFURBISHED CEBAF CRYOMODULES*

M. Drury, E. F. Daly, G. K. Davis, J. Fischer, C. Grenoble, J. Hogan, F. Humphry, L. King, J. Preble, K. Worland, Jefferson Lab, Newport News, VA 23606, USA

Abstract

The Thomas Jefferson National Accelerator Facility is currently engaged in a cryomodule refurbishment project known as the C50 project. The goal of this project is robust 6 GeV, 5 pass operation of the Continuous Electron Beam Accelerator Facility (CEBAF). The scope of the project includes removing, refurbishing and replacing ten CEBAF cryomodules at a rate of three per year. Refurbishment includes reprocessing of SRF cavities to eliminate field emission and increase the nominal gradient from the original 5 MV/m to 12.5 MV/m. New "dogleg" couplers between the cavity and helium vessel flanges will intercept secondary electrons that produce arcing at the 2 K ceramic window in the fundamental Power Coupler (FPC). Modifications of the external Q (Qext) of the FPC will allow higher gradient operations. Other changes include new ceramic RF windows for the air to vacuum interface of the FPC and improvements to the mechanical tuner. Any damaged or worn components are replaced as well. Currently, six refurbished cryomodules are installed in CEBAF. Five have completed testing and are operational. This paper will summarize the test results and operational experience for the first five cryomodules.

INTRODUCTION

The first of the refurbished cryomodules (C50-01) was installed in the North Linac of CEBAF in January, 2007. The fifth refurbished CEBAF cryomodule (C50-05) was installed in the South Linac of CEBAF in February, 2008. All five of these cryomodules had previously been in service in the accelerator tunnel since 1992. During the refurbishment process, each cryomodule was disassembled and its cavities removed. Improved processing methods were used to eliminate field emission and increase the gradient from the original 5 MV/m to an average of 12.5 MV/m. "Dogleg" waveguides were installed between the cavity and helium vessel flanges to intercept the secondary electrons that produce arcing on the cold ceramic window of the FPC. Improved warm ceramic windows were added as well. Improvements were made to the mechanical tuners to reduce backlash. Components that were subject to mechanical wear or radiation damage over the years were replaced.

As these cryomodules are installed, they are subjected to a commissioning process prior to being released for operation in the accelerator. During the commissioning process, each cavity is tested individually to determine the maximum gradient (Emax), and the maximum operating gradient (Emaxop). Measurements of the unloaded Q (Qo) and of field emission are made across the available gradient range. This paper compares the results of commissioning after refurbishment to the results of the original commissioning in 1992. This paper also takes a brief look at the operational history of the refurbished cryomodules.

* This manuscript has been authored by Jefferson Science Associates, LLC under U.S. DOE Contract No. DE-AC05-06OR23177. T he U.S. Government retains a non-exclusive, paid-up, irrevocable, worldwide license to publish or reproduce this manuscript for U.S. Government purposes.

GRADIENT IMPROVEMENT

One of the goals of the refurbishment project is to increase the energy gain from 20 MV to a nominal 50 MV. This goal required an increase in the nominal cavity gradient from 5 MV/m to 12.5 MV/m. Improvements in cavity processing are used to increase the quench gradient and eliminate field emission. The dogleg waveguides are designed to eliminate arcing as a limitation on gradient. The improved RF window design reduces FPC operating temperatures and allows higher forward power levels.

Figure 1 shows the distribution of Emax before and after rebuilding. Emax is defined as the highest gradient that can be reached without quenching the cavity or activating one of the machine protection interlocks. These interlocks include arc detectors looking at the waveguide vacuum space, warm window temperature, or beamline and waveguide vacuum set points.

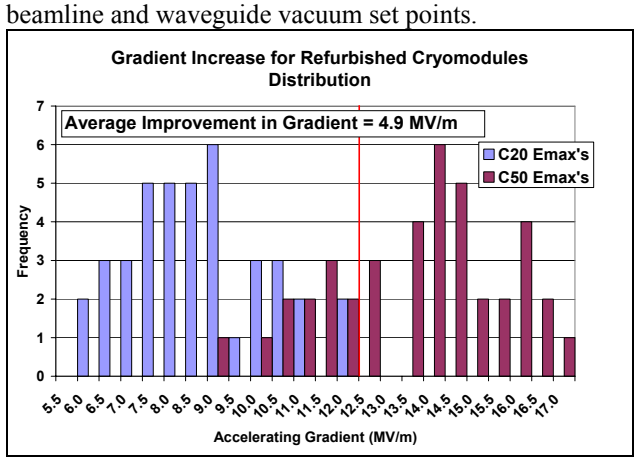

Figure 1: Gradient Improvement

Before reprocessing, these cavities had an average Emax of 8.5 MV/m. The average maximum gradient for the forty cavities has increased to 13.4 MV/m, an increase of 4.9 MV/m or 58%.

Table 1 lists the gradient limits for these cryomodules. The majority of cavities are quench limited. Nine cavities were limited by the warm window temperature. An older style of window had been installed temporarily because of window production delays. These windows were recently replaced with the correct type of ceramic window and the

CONSTRUCTION OF THE MAGNETS AND SUPPORTS FOR THE LINAC COHERENT LIGHT SOURCE (LCLS) UNDULATOR SYSTEM*

M. White#, J. Collins, M. Jaski, G. Pile, B. Rusthoven, S. Sasaki, S. Shoaf, J. Stein, E. Trakhtenberg, I. Vasserman, and J. Xu, ANL, Argonne, IL 60439, U.S.A.

Abstract

The LCLS [1], nearing completion at the Stanford Linear Accelerator Center (SLAC) in California, will be the world's first x-ray free-electron laser when it comes online in mid-2009. Design and production of the undulator system was the responsibility of a team from the Advanced Photon Source (APS) at Argonne National Laboratory. Forty 3.4-m-long precision undulators, 37 laminated quadrupole magnets, and 38 precision support and motion systems with micron-level adjustability and stability were constructed and delivered to SLAC for tuning, fiducialization, final assembly, and installation in the LCLS tunnel. In addition to the magnets and supports, Argonne provided vacuum and diagnostics systems for the undulator line and a computer control and monitoring system that enables undulator girders and all components mounted on them to be accurately positioned [2]. An overview of the magnet and support construction is presented herein.

INTRODUCTION

The LCLS construction project is nearing completion at the Stanford Linear Accelerator Center (SLAC) in California, and LCLS will be the world's first x-ray free-electron laser when it comes online in mid-2009. LCLS design and construction were accomplished primarily by a partnership of three U. S. national laboratories: Argonne National Laboratory (ANL), Lawrence Livermore National Laboratory (LLNL), and SLAC. A team from Argonne's Advanced Photon Source was responsible for design and construction of the high-precision undulator system, including the undulator and quadrupole magnets, vacuum system, beam diagnostics, ultra-stable support and motion system, and computer control and monitoring of the undulator system. At the time of this paper, the magnets and supports, vacuum system, and undulator controls system are all delivered, and component installation in the LCLS tunnel is well underway.

MAGNETS AND SUPPORTS

Undulators

Forty planar-hybrid, fixed-gap precision undulators were designed for LCLS by the Argonne team [3,4], and were optimized for efficient, cost-effective industrial mass production. The magnets are made of NdFeB, and poles are vanadium permendur. Magnets and poles are installed on an aluminum structure that defines their precise locations; the aluminum structure is bolted into a strong titanium housing. The most important undulator physics requirements are listed in Table 1. Undulator assembly was accomplished ahead of schedule and with significant cost savings. Bidders on the fabrication and assembly contracts were prequalified to ensure that they were capable of performing the job safely and correctly. The Argonne team devoted time up front to procedure development, vendor safety training, and completion of the necessary documentation. Vendor oversight, communication, and QA were continuous and thorough throughout the duration.

Table 1: Undulator Physics Requirements

Parameter	Value	Units
# of 3.4-m-long und. segments	33 + 7	
Total installed undulator length	131.520	m
Min. expected undulator sys. life	20	years
Undulator period length	30.00±0.05	mm
Undulator gap height	≥ 6.8	mm
Wiggle plane	horizontal	
Horiz. und. seg. good field region	±5.0	mm
Vert. und. seg. good field region	±200	μm
Total pole cant angle	4.5	mrad
Phase slippage distance of 113×2π	3.656	m
Phase slip. tolerance (@ 1.5 Å)	±175	mrad
Max. acc. seg. ph. err. (@ 1.5Å)	±175	mrad
Abs. 1st field int. along und. seg.	$<40\times10^{-6}$	Tm
Abs. 2nd field int. along und. seg.	$<50\times10^{-6}$	Tm^2
Undulator system temp. range	20.00±0.56	°C

The final undulator was ready 27 months after award of the first long-lead contract. The first undulator from each of the assembly vendors [5,6] was magnetically tuned and mechanically verified at Argonne. All other undulators were delivered directly to SLAC for final tuning and fiducialization. Average peak fields of all undulators were measured at factory acceptance using a portable Hall probe. Results for 38 devices are shown in Figure 1.

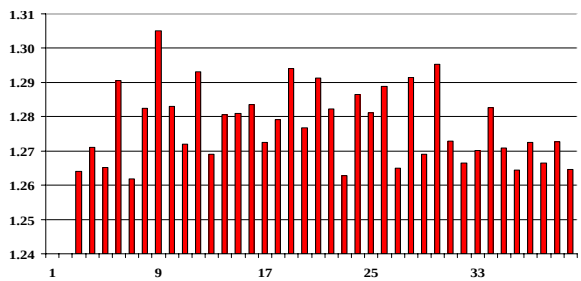

Figure 1: Average peak fields measured during factory acceptance of LCLS undulators.

*Work at Argonne was supported by the U. S. Department of Energy, Office of Science, Office of Basic Energy Sciences under Contract No. DE-AC02-06CH11357.

mwhite@aps.anl.gov

8-GeV C-BAND ACCELERATOR CONSTRUCTION FOR XFEL/SPring-8

Takahiro Inagaki#, on behalf of the members of the XFEL/SPring-8 project,
XFEL joint project of RIKEN and JASRI,
1-1-1 Kouto, Sayo-cho, Sayo-gun, Hyogo, 679-5148, Japan

Abstract

The C-band (5712 MHz) accelerator is used as the main accelerator of the X-ray free electron laser (XFEL) facility in SPring-8. We will use 64 units of them for the 8 GeV XFEL accelerator. Since the C-band generates a high accelerator gradient, as high as 35 MV/m, it makes the accelerator compact. Since May 2008, we have operated one of the C-band units in the SCSS test accelerator with a high accelerator gradient of 37 MV/m. We have experienced no trouble, no serious rf discharge, and no degradation of FEL performance. We confirmed high reliability of the C-band accelerator at high-gradient.

Mass-production of high-power rf components was started in 2007. They have been delivered on schedule. In order to maintain the production quality, we constructed a high-power rf test bunker.

For the power supply, special design was taken to improve stability. The new high-voltage charger has extremely high stability, which satisfies the requirement for the XFEL.

INTRODUCTION

The Japanese X-ray free electron laser (XFEL/SPring-8) is under construction at the SPring-8 site [1,2]. It aims to achieve excellent laser performance with a compact, low-cost, highly reliable machine. It is based on three key technologies; 1) a low-emittance injector using the thermonic electron gun, 2) a C-band high-gradient accelerator, 3) an in-vacuum short-period undulator. The frequency of C-band is 5712 MHz, which is double of conventional S-band accelerator. Higher frequency is chosen due to the higher power efficiency, which makes the accelerator compact. Since the C-band generates a high accelerator gradient, as high as 35 MV/m, the total length of the accelerator fits within 400 m, including the injector and three bunch compressors. The C-band uses normal conducting rf technology, thus it runs in the pulse mode at 60 pps, which is well suited for XFEL operation, and is less expensive.

Figure 1 shows a computer image of our facility. The total length of the FEL facility is 700 m, which fits with available length in our site.

Figure 2 shows the accelerator layout. After the injector and S-band sector, the first C-band sector with 12 C-band units accelerates an electron beam from 415 MeV to 1.45 GeV. At this sector, the rf phase is set at 42 degrees from the crest, which makes energy chirp for the bunch compression chicane (BC3). After BC3, 52 C-band units accelerate the beam to 8 GeV.

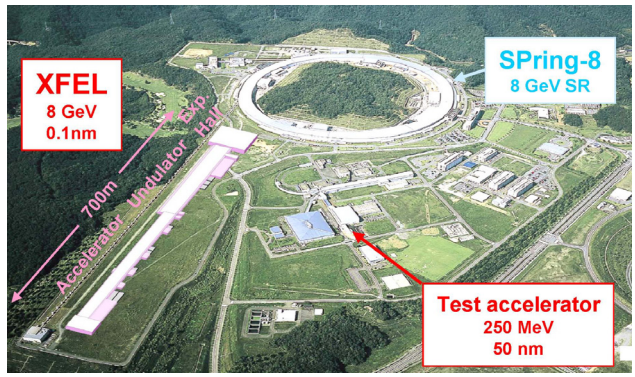

Figure 1: Computer image of the XFEL facility in SPring-8 site.

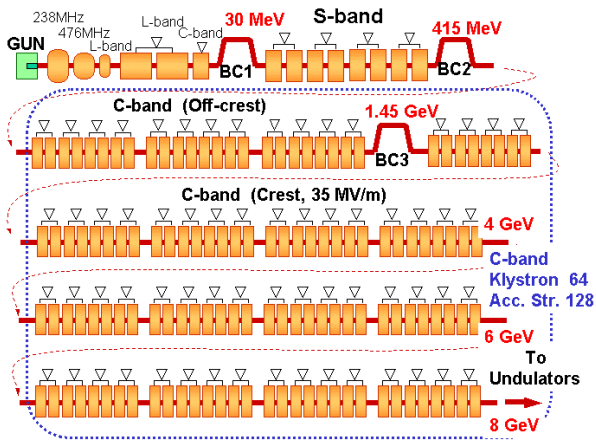

Figure 2: Accelerator layout of XFEL/SPring-8.

C-BAND ACCELERATOR SYSTEM

Figure 3 shows one unit of the C-band accelerator system. The rf source is the 50 MW pulse klystron. An rf pulse compressor compresses a 50 MW, 2.5 μs square pulse to a 150 MW, 0.5 μs pulse. It is then fed to two 1.8 m accelerating structures.

The C-band accelerator was initially developed for the e^+e^- linear collider project. At KEK, the first model of the accelerating structure, the rf pulse compressor, waveguide components, and the klystron were developed [3,4,5,6]. We adopted C-band technology for XFEL. XFEL is the first practical application of the C-band accelerator in a large facility..

#inagaki@spring8.or.jp

COMMISSIONING OF THE LCLS LINAC*

H. Loos†, R. Akre, A. Brachmann, F.-J. Decker, Y. Ding, D. Dowell, P. Emma, J. Frisch, S. Gilevich, G. Hays, Ph. Hering, Z. Huang, R. Iverson, C. Limborg-Deprey, A. Miahnahri, S. Molloy, H.-D. Nuhn, J. Turner, J. Welch, W. White, J. Wu, SLAC, Menlo Park, CA 94025, USA
D. Ratner, Stanford University, Stanford, CA 94305, USA

Abstract

The Linac Coherent Light Source (LCLS) X-ray free electron laser project is currently under construction at the Stanford Linear Accelerator Center (SLAC). A new injector and upgrades to the existing accelerator were installed in two phases in 2006 and 2007. We report on the commissioning of the injector, the two new bunch compressors at 250 MeV and 4.3 GeV, and transverse and longitudinal beam diagnostics up to the end of the existing linac at 13.6 GeV. The commissioning of the new transfer line from the end of the linac to the undulator is scheduled to start in November 2008 and for the undulator in March 2009 with first light to be expected in July 2009.

INTRODUCTION

The Linac Coherent Light Source (LCLS) [1] is an X-ray free electron laser project aimed at generating coherent radiation at wavelengths from 15 Å to 1.5 Å using the final third of the existing SLAC 2-mile accelerator to deliver electrons with an energy of up to 13.6 GeV into an undulator with a length of 130 m. The requirements of a small transverse normalized emittance of 1.2 μm and a peak current of 3 kA to achieve saturation within the length of the undulator are met with the addition of a high brightness photo-injector at the 2/3 point in the linac and two subsequent magnetic chicane bunch compressors. The photo-injector and first bunch compressor was constructed in 2006 and commissioned from April to August 2007 [2, 3]. The second bunch compressor was installed in the fall of 2007 and the second phase of commissioning took place from January to August of 2008 [3].

The layout of the LCLS is depicted in Fig. 1, showing the injector oriented at 35° to the main linac, the two bunch compressors, and some of the diagnostics (LTU and undulator not shown). The main design parameters of the LCLS linac and the achieved values are listed in Table 1.

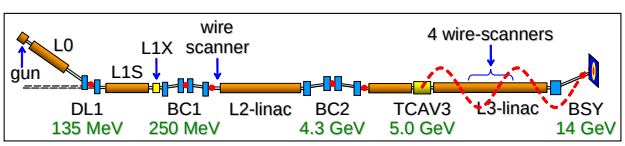

Figure 1: Layout of the LCLS accelerator.

Table 1: LCLS Accelerator Specifications

	Design	Meas.	Unit
Repetition rate	120	30	Hz
Energy	13.6	13.6	GeV
Charge	1	0.25	nC
Bunch length	20	8-10	μm
Peak current	3	3	kA
Emittance (injector)	1.2	0.7-1	μm
Slice emittance (inj.)	1.0	0.6	μm
Emittance (linac end)	1.5	0.7-1.6	μm
Laser energy	250	20-150	μJ
Gun field at cathode	120	115	MV/m
Quantum efficiency	6	0.7-7	10^{-5}

Most of the diagnostics for the electron beam were commissioned in the first phase with some additions during the second phase. New beam position monitors in the injector and bunch compressors and upgraded ones in the existing linac achieve between $5 - 10\,\mu$m resolution. Images of the beam are obtained with YAG screens in the gun and low energy area of the injector, and OTR foils with up to 10 μm resolution throughout the rest of the machine. Their functioning is presently compromised by the occurrence of coherent optical transition radiation and are expected to become reliable with the installation of a laser heater in the injector, which will suppress coherent effects in the beam. Projected transverse emittance can be measured with OTR screens and wire scanners located in the injector at 135 MeV and after BC1 at 250 MeV with 3-screen or quadrupole scan technique. Four wire scanners halfway in the third linac (L3) at 9 GeV are used to obtain the emittance after the second bunch compressor.

A transverse deflector cavity in the injector and one after BC2 make it possible to measure the longitudinal bunch profile and longitudinal phase space on OTR screens in the injector and a phosphorus screen in a dispersive section downstream of the main linac. The vertically deflecting cavity is also used to obtain the horizontal slice emittance in the injector. A number of phase cavities in the injector and after each bunch compressor give the bunch arrival time. Two relative bunch length monitors after BC1 and BC2 which detect coherent edge radiation from the bunch compressor dipoles provide a non-interceptive signal related to the bunch length. The signals are calibrated against an absolute measurement with the transverse cavity.

* Work supported by US DOE contract DE-AC02-76SF00515.
† loos@slac.stanford.edu

OPERATION OF FLASH AS AN FEL USER FACILITY

K. Honkavaara*, DESY, Hamburg, Germany †

Abstract

FLASH, the FEL user facility at DESY, is operated with an electron beam energy up to 1 GeV corresponding to a photon wavelength down to 6.5 nm. The full year 2008 is dedicated to beam operation: about half of the time is scheduled for FEL users, and the rest for accelerator and FEL physics studies. Operational experience gathered at FLASH is very important not only for further improvements of the FLASH facility itself, but also for the European XFEL and for the ILC R&D effort. This paper reports our experience to operate FLASH as a user facility.

INTRODUCTION

FLASH is a free-electron laser (FEL) user facility at DESY (Hamburg, Germany). It is a high-gain single-pass FEL based on self-amplified spontaneous emission (SASE). FLASH is a world-wide unique light source providing ultrashort radiation pulses (femtosecond range) with an unprecedented brilliance.

FLASH is based on the TTF-FEL [1] operated at DESY until end of 2002 with a photon wavelength range from 120 nm to 80 nm [2, 3]. The first lasing of FLASH at 32 nm was achieved in January 2005 [4]. Since summer 2005, FLASH is an FEL user facility. The first two years it provided FEL radiation for user experiments with photon wavelengths from 47 nm to 13 nm [5]. An energy upgrade to 1 GeV in summer 2007 extended the wavelength range down to 6.5 nm. The second user period started end of November 2007.

The complete year 2008, as well as the first half of 2009, is dedicated to beam operation. About half of the time is scheduled for FEL user experiments. The other half is shared between accelerator and FEL physics studies, and maintenance periods.

The experience gathered at FLASH is important not only for further improvements of the FLASH facility itself, but also for the European XFEL project [6] and for the R&D effort of the International Linear Collider (ILC) [7]. We report here our experience to operate FLASH as a user facility. Part of this material has already been presented in [8] and [9].

PRODUCTION OF ELECTRON BUNCHES

Figure 1 shows a schematic layout of the FLASH linac.

A laser driven pulsed RF-gun provides up to 800 electron bunches per bunch train. The macro-pulse repetition rate is 5 Hz. The photocathode laser is based on a mode-locked pulse train oscillator synchronized to the 1.3 GHz of the accelerator. A chain of single-pass Nd:YLF amplifiers provides enough power to convert the initial infra-red wavelengths to ultraviolet (262 nm). The laser beam is guided to a Ce_2Te cathode, which is inserted to the backplane of the RF-gun. The RF-gun is a 1.5 cell normal conducting L-band cavity (1.3 GHz). The maximum accelerating gradient on the photocathode is 46 MV/m, and the electron beam energy at the gun exit $\sim$5 MeV.

Table 1: Some FLASH Parameters

Electron beam		
Energy	MeV	370 - 1000
Peak current	kA	1-2
Emittance, norm. (x,y)	μmrad	1.5 - 2
nb. of bunches / train		1 - 800
Bunch train length	ms	up to 0.8
Rep. rate	Hz	5
Undulator		
Period	cm	2.73
Gap	mm	12
Peak magnetic field	T	0.48
K		1.23
Total length	m	27.3
FEL radiation		
Wavelength	nm	47 - 6.5
Average pulse energy (typ.)	μJ	10 - 50
Average pulse energy (max)	μJ	70
Bandwidth (fwhm)	%	$\sim$1
Pulse duration (fwhm)	fs	10 - 50
Peak power	GW	1 - 5
Peak spectral brilliance	*	10^{29} - 10^{30}

* photons/s/mrad^2/mm^2/(0.1% bw)

The number of bunches in the bunch train as well as the bunch spacing can be varied: the standard spacing is 1 MHz, other spacings like 500 kHz, 250 kHz, or 100 kHz have been realized as well. The electron bunch charge is variable to a certain extend. During FEL operation, a charge between 0.5 nC and 1 nC is used. Some main electron beam parameters are listed in Table 1.

FLASH uses TESLA type accelerating modules. Each module contains eight superconducting niobium 9-cell cavities, a quadrupole doublet with integrated steerers and a beam position monitor. The first accelerating module boosts the electron beam energy to 130 MeV. In order to reduce space charge effects, its first four cavities are operated with a moderate gradient (12-15 MV/m). The first bunch compressor is followed by two modules (ACC2 and

* katja.honkavaara@desy.de
† for the FLASH team

REVIEW OF ADVANCED LASER TECHNOLOGIES FOR PHOTOCATHODE HIGH BRIGHTNESS GUNS

H. Tomizawa, H. Dewa, T. Taniuchi, A. Mizuno, and H. Hanaki,
Accelerator Division, Japan Synchrotron Radiation Research Institute (JASRI/SPring-8),
Kouto, Sayo-cho, Sayo-gun, Hyogo 679-5198, Japan

Abstract

We developed an adaptive 3D shaping UV pulse laser system (based on a Ti:S laser) as an ideal light source for yearlong stable generation of low-emittance electron beams with a charge of 1 nC/bunch. From 2005 onwards, the laser's pulse-energy stability was continuously kept at <1.4% for THG (263 nm) for several months (flashlamp lifetime). In addition, in order to suppress the emittance growth caused by the space charge effect, the 3D cylindrical "beer-can" shape of the laser pulse was optimized spatially as a top-hat (flattop) and temporally as a square stacked chirped pulse. We utilized a deformable mirror that automatically shapes the spatial profile with a feedback routine, which is based on a genetic algorithm, and an UV pulse stacker consisting of three birefringent Alpha-BBO crystal rods for temporal shaping at the same time. Using this "beer-can" 3D-shaped laser pulse, so far we have obtained a minimum horizontal normalized emittance of 1.4 π mm mrad. In 2006, we proposed a laser-induced Schottky-effect-gated photocathode gun for the realization of a water bag beam in Luiten's scheme by using Z-polarization of the laser on the cathode. A hollow laser incidence was applied with convex lens focusing after passing the beam through a radial polarizer. According to our calculations (NA=0.15), a Z-field of 1 GV/m needs 1.26 MW at peak power for the fundamental wavelength (790 nm) and 0.316 MW for the SHG (395 nm).

INTRODUCTION

Since 1996, we have been developing a stable and highly effective UV laser pulse as the light source for a photo-cathode RF gun [1] which in turn provides high-brightness electron beams for future X-ray light sources at SPring-8. The electron source for several X-ray FEL projects [2-4] requires electron beams with very low emittance (high brightness), often as low as 1 π mm mrad, and a charge of 1 nC/bunch. One of the most reliable candidates for this high-brightness electron source is a photocathode RF gun. This type of gun generates an electron beam pulse from a photocathode illuminated by a laser pulse. The development of this gun is oriented toward the creation of a yearlong stable system for user facilities. Since we started developing the laser test facility in 2001, two issues related to the source of laser light have arisen. One is the energy stability of the UV laser light source. In this regard, we successfully stabilized the third-harmonic generation (THG) of a CPA (chirped pulse amplification) Ti:Sapphire terawatt laser system as the laser light source for the SPring-8 RF gun. From 2005 onwards, the laser's pulse-energy stability was continuously kept at <1.4% for THG (263 nm) for several months limited by flashlamp lifetime. This improvement reflects the ability to stabilize the laser system in the pumping sources (Q-switched YAG) of the amplifiers with a temperature-controlled base plate in a clean room where the relative humidity was maintained at 55%. This system keeps dust particles away from the charged optical elements (typically insulator) and thus avoids burn-out damage with the laser incidence.

The other problem concerns the spatial and temporal laser profiles. In order to minimize the beam emittance of a photocathode RF gun, the laser pulse shape should be optimized in three dimensions. One of the candidates for a reliable 3D laser pulse shape has been the cylindrical "beer-can" shaped (spatially top-hat and temporally square) pulse. Over the past seven years, at the test facility for photocathode laser light sources at SPring-8, several 3D shaping systems in the UV region have been developed from combinations of spatial (transverse: x-, y-axes) and temporal (longitudinal: z-axis) pulse-shaping methods (Fig. 1). It was necessary to modify the spatial profile with a microlens array [5] or a deformable mirror (DM) [6], as well as to alter the temporal profile with a spatial light modulator (SLM) [6] or a pulse stacker. In its current form, we have applied a deformable mirror which automatically shapes the spatial profile with a feedback routine based on a genetic algorithm and a UV pulse stacker consisting of three or four birefringent Alpha-BBO crystal rods for temporal shaping at the same time [7]. In 2006, we demonstrated a cylindrical 3D UV laser pulse with the shaping system described above. By precisely optimizing the 3D shape of the laser pulse, we are striving toward the generation of a beam with as high a brightness and as low an emittance as possible. The perfect homogeneity of temporal stacking is automatically optimized with a feedback routine between a AOPDF UV pulse measurement (spectral phase interferometry in the UV region) and a high-resolution DAZZLER as a micro pulse shaper. Using this "beer-can" 3D-shaped laser pulse (diameter: 0.8 mm; pulse duration: 10 ps), so far we have obtained a minimum horizontal normalized emittance of 1.4 π mm mrad [7].

Recently, another candidate for the generation of a reliable 3D pulse shape was proposed for even lower emittance values [8], which comprises an ellipsoid with equivalent fluence along the temporal axis. Such uniform 3D ellipsoidal distributions of charge are one of the ultimate goals in high-brightness beams due to their linear internal force fields. O. J. Luiten simulated a method for the actual production of such bunches, which are based on

BILLION PARTICLE LINAC SIMULATIONS FOR FUTURE LIGHT SOURCES*

J. Qiang#, R. D. Ryne, M. Venturini, A. A. Zholents, LBNL, Berkeley, CA 94720, U.S.A.

Abstract

In this paper we report on multi-physics, multi-billion macroparticle simulation of beam transport in a free electron laser (FEL) linac for future light source applications. The simulation includes a self-consistent calculation of 3D space-charge effects, short-range geometry wakefields, longitudinal coherent synchrotron radiation (CSR) wakefields, and detailed modeling of RF acceleration and focusing. We discuss the need for and the challenges associated with such large-scale simulation. Applications to the study of the microbunching instability in an FEL linac are also presented.

INTRODUCTION

The electron beam quality at the entrance to FEL undulators plays a crucial role for the success of next generation X-ray light sources. In order to achieve good performance of X-ray output with reasonable cost, the emittance of the electron beam and the energy spread of the electron beam need to be controlled within the tolerance level subject to a high peak current. However, collective effects such as the microbunching instability driven by space-charge, wakefields, and CSR can pose a particular challenge that leads to irreversible degradation in beam quality. In order to accurately predict the beam properties at the end of linac subject to those collective effects and to optimize the linac design, large-scale self-consistent simulation is needed. As will be shown, the use of on the order of a billion macroparticles or close to real number of electrons per bunch in self-consistent particle tracking helps to correctly simulate the shot noise inside the electron beam that can be amplified by the microbunching instability.

COMPUTATIONAL AND PHYSICAL MODELS

In this study, we have used the IMPACT code [1], a parallel beam dynamics macroparticle tracking code, as our major simulation tool. The IMPACT code is an object-based parallel particle-in-cell code to simulate high intensity, high brightness beam transport in a beam delivery system. It uses a split-operator method to separate the particle advance subject to the given external fields from the particle advance subject to the collective self-consistent space-charge or wakefield forces. The space-charge forces are calculated from the solution of the 3D Poisson equation in the beam frame using a convolution of the charge density with the Green function for open boundary conditions (in most applications). This convolution is calculated numerically on a 3D grid using an integrated Green function method [2] with FFT calculation of a cyclic summation in a doubled computational domain [3]. The space-charge fields are Lorentz transformed back to the laboratory frame to advance particle momentum. The wakefield forces are calculated in the laboratory frame using a convolution of the wake function and the particle density. This convolution is also computed using the FFT based method. The CSR effects inside a chicane are calculated using a one-dimensional longitudinal CSR wake model [4]. As a test of our space-charge model, we computed the energy modulation amplitude of an initial 120 MeV round uniform electron beam with 120 A current, 5% modulation, and zero initial temperature propagating through a drift space. Figure 1 shows the amplitude of energy modulation as a function of distance in comparison with an often used analytical model of longitudinal space-charge impedance [5]. This analytical model presupposes that the longitudinal component of the electric field across the beam is uniform and equal to the value on the beam axis. This is a good approximation if the wavelength of the perturbation as measured in the beam commoving frame is large compared to the beam transverse radius (or $k*r_b/\gamma \ll 1$, where $k=2\pi/\lambda$ is the perturbation wavenumber in the lab frame.) However, as shown in the picture at smaller wavelengths the analytical model tends to overestimate the energy modulation when this is averaged over the beam tranasverse density. See also [6].

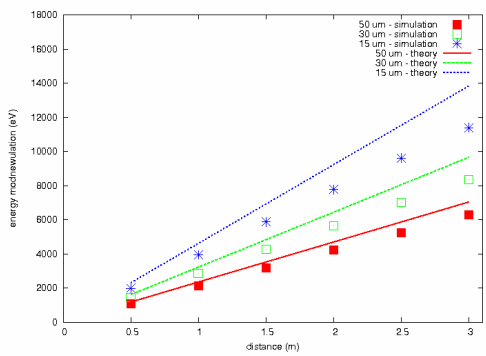

Figure 1: Energy modulation amplitude as a function of distance with initial 5% current modulation at 15 um, 30 um and 50 um wavelength.

The code is implemented on parallel computers using both a domain-decomposition method and a particle-field decomposition method. In the domain-decomposition method, the spatial physical domain is decomposed

*Work supported by the U.S. Department of Energy under Contract No. DE-AC02-05CH11231.
#jqiang@lbl.gov

THE IFMIF 5 MW LINACS

A. Mosnier, CEA, IRFU, F-91191 Gif-sur-Yvette, France.

Abstract

The International Fusion Materials Irradiation Facility (IFMIF) is based on two high power cw accelerator drivers, each delivering a 125 mA deuteron beam at 40 MeV to the common lithium target. The present design of the 5 MW IFMIF Linacs, as well as the description of the prototype accelerator to be built in Japan are presented: the injector including the 140 mA ion source and the magnetic focusing LEBT, the RFQ for the bunching and acceleration to 5 MeV, the MEBT for the proper injection into the Drift-Tube-Linac where the beam is accelerated to the final energy of 40 MeV. Recently, the Alvarez type DTL was replaced by a superconducting Half-Wave Resonator Linac to benefit from the advantages of the SRF technology, in particular the rf power reduction, plug power saving, ability to accelerate high intensity cw beams with high flexibility and reliability. Last, a HEBT section transports and tailors the beam as a flat rectangular profile on the flowing Lithium target. The design and technology choices will be validated during the EVEDA phase, which includes the construction of one full-intensity deuteron linac, but at a lower energy (9 MeV) at Rokkasho Mura in Japan.

INTRODUCTION

The International Fusion Materials Irradiation Facility (IFMIF) is an accelerator driven neutron source for the investigation of the fusion plasma facing materials [1]. The accelerator consists of two high power linacs, each delivering 125 mA deuteron beams at the energy of 40 MeV to the common lithium target. The Engineering Validation and Engineering Design Activities (EVEDA), launched in the framework of a bilateral agreement between Euratom and the Government of Japan in the middle of 2007 aims at producing the detailed design file enabling the further construction of IFMIF, as well as the construction and test at full current of the low energy part of one accelerator at Rokkasho in Japan. The components of the prototype accelerator are provided by European institutions (CEA, INFN, CIEMAT): the injector, the RFQ, the transport line to the 1.2 MW beam dump, the 175 MHz RF systems, the matching section and the DTL, the local control systems and the beam instrumentation, required for tuning, commissioning and operation of the accelerator. The building constructed at Rokkasho Broader Approach site, the supervision of the accelerator control system, as well as the RFQ couplers, are provided by JAEA. From the IFMIF Conceptual Design Report [2], technical updates have been brought in order to optimise the design of the entire linac. In addition to the RFQ, which looks now shorter, the major change is the switch from the room temperature DTL to superconducting technology for the high energy portion of the linac and a linked complete redesign of the RF system.

INJECTOR

The injector has to deliver a 140 mA, low emittance deuteron beam with high reliability. An ECR type (Electron Cyclotron Resonance) ion source has been selected owing to its intrinsic high efficiency, high availability and limitless lifetime. Starting from the SILHI source, developed at CEA-Saclay, with a frequency of 2.45 GHz at 875 Gauss, the extracted energy has been increased from 95 keV to 100 keV, then the extracted intensity from 150 mA to 175 mA in order to meet the 140 mA D^+ requirement (26 mA D_2^+, 9 mA D_3^+). Simulations have been carried out to optimize the electrode number, electrode shape, aperture diameter and to minimize the electric field (Figure 1). A four electrode extraction system was finally chosen since it allows an easy tuning with minimum beam losses and back-streamed electrons. In order to decrease the risk of sparking, the maximum electric field has been kept around 100 kV/cm.

The Low Energy Beam Transport (LEBT) is a dual solenoid transport system with space charge compensation. The total length was minimized to about 2 m to restrain the emittance growth, but even so it allows to include classical diagnostics (movable Faraday cup and insulated screens associated with cameras, current transformers, emittance measurement unit) as well as non destructive optical diagnostic based on residual gas fluorescence to measure steadily the species fraction by Doppler shift analysis. Numerical simulations [3], using a back-and-forth process between the TRACEWIN code and a specially developed code, capable of calculating the space charge compensation, showed that the emittance at the RFQ entrance could come close to the challenging requirement (0.25 π.mm.mrad for the total current of 175 mA) provided that a Krypton gas is injected in addition to deuterium in order to better compensate the space charge effect (P_{D2} = 1.10^{-5} hPa, P_{Kr} = 4.10^{-5} hPa). The loss rate of the incoming D^+ beam by neutralization on the gas is about 2.4% under these pressure conditions.

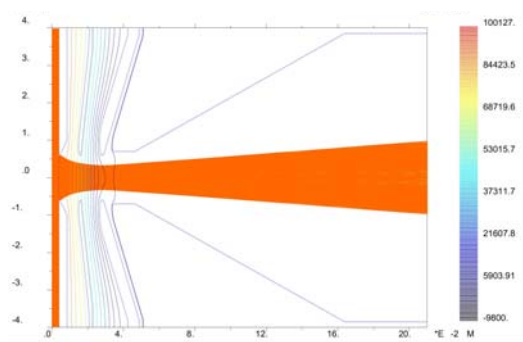

Figure 1: Plot of trajectory simulation for the 4 electrode extraction system (175 mA, 100 kV).

LINACS FOR FUTURE MUON FACILITIES*

S.A. Bogacz#, Jefferson Lab, Newport News, VA, USA
R.P. Johnson, Muons, Inc., Batavia IL, USA.

Abstract

Future Muon Colliders (MC) and Neutrino Factories (NF) based on muon storage rings will require innovative linacs to: produce the muons, cool them, compress longitudinally and 'shape' them into a beam and finally to rapidly accelerate them to multi-GeV (NF) and TeV (MC) energies. Each of these four linac applications has new requirements and opportunities that follow from the nature of the muon in that it has a short lifetime (τ = 2.2 μsec) in its own rest frame, it is produced in a tertiary process into a large emittance, and its electron, photon, and neutrino decay products can be more than an annoyance. As an example, for optimum performance, the linac repetition rates should scale inversely with the laboratory lifetime of the muon in its storage ring, something as high as 1 kHz for a 40 GeV Neutrino Factory or as low as 20 Hz for a 5 TeV Muon Collider. A superconducting 8 GeV Linac capable of CW operation is being studied as a versatile option for muon production [1] for colliders, factories, and muon beams for diverse purposes. A linac filled with high pressure hydrogen gas and imbedded in strong magnetic fields has been proposed to rapidly cool muon beams [2]. Recirculating Linear Accelerators (RLA) are possible because muons do not generate significant synchrotron radiation even at extremely high energy and in strong magnetic fields. We will describe the present status of linacs for muon applications; in particular the longitudinal bunch compression in a single pass linac and multi-pass acceleration in the RLA, especially the optics and technical requirements for RLA designs, using superconducting RF cavities capable of simultaneous acceleration of both μ^+ and μ^- species, with pulsed linac quadrupoles to allow the maximum number of passes. The design will include the optics for the multi-pass linac and droplet-shaped return arcs.

MUON PRODUCTION AND COOLING

Proton Driver Linac

The first linac in the accelerator chain for intense muon beams is for the proton driver. Proposals for various types of linacs and synchrotrons for this purpose have been to use charge exchange injection of H^- ions to overcome the Laslett space charge tune spread. The ultimate expression of this idea is to eliminate acceleration in the synchrotron, such that it becomes an accumulation and bunching ring, and provide all of the acceleration in an 8 GeV linac [1]. To provide sufficient muon flux for a collider of acceptable luminosity will require over 4 MW of beam power at some energy greater than 6 GeV [3].

*Work supported in part by DOE STTR grant DE-FG02-08ER86251
#bogacz@jlab.org

Multi-Megawatt Target

Once the intense proton bunches have been formed at 8 GeV they are tightly focused onto a target capable of many MW operation [4] to produce an intense pion beam. The pions are captured in a strong solenoidal field where they decay into muons (and neutrinos). At the end of the 40 m pion decay channel the muon beam has transverse normalized emittances of around 40,000 mm-mr and is spread in time over tens of ns. The transverse dimensions of the beam must be cooled to be small enough and bunches must be formed to fit into reasonable accelerating structures, depending on their intended NF or MC use.

Ionization Cooling and Emittance Exchange

The only method fast enough to cool a muon beam is ionization cooling in which the muons pass through a low Z material to lose energy in all three directions, have only the longitudinal component replenished by RF, and thereby reduce their angular divergence. Doing the same thing after ninety degrees in betatron phase advance allows the transverse dimensions of the beam to be reduced, but to reduce the bunch length by ionization cooling requires the longitudinal emittance to be exchanged with the transverse emittance. This exchange can be accomplished by placing the energy absorbing material in a dispersive region, either as a wedge-shaped absorber or as a continuous homogeneous absorber [5].

Linacs for Bunching and Cooling

The reduction in each transverse emittance by a factor of 1/e from ionization cooling requires that the energy lost in the absorber be equal to the energy of the beam. Thus for a 250 MeV beam, a linac of about 7×250 = 1750 MeV energy would be needed to achieve a factor of a thousand in each transverse plane, or a factor of a million in six-dimensional emittance reduction as is required for a MC. In muon ionization cooling, intense magnetic fields are required which imply either sequential energy absorption and RF segments or the use of normal conducting RF filled with high-pressure gas [6].

CHOICE OF ACCELERATION TECHNOLOGY

Since muons are generated as a tertiary beam they occupy large phase-space volume and the accelerator must provide very large transverse and longitudinal acceptances. The above requirements drive the design to low RF frequency, as low as 200 MHz for the initial bunching and cooling sections. If normal-conducting cavities were used, the required high gradients of order of ~15 MV/m would demand uneconomically high peak power of RF sources. Superconducting RF (SRF) cavities are a much

NEUTRONS AND PHOTONS: PROBES OF CONDENSED MATTER

W. G. Stirling, ESRF, Grenoble

Abstract

Synchrotron X-rays and neutrons provide unique microscopic information on the structures and dynamics of condensed matter. These probes are essential tools for biologists, chemists, physicists and materials scientists and have become increasingly important in a remarkably wide range of disciplines, from palaeontology to medicine. The electron storage rings producing synchrotron radiation, and fission reactor or spallation neutron sources, are usually situated at major national or international laboratories. Such central research facilities are exemplified by the two international laboratories in Grenoble, the European Synchrotron Radiation Facility and the Institut Laue-Langevin. After a discussion of the sources used to produce synchrotron radiation and neutron beams, some of the instrumentation and methods used in the investigation of materials will be described, with illustrative examples of recent research. Finally, some major X-ray and neutron sources under construction or at the planning stage will be described, including several where linac technology plays an important role (e.g. the XFEL at DESY and the SNS at ORNL).

CONTRIBUTION NOT RECEIVED

THE HIGGS BOSON HOLY GRAIL OF PARTICLE PHYSICS

Nigel Lockyer, TRIUMF, 4004 Wesbrook Mall, Vancouver, BC Canada V6T 2A3

Abstract

The most sought after particle in history is the Higgs Boson. Arguably, the Large Hadron Collider (LHC) at CERN has been built to find the Higgs. Some kind of Higgs mechanism is needed in the Standard Model to give mass to the intermediate vector bosons, the carriers of the weak force. The same mechanism gives mass to the quarks and leptons as well. An elementary introduction to the Higgs Boson is presented.

INTRODUCTION

There are several motivating questions that drive research in particle physics and for more than half of these it can be argued the Higgs boson sheds some light on the question.

1. Are there undiscovered new symmetries or laws in nature?
2. Are there extra dimensions of space? (small or large)
3. Do all the forces become one?
4. How can we solve the mystery of Dark Energy?
5. What is Dark Matter?
6. Where is all the anti-matter?
7. How to combine quantum mechanics & gravity?

Items 1) and 2) motivated by new physics to stabilize Higgs mass calculation-no fine tuning assumption. Item 3) Hints exist & needs spontaneous symmetry breaking. Item 4) Higgs may be part of the puzzle. Items 5) 6) require experimenters to get more data since theory cannot lead. Item 7) String theory has much to say about this since it is the only theory to include gravitational interactions and particle physics.

In this paper we'll discuss: What is the Higgs Boson? What is the Higgs Mechanism? Why are weak interactions weak? Connections to Nuclear Physics & Astrophysics? Higgs Search Status at Tevatron and a few words about the ILC as a Higgs Factory.

Peter Higgs is a theoretical physicist from the University of Edinburgh. He did his seminal work over 40-years ago. He was motivated by the work of Schrieffer and Nambu amongst others, who had been studying superconductivity. It was recognized that the Higgs field was a form of superconductivity in vacuum, a relativistic quantum fluid that fills all of space.

In a superconductor, Cooper pairs form a condensate which breaks the electromagnetic gauge symmetry and expels magnetic fields from inside the superconductor, a phenomena called the Meisner Effect. One interpretation of the Meisner effect is that the electromagnetic fields in the superconductor are short range and therefore cannot penetrate the surface more than a short distance. In an ordinary metal, we know electric fields inside the conductor are zero due to a rearrangement of the electric charges on the surface of the conductor. However, magnetic fields can fully penetrate a conductor. In a superconductor, the photon becomes massive and consequently has a short range, inversely proportional to the mass.

The Higgs mechanism is a form of superconductivity in vacuum. The Higgs field fills all space and prevents the weak force from propagating over infinite distance. In the simplest case, the Higgs field consists of 2 neutral and 2 charged components. When the Higgs acquires a non-zero vacuum expectation value, the Higgs field then has a non-zero value throughout space. The value is given in the standard model as 246 GeV. Three of the fields, the two neutral and one charged field mixes with the three W and Z bosons, giving them mass, and the other remaining field is the scalar Higgs boson. The weak force range is inversely proportional to the mass of the W and Z bosons.

Now for a few simple definitions to set the stage for further discussion. A particle is a disturbance in a field. An example of a field, such as a temperature field, is a number at every point in space that describes the temperature at that point. If one number describes each point, it is called a scalar field. If two numbers are required, such as with a wind field or a magnetic field, where you need a number and a direction, it is a vector field. The Higgs field is a neutral scalar field that fills the entire universe. Particles travelling through the universe interact with the field and become massive. Importantly, the W and Z become massive and the photon must have a mass identical to zero in the standard model.

We wish to introduce the concept of spontaneous symmetry breaking in a non-rigorous manner. Firstly, symmetry is a concept we are all familiar with, especially in art. M.C. Escher is a good example. It is however more precisely defined in physics and this leads to some confusion. Often, non-scientists think a snow-flake has a great deal of symmetry (6-fold) and yet steam does not. However, if we define a perfectly symmetric system as one where every direction for example, is identical, then steam is more symmetric than a snow flake. Therefore, steam, after it cools, loses symmetry. The original symmetry is broken.